



NASA CR-159,802
V.I

NASA-CR-159802
19800019998

NASA CR-159802
VOLUME 1 OF 2



MATERIALS FOR ADVANCED TURBINE ENGINES

PROJECT COMPLETION REPORT PROJECT 1

POWDER METALLURGY RENÉ 95 ROTATING TURBINE ENGINE PARTS

Volume 1

by

W.R. Pfouts
C.E. Shamblen
J.S. Mosier
R.E. Peebles
R.W. Gorsler

LIBRARY COPY

JUNE 1979

AUG 22 1980

LANGLEY RESEARCH CENTER
LIBRARY, NASA
HAMPTON, VIRGINIA

Prepared for:
National Aeronautics and Space Administration
NASA-Lewis Research Center
Contract NAS3-20074

1. Report No. NASA CR-159802		2. Government Accession No.		3. Recipient's Catalog No.	
4. Title and Subtitle Powder Metallurgy René 95 Rotating Turbine Engine Parts				5. Report Date June 1979	
				6. Performing Organization Code	
7. Author(s) W.R. Pfouts, C.E., Shamblen, J.S. Mosier, R.E. Peebles, and R.W. Gorsler				8. Performing Organization Report No. R79AEG416	
				10. Work Unit No.	
9. Performing Organization Name and Address General Electric Company Aircraft Engine Group Advanced Engineering and Technology Programs Department Cincinnati, Ohio 45215				11. Contract or Grant No. NAS3-20074	
				13. Type of Report and Period Covered Final (Project 1, Volume 1)	
12. Sponsoring Agency Name and Address National Aeronautics and Space Administration Washington, D.C. 20456				14. Sponsoring Agency Code	
15. Supplementary Notes Project Manager: Robert L. Dreshfield, Materials and Structures, NASA Lewis Research Center, Cleveland, Ohio					
16. Abstract Project 1, a five year cooperative Government/Industry effort, Materials for Advanced Turbine Engines (MATE), was conducted to refine methods for producing powder metallurgy aircraft gas turbine engine rotating parts from the nickel-base superalloy known as René 95. The parts produced were the high pressure turbine aft shaft for the CF6-50 engine and the stages 5 through 9 compressor disk forgings for the CFM56/F101 engines. The goal of the project was to achieve a 50% cost reduction as compared to conventional cast and wrought processing practices. The project consisted of an integrated effort involving several powder producers and a major forging source. The project was divided into five principal tasks. Task I included material envelope design for both the As-HIP and the HIP - Forge parts. Task II, Process Development, included the development of processing methods, heat treatment parameters, and the effect of process variables on the mechanical properties and producibility of the selected components. Task III, Manufacturing, covered the manufacture of the selected parts for mechanical property verification and for inspection and finish machining of parts for engine test. Task IV, Engine Testing, covered the engine testing of one of each of the selected parts in a typical ground based test. Task V analyzed the results of the overall program. A separate report will be issued describing the results of the last two tasks. Mechanical properties of both As-HIP and HIP + Forge René 95 components met or exceeded all mechanical property goals. An input weight reduction of 54% and a cost reduction of 35% was achieved for HIP + Forge components as compared to conventionally processed René 95. Both the As-HIP and HIP + Forge processes developed here are being used to produce production components for the CFM56 engine, scheduled for utilization in commercial aviation service in the early 1980's, and other engines currently under development or production by General Electric.					
17. Key Words (Suggested by Author(s)) HIP René 95 Forging Powder Metallurgy			18. Distribution Statement Hot Isostatic Pressing Rotating Parts Disks		
19. Security Classif. (of this report)		20. Security Classif. (of this page)		21. No. of Pages	22. Price*

* For sale by the National Technical Information Service, Springfield, Virginia 22161

N80-28499 #

FOREWORD

This report was prepared for the National Aeronautic and Space Administration, Lewis Research Center, under Contract NAS3-20074. It presents the results of a three year program to establish manufacturing methods for producing powder metallurgy René 95 rotating parts by both as-hot isostatically pressed (as-HIP) processes and by a combination process consisting of hot isostatic pressing followed by hot die forging (HIP + Forge). The goal was to produce parts by these powder metallurgy processes with component quality and mechanical properties comparable to parts produced from René 95 alloy and IN718 by conventional forging of vacuum arc-cast ingot material.

Appreciation is expressed for the contributions of Messrs E.N. Bamberger and D.B. Arnold who were involved in Program Management of Project 1. Dr. W.R. Pfouts and Mr. R.E. Peebles were principal investigators for the as-HIP portion of the project and Mr. C.E. Shamblen was principal investigator for the HIP + Forge portion of the project. Mr. J.S. Mosier acted as project manager throughout the course of Project 1. Appreciation is also expressed to Dr. Robert L. Dreshfield of NASA Research Center, project manager of Project 1, whose guidance and counsel were invaluable to the overall success of Project 1.

TABLE OF CONTENTS

<u>Section</u>		<u>Page</u>
1.0	SUMMARY	1
2.0	INTRODUCTION	3
2.1	Background	3
2.2	Program Outline	11
3.0	AS-HIP PROCESSING	16
3.1	Material Envelope Design - As-HIP	16
3.1.1	Task I - Envelope Design	16
3.1.2	Task II - Process Development	17
3.1.3	Task III - Manufacturing Shape Development	31
3.2	Processing and Properties of As-HIP Shapes	43
3.2.1	Task II - Process Development	43
3.2.1.1	Powder Production	43
3.2.1.2	Heat Treatment Development	43
3.2.1.3	Detailed Heat Treatment Evaluation	55
3.2.1.4	Process Variable Studies	74
3.2.1.5	Process Deviation Effects	103
3.2.2	Task III - Manufacturing	133
3.2.2.1	Mechanical Properties: CF6-50 HPT Aft Shaft	133
3.2.2.2	Product Acceptance Testing	157
3.2.2.3	René 95 Machinability Studies	157
4.0	HIP + FORGE PROCESSING	175
4.1	Hot Die Forging Preform Shape and Forging Parameters	175
4.1.1	Die Cavity Design	175
4.1.2	Preform Shape Design	175
4.1.3	Subscale CFM56/F101 Disk Hot Die Forging Parameter Development	177
4.1.4	Full Scale Forging Parameter Selection	182

TABLE OF CONTENTS (Concluded)

<u>Section</u>	<u>Page</u>
4.2 Task II - Process Development	184
4.2.1 Development Approach and Materials Characterization	184
4.2.2 Subscale Shape Development	186
4.2.3 Full-Scale Forging Preform Process Development	209
4.2.4 Alternate Approach to Near-Net-Shape Preforms	212
4.3 Task III - Manufacturing	214
4.3.1 Forging Die Production	214
4.3.2 Oversize Preform Production	214
4.3.3 Net Size Preform Production	218
4.3.4 Forging of Preforms	223
4.3.5 Analyses of Forge Cracking Problems	228
4.3.6 Mechanical Property Evaluation	244
5.0 TASK IV - ENGINE DEMONSTRATION TEST	277
6.0 TASK V - POST ENGINE TEST ANALYSIS	278
7.0 ANALYSIS/RECOMMENDATIONS	279
8.0 CONCLUSIONS	282
9.0 GLOSSARY	284
Appendix A - Vendor Certificate of Test for CF6-50 HPT Aft Shaft SM-586	285
Appendix B - Vendor Certificate of Test for CF6-50 Aft Shafts SM-582, SM-587, SM-589, SM-590, and SM-531.	293
Appendix C - Process Plan for Manufacturing CF6-50 HPT Aft Shaft	307
Appendix D - Process Plans for Manufacturing CFM56 HIP + Forge Compressor Disc Preforms and Forgings	317
Appendix E - Material Acceptance Criteria and Lower Limit Data for as-HIP René 95	326
Appendix F - Material Acceptance Criteria and Lower Limit Data Curves for Hip + Forged René 95	332

LIST OF ILLUSTRATIONS

<u>Figure</u>		<u>Page</u>
2-1.	Ultimate Strength Comparison of René 95 Versus Other Disk Alloys.	5
2-2.	Conventional As-HIP PM Hot Die, and As-HIP PM Processing Sequences for the Core Compressor Stages 5-9 Disk.	8
2-3.	CF6-50 High Pressure Turbine Rotor Aft Shaft.	9
2-4.	CF6-50 HPTR Rear Shaft.	10
2-5.	Powder Metallurgy René 95 - Rotating Parts.	12
2-6.	Flow Diagram for Task I.	13
2-7.	Flow Diagram for Task II.	14
2-8.	Flow Diagram for Task III.	15
3-1.	Effect of Harperizing on Surface Finish of First Iteration CF6-50 Aft Shaft Shape (SM389).	19
3-2.	Surface Contour of Typical As-HIP Surface Before Harperizing (Aft Shaft Shape SM-389, Area A).	20
3-3.	Surface Contour of Typical As-HIP Surface After Harperizing (Aft Shaft Shape SM-389, Area A).	21
3-4.	Schematic of Ultrasonic Response Signals from Area A (Figure 3-2), Harperized Aft Shaft Shape.	22
3-5.	As-HIP CF6 HPTR Rear Shaft - 1st Shape Trial (SM-389).	24
3-6.	As-HIP CF6 HPTR Rear Shaft Dimension Locations.	25
3-7.	Relationship of 1st Shape Trial Part (SM-389) to HIP Target Shape and Final Part Configuration.	27
3-8.	Minimum and Maximum Material Conditions Found on SM-489.	29

LIST OF ILLUSTRATIONS (Continued)

<u>Figure</u>		<u>Page</u>
3-9.	Minimum Material Envelope Versus Engineering Contour Compact SM-489.	30
3-10.	As-HIP CF6 HPTR Rear Shaft Dimension Locations.	32
3-11.	3rd Shape Trial Part (SM-531) Showing Minimum Envelope, Sonic Target and Final Part.	34
3-12.	Wax Patterns for CF6 HPTR Rear Shaft.	35
3-13.	Comparison of Total Envelope Variance (Patterns and Compacts) and Deviation from Target Dimension.	37
3-14.	SEM Photomicrographs of Typical Crucible René 95 Powder.	44
3-15.	Temperature Versus Time Curves for Rapid Air Cool from 1093° C (2000° F) and 1121° C (2050° F) Solution Temperatures.	48
3-16.	Cooling Rate Versus Section Size Curves for Rapid Air Cool from 1093° C (2000° F) and 1121° C (2050° F) Solution Temperatures.	49
3-17.	Microstructure of AS-HIP René 95 Solution Treated at 1093° C (2000° F) and 1121° C (2050° F) and Aged at 760° C (1400° F) 16 Hours (Walker's Etch).	54
3-18.	Cut Up Plan for Plates 1, 3, and 5 of Detailed Mechanical Property Evaluation.	57
3-19.	Cut Up Plan for Plates 2, 4 and 6 of Detailed Mechanical Property Evaluation.	58
3-20.	Tensile and Stress Rupture Test Specimens.	59
3-21.	Tensile, Stress Rupture, and Creep Specimen and Double Reduced Notch Bar Cycle Rupture Test Specimen.	60
3-22.	Notch Bar Low Cycle Fatigue (Load Control) Test Specimen.	61
3-23.	Crack Propagation (K_P) Test Specimen.	61
3-24.	Microstructure of Material Given Heat Treatment A.	63
3-25.	Microstructure of Material Given Heat Treatment B.	64

LIST OF ILLUSTRATIONS (Continued)

<u>Figure</u>		<u>Page</u>
3-26.	Microstructure of Material Given Heat Treatment C.	65
3-27.	Stress Rupture Data for Detailed Evaluation Heat Treatments Compared to IN718 Average Properties.	68
3-28.	0.1% Creep for Detailed Evaluation Heat Treatments Compared to IN718 Average Properties.	69
3-29.	Notched ($K_t = 3.5$) Low Cycle Fatigue Data for Detailed Evaluation Heat Treatments Compared to IN718 Properties.	71
3-30.	Sustained Peak Low Cycle Fatigue Data for Detailed Evaluation Heat Treatments Compared to IN718 Properties.	73
3-31.	Cooling Rate Versus Section Size Curve for 704, 760, and 816° C (1300, 1400, and 1500° F) Salt Bath Quenches from 1121° C (2050° F) Salt Solution Treatment.	75
3-32.	Smooth Bar Low Cycle Fatigue (Strain Control) Test Specimen.	79
3-33.	Typical Blank Cut-Up for Test Specimens.	80
3-34.	Examples of Defects Found in Billets Seeded with Oxide Inclusions.	82
3-35.	Examples of LC Astroloy and M2 Tool Steel Contaminants Found in Billets Seeded with These Foreign Alloy Contaminants.	83
3-36.	Surface Defects Noted Prior to Test and Fracture Surface of Specimen T54.	88
3-37.	Surface Defect Noted Prior to Test and Fracture Surface of Specimen T52.	89
3-38.	Effect of Oxide Inclusion Size on Room Temperature Tensile Properties.	90
3-39.	Effect of Defect Area on 649° C (1200° F) Tensile Properties.	91

LIST OF ILLUSTRATIONS (Continued)

<u>Figure</u>		<u>Page</u>
3-40.	Effect of Foreign Alloy Contaminants on RT Tensile Properties.	92
3-41.	Effect of Foreign Alloy Contaminants on 1200° F Tensile Properties.	93
3-42.	Effect of Percent Tip on RT Tensile Properties.	95
3-43.	Effect of Percent Tip on 649° C (1200° F) Tensile Properties.	96
3-44.	Effect of Oxide Inclusion Size on 649° C/965 MPa (1200° F/140 ksi) Stress Rupture.	98
3-45.	Effect of Foreign Alloy Contaminants on 649° C/965 MPa (1200° F/140 ksi) Stress Rupture.	99
3-46.	Effect of Percent Tip on 649° C/695 MPa (1200° F/140 ksi) Stress Rupture.	100
3-47.	Fracture Surface of LCF Specimen LS4 Showing Example of Fatigue Initiation at a Pore.	104
3-48.	Effect of Oxide Inclusions on 538° C (1000° F) Strain Control R = 0 (A = 1, K _t = 1) LCF.	105
3-49.	Fracture Surface of LCF Specimen LS29 Showing Example of Fatigue Initiation at Surface Oxide Inclusion.	106
3-50.	Fracture Surface of LCF Specimen LS23 Showing Example of Fatigue Initiation at Subsurface Oxide Inclusion.	107
3-51.	Fracture Surface of LCF Specimen LS35 Showing Example of Fatigue Initiation at M2 Tool Steel Particle.	108
3-52.	Effect of M2 Tool Steel, LC Astroloy, and Percent Tip on 538° C (1000° F) Strain Control (A = 1), K _t = 1 LCF.	109
3-53.	Microstructure of Standard -60 Mesh Product Fabricated Using Nominal HIP and Heat Treatment Parameters (Disk B462-1).	111
3-54.	SEM Photomicrographs of Crucible -60 +150 Mesh René' 95 Powder (MB048).	114

LIST OF ILLUSTRATIONS (Continued)

<u>Figure</u>		<u>Page</u>
3-55.	SEM Photomicrographs of Crucible -50 Mesh René 95 Powder (MB048).	115
3-56.	Microstructures of Disks Made From -60 +150 (B468) and -150 (B487) Mesh Powder with Nominal HIP and Heat Treatment Parameters.	116
3-57.	Microstructures of Disks Compacted at 28° C (50° F) Below 1093° C (2000° F) - B464, and 28° C (50° F) Above 1149° C (2100° F) - B465, the Nominal HIP Temperature 1121° C (2050° F) and Given the Nominal Heat Treatment.	117
3-58.	Microstructures of Disks HIP Under Nominal Conditions and Then Solution Treated 28° C (50° F) Above 1149° C (2100° F) - B463-1 and 28° C (50° F) Below 1903° C (2000° F) - B463-3 Nominal Solution Temperature.	119
3-59.	Effect of Particle Size Distribution on Tensile Properties of As-HIP René 95.	122
3-60.	Effect of HIP Temperature on Tensile Properties of As-HIP René 95.	123
3-61.	Effect of Solution Temperature on Tensile Properties of As-HIP René 95.	124
3-62.	Effect of Solution Temperature and Powder Size Distribution on Stress Rupture Properties of As-HIP René 95.	127
3-63.	Effect of Particle Size Distribution on 538° C (1000° F) Notched ($K_t = 3.5$) Load Control Low Cycle Fatigue.	130
3-64.	Effect of HIP Temperature on 538° C (1000° F) Notched ($K_t = 3.5$) Load Control Low Cycle Fatigue.	131
3-65.	Effect of Solution Temperature on 538° C (1000° F) Notched $K_t = 3.5$ Load Control Low Cycle Fatigue.	132
3-66.	Effect of Process Deviations on 538° C (1000° F) Strain Control Low Cycle Fatigue $R = 0$, $(A = 1)$, $K_t = 1$.	135

LIST OF ILLUSTRATIONS. (Continued)

<u>Figure</u>		<u>Page</u>
3-67.	As-HIP CF6-50 Shaft Test Specimen Layout.	137
3-68.	As-HIP CF6-50 Test Specimen Layout.	138
3-69.	Photomicrographs Showing Typical Microstructures of As-HIP René 95 CF6-50 HPT Rear Shafts SM 582 and SM 590.	139
3-70.	Density and TIP Measurements for As-HIP René 95 CF6-50 HPT Rear Shafts SM590 and SM582.	141
3-71.	0.2% Yield Strength and Ultimate Tensile Strength Versus Temperature for As-HIP René 95 CF6-50 HPT Rear Shaft.	143
3-72.	Percent Elongation and Percent Reduction of Area Versus Temperature for As-HIP René 95 CF6-50 HPT Rear Shaft.	144
3-73.	Larson-Miller Parameter Plot of Stress Rupture Data from As-HIP René 95 CF6 HPT Rear Shafts.	146
3-74.	Double Reduced Notched Bar Sustained Peak Low Cycle Fatigue (SPLCF) Test Specimen.	148
3-75.	Smooth Bar Low Cycle Fatigue (Strain Control) Test Specimen.	150
3-76.	Smooth Bar Load Control Low Cycle Fatigue Test Specimen.	152
3-77.	482° C (900° F) Notched ($K_t = 1.5$) Load Control LCF Data from As-HIP René 95 CF6-50 HPT Shafts ($A = 0.95$).	154
3-78.	Notched Bar Low Cycle Fatigue (Load Control) Test Specimen.	155
3-79.	371° C (700° F) Notched ($K_t = 3.5$) Load Control LCF Data from As-HIP René 95 CF6-50 HPT Rear Shafts $R = .03$ ($A = .95$).	156
3-80.	538° C (1100° F) Sustained Peak Low Cycle Fatigue Data from As-HIP René 95 CF6-50 HPT Rear Shaft 10-90-10, sec - $K_t = 2$, $A = 0.95$, $R = 0.03$).	159

LIST OF ILLUSTRATIONS (Continued)

<u>Figure</u>		<u>Page</u>
3-81.	Crack Propagation (K_B) Test Specimen.	160
3-82.	Stiffness Comparison of Tee Lock and Preloaded Pin Design.	164
3-83.	Milling Setups.	166
3-84.	Tool Life-Linear Milling.	169
3-85.	Effect of Hole Depth on Drill Life*, 6.35 mm (1/4") Diameter Carbide Drills.	171
3-86.	Effect of Hole Depth on Drill Life, 1.6 mm (1/16") Diameter Carbide Drills.	172
4-1.	CFM56/F101 Stages 5-9 Compressor Rotor Disk Forging Configuration.	176
4-2.	Typical Subscale F101 Stage(s) 5-9 Compressor Disk(s) Forging Microstructures at 250X (Phosphoric Electrolytic Etch).	181
4-3.	Schematic Diagram of Striation Development.	194
4-4.	Striations Pattern Formation as a Function Container Filling Procedure.	196
4-5.	Acceptable Forgeability for Subscale CFM56/F101 Stage 5-9 Compressor Disk Forging.	197
4-6.	Subscale F101 Stage(s) 5-9 Compressor Disk(s) Forging.	198
4-7.	Subscale CFJ56/F101 5-9 Compressor Disk Forging.	199
4-8.	Udimet 1008 Can Material - 1st Subscale Run Forged Preforms Surface Reactions (Walker's Etch, 250X).	200
4-9.	Udimet 1st Subscale Run (250X).	202
4-10.	MATE CFM56/F101 Compressor Disk Forging.	224
4-11.	Compressor Disk Forgings Produced from the Cartech Three-Piece Preform Multiple Log.	226
4-12.	Stage 5-9 Compressor Disks Produced from 1204° C (2200 °F) HIP Udimet Preforms.	227
4-13.	Stage 5-9 Compressor Disk Forging Preform Showing Powder F111 Striations.	229

LIST OF ILLUSTRATIONS (Continued)

<u>Figure</u>		<u>Page</u>
4-14.	Section of Stage 5-9 Compressor Disk Forging Showing Striations and Attempt to Grind Out Striation Cracks at the Rim (Bottom).	230
4-15.	Section of the 1121° C (2050° F) HIP Plus 1201° C (2200° F) Re-HIP Preform Compressor Disk Forging Showing Striations and Associated Cracking.	231
4-16.	Compressor Disk Forging Microstructure After 1121° C (2050° F) HIP + 1190° C (2175° F) Preforge Heat Treatment + 1107° C (2025° F) Forge and Final Heat Treatment. Note Outlining of PPB.	232
4-17.	CFM56/F101 Compressor Disk Forging Microstructure After 1121° C (2050° F) HIP + 1204° C (2200° F) Re-HIP + 1190° C (2175° F) Preforge Heat Treatment + 1107° C (2025° F) Forge. Note Outlining of PPB.	233
4-18.	Microstructure of the CarTech Preforms in the HIP Condition (Walker's Etchant).	236
4-19.	Microstructure of the Udimet Preforms in the 1204° C (2200° F) HIP Condition (Walker's Etchant).	237
4-20.	Typical Forged Microstructures of Compressor Disk Forgings Produced from CarTech Three-Piece Preform Multiple Log (Walker's Etch, 200X). Note Prior Particle Delineation.	239
4-21.	Illustration of Prior Particle Boundary Separation During Forging of CarTech Preforms (Forging S/N 9982, Walker's Etch).	240
4-22.	Illustration of Prior Particle Boundary Separation Leading to Cracking During Forging of CarTech Preforms. (Unetched Forging S/N 9982).	241
4-23.	Typical Forged Microstructures of the CFM56/F101 Forging (FAH 86) Produced from Udimet Preforms (Walker's Etch). Note Absence of Prior Particle Boundary Delineation.	245
4-24.	Forging Schematic Cut-Up Plan Used for DDA4, FWA67, and FAH86 René 95 HIP + Forge Disks.	248

LIST OF ILLUSTRATIONS (Concluded)

<u>Figure</u>		<u>Page</u>
4-25.	PM René 95 HIP Plus Forge Compressor Stage 5-9 Disk (S/N MZS 27C73) Forging Schematic Cutup Plan.	249
4-26.	PM René 95 HIP Plus Forge Average Tensile Data Strength Values.	255
4-27.	PM René 95 HIP Plus Forge Average Tensile Ductility Values.	256
4-28.	PM René 95 HIP Plus Forge Stress Rupture Data.	259
4-29.	PM René 95 HIP Plus Forge Creep Data.	262
4-30.	PM René 95 HIP Plus Forge Cycle Rupture Data at 649° C (1200° F), A = 1, K _t = 2, 10-90-10 Seconds.	266
4-31.	Hot Die Forged PM René 95 Strain Control Low Cycle Fatigue at A _ε = 1.0.	269
4-32.	Maximum Stress Versus Cycles to Failure for the Residual Cyclic Life Specimens.	273
4-33.	Crack Propagation Rate of HIP + Forged René 95, 538° C (1000° F), A = 0.95, 20 Hz.	274
7-1.	Cost Comparisons for As-HIP René 95.	280

LIST OF TABLES

<u>Table</u>		<u>Page</u>
2-1.	René 95 Powder Composition.	4
3-1.	Target and Part Dimensions for CF6 HPTR Rear Shaft.	26
3-2.	Target and Part Dimensions for CF6 HPTR Rear Shaft.	28
3-3.	Target and Part Dimensions for CF6 HPTR Rear Shaft.	33
3-4.	Target and Part Dimensions for CF6 HPTR Rear Shaft.	39
3-5.	Target and Part Dimensions for CF6 HPTR Rear Shaft.	40
3-6.	Summary of Test Ring Data.	42
3-7.	Chemical Analysis of Crucible Blends Produced in Task II.	45
3-8.	Crucible Powder Characteristics.	46
3-9.	Preliminary Heat Treatment Study Tensile Property Versus Cooling Rate.	50
3-10.	Tensile Properties for Bars Solutioned at 1093° C (2000° F).	51
3-11.	Tensile Properties for Bars Solutioned at 1121° C (2050° F).	52
3-12.	Density and Tip Results from Detailed Mechanical Property Material.	62
3-13.	Detailed Evaluation Tensile Properties.	66
3-14.	Stress Rupture and Creep Properties for Detailed Heat Treatment Evaluation.	67
3-15.	Low Cycle Fatigue, Sustained Peak Low Cycle Fatigue and Residual Cyclic Life Data for Detailed Heat Treatment Evaluation.	70
3-16.	Tensile Properties for 816° C (1500° F) SQ VS RAC.	76
3-17.	Process Variables.	77
3-18.	Density and Tip Response for René 95 Compacts.	78

LIST OF TABLES (Continued)

<u>Table</u>		<u>Page</u>
3-19.	Test Specimen Identification for Material Having Powder Cleanliness Variations.	84
3-20.	Effect of Material Defects on As-HIP René 95 Properties Room Temperature Tensile Properties.	86
3-21.	Effect of Material Defects on As-HIP René 95 Properties 649° C (1200° F) Tensile Properties.	87
3-22.	Effect of Material Defects on As-HIP René 95 Properties 649° C/695 MPa (1200° F/140 ksi) Rupture Properties.	97
3-23.	Effect of Material Defects on As-HIP René 95 Properties 538° C (1000° F) Strain Control.	101
3-24.	Powder Compositions.	112
3-25.	Powder Characteristics of MB048.	113
3-26.	Test Specimen Identification for Material Having Process Deviations.	120
3-27.	Tensile Properties of Material Having Process Deviations.	121
3-28.	Stress Rupture and SPLCF Properties of Material Having Process Deviations.	126
3-29.	Effect of Process Variables on As-HIP René 95 Properties.	128
3-30.	Effect of Process Deviations on As-HIP René 95 Properties Notched Load Control Low Cycle Fatigue.	129
3-31.	Effect of Process Deviations on As-HIP René 95 Properties 538° C (1000° F) Strain Control LCF.	134
3-32.	Summary of Mechanical Property Tests on HPT Rear Shaft.	136
3-33.	Tensile Properties of CF6 HPT Rear Shafts.	142
3-34.	Stress Rupture Properties of CF6 HPT Rear Shaft.	145

LIST OF TABLES (Continued)

<u>Table</u>		<u>Page</u>
3-35.	Creep Properties of As-HIP René 95.	147
3-36.	Notched ($K_t = 2$) Bar Tensile Properties of As-HIP.	149
3-37.	Strain Low Control Fatigue Properties of CF6 HPT Rear Shafts.	151
3-38.	Smooth and Notched Bar Load Control Low Cycle Fatigue Data from As-HIP René 95 CF6-50 HPT Rear Shaft R = .03-0 (A = 0.95-1.0).	153
3-39.	Sustained-Peak Low Cycle Fatigue Data of CF6 HPT Rear Shafts.	158
3-40.	538° C (1000° F) Residual Cyclic Life (K_B) Data from As-HIP René 95 CF6-50 HPT Rear Shafts.	158
3-41.	Dynamic Modulus Properties of CF6 HPT Rear Shafts..	161
3-42.	Thermal Expansion Properties of CF6 HPT Rear Shafts.	162
3-43.	Experimental Designs and Results.	167
3-44.	Borazon Turning Design and Results.	168
4-1.	CarTech B-093 Characterization.	178
4-2.	Subscale Forge Development Mechanical Property Tests.	180
4-3.	Subscale Forgeable Surface Development Master Powder Blends Characterization.	185
4-4.	First Series Net Shape Subscale Forging Preform Surface Preparation Conditions.	188
4-5.	Container Material Characterization.	189
4-6.	Net-Shape Subscale Forgeable Surface Hot Compression Test Metallographic Observations.	191
4-7.	Initial Net Shape Forgeable Surface Hot Compression Test Evaluation Summary.	192
4-8.	Second Series Subscale Preform Results.	206

LIST OF TABLES (Continued)

<u>Table</u>		<u>Page</u>
4-9.	CarTech B146 Characterization.	216
4-10.	Oxygen Data - CarTech Three-Piece Preform Multiple Log.	217
4-11.	Characterization of the Udimet Master Powder Blends.	219
4-12.	René Master Powder Blends Characterization.	220
4-13.	Near-Net-Shape Preform Oxygen Analyses.	222
4-14.	1093° C (2000° F) Tensile Data on CarTech Preforms.	242
4-15.	CarTech Al382 Material Characterization.	243
4-16.	Summary of Mechanical Property Tests on Hot Die Forged René 95 in Task III.	246
4-17.	Hot Die Forged PM René 95 Tensile Data.	250
4-18.	Hot Die Forged PM René 95 Stress Rupture Data at 649° C/1034 MPa (120° F/150 ksi).	257
4-19.	Hot Die Forged PM René 95 Stress Rupture Data.	258
4-20.	Hot Die Forged PM René 95 Creep Data at 593° C/1034 MPa (1100° F/150 ksi).	260
4-21.	Hot Die Forged PM René Creep Data.	261
4-22.	Hot Die Forged PM René 95 Cyclic Rupture Data.	264
4-23.	Hot Die Forged PM René 95 Cyclic Rupture Data.	265
4-24.	Hot Die Forged PM René 95 Strain Control Low Cycle Fatigue Data 6.35 mm (0.25 inch) Diameter, R = 0, (A _E = 1).	267
4-25.	Hot Die Forged PM René 95 Strain Control Low Cycle Fatigue Data - 10.16 mm (0.4 inch) Diameter, (R = 0, A _E = 1).	268
4-26.	Hot Die Forged PM René 95 Residual Cyclic Life Data.	270
4-27.	Hot Die Forged PM René 95 Crack Growth Rate Data from the Residual Cyclic Life (KB) Specimen.	272

LIST OF TABLES (Concluded)

<u>Table</u>		<u>Page</u>
4-28.	Hot Die Forged PM René 95 Dynamic Modulus Data.	275
4-29.	Hot Die Forged PM René 95 Density Data.	276

1.0 SUMMARY

This project consisted of refinement of powder metallurgical processing procedures to produce near-net-shape rotating turbine engine parts, using the René 95 alloy, to achieve significant cost reductions when compared to conventional processing techniques. Conservation of material, reduced conversion costs, and reduced metal machining time were realized by application of two technologies - first by the use of powder as-hot-isostatically-pressed (as-HIP) in components and second by the use of as-HIP preforms for use in isothermal finish forge operations. The CF6-50 high pressure turbine rear shaft, used in applications such as the DC10-30 and A300 aircraft, was the configuration selected to refine the as-HIP technology and the CFM56/F101 compressor common rotor disk (Stage 5-9), used in applications such as retrofit of the DC-8 and 707 aircraft, was selected to refine the process for the hot die forging of as-HIP preforms (HIP + Forge). Each of these technologies have been successfully demonstrated and production utilization on the CFM56 engine has been realized.

The as-HIP near-net-shape capability for the shaft part was attained through a series of iterative trials. A ceramic mold, developed by Crucible, was employed as the powder container for compaction. Three shape iterations incorporating progressive tooling modifications, and two hard tooling production runs of five and three pieces respectively, demonstrated an envelope capability of 2.5 mm (100 mil). In addition, it was also demonstrated that a low cost Harperizing procedure produced an ultrasonically inspectable as-HIP surface without the aid of conventional machining. This successful demonstration of this surface conditioning procedure will have widespread applicability beyond the scope of the subject project.

Concurrent with this as-HIP near-net-shape development effort, a process variable study was conducted to evaluate variations of powder particle size distribution, HIP temperature, solution heat temperature, contamination by foreign materials (SiO_2 , Al_2O_3 , Astroloy, M-2 tool steel), as well as the effect of argon entrapment on selected mechanical properties. No major effect on properties was observed for variations in René 95 powder particle size ranges of -60, -60 + 150, and -150 mesh. A tolerance of $\pm 28^\circ \text{C}$ ($\pm 50^\circ \text{F}$) was found acceptable for HIP and solution heat treat temperatures. This range is well within the capability of commercial facilities.

Degradation of all mechanical properties, which increased with defect size, was observed for oxide inclusions above 0.15 mm (6 mils) diameter. While a contamination level of 0.1 volume percent Astroloy powder had no significant effect on properties, similar contamination with tool steel powder particles reduced rupture life. Argon entrapment above the 0.3% porosity limit reduced properties.

All shaft part shapes and their test rings produced in the full scale

part manufacturing task met target properties for the CF6-50 shaft and two engine quality finished machined parts have been produced. One of these parts is currently being tested on a CF6-50 test engine.

Forging of the CFM56/F101 compressor disks from as-HIP preforms required the definition of acceptable hot die forging parameters. This definition was initially accomplished at the Ladish Company with 1/4-scale disks. After the initial forging parameters were established, iterative development of full-scale as-HIP preforms was completed with Special Metals and Carpenter Technology as both powder and preform vendors.

Application of subscale forging parameters to full-scale forgings at Ladish using near-net-shape stage 5-9 disk preforms resulted in unanticipated technical problems due to a prior particle boundary condition. Modifications to the preform process, including fill practice, reduced carbon level, and increased HIP temperature, did not fully resolve the technical problems. However, subsequent forging of near-net-shape preforms was successfully demonstrated on other parts of the same final forging configuration which, although not initially part of the subject project, utilized the technology refined under this project.

Full-scale parts were successfully manufactured from preforms cut as slices of hollow as-HIP logs. This method is now the current production procedure used by General Electric on these parts. All mechanical properties measured on these full scale CFM56/F101 compressor disks met or exceeded the conventional cast and wrought René 95 target properties. Parts were successfully inertia welded and finished machined into a stage 5-9 compressor spool and engine testing is underway for these parts on a CFM56 test engine.

The HIP+Forge process demonstrated a 54% decrease in input material weight and a cost reduction of 35% as compared to conventional cast and wrought René 95 forgings. The as-HIP process used for the aft shaft component demonstrated a 50% input weight reduction and a 40% cost reduction as compared to cast and wrought René 95. A cost reduction was not realized as compared to cast and wrought Inco 718 because of the greater increase in René 95 raw material cost resulting from the large increase in cobalt prices between 1974 and 1979.

The results of Project 1 have clearly demonstrated the capability of low-cost near-net-shape manufacturing methods for both as-HIP and HIP + Forge René 95 engine rotating components. These processes are now in use for manufacturing production parts for the CFM56 commercial engine, for several military engines, and for an advanced Energy Efficient Engine (E³) now in the development stage. The work accomplished here served to advance significantly the state of the art for nickel-base superalloys produced by powder metallurgy techniques both from the manufacturing standpoint and from the understanding gained concerning the metallurgical behavior of these materials and has been directly transitioned into the powder production industry.

2.0 INTRODUCTION

2.1 BACKGROUND

The NASA-MATE Program has as its primary objective the introduction of new materials technologies into advanced aircraft turbine engines to more rapidly achieve potential economic and operational performance advantages. The Program encompasses the accelerated transfer of selected materials technologies by scaling them up from the feasibility stage to engine demonstration as well as performing cost/benefit analyses to provide guidance in the selection of the candidate material technologies to be scaled up.

The first MATE project conducted by the General Electric Company described in this report involved the scale-up of powder metallurgy processes for the manufacture of aircraft gas turbine engine components using the René 95 nickel-base alloy. The following paragraphs describe some of the characteristics of this alloy together with the objectives of the MATE project effort.

Of the wrought nickel-base superalloys used for turbine and compressor disks, shafts, rotating seals, and related parts, René 95 is the strongest of the commercially available superalloys over the use temperature range from ambient to about 650° C (1200° F). Table 2-1 shows the specified composition for the René 95 alloy.

The superiority of René 95 is illustrated by Figure 2-1, which compares the tensile strength versus temperature of René 95 with those of three other disk alloys, Inconel 718, Waspaloy, and isothermally forged IN100 produced by powder metallurgy processes. The superior strength of René 95 resulted in its selection as the material of choice for hot rotating parts in several advanced, development and production engines at General Electric. The alloy is used today in the CFM56, F101, T700, and F404 engines which have been selected to power various fighters, helicopters, and transport aircraft. The CFM56 engine has been selected to retrofit DC8 aircraft with a more modern engine and is a candidate for powering several medium size commercial aircraft scheduled for production in the 1980's as well as for retrofitting other aircraft.

Today's military and commercial customers are emphasizing the reduction of total operating cost of their aircraft systems. This effort focuses on improving component life, reliability, and field utility/repair during the development and operational phases of advanced systems. Current advanced engines are being developed against new and more stringent performance criteria: e.g., higher thrust-to-weight ratios, single stage turbines, and high stage loaded compressors. These performance criteria result in the need for higher strength materials in both the compressor and turbine sections.

The development of René 95 has made practical the technical advancements apparent in today's advanced technology engines. The design of high speed,

Table 2-1. René 95 Powder Composition.

<u>Element</u>	<u>Weight % Alloy</u>	
	<u>Minimum</u>	<u>Maximum</u>
C	0.04	0.09
Mn	---	0.15
Si	---	0.20
S	---	0.015
P	---	0.015
Cr	12.0	14.0
Co	7.0	9.0
Mo	3.3	3.7
Fe	---	0.5
Ta	---	0.2
Cb	3.3	3.7
Zr	0.03	0.07
Ti	2.3	2.7
Al	3.3	3.7
B	0.006	0.015
W	3.3	3.7
O	---	0.010
N	---	0.005
H	---	0.001
Ni	Balance	Balance

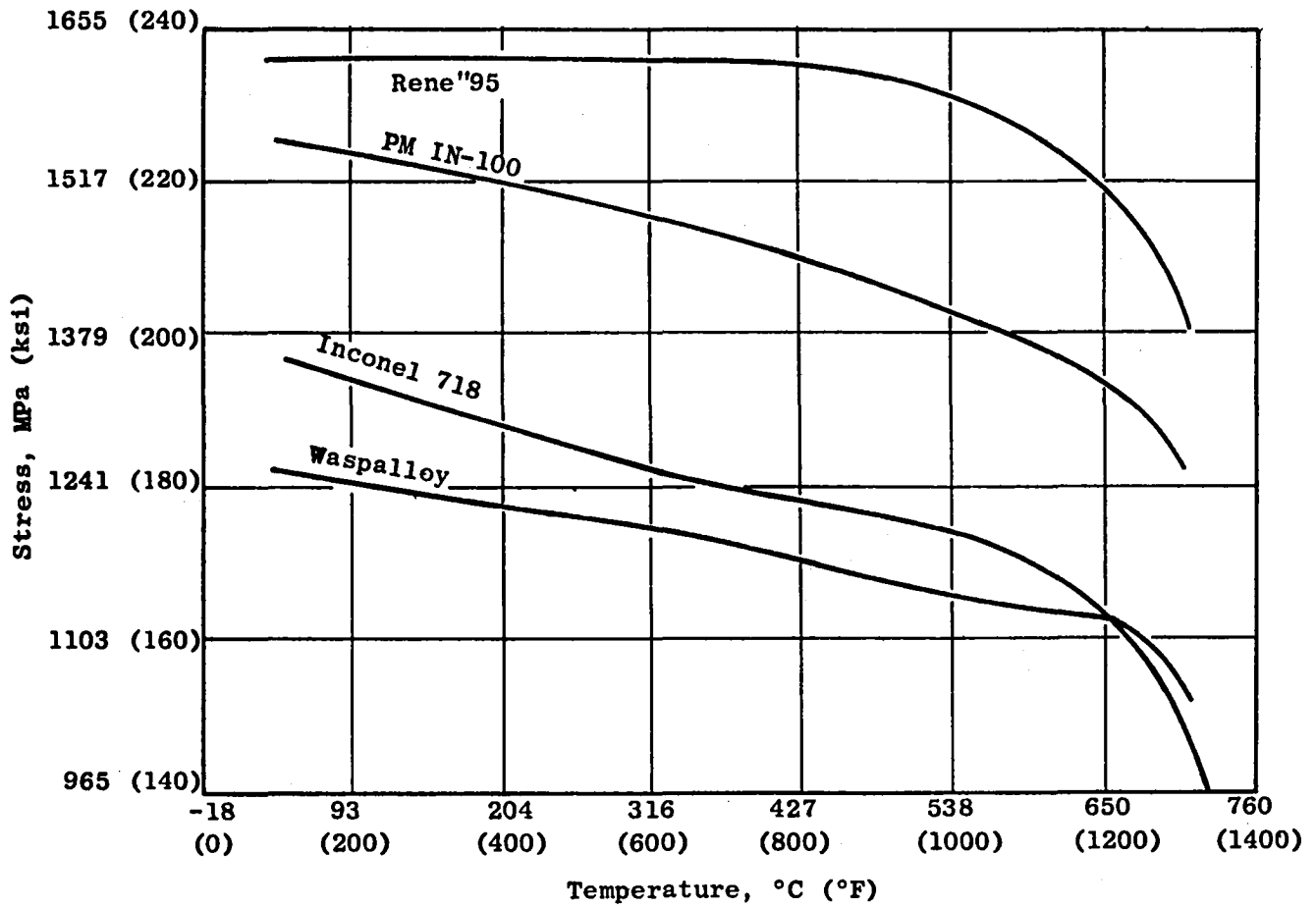


Figure 2-1. Ultimate Strength Comparison of Rene' 95 Versus Other Disk Alloys.

high pressure ratio compressors and single-stage, high speed, high pressure turbines would become considerably more cumbersome and complex without René 95. For example, the inertia welded CFM56/F101 aft compressor spool using René 95 weighs 30% less than a similar Inconel 718 part.

More specifically, in the case of high speed turbines, some 65% of the average disk tangential stress is induced by the weight of the disk itself. Therefore, the significance of disk weight becomes doubly important, i.e., not only because of its effect on engine thrust to weight ratio but also disk life. A doubling of a turbine disk weight, for example, would lower the bore tangential stress only approximately 20%.

The René 95 alloy combined with the development of the inertia welding process made possible the design of the integral aft compressor spool of the CFM56/F101 engine, comprising five individual disks inertia welded to one another to form the spool. The design of this spool made possible:

- The manufacture of five compressor disk stages from a forged shape of one configuration
- Common tooling for fabricating and inertia welding these stages
- The elimination of internal bolted flanges which in turn
 - Reduced rotor weight
 - Reduced the number of component parts
 - Eliminated bolt hole stress concentrations
 - Increased rotor stiffness

The exceptionally high strength and temperature capability of René 95 permitted a large bore, thin web disk design, resulting in an exceptionally light-weight aft compressor spool.

René 95 was initially developed by General Electric under Air Force sponsorship. The original alloy development was performed using double vacuum melting with vacuum arc remelting as the final step. Forging and heat treating procedures were developed for René 95 to produce a unique microstructure by controlled forging processes for the arc-cast ingot dubbed the "necklace" structure. This structure consists of warm-worked grains surrounded by a necklace of fine recrystallized grains. René 95 with the necklace structure exhibited superior crack propagation resistance and notched low cycle fatigue strength as compared to fine-grained material and attainment of the necklace structure became a major requirement in forging and heat treating arc-cast ingots of René 95.

Despite the extremely high strength of René 95, parts made by conventional process technology cost about twice as much as similar parts made of the lower strength alloys which were used for turbine and compressor rotating

parts in earlier engines. This cost problem prompted the initiation of major cost reduction efforts on René 95 parts.

Cost reduction approaches involved the use of high purity prealloyed powders consolidated into shapes by hot isostatic pressing (HIP). Preforms made by HIP consolidation may be subsequently forged to near finished size shapes or parts can be HIP directly to a near net shape (NNS) without using forging processes. Initial feasibility demonstrations of the HIP + Forge approach were made in 1974 using the CFM56/F101 stage 5-9 compressor disk as the demonstrator part. This work showed that both processes (as-HIP and HIP plus hot die forging), coupled with appropriate heat treatments, could produce properties equivalent to those of conventional cast and wrought René 95.

Although these results indicated that major (circa 50%) cost reductions were achievable in several engines by changing from arc casting followed by conventional forging to parts having a common origin in HIP-consolidated René 95 powder, attaining this goal required a major scale up-effort.

The overall objective of the General Electric MATE Project 1 program was to refine René 95 superalloy powder metallurgy processing technology to permit the fabrication of turbine engine rotating parts at significant cost reductions as compared to similar parts produced by more conventional methods. It was predicted that process technology advancements could be achieved which would permit production engine finished part cost reductions of at least 50% as compared to conventionally processed René 95. These very significant cost reductions were to be achieved with the introduction of parts produced by hot die forging of hot isostatically pressed (HIP) René 95 powder shapes as well as parts produced by HIP compaction alone (as-HIP).

The HIP and hot die forged René 95 powder parts would be made by producing minimum weight preforms to be subsequently hot die forged and heat treated. The engine components chosen to demonstrate this latter technology were the Stages 5-9 disks of the CFM56/F101 compressor rotor. Each of these compressor disks are machined and then inertia welded together using a common input forging. Figure 2-2 shows a comparison of the conventional process to the projected powder metallurgy process for this part.

As-HIP René 95 parts were to be developed to minimum envelope shapes for replacement of certain conventionally forged and heat-treated Inconel 718 parts in the CF6-50 engine. The engine component chosen to demonstrate this technology was the CF6-50 high pressure turbine rotor rear shaft shown in Figures 2-3 and 2-4.

Superalloy shapes manufactured by these powder metallurgy processes were predicted to possess mechanical properties and quality at least equivalent to those being achieved now in conventionally forged René 95 (for HIP + hot die forged René 95) and conventionally forged Inconel 718 (for as-HIP René 95).

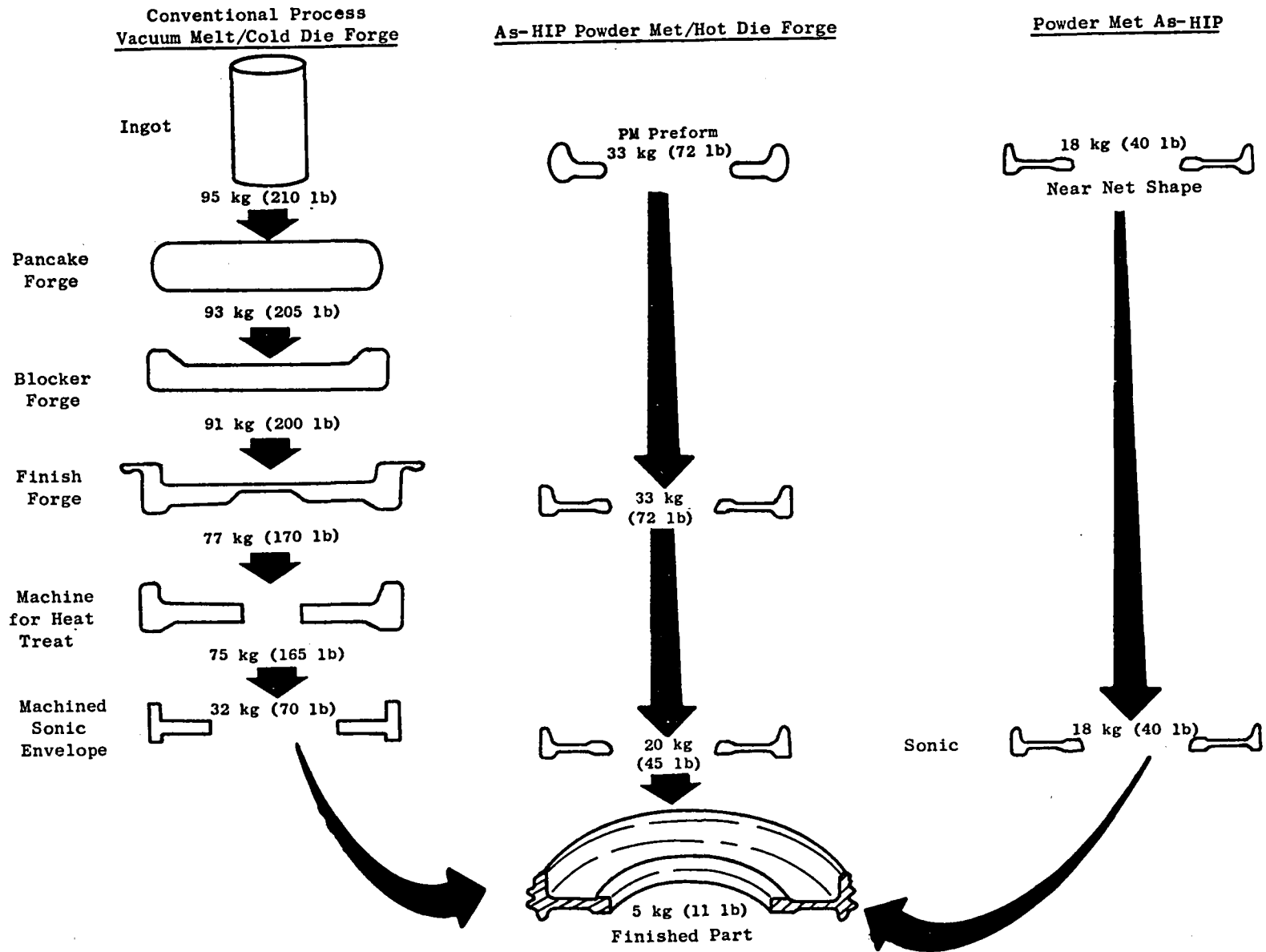


Figure 2-2. Conventional as-HIP PM Hot Die, and as-HIP PM Processing Sequences for the Core Compressor Stages 5-9 Disk.



0702060

Figure 2-3. CF6-50 High Pressure Turbine Rotor Aft Shaft

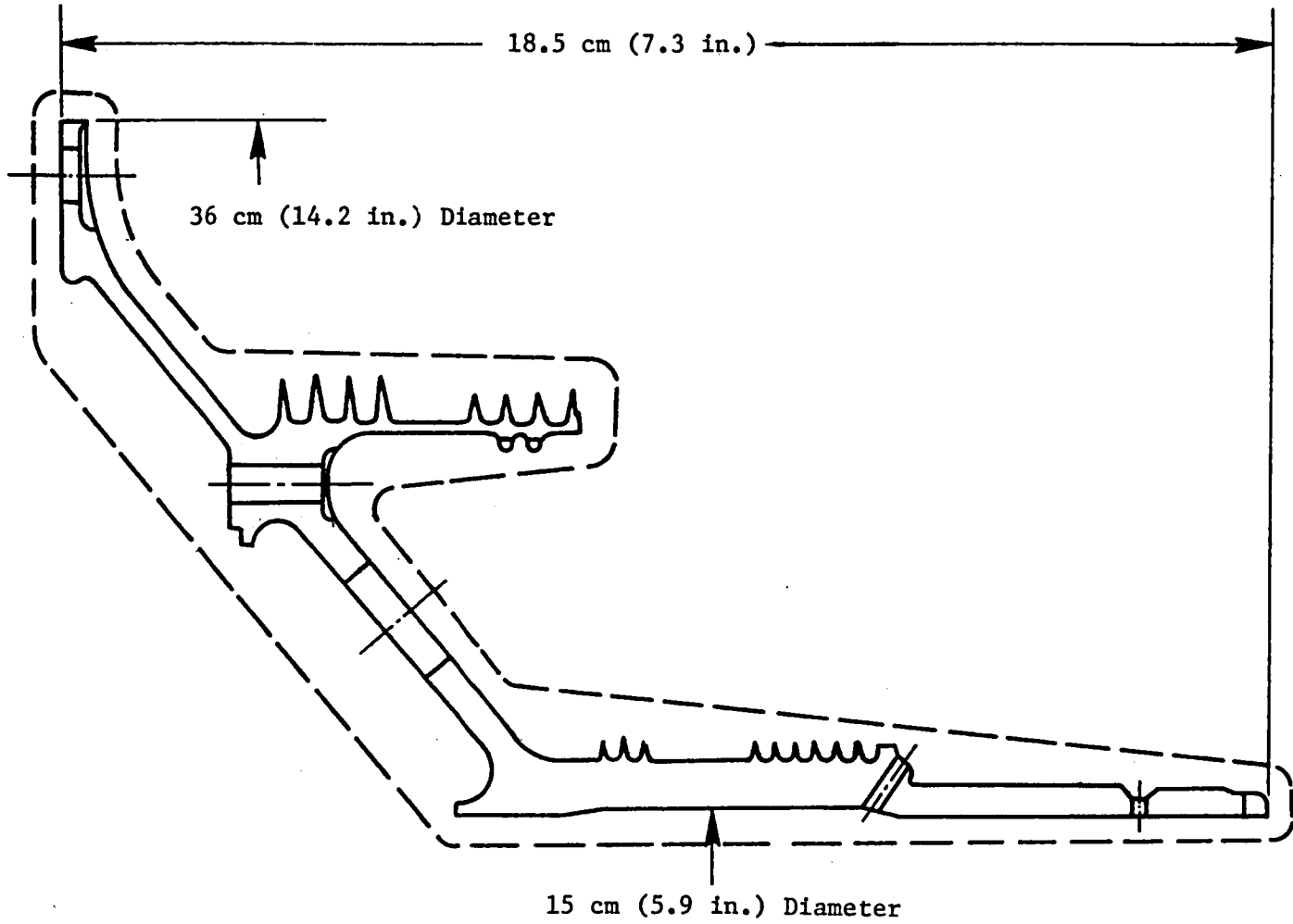


Figure 2-4. CF6-50 HPTR Rear Shaft.

The key to success in both elements of this project was the production of acceptable quality, minimum envelope preforms and HIP shapes. Feasibility demonstrations performed earlier strongly indicated that this goal could be met.

2.2 PROGRAM OUTLINE

As discussed briefly above, the initial technology scale-up project performed by the General Electric Company under the MATE Program was Project 1 "Powder Metallurgy René 95 Rotating Parts." The objective of this Project was to refine powder metallurgy processing of René 95 to permit significant cost reductions in rotating turbine engine parts compared to current practices. To demonstrate this technology, two turbine engine components were manufactured using related powder metallurgical processing methods. One component was the aft shaft of the CF6-50 engine high pressure turbine which was fabricated by hot isostatic pressing René 95 powder to near final size followed by heat treatment. The second component was a compressor rotor disk for use in the fifth through ninth stages of the F101 and CFM56 engines. It was produced by hot-die forging of HIP René 95 preforms which were subsequently inertia welded and machined into a compressor rotor. The powder metallurgy (PM) processing of both components required close tolerance hot isostatic pressing of powder to a desired shape and providing a surface amenable to further processing and inspection. The target goal of this Project was to reduce the costs of these parts by at least 50 percent from the costs of the same parts produced by conventional processes.

The Program Task structure of Project 1 was as follows:

- Task I - Material Envelope Design
- Task II - Process Development
- Task III - Manufacturing
- Task IV - Engine Test
- Task V - Posttest Analysis

A flow chart showing the overall program structure is shown in Figure 2-5. Figures 2-6, 2-7, and 2-8 show the flow diagrams for each of the principal technical tasks I, II, and III.

Since the as-HIP CF6-50 high pressure turbine rotor (HPTR) aft shaft required quite different processing as compared to the HIP + Forge process for the CFM56/F101 compressor disks, this report is organized into two sections, each dealing with processing and evaluation of one of these parts. However, each type of processing followed the general task and subtask sequence illustrated in Figures 2-5 through 2-8 and the results are presented in the following sections of this report.

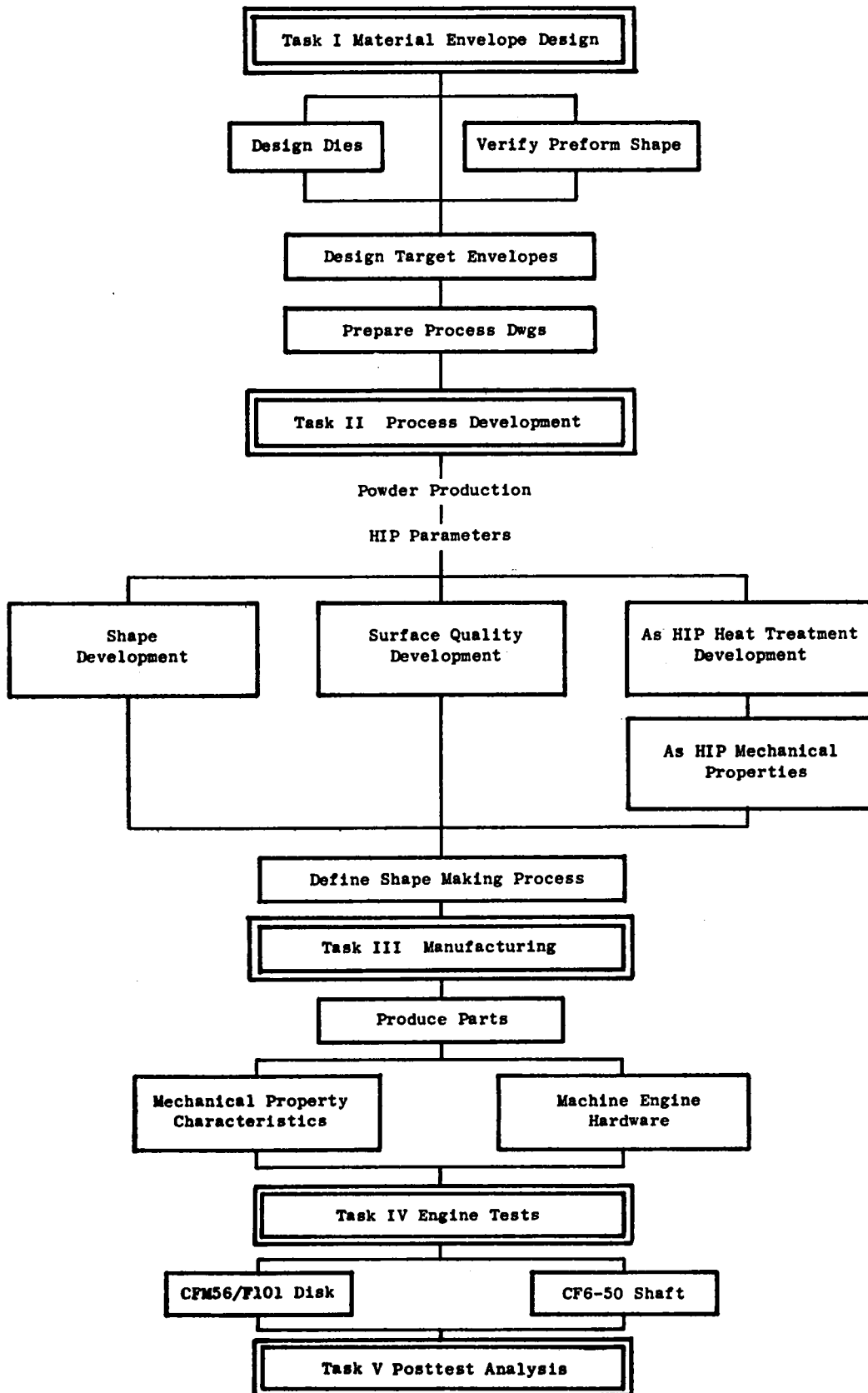


Figure 2-5. Powder Metallurgy René 95 - Rotating Parts.

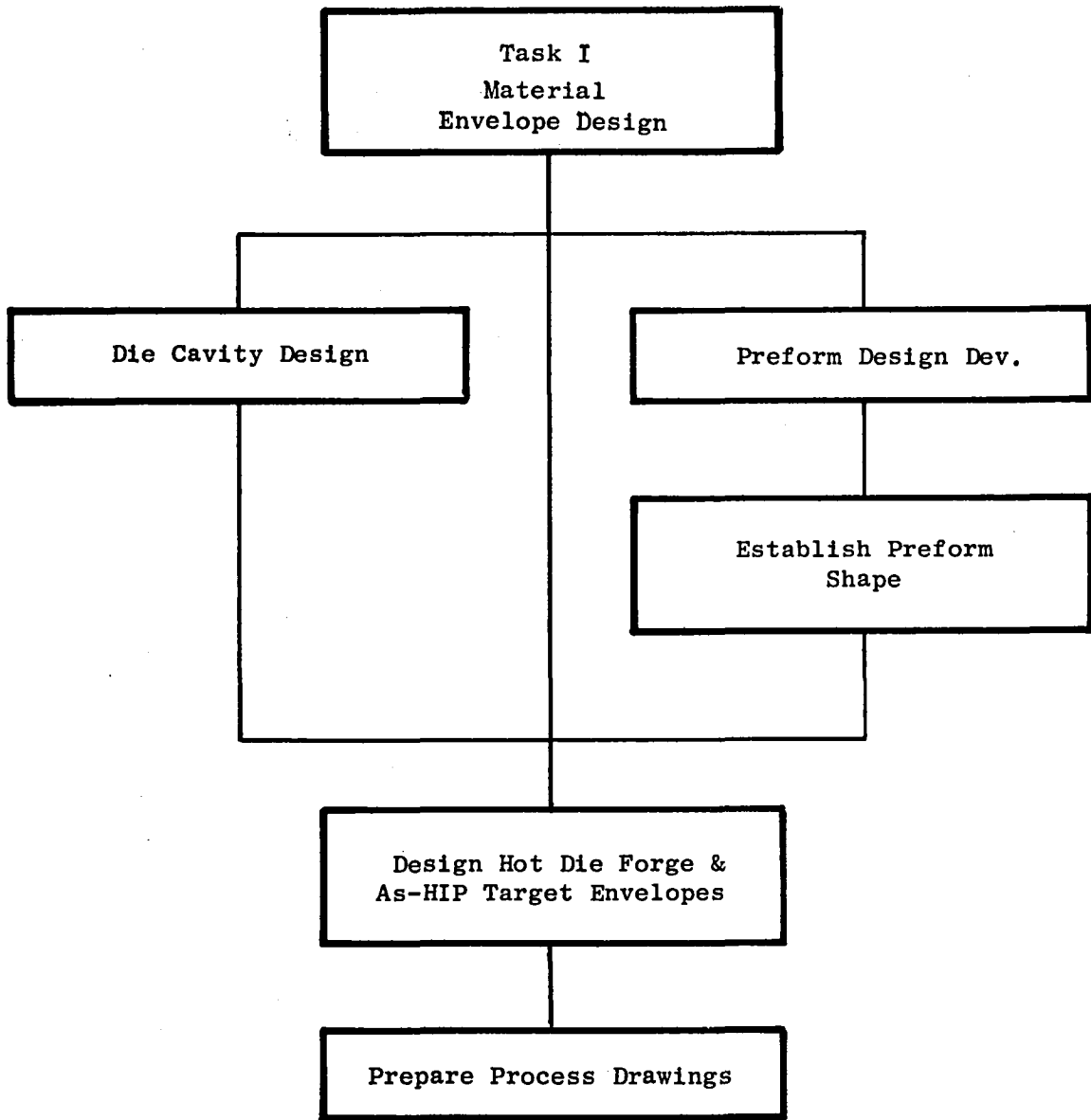


Figure 2-6. Flow Diagram for Task I.

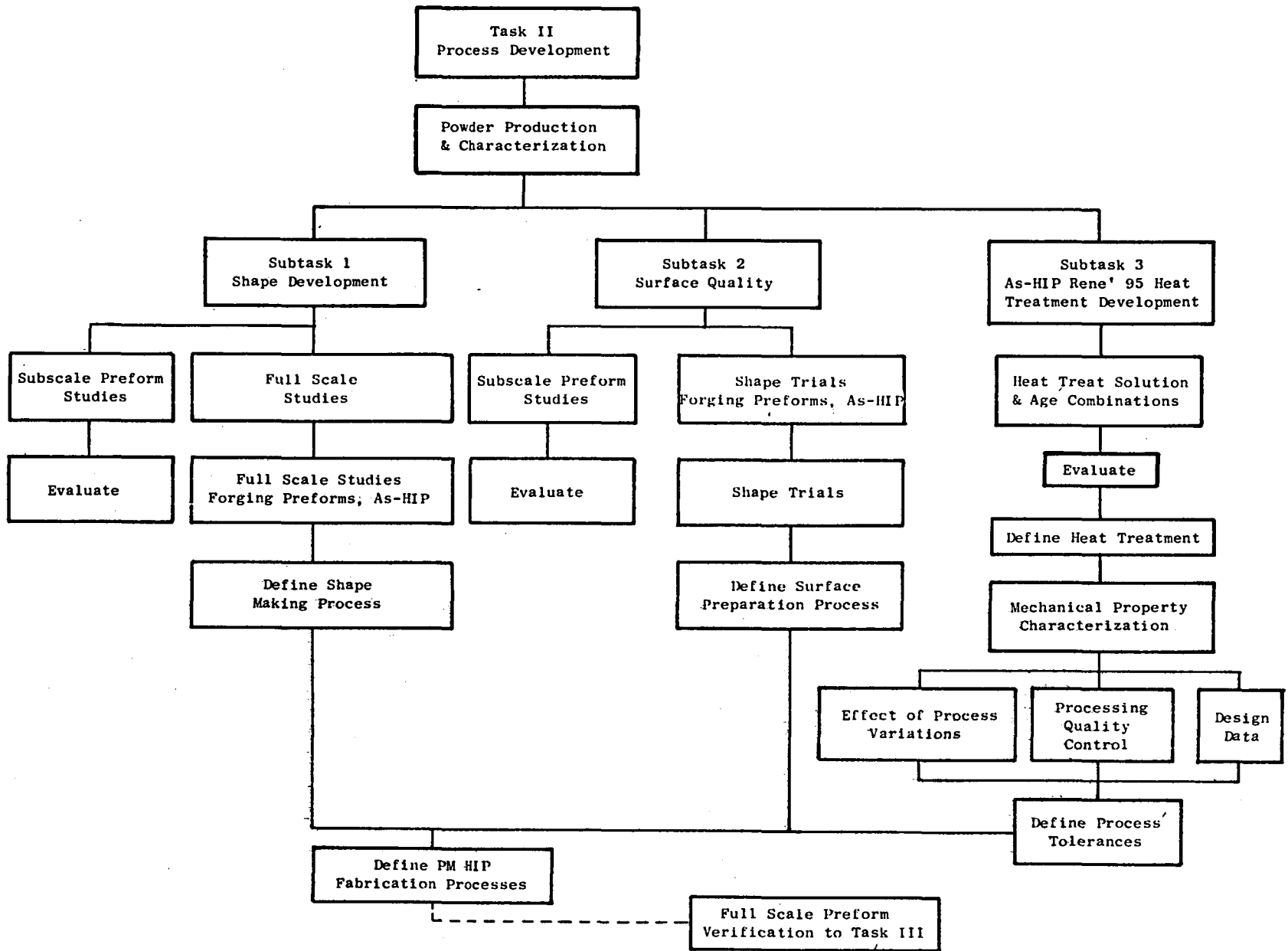


Figure 2-7. Flow Diagram for Task II.

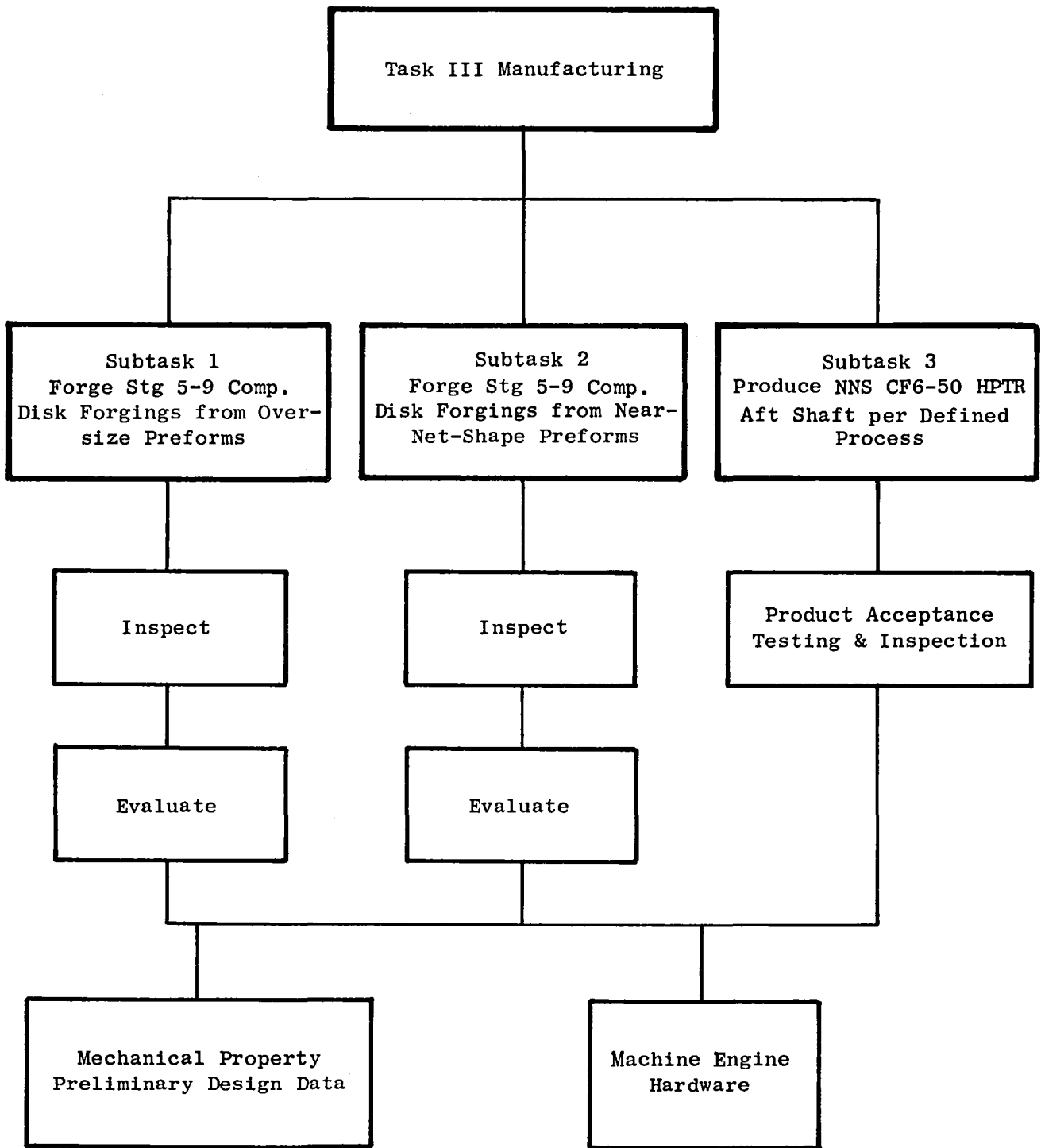


Figure 2-8. Flow Diagram for Task III.

3.0 AS-HIP PROCESSING

The component selected for as-HIP processing was the CF6-50 engine high pressure turbine rotor (HPTR) aft shaft which is currently manufactured from arc-cast and forged Inconel 718 alloy. The following sections describe the process development effort and mechanical property evaluations connected with the manufacture and qualification of this part for engine testing.

3.1 MATERIAL ENVELOPE DESIGN - AS-HIP

The selection of the part to be used for hot isostatic pressing (HIP) consolidation was based on several criteria: (1) a complex part of sufficient size to offer a challenge to the mold making technology, (2) ease of assembly/inspectability in the CF6-50 engine, and (3) the potential for a cost reduction. The CF6-50 high pressure turbine (HPT) aft shaft met these criteria and was selected as the demonstration part.

A chronology of the development of the Crucible Research Center (CRC) ceramic mold technology was (1) to establish the required envelope (Task I), (2) to produce three shape iterations to achieve the agree to configuration, and (3) to produce five parts for evaluation or machining to final part configuration for engine test. This chronology was followed with one exception, the five production parts indicated greater dimensional variation than CRC believed was the "process capability" due to assignable cause(s). Therefore, CRC produced, at no cost to the MATE project, three additional parts using slightly modified ceramic mold shape and a modified handling procedure, the dimensional inspection results for these three parts showed substantial improvement.

One other task, not mentioned above, was to identify a low cost technique whereby the rough as-HIP surface could be improved to a degree which would permit ultrasonic testing.

3.1.1 Task I - Envelope Design

A drawing was issued which met the weight objective, but in some places allowed only ± 0.25 mm (± 0.01 in) above the described final shape. After consultation with CRC a second drawing was issued which indicated minimum dimensions and a maximum weight. This drawing allowed CRC about 3.18 kilograms (7 pounds) discretionary material to be placed where CRC believed necessary to protect the minimum dimension. With process improvements, the discretionary weight would be reduced or removed entirely.

3.1.2 Task II - Process Development

3.1.2.1 Surface Improvement

The purpose of this effort was to develop an economical surface preparation for heat treatment and subsequent ultrasonic inspection. It was believed that the parts might crack during heat treatment if the rough as-HIP surface remained. Also it was obvious that to obtain a satisfactory ultrasonic inspection the as-HIP surface roughness would have to be improved.

After a preliminary evaluation, three surface improvement processes were selected for evaluation on as-HIP surfaces: (1) abrasive flow machining (AFM), (2) Harperizing, and (3) vibratory tub finishing.

Abrasive flow machining was not successful when attempted on an as-HIP part of the same basic configuration. The surface finish was approximately 140AA before AFM, and improved only slightly to a 120AA after (2-5) hours (142 cycles). AFM tends to "reproduce" or remove equal amounts from a surface, thus additional efforts using this process were not performed. AFM has shown promise on smaller bores [>7.6 mm (~ 3 inches)], on surfaces with some prior hand polishing or on surfaces produced by metal cans. For these reasons, this process should not be ruled out for as-HIP parts which meet one or more of the above requirements.

The initial results on Harperizing, a process wherein, a part (or in this case, an as-HIP compact) is either fixtured or tumbled loose in a mixture of water and coarse abrasive media. Vibratory tub finishing is basically the same except that a finer media is used and the part is "free floating". Although both indicated promise, the Harperizer was selected for economic reasons.

The first iteration (SM389) was processed through a model 2HA-18 Harperizer under these parameters:

	<u>Rough</u>	<u>Finish</u>
Turret Speed	15 g's	5 g's
Process Time	4 hr	0.5 hr
Media	848 @ 7/8 (Sic) with MFC No. 7	666T1 (Ceramic) with MFC No. 115
Height of Media	about 2/3 full	about 2/3 full

The results are shown in Figure 3-1. The greatest improvement was noted on the external surface, except for a one inch wide area masked by the handling fixture. There was a definite improvement on the internal surface as well.

The surface contours of Area A (Figure 3-1) are shown in Figure 3-2, before Harperizing, and Figure 3-3 after Harperizing. This surface was very adequate for ultrasonic inspection as noted in Figure 3-4 which shows the signal response from Area A in both the longitudinal and shear mode. These results show that an economical surface preparation technique was identified and the process was used on all subsequent parts with equivalent success.

3.1.2.2 Shape Development Utilizing the Ceramic Mold

A brief description of CRC's patented ceramic mold process is given here to acquaint those unfamiliar with this process.

The process is patterned after the "lost wax" process for the production of precision castings. A wax pattern is generated by machining (or injection molding in larger quantities) which conforms to the configuration desired, except for fill tubes. The mold is oversized by a predetermined amount to compensate for shrinkage as the loose powder consolidates to 100% theoretical density during the HIP autoclave cycle.

The ceramic mold is built up over the wax patterns by sequential dipping and drying. When the walls are thick enough the entire mold is heated to remove the wax and the ceramic is fired at an elevated temperature. This firing is adequate to yield a hard interior surface, however, the walls are not impervious to the passage of gas.

The next operation involves placing the fired mold on a bed of "pressure-transmitting media" in a large steel outer container. More media (fine Al_2O_3) is filled in between the exterior of the mold and the container. A predetermined quantity of metal powder is then charged through one or more fill tubes into the ceramic mold, using various vibratory techniques to improve the packing density.

The steel container is then completely filled with the pressure transmitting media, a lid welded on, and the entire assembly evacuated. This removes the residual air from the packing media, and, due to the permeable nature of the ceramic mold walls, residual gas is also removed from the contained metal powder. The degassing is initially conducted cold and subsequently hot. At a predetermined pressure and temperature, the vacuum outlet from the steel container is sealed, and the assembly is ready for the autoclave cycle.

The containers are heated in the autoclave 1020° C (2050° F) and pressurized to 103 MPa (15,000 psi). At these temperatures and pressures the ceramic mold first densifies, which accommodates most of the powder shrinkage, the remainder being accommodated by a quasi-plastic state of the assembly.

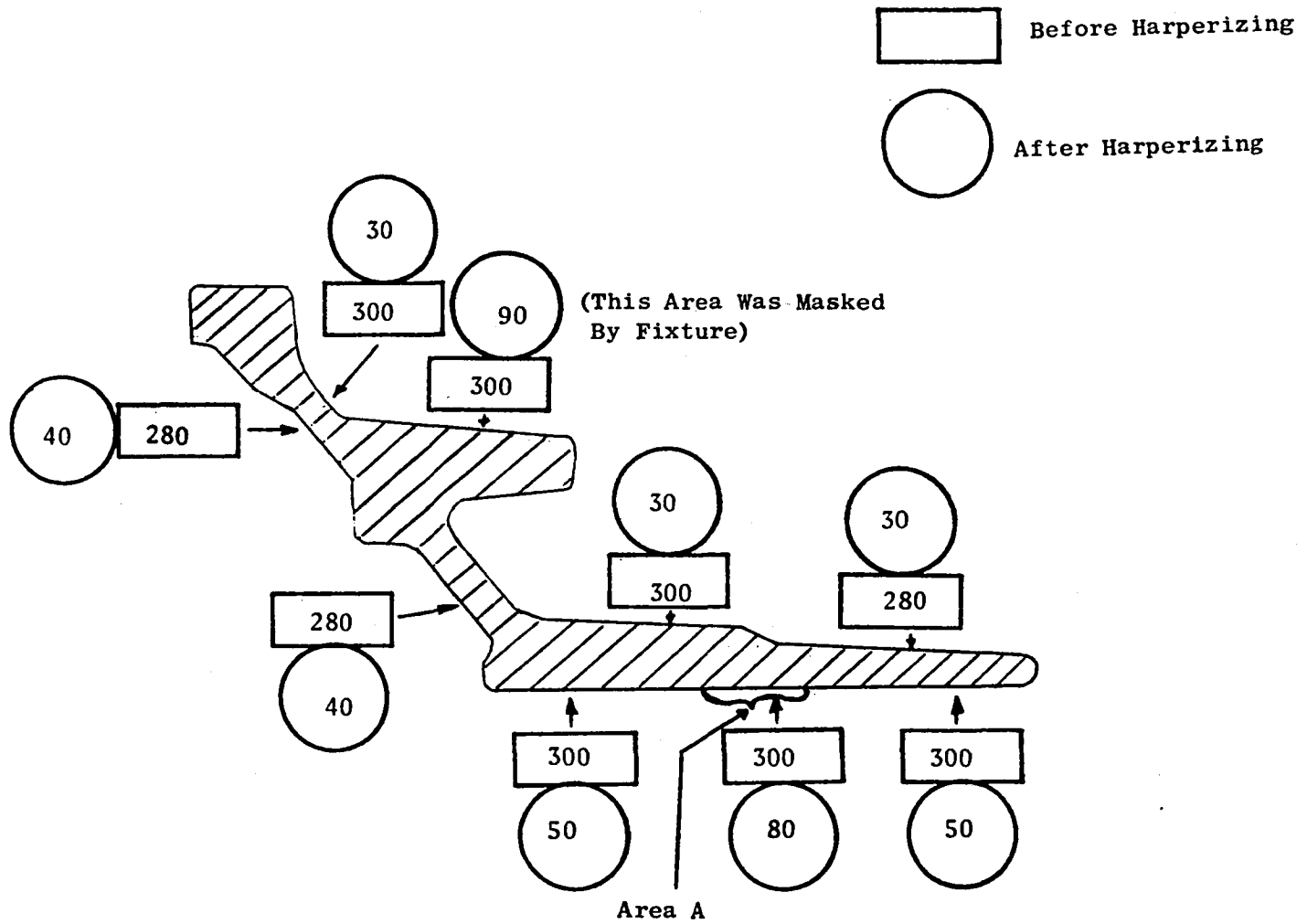


Figure 3-1. Effect of Harperizing on Surface Finish of First Iteration CF6-50 Aft Shaft Shape (SM-389).

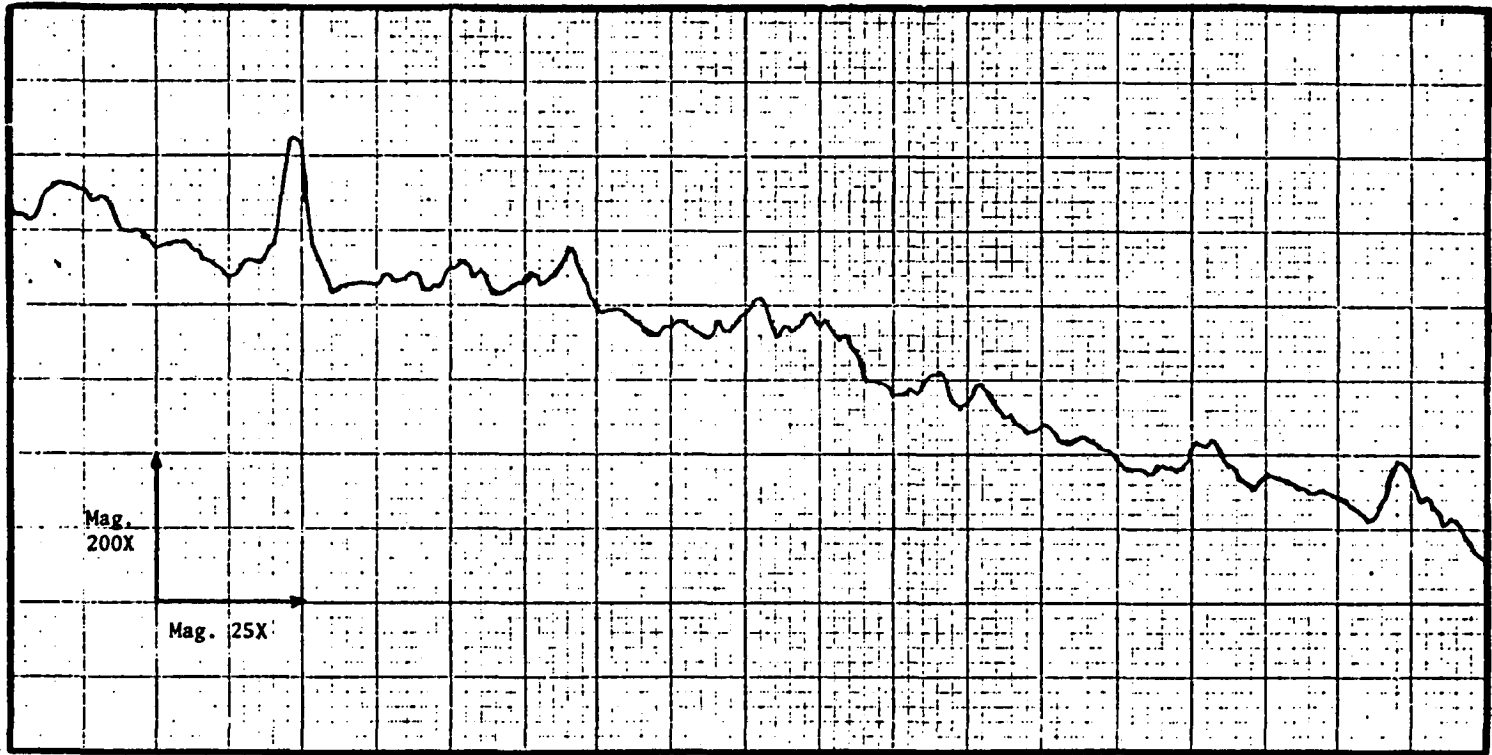


Figure 3-2. Surface Contour of Typical as-HIP Surface Before Harperizing (Aft Shaft Shape SM-389, Area A).

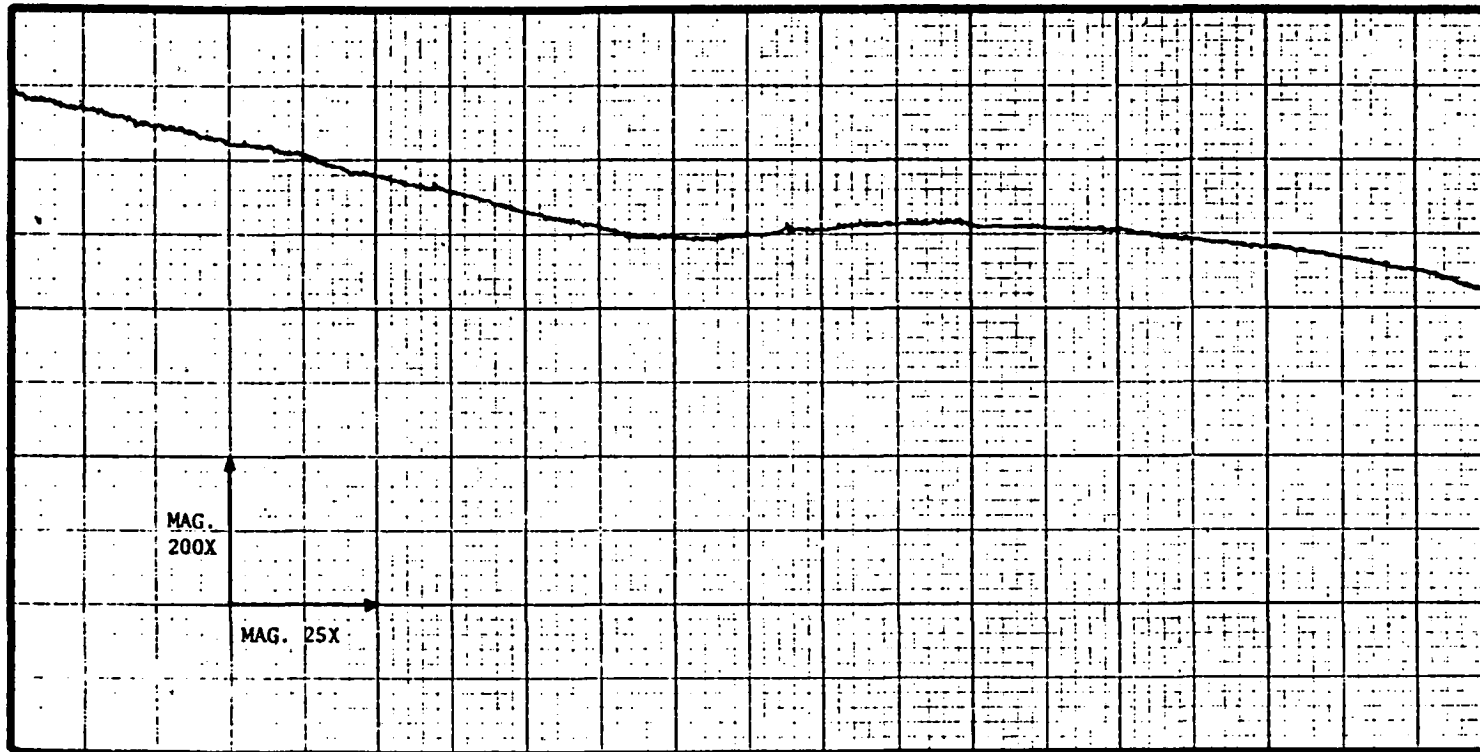
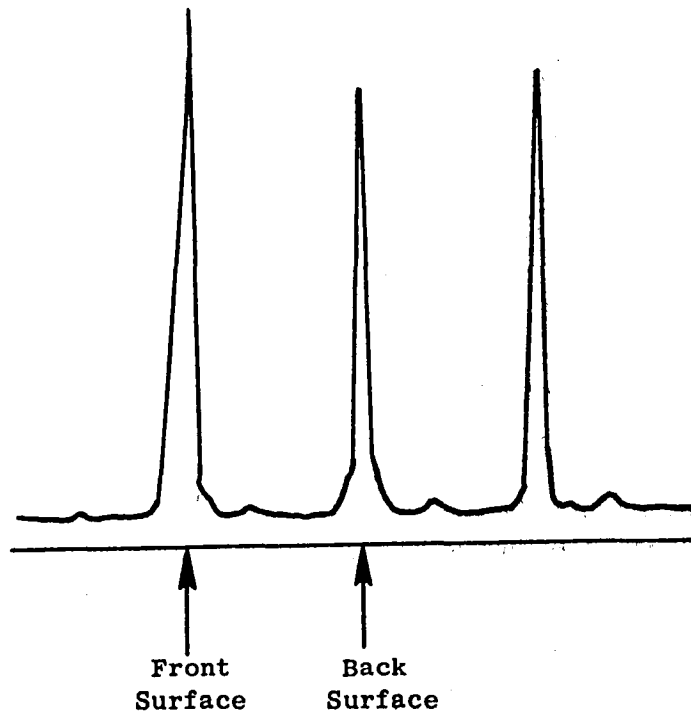
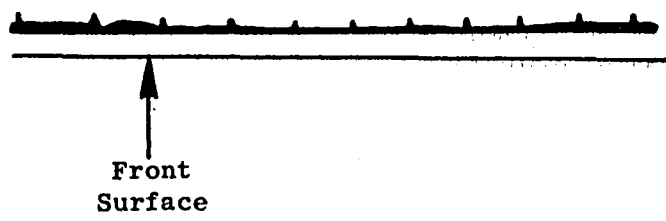


Figure 3-3. Surface Contour of Typical as-HIP Surface After Harperizing (Aft Shaft Shape SM-389, Area A).



(a) Longitudinal Mode



(b) Shear Mode

Figure 3-4. Schematic of Ultrasonic Response Signals from Area A (Figure 3-1), Harperized Aft Shaft Shape.

On cooling, the ceramic tends to spall from the HIP shape as a result of the difference in coefficient of thermal expansion between the metal and ceramic. The steel containers are removed from the autoclave, opened, and the finished compact is removed and prepared for further processing.

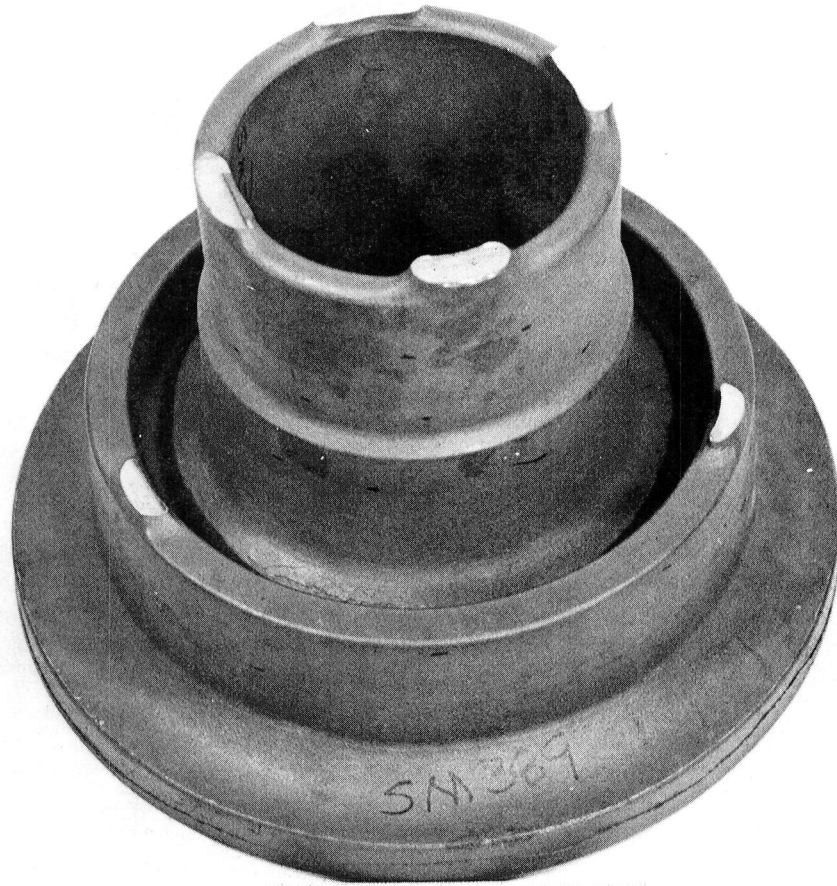
Using the drawing supplied by GE-AEG, and adding material where necessary, CRC machined the first wax and produced the ceramic mold for the first iteration. The mold was filled with minus 60 mesh R95 powder (MB033 and MB035) and consolidated in the large autoclave system (LAS) at Battelle Columbus Laboratories (BCL). The parameters used were 1120° C - 103 MPa (2050° F - 15,000 psi) with total autoclave cycle time sufficient to assure the compact was at temperature for three hours. The resulting compact number SM-389 with the fill stems removed is shown in Figure 3-5, the location of the dimensions in Figure 3-6, the desired and achieved dimensions in Table 3-1, and a schematic drawing indicating the areas of concern in Figure 3-7. The dimensional measurement was performed at GE-AEG's Lynn, Mass. facility using a Brown and Sharp Verifier. The schematic (Figure 3-7) shows the minimum envelope about the described configuration. The location of the finish machined part shape is also shown. These lines represent the minimum dimensions measured and therefore could represent a local "suck in" area, or other anomaly; however, these local variations preclude producing an acceptable shaped part from this type compact.

A wax was machined incorporating the dimensional modifications suggested by the results of the first iteration. This compact (SM489) was consolidated in the BCL autoclave using the same HIP parameters as the previous iteration.

The resulting compact was dimensionally analyzed by CRC utilizing conventional plate layout techniques. The compact was subsequently shipped to GE Lynn where a second dimensional analysis was performed in the Brown and Sharp Verifier. The results of the CRC and GE dimensional analyses were substantially the same.

The dimensional data as determined by GE are presented in Table 3-2, for the dimension location numbers given earlier in Figure 3-6. The maximum and minimum dimensions obtained are shown in Figure 3-8. The radial difference between the maximum and minimum envelope is equivalent to the FIR (full indicated runout which is a measure of eccentricity) when the compact is rotated about its centerline. The compact indicated good FIR except in areas A and B. The greater runout in Area A may be attributed to the fill stems which were attached to the aft end of the seal teeth area.

The outline of the finish machined part is shown with the minimum envelope in Figure 3-9. An infringement of the compact into the finished part outline is noted in the diameter at Area A. With the exception of the ID seal teeth area, SM 489 would be acceptable for the production of a finished part.



Colt Industries  Crucible
Metals Research Center

Figure 3-5. As-HIP CF6 HPTR Rear Shaft -
1st Shape Trial (SM-389).

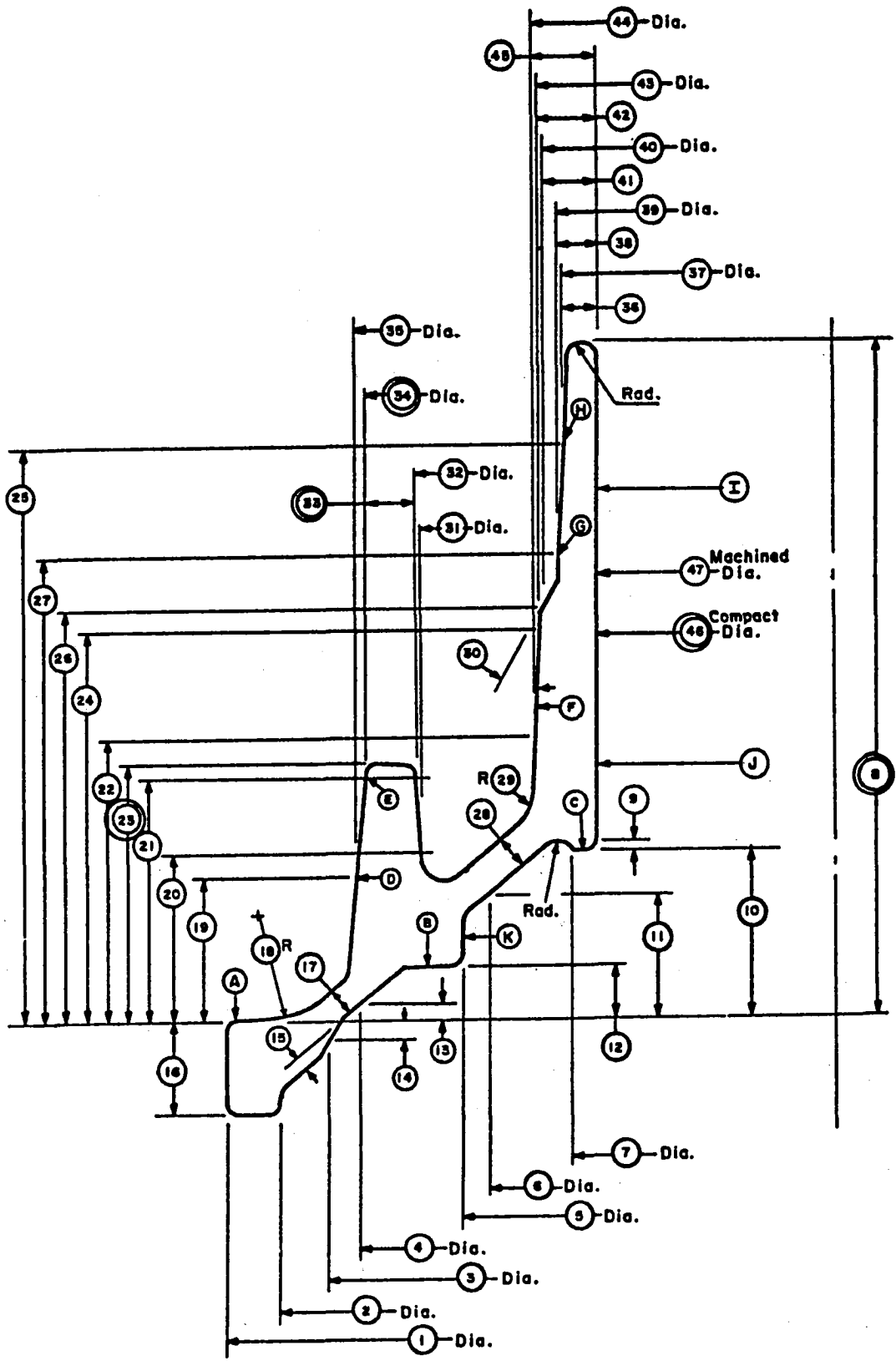


Figure 3-6. As-HIP CF6 HPTR Rear Shaft Dimension Locations.

Table 3-1. Target and Part Dimensions for CF6 HPTR Rear Shaft

Dimension No. ^a	Target Dimension		1st Trial - SM-389		2nd Trial - SM-489	
	(in.)	(mm)	Part Dimension		Part Dimension	
			(in.)	(mm)	(in.)	(mm)
1	14.40	365.8	14.50	368.3	14.52	368.8
2	13.15	334.0	-	-	12.72	323.2
3	11.98	304.3	11.94	303.2	11.96	303.8
4	11.24	285.5	11.20	284.5	11.25	285.8
5	8.82	224.0	8.69	220.7	8.73	221.9
6	8.18	207.8	7.94	201.7	8.17	207.6
7	6.12	155.4	6.17	156.7	6.18	157.0
8	8.00	203.2	8.02	203.7	8.07	205.1
9	.10	2.5	.08	2.0	.10	2.5
10	1.99	50.5	1.96	49.8	2.07	52.7
11	1.50 ^b	38.1	1.50	38.1	1.50	38.1
12	.64	16.3	.62	15.7	.59	15.0
13	.20 ^b	5.1	.20	5.1	.20	5.1
14	.215 ^b	5.5	.22	5.6	.21	5.5
15	.19	4.8	-	-	-	-
16	1.10	27.9	1.21	30.7	1.15	29.2
17	.34	8.6	.30	7.6	.40	10.2
18	1.25	31.7	1.25	31.7	1.00	25.4
19	1.70 ^b	43.2	1.70	43.2	1.70	43.2
20	2.00 ^b	50.8	2.00	50.8	2.00	50.8
21	2.875 ^b	73.0	2.875	73.0	2.87	73.0
22	3.33 ^b	84.6	3.33	84.6	3.33	84.6
23	3.05 ^b	77.5	3.05	77.5	3.05	77.5
24	4.61	117.1	4.61	117.1	4.61	117.1
25	6.81 ^b	173.0	6.81	173.0	6.81	173.0
26	4.86 ^b	123.4	4.86	123.4	4.86	123.4
27	5.50 ^b	139.7	5.50	139.7	5.50	139.7
28	.42	10.7	3.8	9.7	.45	11.5
29	.48	12.2	.50	12.7	.50	12.7
30	30°	-	-	-	28°	28°
31	9.79	248.7	9.30	236.2	10.00	254.0
32	9.94	252.5	9.50	241.3	10.02	254.6
33	.59	15.0	.71	18.0	.70	17.8
34	11.12	282.4	10.92	277.4	11.30	287.0
35	11.32	287.5	11.14	283.0	11.38	289.1
36	.39	9.9	.58	14.7	.41	10.4
37	6.375	161.9	6.41	162.8	6.50	165.1
38	.455	11.6	.60	15.2	.44	11.2
39	6.51	165.4	6.45	166.1	6.52	165.6
40	6.86	174.2	6.91	175.5	6.96	176.8
41	.63	16.0	.83	21.1	.64	16.3
42	.68	17.3	.84	21.3	.70	17.8
43	6.96	176.8	6.93	176.0	7.07	179.6
44	7.09	180.1	7.07	179.6	7.20	182.9
45	.74	18.9	.91	23.1	.75	19.2
46	5.47	138.9	5.25	133.4	5.72	14.5
47	5.60	142.2	-	-	-	-

a) Refer to Figure 3-6 for dimension location.

b) Reference dimensions.

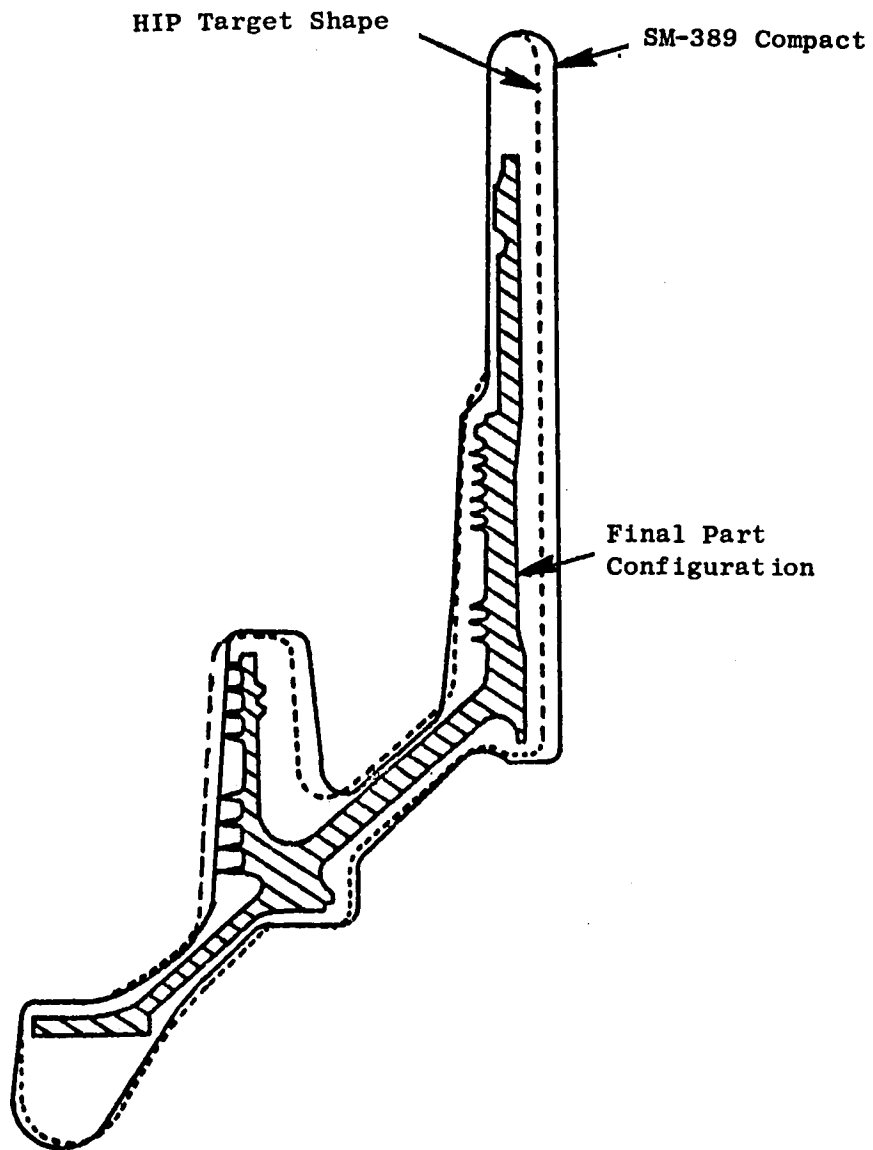


Figure 3-7. Relationship of 1st Shape Trial Part (SM-389) to HIP Target Shape and Final Part Configuration.

Table 3-2. Target and Part Dimensions
for CF6 HPTR Rear Shaft.

Dimension No. ^a	Target Dimension		SM-489 Part Dimension	
	(in.)	(mm)	(in.)	(mm)
1	14.40	365.8	14.52	368.8
2	13.15	334.0	12.72	323.2
3	11.98	304.3	11.96	303.8
4	11.24	285.5	11.25	285.8
5	8.82	224.0	8.73	221.9
6	8.18	207.8	8.17	207.6
7	6.12	155.4	6.18	157.0
8	8.00	203.2	8.07	205.1
9	.10	2.5	.10	2.5
10	1.99	50.5	2.07	52.7
11	1.50 ^b	38.1	1.50	38.1
12	.64	16.3	.59	15.0
13	.20 ^b	5.1	.20	5.1
14	.215 ^b	5.5	.21	5.5
15	.19	4.8	---	---
16	1.10	27.9	1.15	29.2
17	.34	8.6	.40	10.2
18	1.25	31.7	1.00	25.4
19	1.70 ^b	43.2	1.70	43.2
20	2.00 ^b	50.8	2.00	50.8
21	2.875 ^b	73.0	2.87	73.0
22	3.33 ^b	84.6	3.33	84.6
23	3.05 ^b	77.5	3.05	77.5
24	4.61	117.1	4.61	117.1
25	6.81 ^b	173.0	6.81	173.0
26	4.86 ^b	123.4	4.86	123.4
27	5.50 ^b	139.7	5.50	139.7
28	.42	10.7	.45	11.5
29	.48	12.2	.50	12.7
30	30°	---	28°	28°
31	9.79	248.7	10.00	254.0
32	9.94	252.5	10.02	254.6
33	.59	15.0	.70	17.8
34	11.12	282.4	11.30	287.0
35	11.32	287.5	11.38	289.1
36	.39	9.9	.41	10.4
37	6.375	161.9	6.50	165.1
38	.455	11.6	.44	11.2
39	6.51	165.4	6.52	165.6
40	6.86	174.2	6.96	176.8
41	.63	16.0	.64	16.3
42	.68	17.3	.70	17.8
43	6.96	176.8	7.07	179.6
44	7.09	180.1	7.20	182.9
45	.74	18.9	.75	19.2
46	5.47	138.9	5.72	14.5
47	5.60	142.2	---	---

^a Refer to Figure 3-6 for dimension location.
Part dimensions are averaged.

^b Reference dimensions.

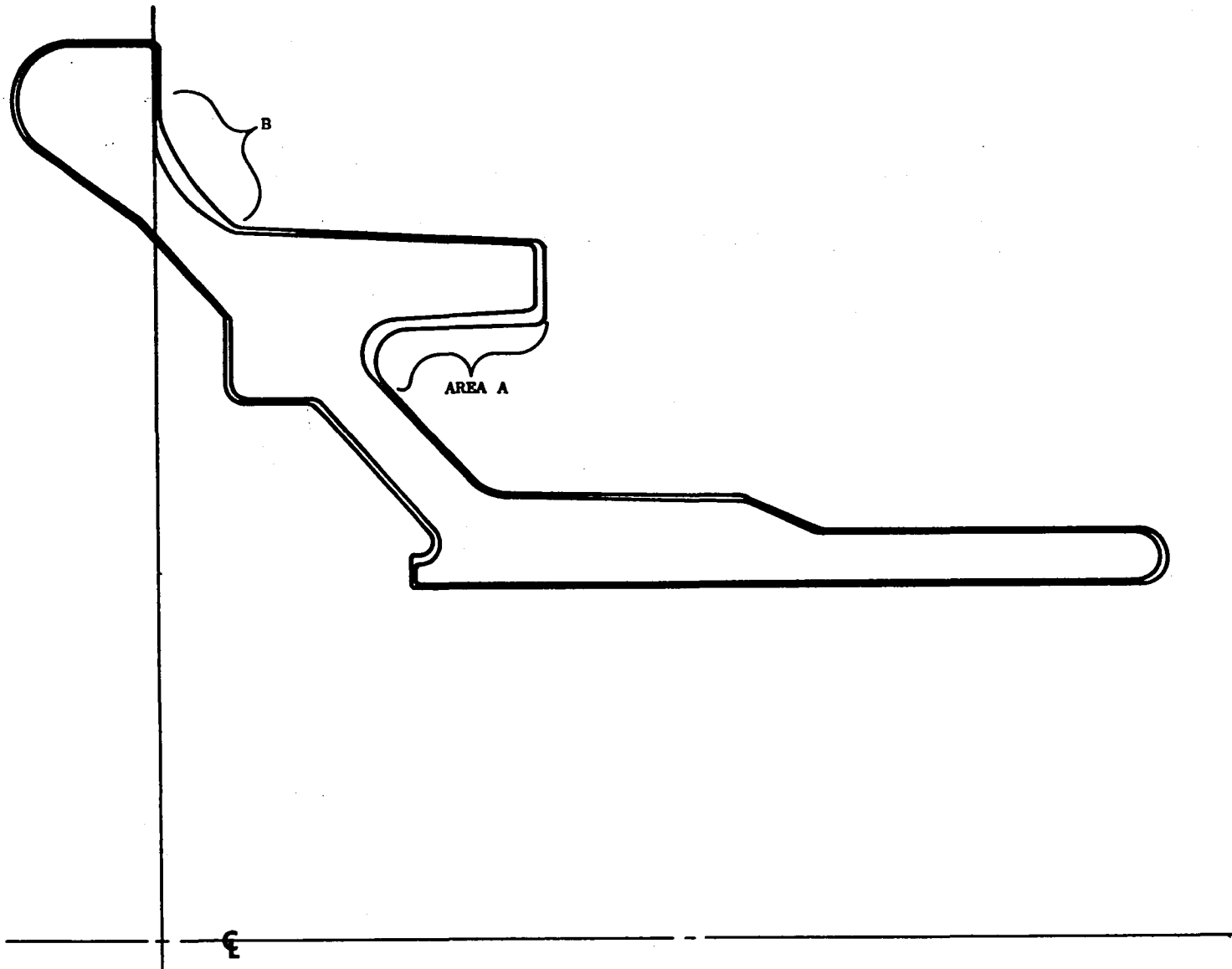


Figure 3-8. Minimum and Maximum Material Conditions Found on SM-489.

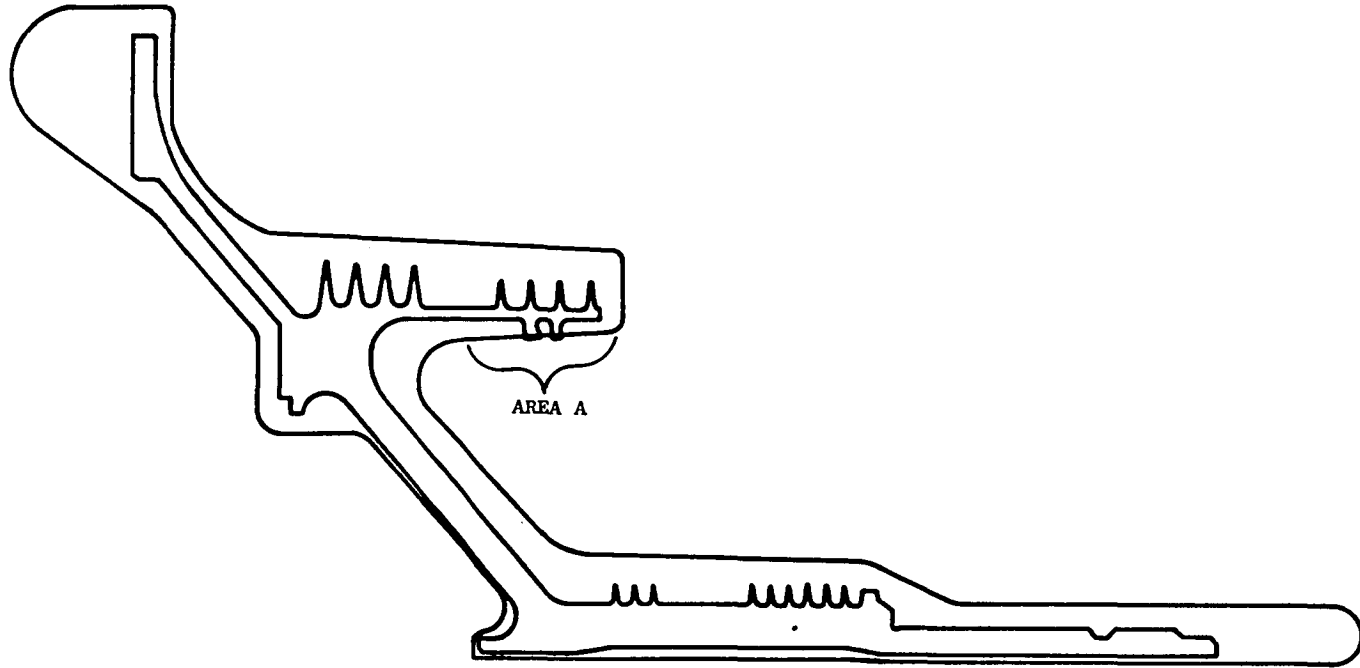


Figure 3-9. Minimum Material Envelope Versus Engineering Contour Compact SM-489.

The third shape iteration wax was machined to dimensionally correct for the discrepant areas in the previous iterations. The compact was consolidated in the BCL autoclave under the same conditions as the previous two. After consolidation the compact (SM531) was delivered to GE Lynn for dimensional inspection again using the Brown and Sharp Verifier.

A new drawing was issued between the second and third iterations with the primary difference being that minimum dimensions were imposed, along with a maximum weight. This maximum weight allowed CRC about seven pounds of "discretionary metal."

The location of the "new" dimensions are indicated in Figure 3-10, and the target dimensions of each are recorded in Table 3-3. Table 3-3 also records the dimensions of the third iteration (SM531) at the indicated points. (It should be noted that basically the same dimensions are measured by the two techniques - the old method defining the coordinates on the drawing whereas the "new" method lists either the radius at which point "Z" dim. are measured, or "Z" dimensions denoting the height at which a radius is to be determined.)

Figure 3-11 shows the finish machined part, the target envelope, and the minimum dimension of the achieved envelope. Examination of Figure 3-11 shows that the finish machined part can be derived from the compact.

The achievement of the desired configuration concluded the shape making iterations by CRC in this Task.

3.1.3 Task III - Manufacturing Shape Development

The purpose of this task was to make a pilot production run to produce five near net shape CF6-50 HPT aft shafts using the production process defined in Task II of this program. A process plan for production of as-HIP parts of this general configuration was approved by NASA. This document is included in Appendix C to this report.

The beginning of Task III at CRC included production of an injection mold die using the dimensions of the wax which produced the third iteration. Five wax patterns were produced using the injection mold for "proof" testing. These five wax patterns were dimensionally measured using an Iota-PDEA coordinate checked at a nearby vendor. An analysis of the results indicted the five patterns were all undersize due to greater wax shrinkage than anticipated. The decision was made to rework the die and prepare new wax patterns. CRC had seven wax patterns produced and dimensionally measured at 0°, 90°, 180°, and 270° on the same coordinate checker. A photograph of typical wax patterns is given in Figure 3-12.

The wax patterns contained three small protrusions on the top of the large flange about 1.99 - 2.54 mm. (0.090 in. - 0.100 in.) high. Two of these were circular, approximately 2.54 mm (0.100 in.) in diameter, the third was square, approximately 3.16 mm (0.125 in.) on a side. All measurements of

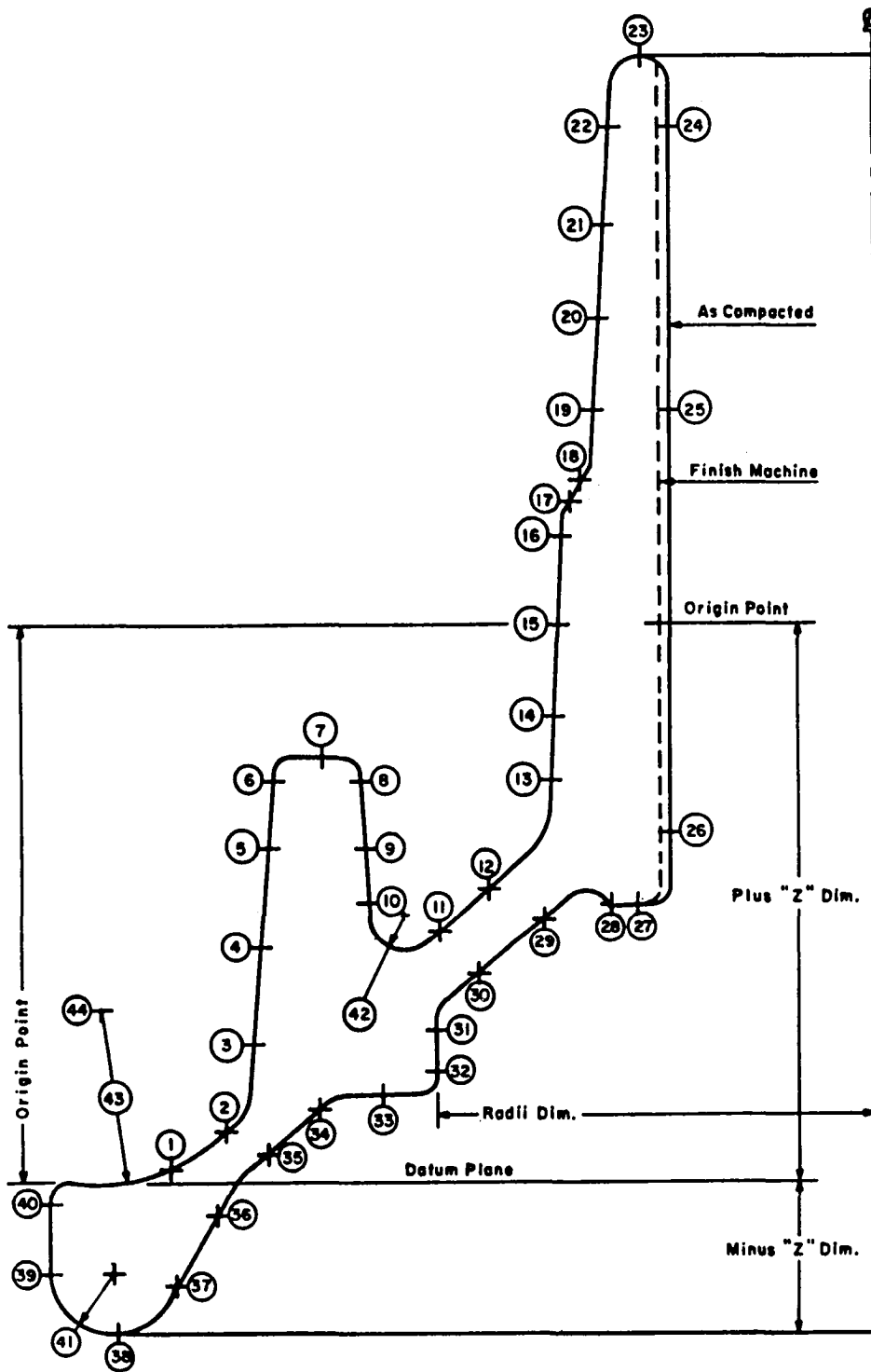


Figure 3-10. As-HIP CF6 HPTR Rear Shaft Dimension Locations.

Table 3-3. Target and Part Dimensions for CF6 HPTR Rear Shaft.

Dimension No. ^a	"z" Dimension		Target Dimension ^b		Compact Dimensions ^b - SM-531			
					Min. Envelope		Max. Envelope	
	(in)	(mm)	(in)	(mm)	(in)	(mm)	(in)	(mm)
1	.025	0.6	-	-	6.502	165.2	6.575	167.0
2	.500	12.7	-	-	5.833	148.2	5.873	149.2
3	1.000	25.4	5.720	145.3	5.684	144.4	5.728	145.5
4	1.700	43.2	5.666	143.9	5.624	142.8	5.686	144.4
5	2.150	54.6	-	-	5.586	141.8	5.638	143.2
6	2.875	73.0	5.560	141.2	5.555	141.1	5.588	141.9
7	3.040	77.2	3.040*	77.2*	3.121*	79.3*	3.167*	80.4*
8	2.875	73.0	4.970	126.2	4.893	124.3	4.808	122.1
9	2.450	62.2	-	-	4.891	124.2	4.809	122.1
10	2.000	50.8	4.895	124.3	4.898	124.4	4.789	121.6
11	2.000	50.8	-	-	4.255	108.1	4.346	110.4
12	2.150	54.6	-	-	4.042	102.7	4.149	105.4
13	2.800	71.1	-	-	3.643	92.5	3.717	94.4
14	3.330	84.6	3.545	90.0	3.593	91.3	3.633	92.3
15	4.330	61.8	-	-	3.539	89.9	3.578	90.9
16	4.610	117.1	3.480	88.4	3.532	89.7	3.569	90.7
17	4.860	123.4	3.430	87.1	3.515	89.3	3.553	90.2
18	5.000	127.0	3.349	85.1	-	-	-	-
19	5.500	139.7	3.255	82.7	3.293	83.6	3.325	84.5
20	6.500	165.1	-	-	3.266	83.0	3.300	83.8
21	6.810	173.0	3.188	81.0	3.252	82.6	3.290	83.6
22	7.550	191.8	-	-	3.209	81.5	3.281	83.3
23	8.000	203.2	8.000*	203.2*	8.030*	204.0*	8.081*	205.3*
24	7.500	190.5	2.800	71.1	2.770	70.4	2.712	68.9
25	5.500	139.7	2.800	71.1	2.778	70.6	2.744	69.7
26	2.680	68.1	2.800	71.1	2.742	69.6	2.716	69.0
27	1.990	50.5	1.990*	50.5*	2.089*	53.1*	2.082*	52.9*
28	2.089	53.1	3.100	78.7	3.108	78.9	3.130	79.5
29	1.850	47.0	-	-	3.731	94.8	3.637	92.4
30	1.500	38.1	4.090	103.8	4.164	105.8	4.127	104.8
31	1.100	27.9	4.410	112.0	4.374	111.1	4.350	110.5
32	.800	20.3	4.410	112.0	4.370	111.0	4.348	110.4
33	.640	16.3	.640*	16.3*	.688*	17.5*	.669*	17.0*
34	.300	7.6	-	-	5.457	138.6	5.411	137.4
35	.210	5.3	-	-	5.560	141.2	5.514	140.1
36	-.215	-5.5	5.990	152.1	5.977	152.3	5.926	150.5
37	-.750	-19.0	6.299	160.0	6.270	159.3	6.217	157.9
38	-1.110	-28.2	-1.110*	-28.2*	-1.112*	-28.2*	-1.127*	-28.6*
39	-.675	-17.1	7.200	182.9	7.321	186.0	7.359	186.9
40	-.200	-5.1	7.200	182.9	7.294	185.3	7.334	186.3
41	-	-	.439R	11.2R	-	-	-	-
42	-	-	.250R	6.3R	-	-	-	-
43	-	-	1.250R	31.8R	-	-	-	-
44	1.250	31.7	6.840	173.7	-	-	-	-

a) Refer to Figure 3-6 for dimension locations.

b) All dimensions are radii except those marked "*" which are Z dimensions.

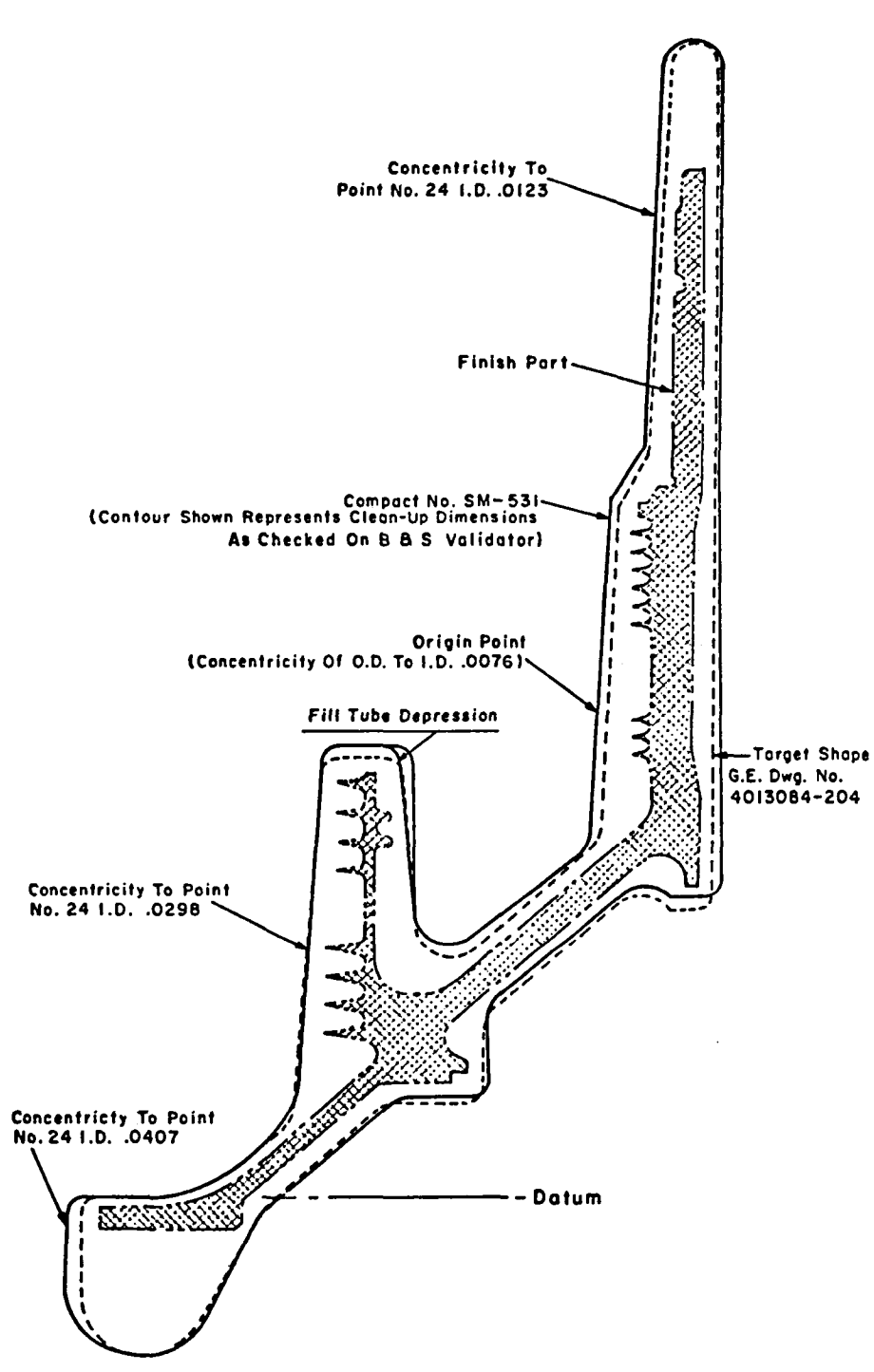


Figure 3-11. 3rd Shape Trial Part (SM-531) Showing Minimum Envelope, Sonic Target and Final Part.

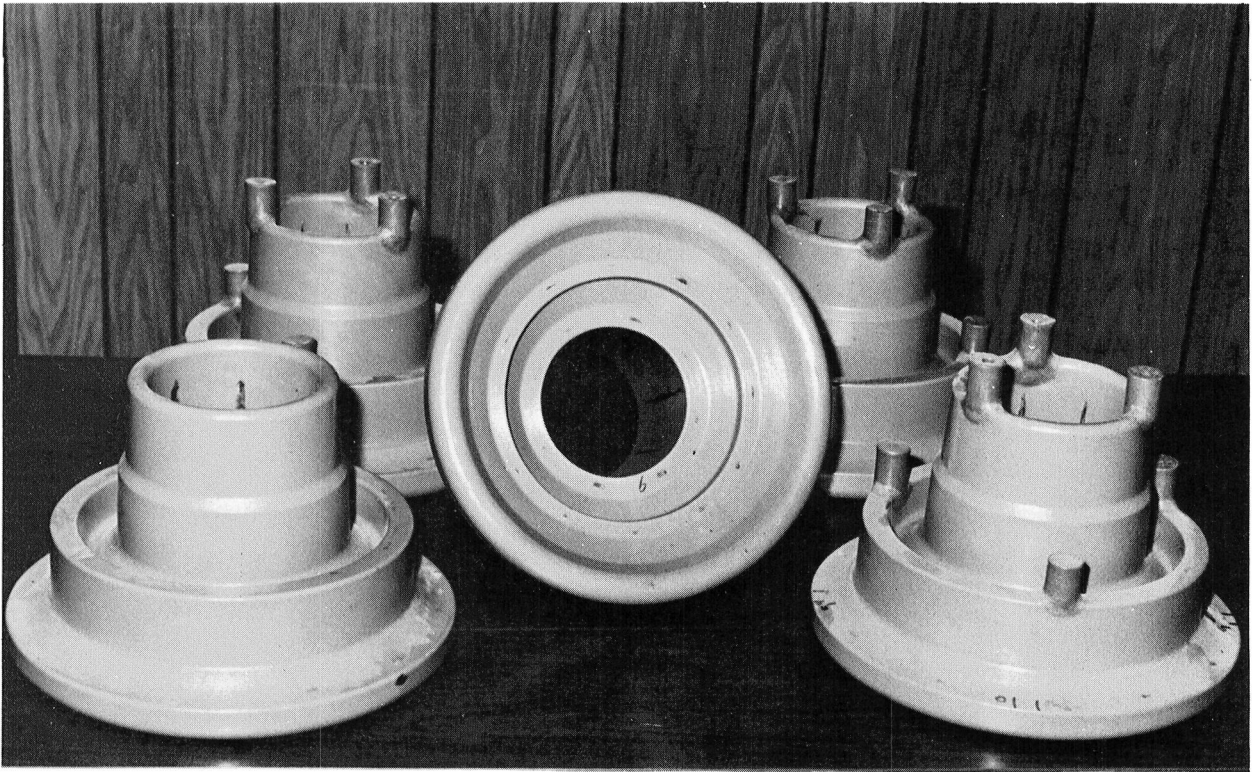


Figure 3-12. Wax Patterns for CF6 HPTR Rear Shaft.

the wax patterns and compacts used this square protrusion as the "0" for angular orientation. An attempt was made to follow this zero through all operations to determine if location or placement in the container, autoclave, or heat treat rack made any significant difference in dimensional control. We found the none of these contributed to any significant extent, to the dimensional variations encountered.

The wax patterns were dimensionally inspected per Figure 3-10 and the range of deviations from the target dimension of all seven wax patterns are shown in Figure 3-13. A positive variation indicates an excess envelope (larger OD or smaller ID) and negative variations the opposite.

These incorporated the maximum envelope at any dimension (four per wax) to the minimum envelop at that same dimensions on any wax. Thus for each dimension shown the maximum and minimum of about 28 readings are represented.

Ceramic molds were produced and filed with René 95 powder from five of these wax patterns:

SN/582 - Pattern No. 7
SN/586 - Pattern No. 8
SN/587 - Pattern No. 9
SN/589 - Pattern No. 6
SN/590 - Pattern No. 10

These five were consolidated in one cycle of the large autoclave at the same parameters as those used on the earlier iteration.

Subsequent to consolidation, the fill stems (six per compact) were removed, examined, and accepted as fully dense on the basis of the microstruc-tive observed.

Prior to dimensional inspection, the compacts were target machined using the following procedure:

1. Each compact was held in a four jaw chuck in a lathe at dimensions points 39 and 40 (Figure 3-10). The datum surface was then indicated and adjusted until the indicated runouts were balanced. The same procedure was used to balance the diameter a point 4 (Figure 3-10) and light target machining cuts were then made at dimensions 7, 24, and 26.
2. The compact was then reversed in the lathe and held at dimension point 22. The compact was then balanced using the previously machined points 7 and 24. A light target machining cut was then made at dimension point 38.

The five compacts were shipped to the GE, Lynn, Mass. facility for dimensional inspection using the Brown and Sharp verifier. To accomplish this inspection, the compacts were set up and balanced using the machined surfaces

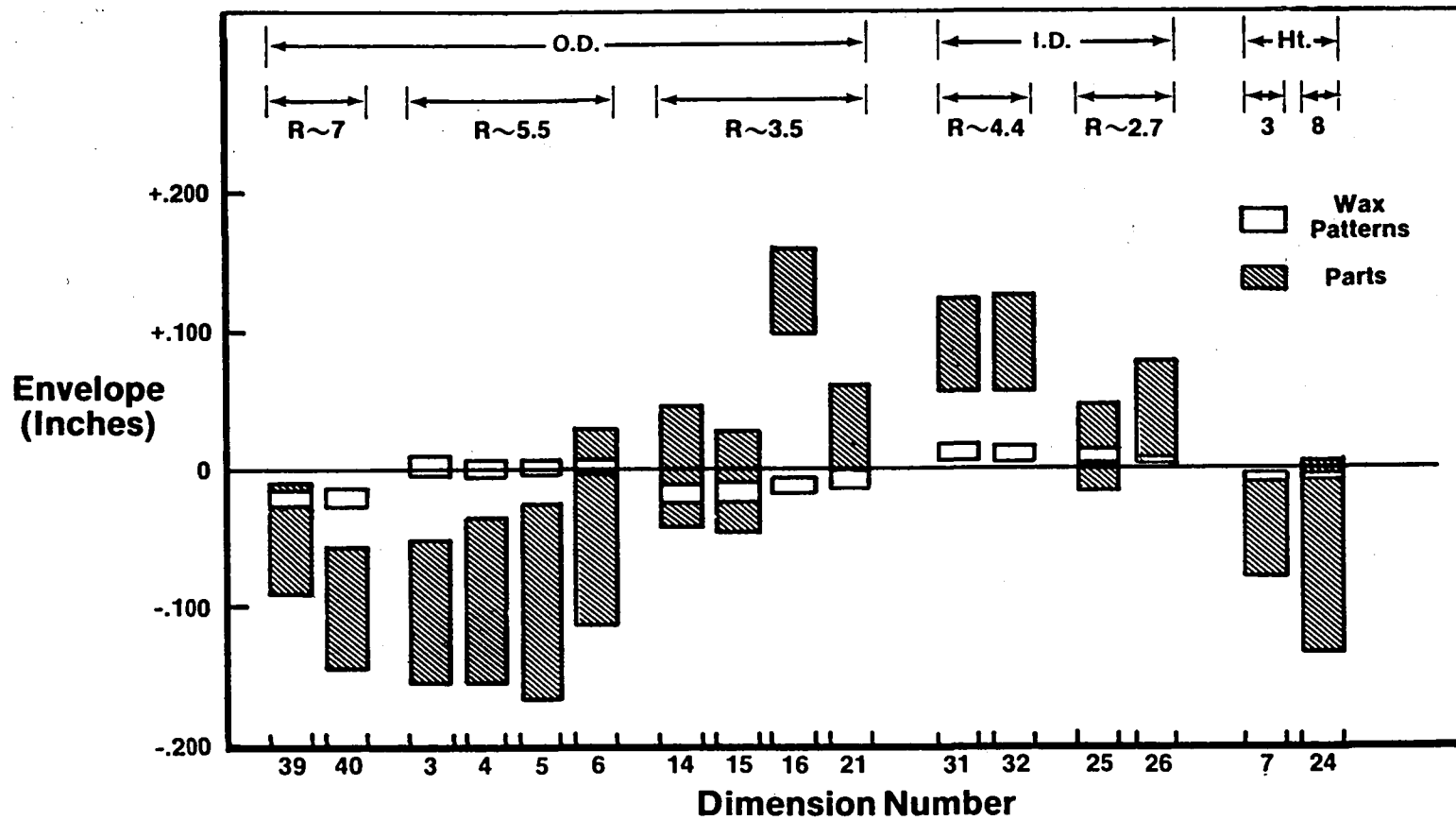


Figure 3-13. Comparison of Total Envelope Variance (Patterns and Campacts) and Deviation From Target Dimension.

as reference planes. The results of this inspection are given in Table 3-4. Several compacts were set up using the surface of the small locator protrusions as a reference plane and the as-compacted dimensions were measured. These results were in very close agreement with those reported in Table 3-4 and therefore are not reported here.

Analysis of these data indicated that the compacts did not fully achieve the target dimensions, although one, (SM587), was close to the desired shape. This nonconformance was manifest in two areas:

1. All dimensions (ID and OD) reduced during HIP to a greater extent than predicted on the basis of the previous trial shapes.
2. The compacts exhibited a greater point-to-point variation than anticipated based on previous experience.

A review of the dimensions showed that two shapes would yield finish machined parts. To meet the GE requirement of two compacts to supply the production machining line, it was decided that the third shape iteration (SM 531) produced from a different but qualified master powder blend should be heat treated along with the five.

The dimensional discrepancies were traced to two related problems: (1) faulty wax pattern injection molding techniques that allowed porosity to develop within the wax, thus, when weighed to determine the weight of R95 powder, an error on the low side was introduced. The loading procedure was modified in the same time period, and the modification was used on four of the five. The most acceptable compact was loaded by the old procedure. CRC reported these variations and produced three additional compacts at no cost to the contract using revised techniques and procedures. In addition certain dimensions of the wax patterns were revised slightly. These were slightly heavier 3.6 kg (~8 lbs) than the previous compacts but weight could be reduced, if a new injection mold cavity was produced.

The dimensions of these additional compacts were measured by CRC using a Bendix Cordax coordinate checker. These data are given in Table 3-5. Based on these data it appears that a maximum 2.54 mm (0.100 in.) envelope can be achieved on compacts of similar shape and size after one or two shape iterations.

The five production compacts, plus the third iteration part were heat treated in two lots of three each (SM531, 582, 589 in one lot and SM586, 587, and 590 in the other) using a molten salt quench. The heat treatment sequence as previously established included solution treatment at a temperature of 1120° C (2050° F) for one hour followed by a quench into a 816° C (1500° F) salt bath which was manually agitated. The solution treatment was followed by a double age: 870° C (1600° F) for one hour, air cooled plus 650° C (1200° F) for sixteen hours and air cooled. All six compacts were visually inspected after heat treatment and no cracks were observed.

Table 3-4. Target and Part Dimensions for CF6 HPTR Rear Shaft.

Dimension No. ^a	Target Dimensions (in.)		Compact Dimensions (in.) ^b									
			SM-582		SM-586		SM-587		SM-589		SM-590	
	Z	Radius	Minimum Envelope	Maximum Envelope	Minimum Envelope	Maximum Envelope	Minimum Envelope	Maximum Envelope	Minimum Envelope	Maximum Envelope	Minimum Envelope	Maximum Envelope
1	.100	6.350	6.353	6.423	6.346	6.428	6.318	6.442	6.345	6.380	6.335	6.411
2	.375	5.939	5.968	6.050	5.956	6.015	5.956	6.054	5.965	6.008	5.972	6.018
3	1.000	5.720	5.568	5.684	5.568	5.620	5.611	5.684	5.617	5.662	5.606	5.643
4	1.700	5.660	5.504	5.642	5.517	5.560	5.571	5.598	5.538	5.612	5.540	5.585
5	2.375	5.618	5.464	5.604	5.441	5.520	5.541	5.592	5.467	5.577	5.498	5.530
6	2.875	5.560	5.478	5.592	5.434	5.531	5.532	5.578	5.482	5.570	5.469	5.524
7	3.040	-	-	-	2.957*	3.027*	2.987*	3.094*	3.004*	3.030*	2.994*	3.038*
8	2.875	4.970	4.827	4.743	4.794	4.702	4.773	4.707	4.803	4.720	4.826	4.717
9	2.375	4.927	4.812	4.705	4.785	4.720	4.737	4.659	4.860	4.663	4.822	4.683
10	2.000	4.895	-	-	4.798	4.697	4.711	4.630	4.825	4.651	4.826	4.661
10	2.050	-	4.828	4.681	-	-	-	-	-	-	-	-
11	1.800	4.384	-	-	-	-	-	-	-	-	-	-
11	2.050	-	4.093	4.161	-	-	-	-	-	-	-	-
11	2.000	-	-	-	4.104	4.200	-	-	4.109	4.179	4.075	4.182
12	2.100	4.031	-	-	3.962	4.049	3.865	3.974	3.969	4.042	3.937	4.037
12	2.150	-	3.956	4.024	-	-	-	-	-	-	-	-
13	2.875	3.568	3.557	3.638	3.544	3.619	3.508	3.598	3.542	3.668	3.533	3.633
14	3.330	3.545	3.517	3.549	3.497	3.560	3.480	3.561	3.511	3.591	3.490	3.571
15	4.000	3.511	3.474	3.546	3.457	3.533	3.457	3.528	3.475	3.563	3.453	3.520
16	4.610	3.480	3.453	3.518	3.438	3.500	3.441	3.504	3.454	3.514	3.432	3.491
17	4.860	3.430	-	-	3.372	3.427	3.393	3.435	3.409	3.481	3.387	3.431
17	4.900	-	3.388	3.464	-	-	-	-	-	-	-	-
18	5.000	3.349	-	-	3.296	3.351	3.317	3.357	3.334	3.399	3.313	3.355
18	5.100	-	3.286	3.366	-	-	-	-	-	-	-	-
19	5.500	3.255	3.217	3.292	3.210	3.261	3.216	3.257	3.222	3.277	3.201	3.252
20	6.150	3.222	3.200	3.271	3.190	3.242	3.211	3.240	3.205	3.246	3.186	3.241
21	6.810	3.188	3.177	3.260	3.171	3.227	3.196	3.228	3.167	3.208	3.177	3.228
22	7.500	3.153	3.153	3.246	3.159	3.208	3.190	3.216	3.163	3.208	3.159	3.227
23	8.000	-	7.936*	8.107*	7.857*	7.893*	7.866*	7.931*	7.882*	7.914*	7.890*	7.940*
24	7.500	2.735	2.739	-	2.676	2.618	2.694	2.654	2.779	2.648	2.690	2.629
25	5.500	2.735	2.736	2.674	2.716	2.667	2.693	2.665	2.717	2.674	2.718	2.684
26	2.500	2.735	2.740	2.736	2.715	2.703	2.706	2.701	2.727	2.717	2.735	2.670
27	1.990	-	1.950*	1.939*	1.917*	1.898*	1.841*	1.817*	1.926*	1.911*	1.891*	1.870*
28	1.990	-	1.950*	1.933*	1.919*	1.888*	1.834*	1.805*	1.927*	1.910*	1.881*	1.862*
29	1.900	3.619	-	-	-	-	-	-	-	-	-	-
29	1.700	-	3.845	3.778	3.792	3.732	3.673	3.596	3.851	3.731	3.751	3.678
30	1.500	4.090	4.085	4.004	4.036	3.956	3.922	3.851	4.072	3.956	4.010	3.907
31	1.100	4.410	4.357	4.287	-	-	-	-	-	-	-	-
31	1.000	-	-	-	4.353	4.289	-	-	-	-	-	-
31	.950	-	-	-	-	-	4.353	4.290	4.355	4.287	4.342	4.296
32	.800	4.410	4.341	4.290	4.324	4.290	-	-	-	-	4.337	4.299
32	.650	-	-	-	-	-	4.362	4.301	-	-	-	-
32	.700	-	-	-	-	-	-	-	4.375	4.300	-	-
33	.640	-	.643*	.609*	.648*	.600*	.535*	.501*	.615*	.547*	.594*	.549*
34	.500	5.267	5.150	5.088	5.132	5.063	-	-	5.150	5.003	-	-
34	.400	-	-	-	-	-	5.187	5.087	-	-	5.219	5.153
35	.200	5.620	-	-	-	-	-	-	-	-	-	-
35	.100	-	5.611	5.542	5.597	5.529	5.790	5.690	5.586	5.500	5.575	5.521
36	-.215	5.990	-	-	-	-	-	-	-	-	-	-
36	-.300	-	5.964	5.901	5.945	5.882	5.961	5.887	5.945	5.883	5.946	5.919
37	-.750	6.299	6.216	6.153	6.210	6.153	6.220	6.146	6.207	6.146	6.223	6.188
38 ^c	-1.110	-	-1.039*	-1.039*	-1.029*	-1.054*	-1.081*	-1.083*	-1.035*	-1.071*	-1.043*	-1.078*
39	-.650	7.200	7.114	7.186	7.106	7.156	7.149	7.206	7.134	7.183	7.164	7.194
40	-.150	7.200	7.060	7.152	7.044	7.104	7.103	7.155	7.089	7.131	7.097	7.134

- a) Refer to Figure 3-6 for dimension locations.
- b) All dimensions are radii except those marked "*" which are Z dimensions.
- c) Target machined location.

Table 3-5. Target and Part Dimensions for CF6 HPTR Rear Shafts.

Dimension No. ^a	Target Dimensions (in.)		Compact Dimensions (in.)					
			Wax #4		Wax #7		Wax #5	
			SM-627		SM-628		SM-630	
			Z	Radius	Minimum Envelope	Maximum Envelope	Minimum Envelope	Maximum Envelope
1	.147	6.252	6.263	6.302	6.206	6.260	6.204	6.260
2	.422	5.904	5.910	5.936	5.849	5.912	5.853	5.914
3	1.047	5.716	5.699	5.737	5.647	5.697	5.658	5.705
4	1.747	5.656	5.619	5.653	5.566	5.613	5.592	5.635
5	2.422	5.599	5.563	5.582	5.506	5.546	5.529	5.565
6	2.747	5.571	5.537	5.548	5.474	5.515	5.503	5.521
7 ^b	2.993	5.152	2.992	3.028	2.986	3.007	2.950	3.009
8	2.922	4.974	4.750	4.721	4.737	4.684	4.743	4.700
9	2.422	4.931	4.737	4.701	4.709	4.679	4.728	4.675
10	2.047	4.900	4.713	4.676	4.689	4.633	4.695	4.625
11 ^c	2.058	4.080	1.972	2.027	1.953	2.013	1.959	2.131
12 ^c	2.337	3.752	2.222	2.288	2.203	2.275	2.213	2.276
13	2.922	3.566	3.542	3.592	3.515	3.581	3.529	3.592
14	3.377	3.538	3.502	3.548	3.479	3.539	3.481	3.521
15	4.047	3.509	3.474	3.519	3.450	3.512	3.449	3.496
16	4.657	3.478	3.452	3.490	3.432	3.481	3.427	3.459
17	4.907	3.403	3.356	3.404	3.348	3.389	3.338	3.378
18	5.047	3.322	3.290	3.335	3.268	3.323	3.264	3.302
19	5.547	3.253	3.223	3.249	3.197	3.233	3.190	3.225
20	6.197	3.220	3.203	3.233	3.183	3.220	3.177	3.212
21	6.857	3.186	3.201	3.219	3.178	3.212	3.174	3.237
22	7.497	3.153	3.192	3.233	3.162	3.201	3.196	3.249
23 ^b	8.000	2.850	7.876	7.891	7.861	7.903	7.864	7.876
24	7.547	2.735	2.634	2.617	2.620	2.593	2.630	2.575
25	5.547	2.735	2.678	2.653	2.676	2.646	2.671	2.635
26	2.497	2.735	2.667	2.653	2.687	2.641	2.664	2.646
27 ^b	1.943	2.850	1.886	1.857	1.824	1.810	1.880	1.860
28 ^b	1.943	3.100	1.879	1.844	1.819	1.802	1.869	1.848
29	1.647	3.917	3.757	3.667	3.704	3.650	3.721	3.665
30	1.347	4.270	4.108	4.052	4.043	3.994	4.054	4.006
31	.947	4.410	4.308	4.289	4.300	4.253	4.280	4.263
32	.747	4.410	4.310	4.290	4.296	4.246	4.283	4.258
33 ^b	.593	4.500	0.557	0.533	0.512	0.490	0.550	0.518
34	.322	5.477	5.246	5.187	5.203	5.138	5.212	5.135
35	.197	5.624	5.391	5.334	5.701	5.641	5.360	5.292
36	-.168	6.099	5.962	5.908	5.931	5.883	5.922	5.891
37	-.703	6.243	6.100	6.055	6.066	6.032	6.071	6.044
38 ^b	-1.063	6.750	-1.120	-1.160	-1.119	-1.139	-1.133	-1.150
39	-.603	7.200	7.225	7.249	7.183	7.235	7.192	7.232
40	-.103	7.200	7.190	7.203	7.142	7.185	7.132	7.178

- a) See Figure 3-6 for dimension locations.
- b) Z dimensions.
- c) On all previous parts these dimensions were measured as radii, but on these three parts they were measured as Z dimensions.

The two test rings were parted for testing, TR_A (aft or small diameter) and TR_B. CRC retained all the test rings plus one compact (SM586) for cut up evaluation. The remaining five compacts were forwarded to GE-AEG Evendale, Ohio.

The test ring cut-up plan and results are reported in Appendices A and B to this report. All of the mechanical properties determined from the test rings met the aim properties. A summary of the test ring properties is reported in Table 3-6. These values are averages of the data given in the Appendices.

Upon receipt of the five compacts, the two compacts closest to the aim dimensions were introduced into the manufacturing cycle. These parts were Harperized by the identified procedure, to produce an ultrasonically inspectable surface, checked for whole part density (acceptable), ultrasonically inspected (acceptable), and fluorescent penetrant inspected with no indications interpretable as cracks being noted.

This particular part, the HPT aft shaft, for the CF6-50, is machined by an outside vendor. The similar part for the CF6-6 is machined at Evendale, therefore the NC tapes were modified to produce the CF6-50 part and all machining was accomplished in-house which allowed close surveillance throughout the manufacturing operations. Two parts were finish machined to acceptable blueprint dimensions. The finished HPT aft shaft is shown in Figure 2-3.

Table 3-6. Summary of Test Ring Data (1).

	Ultimate Tensile Strength		0.2% Yield Strength		Elong (%)	Red Area (%)	
	(MPa)	(ksi)	(MPa)	(ksi)			
<u>Room Temp.</u>							
SM531	1586	(230)	1165	(169)	16.6	18.8	
SM582	1593	(231)	1165	(169)	16.8	19.0	
SM587	1586	(230)	1186	(172)	14.9	17.7	
SM589	1593	(231)	1158	(168)	18.0	19.7	
SM590	1531	(222)	1193	(173)	11.3	15.2	
Drawing Req.	1276	(185)	1034	(150)	10	12	
<u>650° C (1200° F)</u>							
SM531	1454	(211)	1089	(158)	15.8	17.2	
SM582	1454	(211)	1103	(160)	12.4	18.3	
SM587	1420	(206)	1124	(163)	10.1	15.7	
SM589	1434	(208)	1089	(158)	11.4	15.7	
SM590	1441	(209)	1089	(158)	9.7	13.8	
Drawing Req.	1000	(145)	862	(125)	8	10	
<u>650° C (1250° F), 690 MPa(100 ksi) Stress Rupture</u>					<u>Life Hours</u>	<u>Elong (%)</u>	<u>Red Area (%)</u>
SM531				266	3.9	7.3	
SM582				310	4.7	7.3	
SM587				331	4.3	6.5	
SM589				373	7.0	7.5	
SM590				316	3.9	4.8	
Drawing Req.				25	6(2)	---	

(1) Complete data are given in Appendix A and B.

(2) Only if failure occurs in less than 150 hrs.

3.2 PROCESSING AND PROPERTIES OF As-HIP SHAPES

3.2.1 Task II - Process Development

3.2.1.1 Powder Production

The objective of this subtask was to produce, at Crucible, sufficient -60 mesh René 95 powder for use in the as-HIP portion of Task II which included the CF6 rear shaft shape trials, the heat treatment identification study, and the process variable study.

Powder was produced at Crucible by argon gas atomizing a vacuum induction melted charge, consisting of virgin materials and revert powder with nominal heat sizes of 238 kg (525 lb). Following atomization, the powder was screened to -60 mesh. Individual heats were then blended to insure particle size uniformity, following which they were sampled for cleanliness. When qualified on the basis of composition and cleanliness, multiple heats are blended together to form a master blend. All powder handling operations were conducted in clean rooms to maintain powder cleanliness. SEM photomicrographs of typical Crucible René 95 powder are shown in Figure 3-14. The certification data for the blends produced by Crucible in Task II are shown in Tables 3-7 and 3-8.

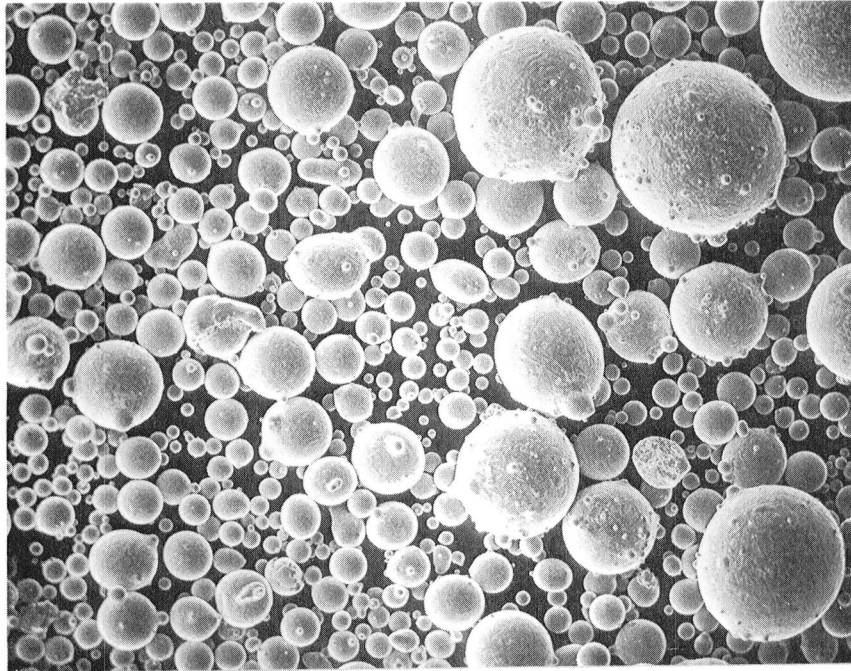
Master powder blend (MPB) MB022 was used to produce the billet used in the heat treatment identification study. Four different blends were used to fabricate the three CF6 shaft shape trial parts: MB033 and MB035 for the first shape trial (SM389), MB045 for the second (SM489), and MB047 for the third. Blend MB048 was used to fabricate the billets for the process variable study and was also used to produce the five shafts in the pilot production run for Task III.

3.2.1.2 Heat Treatment Development

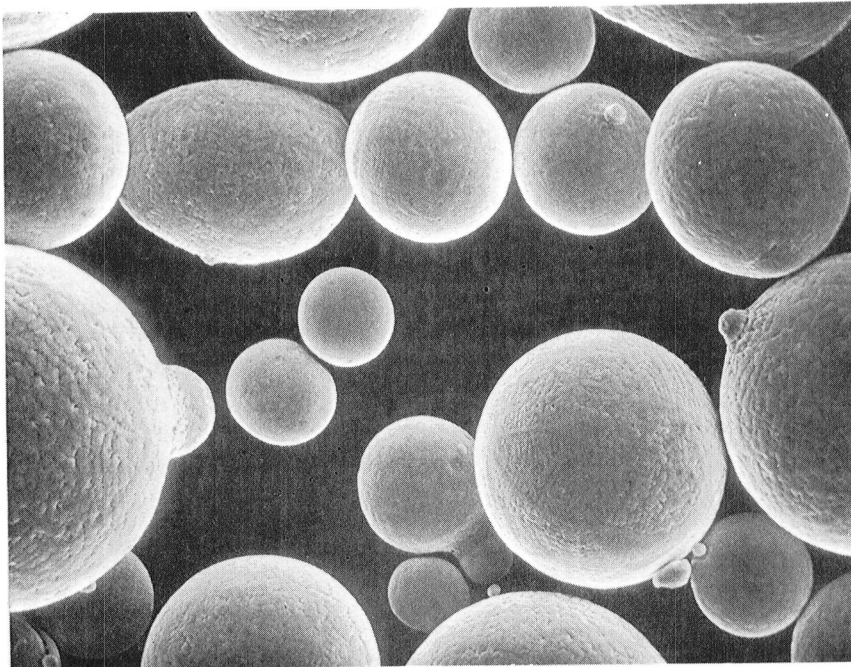
The objective of the heat treatment study was to identify the heat treatment parameters for as-HIP René 95 which would provide mechanical properties required for IN718 replacement. The study was conducted utilizing a -60 mesh Crucible powder billet compacted at 1121° C/103 MPa (2050° F/15 ksi). The billet was produced from blend MB022 and the certification data was given in Tables 3-7 and 3-8. The heat treatment evaluation was conducted in two phases consisting of a preliminary study followed by a detailed mechanical property analysis of the three best heat treatments selected from the preliminary evaluation.

Preliminary Heat Treatment Study

Based on prior experience with as-HIP René 95, solution treatments of 1093° C/RAC (2000° F) (Rapid Air Cool) and aging treatments of 760° C/16 hrs (1400° F), 760° C/16 hrs (1400° F) + 649° C/16 hrs (1200° F), and 872° C/1 hr (1600° F) + 649° C/16 hrs (1200° F) were selected for evaluation. The



100X



1000X

Figure 3-14. SEM Photomicrographs of Typical Crucible René 95 Powder.

Table 3-7. Chemical Analysis of Crucible Blends Produced in Task II.

Element	Weight % Alloy						Specification Limits (C50TF64-S1)
	MB022	MB033	MB035	MB045	MB047	MB048	
C	0.055	0.052	0.054	0.056	0.050	0.050	0.04/0.09
Mn	<0.01	<0.01	<0.01	<0.01	<0.01	<0.01	0.15 max
Si	0.08	0.08	0.07	0.064	0.08	0.08	0.20 max
S	0.001	0.004	0.005	0.004	0.006	0.005	0.015 max
P	<0.003	<0.003	<0.003	<0.002	<0.003	---	0.015 max
Cr	12.79	12.95	12.99	12.86	12.86	12.86	12/14
Co	8.13	8.17	8.15	8.19	8.23	8.28	7/9
Mo	3.55	3.54	3.49	3.56	3.53	3.53	3.3/3.7
Fe	0.16	0.08	0.10	0.10	0.06	0.05	0.5 max
Ta	<0.01	<0.01	<0.01	<0.01	<0.01	<0.01	0.2 max
Cb	3.53	3.60	3.60	3.42	3.47	3.50	3.3/3.7
Zr	0.06	0.04	0.05	0.03	0.04	0.04	0.03/0.07
Ti	2.60	2.59	2.53	2.52	2.49	2.49	2.3/2.7
Al	3.41	3.56	3.47	3.50	3.54	3.61	3.3/3.7
B	0.007	0.009	0.009	0.009	0.008	0.009	0.006/0.015
W	3.41	3.40	3.46	3.41	3.42	3.42	3.3/3.7
O	0.0071	0.0069	0.0067	0.0028	0.0076	0.0065	0.010 max
N	0.0023	0.0023	0.0010	0.0030	0.0021	0.0030	0.005 max
H	0.0001	0.00028	0.00028	0.00012	0.00024	0.00024	0.001 max
Ni	Balance	Balance	Balance	Balance	Balance	Balance	Balance

Table 3-8. Crucible Powder Characteristics.

	Lot Number					
	MB022	MB033	MB035	MB045	MB047	MB048
Screen Analysis (%)						
+ 60	0.0	0.0	0.0	0.0	0.1	0.5
- 60 + 100	24.5	17.3	21.0	26.2	26.9	29.2
-100 + 325	54.8	58.4	58.2	57.8	54.2	55.0
- 325	20.3	24.1	20.4	15.6	18.8	15.3
Apparent Density kg/m ³ (lb/in ³)	---	4887 (0.1766)	4891 (0.1767)	4889 (0.1766)	4892 (0.1767)	5000 (0.1806)
Consolidated Density kg/m ³ (lb/in ³)	8265 (0.2986)	8265 (0.2986)	8265 (0.2986)	8251 (0.2981)	8249 (0.2980)	8251 (0.2981)
γ' Solvus Temperature °C (°F)	1166 (2130)	1166 (2130)	1160 (2120)	1160 (2120)	1160 (2120)	1169 (2135)

Disposition:

- MB022 - Heat Treatment Study
- MB033, MB035 - 1st Shape Trial
- MB045 - 2nd Shape Trial
- MB047 - 3rd Shape Trial
- MB048 - Process Variable Study, Pilot Production

near net shape shaft ranges in section size from 9.5 mm (0.375 inch) to 31.8 mm (1.25 inch), and variations in properties caused by differential cooling rates could be expected. Consequently the influence of section size on cooling rate from the solution temperature was of primary interest.

The cooling rate versus section size data were generated using two 3.81 cm (1.5 inch) and two 1.27 cm (0.5 inch) thick plates 12.7 cm x 12.7 cm (5 inch x 5 inch) which were sectioned from the billet and then ground to obtain flat and parallel faces. Thermocouple holes were drilled into the midplane section of the plates, and each plate was then fitted with chromel-alumel thermocouples sheathed in stainless steel. One plate of each section size was solutioned at 1093° C (2000° F) and at 1121° C (2050° F) and the temperature recorded at 15 second intervals during the rapid air cool until the plate temperature reached 649° C (1200° F). The resultant data are presented in Figure 3-15.

The purpose of the solution treatment is to place the γ' into solution and then to cool at a sufficiently rapid rate to prevent precipitation, thereby assuring that the γ' will be available for the precipitation during the subsequent aging treatment. Reprecipitation of γ' during the cooling from the solution temperature is most likely (and rapid) at the higher temperatures so that the cooling rate from the solution temperature to 927° C (1700° F) has the most significant effect on mechanical properties. In view of this, cooling rate determinations were made by taking the slopes of the temperature versus time curves (Figure 3-15) between the the solution temperature and 927° C (1700° F). These data are plotted in Figure 3-16 showing cooling rate as a function of section size. The data show that the cooling rate increases with decreasing section size, as expected, and that there is no significant difference between the cooling rates from the two solution temperatures. The data also indicate that the cooling rate will vary from $\approx 105^\circ\text{C}$ (190° F) min to $\approx 250^\circ\text{C}$ (450° F) min depending on location in the NNS CF6 shaft.

Having identified the cooling rates obtainable with the selected solution treatments, the tensile properties corresponding to these cooling rates were determined using 48 tensile specimens machined from the heat treatment study billet. The bars were solution treated in vacuum and cooled at controlled rates, the cooling rates being measured by thermocouples implanted in a hollow specimen accompanying the test specimens. The specimens were then aged in vacuum at the desired temperatures and times. The cooling rates achieved for each solution temperature are shown in Table 3-9 together with the aging cycles applied to each solution temperature/cooling rate combination.

Eight bars were tested for each of the four solution temperature/age combinations, four at room temperature and four at 649° C (1200° F.) The remaining bars were tested at selected conditions, and served primarily as duplicate tests. The results for the 1093 and 1121° C (2000 and 2050° F) solution temperatures, together with cooling rate and age for each specimen are shown in Tables 3-10 and 3-11. Also indicated are the Inconel 718 specification UTS and YS minimums, which are the minimum properties required in the current program. Ductility properties (% Elongation and RA) are to meet the minimum properties

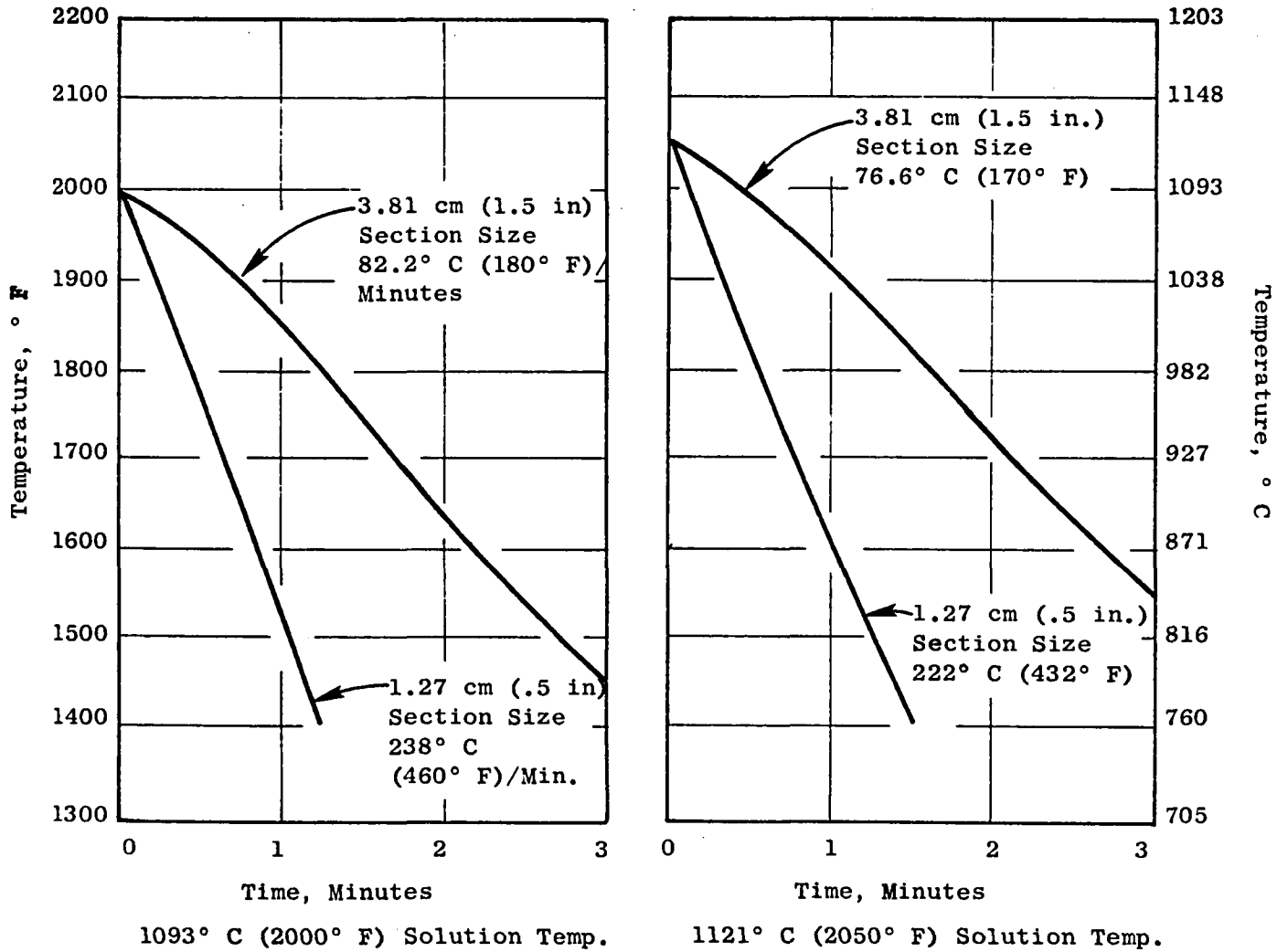


Figure 3-15. Temperature Versus Time Curves for Rapid Air Cool From 1093° C (2000° F) and 1121° C (2050° F) Solution Temperatures.

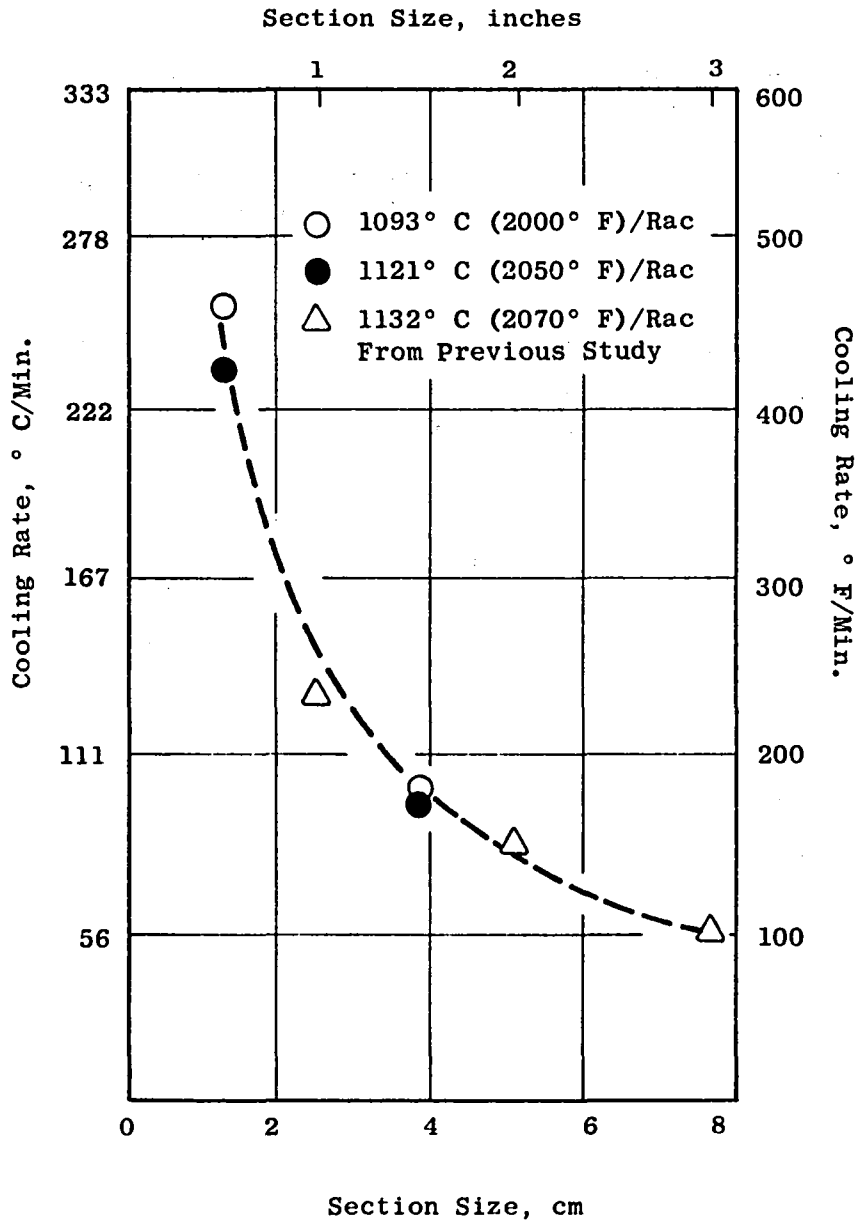


Figure 3-16. Cooling Rate Versus Section Size Curves for Rapid Air Cool From 1093° C (2000° F) and 1121° C (2050° F) Solution Temperatures.

Table 3-9. Preliminary Heat Treatment Study Tensile Property Versus Cooling Rate.

Heat Treatment Configuration - tensile specimen
 Heat Treatment Atmosphere - vacuum
 Test Conditions - RT and 649° C (1200° F) tensile
 No. of Specimens - 3 at each solution temp./cooling rate/age combination below

Solution Temperature		Cooling Rates		Aging Treatments
° C	(° F)	° C/min.	(° F/min.)	° C (° F)/hrs.
1093	(2000)	42	(75)	760(1400)/16
		94	(170)	760(1400)/16 + 649(1200)/16
		206	(370)	
		328	(590)	
1121	(2050)	53	(95)	760(1400)/16
		108	(195)	871(1600)/1 + 649(1200)/16

Table 3-10. Tensile Properties for Bars Solutioned at 1093° C (2000° F).

Spec No.	Cooling Rate (° C/min) (° F/min)	Age	Test Temp.		UTS		0.2% YS		El %	RA %
			(° C)	(° F)	MPa	(ksi)	MPa	(ksi)		
1	42.0	(75)	A	RT	1597	(231.6)	1099	(159.4)	23.4	21.8
4	42.0	(75)	B	RT	1604	(232.7)	1126	(163.4)	20.5	19.0
7	94.0	(170)	A	RT	1618	(234.6)	1155	(167.5)	20.4	20.7
9	94.0	(170)	A	RT	1616	(234.4)	*	*	19.4	20.4
10	94.0	(170)	B	RT	1620	(235.0)	1172	(170.0)	17.3	18.3
13	104.0	(370)	A	RT	1620	(235.0)	*	*	19.3	19.0
15	104.0	(370)	A	RT	1613	(233.9)	1173	(170.1)	17.4	17.8
16	104.0	(370)	B	RT	1642	(238.1)	1211	(175.7)	15.8	15.9
19	328.0	(590)	A	RT	1647	(238.9)	1198	(173.7)	22.1	19.9
22	328.0	(590)	B	RT	1590	(230.6)	1224	(177.5)	13.4	15.7
24	328.0	(590)	B	RT	1653	(239.7)	1249	(181.1)	15.3	16.0
Inconel 718 Specification Min. René 95 Specification Min.					1276	(185.0)	1034	(150.0)	---	---
						---		---	10.0	12.0
2	42.0	(75)	A	649 (1200)	1376	(199.6)	1029	(149.3)	14.4	13.1
3	42.0	(75)	A	649 (1200)	1346	(195.3)	1008	(146.2)	15.3	15.3
5	42.0	(75)	B	649 (1200)	1398	(202.8)	*	*	15.7	16.0
6	42.0	(75)	B	649 (1200)	1370	(198.8)	1034	(149.9)	15.9	14.7
8	94.0	(170)	A	649 (1200)	1413	(204.9)	1059	(153.6)	15.3	14.7
11	94.0	(170)	B	649 (1200)	1440	(208.8)	1094	(158.7)	14.8	13.8
12	94.0	(170)	B	649 (1200)	1431	(207.6)	1082	(156.9)	10.7	11.2
14	104.0	(370)	A	649 (1200)	1433	(207.9)	1094	(158.6)	12.3	13.9
17	104.0	(370)	B	649 (1200)	1444	(209.4)	1119	(162.3)	12.8	13.0
18	104.0	(370)	B	649 (1200)	1444	(209.5)	1118	(162.2)	10.6	11.6
20	328.0	(590)	A	649 (1200)	1432	(207.7)	1128	(163.6)	7.7	10.9
21	328.0	(590)	A	649 (1200)	1417	(205.5)	1085	(157.4)	9.4	8.6
23	328.0	(590)	B	649 (1200)	1462	(212.1)	1156	(167.7)	9.2	8.7
Inconel 718 Specification Min. René 95 Specification Min.					1000	(145.0)	862	(125.0)	---	---
						---		---	8.0	10.0
*Extensometer Slip					Ages					
° Premature Failure due to Inclusion					A - 760° C (1400° F)/16 hrs.					
					B - 760° C (1400° F)/16 hrs. + 649° C (1200° F)/16 hrs.					

of René 95. As can be seen in the tables, the UTS, 0.2% YS and ductilities meet these minimum requirements, except for three isolated cases (all at same solution temperature and cooling rate) where the 649° C (1200° F) ductility does not fully attain the René 95 minimum.

These data were used to construct property versus cooling rate curves for the selected heat treatments. To permit separate evaluation of the effects of (1) solution temperature, (2) age condition on material solutioned at 1093° C (2000° F), and (3) age condition on material solutioned at 1121° C (2050° F), the curves were compared and all showed the expected increase in strength and decrease in ductility with increasing cooling rate. The duplicate tests showed good reproducibility.

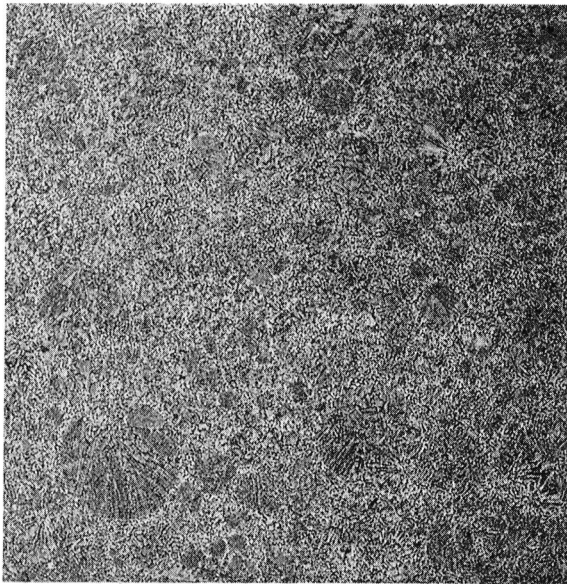
The first comparison made was of the two different solution temperatures with the same age condition 760° C (1400° F)/16 hrs. At room temperature the 1121° C (2050° F) solution temperature provided a slight increase in 0.2% YS 6.9 - 13.8 MPa (1-2 ksi) while UTS and ductility of the two solution temperatures were approximately equivalent. At 649° C (1200° F), the 1121° C (2050° F) solution temperature produced a more significant increase in both YS and UTS with approximately equivalent ductilities. The reason for the increase in properties provided by the 1121° C (2050° F) solution temperature is illustrated in Figure 3-17, which shows the microstructures obtained from the two solution temperatures (both aged at 760° C (1400° F)/16 hrs. Comparison of the microstructures at 500X shows that a greater percentage of coarse γ' remains in the material solutioned at 1093° C (2000° F). The higher solution temperature 1121° C (2050° F) tends to put more γ' into solution, thus, making a greater percentage of γ' available for precipitation during aging and thereby improving strength.

A comparison was made of the two age conditions on the material solutioned at 1093° C (2000° F). The double age 760° C (1400° F)/16 hrs + 649° C (1200° F)/16 hrs provides a significant increase in 0.2% YS at room temperature with an associated decrease in ductility. The two age conditions also yielded an approximately equivalent UTS at RT. The double age provided increased yield and tensile strengths at 649° C (1200° F) although ductilities were not degraded below that of the single 760° C (1400° F)/16 hrs age.

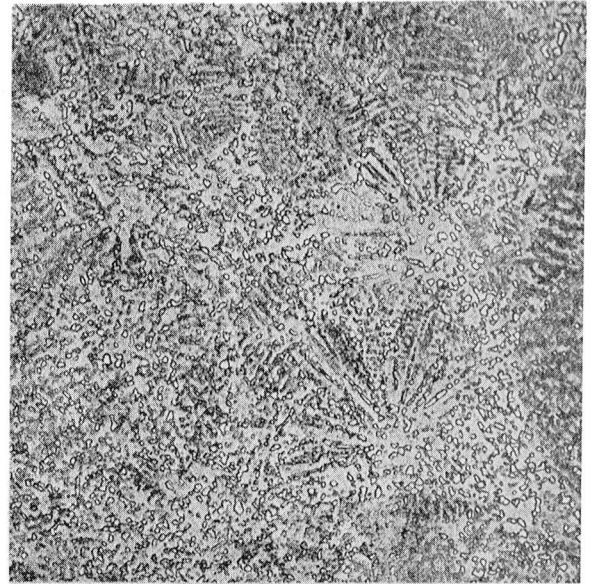
The effect of the two age conditions 760° C (1400° F)/16 hrs and 871° C (1600° F)/1 hr + 649° C (1200° F)/16 hrs on the bars solutioned at 1121° C (2050° F) indicated that there is no significant difference in tensile properties between the two age conditions.

In summary, the data indicate that:

- 1) Yield and tensile strength increase, and ductility decreases with increasing cooling rate for each of the solution temperature/age combinations tested.
- 2) The 1121° C (2050° F) solution temperature provides greater YS and UTS over the 1093° C (2000° F) solution temperature [particularly at 649° C (1200° F)] with no apparent loss of ductility.

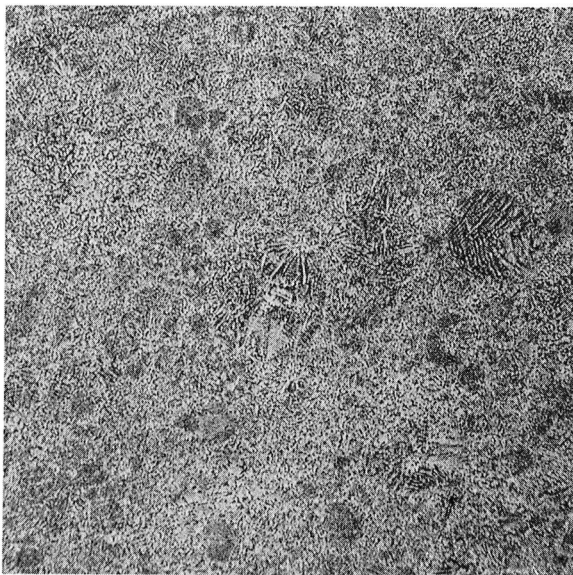


100X

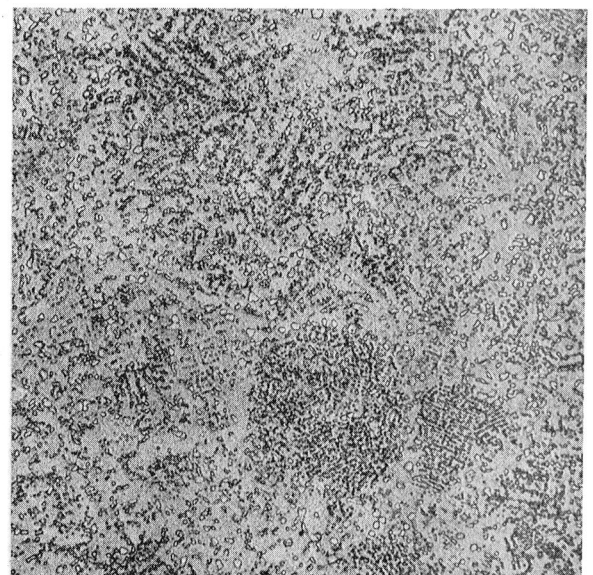


500X

(a) 1093° C (2000° F) Solution Treatment (Specimen 19).



100X



500X

(b) 1121° C (2050° F) Solution Treatment (Specimen 43).

Figure 3-17. Microstructure of As-HIP René 95 Solution Treated at 1093° C (2000° F) and 1121° C (2050° F) and Aged at 760° C (1400° F) 16 Hours (Walker's Etch).

- 3) The 871° C (1600° F)/1 hr + 649° C (1200° F)/16 hrs and the 760° C (1400° F)/16 hrs age yield approximately equivalent strengths and ductilities.
- 4) The 760° C (1400° F)/16 hrs + 649° C (1200° F)/16 hrs age offers a significant improvement in strength over the 760° C (1400° F)/16 hrs age with some loss in ductility.

The selection of the three heat treatments to be evaluated in the detailed mechanical property evaluation were made on the basis of the above results. Because the 1121° C (2050° F) solution temperature offered improved strengths over the 1093° C (2000° F) solution temperature, with no apparent loss in ductility, only the 1121° C (2050° F) solution temperature was evaluated. In conjunction with the 1121° C (2050° F) solution anneal, the following aging cycles were utilized.

- 760° C (1400° F)/16 hrs + 649° C (1200° F)/16 hrs - to produce highest tensile strengths but lowest ductilities.
- 760° C (1400° F)/16 hrs - to produce lower tensile properties than above, but with increased ductilities.
- 871° C (1600° F)/1 hr + 649° C (1200° F)/16 hrs - to produce equivalent tensile properties to the 760° C (1400° F)/16 hrs age, but has the advantage of relieving, residual quenching stresses more fully, an important consideration for minimizing distortion when machining the near-net-shape components.

3.2.1.3 Detailed Heat Treatment Evaluation

Six 3.2 cm (1.25 in.) thick plates (12.7 cm x 12.7 cm (5 in. x 5 in.)), representing the maximum section thickness of the NNS CF6-50 shaft, were sectioned from the Crucible billet for use in the detailed heat treatment evaluation. Duplicate plates were used for each heat treatment. The plates were heat treated at Indiana Metal Treating as follows:

<u>Plate No.</u>	<u>Heat Treatment</u>
1, 2	A. Solution Treatment - 1121° C (2050° F)/RAC Age - 871° C (1600° F)/1 hr/AC + 649° C (1200° F)/16 hrs/AC
3, 4	B. Solution Treatment - 1121° C (2050° F)/RAC Age - 760° C (1400° F)/16 hrs/AC + 649° C (1200° F)/16 hrs/AC
5, 6	C. Solution Treatment - 1121° C (2050° F)/RAC Age - 760° C (1400° F)/16 hrs

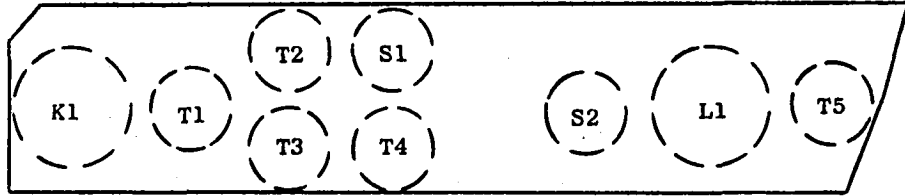
Following heat treatment, the plates were cut up for the mechanical property testing including tensile, stress rupture, creep, low cycle fatigue, sustained peak low cycle fatigue, and residual cyclic life. The cut up plan for two plates for each heat treatment is shown in Figures 3-18 and 3-19 and the test specimen configurations are illustrated in Figures 3-20 through 3-23. In general, the test conditions were selected to permit comparison of data with Inconel 718 properties. The 538° C (1000° F) notched ($K_t = 3.5$) low cycle fatigue condition was selected because it is one of the conditions of design interest for the shaft.

Optical and electron microscopy, density, and thermally induced porosity (TIP) evaluations were also conducted on the material following heat treatment. The density and TIP results (Table 3-12) show that all the material met specification requirements. The microstructures following the three different heat treatments are approximately equivalent as shown in Figures 3-24 through 3-26. The grain size is not well-defined due to the coarse γ' background, but all of the heat treatments resulted in grain sizes of ASTM 8 or finer. The electron micrographs show the coarse γ' which is not solutioned during the solution treatment, and the much finer γ' which precipitates during the rapid air cool from the solution temperature. As seen in Figures 3-24 through 3-26, the three heat treatments produced similar γ' distributions. This is as expected, since they all had the same solution temperature and cooling rate. The effect of the different age treatments on γ' distribution cannot be discerned at these magnifications.

The tensile properties are presented in Table 3-13. A total of four tensile tests were performed for each heat treatment, two at room temperature (RT) and two at 649° C (1200° F.). The RT tensile properties are approximately equivalent for all three conditions, although B may provide a slight advantage in 0.2% Y.S. All of the RT yield and tensile strengths exceed the minimum requirements by a wide margin and, with the exception of specimen T13 which failed at a non metallic inclusion, very good ductilities were achieved. The 649° C (1200° F) data suggest that heat treatment A produces a 0.2% Y.S. slightly lower than the other two heat treatments, but UTS and ductility are approximately equivalent for all three heat treatments.

The stress rupture and creep data are shown in Table 3-14. There is no significant difference between the rupture properties after each heat treatment, and each exceeded the rupture capabilities of Inconel 718 as shown in Figure 3-27. The creep data also indicate a capability in excess of that obtainable with Inconel 718 (Figure 3-28). In summary, the tensile, rupture, and creep properties of the three candidate heat treatments exceed the program goals and on the basis of these tests--there is no clear cut advantage of any one of the three heat treatments.

Table 3-15 shows the results of the low cycle fatigue (LCF), sustained peak low cycle fatigue (SPLCF), and residual cyclic life (RCL) testing conducted after the three heat treatments. The notched ($K_t = 3.5$) LCF data are shown in Figure 3-29 as compared to Inconel 718. It should be noted that there are two data points at both 241 and 276 MPa (35 and 40 ksi) for heat



Top View Plate 1

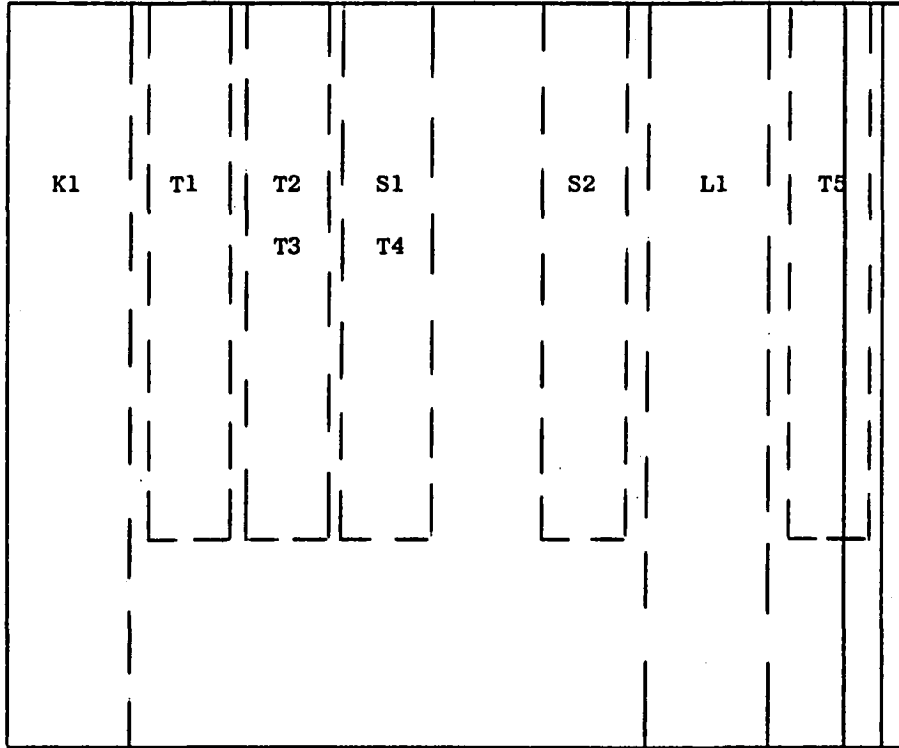
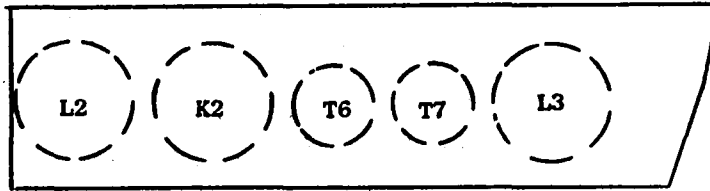


Plate 1

Specimen Blank Allocations For Plates 1,3, and 5.
Patterns are Similiar to Plate 1.

PLATE	MICRO	TENSILE	SPLCF	K_B	LCF
1	A	T1 → T5	S1 & S2	K1	L1
3	B	T8 → T12	S3 & S4	K3	L4
5	C	T15 → T19	S5 & S6	K5	L7

Figure 3-18. Cut Up Plan for Plates 1,3, and 5 of Detailed Mechanical Property Evaluation.



Top View Plate 2

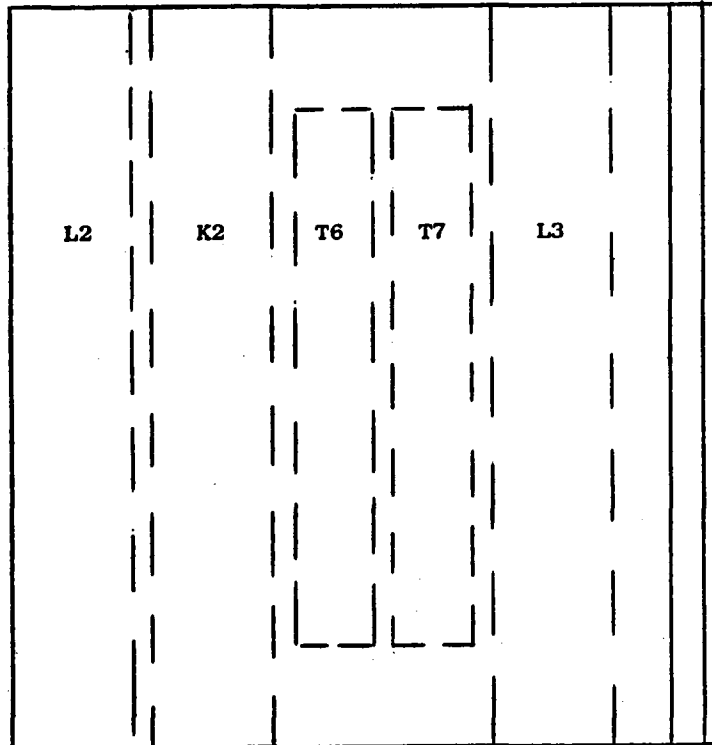


Plate 2

Specimen Blank Allocations For Plates 2,4, and 6.
Patterns are Similar to Plate 2.

PLATE	DENSITY	TENSILE	K_B	LCF
2	A	T6 & T7	K2	L2 & L3
4	B	T13 & T14	K4	L5 & L6
6	C	T20 & T21	K6	L8 & L9

Figure 3-19. Cut Up Plan for Plates 2,4 and 6 of Detailed Mechanical Property Evaluation.

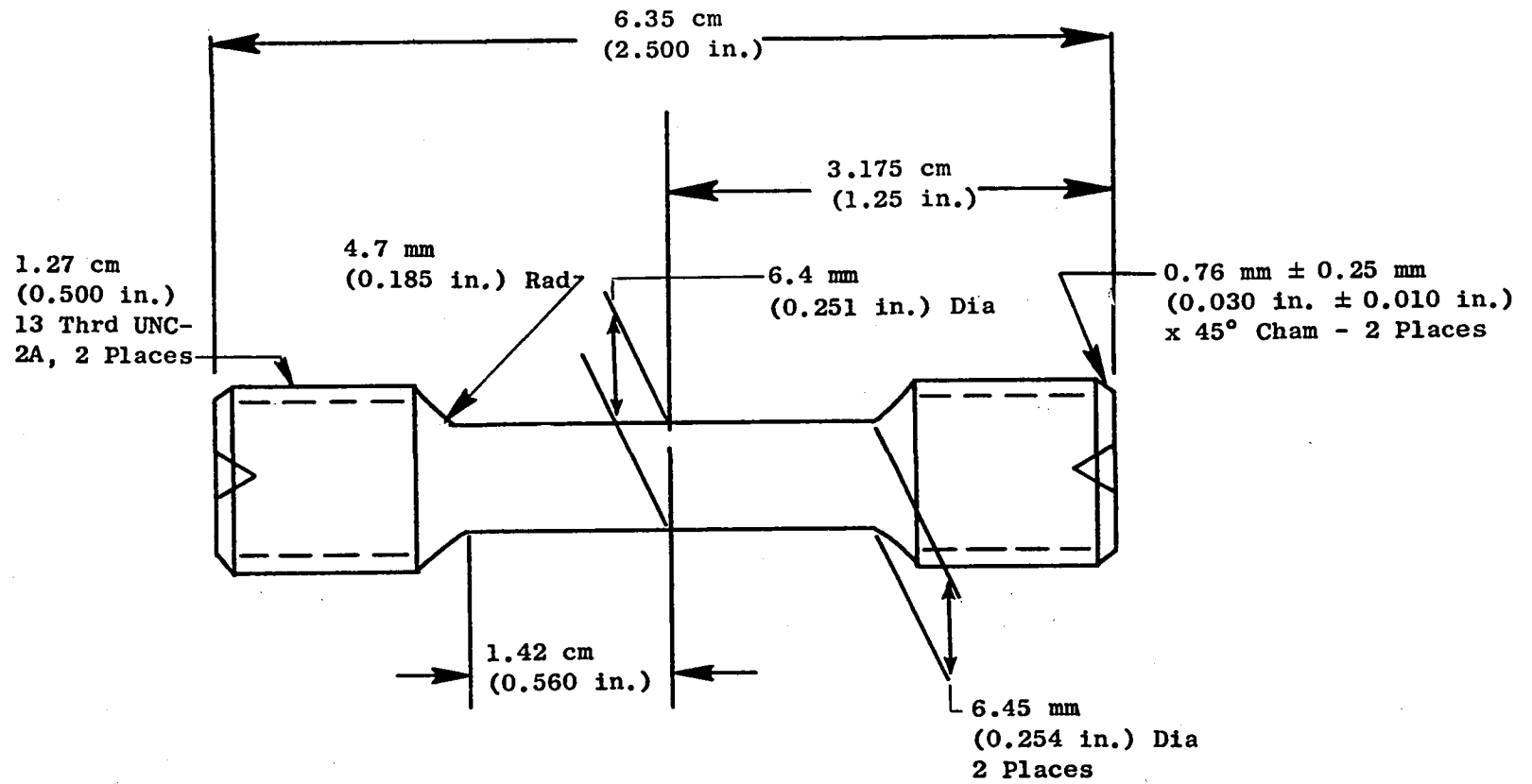
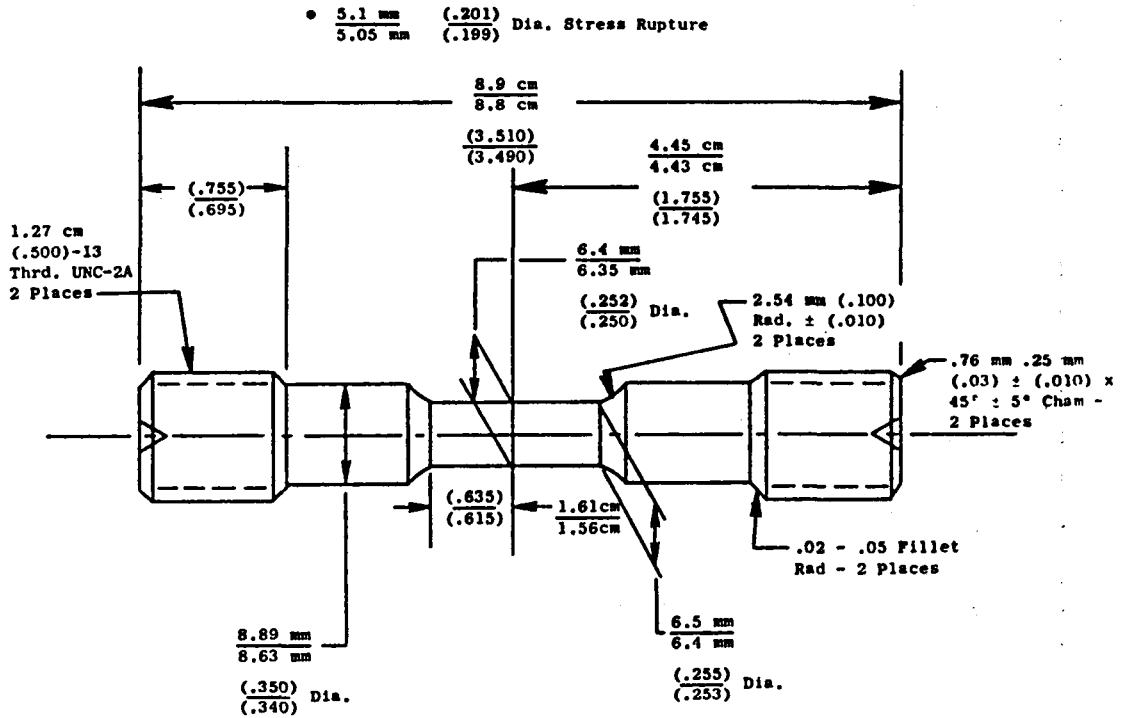
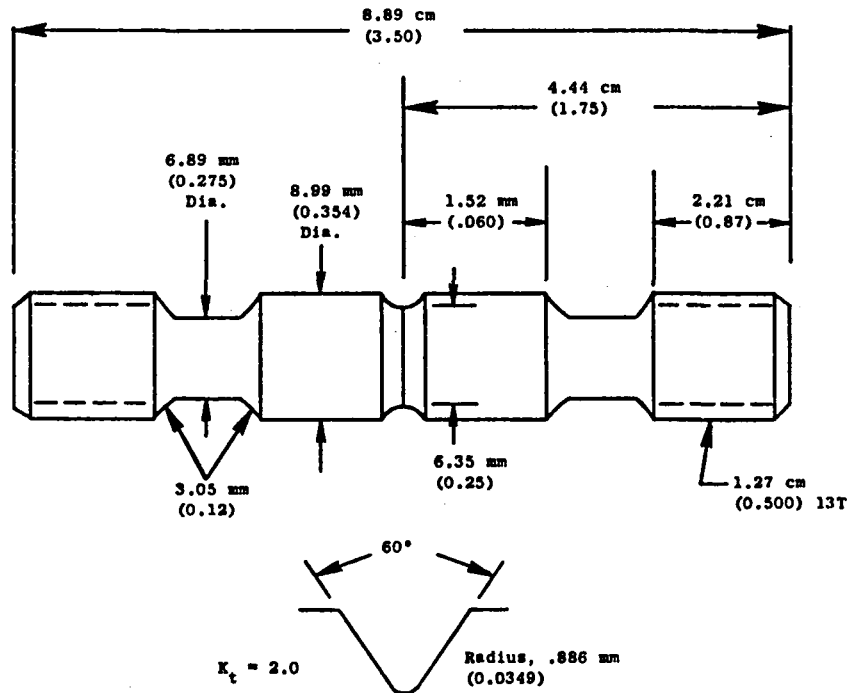


Figure 3-20. Tensile and Stress Rupture Test Specimens.



Tensile, Stress Rupture, and Creep Specimen



Double Reduced Notch Bar Cyclic Rupture (SPLCF) Test Specimen

Figure 3-21. Tensile, Stress Rupture, and Creep Specimen and Double Reduced Notch Bar Cycle Rupture Test Specimen.

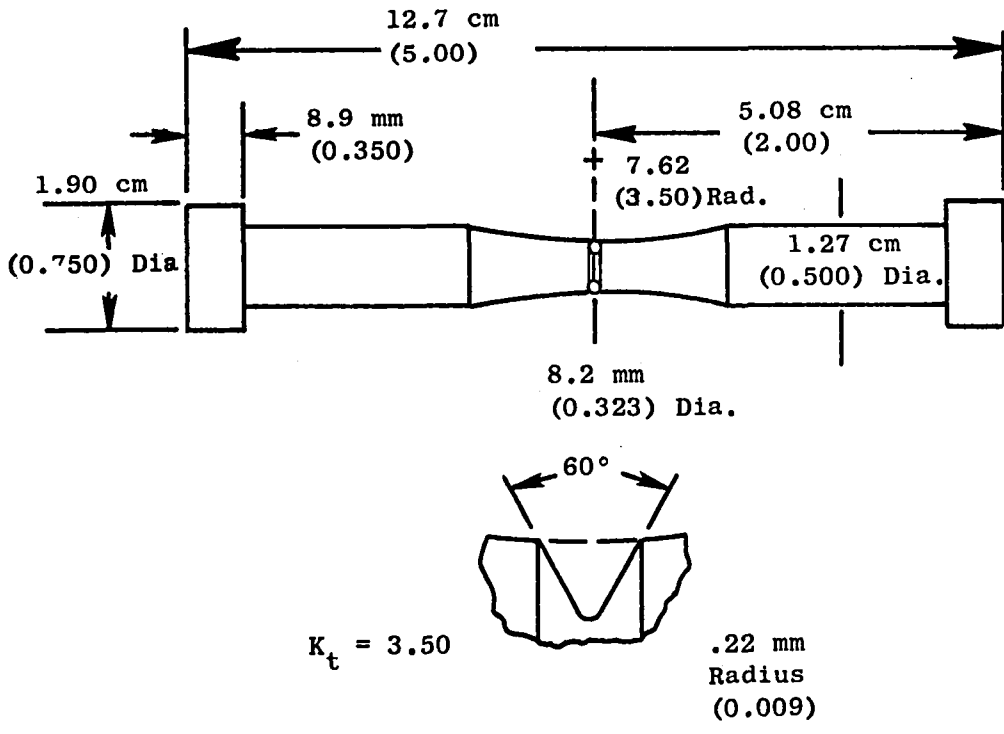


Figure 3-22. Notch Bar Low Cycle Fatigue (Load Control) Test Specimen.

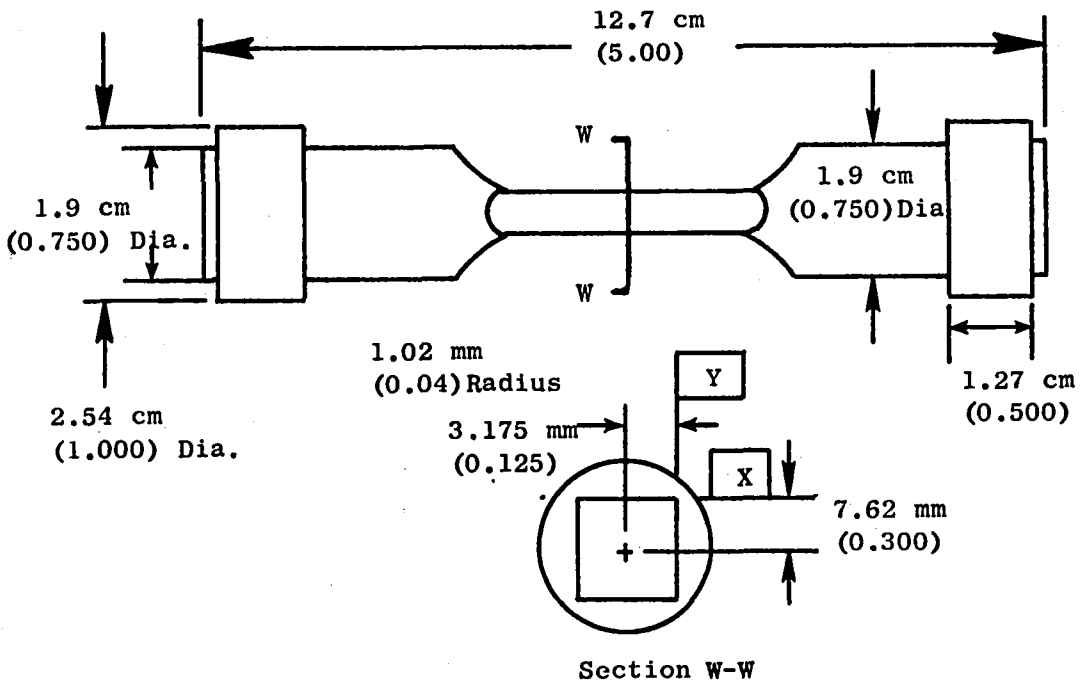
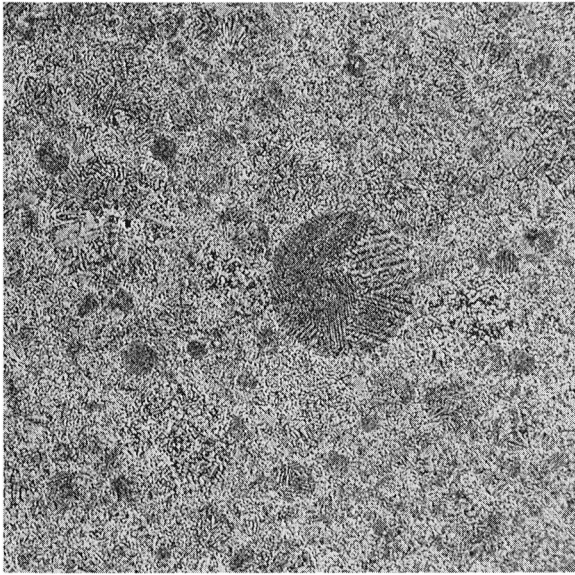


Figure 3-23. Crack Propagation (K_B) Test Specimen.

Table 3-12. Density and Tip Results From Detailed Mechanical Property Material.

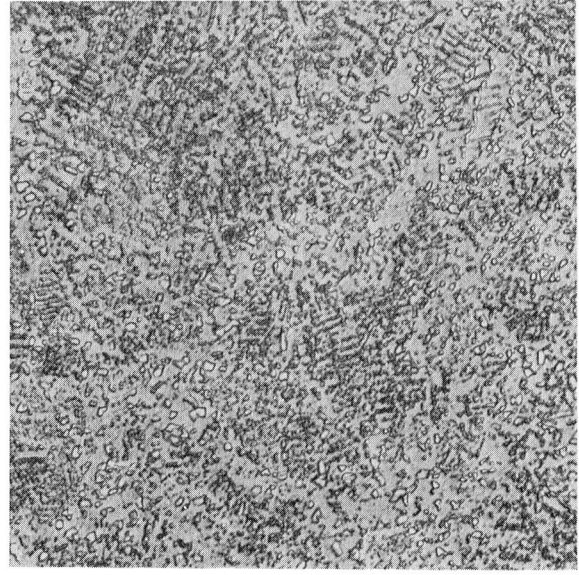
Sample	Heat Treatment	Density, kg/m ³ (lbs/in ³)			% Tip Change+
		As-HIP	Heat Treated	Tip*	
1	A	8265.2 (0.2986)	8262.4 (0.2985)	8240.3 (0.2977)	0.27
3	B	8265.2 (0.2986)	8259.7 (0.2984)	8240.3 (0.2977)	0.23
6	C	8265.2 (0.2986)	8262.4 (0.2985)	8243.1 (0.2978)	0.23

*Tip Treatment - 1204° C (2200° F)/4 hours/AC
+Specification Requirement <0.3% Change due to TIP



13443

100X



13443

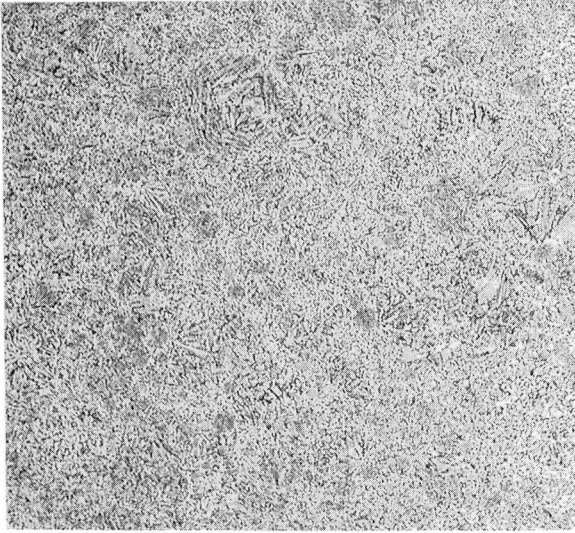
500X



13443

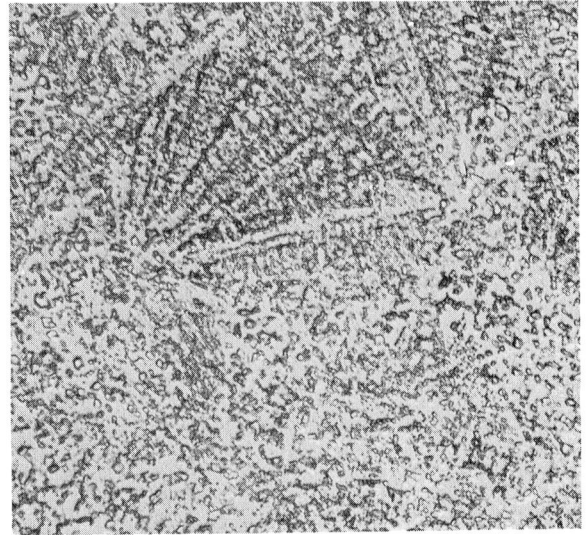
5000X

Figure 3-24. Microstructure of Material Given Heat Treatment A.



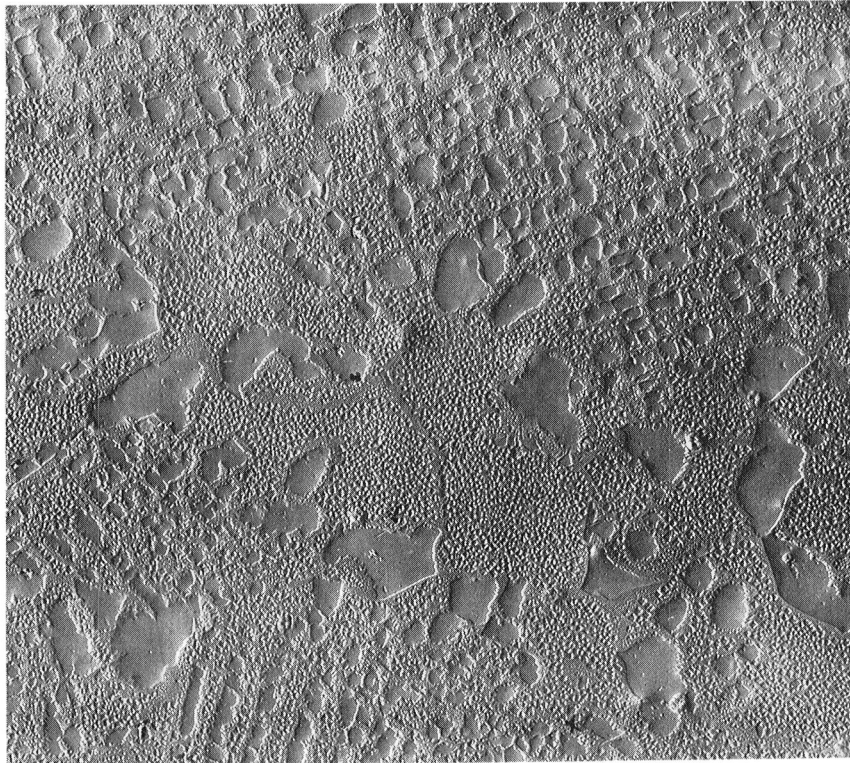
13444

100X



13444

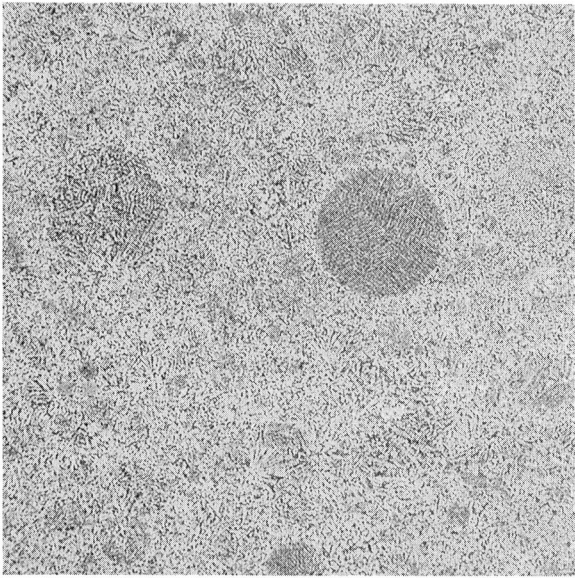
500X



13444

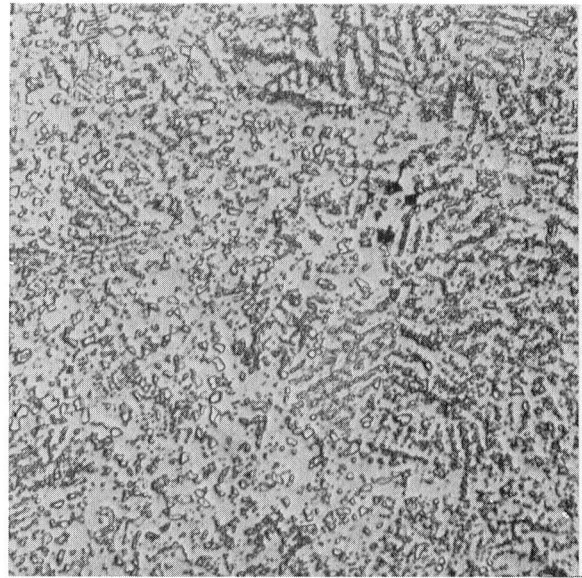
5000X

Figure 3-25. Microstructure of Material Given Heat Treatment B.



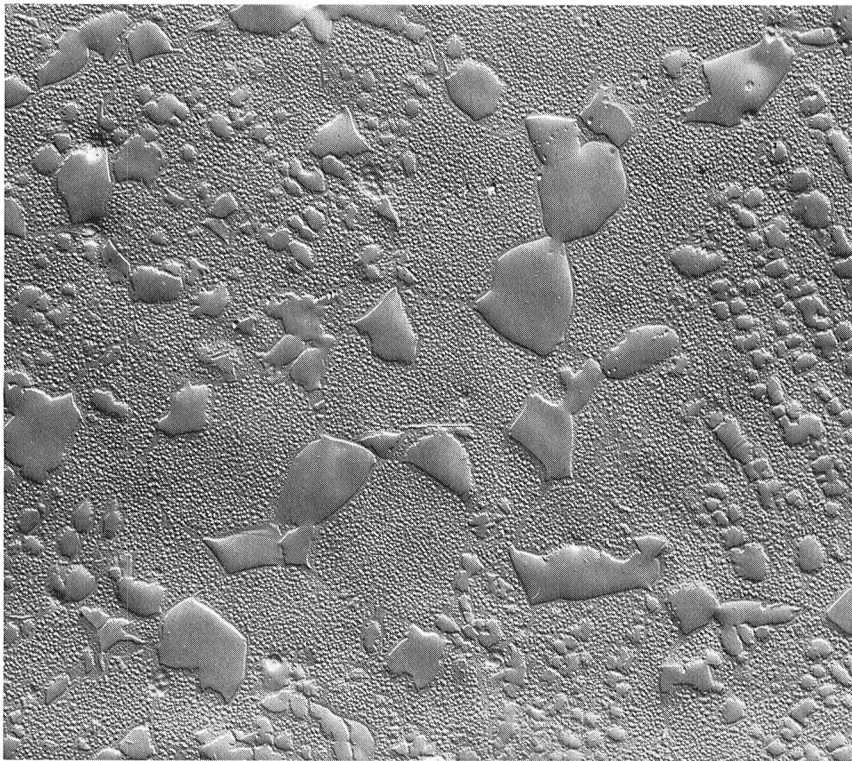
13445

100X



13445

500X



13445

5000X

Figure 3-26. Microstructure of Material Given Heat Treatment C.

Table 3-13. Detailed Evaluation Tensile Properties.

Spec. No.	Heat Treatment	Test Temp.		UTS		0.2% YS		El %	RA %
		° C	(° F)	MPa	(ksi)	MPa	(ksi)		
T1	A	RT		1604	(232.7)	1171	(169.8)	17.4	20.0
T6	A	RT		1589	(230.5)	1151	(167.0)	18.1	18.3
T8	B	RT		1613	(233.9)	1175	(170.4)	15.4	16.8
T13	B	RT		1509	(218.8)	1184	(171.7)	10.0	13.5
T15	C	RT		1629	(236.3)	1158	(168.0)	18.5	21.8
T20	C	RT		1620	(234.9)	1169	(169.5)	18.0	19.3
		Inconel 718 Spec. Min.		1276	(185.0)	1034	(150.0)	N/A	N/A
		René 95 Spec. Min.		N/A	N/A	N/A	N/A	10.0	12.0
T2	A	649	(1200)	1422	(206.3)	1051	(152.5)	15.5	16.6
T7	A	649	(1200)	1429	(207.3)	1049	(152.1)	14.2	14.2
T9	B	649	(1200)	1429	(207.3)	1084	(157.2)	13.4	16.8
T14	B	649	(1200)	1453	(210.8)	1093	(158.5)	14.7	16.9
T16	C	649	(1200)	1444	(209.5)	*	*	15.0	15.0
T19	C	649	(1200)	1449	(210.2)	1111	(161.1)	10.4	12.4
		Inconel 718 Spec. Min.		1000	(145.0)	862	(125.0)	N/A	N/A
		René 95 Spec. Min.		N/A	N/A	N/A	N/A	8.0	10.0
Heat Treatments:									
All Given 1121° C (2050° F)/RAC Solution Treatment									
Ages A - 871° C (1600° F)/1 hour/AC + 649° C (1200° F)/16 hours/AC									
B - 760° C (1400° F)/16 hours/AC + 649° C (1200° F)/16 hours/AC									
C - 760° C (1400° F)/16 hours									
*Indicates Extensiometer Slip, Missed Yield Point									
N/A = Not Applicable									

Table 3-14. Stress Rupture and Creep Properties for Detailed Heat Treatment Evaluation.

649° C/965 MPa (1200° F/140 ksi) Stress Rupture

<u>Spec. No.</u>	<u>Heat Treatment</u>	<u>Life (hrs)</u>	<u>EL %</u>	<u>RA %</u>
T5	A	248.7	3.1	3.9
T10	B	252.9	3.2	5.5
T17	C	399.3	2.5	4.0

593° C/965 MPa (1100° F/140 ksi) Creep

<u>Spec. No.</u>	<u>Heat Treatment</u>	<u>Time to 0.1% Creep (hrs.)</u>
T4	A	278
T11	B	62
T18	C	287

- 871° C (1600° F)- 1 hr. -AC + 649° C (1200° F)-16 hrs.-AC-A
- ▲ 760° C (1400° F)-16 hrs.-AC + 649° C (1200° F)-16 hrs.-AC-B
- 760° C (1400° F)-16 hrs.-AC -C
- IN 718 Average

649° C/965.3 MPa (1200° F/140 ksi) Stress Rupture

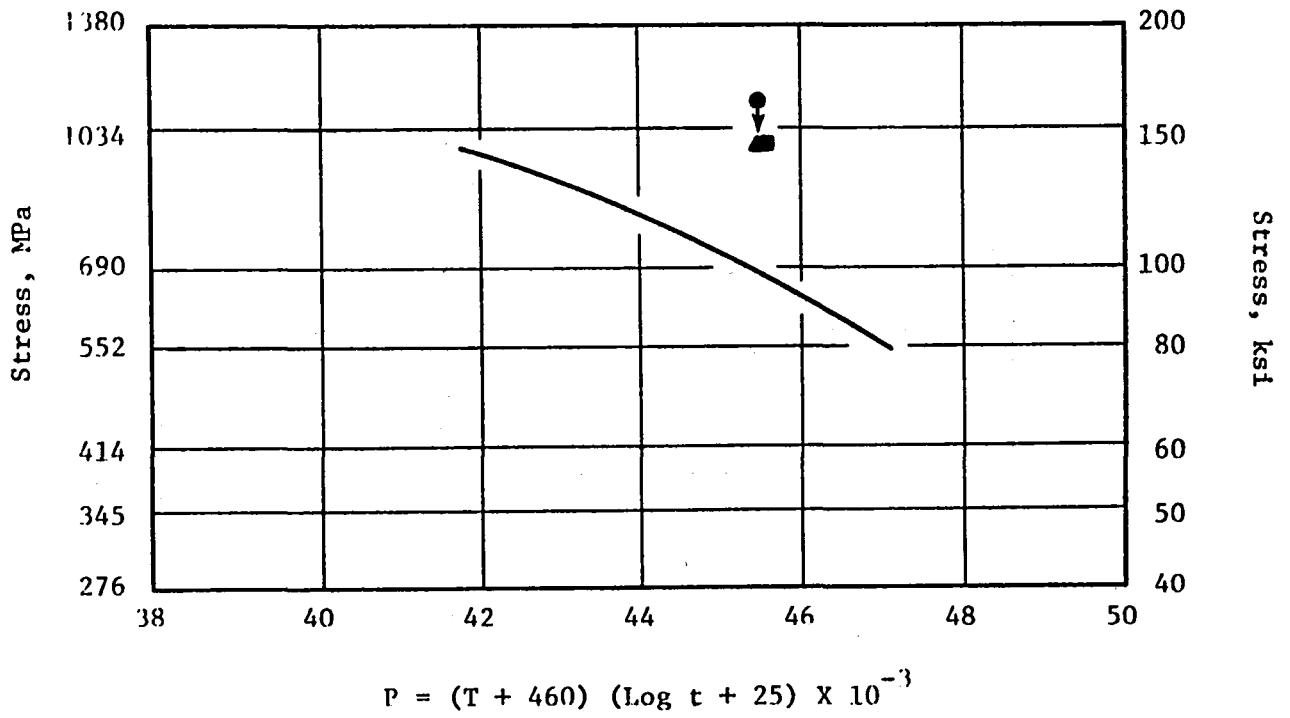


Figure 3-27. Stress Rupture Data for Detailed Evaluation Heat Treatments Compared to IN718 Average Properties.

- 871° C (1600° F)- 1 hr. -AC + 649° C (1200° F)-16 hrs.-AC-A
- ▲ 760° C (1400° F)-16 hrs.-AC + 649° C (1200° F)-16 hrs.-AC-B
- 760° C (1400° F)-16 hrs.-AC -C
- IN 718 Average

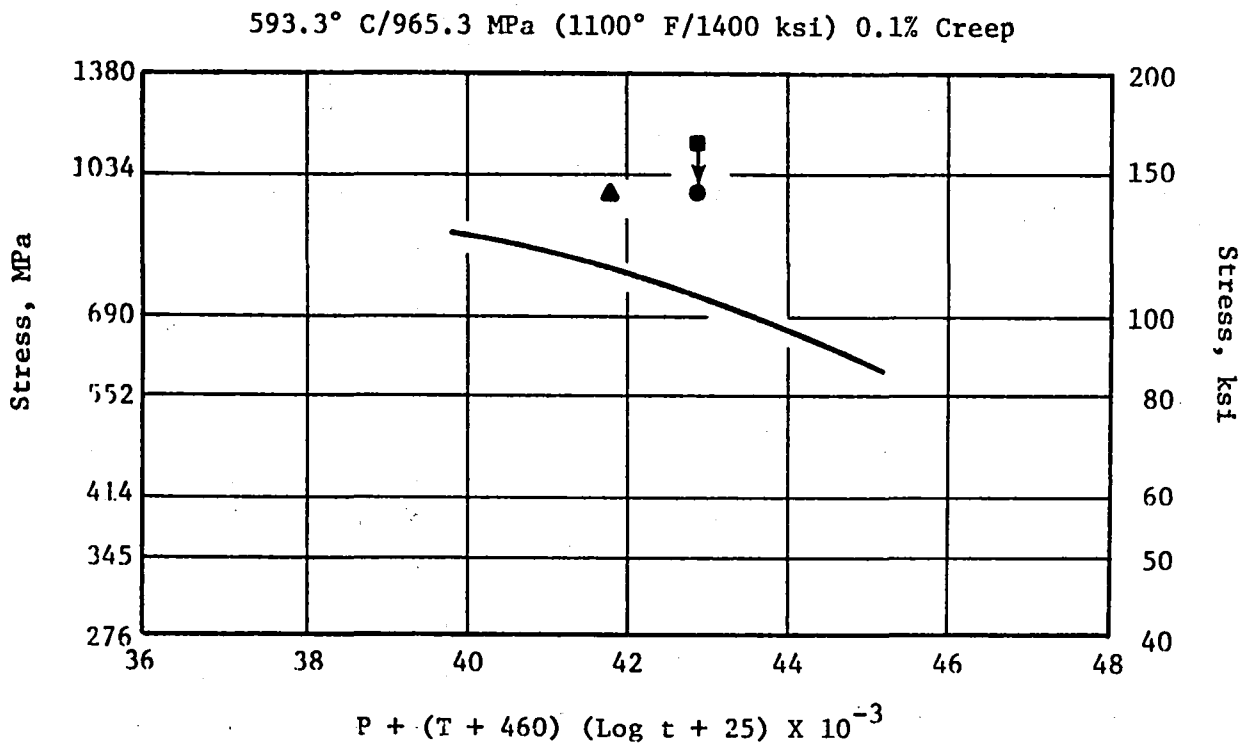


Figure 3-28. 0.1% Creep for Detailed Evaluation Heat Treatments Compared to IN718 Average Properties.

Table 3-15. Low Cycle Fatigue, Sustained Peak Low Cycle Fatigue and Residual Cyclic Life Data for Detailed Heat Treatment Evaluation.

538° C (1000° F) Notched Low Cycle Fatigue, $K_t = 3.5$; $R = 0.03$ ($A = 0.95$)						
	Spec. No.	Heat Treatment*	Alt. Stress		N_f (Cycles)	In 718 (Ave)
			MPa	(ksi)		
	L1	A	241	(35.0)	177,617 ⁺	20,000
	L1C	A	276	(40.1)	13,438	10,000
	L2	A	276	(40.1)	10,198	10,200
	L3	A	241	(35.0)	13,011	20,000
	L10	A	207	(30.0)	137,000 ⁺	40,000
	L4	B	207	(30.0)	80,154 ⁺	40,000
	L5	B	276	(40.1)	5,463	10,000
	L6	B	242	(35.1)	51,543	20,000
	L7	C	207	(30.0)	88,890 ⁺	40,000
	L8	C	276	(40.1)	5,923	10,000
	L9	C	242	(35.1)	25,664	20,000
593.3° C (1100° F) Sustained Peak Low Cycle Fatigue, $K_t = 2.0$; $R = 0.03$ ($A = 0.95$), 10-90-10 Seconds						
	S1	A	504	(73.5)	1100	700
	S2	A	470	(68.2)	1918	1000
	S3	B	504	(73.0)	858	700
	S4	B	470	(68.2)	1509	1000
	S5	C	504	(73.0)	754	700
	S6	C	470	(68.2)	1008	1000
538° C (1000° F) Residual Cyclic Life, 0.51 x 1.52 mm (0.02 x 0.06) crack; $R = 0.03$ ($A = 0.95$)						
			Max. Stress			
			MPa	(ksi)		
	K1	A	707	(102.6)	5718	6000
	K2	A	690	(100.0)	4508	6000
	K3	B	707	(102.6)	5498	6000
	K4	B	707	(102.6)	4745	6000
	K5	C	Invalid Test Due to Malfunction			
	K6	C	707	(102.6)	4510	6000
*For Heat Treatment see Table 3-13						
+Indicates Test Stopped at Indicated Cycles						

treatment A. The first test of material given heat treatment A at 241 MPa (35 ksi) (L3) failed low and SEM analysis revealed that failure initiated at small nonmetallic inclusions. Because of this, bar L1 was also tested at 241 MPa (35 ksi) to repeat the first low point test condition and it did not fail after 177,000 cycles. This bar was then loaded to 276 MPa (40 ksi) alternating stress (and identified as LIC), and it failed after 13,438 cycles. In general, the data from all three of the heat treatments indicate that at 276 MPa (40 ksi) alternating stress, the René 95 is approximately equivalent or slightly below Inconel 718, while at lower stress levels the René 95 is well above IN 718 average properties. In comparing the heat treatments against one another, it appears that heat treatment A provides some advantages, producing longer life at both 241 and 276 MPa (35 and 40 ksi) alternating stress.

The SPLCF data are plotted in Figure 3-30 in comparison to the typical Inconel 718 curve. All three heat treatments meet or exceed the Inconel 718 values and the trend in the data suggests that heat treatment A provides improved SPLCF as compared to the other two heat treatments.

The residual cyclic life (K_B) data indicate that all of the heat treatments result in approximately equal values and all are close to Inconel 718 properties.

The evaluation of the candidate heat treatments led to the following conclusions:

- Tensile, stress rupture and creep properties for all three heat treatments are approximately equivalent and exceed program goals.
- Notched low cycle fatigue and SPLCF data indicate that heat treatment A provides improved life.
- Residual cyclic life data for all three heat treatments are approximately equivalent.

Based on these conclusions, heat treatment A 1121° C (2050° F)/RAC + 871° C (1600° F)/1 hr/AC + 649° C (1200° F)/16 hrs/AC) resulted in the best combination of properties and was selected as the heat treatment cycle for the as-HIP René 95 CF6-50 shaft.

Subsequent to the selection of the 1121° C (2050° F)/RAC (air furnace/fan cool) solution treatment, General Electric identified a salt solution/salt quench heat treatment which offered the advantage of improved temperature control and greater production capability as compared to the air furnace/fan cool method. To determine the proper salt-to-salt heat treatment cycle, cooling rate studies were conducted to determine the salt quench temperature required to provide cooling rates, and thus properties, similar to the approved RAC.

Salt-to-salt cooling rate versus section size data were generated utilizing the same 1.3 and 3.8 cm (0.5 and 1.5 inch) thick plates which were used to determine the RAC cooling rate curves. The thermocoupled plates were

- 871° C (1600° F)- 1 hr. -AC + 649° C (1200° F)-16 hrs.-AC-A
- ▲ 760° C (1400° F)-16 hrs.-AC + 649° C (1200° F)-16 hrs.-AC-B
- 760° C (1400° F)-16 hrs.-AC -C
- IN 718 Average

593° C (1100° F) SPLCF $K_t = 2.0$ (A = 0.95) 10-90-10 seconds

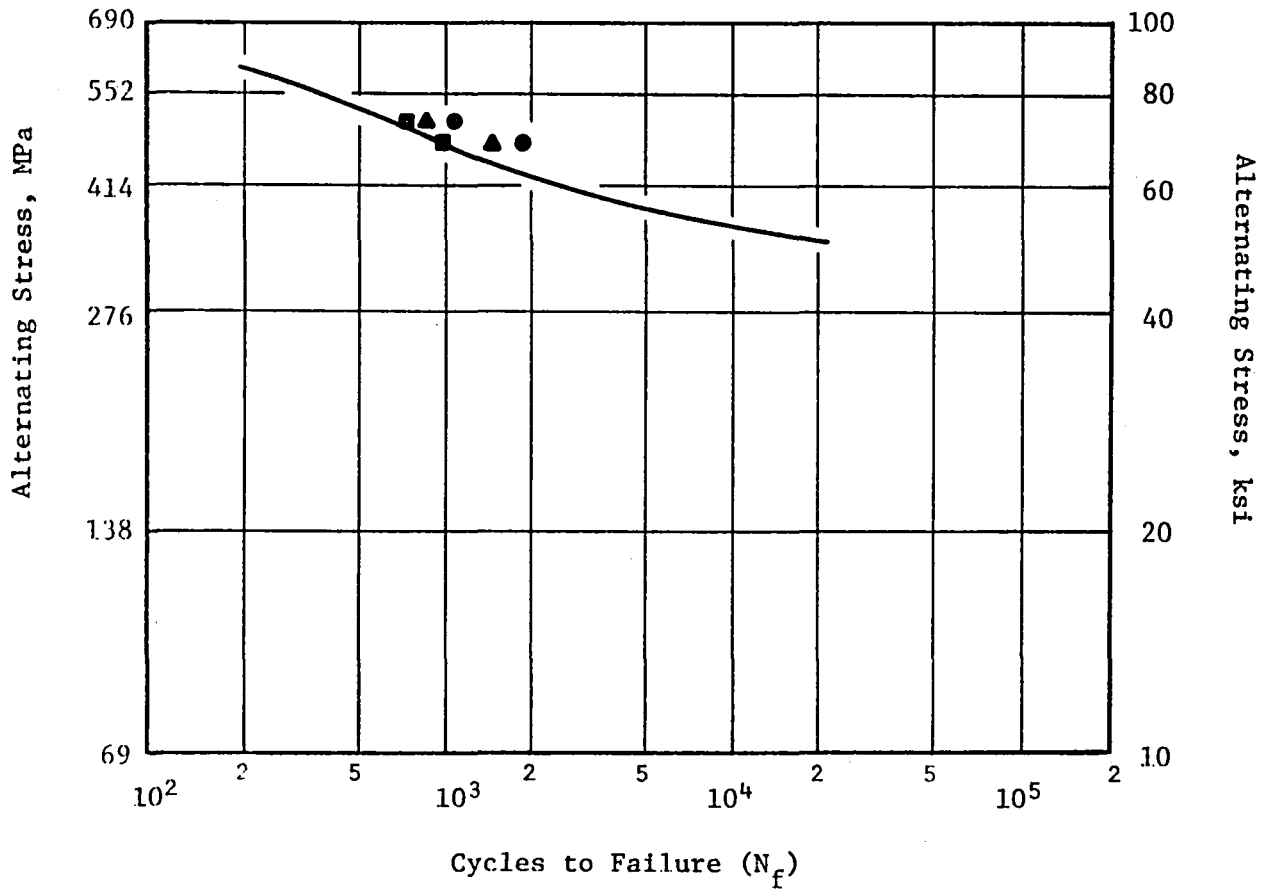


Figure 3-30. Sustained Peak Low Cycle Fatigue Data for Detailed Evaluation Heat Treatments Compared TO IN 718 Properties.

solution treated in 1121° C (2050° F) salt and then transferred to one of the three 704°, 760°, or 816° C (1300°, 1400°, or 1500° F) salt quench baths. The resulting cooling rates, as a function of section size, are shown in Figure 3-31 together with comparative RAC cooling rate data. This figure indicates that the 816° C (1500° F) salt quench produces cooling rates approximately equivalent to the RAC treatment.

In order to further verify that the 816° C (1500° F) SQ is acceptable, a 3.7 cm (1.25 inch) thick disk from the process variable study (B462) was given the 1121° C (2050° F) SQ + double age heat treatment and sectioned for tensile testing. The tensile results are shown in Table 3-16 together with predicted properties and with properties obtained with the 1121° C (2050° F)/RAC. As shown in this table, the 816° C (1500° F) salt quench results in mechanical properties approximately equivalent to the RAC. Based on this result and the cooling rate data, the salt-to-salt 1121° C/816° C (2050° F/1500° F) SQ treatment was adopted for the remainder of the program.

3.2.1.4 Process Variable Studies

The objective of the process variable study was to determine the effect of deviations from normal processing on the mechanical properties of as-HIP René 95. Two types of process variables were evaluated: (1) powder cleanliness including oxide inclusions, foreign alloy contaminants, and argon entrapment and (2) process deviations including particle size distribution, HIP temperature, and solution temperature. A listing of the billets 15.2 cm (~ 6 inch diameter) produced and the associated process variables is shown in Table 3-17. All of these compacts were made from blend MB048 and were hot isostatically pressed in a single cycle at 1121° C (2050° F) and 103 MPa (15 KSI) with the exception of B464 and B465, which were compacted at 1093° C/103 MPa (2000° F/15 ksi and 1149° C/103 MPa (2100° F/15 KSI) respectively.

Following compaction, each billet was sectioned into 3.18 cm (1.25 inch) thick disks to simulate the thickest section of the CF6-50 HPTR aft shaft. All of the disks were heat treated (at Sun Steel) using a salt bath solution treatment followed by a salt bath quench according to the conditions shown in Table 3-17. The evaluation performed on material from each billet indicated acceptable microstructures and, with the exception of billets B466 and A106 which were intended to have high TIP, each of the billets met density and TIP requirements as shown in Table 3-18.

Following heat treatment, the disks were cut up for mechanical property testing. The specimen configurations used were the same as those used in the heat treatment study with the addition of the smooth low cycle fatigue specimen shown in Figure 3-32. A typical cut up plan is shown in Figure 3-33.

The B462 billet was produced to nominal processing parameters [-60 mesh powder, 1121° C (2050° F) HIP, and 1121° C (2050° F) solution temperature] and was the baseline condition against which each of the process variables were compared.

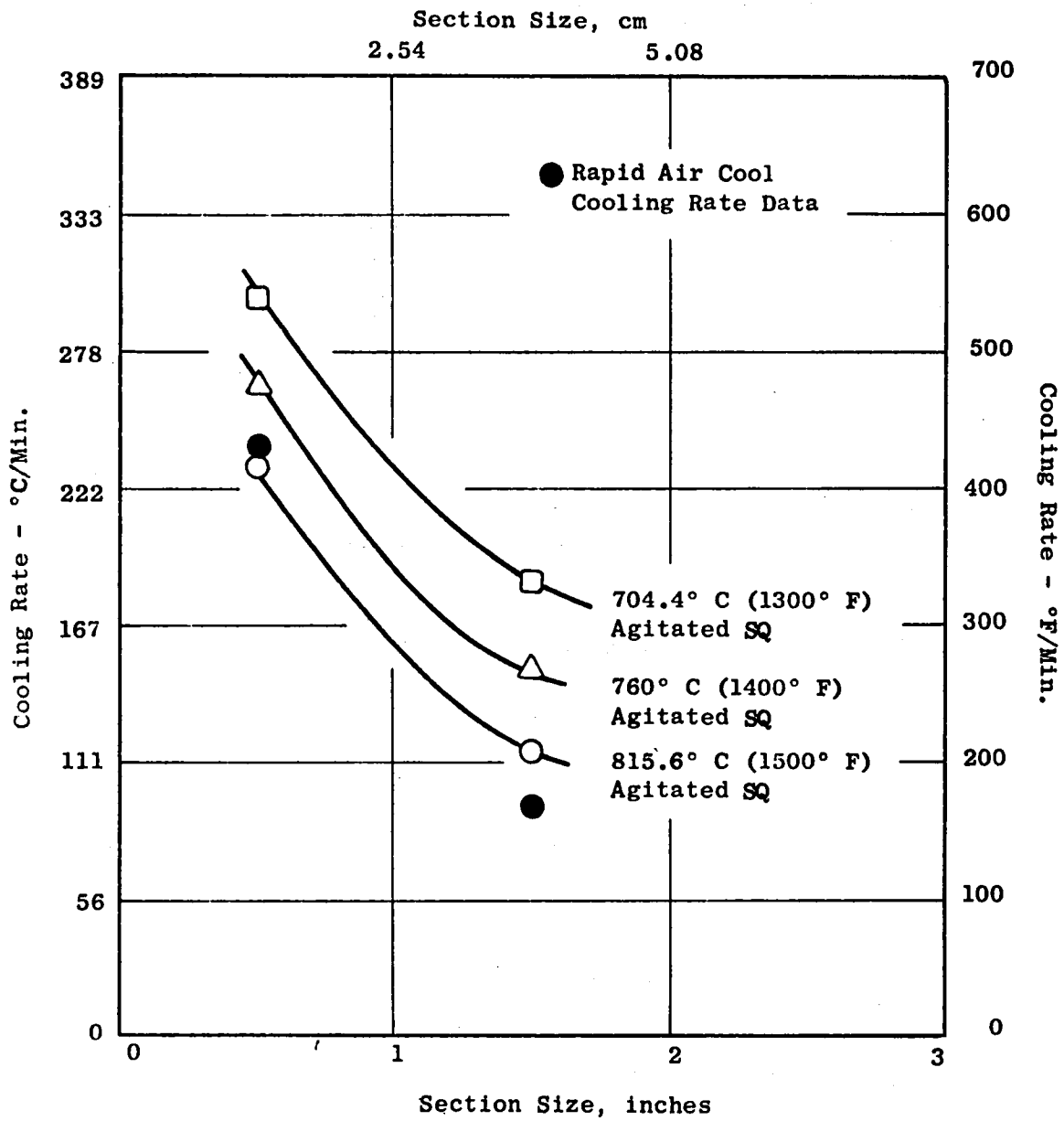


Figure 3-31. Cooling Rate Versus Section Size Curve for 704, 760, and 816° C (1300, 1400, and 1500° F) Salt Bath Quenches from 1121° C (2050° F) Salt Solution Treatment.

Table 3-16. Tensile Properties for 816° C (1500° F) SQ VS RAC.

Spec No.	Heat Treatment*	Test Temp.		UTS		0.2% YS		El %	RA %
		° C	(° F)	MPa	(ksi)	MPa	(ksi)		
M1	1121° C/816° C (2050° F)(1500° F) SQ		RT	1618	(234.6)	1198	(173.7)	17.9	16.6
M4	(2050° F)(1500° F) SQ		RT	1618	(234.6)	1174	(170.3)	17.7	17.1
---	Predicted (+)		RT	1634	(237.0)	1186	(172.0)	19.0	18.5
---	1121° C(2050° F)/ RAC Typical		RT	1604	(232.7)	1171	(169.8)	17.4	20.0
M2	1121° C(2050° F)/ 816° C(1500° F) SQ	649	(1200)	1411	(204.6)	1089	(157.9)	14.5	14.8
M5	1121° C(2050° F)/ 816° C(1500° F) SQ	649	(1200)	1455	(211.0)	1082	(156.9)	15.5	17.1
---	Predicted	649	(1200)	1434	(208.0)	1089	(158.0)	14.0	14.5
---	1121° C(2050° F)/ RAC Typical	649	(1200)	1422	(206.3)	1051	(152.5)	15.5	16.6

*All Material Given 871° C (1600° F)/1 hr + 649° C (1200° F)/16 hr Double Age.

+Properties Predicted for 115.5° C (240° F)/Min Cooling Rate From Property Versus Cooling Rate Curves.

Table 3-17. Process Variables.

Compact Code	Powder ^a Mesh Size	HIP Temperature		Solution Treatment Temperature ^b		Added Defects
		C	F	C	F	
B468	-60 +150	1121	2050	1121	2050	None
B487 ^c	-150	1121	2050	1121	2050	None
B464	-60	1093	2000	1121	2050	None
B465	-60	1149	2100	1121	2050	None
B463	-60	1121	2050	1093	2000	None
B463	-60	1121	2050	1149	2100	None
A106	-60	1121	2050	1121	2050	Argon, 1.4% TIP
B466	-60	1121	2050	1121	2050	Argon, .4% TIP
B470	-60	1121	2050	1121	2050	SiO ₂ + Al ₂ O ₃ .152 to .254 mm (.006 to .010 in.)
B471	-60	1121	2050	1121	2050	SiO ₂ + Al ₂ O ₃ .508 to .838 mm (.020 to .033 in.)
B472	-60	1121	2050	1121	2050	SiO ₂ + Al ₂ O ₃ .838 to 1.19 mm (.033 to .047 in.)
B473	-60	1121	2050	1121	2050	SiO ₂ + Al ₂ O ₃ 1.19 to 1.65 mm (.047 to .065 in.)
B474	-60	1121	2050	1121	2050	LC Astroloy; 0.1 vol. %
B475	-60	1121	2050	1121	2050	M2 Tool Steel, 0.1 vol. %
B462	-60	1121	2050	1121	2050	None

^aMB048

^bSolution treated at the indicated temperature/1 hr/816 C (1500 F) salt quench + 871 C (1600 F)/1 hr/AC + 649 C (1200 F)/6 hr/AC.

^cB487 replaced B469 which leaked during processing.

Table 3-18. Density and Tip Response for René 95 Compacts.

Compact Code	Density	Tip ^a
	kg/m ³ (lb/in. ³)	%
B462	8247 (0.2979)	0.19
B463	8248 (0.2980)	0.20
B464	8250 (0.2980)	0.24
B465	8249 (0.2980)	0.19
B466	8249 (0.2980)	0.39
A106	8249 (0.2980)	1.4
B468	8249 (0.2980)	0.26
B469	8247 (0.2979)	0.17
B470	8250 (0.2980)	0.20
B471	8248 (0.2980)	0.19
B472	8246 (0.2979)	0.19
B473	8246 (0.2979)	0.20
B474	8248 (0.2980)	0.21
B475	8247 (0.2979)	0.19
Double HIP Standard MB048	8251 (0.2981)	---

^aDensity Change Resulting From a 1204 °C (2200 °F) 4-hour Exposure.

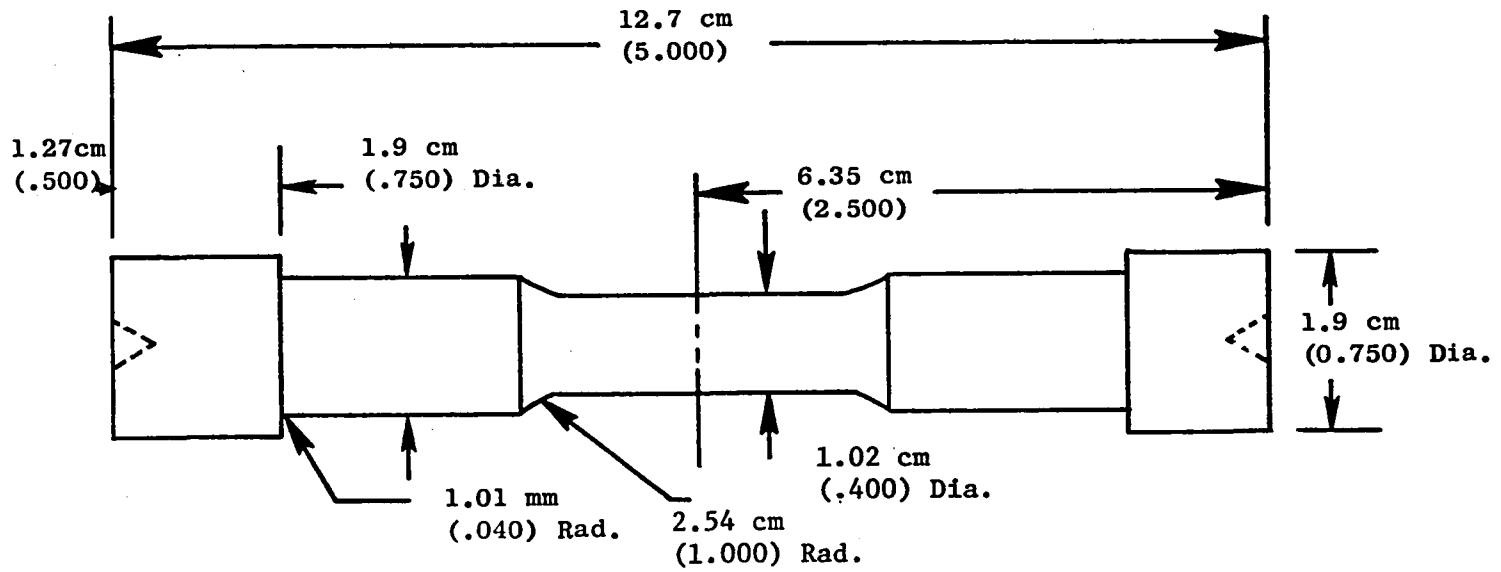


Figure 3-32. Smooth Bar Low Cycle Fatigue (Strain Control) Test Specimen.

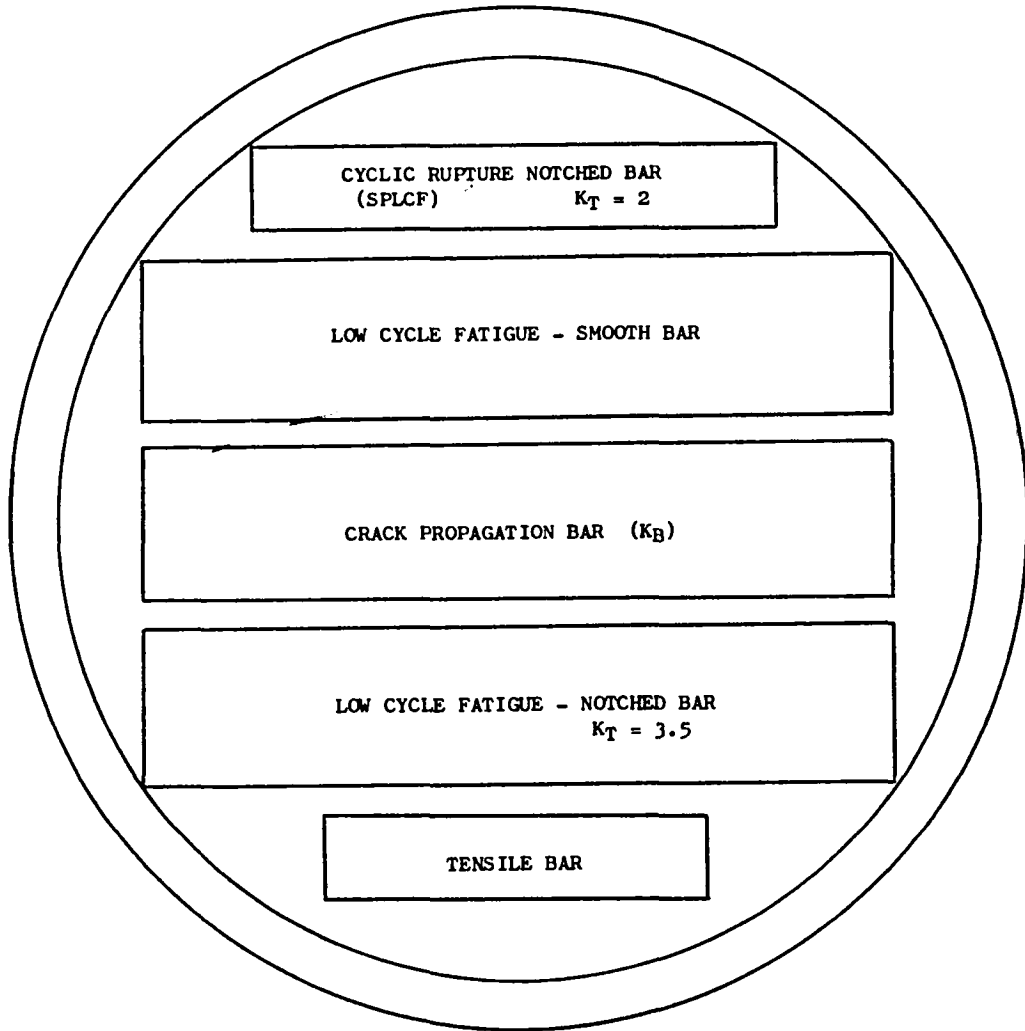


Figure 3-33. Typical Blank Cut-Up for Test Specimens.

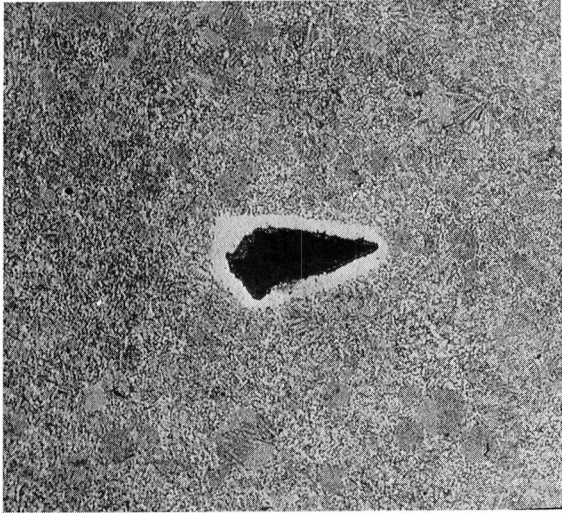
Powder Cleanliness

The objective of the powder cleanliness portion of the process variable study was to determine the influence of material defects on as-HIP René 95 mechanical properties. Three types of material defects (oxide inclusions, foreign alloy contaminants, and argon entrapment) were evaluated with the test material prepared as follows:

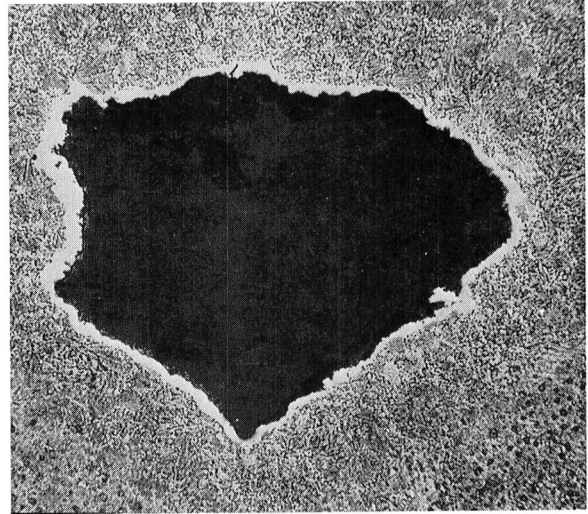
- Oxide inclusions - four billets, one for each inclusion size, 0.15 - 0.25, 0.51 - 0.84, 0.84 - 1.19, and 1.19 - 1.7 mm (0.006-0.10 inch, 0.020-0.033 inch, 0.033-0.047 inch, and 0.047-0.067 inch), were prepared by intentionally seeding the powder with oxides (SiO_2 and Al_2O_3) and processing with the nominal particle size distribution, HIP cycle, and heat treatment conditions. The oxides were screened to the proper size ranges and blended into the René 95 powder using approximately 70 oxide particles per pound of powder. Examples of the oxide inclusions as they appear in the René 95 structure are shown in Figure 3-34.
- Foreign alloy contaminants - two billets, one for each foreign alloy particle [Low Carbon (LC) Astroloy and M2 tool steel], were prepared by blending 0.1 volume percent of -60 mesh foreign alloy powder with standard -60 mesh René 95 powder and processed utilizing standard HIP cycle and heat treatment conditions. Examples of the foreign alloy contaminants as they appear in the as-HIP René 95 structure are shown in Figure 3-35.
- Argon entrapment - two billets having argon levels greater than the specification limit (0.3% TIP) were prepared utilizing standard particle size distribution, HIP cycle, and heat treatment conditions. One billet (B466) having 0.4% TIP was prepared by backfilling with argon and the second billet (A106) having 1.4% TIP leaked during the autoclave cycle.

The identification of the disks cut from the billets and the type, number, and specimen codes of the test performed are outlined in Table 3-19. It should be noted that posttest analysis consisted of visual examination (10-30X) of each fracture surface and, if required to further characterize the failure, analysis of the fracture surface on the scanning electron microscope (SEM). The tables summarizing the data contain failure initiation site information obtained from visual/SEM analysis with the initiation sites characterized as follows:

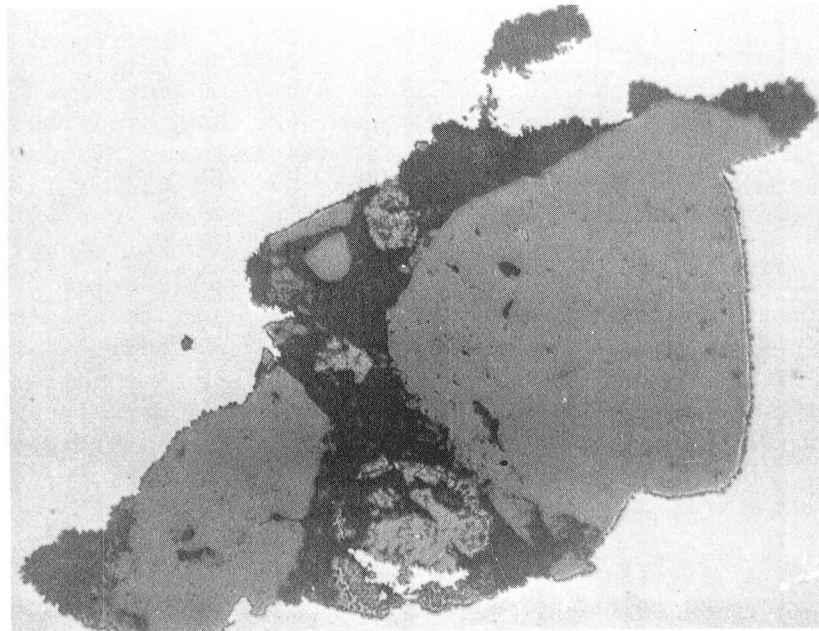
- Location is categorized as being (1) surface (SURF) indicating that initiation occurred at a site which intersects the specimen surface or (2) subsurface (SUB) indicating initiation at a site away from the specimen surface.
- Type indicates the nature of the initiation site such as pore, oxide inclusion, etc.



11320 0.015-0.025 cm 100X
(0.006-0.010 in.) Oxides

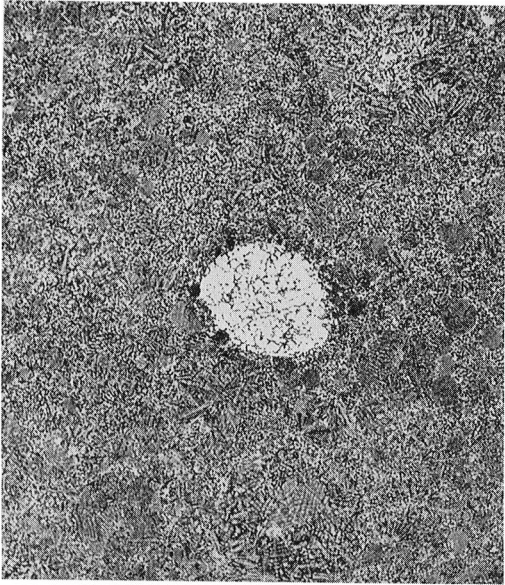


11316 0.05-0.08 cm 100X
(0.020-0.033 in.) Oxides

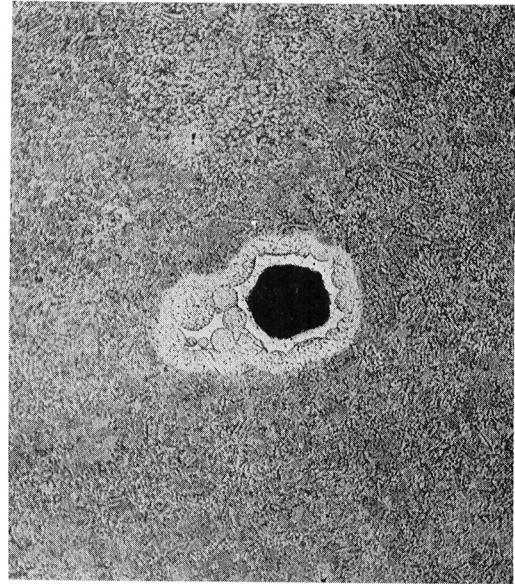


11321 0.08-0.12 cm 50X
(0.033-0.047 in.) Oxides

Figure 3-34. Examples of Defects Found in Billets Seeded With Oxide Inclusions



11309 LC ASTROLOY 100X



11311 M2 TOOL STEEL 100X

Figure 3-35. Examples of LC Astroloy and M2 Tool Steel Contaminants Found in Billets Seeded With These Foreign Alloy Contaminants.

Table 3-19. Test Specimen Identification for Material Having Powder Cleanliness Variations.

Disk No.	Defects	Type of Test					
		Tensile 649° C RT (1200° F)		Rupture	LCF-S	K _B	SPLCF
B466-1	Argon (0.4% TIP)	T76	T80	T77	LS38		S5
B466-2	Argon (0.4% TIP)	T78	T81	T79	LS39	K5	S6
B470-1	0.15 -0.25mm SiO ₂ +Al ₂ O ₃ (0.006-0.010)	T42	T40	T41	LS20,LS21		
B470-2	0.15 -0.25mm SiO ₂ +Al ₂ O ₃ (0.006-0.010)	T45	T43	T44	LS22		
B471-1	0.51 -0.84mm SiO ₂ +Al ₂ O ₃ (0.020-0.033)	T48	T46	T47	LS23,LS24		
B472-1	0.84 -1.2mm SiO ₂ +Al ₂ O ₃ (0.033-0.047)	T54	T52	T53	LS26,LS27		
B472-2	0.84 -1.2mm SiO ₂ +Al ₂ O ₃ (0.033-0.047)	T57	T55	T56	LS28		
B473-1	1.2 -0.64mm SiO ₂ +Al ₂ O ₃ (0.047-0.065)	T60	T58	T59	LS29,LS30		
B473-2	1.2 -1.65mm SiO ₂ +Al ₂ O ₃ (0.047-0.065)	T63	T61	T62	LS31		
B474-1	LC Astroloy	T66	T64	T65	LS32,LS33		
B474-2	LC Astroloy	T69	T67	T68	LS34		
B475-1	M2 Tool Steel	T72	T70	T71	LS35,LS36		
B475-2	M2 Tool Steel	T75	T73	T74	LS37		
A106	Argon (1.4% TIP)	T82	T84	T83	LS40	K6	S7
		T87	T86	T85	LS44		S8

Specimen Code	Type of Test	Qty.
T	Tensile & Rupture Bar	48
LS	Low Cycle Fatigue - Smooth Bar	22
K	Crack Propagation Bar (K _B)	2
S	Notch Bar Cyclic Rupture (Sustained Peak Low Cycle Fatigue- K _T =2)	4

- Size measurements are the minimum and maximum dimensions in mils of the initiation site assuming a rectangular shape (an approximation because most of the defects were irregularly shaped).
- Area mm^2 (mil^2) is the product of the minimum and maximum dimensions again assuming a rectangular shape.

Effect of Material Defects on As-HIP Rene Mechanical Properties

- Oxide Inclusions
 - Degrade all mechanical properties
 - Degree dependent on defect size/location
- Foreign Alloy Contaminants
 - M2 tool steel
 - no significant effect on tensile properties
 - reduces rupture life/ductility
 - acts as fatigue initiation site
 - LC Astroloy
 - no significant effect on properties
- Argon Entrapment
 - Properties decrease with increasing argon content
 - 0.3% TIP is an acceptable limit
 - Pores act as fatigue initiation sites

The following is a more detailed description of the powder cleanliness test program results.

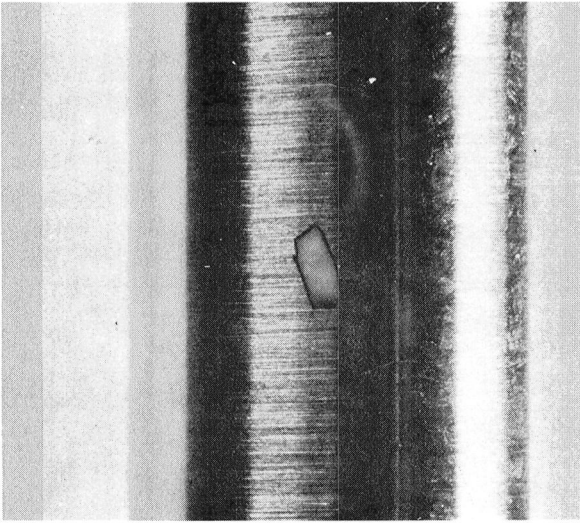
- Tensile Properties - Room temperature (RT) and 649° C (1200° F) tensile test results on material with intentionally seeded defects are given in Tables 3-20 and 3-21 and discussed below for each type of contaminant.
- Oxide Inclusions - Macrophotographs showing examples of fracture surfaces are shown in Figures 3-36 and 3-37. It should be noted that some of the bars did not fail at an oxide inclusion indicating that there probably was no defect in the gage section. Figures 3-38 and 3-39 are plots of the RT and 649° C (1200° F) data versus defect area and illustrate the reduction in ultimate strength and ductility with increasing defect size. The figures also show that the 0.2%YS was relatively unaffected for the inclusion size range tested.
- Foreign Alloy Contaminants - As shown in Figures 3-40 and 3-41 neither the LC Astroloy nor the tool steel had any significant effect on 0.2YS or UTS at RT or 649° C (1200° F) but did cause a slight reduction in ductility. However, all of the property levels exceeded the requirements of this program.

Table 3-20. Effect of Material Defects on As-HIP René 95 Properties Room Temperature Tensile Properties.

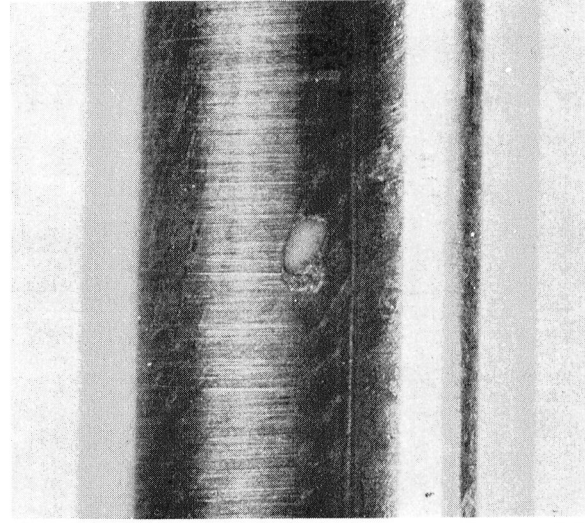
Spec. No.	Disk No.	Added Defects	0.2% YS		UTS		EI (%)	RA (%)	Location	Initiation Site		
			MPa	(KSI)	MPa	(KSI)				Type	Size, mm (Mils)	Area, mm ² (Mils)
T2	B462-2	Standard	1169	(169.6)	1618	(234.7)	18.3	16.5	No Defect			
M1	B462-1	Standard	1198	(173.7)	1618	(234.6)	17.9	16.6	No Defect			
M4	B462-1	Standard	1174	(170.3)	1618	(234.6)	17.7	17.1	No Defect			
T42	B470-1	0.15 -0.25mm (0.006-0.010") Oxides	1187	(172.1)	1613	(234.0)	16.6	17.6	Sub	Oxide	0.15 x 0.20 (6 x 8)	0.031 (48)
T45	B470-2	0.15 -0.25mm (0.006-0.010") Oxides	1193	(173.0)	1587	(230.1)	14.6	15.7	Surf	Pore	0.076 x 0.076 (3 x 3)	0.006 (9)
T48	B471-1	0.51 -0.84mm (0.020-0.033") Oxides	1174	(170.5)	1615	(234.2)	11.9	9.9	Surf	Oxide	0.34 x 0.84 (13.5 x 33)	0.287 (446)
T51	B471-2	0.51 -0.84mm (0.020-0.033") Oxides	1181	(171.3)	1530	(221.9)	17.3	17.3	No Defect			
T54	B472-1	0.84 -1.19mm (0.033-0.047") Oxides	1193	(173.1)	1257	(182.3)	3.8	5.0	Sub	Oxide	0.737 x 1.55 (29 x 61)	1.141 (1769)
T57	B472-2	(0.033-0.047") Oxides	1187	(172.2)	1532	(222.2)	11.5	10.8	No Defect			
T60	B473-1	1.19 -1.71mm (0.047-0.065") Oxides	1182	(171.4)	1276	(185.1)	4.5	7.1	Surf	Oxide	0.61 x 1.07 (24 x 42)	0.650 (1008)
T63	B473-2	1.19 -1.71mm (0.047-0.065") Oxides	1038	(150.6)	1186	(172.0)	1.9	5.6	Surf	Oxide	1.12 x 0.94 (44 x 37)	1.050 (1628)
T66	B474-1	LC Astroloy	1205	(174.8)	1609	(233.3)	15.7	12.7	No Defect			
T69	B474-2	LC Astroloy	1182	(171.4)	1607	(233.0)	15.3	16.0	No Defect			
T72	B475-1	M2 Tool Steel	1191	(172.7)	1551	(225.0)	12.8	13.8	Tool Steel			
T75	B475-2	M2 Tool Steel	1175	(170.4)	1557	(225.8)	13.1	14.5	Tool Steel			
T76	B466-1	Argon (0.4% TIP)	1150	(166.8)	1487	(215.7)	11.3	11.6	Extensometer Mark			
T78	B466-2	Argon (0.4% TIP)	1161	(168.4)	1571	(227.8)	15.8	14.6	No Defect			
T82	A106	Argon (1.4% TIP)	1155	(167.5)	1460	(211.7)	9.5	13.3	Pores			
T87	A106	Argon (1.4% TIP)	1194	(173.1)	1537	(222.9)	11.8	13.4	Pores			
		Program Requirements	1034	(150.0)	1276	(185.0)	10.0	12.0				

Table 3-21. Effect of Material Defects on As-HIP René 95 Properties 649° C (1200° F) Tensile Properties.

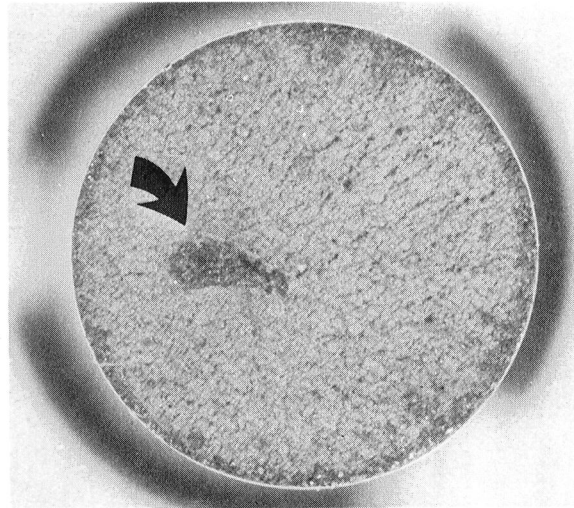
Spec. No.	Disk No.	Added Defects	0.2% YS		UTS		El (%)	RA (%)	Location	Initiation Site		
			MPa	(KSI)	MPa	(KSI)				Type	Size, mm (Mils)	Area, mm ² (Mils)
T4	B462-3	Standard	1048	(152.0)	1403	(203.5)	13.9	14.5	No Defect			
M2	B462-1	Standard	1089	(157.9)	1411	(204.6)	14.5	14.8	No Defect			
M3	B462-1	Standard	1084	(157.2)	1476	(214.0)	16.0	17.4	No Defect			
M5	B462-1	Standard	1079	(156.5)	1452	(210.6)	15.5	17.1	No Defect			
T40	B470-1	0.15 -0.25mm (0.006-0.010") Oxides	1094	(158.7)	1420	(206.0)	13.9	14.9	No Defect			
T43	B470-2	0.15 -0.25mm (0.006-0.010") Oxides	1094	(158.6)	1433	(207.8)	12.9	12.9	No Defect			
T46	B471-1	0.51 -0.84mm (0.020-0.033") Oxides	1069	(155.1)	1427	(207.0)	14.8	17.0	No Defect			
T49	B471-2	0.51 -0.84mm (0.020-0.033") Oxides	1101	(159.7)	1431	(207.6)	12.6	13.9	Surf	Oxide	0.23 x 0.36 (9 x 14)	0.083 (126)
T52	B472-1	0.84 -1.19mm (0.033-0.047") Oxides	1103	(159.9)	1142	(165.6)	2.0	3.0	Surf	Oxide	1.27 x 1.32 (50 x 52)	1.68 (2600)
T55	B472-2	0.84 -1.19mm (0.033-0.047") Oxides	1083	(157.1)	1245	(180.6)	3.8	6.6	Sub	Oxide	0.61 x 1.55 (24 x 61)	0.94 (1464)
T58	B473-1	1.19 -1.71mm (0.047-0.065") Oxides	1080	(156.6)	1428	(207.1)	13.8	16.8	No Defect			
T61	B473-2	1.19 -1.71mm (0.047-0.065") Oxides	1076	(156.1)	1140	(165.4)	1.9	5.9	Surf	Oxide	1.40 x 1.78 (55 x 70)	2.49 (3850)
T64	B474-1	LC Astroloy	1099	(159.4)	1400	(203.1)	8.1	11.9				
T67	B474-2	LC Astroloy	1094	(158.6)	1432	(207.7)	12.6	14.6				
T70	B475-1	M2 Tool Steel	1100	(159.6)	1413	(204.9)	9.1	13.8	Tool Steel			
T73	B475-2	M2 Tool Steel	1098	(159.3)	1420	(205.9)	9.6	14.7	Tool Steel			
T80	B466-1	Argon (0.4% TIP)	1059	(153.6)	1383	(200.6)	14.6	16.3				
T81	B466-2	Argon (0.4% TIP)	1065	(154.4)	1413	(204.9)	14.2	14.6				
T84	A106	Argon (1.4% TIP)	1059	(153.6)	1360	(197.3)	7.9	7.7				
T86	A106	Argon (1.4% TIP)	1087	(157.6)	1422	(206.3)	10.9	12.3				
		Program Requirements	862	(125.0)	1000	(145.0)	8.0	10.0				



T54 10X
Defect 3.30 cm (1.3 in.) From End

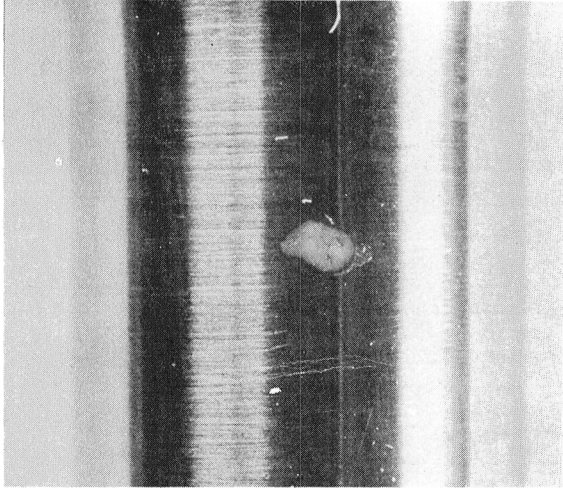


T54 10X
Defect 3.68 cm (1.45 in.) From End

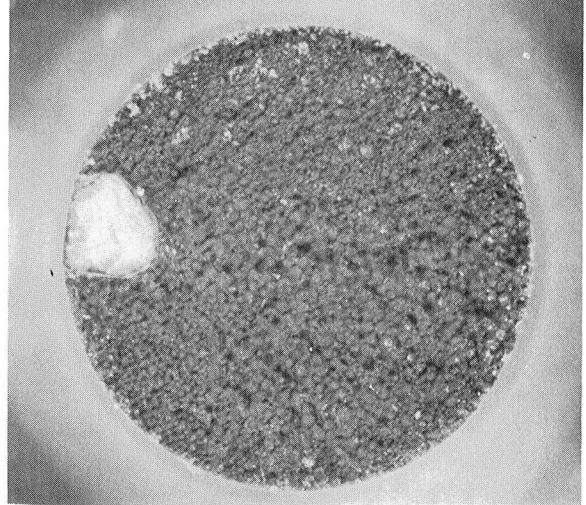


T54 10X
Failure at Subsurface Defect 3.96 cm
(1.56 in.) From End

Figure 3-36. Surface Defects Noted Prior to Test and Fracture Surface of Specimen T54



T52 10X
Defect 4.37 cm (1.72 in.) From End



T52 10X
Failure at Surface Defect 4.37 cm
(1.72 in.) From End

Figure 3-37. Surface Defect Noted Prior to Test and Fracture Surface of Specimen T52

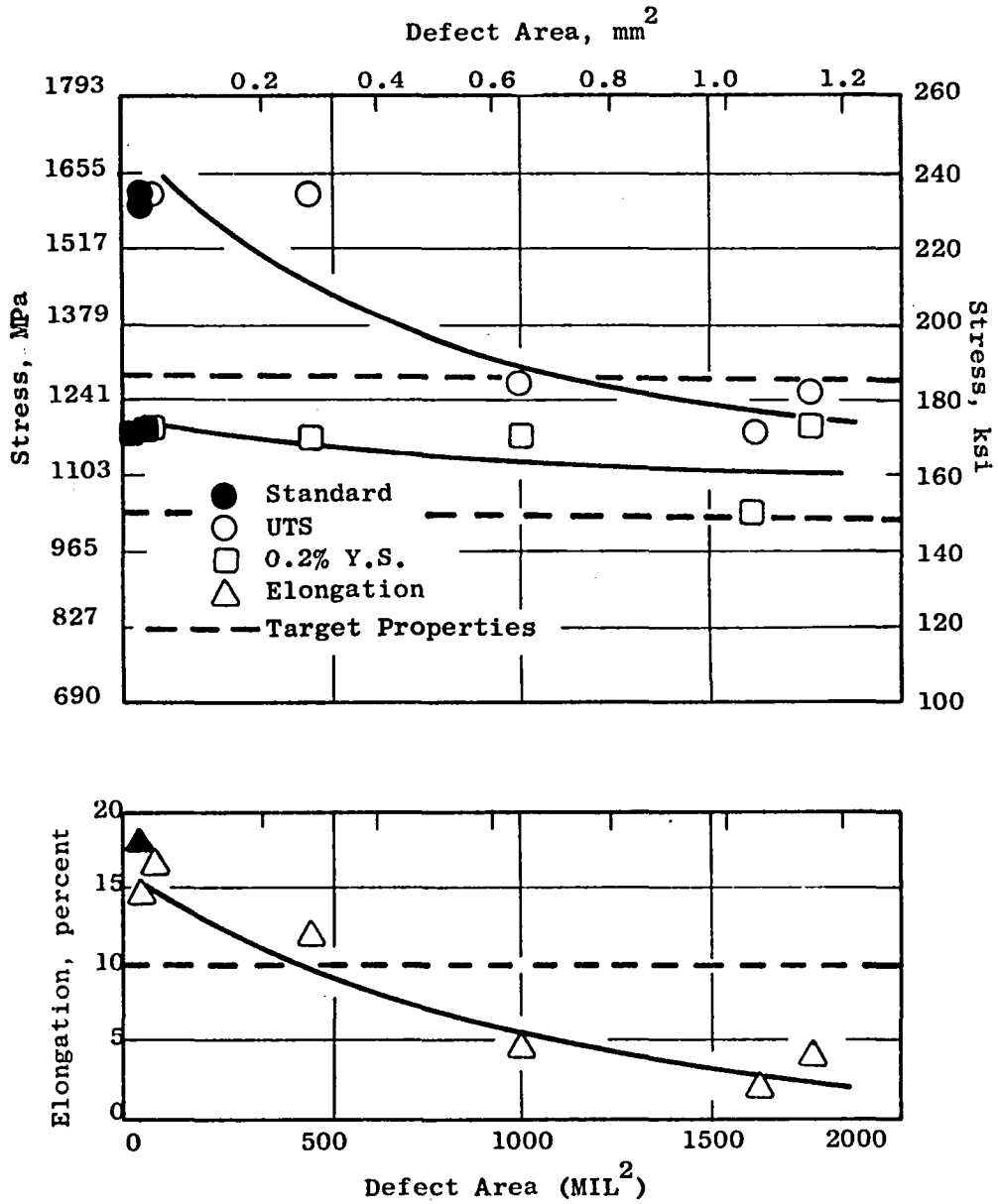


Figure 3-38. Effect of Oxide Inclusion Size on Room Temperature Tensile Properties.

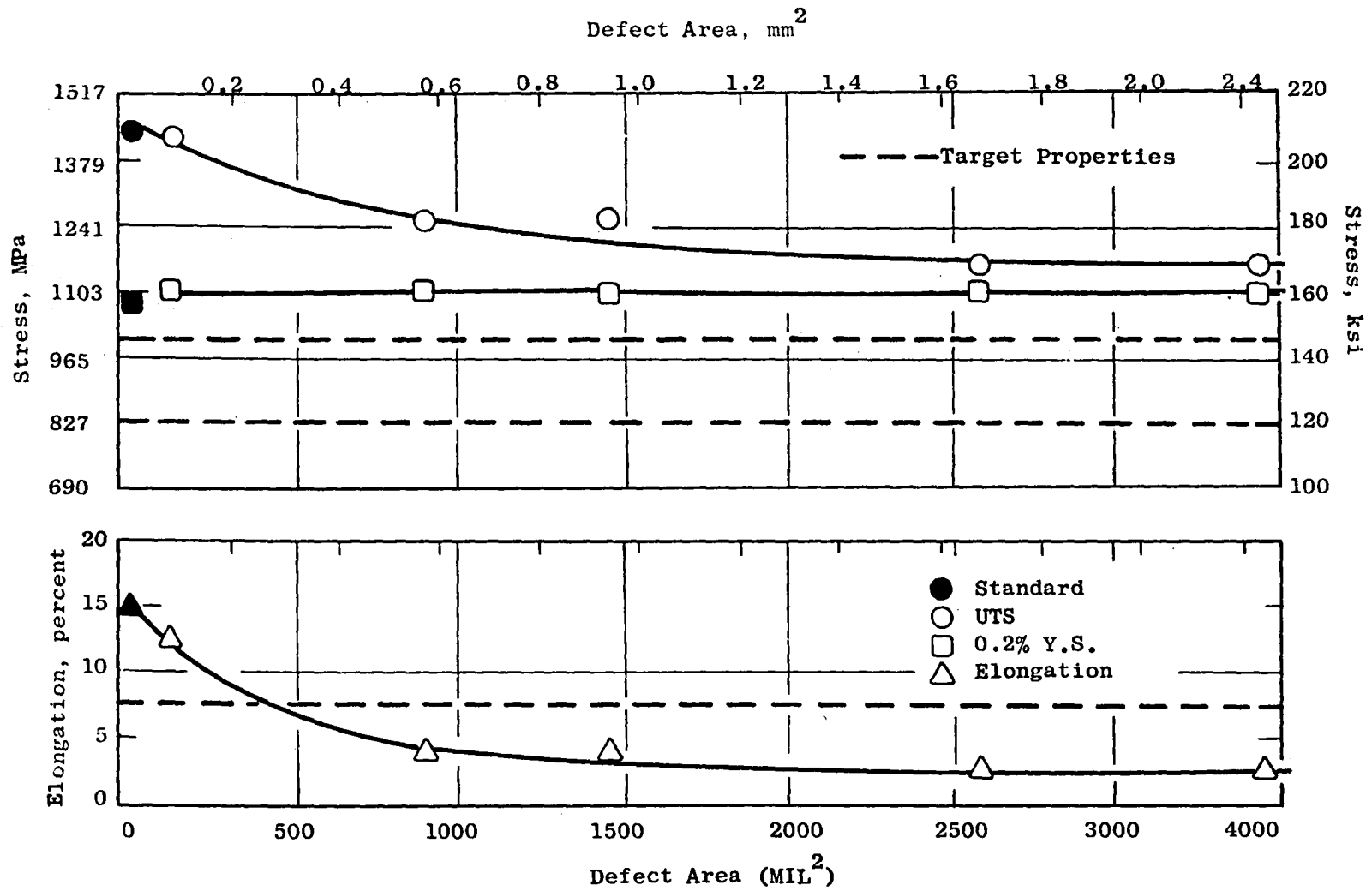


Figure 3-39. Effect of Defect Area on 649° C (1200° F) Tensile Properties.

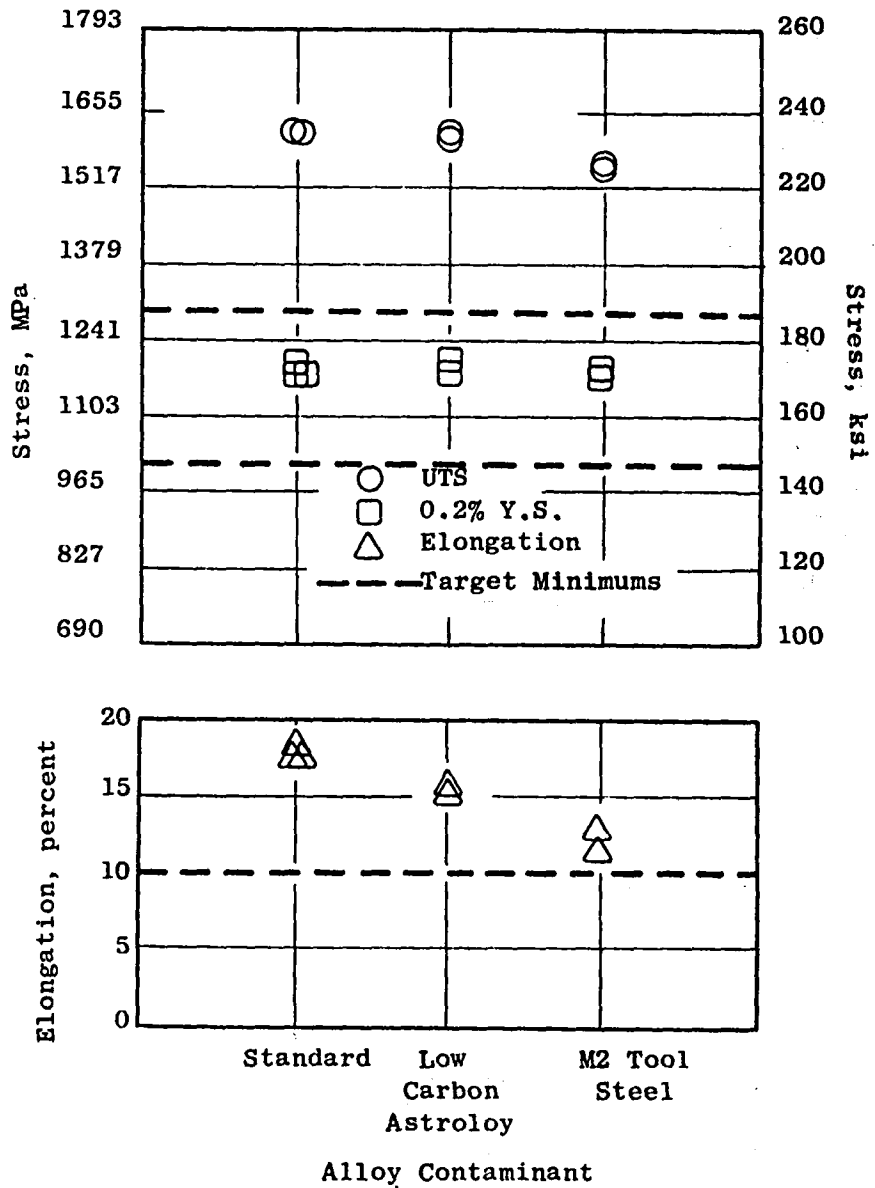


Figure 3-40. Effect of Foreign Alloy Contaminants on RT Tensile Properties.

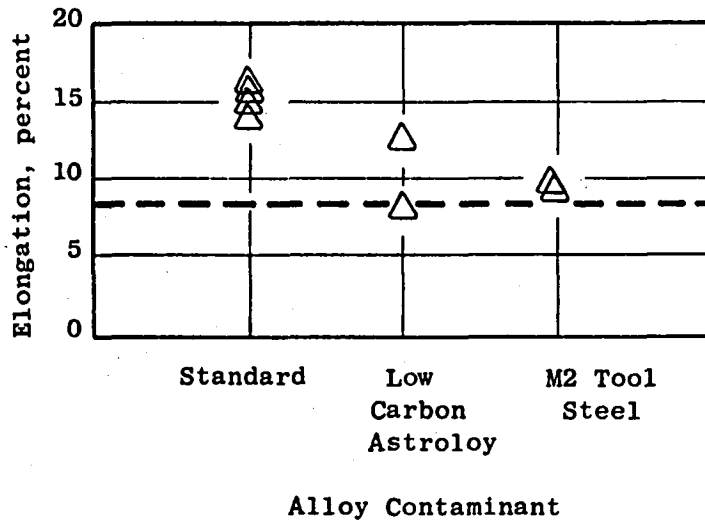
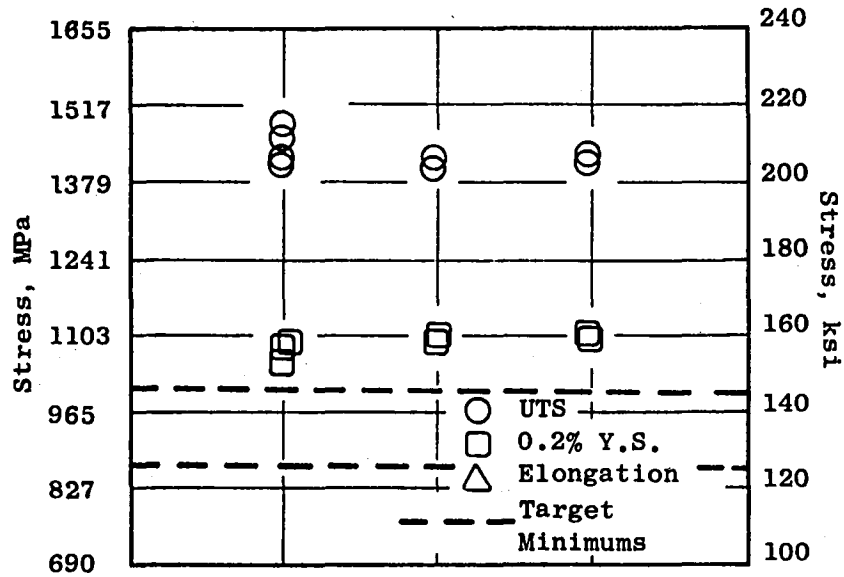


Figure 3-41. Effect of Foreign Alloy Contaminants on 1200° F Tensile Properties.

- Argon Entrapment - Plots of RT and 1200° F tensile properties versus % TIP are shown in Figures 3-42 and 3-43 respectively and indicate that ultimate strength and ductility decrease with increasing argon content as indicated by % TIP while 0.2%YS is unaffected. With the exception of the ductility value on specimen T82, the material with greater argon content than specification limits had properties which exceeded program requirements.

Stress Rupture Properties

The 649° C/965 MPa (1200° F/140 ksi) stress rupture properties of material with intentionally seeded defects are shown in Table 3-22 and the results are described below.

- Oxide Inclusions - As shown in Table 3-22, several of the specimens did not fail at oxide inclusions. A plot of the data from specimens which did fail at oxides is shown in Figure 3-44 and illustrates the decrease in rupture life and ductility with increasing defect size. Three of the bars (T53, T59 and T62) failed to meet program life requirements and the same three plus specimen T50 failed to meet ductility requirements.
- Foreign Alloy Contaminants - Figure 3-45 shows the rupture properties of the material doped with LC astroloy and M2 tool steel versus the standard. These data indicate that LC astroloy results in a slight reduction in life and ductility while M2 tool steel shows a greater reduction, particularly in ductility. Failures in the bars containing M2 tool steel initiated at surface tool steel particles which had oxidized during the 649° C (1200° F) test and this resulted in the lower ductility. Neither contaminant caused rupture lives to fall below program requirements but the tool steel resulted in ductilities below the requirements defined for this program.
- Argon Entrapment - Figure 3-46 compares the rupture properties of the material having argon levels above specification with the standard material (0.2% TIP). As seen in the figure, rupture life and ductility decreased with increasing argon content (specimen T85 over-temperatured during the test and resulted in an invalid test point). The rupture properties of specimens containing the argon (% TIP) levels tested in this study exceeded the program requirements.

Low Cycle Fatigue

The low cycle fatigue (strain control), axial-axial, $A=1$, $K_t=1$, 538°C (1000° F) properties of material with intentionally seeded defects are presented in Table 3-23 and the results for each type of material defect are discussed below.

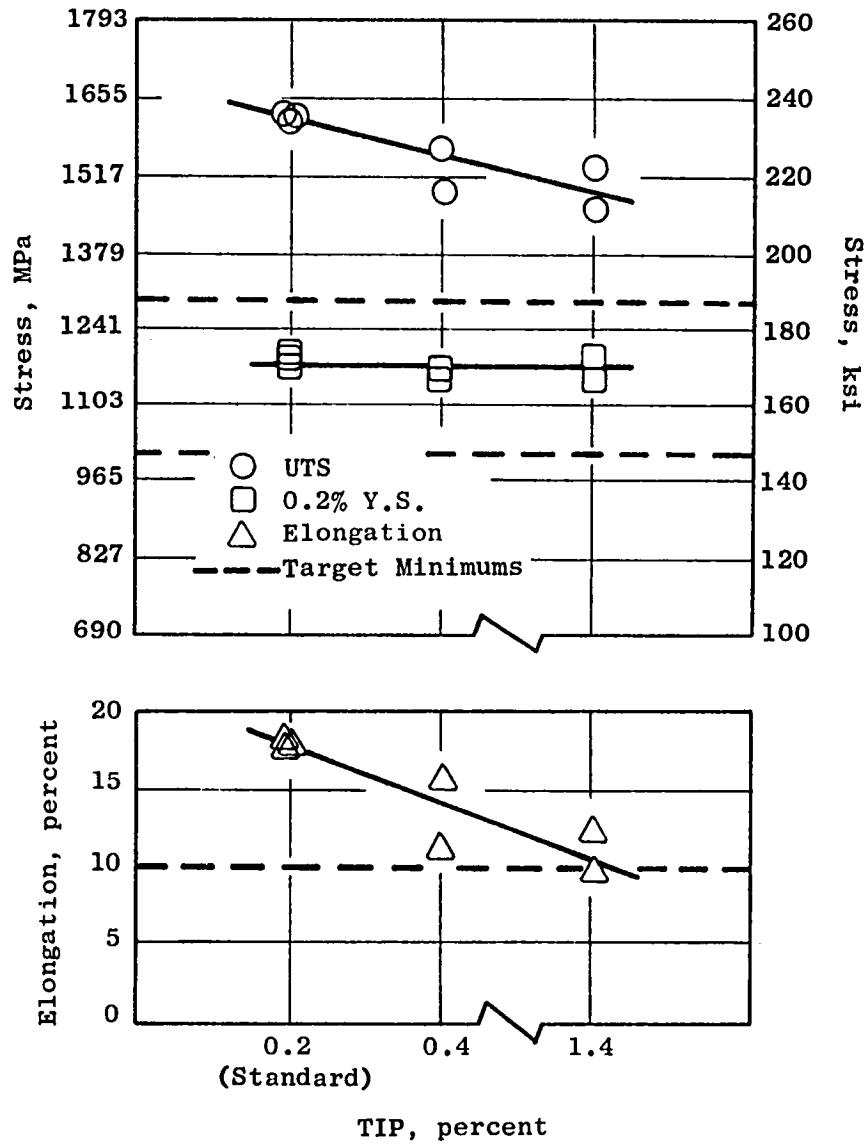


Figure 3-42. Effect of Percent TIP on RT Tensile Properties.

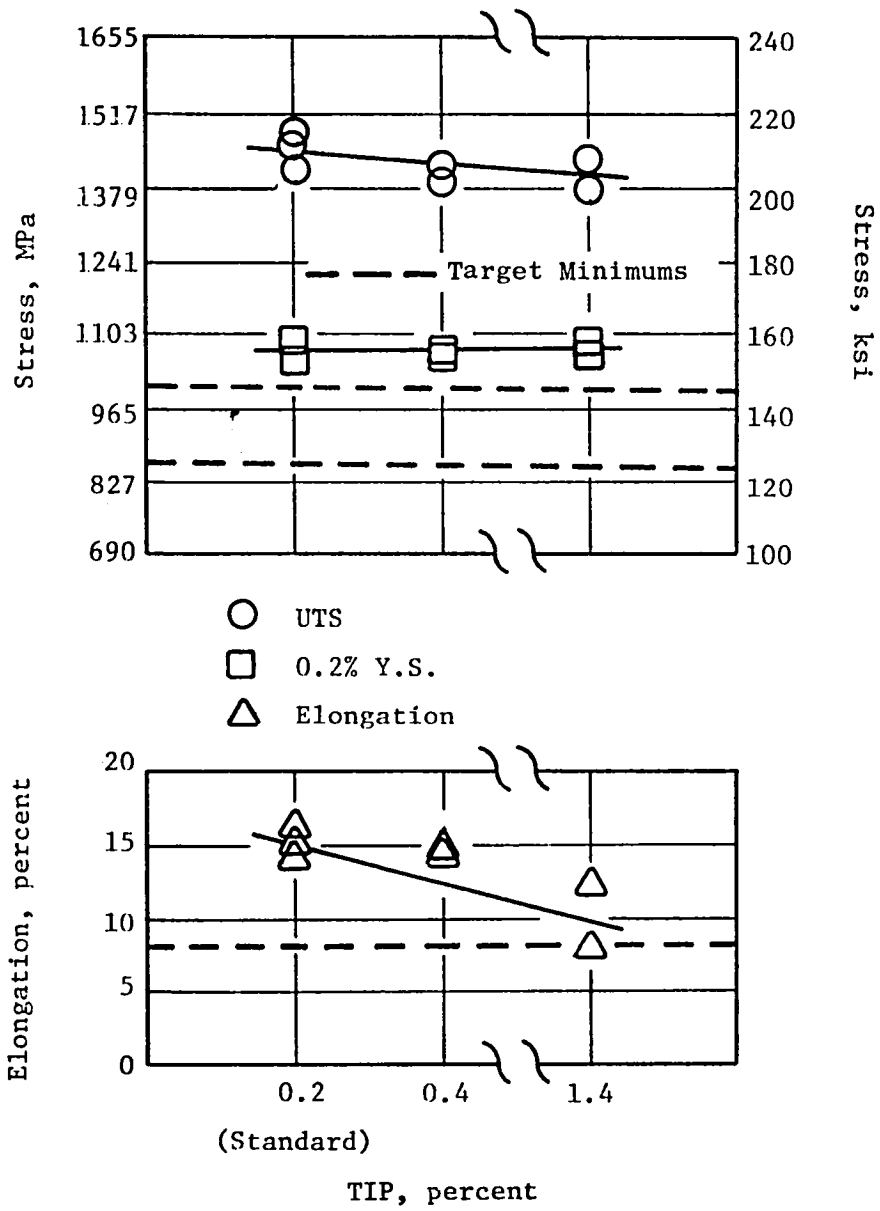


Figure 3-43. Effect of Percent TIP on 649° C (1200° F) Tensile Properties.

Table 3-22. Effect of Material Defects on As-HIP René 95 Properties 649° C / 695 MPa (1200° F/140 ksi) Rupture Properties.

Spec. No.	Disk No.	Added Defects	Life (Hrs)	E1 (%)	RA (%)	Location	Type	Size, mm (Mils)	Area, mm ² (Mils)
T1	B462-1	Standard	399.8	4.3	6.3	No Defect			
T3	B462-3	Standard	129.0	3.6	5.1	No Defect			
T41	B470-1	0.15 -0.25mm (0.006-0.010") Oxides	317.4	3.8	3.2	No Defect			
T44	B470-2	0.15 -0.25mm Oxides	151.2	4.5	5.5	Sub	Oxide	0.20 x 0.30 (8 x 12)	0.06 (96)
T47	B471-1	0.51 -0.84mm (0.020-0.033") Oxides	247.1	4.4	4.7	No Defect			
T50	B471-2	0.51 -0.84mm (0.020-0.033") Oxides	106.05	1.5	3.1	Surf	Oxide	0.20 x 0.56 (8 x 22)	0.112 (176)
T53	B472-1	0.84 -1.19mm (0.033-0.047") Oxides	5.3	0.6	1.2	Surf	Oxide	0.96 x 1.52 (38 x 60)	1.46 (2280)
T56	B472-2	0.84 -1.19mm (0.033-0.047") Oxides	89.5	2.4	4.0	No Defect			
T59	B473-1	1.19 -1.71mm (0.047-0.065") Oxides	23.7	1.0	3.6	Surf	Oxide	0.43 x 1.19 (17 x 47)	0.51 (799)
T62	B473-2	1.19 -1.71mm (0.047-0.065") Oxides	7.6	0.9	1.6	Surf	Oxide	0.79 x 1.19 (31 x 47)	0.94 (1457)
T65	B474-1	LC Astroloy	85.3	2.9	3.9	No Defect			
T68	B474-2	LC Astroloy	191.0	3.8	3.5	No Defect			
T71	B475-1	M2 Tool Steel	109.4	0.8	0.8	Surf	Tool Steel	0.035 x 0.043 (1.4 x 1.7)	0.002 (2.4)
T74	B475-2	M2 Tool Steel	115.2	2.0	2.0	Surf	Tool Steel		
T77	B466-1	Argon (0.4% TIP)	146.10	3.3	3.2	No Defect			
T79	B466-2	Argon (0.4% TIP)	119.86	2.0	5.1	No Defect			
T83	A106	Argon (1.4% TIP)	98.30	2.4	2.4	Surf	Pores		
T85	A106	Argon (1.4% TIP)	1.8	5.4	6.3	Overtemp 777° C (1430° F) During Test			
		Program Requirements	25	2					

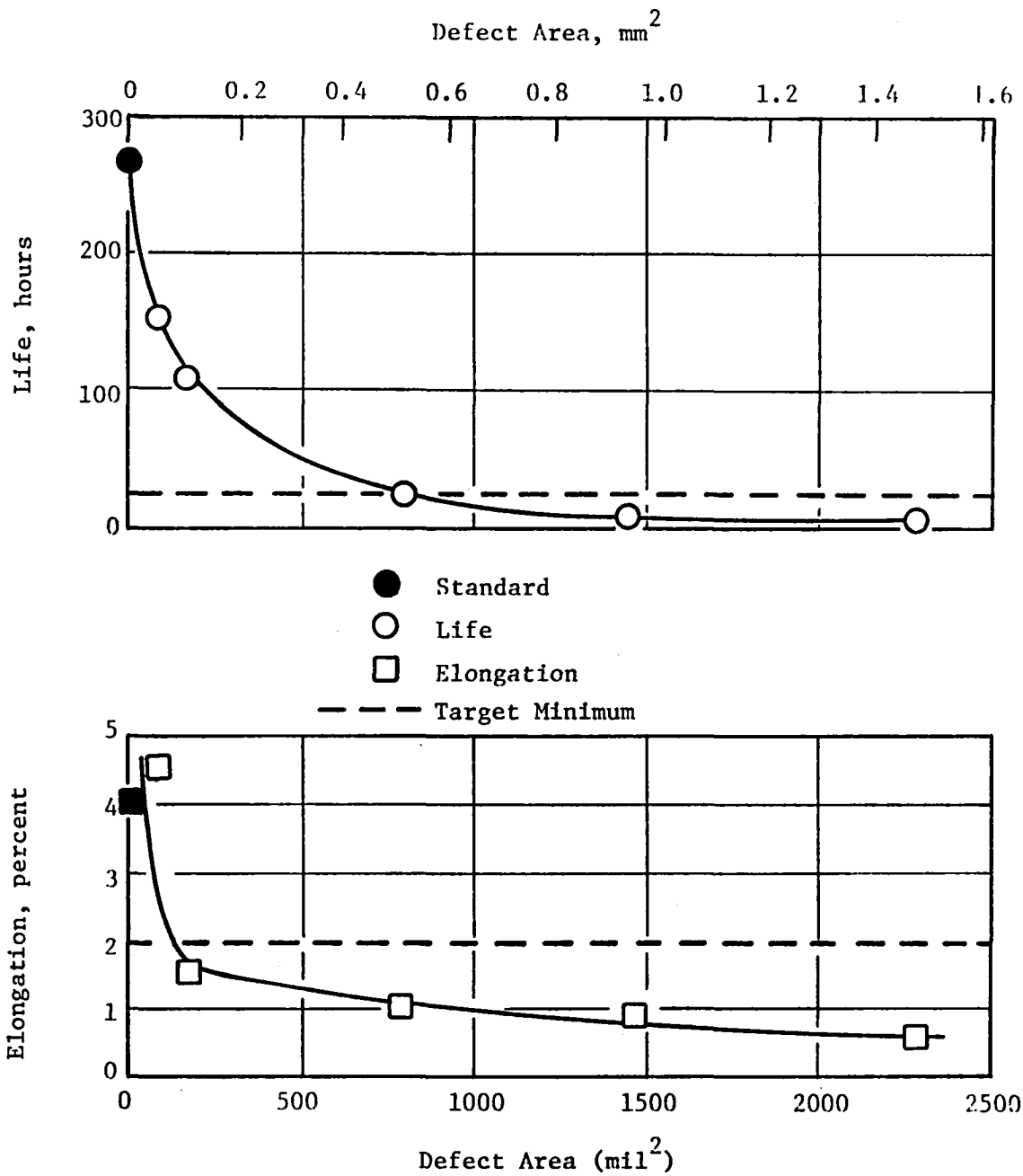


Figure 3-44. Effect of Oxide Inclusion Size on 649° C/965 MPa (1200° F/140 ksi) Stress Rupture.

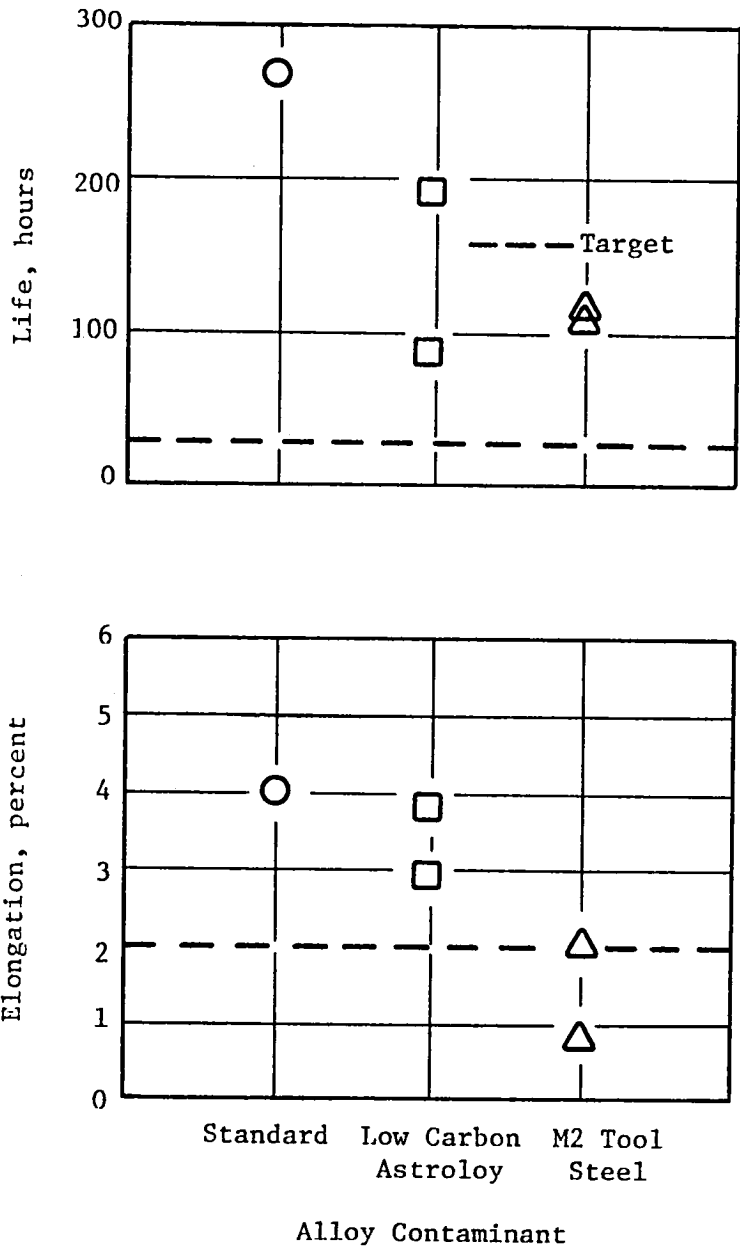


Figure 3-45. Effect of Foreign Alloy Contaminants on 649° C/965 MPa (1200° F/140 ksi) Stress Rupture.

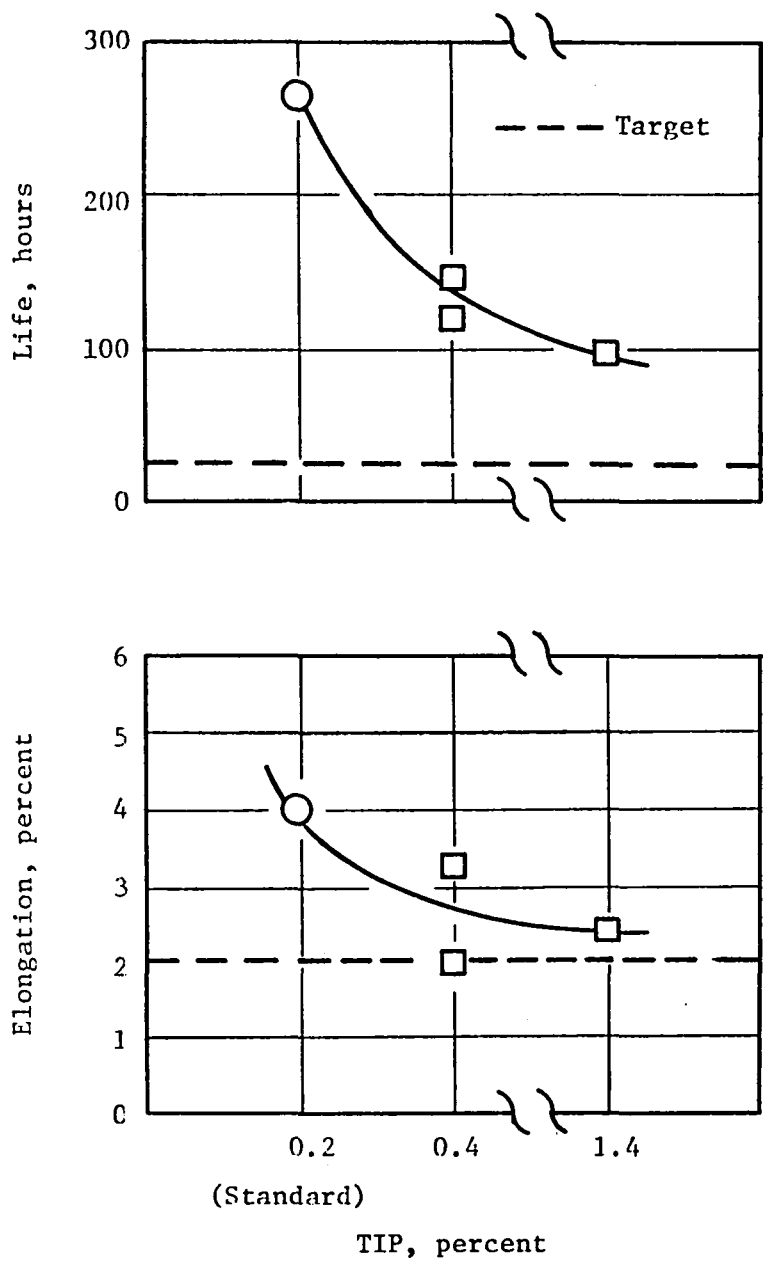


Figure 3-46. Effect of Percent TIP on 649° C/ 695 MPa (1200° F/1400 ksi) Stress Rupture.

Table 3-23. Effect of Material Defects on As-HIP René 95 Properties 538° C (1000° F)
Strain Control.

R=0 (A=1), $K_t=1$

Spec. No.	Disk No.	Added Defects	Strain Range %	Modulus		Alternating Pseudo Stress		Life (Cycles)	Location	Type	Size, mm (Mils)	Area, mm ² (Mils) ²
				GPa	(x 10 ⁶ PSI)	MPa	(KSI)					
LS1	B462-1	Standard	0.68	0.194	(28.2)	661	(95.9)	31,806	Sub	Pore	0.08 x 0.10 (3 x 4)	0.008 (12)
LS2	B462-2	Standard	0.68	0.196	(28.5)	668	(96.9)	14,196	Surf	Pore	0.05 x 0.05 (2 x 2)	0.002 (4)
LS3	B462-3	Standard	0.62	0.197	(28.6)	612	(88.7)	53,380	Sub	Pore	0.08 x 0.08 (3 x 3)	0.006 (9)
LS20	B470-1	0.15-0.25mm (0.006-0.010") Oxides	0.67	0.194	(28.1)	649	(94.1)	26,330	Surf	Pore	0.025 x 0.08 (1 x 3)	0.002 (3)
LS21	B470-1	0.15-0.25mm (0.006-0.010") Oxides	0.61	0.192	(27.9)	592	(85.8)	17,292	Surf	Pore	0.025 x 0.05 (1 x 2)	0.001 (2)
LS22	B470-2	0.15-0.25mm (0.006-0.010") Oxides	0.62	0.188	(27.2)	578	(83.8)	27,884	Surf	Pore	0.05 x 0.08 (2 x 3)	0.004 (6)
LS23	B471-1	0.51-0.84mm (0.020-0.033") Oxides	0.68	0.188	(27.2)	637	(92.4)	16,039	Sub	Oxide	0.48 x 0.84 (19 x 33)	0.406 (630)
LS24	B471-1	0.51-0.84mm (0.020-0.033") Oxides	0.63	0.189	(27.4)	590	(85.7)	8,042	Sub	Oxide	0.46 x 0.76 (18 x 30)	0.348 (540)
LS25	B471-2	0.51-0.84mm (0.020-0.033") Oxides	0.60	0.202	(29.3)	609	(88.3)	15,665	Sub	Oxide	0.56 x 0.79 (22 x 31)	0.439 (680)
LS26	B472-1	0.84-1.19mm (0.033-0.047") Oxides	0.69	0.184	(26.7)	633	(91.8)	1,454	Surf	Oxide	0.74 x 1.62 (29 x 64)	1.19 (1850)
LS27	B472-2	0.84-1.19mm (0.033-0.047") Oxides	0.50	0.196	(28.4)	493	(71.5)	24,413	Sub	Oxide	0.61 x 0.68 (24 x 27)	0.419 (650)

Table 3-23. Effect of Material Defects on As-HIP René 95 Properties 538° C (1000° F)
Strain Control. (Concluded)

R=0 (A=1), $K_t=1$.

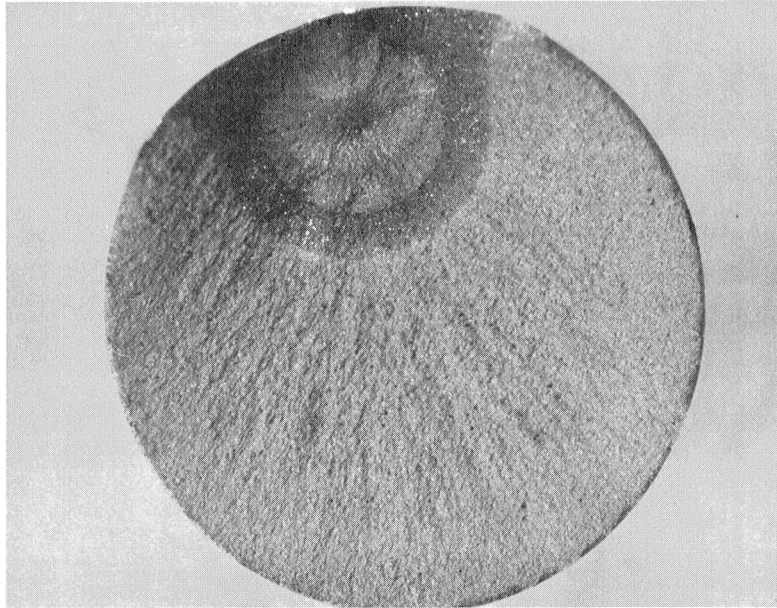
Spec. No.	Disk No.	Added Defects	Strain Range %	Modulus		Alternating Pseudo Stress		Life (Cycles)	Location	Type	Size, mm (Mils)	Area, mm ² (Mils) ²
				TPa	(x 10 ⁶ PSI)	MPa	(KSI)					
LS28	B472-2	0.84-1.19mm (0.033-0.047") Oxides	0.62	0.195	(28.3)	605	(87.7)	3,845	Surf	Oxide	0.71 x 1.19 (28 x 47)	0.871 (1350)
LS29	B473-1	1.19-1.71mm (0.047-0.065") Oxides	0.75	0.183	(26.5)	683	(99.1)	375	Surf	Oxide	0.99 x 2.00 (39 x 79)	2.0 (3100)
LS30	B473-1	1.19-1.37mm (0.047-0.054") Oxides	0.63	0.185	(26.8)	582	(84.4)	2,605	Surf	Oxide	0.38 x 1.17 (15 x 46)	0.445 (690)
LS31	B473-2	1.19-1.71mm (0.047-0.065") Oxides	0.50	0.196	(28.5)	489	(70.9)	4,435	Surf	Oxide	0.74 x 1.37 (29 x 54)	1.006 (1560)
LS32	B474-1	LC Astroloy	0.67	0.192	(27.9)	647	(93.9)	10,650	Surf	Pore	0.05 x 0.10 (2 x 4)	0.005 (8)
LS33	B474-1	LC Astroloy	0.61	0.198	(28.8)	610	(88.4)	42,556	Button Head Failure			
LS34	B474-2	LC Astroloy	0.55	0.205	(29.7)	565	(82.0)	42,141	Sub	Oxide	0.10 x 0.13 (4 x 5)	0.013 (20)
LS35	B475-1	M2 Tool Steel	0.68	0.185	(26.9)	629	(91.2)	8,185	Surf	Tool Steel	0.15 x 0.25 (6 x 10)	0.038 (60)
LS36	B475-1	M2 Tool Steel	0.54	0.201	(29.2)	545	(79.0)	54,839	Surf	Tool Steel	0.13 x 0.20 (5 x 8)	0.025 (40)
LS37	B475-2	M2 Tool Steel	0.61	0.192	(27.8)	590	(85.5)	10,830	Surf	Tool Steel	0.18 x 0.20 (7 x 8)	0.036 (56)
LS38	B466-1	Argon (0.4% TIP)	0.68	0.187	(27.1)	637	(92.4)	35,616	Button Head Failure			
LS39	B466-1	Argon (0.4% TIP)	0.61	0.188	(27.2)	574	(83.2)	33,725	Button Head Failure			
LS40	A106	Argon (1.4% TIP)	0.62	0.203	(29.4)	632	(91.7)	8,155	Surf		0.05 x 0.13 (2 x 5)	0.006 (10)
LS41	A106	Argon (1.4% TIP)	0.68	0.185	(26.8)	632	(91.6)	2,496	Surf	Multiple Sites at Pores		

- Standard - Three LCF specimens taken from standard material were tested and in each case failure initiated at small pores which are inherent in the argon atomized material. Figure 3-47 shows an example of fatigue initiation at a pore.
- Oxide Inclusions - A total of 12 LCF specimens were tested from the material intentionally seeded with oxide inclusions. As shown in Table 3-23 the specimens with 0.15-0.25 mm (0.006-0.010 inch) oxides (LS 20-22) failed at surface pores rather than oxide inclusions. All of the other failures in specimens with intentional oxides initiated at oxide inclusions as shown in the table. The data are plotted (life versus alternating pseudo stress) in Figure 3-48 which shows the trend of decreasing life with increasing oxide inclusion size. Figures 3-49 and 3-50 illustrate examples of fatigue initiation at surface and sub-surface oxide inclusions.
- Foreign Alloy Contaminants - A total of six LCF tests were conducted on the material seeded with foreign alloy powder three for LC astroloy specimens initiated at pores or oxide inclusions indicating that the LC astroloy contaminant does not play a significant role in the fatigue process, at least in the range of lives observed. On the other hand, the failures in the tool-steel-doped specimens all initiated at surface tool steel particles, an example of which is shown in Figure 3-51. The data are plotted in Figure 3-52 which illustrates the reduction in life resulting from the surface initiation at the tool steel particles.
- Argon Entrapment - Two LCF specimens were tested at each of the two TIP levels evaluated. Both of the specimens having 0.4% TIP failed in the button head so that the data could not be used to provide a valid comparison with the standard. The two bars having 1.4% TIP both had failures that initiated at surface porosity which resulted in reduced life.

In summary, the LCF data from the material with intentionally seeded defects indicates that oxide inclusions, tool steel particles, and porosity act as fatigue crack initiation sites. The effect of these defects is dependent both on defect size, with LCF life decreasing with increasing defect size, and on defect location. A comparison of specimens LS25 and LS30 (Table 3-23) provides an indication of the influence of defect location. For both specimens, run at approximately the same strain range, fatigue initiation occurred at approximately the same size defect but LS25, with initiation internal to the specimen surface, failed at 15,665 cycles while LS30, with initiation on the surface, failed at 2,605 cycles.

3.2.1.5 Process Deviation Effects

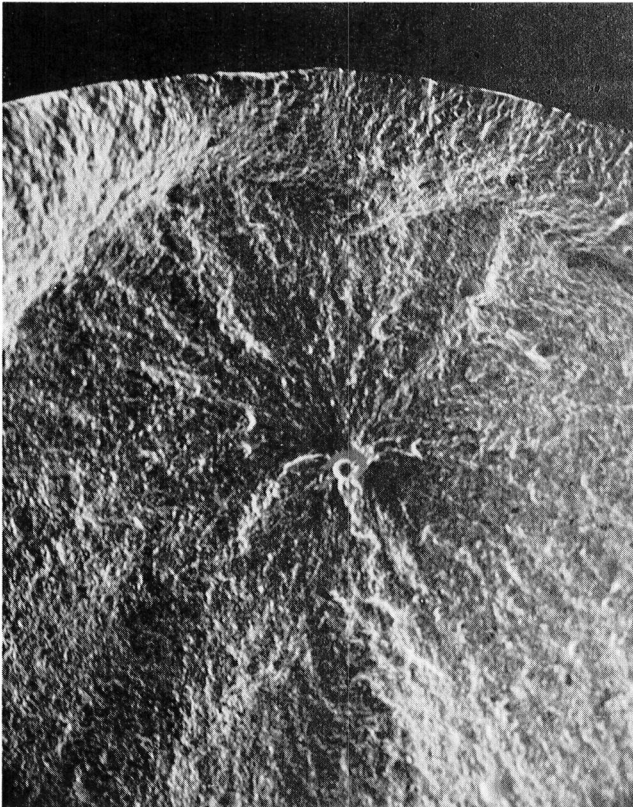
The objective of the process deviation portion of the process variable study was to determine the effect of deviations from nominal conditions on



LS4

8X

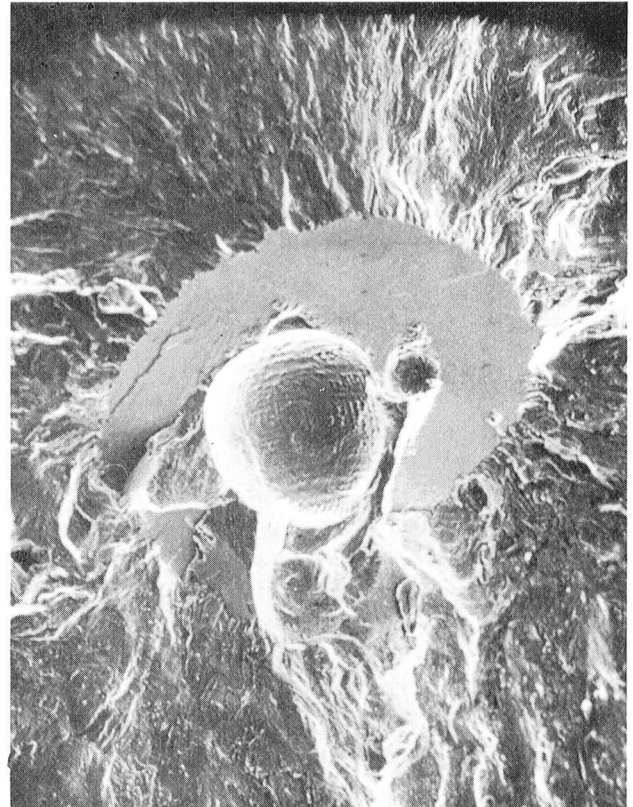
FATIGUE INITIATION AT SUBSURFACE SITE



LS4

27X

PORE AT INITIATION SITE



LS4

270X

PORE AT INITIATION SITE

Figure 3-47. Fracture Surface of LCF Specimen LS4 Showing Example of Fatigue Initiation at a Pore (See Table 3-31).

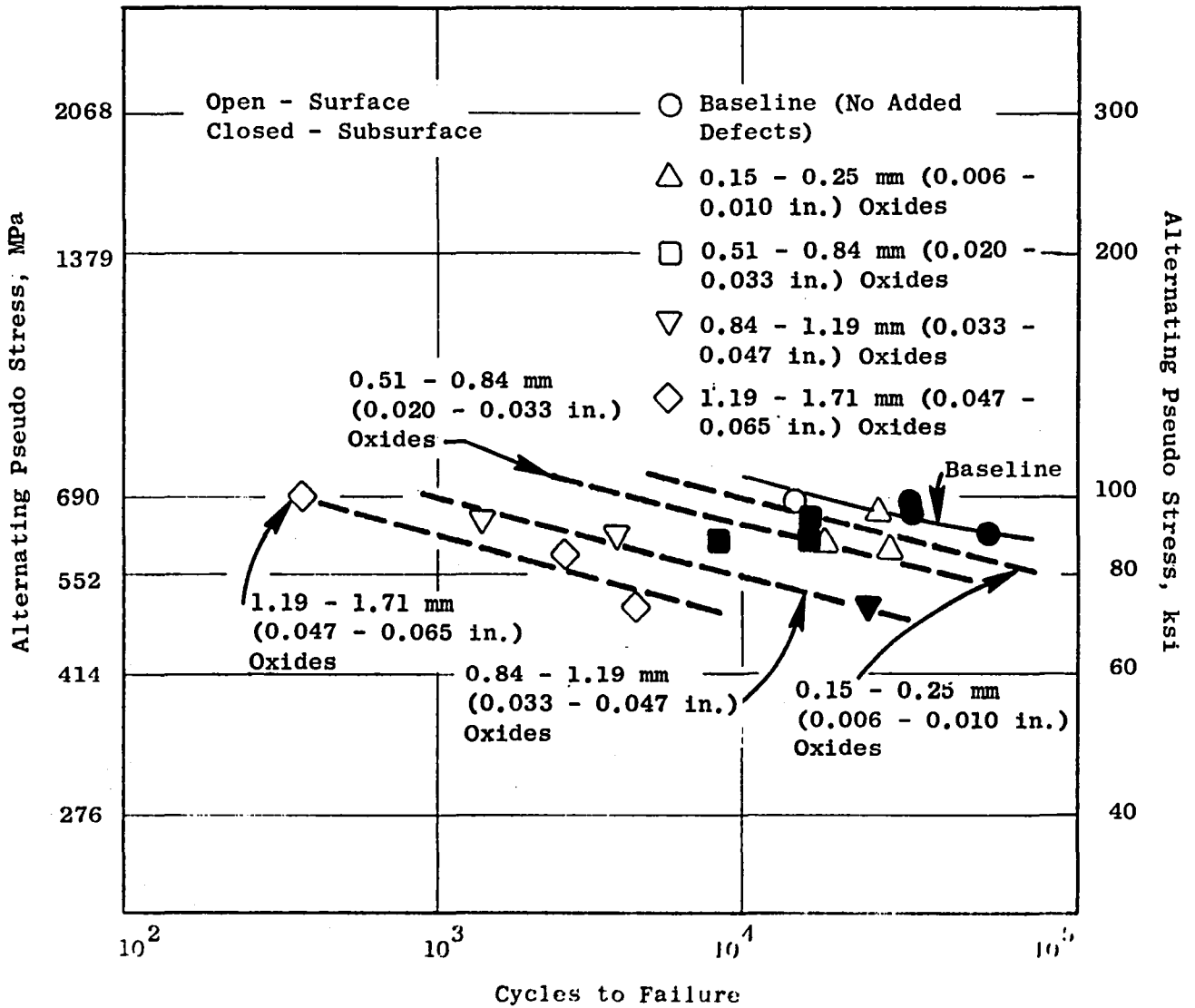
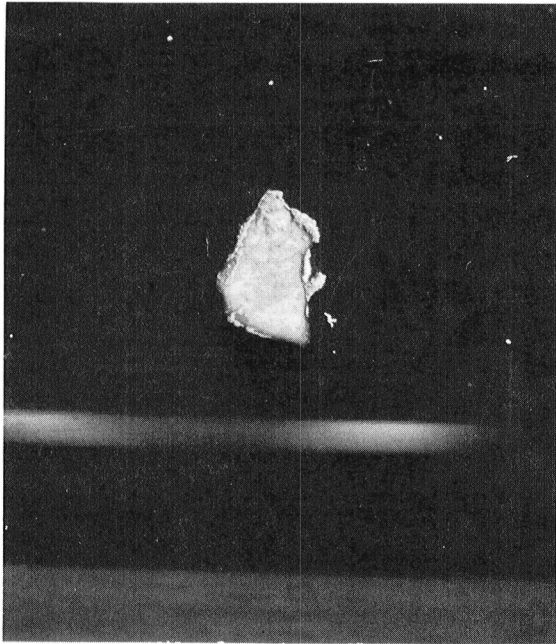


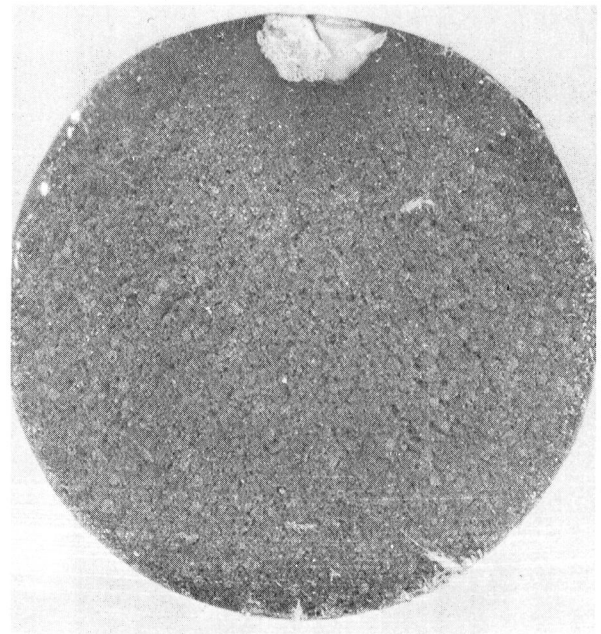
Figure 3-48. Effect of Oxide Inclusions on 538° C (1000° F) Strain Control $R = 0$ ($A = 1$, $K_t = 1$) LCF.



LS29

10X

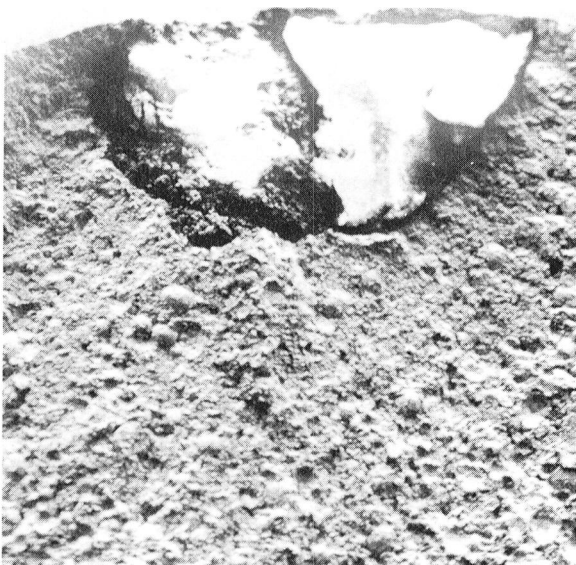
Surface Defect 67.6 cm (2.66 in.) From End (Noted Prior to Test)



LS29

8X

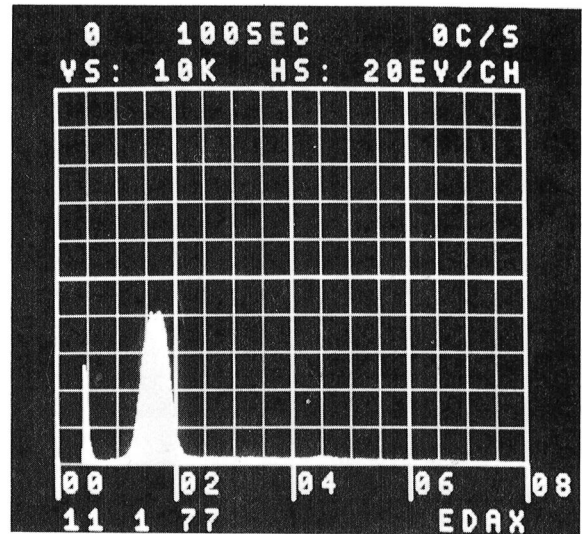
Fatigue Initiation at Surface Defect 67.6 cm (2.66 in.) From End



LS29

29X

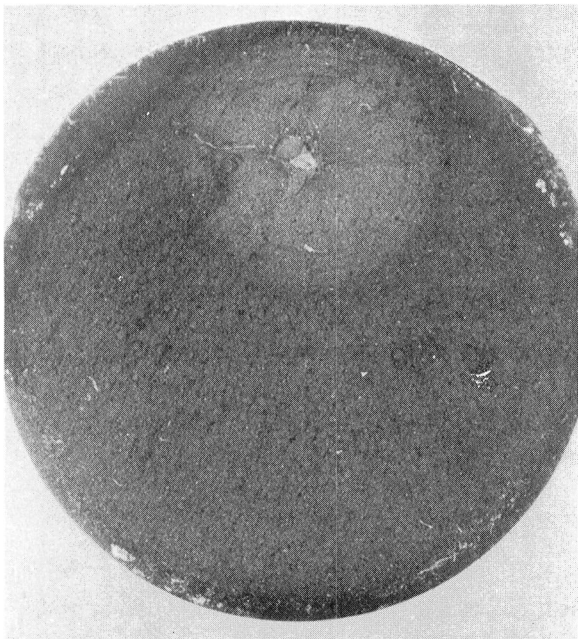
OXIDE INCLUSION AT INITIATION SITE



Al/Si

EDAX INDICATING OXIDE HIGH IN Al/Si

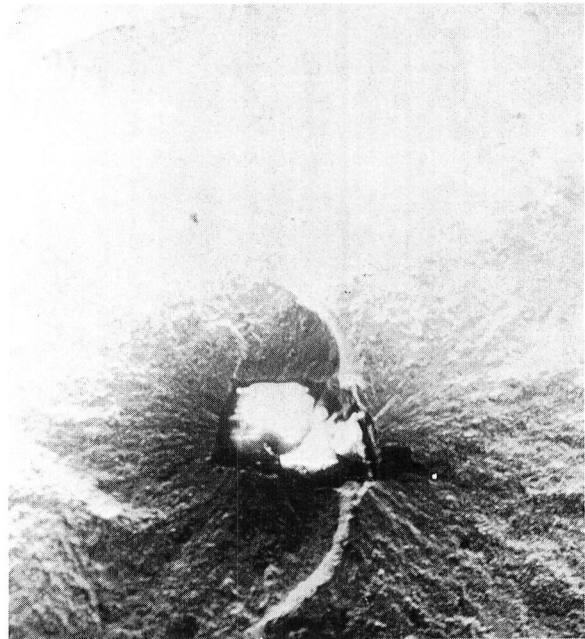
Figure 3-49. Fracture Surface of LCF Specimen LS29 Showing Example of Fatigue Initiation at Surface Oxide Inclusion



LS23

8X

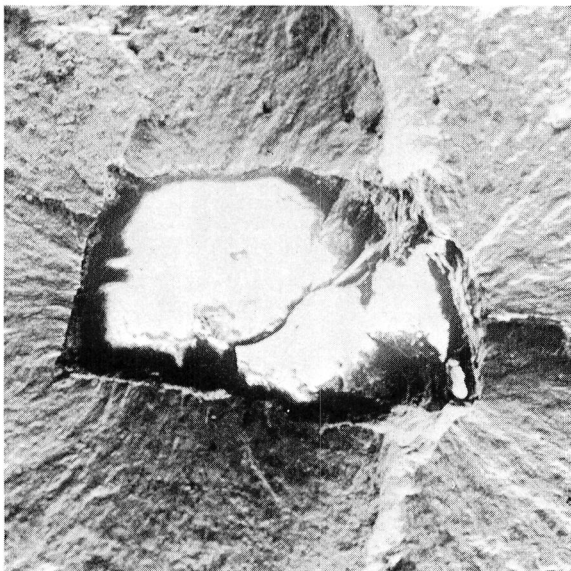
FATIGUE INITIATION AT
SUBSURFACE SITE



LS23

27X

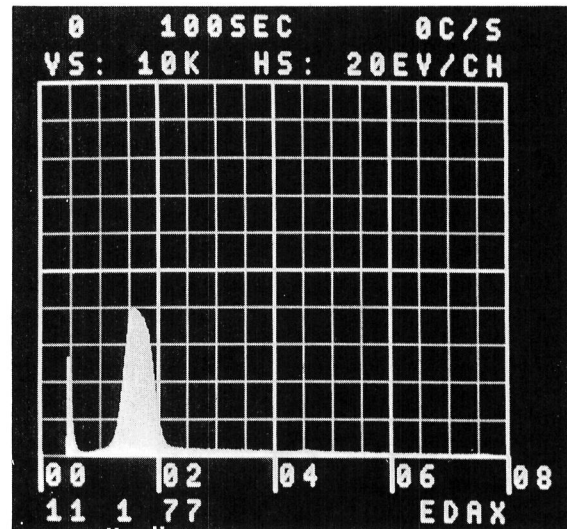
OXIDE INCLUSION AT
INITIATION SITE



LS23

67X

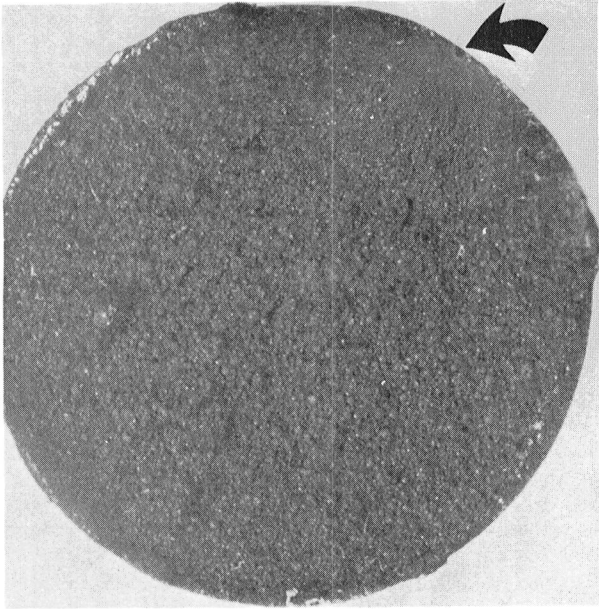
OXIDE INCLUSION AT
INITIATION SITE



Al/Si

EDAX INDICATING OXIDE
HIGH IN Al/Si

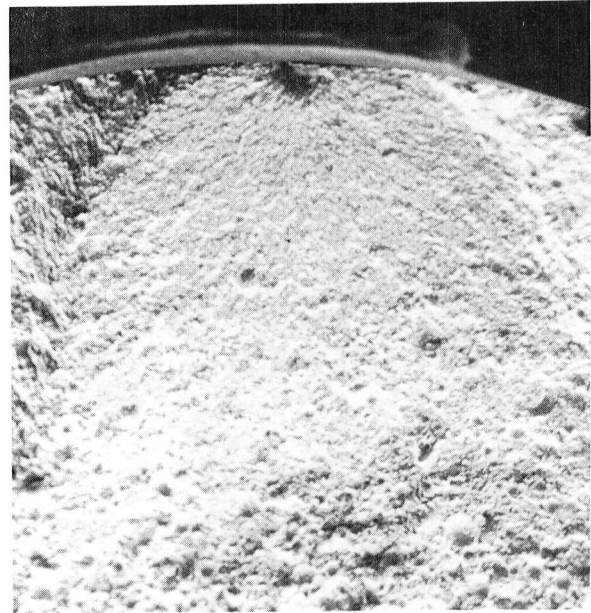
Figure 3-50. Fracture Surface of LCF Specimen LS23 Showing Example of Fatigue Initiation at Subsurface Oxide Inclusion



LS35

8X

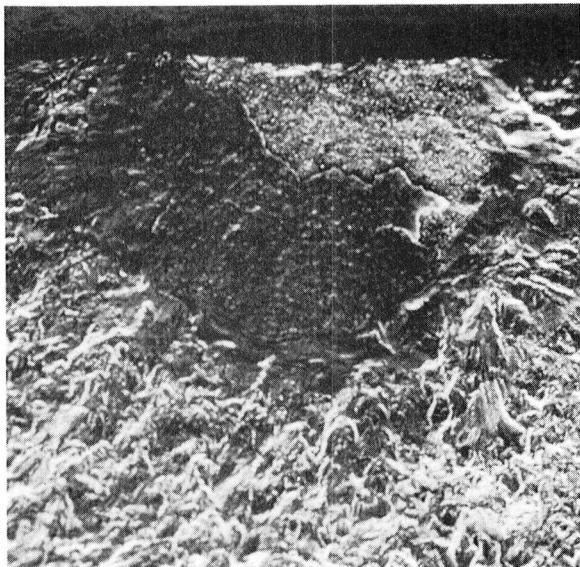
FATIGUE INITIATION AT SURFACE SITE



LS35

27X

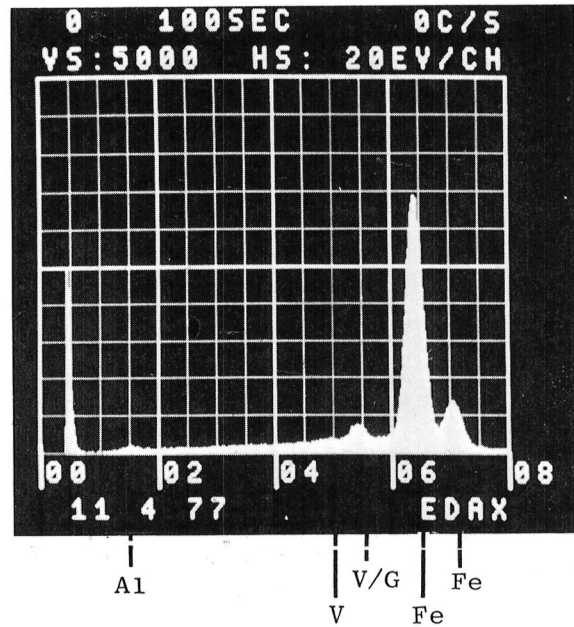
FATIGUE INITIATION AT SURFACE SITE



LS35

285X

M2 TOOL STEEL PARTICLE AT INITIATION SITE



EDAX INDICATING IRON RICH (M2 T.S.) INITIATION SITE

Figure 3-51. Fracture Surface of LCF Specimen LS35 Showing Example of Fatigue Initiation at M2 Tool Steel Particle

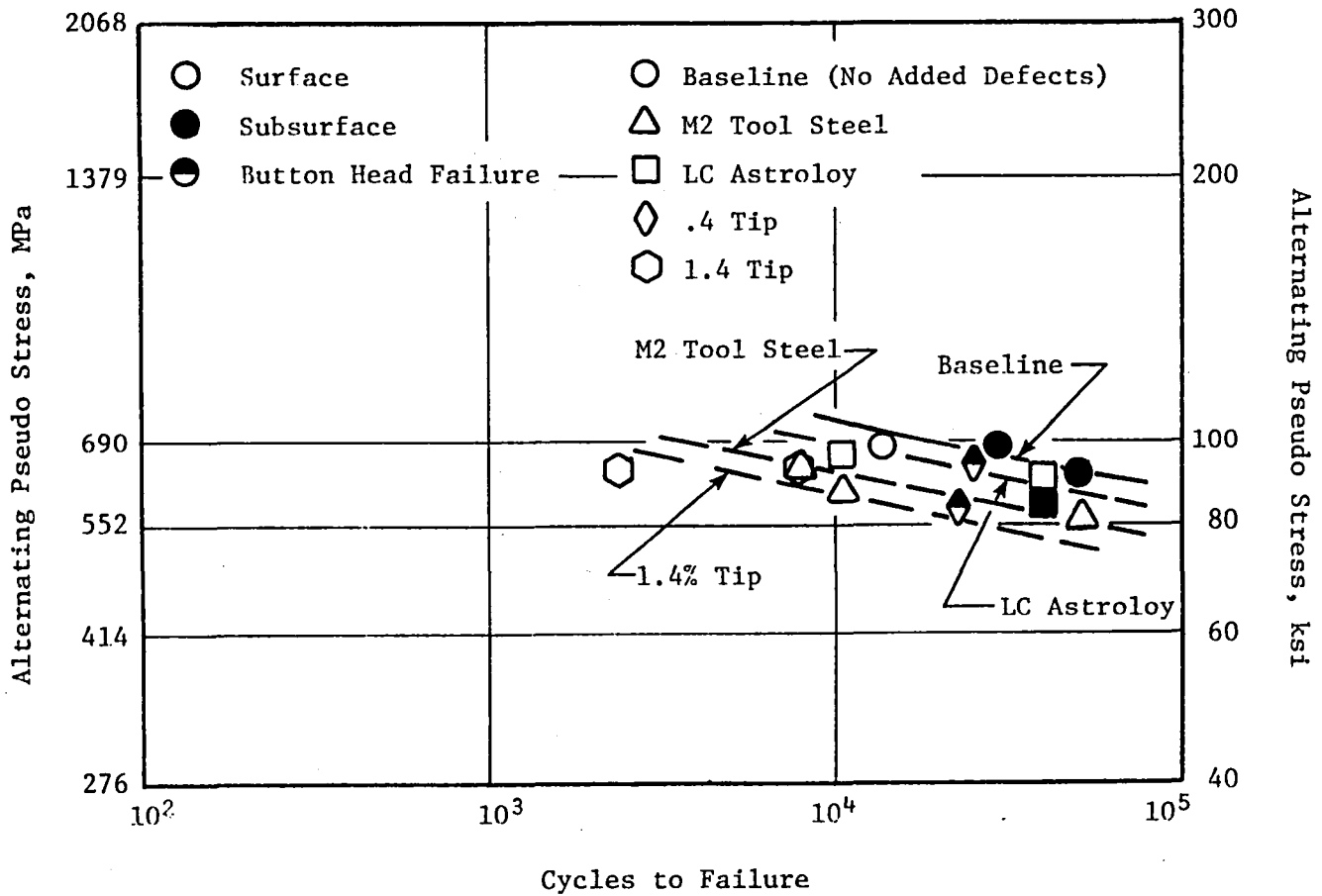


Figure 3-52. Effect of M2 Tool Steel, LC Astroloy, and Percent Tip on 538° C (1000° F) Strain Control ($A = 1$), $K_t = 1$ LCF.

as-HIP René 95 mechanical properties. Three different process deviations were evaluated with the test material prepared as follows:

- Standard -60 mesh point: Billet B462 was fabricated using standard -60 mesh powder with no intentional process deviations and was tested to establish baseline properties against which all of the other process variations were compared. The microstructure typical of the heat treated disks (B462-1, 2, and 3) is shown in Figure 3-53 and is representative of the as-HIP product given the standard processing cycle utilized in this program. The grain structure is not evident in the photomicrographs but the grain size is ~ASTM 8-10 which is typical of that obtained utilizing standard processing parameters.
- Particle Size Distribution: Two billets one with powder coarser than nominal (B468) and one with powder finer than nominal (B487), were prepared by screening standard -60 mesh powder through a 150 mesh screen to separate the powder into -60 +150 (coarse) and -150 (fine) mesh fractions. Analyses were performed on the three size fractions and, as shown in Table 3-24, the compositions are quite similar and meet specification requirements except for a slightly higher oxygen content (115 ppm) in the -150 mesh product. This increase in oxygen content is attributed to the high surface-to-volume ratio of this finer powder fraction. Table 3-25 lists the screen analysis, apparent density, consolidated density, and γ' solvus temperature for the different size fractions. Figures 3-54 and 3-55 are SEM photomicrographs showing the particle morphology of the -60 +150 and -150 mesh powder. Both billets were compacted under nominal HIP conditions 1121° C/103 MPa (2050° F/15 ksi) and heat treated to standard heat treat parameters 1121° C/816° C [(2050° F/1500° F) SQ + 871° C (1600° F)/1 hr + 649° C + (1200° F)/16 hrs]. The microstructures of the two billets are compared in Figure 3-56 and evidence of the difference in particle size distribution can be seen.
- HIP Compaction Temperature: In order to determine the effect of HIP temperature deviations, two billets of standard -60 mesh powder were compacted at HIP temperatures 28° C (50° F) below the nominal 1093° C (2000° F) - B464 and at 28° C (50° F) above the nominal 1149° C (2100° F) - B465. Disks sectioned from the billets were given standard heat treatments of 1121° C (2050° F)/816° C (1500° F) SQ + 811° C (1600° F)/1 hr + 640° C (1200° F)/16 hrs. Microstructures (heat treated condition) from each billet are shown in Figure 3-57.
- Solution Temperature: Two solution temperatures deviating from nominal 1121° C (2050° F) were evaluated to determine the effect on properties. Billet B463 was fabricated utilizing standard -60 mesh powder and compacted under nominal HIP conditions. The billet was then sectioned into four 3.18 cm (1.25 inch) thick disks: two of the disks were solution treated at 1093° C (2000° F) 28° C (50° F) below nominal, and two at 1149° C (2100° F) 28° C (50° F) above nominal. All four of the disks were quenched in 816° C (1500° F) salt and

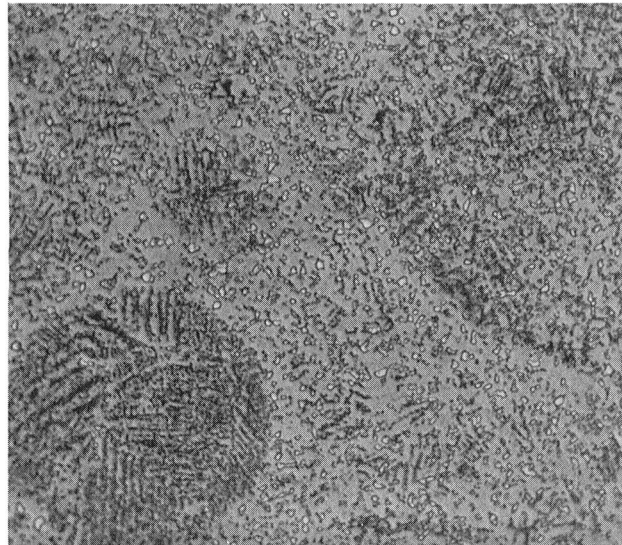
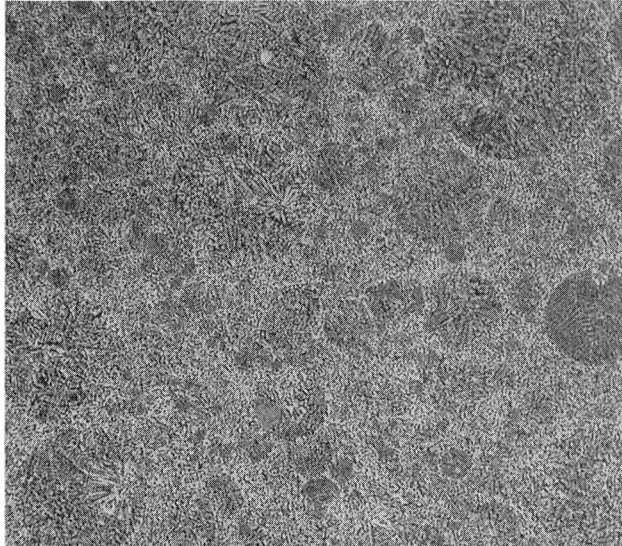


Figure 3-53. Microstructure of Standard -60 Mesh Product Fabricated Using Nominal HIP and Heat Treatment Parameters (Disk B462-1)

Table 3-24. Powder Compositions.

Element	MB048 - Weight %			C50TF64-S1
	-60 mesh	-60 +150 mesh	-150 mesh	
C	.050	.049	.050	.04/.09
Mn	<.01	<.01	<.01	.15 max
Si	.08	.08	.08	.20 max
S	.005	.004	.005	.015 max
P	≤.003	≤.003	≤.003	.015 max
Cr	12.86	12.90	12.87	12/14
Co	8.28	8.18	8.19	7/9
Mo	3.53	3.52	3.53	3.3/3.7
Fe	.05	.09	.09	.5 max
Ta	<.01	<.01	<.01	.2 max
Cb	3.50	3.52	3.50	3.3/3.7
Zr	.04	.05	.04	.03/.07
Ti	2.49	2.66	2.45	2.3/2.7
Al	3.61	3.49	3.53	3.3/3.7
B	.009	.008	.009	.006/.015
W	3.42	3.47	3.46	3.3/3.7
O	.0065	.0069	.0115	.010 max
N	.0030	.0026	.0027	.005 max
H	.00024	.00017	.00034	.001 max
Ni	Balance	Balance	Balance	Balance

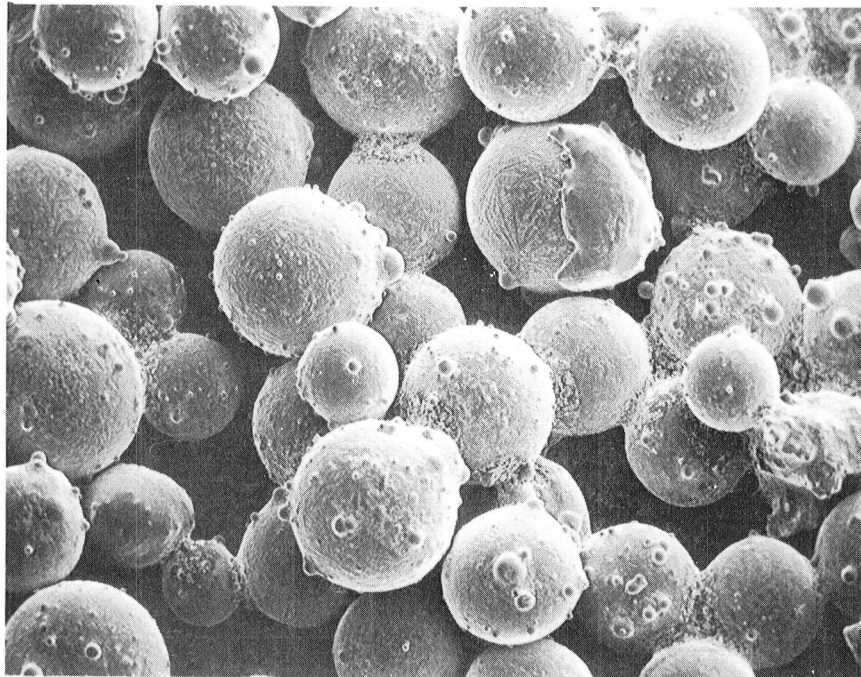
Table 3-25. Powder Characteristics of MB048.

Screen Analyses - %		
-60 mesh	-60 +150 mesh	-150 mesh
+60 - .5	+60 - .1	+150 - .2
-60 +100 - 29.2	-60 +80 - 30.8	-150 +170 - 10.1
-100 +325 - 55.0	-80 +100 - 21.1	-170 +200 - 11.4
-325 - 15.3	-100 +120 - 12.2	-200 +270 - 20.5
	-120 - 35.3	-270 +325 - 10.5
		-325 - 45.0

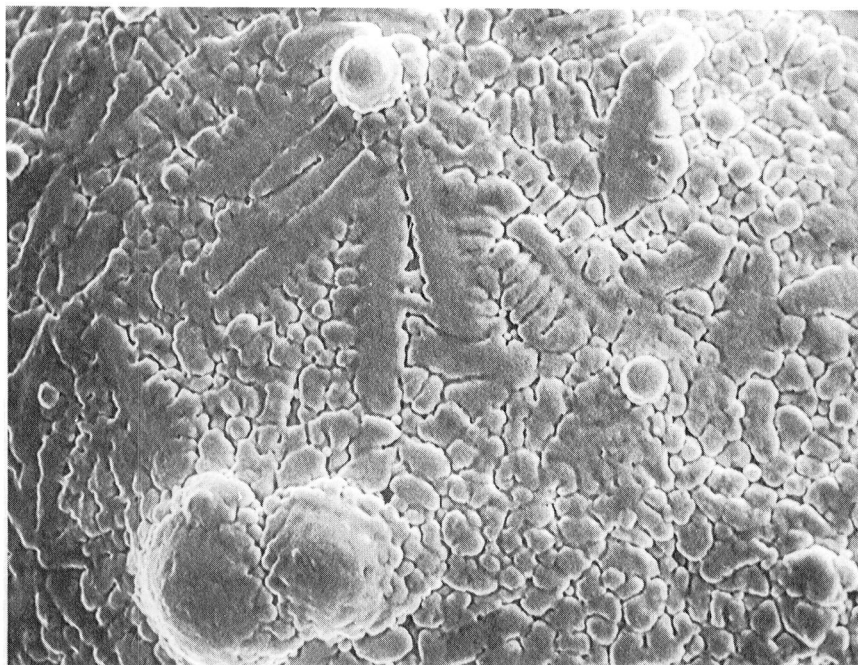
Apparent Density kg/m^3 (lb/in. ³)		
-60 mesh	-60 +150 mesh	-150 mesh
5000 (.1806)	4390 (.1586)	4880 (.1763)

Consolidated Density kg/m^3 (lb/in. ³)		
-60 mesh (B463)	-60 +150 mesh (B468)	-150 mesh (B469)
8248 (.2980)	8249 (.2980)	8247 (.2979)

γ' Solvus Temperature C (F)		
-60 mesh	-60 +150 mesh	-150 mesh
1169 (2135)	1169 (2135)	1169 (2135)

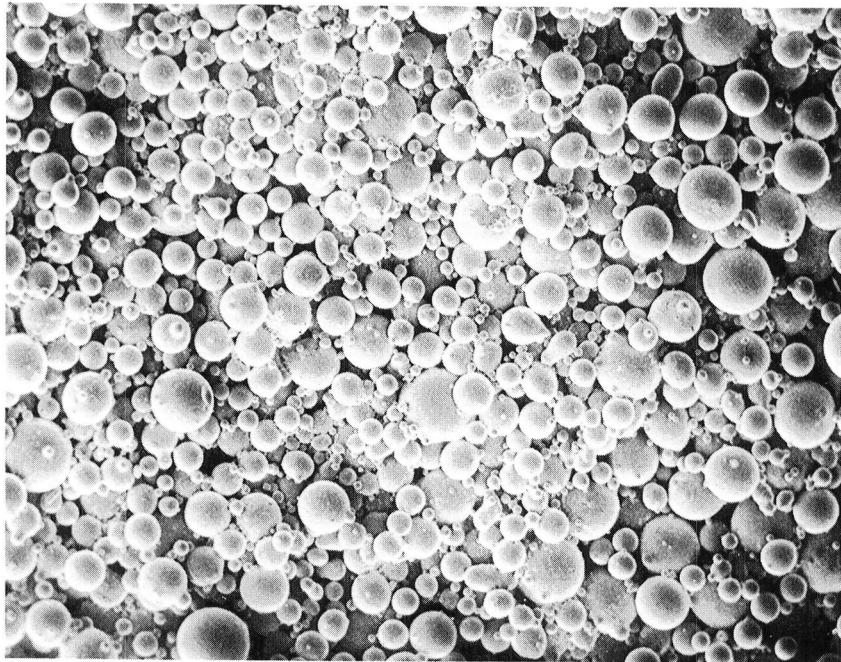


100X

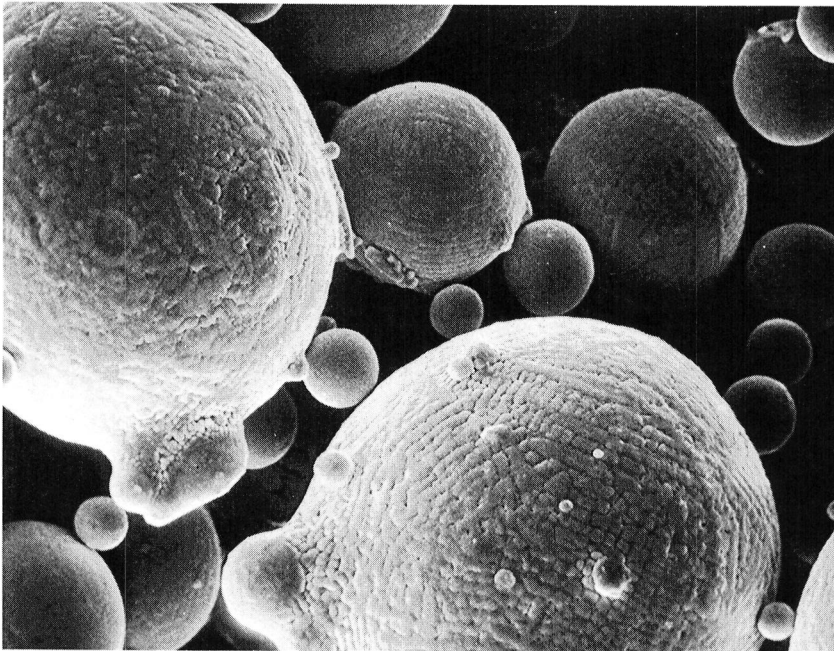


1000X

Figure 3-54. SEM Photomicrographs of Crucible
-60 +150 Mesh René 95 Powder (MB048).

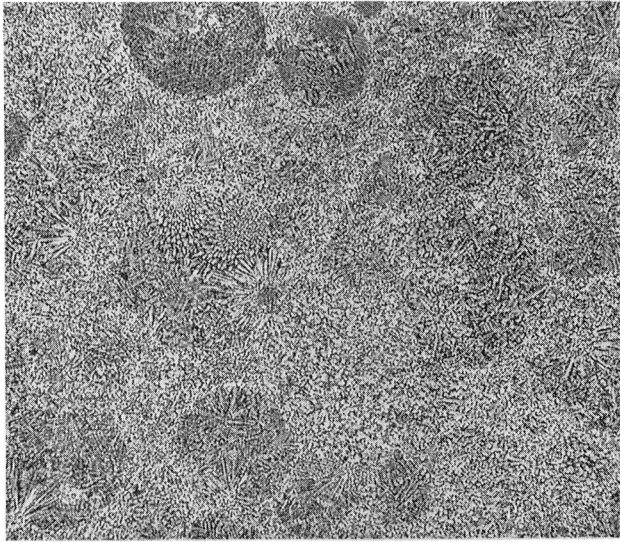


100X



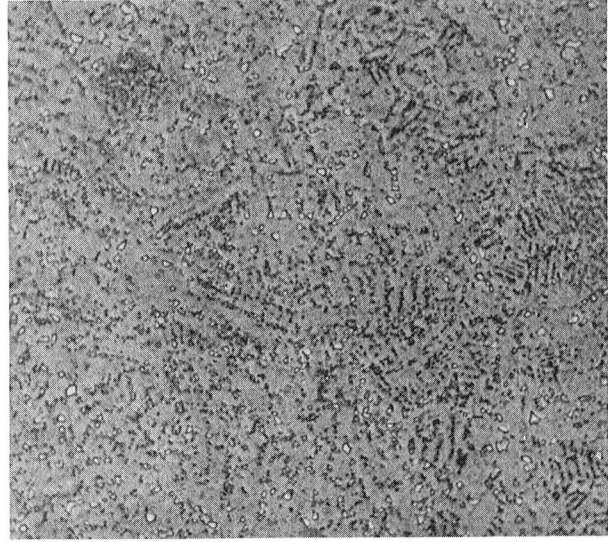
1000X

Figure 3-55. SEM Photomicrographs of Crucible
-150 Mesh René 95 Powder (MBO48).



8661

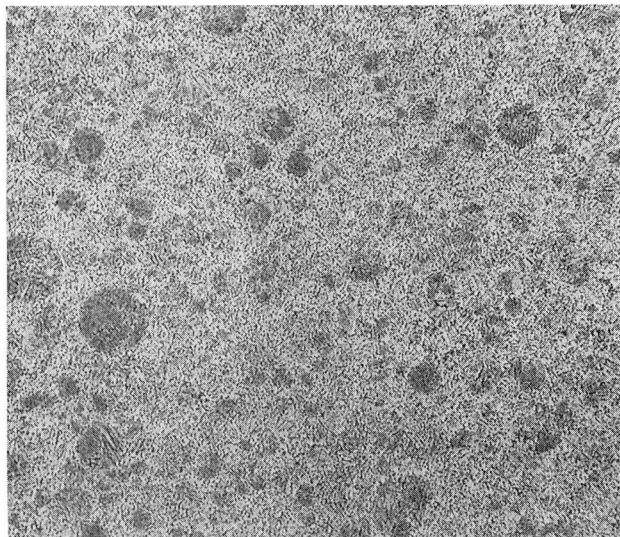
100X



8660

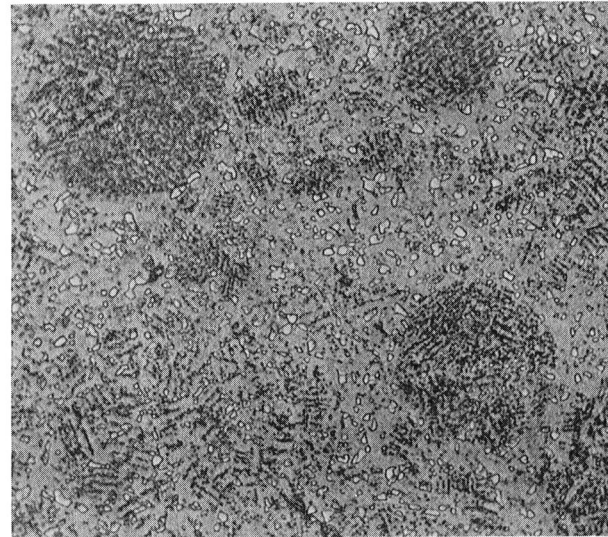
500X

BILLET B468 - -60 +150 MESH POWDER



8662

100X

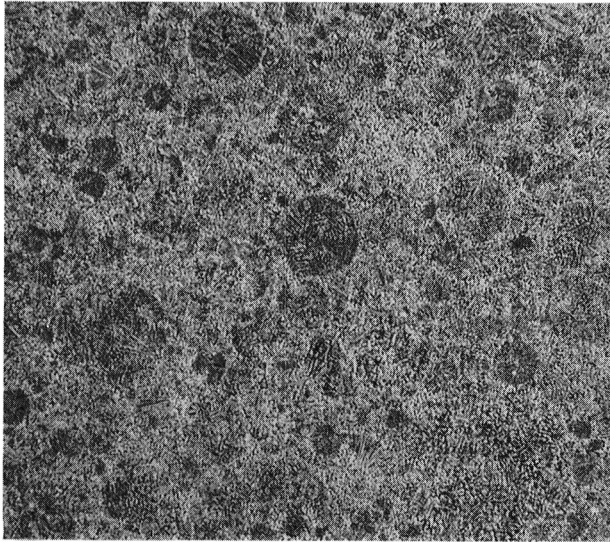


8662

500X

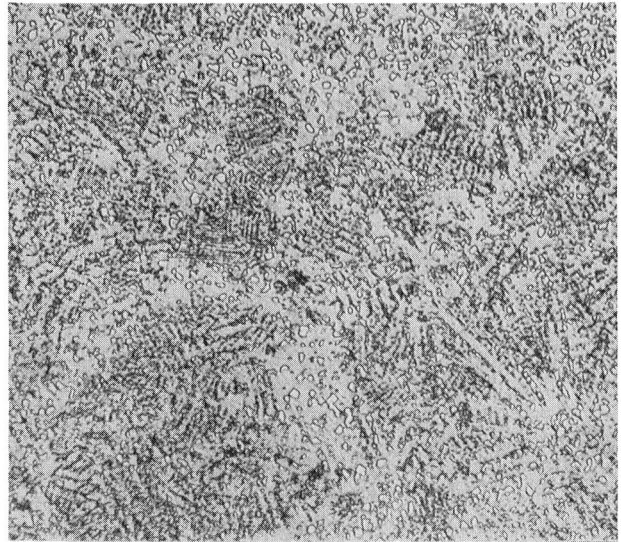
BILLET B487 - -150 MESH POWDER

Figure 3-56. Microstructures of Disks Made From -60 +150 (B468) and -150 (B487) Mesh Powder With Nominal HIP and Heat Treatment Parameters



8657

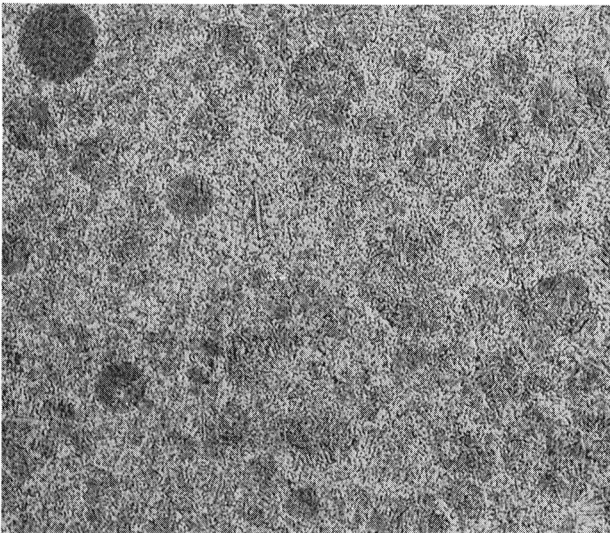
100X



8656

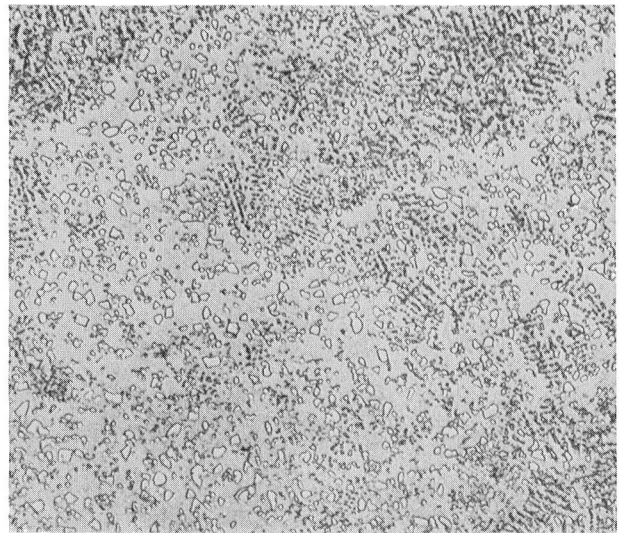
500X

Billet B464 - 1193° C (2000° F) HIP



8658

100X



8658

500X

Billet B465 - 1149° C (2100° F) HIP

Figure 3-57. Microstructures of Disks Compacted at 28° C (50° F) Below 1093° C (2000° F) - B464, and 28° C (50° F) Above 1149° C (2100° F) - B465, the Nominal HIP Temperature 1121° C (2050° F) and Given the Nominal Heat Treatment.

given the nominal aging treatment 871° C (1600° F)/1 hr + 649° C (1200° F)/16 hrs. Again, the 1149° C (2100° F) solution treatment resulted in an increased volume fraction of γ' in solution as shown in Figure 3-58.

The identification of the disks cut from the billets and the type, number, and specimen codes of the tests performed are outlined in Table 3-26. The methods used in the posttest analyses and the initiation site characterization for the process deviation study are the same as those described for the powder cleanliness portion of the program. The test results are summarized below:

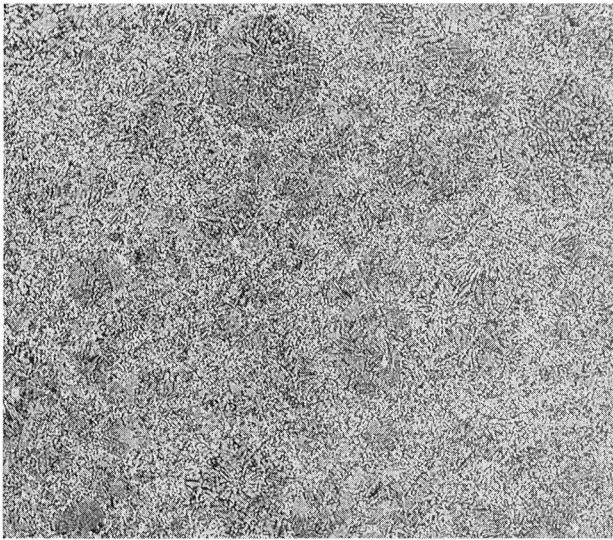
Effects of Process Deviations on As-HIP René 95 Mechanical Properties

- Particle size distribution
 - No major effect on properties
 - Trend toward improved LCF with -150 mesh
- HIP temperature
 - No significant effect on properties
 - $\pm 28^\circ$ C (50° F) tolerance acceptable with nominal 1121° C (2050° F) HIP temperature
- Solution temperature
 - No significant effect on properties
 - $\pm 28^\circ$ C (50° F) tolerance acceptable with nominal 1121° C (2050° F) solution temperature

A more detailed description of the effect of process deviations is presented below with respect to each test condition.

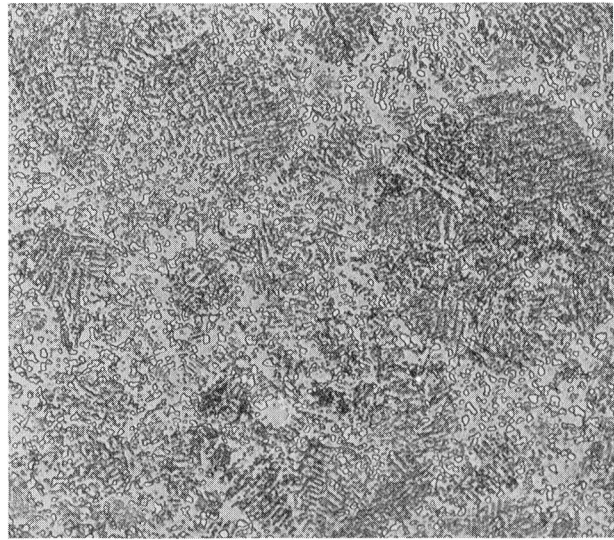
- Tensile Properties

The results of the RT and 649° C (1200° F) tensile tests are presented in Table 3-27. Tensile properties versus particle size distribution are plotted in Figure 3-59 which indicates no significant effect of powder particle size on 0.2%YS and UTS but shows a trend of increasing ductility with decreasing powder particle size. Figure 3-60 is a plot of tensile properties versus HIP temperature and indicates that there is no significant effect of HIP temperature on either RT or 649° C (1200° F) tensile properties, although the 1149° C (2100° F) HIP gave a slightly lower 0.2%YS at RT. Figure 3-61, a plot of tensile properties versus solution temperature, shows a trend of increasing strength and decreasing ductility with increasing solution temperature, particularly at 649° C (1200° F.) In summary only minor effects on tensile properties were observed for any of the process deviations and all conditions exceeded program requirements.



8654

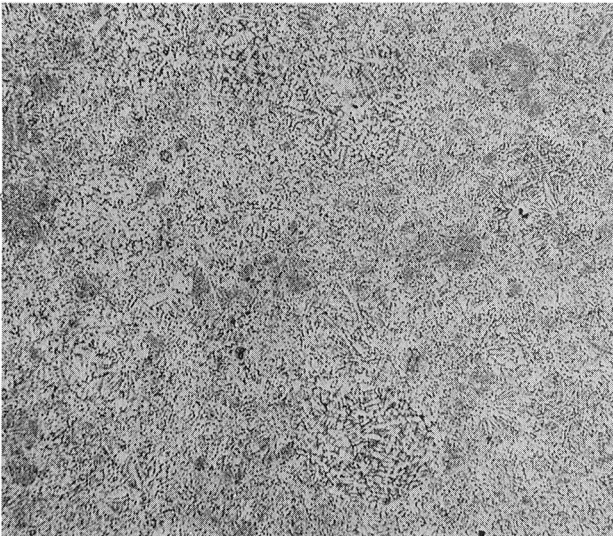
100X



8654

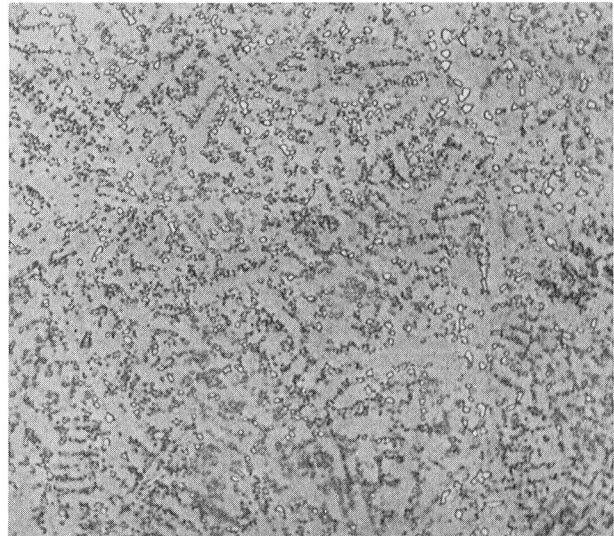
500X

Disk B463-3 - 1093° C (2000° F) Solution Temperature.



8652

100X



8652

500X

Disk B463-1 - 1149° C (2100° F) Solution Temperature.

Figure 3-58. Microstructures of Disks HIP Under Nominal Conditions and Then Solution Treated 28° C (50° F) Above 1149° C (2100° F) - B463-1 and 28° C (50° F) Below 1093° C (2000° F) - B463-3 Nominal Solution Temperature.

Table 3-26. Test Specimen Identification for Material Having Process Deviations.

Disk No.	Type of Test							
	Tensile RT		Rupture	LCF-S	LCF-N	K _B	Creep	SPLCF
	649° C	(1200° F)						
B462-1			T1	LS1			C1	S1
B462-2	T2			LS2	LN1	K1		S2
B462-3		T4	T3	LS3	LN2	K2		
B463-1	T5	T6		LS4	LN3, LN4			
B463-2	T9	T7	T8	LS5	LN5			
B463-3	T10	T11		LS6	LN6, LN7			
B463-4	T14	T12	T13	LS7	LN8			
B464-1	T15	T16		LS8	LN9, LN10			
B464-2	T19	T17	T18	LS9	LN11			
B465-1	T20	T21		LS10	LN12, LN13			
B465-2	T24	T22	T23	LS11	LN14			
B468-1	T26	T25		LS12	LN15	K3		
B468-2	T27	T28	T29	LS13	LN16		C2	S3
B487-1	T30			LS14	LN17		C3	
B487-2	T31	T33	T32			K4		
B487-3		T34		LS15	LN18			S4

Specimen Code	Type of Test	Qty.
T	Tensile & Rupture Bar	34
LS	Low Cycle Fatigue - Smooth Bar	15
LN	Low Cycle Fatigue - Notched Bar (K _T =3.5)	18
K	Residual Cyclic Life (K _B)	4
C	Creep	3
S	(Sustained Peak Low Cycle Fatigue- K _T =2)	

Table 3-27. Tensile Properties of Material Having Process Deviations.

Spec. No.	Disk No.	Process Deviation	0.2YS		UTS		EL (%)	RA (%)
			(MPa)	(KSI)	(MPa)	(KSI)		
Room Temperature								
T2	462-2	Standard	1169	(169.6)	1618	(234.7)	18.3	16.5
M1	462-1	Standard	1198	(173.7)	1617	(234.6)	17.9	16.6
M4	462-1	Standard	1174	(170.3)	1617	(234.6)	17.7	17.1
T5	B463-1	1149° C (2100° F) Sol Temp	1196	(173.5)	1621	(235.2)	15.7	17.8
T9	B463-2	1149° C (2100° F) Sol Temp	1167	(169.3)	1604	(232.7)	16.2	17.9
T10	B463-3	1093° C (2000° F) Sol Temp	1187	(172.2)	1536	(222.8)	12.5	14.4
T14	B463-4	1093° C (2000° F) Sol Temp	1166	(169.1)	1604	(232.7)	18.5	18.5
T15	B464-1	1093° C (2000° F) HIP	1167	(169.2)	1619	(234.9)	19.0	19.8
T19	B464-2	1093° C (2000° F) HIP	1175	(170.4)	1593	(231.1)	16.8	17.8
T20	B465-1	1149° C (2100° F) HIP	1150	(166.8)	1605	(232.9)	18.9	18.1
T24	B465-2	1149° C (2100° F) HIP	1124	(163.0)	1586	(230.1)	18.1	18.1
T26	B468-1	-60+150	1156	(167.7)	1580	(229.2)	15.7	17.6
T27	B468-2	-60+150	1162	(168.6)	1609	(233.5)	17.6	17.3
T30	B487-1	-150	1140	(165.3)	1607	(233.1)	20.5	17.1
T31	B487-2	-150	1162	(168.5)	1628	(236.2)	21.2	21.5
		Program Requirements	1034	(150.0)	1275	(185.0)	10.0	12.0
1200° F								
T4	B462-3	Standard	1048	(152.0)	1403	(203.5)	13.9	14.5
M2	B462-1	Standard	1088	(157.9)	1410	(204.6)	14.5	14.8
M3	B462-1	Standard	1084	(157.2)	1475	(214.0)	16.0	17.4
M5	B462-1	Standard	1079	(156.5)	1452	(210.6)	15.5	17.1
T6	B463-1	1149° C (2100° F) Sol Temp	1126	(163.3)	1482	(215.0)	10.2	11.3
T7	B463-2	1149° C (2100° F) Sol Temp	1087	(157.6)	1487	(215.7)	15.6	19.1
T11	B463-3	1093° C (2000° F) Sol Temp	1059	(153.6)	1436	(208.3)	18.2	17.7
T12	B463-4	1093° C (2000° F) Sol Temp	1081	(156.8)	1395	(202.4)	12.7	13.7
T16	B464-1	1093° C (2000° F) HIP	1056	(153.2)	1426	(206.9)	16.3	14.7
T17	B464-2	1093° C (2000° F) HIP	1079	(156.5)	1436	(208.3)	16.1	17.1
T21	B465-1	1149° C (2100° F) HIP	1057	(153.3)	1432	(207.8)	18.9	19.6
T22	B465-2	1149° C (2100° F) HIP	1058	(153.4)	1426	(206.8)	14.5	16.4
T25	B468-1	-60+150	1066	(154.6)	1438	(208.6)	13.7	15.5
T28	B468-2	-60+150	1069	(155.1)	1398	(202.9)	12.9	13.9
T33	B487-2	-150	1055	(153.0)	1434	(208.9)	21.5	17.7
T34	B487-3	-150	1052	(152.6)	1383	(200.6)	13.1	14.7
		Program Requirements	862	(125.0)	1000	(145.0)	8.0	10.0
<p>*Standard Process Parameters HIP Temperature = 1121° C (2050° F) Powder = -60 mesh Solution Temperature = 1121° C (2050° F)</p>								

● Solid Symbols Indicate Standard Minus 60 Mesh Condition

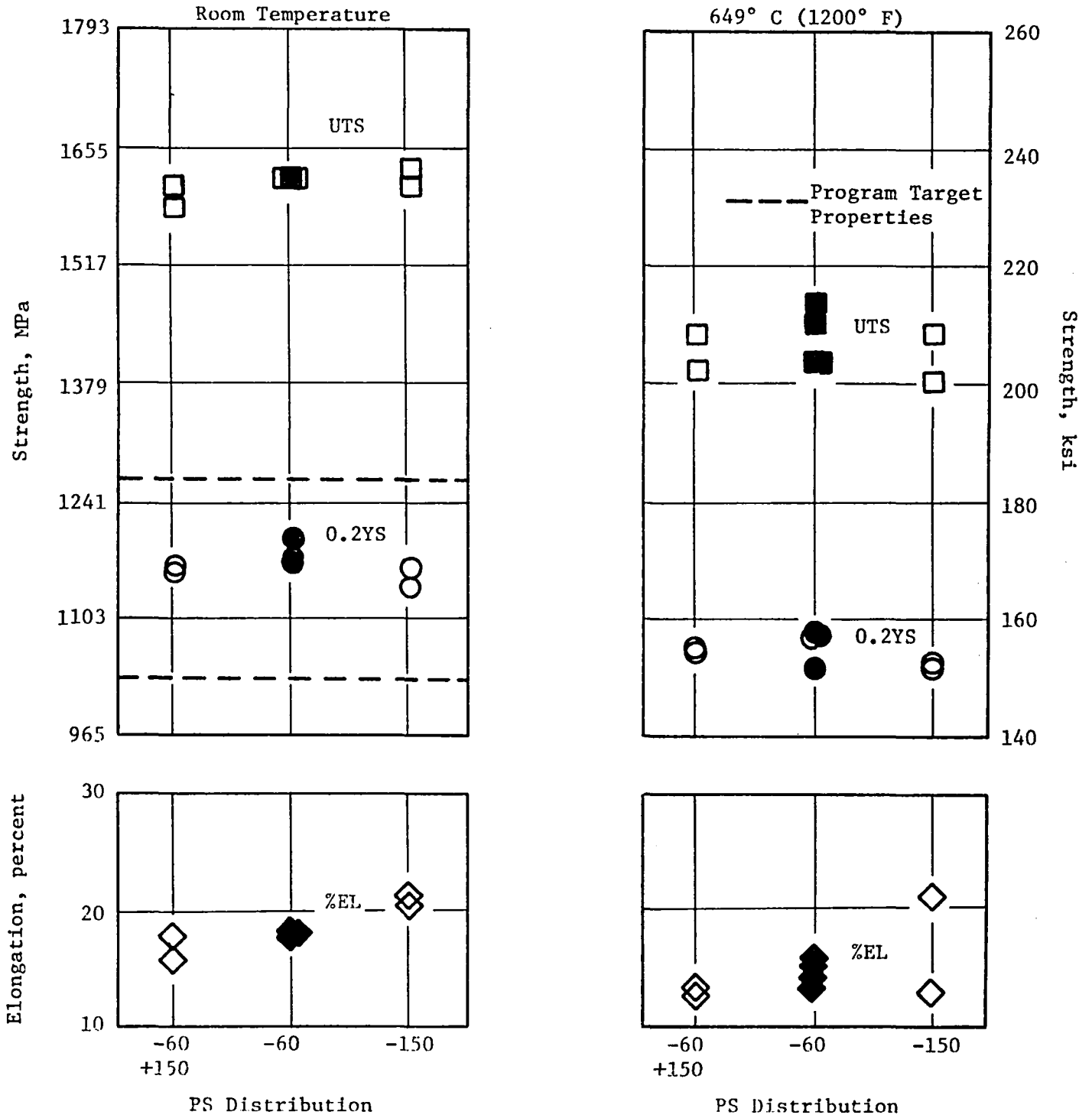


Figure 3-59. Effect of Particle Size Distribution on Tensile Properties of as-HIP René 95.

● Solid Symbols Indicate Standard HIP Condition

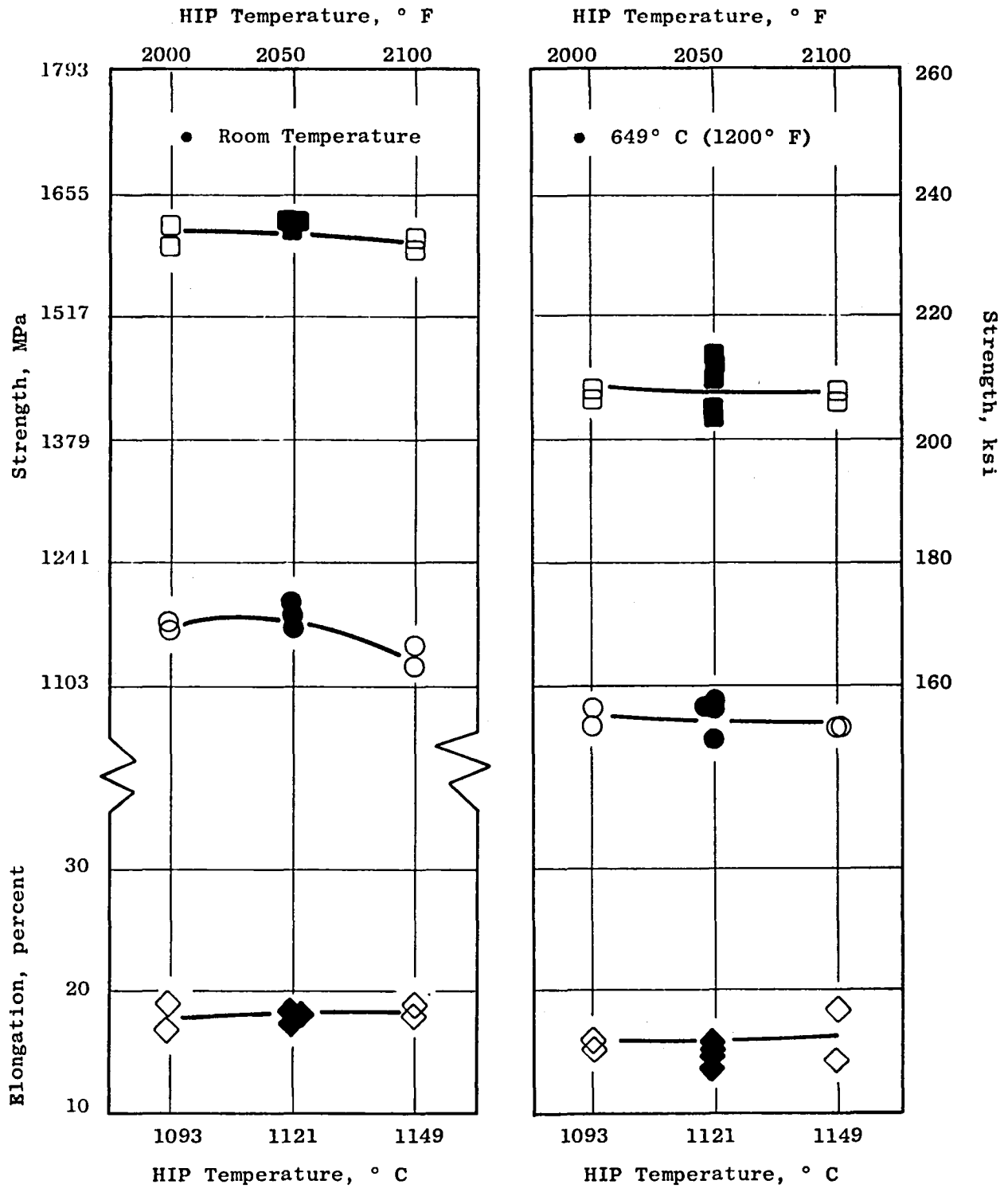


Figure 3-60. Effect of HIP Temperature on Tensile Properties of as-HIP René 95.

● Solid Symbols Indicate Standard 1121° C (2050° F) Heat Treat Condition

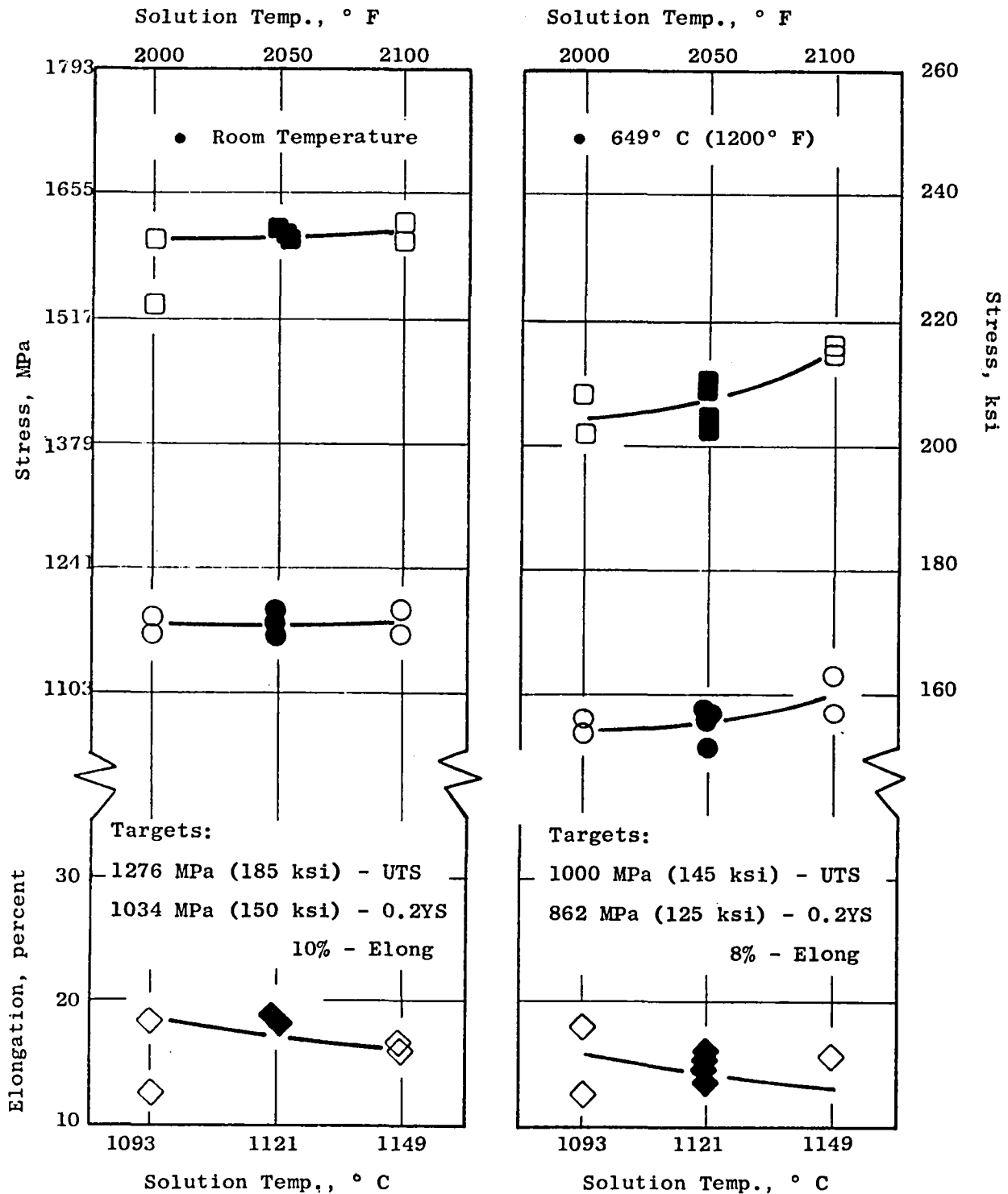


Figure 3-61. Effect of Solution Temperature on Tensile Properties of as-HIP René 95.

- Stress Rupture

The results of the stress rupture testing are presented in Table 3-28 and plotted in Figure 3-62. As seen in Figure 3-62 powder size distribution does not appear to have any significant effect on rupture life or ductility. Figure 3-62b shows a trend of decreasing life and ductility with increasing HIP temperature while Figure 3-62a shows no significant trend with respect to solution temperature. Just as for the tensile properties only minor effects were observed on stress rupture properties and all conditions would appear acceptable.

- Sustained Peak Low Cycle Fatigue (SPLCF)

The 593° C (1100° F) sustained peak low cycle fatigue data for the different powder size distributions are shown in Table 3-28. There is no major effect of size distribution on SPLCF. Also included in the table are the SPLCF data from the high TIP material. At the 1034 MPa (150 ksi) max stress level, there does not appear to be any effect of TIP on SPLCF, but at the lower stress 827 MPa (120 ksi) the material with the higher level of porosity gave reduced SPLCF life. However, in all cases, lives exceeded IN718 data.

- Creep

Creep tests were run only on the standard, -60+150, and -150 mesh products and the results are given in Table 3-29. The differences between the standard (C1) and the two deviations are not considered significant although the test from the -150 mesh material (C3) suggests a reduction in creep resistance possibly due to the finer grain structure obtained with the finer mesh product. The creep strength for all three conditions however far exceed that of Inconel 718.

- Residual Cyclic Life

Residual cyclic life data are also shown in Table 3-29 and indicate that particle size distribution has no significant effect on residual life. The data also suggest that increased porosity, at least at the levels tested, do not significantly degrade residual cyclic life.

- Notched Low Cycle Fatigue

The 538° C (1000° F) notched ($K_t=3.5$) load control low cycle fatigue tests conducted on the process deviation material are reported in Table 3-30. The data are plotted in Figures 3-63 through 3-65 to show the effect of powder size distribution, HIP temperature, and solution temperature, respectively. Each of the figures show a similar trend; that is, little effect of the particular process deviation at 276 MPa (40 ksi) alternating stress while at 241 MPa (35

Table 3-28. Stress Rupture and SPLCF Properties of Material Having Process Deviations.

Stress Rupture 649° C/965 MPa (1200° F/140 KSI)

Spec. No.	Disk No.	Process Deviation	Life (Hrs)	Elong (%)	RA (%)
T1	B462-1	Standard*	399.8	4.3	6.3
T3	B462-3	Standard	129.0	3.6	5.1
T8	B463-2	1149° C (2100° F) Sol Temp	221.1	3.0	5.5
T13	B463-4	1093° C (2000° F) Sol Temp	86.4	2.7	4.3
T18	B464-2	1093° C (2000° F) HIP	287.0	4.1	5.5
T23	B465-2	1149° C (2100° F) HIP	71.0	1.9	4.7
T29	B468-2	-60+150	174.6	4.3	7.8
T32	B487-2	-150	185.1	4.0	11.2
		Program Requirements	25.0	2.0	

Sustained Peak Low Cycle Fatigue (SPLCF)
 $K_t=2.0$, $R=0.03$ ($A=0.95$), 593° C (1100° F)

Spec. No.	Disk No.	Process Deviation	Max MPa Stress, (KSI)	Life (Cycles)
S1	B462-1	Standard*	1034.2 (150)	2009
S2	B462-2	Standard	1034.2 (150)	1005
S3	B468-2	-60+150	1034.2 (150)	967
S4	B487-3	-150	1034.2 (150)	1383
S5	B466-1	0.4% TIP	1034.2 (150)	1408
S6	B466-2	0.4% TIP	827.4 (120)	10015
+S7	A106	1.4% TIP	1034.2 (150)	1223
+S8	A106	1.4% TIP	827.4 (120)	3593

+ Inadvertently Tested at 538° C (1000° F)

* Standard Process Parameters

HIP Temperature 1121° C (2050° F)

Powder -60 mesh

Solution Temperature 1121° C (2050° F)

● 649° C/965.3 MPa (1200° F/140 ksi) Stress Rupture

● Target Properties

- Rupture Life: 25 hours Minimum

- Elongation: 2% Minimum

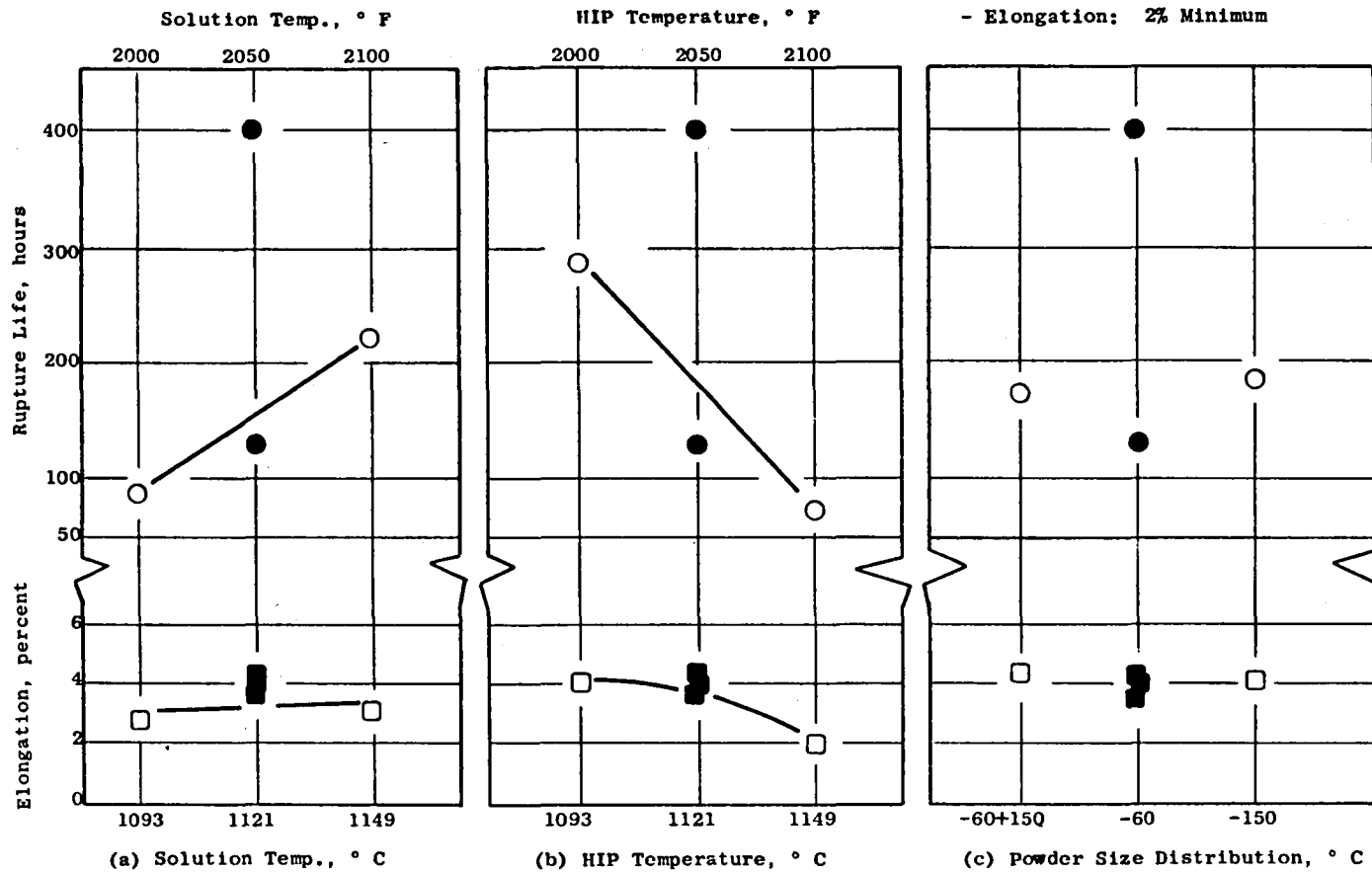


Figure 3-62. Effect of Solution Temperature and Powder Size Distribution on Stress Rupture Properties of as-HIP René 95.

Table 3-29. Effect of Process Variables on As-HIP René 95 Properties.

- Residual Cyclic Life*, 538° C, (1000° F), 0.51 x 1.52mm, (0.02 x 0.06) Crack, R=0.03, (A=0.95)

<u>Spec. No.</u>	<u>Disk No.</u>	<u>Process Variable</u>	<u>Max Stress</u>		<u>Life</u>
			<u>(MPa)</u>	<u>(ksi)</u>	<u>(Cycles)</u>
K1	B462-2	Standard	707	102.6	5572
K2	B462-3	Standard	707	102.6	6173
K3	B468-1	-60+150	707	102.6	6202
K4	B487-2	-150	707	102.6	6245
K5	B466-2	Argon (0.4% TIP)	707	102.6	4773
K6	SA106	Argon (1.4% TIP)	689	100.0	6747

*IN-718 Avg. 6000 Cycles

- Creep+, 593° C/965 MPa (1100° F/140 ksi)

<u>Spec. No.</u>	<u>Disk No.</u>	<u>Process Variable</u>	<u>Creep (%)</u>	<u>Time (Hrs)</u>
C1	B462-1	Standard	0.02	305.6
C2	B468-2	-60+150	0.07	303.8
C3	B487-1	-150	0.10	260.0

+IN-718 0.1% Creep in 300 hrs @ 593° C (1100° F) = 724 MPa (105 ksi)

Table 3-30. Effect of Process Deviations on As-HIP René 95 Properties Notched Load Control Low Cycle Fatigue.

R=0.03 (A=0.95,) 538° C (1000° F,) $K_t=3.5$

Spec. No.	Disk No.	Process Deviation	Alt Stress		Life* (Cycles)
			(MPa)	(ksi)	
L1		Standard	241	35.0	177,617+
L2		Standard	276	40.0	10,198
LN1	B462-2	Standard	241	35.0	16,823
LN2	B462-3	Standard	241	35.0	20,411
LN3	B463-1	1149° C (2100° F) Sol Temp	241	35.0	16,830
LN4	B463-1	1149° C (2100° F) Sol Temp	241	35.0	20,894
LN5	B463-2	1149° C (2100° F) Sol Temp	276	40.0	9,512
LN7	B463-3	1093° C (2000° F) Sol Temp	241	35.0	160,481+
LN8	B463-4	1093° C (2000° F) Sol Temp	276	40.0	8,587
LN9	B464-1	1093° C (2000° F) HIP	241	35.0	24,039
LN10	B464-1	1093° C (2000° F) HIP	276	40.0	7,556
LN11	B464-2	1093° C (2000° F) HIP	276	40.0	4,292
LN12	B465-1	1149° C (2100° F) HIP	241	35.0	101,675+
LN13	B465-1	1149° C (2100° F) HIP	276	40.0	13,472
LN14	B465-2	1149° C (2100° F) HIP	276	40.0	5,543
LN15	B468-1	-60+150	241	35.0	111,010+
LN16	B468-2	-60+150	276	40.0	9,253
LN17	B487-1	-150	241	35.0	109,684+
LN18	B487-3	-150	276	40.0	7,486

*+ Indicates test stopped at indicated cycles without failure.

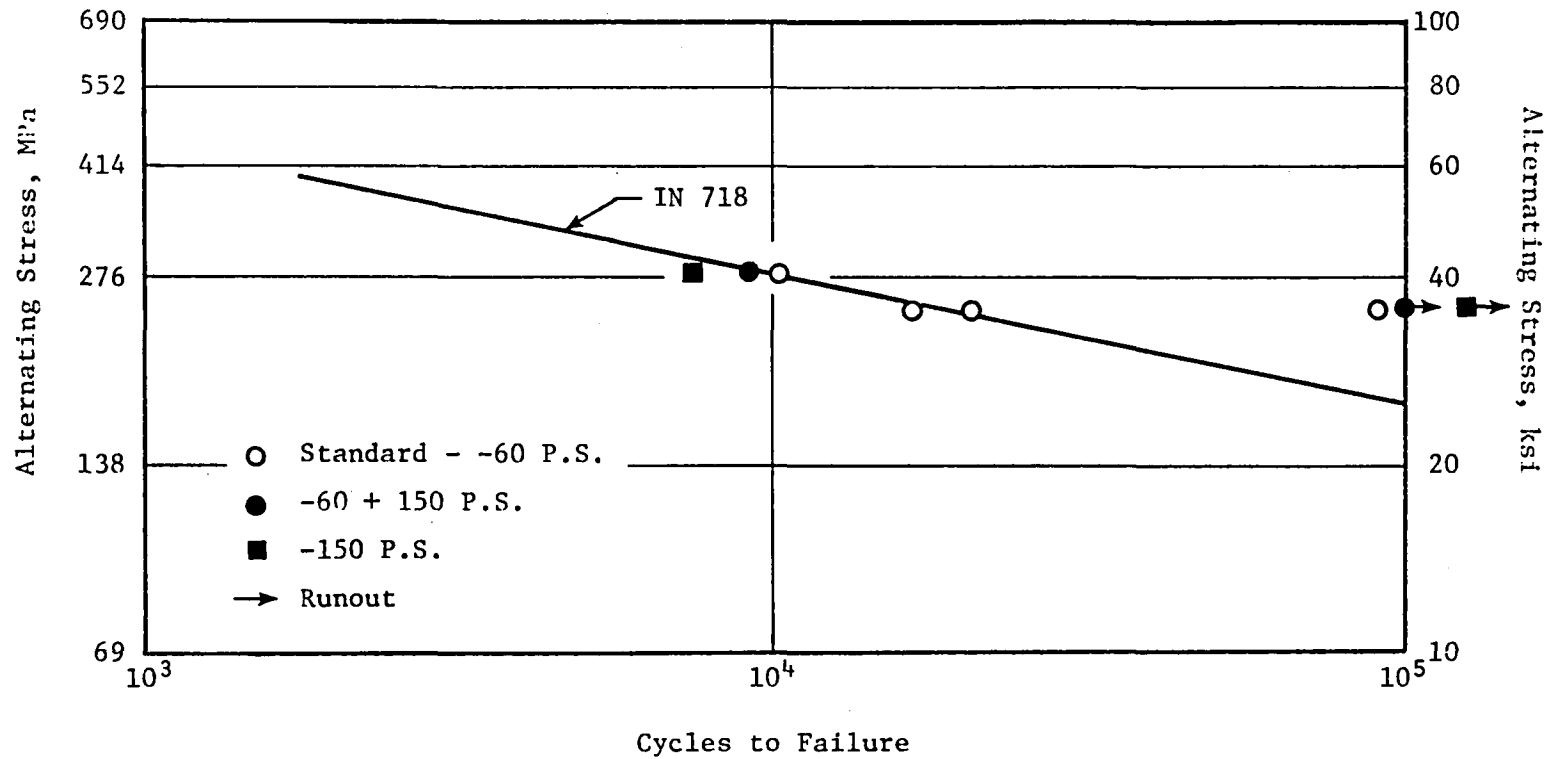


Figure 3-63. Effect of Particle Size Distribution on 538° C (1000° F) Notched ($K_t = 3.5$) Load Control Low Cycle Fatigue.

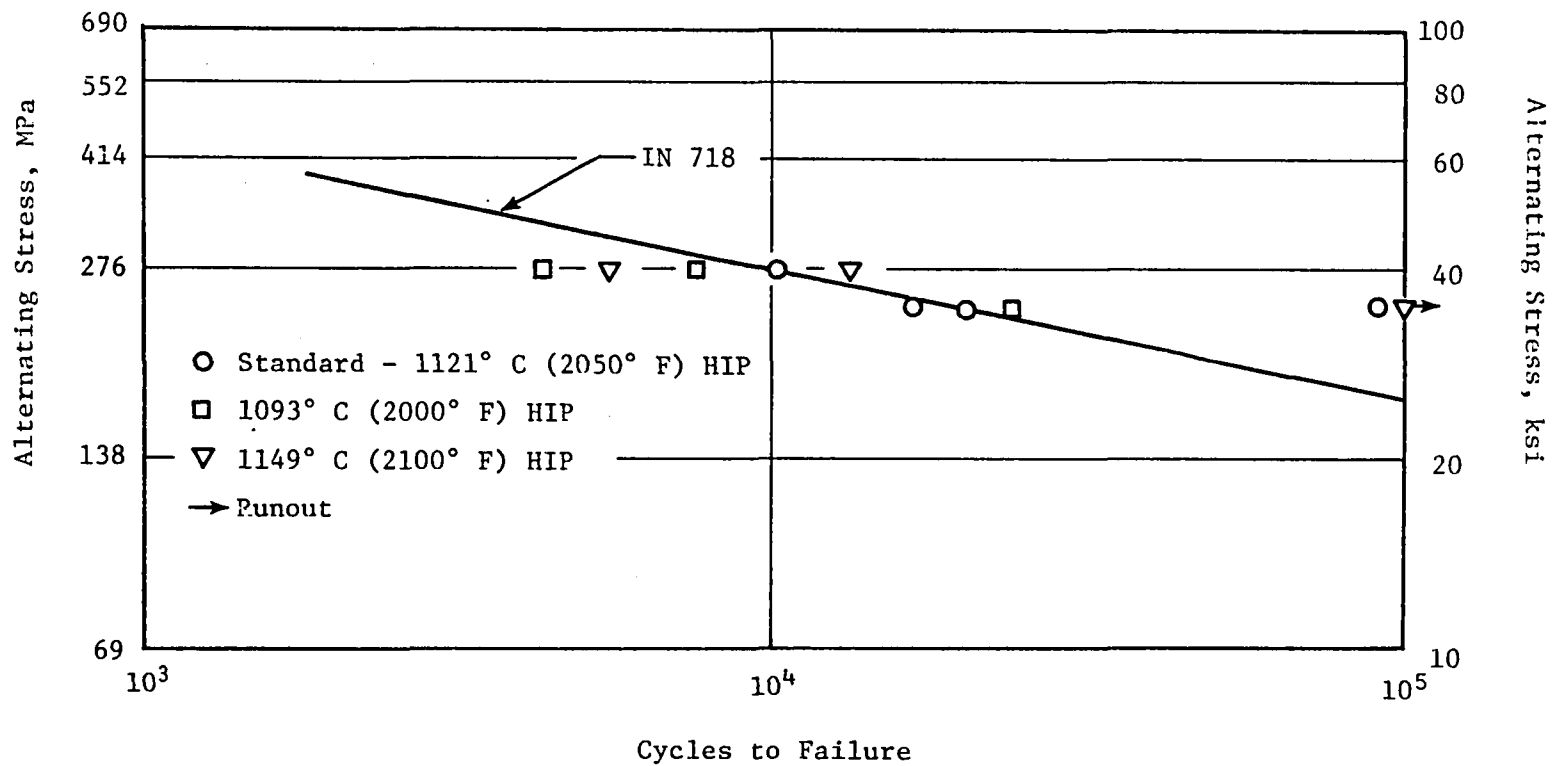


Figure 3-64. Effect of HIP Temperature on 538° C (1000° F) Notched ($K_t = 3.5$) Load Control Low Cycle Fatigue.

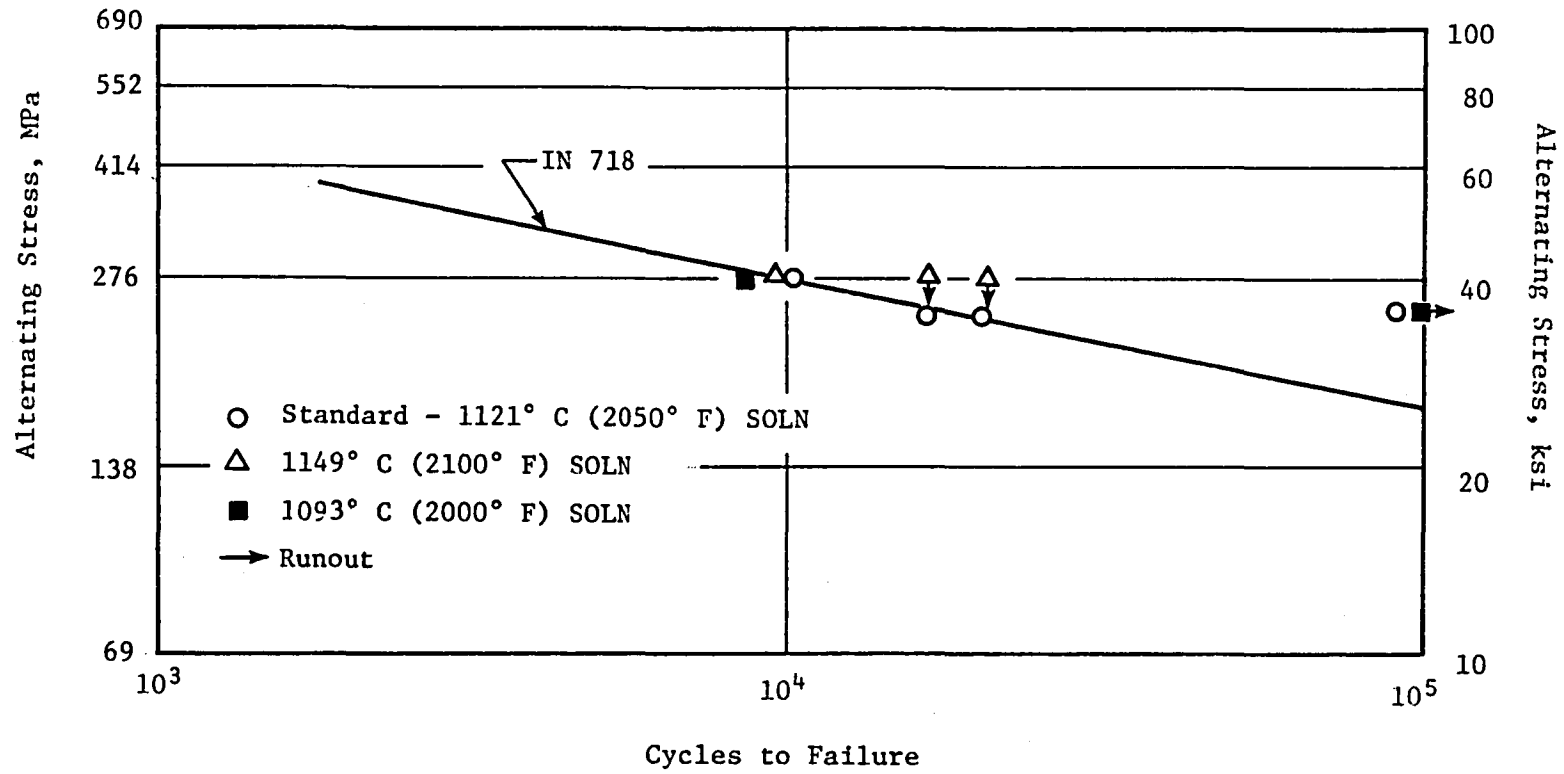


Figure 3-65. Effect of Solution Temperature on 538° C (1000° F) Notched $K_t = 3.5$ Load Control Low Cycle Fatigue.

ksi) alternating stress significant data scatter exists. It is believed that the scatter is not a result of the effect of the process deviations but is a direct result of the as-HIP René 95 curve being very flat (approaching runout) at this low stress level.

- Smooth Bar Low Cycle Fatigue

The 538° C (1000° F) strain control low cycle fatigue [axial-axial R=0 (A=1), $K_t=1$] properties of material processed with deviations from nominal are presented in Table 3-31. As seen in the table, 11 of the 15 specimen failures initiated at subsurface sites, 3 at surface sites, and one specimen (LS15) was a runout. The data are plotted in Figure 3-66 on a life versus alternating pseudo stress basis with a curve drawn through the standard points to represent the baseline LCF capability. All of the data populate the average for the standard material indicating that there is no major influence of any of the process variables on life. However, there are some trends in the data which suggest that (1) failure initiation at surface related inhomogeneities results in lower life than initiation at subsurface sites and (2) -150 mesh powder offers a possible advantage in LCF capability.

In summary, none of the process deviations resulted in a significant variation from the standard, indicating that the process tolerance on HIP temperature, 1121° C $\pm 14^\circ$ C (2050° F $\pm 25^\circ$ F), solution temperature 1121° C $\pm 15^\circ$ F, and particle size distribution are within acceptable production limits.

3.2.2 Task III - Manufacturing As-HIP Shapes

As described earlier in Section 3.1 (as-HIP Material Envelope Design) CF6-50 HPTR aft shaft parts were produced in Task III for demonstrating reproducibility of the process as well as for cut-up mechanical property evaluation, and for final machining and engine testing. The following sections present the results of the mechanical property testing of these parts.

3.2.2.1 Mechanical Properties - CF6-50 HPT Aft Shaft

The objective of this task was to establish the mechanical property levels of the as-HIP René 95 CF6-50 HPT aft shaft. Two parts (SM582 and SM5900) from the pilot production run were selected for the mechanical property characterization. Both parts were made from powder blend MB048. A summary of the testing performed is presented in Table 3-32 and the cut up plans for the two parts are shown in Figures 3-67 and 3-68.

Metallographic sections were taken from various locations in the shafts and showed acceptable microstructures, typical of as-HIP René 95 given the 1121° C (2050° F) solution treatment. Figure 3-69 shows microstructures typical of each shaft and, as seen in the figure, the same structure was obtained

Table 3-31. Effect of Process Deviations on As-HIP René 95 Properties 538° C (1000° F) Strain Control LCF.

R=0.03 (A=0.95,) 538° C (1000° F,) $K_t=3.5$

Spec. No.	Disk No.	Process Deviation	Strain Range (%)	Modulus, TPa (X 10 ⁶ PSI)	Alt Pseudo Stress, MPa (KSI)	Life (Cycles)	Initiation Site Location
LS1	B462-1	Standard	0.68	0.194 (28.2)	661 (95.9)	31,806	Sub
LS2	B462-2	Standard	0.68	0.196 (28.5)	668 (96.9)	14,196	Surf
LS3	B462-3	Standard	0.62	0.197 (28.6)	617 (88.7)	53,380	Sub
LS4	B463-1	1149° C (2100° F) Sol Temp	0.62	0.198 (28.7)	614 (89.0)	36,120	Sub
LS5	B463-2	1149° C (2100° F) Sol Temp	0.68	0.198 (28.8)	675 (97.9)	10,279	Surf
LS6	B463-3	1093° C (2000° F) Sol Temp	0.62	0.200 (29.0)	606 (87.9)	42,827	Sub
LS7	B463-4	1093° C (2000° F) Sol Temp	0.68	0.198 (28.7)	673 (97.6)	32,962	Sub
LS8	B464-1	1093° C (2000° F) HIP Temp	0.62	0.187 (27.1)	579 (84.0)	52,135	Sub
LS9	B464-2	1093° C (2000° F) HIP Temp	0.68	0.199 (28.9)	678 (98.3)	34,280	Sub
LS10	B465-1	1149° C (2100° F) HIP Temp	0.68	0.196 (28.5)	668 (96.9)	43,250	Sub
LS11	B465-2	1149° C (2100° F) HIP Temp	0.62	0.183 (26.6)	569 (82.5)	103,250	Sub
LS12	B468-1	-60+150	0.70	0.198 (28.7)	693 (100.5)	7,766	Surf
LS13	B468-2	-60+150	0.62	0.196 (28.4)	607 (88.1)	47,562	Sub
LS14	B487-1	-150	0.70	0.196 (27.9)	674 (97.7)	55,882	Sub
LS15	B487-3	-150	0.62	0.182 (26.4)	564 (81.8)	143,440+	Did Not Fail

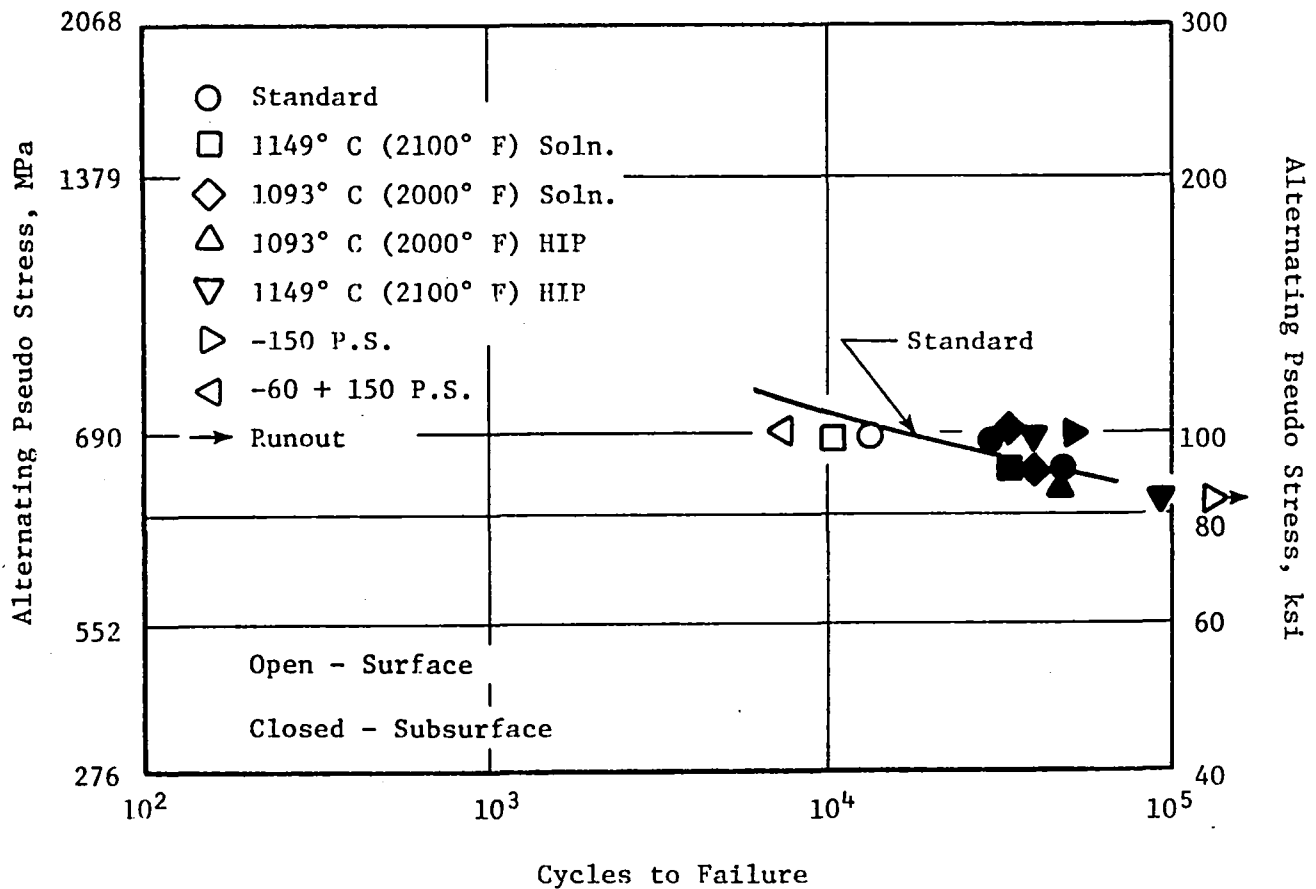


Figure 3-66. Effect of Process Deviations on 538° C (1000° F) Strain Control Low Cycle Fatigue $R = 0$, $(A = 1)$, $K_t = 1$ (Data from Table 3-31).

Table 3-32. Summary of Mechanical Property Tests on HPT Rear Shaft.

	<u>Planned Testing</u>
<u>Tensile</u>	
● Room Temperature	4
● 204° C (400° F)	4
● 427° C (800° F)	5
● 538° C (1000° F)	5
● 649° C (1200° F)	4
<u>Stress Rupture</u>	
● 593° C (1100° F) at stress to product failure	6
● 649° C (1200° F) over the 50-1000 Hr. range	6
● 704° C (1300° F)	6
<u>Creep</u>	
● 649° C (1200° F) at stress to define 0.2% creep	2
● 704° C (1300° F) over the 50-1000 Hr. range	1
<u>Notched Tensile</u>	
● Room Temperature	3
● 427° C (800° F)	2
● 538° C (1000° F)	2
● 649° C (1200° F)	3
<u>Low Cycle Fatigue (Load Control)</u>	
● 371° C (700° F)/ $K_t=3.5A=0.95$	4
● 482° C (900° F)/ $K_t=1.5/A=0.95$	6
● 593° C (1100° F)/ $K_t=1.5/A=0.95$	6
● 427° C (800° F)/ $K_t=1.0/A=0.95$	6
<u>Low Cycle Fatigue (Strain Control)</u>	
● 538° C (1000° F)/ $K_t=1/A=1$	3
<u>Sustained Peak Low Cycle Fatigue, $K_t=2, A=0.95$</u>	
● 594° C (1100° F)	6
<u>Residual Cyclic Life (K_B)</u>	
● 538° C (1000° F) Crack 0.51mm x 1.52mm (.020"x.060")/ $A=0.95$	3
<u>Dynamic Modulus of Elasticity</u>	
● Room Temperature - 816° C (1500° F)	1
<u>Thermal Expansion</u>	
● Over range Room Temperature - 704° C (R.T. - 1200° F)	1
<u>Density</u>	<u>5</u>
Total	92

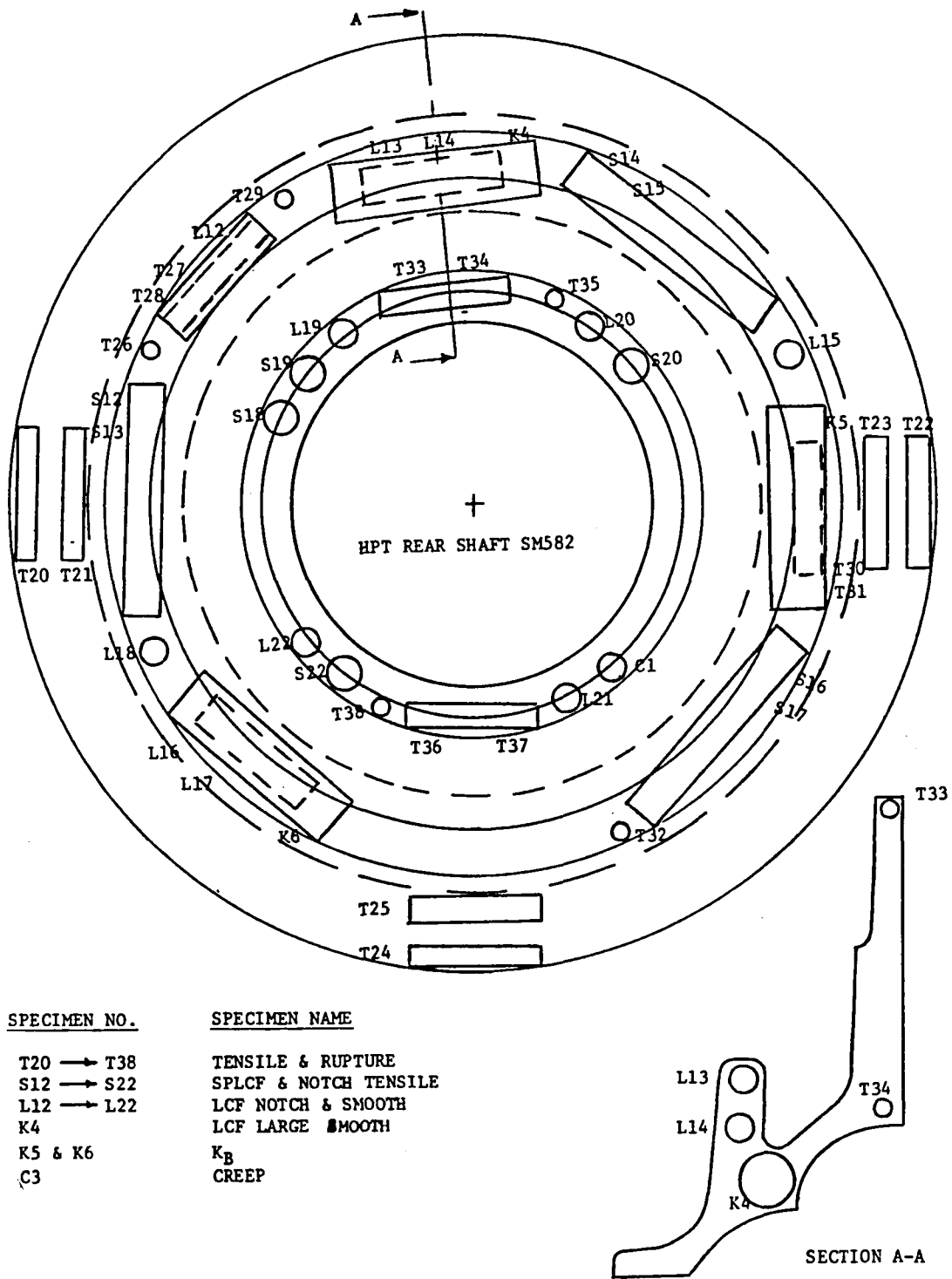
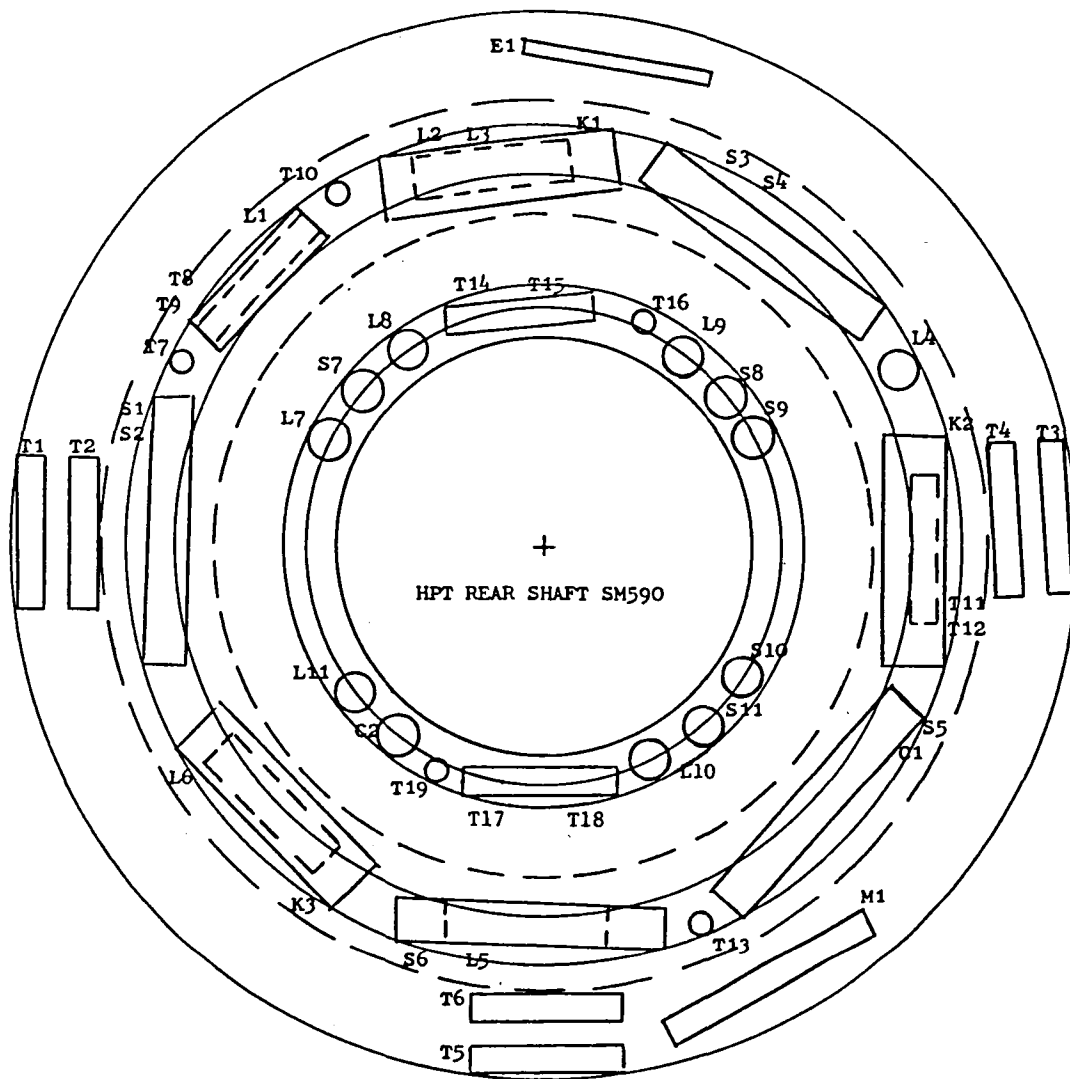
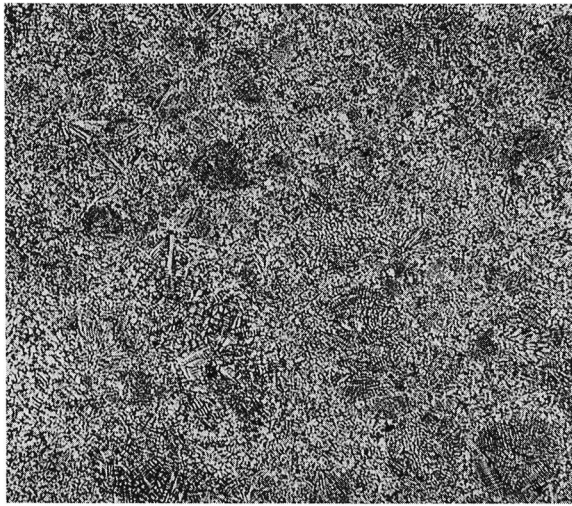


Figure 3-67. As-HIP CF6-50 Shaft Test Specimen Layout.



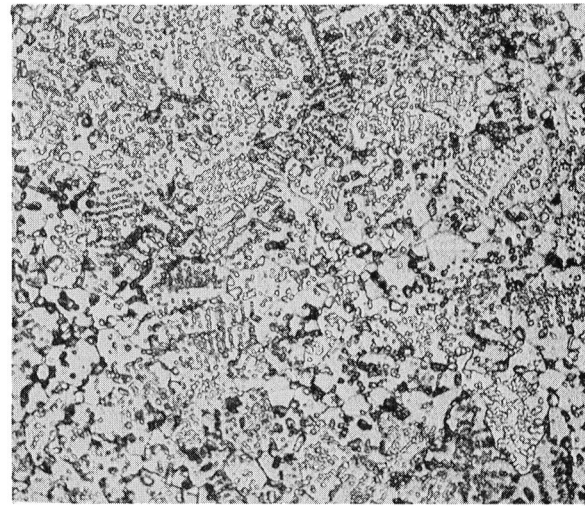
<u>SPECIMEN NO.</u>	<u>SPECIMEN NAME</u>
T1 → T19	Tensile & Rupture
S1 → S11	SPLCF & Notch Tensile
L1 → L11	LCF Notch & Smooth
E1	Thermal Expansion
M1	Dynamic Modulus
K1 & K3	LCF Large Smooth
K2	K_B
C1 & C2	Creep

Figure 3-68. As-HIP CF6-50 Test Specimen Layout.



100X

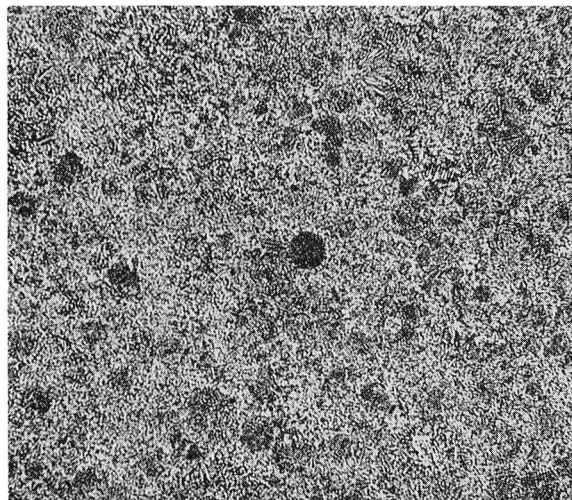
14208



500X

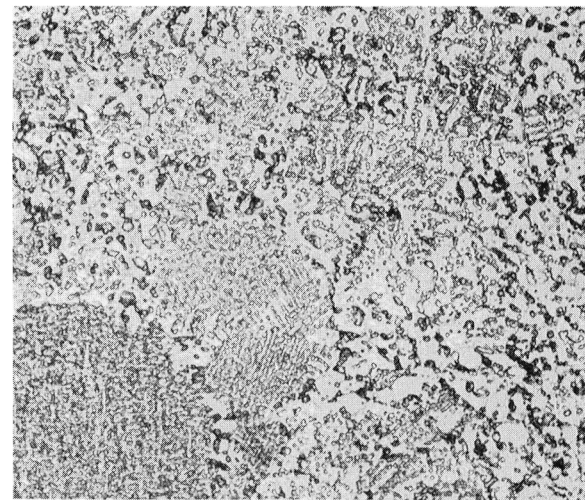
14208

SHAFT SM 582



100X

14205



500X

14205

SHAFT SM 590

Figure 3-69. Photomicrographs Showing Typical Microstructures of As-HIP Rene' 95 CF6-50 HPT Rear Shafts SM 582 and SM 590

in each part. Density and TIP evaluations were also conducted at several locations from each shaft and the data is shown in Figure 3-70 together with the locations from which the test were taken. As can be seen in the figure, the density values compare well with the standard density for this powder blend and the TIP values (density decrease after 1204° C (2200° F) 4 hr. exposure) fall within the 0.3% specification limit. The tensile data, from RT through 649° C (1200° F), is reported in Table 3-33 and plotted in Figures 3-71 and 3-72. All of the test data exceed minimum program requirements.

The stress rupture testing was conducted in the 593° C (1100° F) to 704° C (1300° F) temperature range and the results are shown in Table 3-34. A Larson-Miller parameter plot of the stress rupture data using a C value of 25 is presented in Figure 3-73.

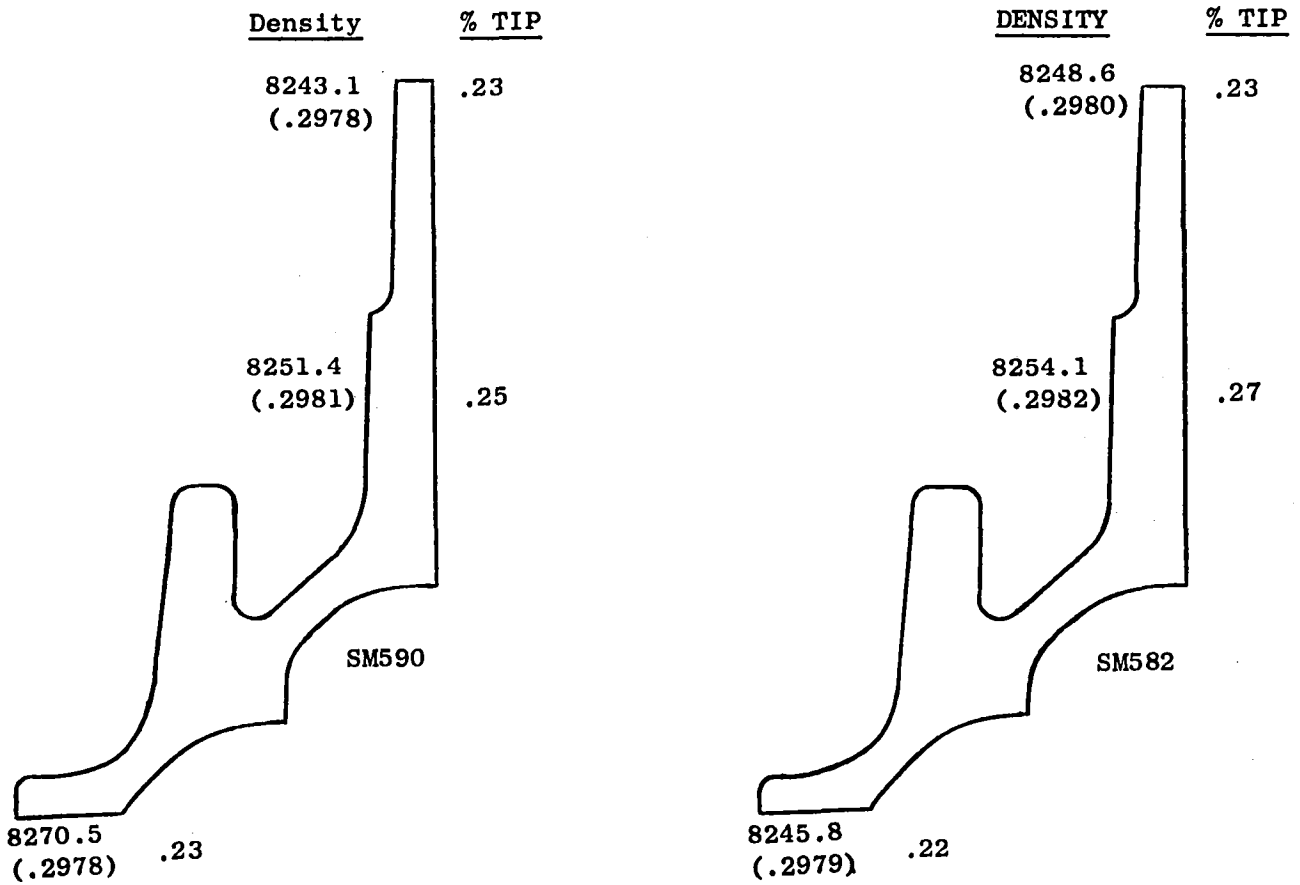
Creep testing was performed at (593° C and 704° C) (1200 and 1300° F) and the data are presented in Table 3-35. Specimen C2 was well below expectations and posttest analysis revealed a test problem, possibly an extensometer slip, which rendered the test invalid. The two valid test points exceeded program requirements.

The notched tensile test data, conducted utilizing the specimen configuration shown in Figure 3-74, is presented in Table 3-36. Several of the specimens failed away from the notch in the reduced section but at expected ultimate tensile strength values for the cross section in which failure occurred. However, specimen S11 failed in the 8.99 mm (.354") cross section at a very low strength value. NDT evaluation of the shaft prior to cut up revealed no evidence of any cracks in the part and no cracks have been found in other specimens or excess material from this shaft. The cracks apparently were introduced during specimen preparation, possibly from the abrasive cutting operation, and this test is considered invalid. The notched tensile data in which failure occurred at the notch shows strengthening at all temperatures evaluated.

Low cycle fatigue testing was conducted at several conditions including smooth bar strain control, smooth bar load control, and notched bar load control. The smooth bar strain control tests were performed at 538° C (1000° F) utilizing a 10.2 mm (0.4 inch) diameter cylindrical gage specimen (Figure 3-75) and the data is presented in Table 3-37. The results are nearly equivalent to those obtained for the baseline condition in the process variable study, as expected.

The smooth bar load control LCF tests were conducted at 427° C (800° F) utilizing a 5 mm (0.2 inch) diameter cylindrical gage section specimen shown in Figure 3-76. The data are presented in Table 3-38 and plotted in Figure 3-77.

Notched bar LCF testing, utilizing the specimen shown in Figure 3-78, was conducted at three conditions: 371° C (700° F), $K_t = 3.5$; 482° C (900° F), $K_t = 1.5$; and 593° C (1100° F), $K_t = 1.5$. Data for all three test conditions were included in Table 3-38 and the results for the 482° C (900), 593° C (1100° F), and 371° C (700° F) tests are shown in Figures 3-77 and 3-79.



Standard (100%) Density for Powder Blend MB048 = 8251 kg/m³,
 .2981 lbs/in³.

Figure 3-70. Density and TIP Measurements for As-HIP René 95
 CF6-50 HPT Rear Shafts SM590 and SM582.

Table 3-33. Tensile Properties of CF6 HPT Rear Shafts.

Spec. No.	Shaft No.	Test Temp.		0.2% YS		UTS		Elong. (%)	R.A. (%)
		(° C)	(° F)	(MPa)	(ksi)	(MPa)	(ksi)		
T1	SM590	RT	RT	1210	175.5	1647	238.9	15.4	17.6
T13	SM590			1148	166.5	1597	231.6	13.5	15.8
T23	SM582			1152	167.1	1650	239.3	16.2	19.6
T26	SM582			1147	166.4	1610	233.5	14.1	17.6
*T6	SM590	204	(400)	1123	162.9	1520	220.5	12.0	11.1
T19	SM590			1140	165.3	1548	224.5	12.8	14.6
*T30	SM582			1135	164.6	1506	218.4	11.4	11.2
T33	SM582			1150	166.8	1570	227.7	14.3	14.5
T3	SM590	427	(800)	1147	166.3	1509	218.9	12.3	17.8
T11	SM590			1117	162.0	1508	218.7	14.5	14.8
T29	SM582			1120	162.5	1543	223.8	16.1	20.2
T32	SM582			1079	156.5	1514	219.6	15.2	15.1
T36	SM582			1105	160.3	1547	224.4	16.4	21.0
T2	SM590	538	(1000)	1129	163.8	1485	215.4	10.9	11.7
T10	SM590			1078	156.4	1512	219.3	14.5	15.0
T15	SM590			1125	163.2	1548	224.5	14.0	15.0
T24	SM582			1129	163.7	1559	226.1	15.4	16.4
T28	SM582			1065	154.4	1520	220.5	16.4	18.4
*T8	SM590	649	(1200)	1134	164.5	1499	217.4	11.7	12.4
T20	SM582			1076	156.1	1530	221.9	13.1	14.4
Program		RT	RT	1034	150.0	1276	185.0	10	12
Requiremnt		649	(1200)	862	125.0	1000	145.0	8	10

*Apparent extensometer mark failure

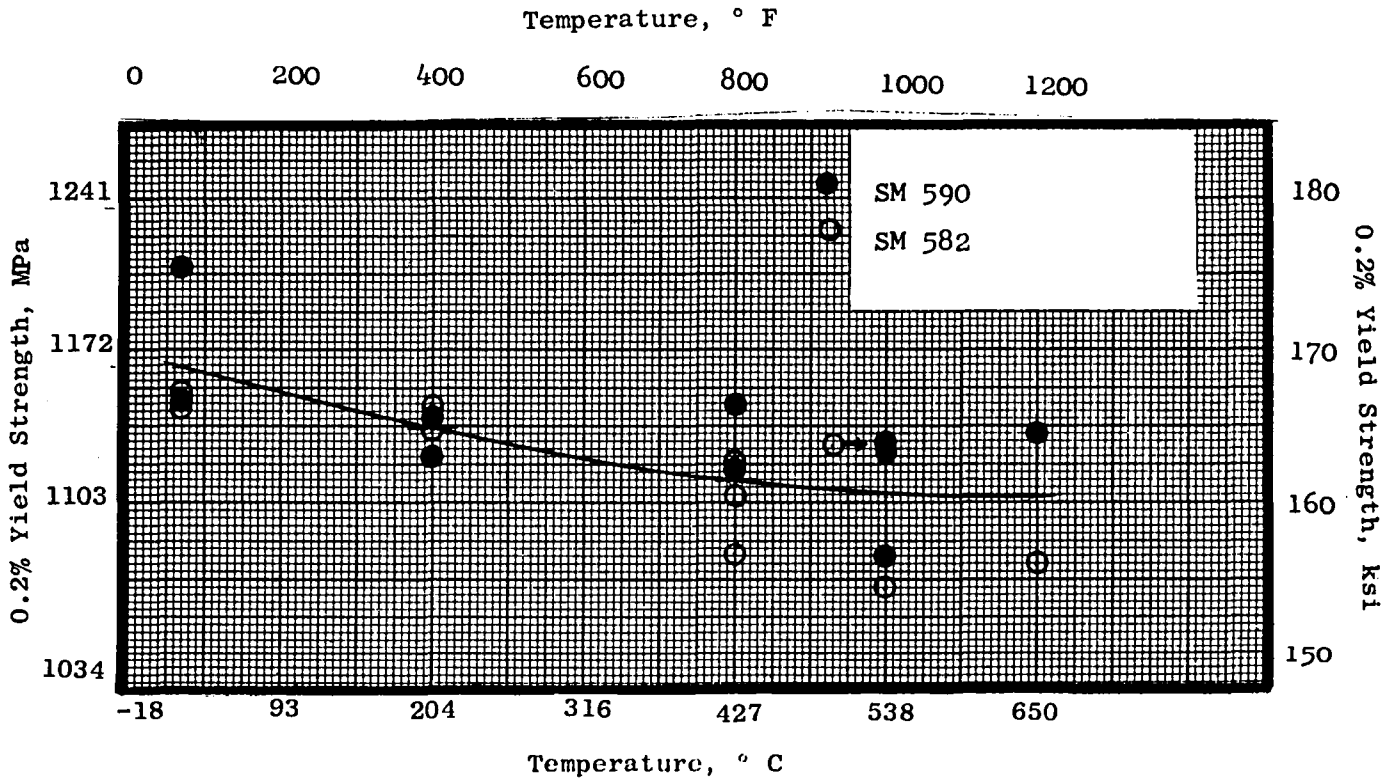
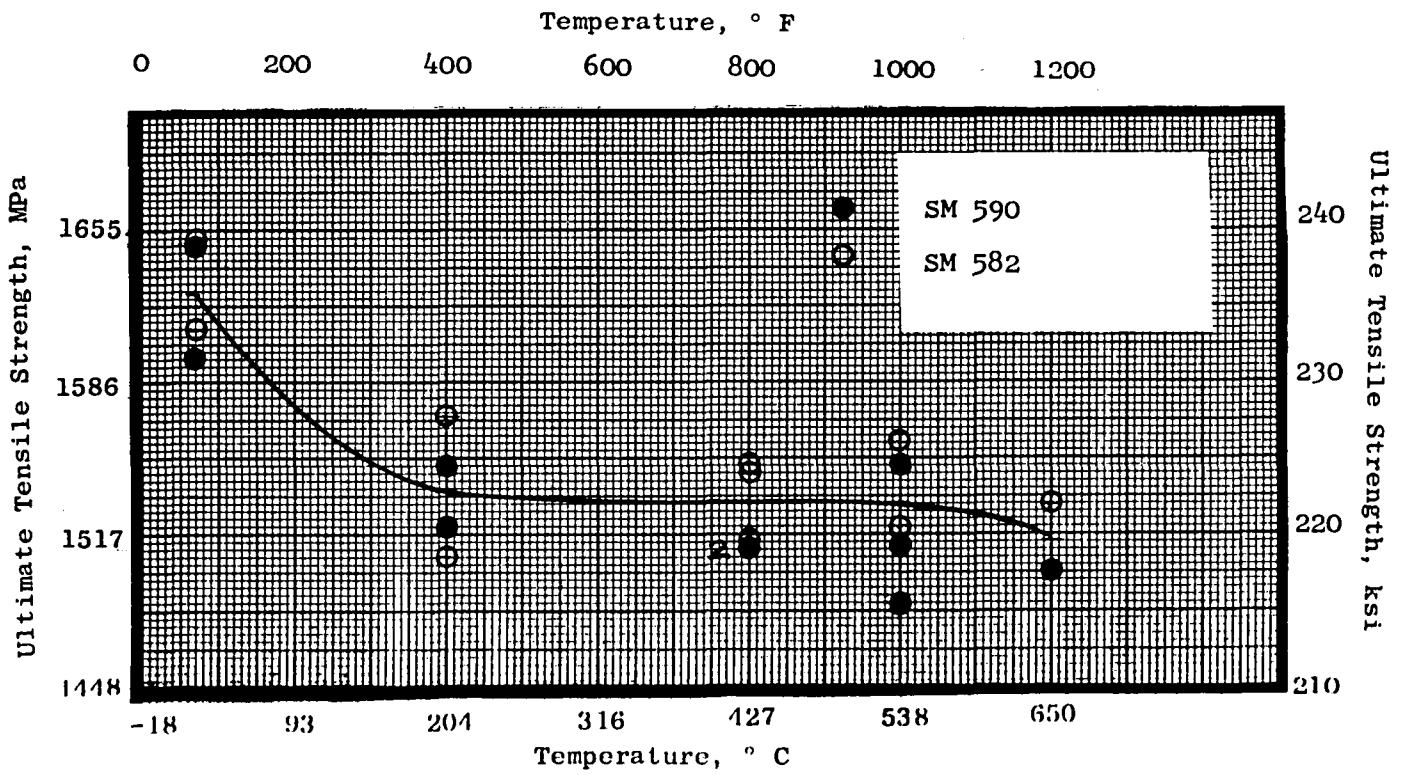


Figure 3-71. 0.2% Yield Strength and Ultimate Tensile Strength Versus Temperature for As-HIP René 95 CF6-50 HPT Rear Shaft.

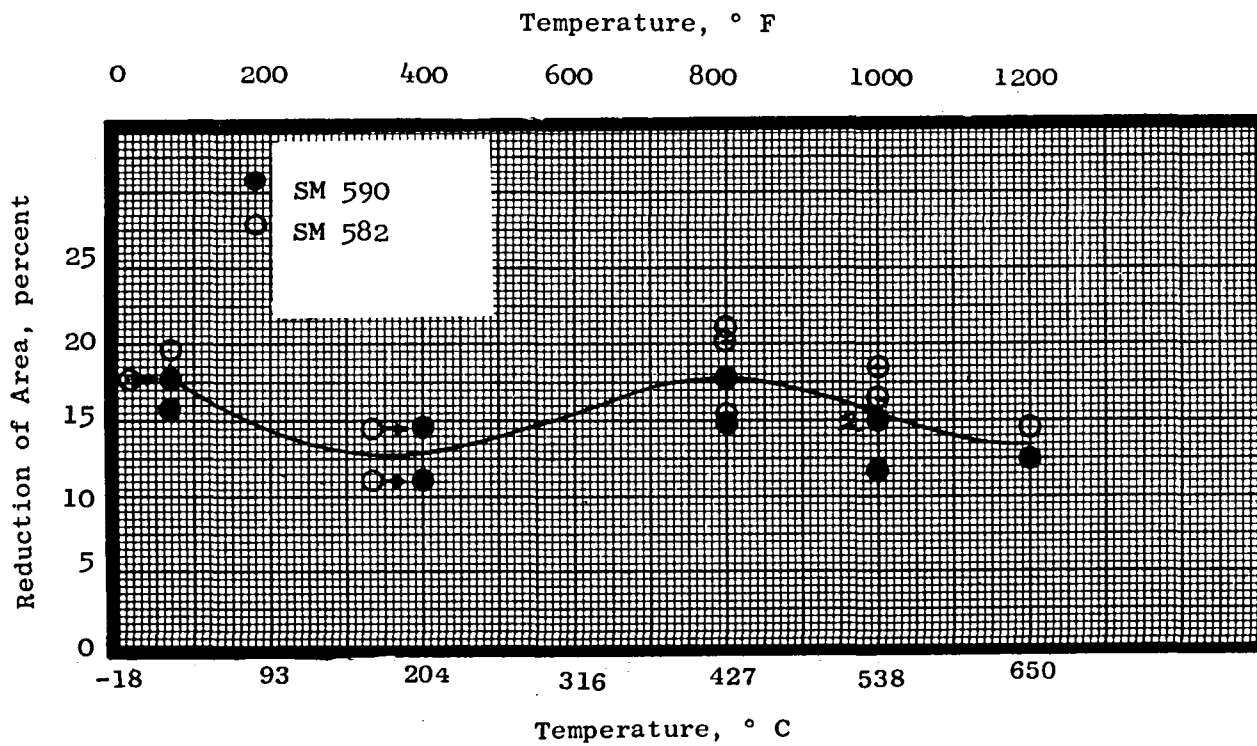
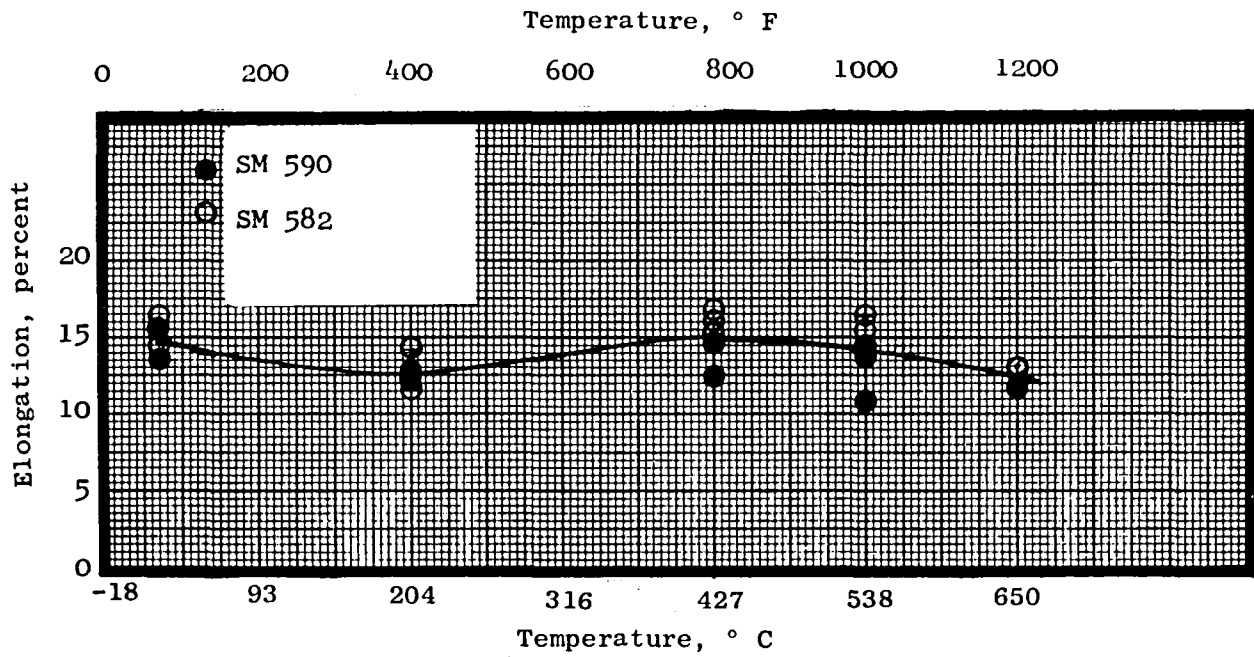


Figure 3-72. Percent Elongation and Percent Reduction of Area Versus Temperature for As-HIP René 95 CF6-50 HPT Rear Shaft.

Table 3-34. Stress Rupture Properties of CF6 HPT Rear Shaft.

Spec. No.	Shaft No.	Test Temp.		Stress		Life (Hrs)	Elong. (%)	R.A. (%)		
		(° C)	(° F)	(MPa)	(ksi)					
T5	SM590	593	1100	1138	165	147.0	0.8	2.8		
T16	SM590			1103	160	855.5	2.9	4.9		
T17	SM590			1207	175	383.2	4.7	19.6		
T25	SM582			1069	155	1453.7	1.9	5.6		
T38	SM582			1172	170	203.3	2.1	4.2		
T7	SM590	649	1200	1034	150	8.3	4.5	4.2		
T12	SM590			793	115	1106.6	0.5	0		
T14	SM590			1000	145	69.9	2.9	5.6		
T21	SM582			862	125	872.8	1.2	4.3		
T31	SM582			965	140	113.8	0.7	0.8		
T34	SM582			896	130	879.1	4.5	6.9		
T35	SM582			827	120	1849.0	4.1	4.2		
T4	SM590			722	1300	690	100	105.8	1.4	1.4
T9	SM590					827	120	27.6	2.1	1.4
T18	SM590					655	95	301.5	2.8	4.2
T22	SM582	621	90			338.4	1.3	1.4		
T27	SM582	724	105			97.1	2.4	2.8		
T37	SM582	758	110			82.8	4.9	5.6		

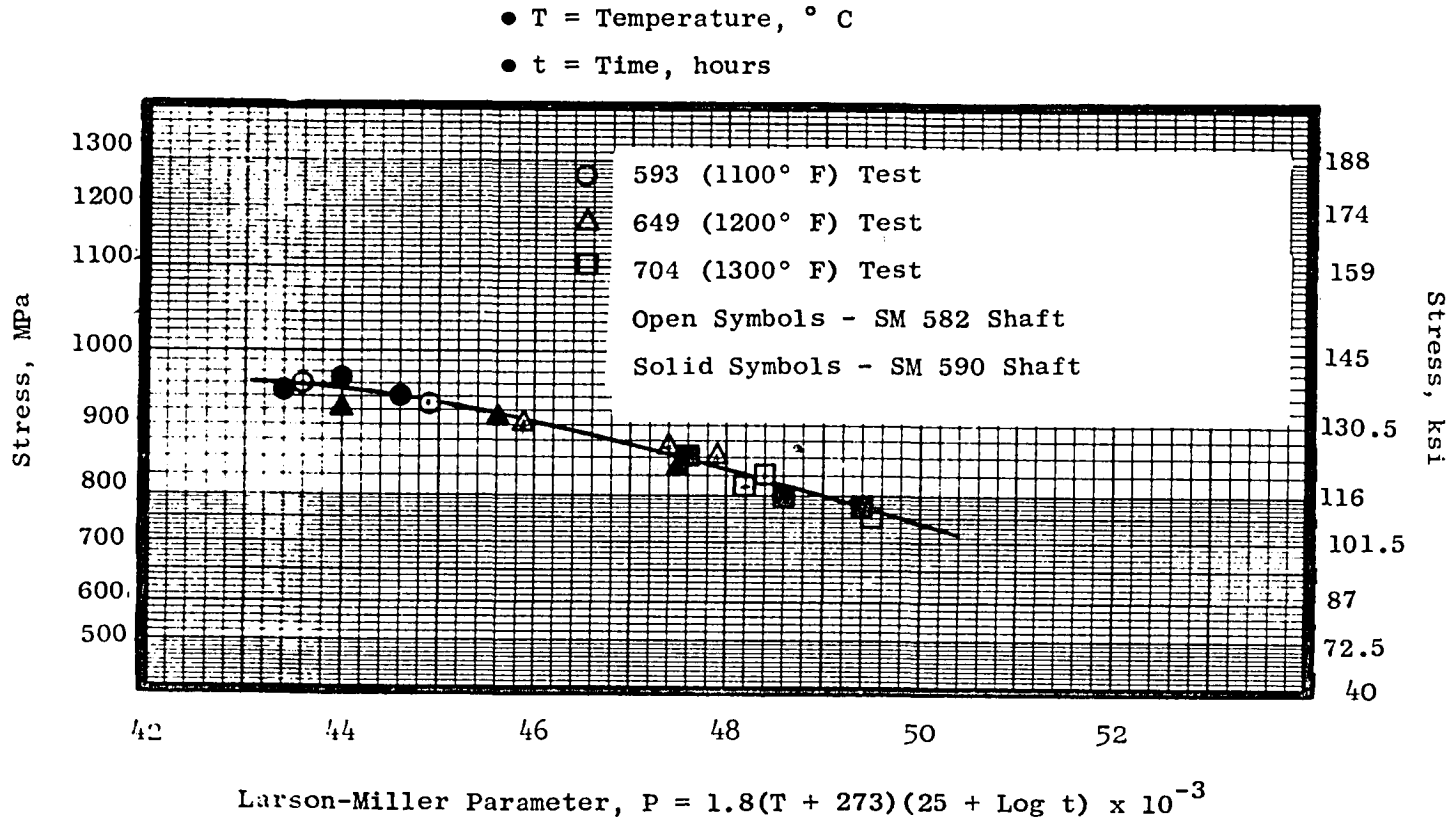


Figure 3-73. Larson-Miller Parameter Plot of Stress Rupture Data from as-HIP René 95 CF6 HPT Rear Shafts.

Table 3-35. Creep Properties of as-HIP René 95.

CF6-50 HPT Rear Shafts

Spec. No.	Shaft No.	Test Temp.		Stress		Time to Creep (Hrs)		
		(° C)	(° F)	(MPa)	(KSI)	0.1%	0.2%	0.3%
C1	SM590	649	1200	655	95	450	680	---
*C2	SM590	704	1300	379	55	10	36.1	89.0
C3	SM582	649	1200	724	105	40	350	---

*Invalid test due to test malfunction.

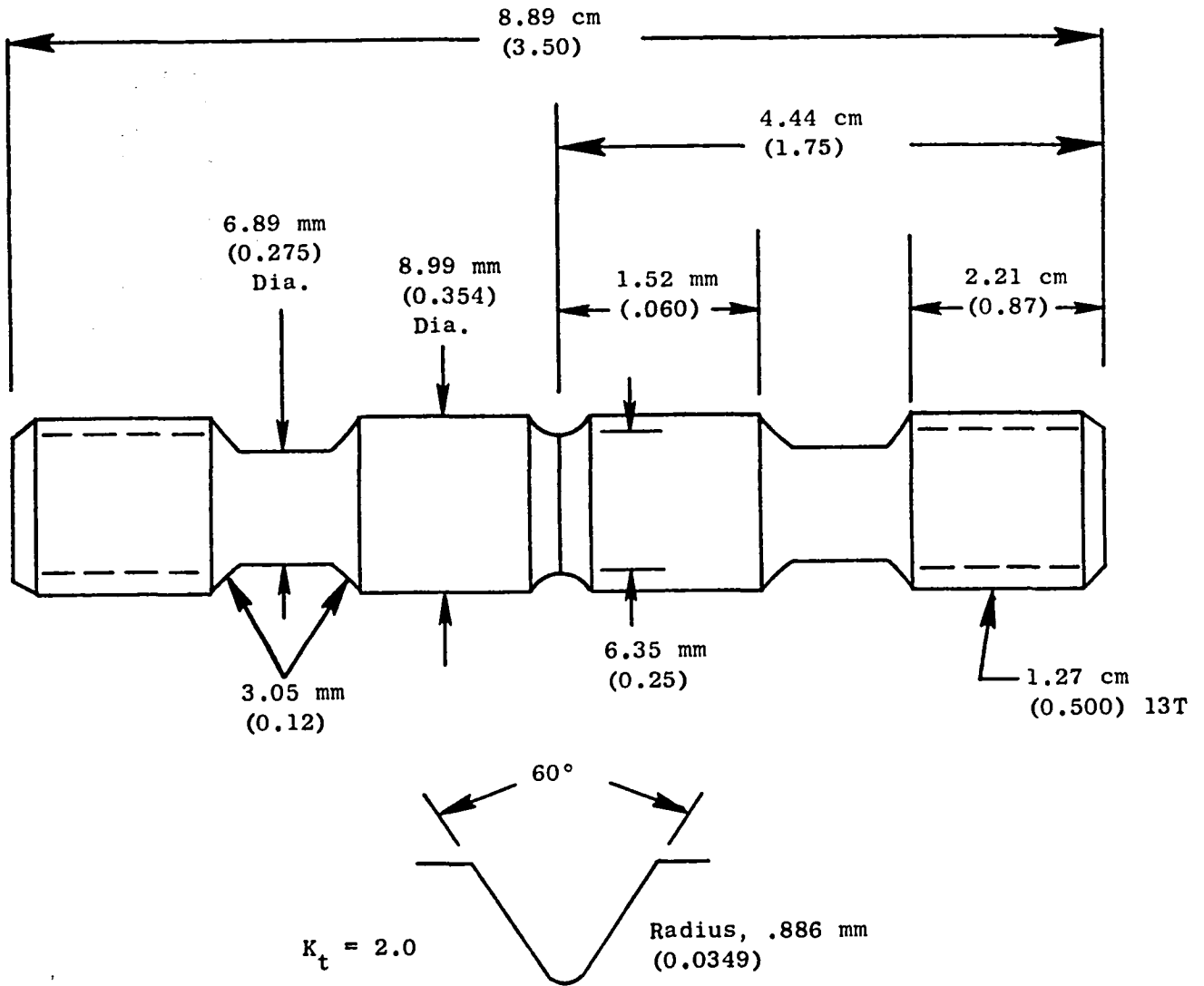


Figure 3-74. Double Reduced Notched Bar Sustained Peak Low Cycle Fatigue (SPLCF) Test Specimen.

Table 3-36. Notched ($K_t = 2$) Bar Tensile Properties of as-HIP.

René 95 CF6- HPT Rear Shafts

Spec. No.	Shaft No.	Test Temp.		UTS		Failure Location	Notch Strength Ratio
		(° C)	(° F)	(MPa)	(KSI)		
S3	SM590	RT	RT	1944	282.0	Notch	1.19
S8	SM590	RT	RT	1939	281.2	Notch	1.19
S14	SM582	RT	RT	1911	277.2	Notch	1.17
S6	SM590	427	800	1532	222.2	6.98 (0.275) Dia.	*
S18	SM582	427	800	1410	204.5	6.98 mm (0.275) Dia.	*
S11	SM590	538	1000	830	120.4**	8.99 mm (0.354) Dia.	**
S15	SM582	538	1000	1878	272.4	Notch	1.23
S2	SM590	649	1200	1520	220.5	6.98 mm (0.275) Dia.	*
S13	SM582	649	1200	1895	274.9	Notch	1.25
S19	SM582	649	1200	1532	222.2	8.99 mm (0.275) Dia.	*

*Failure Stress in Smooth Reduced Section (Outside of Notch) Calculated on Basis of Drawing Dia. of Failed Section.

**Failure in Thick Section Due to Pre-Existing Crack in Specimen, Test Invalid.

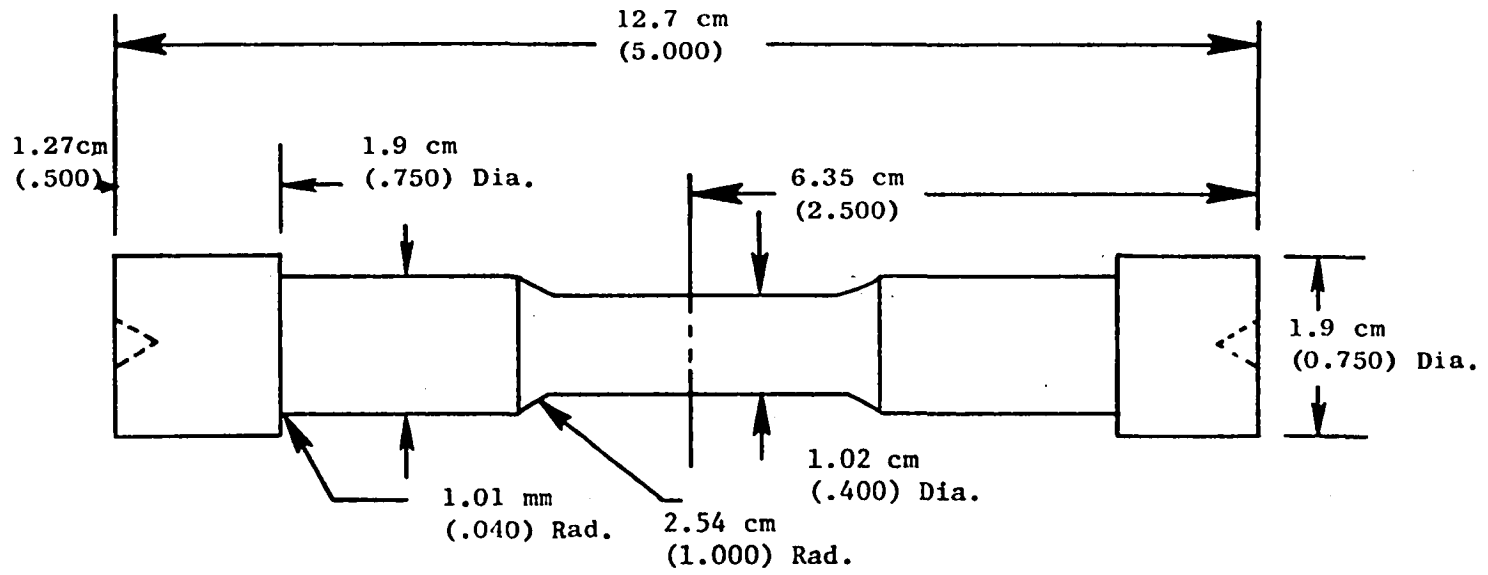


Figure 3-75. Smooth Bar Low Cycle Fatigue (Strain Control) Test Specimen.

Table 3-37. Strain Low Control Fatigue Properties
of CF6 HPT Rear Shafts.

Test Conditions: T=538° C(1000° F), R=0(A=1),(PM5 BAR)
Specimen PM5, Figure 3-75

Spec. No.	Shaft No.	Strain Range (%)	Modulus (TPa)	Modulus (10 ⁶ psi)	Alt. Pseudo Stress		Life (Cycles)	Inco 718 Life, Typical
					(MPa)	(ksi)		
K1	SM590	0.78	0.188	27.2	723.9	105.0	7844	7000
K3	SM590	0.66	0.192	27.9	637.1	92.4	32096	12000
K4	SM582	0.68	0.184	26.7	623.2	90.4	16527	13500

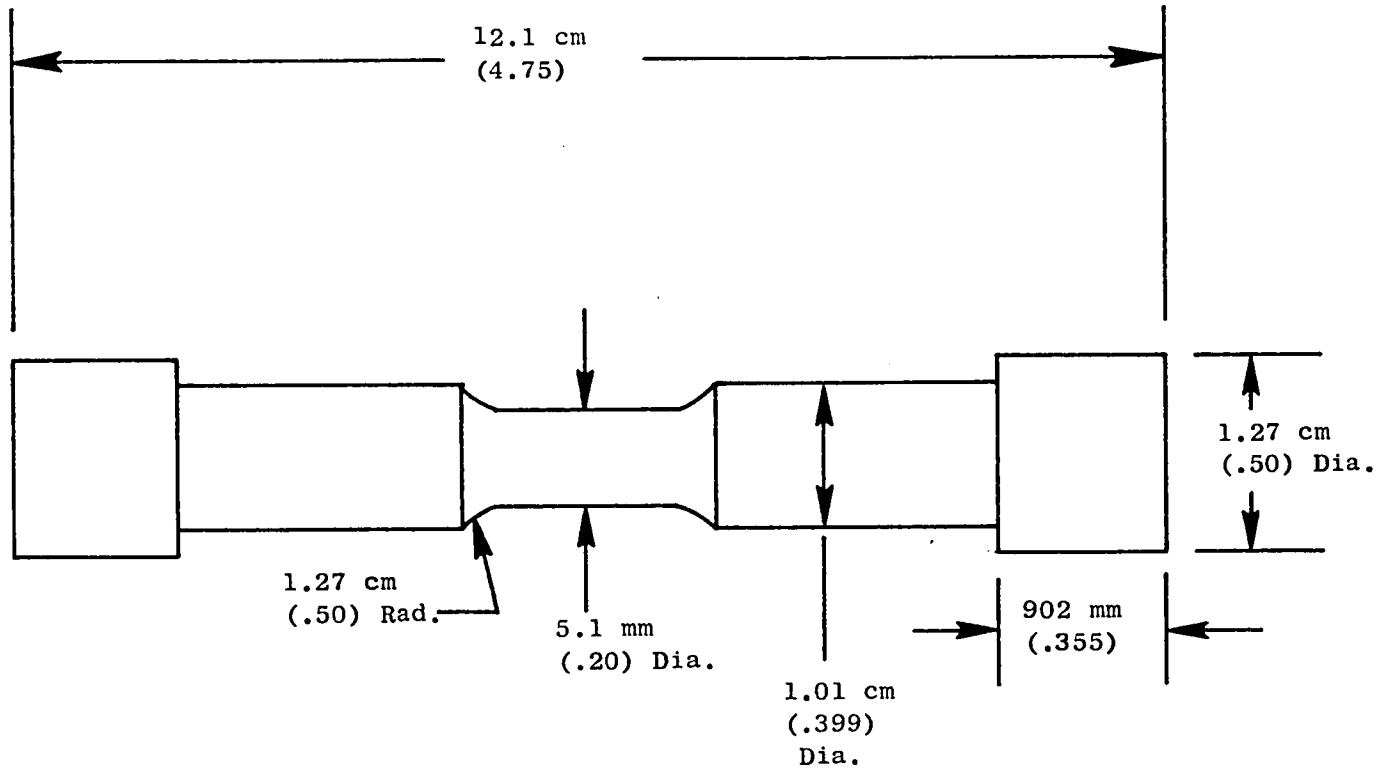
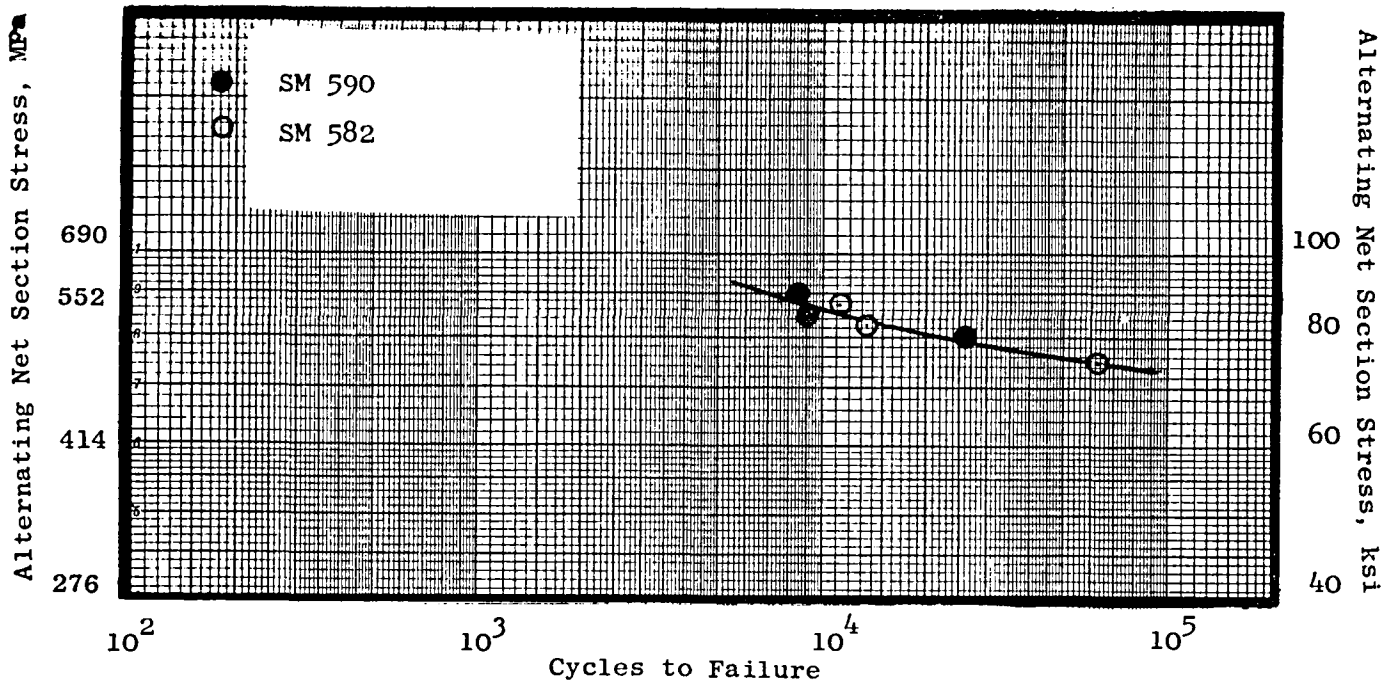


Figure 3-76. Smooth Bar Load Control Low Cycle Fatigue Test Specimen.

Table 3-38. Smooth and Notched Bar Load Control Low Cycle Fatigue Data From as-HIP René 95 CF6-50 HPT Rear Shaft R=.03-0 (A=0.95-1.0).

Spec. No.	Shaft No.	Kt	Test Temp.		Alt. Stress		N _f Cycles	
			(°C)	(°F)	(MPa)	(ksi)		
L2	SM590	1.0	427	800	557	80.0	25712	
L7					586	85.0	9033	
L11					621	90.0	8527	
L14					SM582	569	82.5	13531
L16						517	75.0	62994
L22						603	87.5	11324
L4	SM590	1.5	482	900	403	58.5	17071	
L5					336	48.7	102113 R.O.	
L10					386	56.0	14926 R.O.	
L12	SM582				403	58.4	Mach. Malfunction	
L18					370	53.6	103262	
L19					504	73.1	10286	
L1	SM590	1.5	593	1100	552	80.0	4266	
L6					470	68.2	66716	
L9					604	87.6	3786	
L13					SM582	470	68.2	96154
L17						504	73.1	6963
L20						672	97.4	1986
L3	SM590	3.5	371	700	269	39.0	5782	
L8					188	27.3	112537 R.O.	
L15					SM582	201	29.2	30350
L21						235	34.1	12154

R.O. = Runout



427° C (800° F) Load Control LCF Data From As-HIP René 95 CF6-50 HPT Rear Shafts ($A=1$, $K_t = 1$)

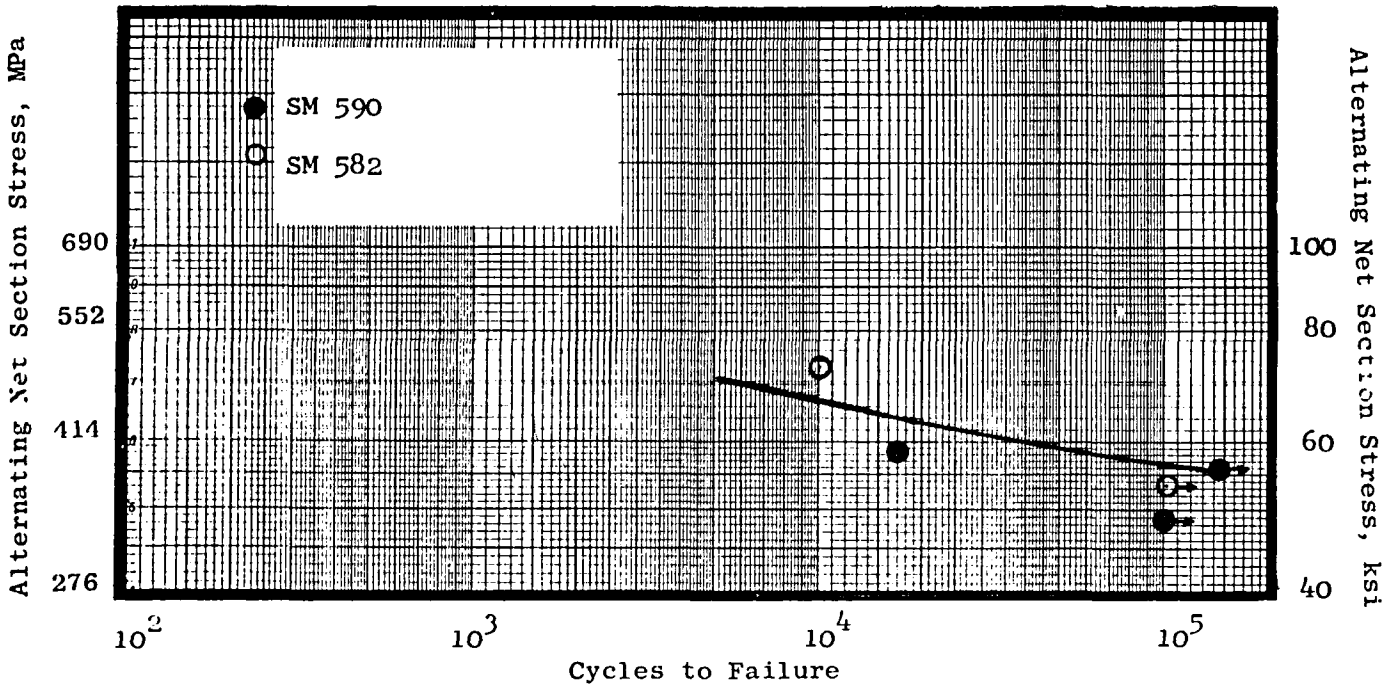


Figure 3-77. 482° C (900° F) Notched ($K_t = 1.5$) Load Control LCF Data from As-HIP René 95 CF6-50 HPT Shafts ($A = 0.95$).

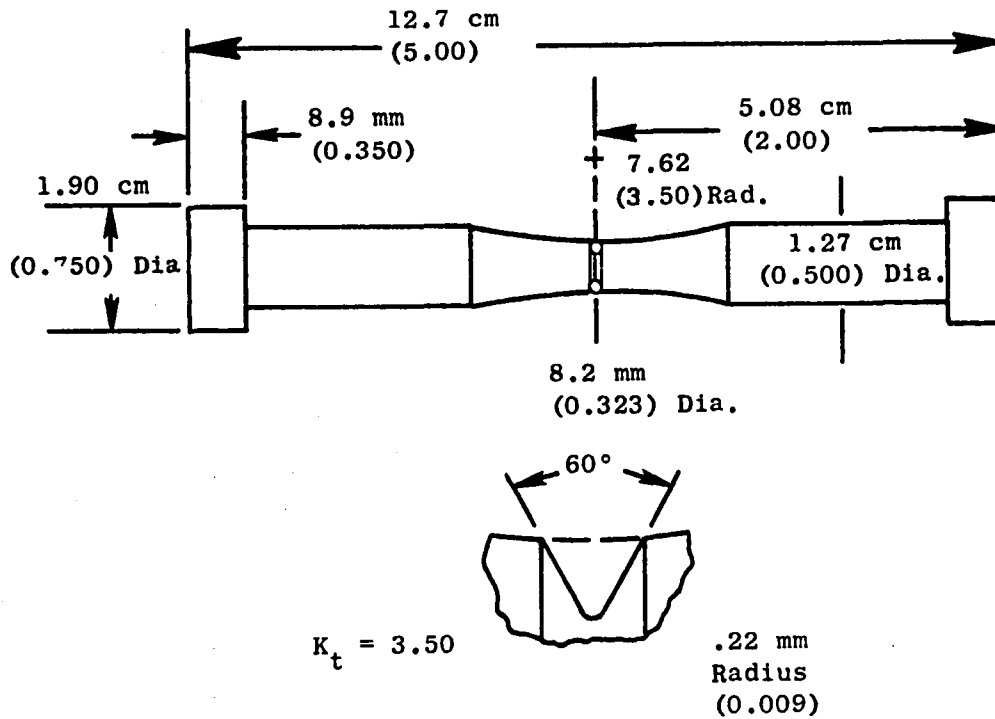


Figure 3-78. Notched Bar Low Cycle Fatigue (Load Control) Test Specimen.

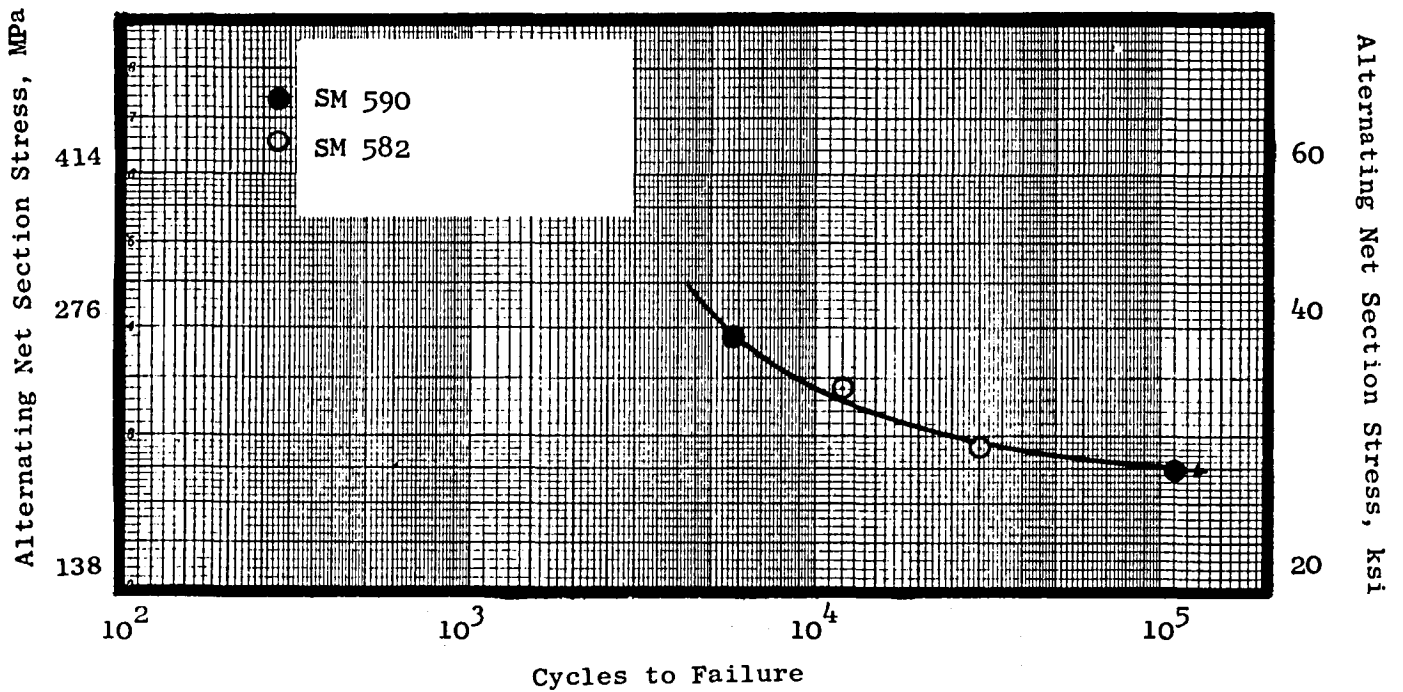
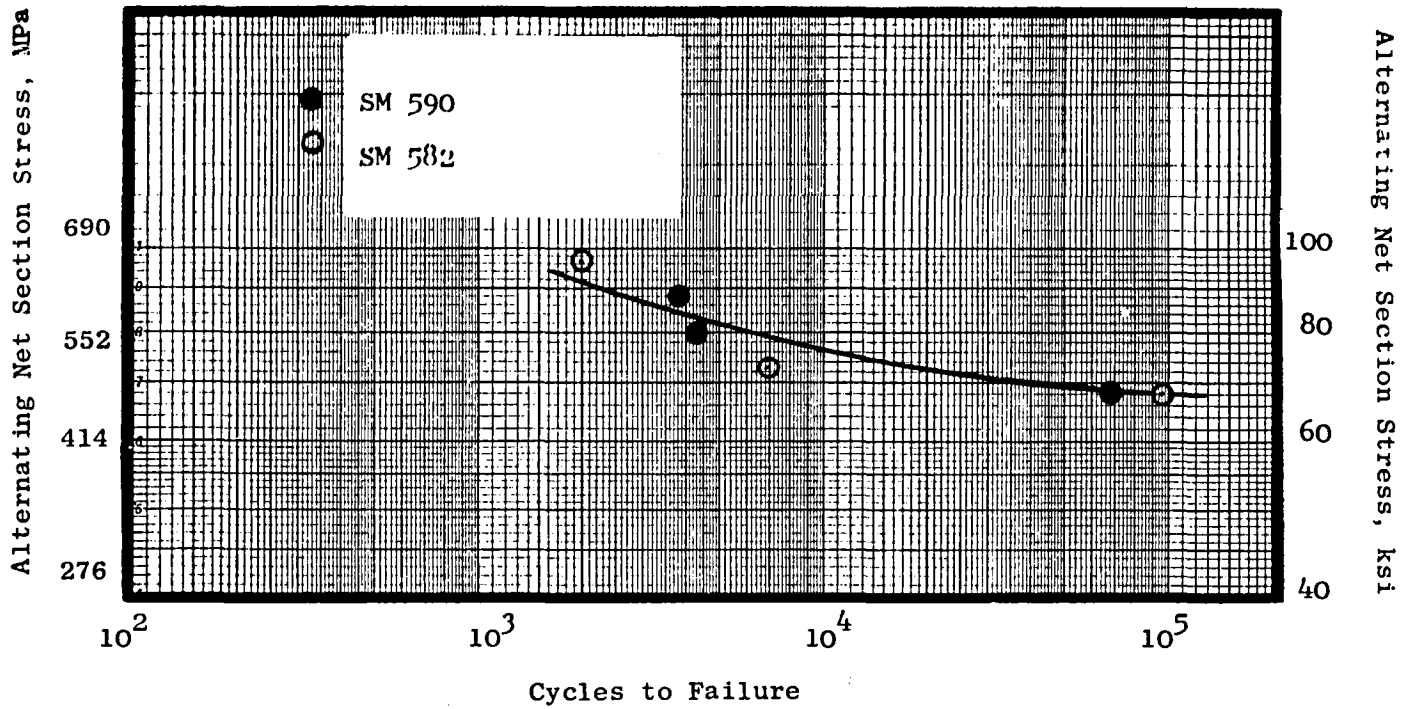


Figure 3-79. 371° C (700° F) Notched ($K_t = 3.5$) Load Control LCF Data from As-HIP René 95 CF6-50 HPT Rear Shafts $R = .03$ ($A = .95$).

Sustained peak low cycle fatigue testing was performed at 593° C (1100° F), $K_t = 2$ with a 10-90-10 second loading cycle (min. to max. load in 10 sec., hold at max. load for 90 sec., max. to min. load in 10 sec.). The results are shown in Table 3-39 and plotted in Figure 3-80.

Residual cyclic life (K_B) testing was conducted utilizing the specimen shown in Figure 3-81. The data, including initial crack size and cycles to failure, is reported in Table 3-40.

Dynamic modulus of elasticity and thermal expansion data are presented in Tables 3-41 and 3-42 respectively. The results are typical of previous results on René 95.

3.2.2.2 Product Acceptance Testing

One of the five pilot production parts was cut up and tested to determine material acceptability. Shaft SM-586 was selected for the cut-up and the certificates of test are presented in the Appendix to this report. The data from the cut-up met or exceeded part requirements and the parts were therefore considered acceptable.

3.2.2.3 René 95 Machinability Studies

Any attempt to assess the cost effectiveness of near-net shapes must include machining cost elements. In order to arrive at a realistic estimate, the latest in cutting tool materials and techniques should be considered. Powder metallurgy René 95 presents some challenges and opportunities as indicated by previous machinability studies and shop experience.

In general, René 95 is not considered machinable with high-speed steel tools. The latest developments in carbide drilling and broaching with micro-grain carbide tooling must be employed. In turning, the as-HIP microstructure lends itself to Borazon tools at a substantial reduction in cost.

Although some advanced machinability data exist from earlier programs, most has been obtained on bar stock and is general in nature. Applications to specific configurations such as the CF6-6 aft shaft required additional development. Experience with other production René 95 parts indicated several difficult and high-cost operations. These include:

- Plunge turning with small diameter round tools
- Broaching Scallops
- Deep-hole drilling of 1.5 mm (0.6 in.) and 6.35 mm (0.25 in.) holes
- Turning HIP and Forge thin wall parts

Table 3-39. Sustained-Peak Low Cycle Fatigue Data of CF6 HPT Rear Shafts.

593° C(1100° F), Kt = 2, R = .03 (A = 0.95)

<u>Spec. No.</u>	<u>Shaft No.</u>	<u>Alternating Stress</u>		<u>Life (N_f) (Cycles)</u>
		<u>(MPa)</u>	<u>(ksi)</u>	
S1	SM590	503	73	8553
S5	SM590	510	74	5024
S10	SM590	552	80	999
S17	SM582	586	85	911
S20	SM582	524	76	1902
S22	SM582	469	68	7094

Table 3-40. 538° C(1000° F) Residual Cyclic Life (K_B) Data From as-HIP René 95 CF6-50 HPT Rear Shafts.

<u>Spec. No.</u>	<u>Shaft No.</u>	<u>Stress Range</u>		<u>Life Cycles</u>	<u>Initial Crack Size, mm (Inches)</u>
		<u>(MPa)</u>	<u>(ksi)</u>		
K2	SM590	571	82.8	8308	0.56 x 1.52 (0.022 x .060)
K5	SM582	672	97.4	4528	0.61 x 1.52 (0.024 x .060)
K6	SM582	738	107.1	4008	0.61 x 1.52 (0.024 x .060)

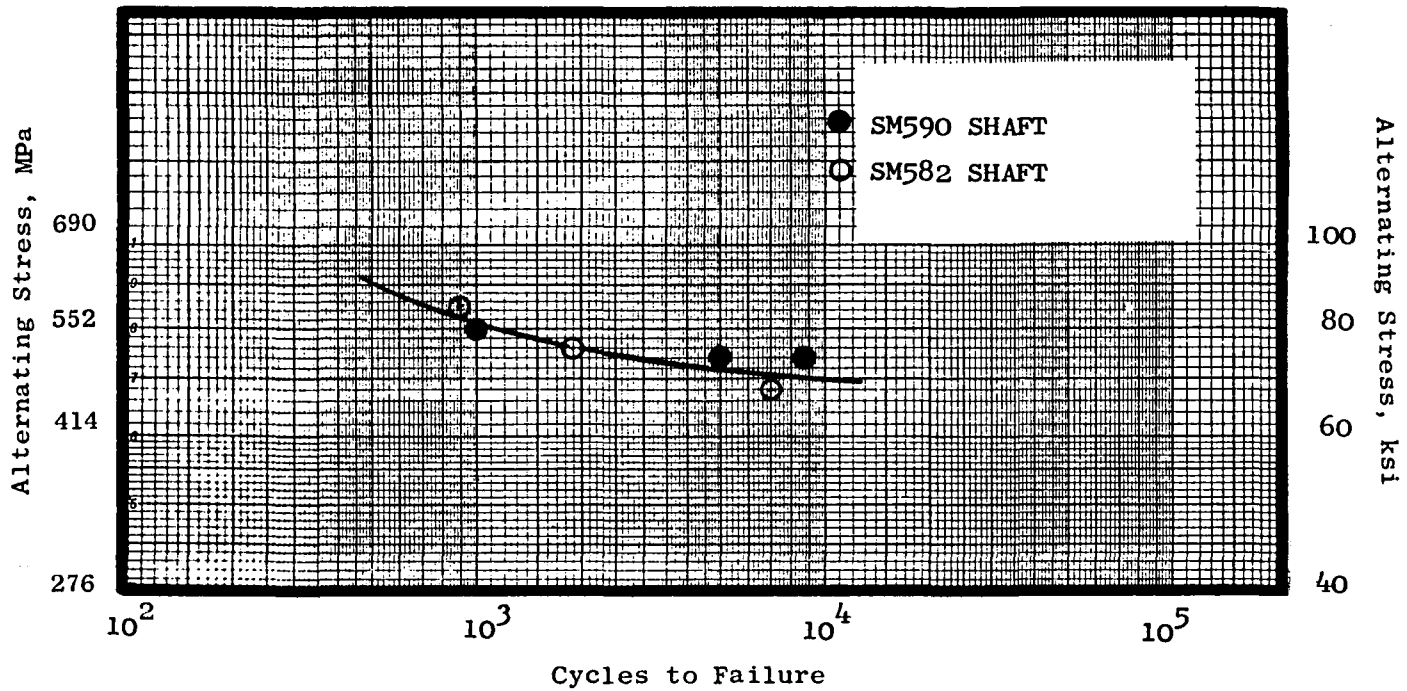


Figure 3-80. 538° C (1100° F) Sustained Peak Low Cycle Fatigue Data from As-HIP René 95 CF6-50 HPT Rear Shaft (10-90-10, sec - $K_t = 2$, $A = 0.95$, $R = .03$).

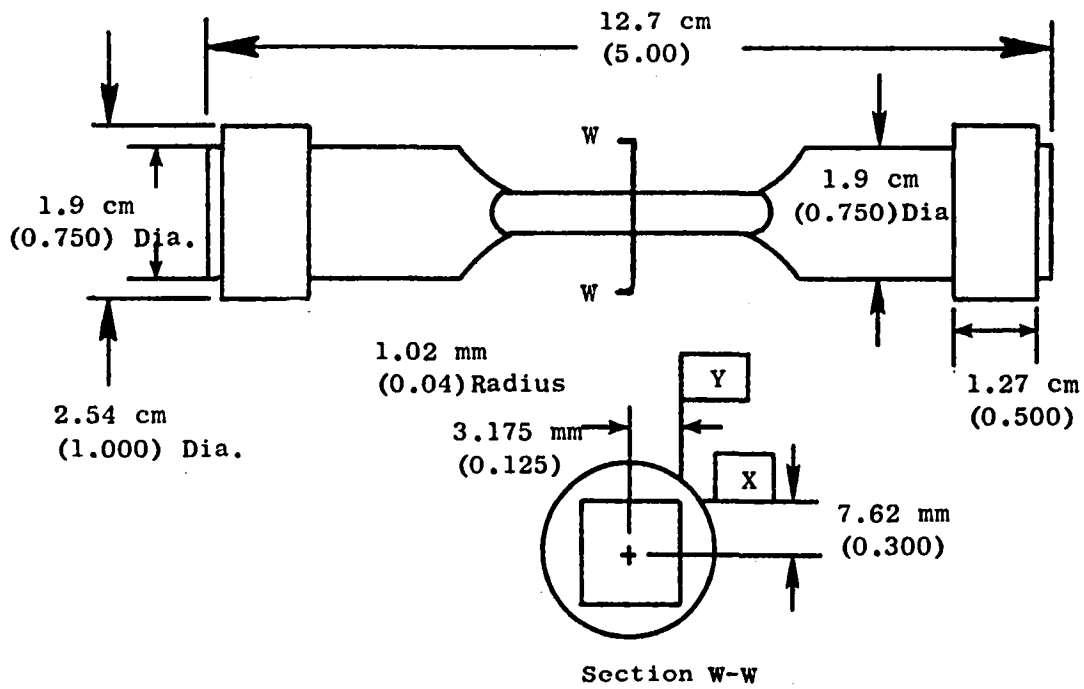


Figure 3-81. Crack Propagation (K_B) Test Specimen.

Table 3-41. Dynamic Modulus Properties of CF6 HPT Rear Shafts.

Temperature		Dynamic Modulus	
(°C)	(°F)	(TPa)	(psi × 10 ⁶)
22	72	0.217	31.49
149	300	0.211	30.60
315	600	0.202	29.35
488	910	0.193	28.02
593	1100	0.187	27.15
704	1300	0.179	25.95
815	1500	0.170	24.73

(Test Specimen MI Taken from SM590 Shaft)

Table 3-42. Thermal Expansion Properties of CF6 HPT Rear Shafts.

Temperature Range (° C) (° F)	Temperature Difference (°C) (°F)		Total Linear Thermal Expansion (in./in. x 10 ⁻³)	Coefficient of Linear Thermal Expansion (in./in./°F x 10 ⁻⁶) (m/m/° C x 10 ⁻⁶)	
25-100 (77-212)	75	135	0.93	6.89	12.4
25-200 (77-392)	175	315	2.12	6.73	12.1
25-300 (77-572)	275	495	3.46	6.99	12.6
25-400 (77-752)	375	675	4.83	7.16	12.9
25-500 (77-932)	475	855	6.33	7.40	13.3
25-600 (77-1112)	575	1035	7.80	7.54	13.6
25-700 (77-1292)	675	1215	9.53	7.85	14.1
25-800 (77-1472)	775	1395	9.97	7.15	12.9

(Test Specimen E1 Taken From SM590 Shaft)

Applications orientated machinability experiments were conducted to investigate these areas and provide reliable data for evaluation. The results are described in the following sections.

Plunge Turning With Small Diameter Round Tools

The first item to be investigated was the difficulty of plunging and OD turning operations with small diameter tools. These operations are inherently time consuming due to the small size (low rigidity) of the tooling involved. Consequently, an assessment of the designs available and their cutting characteristics with carbide and borazon inserts was considered necessary. Tools were screened for static rigidity and subjected to machining tests.

Three tool designs were evaluated. One was a Tee-Lock holder without a backup pocket that was commercially available while a second with a fixed pocket is bought as a special item. The preload pin holder was built especially for this program, and is a scaled-down version of a recent General Electric patented design. The latter appears to be the only practical system for using a succession of a reground borazon inserts.

An indication of the cutting ability of each holder can be obtained by static load testing. For the configurations being investigated, side loading (in contouring or OD turning) is most critical. Good cutting action requires a static holder stiffness in excess of 2500 Kg/mm (140,000 #/in). Lesser values will limit metal removal rate. The Tee Lock inserts were given a light "seating" tap with a mallet, which in itself, is a variable effecting preload. Each insert was loaded to 23 kg, released, and indicators zeroed before proceeding with the test. In most cases several assemblies were evaluated, and average values are plotted in Figure 3-82. The deflection is the difference between insert and shank and does not reflect total system stiffness.

Broaching Versus Carbide End Milling of Scallops

The machinability experiments described here were aimed at reducing the cost of producing the scallops in the CF6-50 HPT Aft Shaft. Experience with early development parts made of as-HIP René 95 pointed to the broaching of scallops with HSS form tools as one of the areas requiring study, since tool life was only 0.5 parts per sharpening. This is attributable to the hot hardness of René 95 as compared to that of HSS tools and was expected. Recent developments in micrograin carbide broach tools may eventually be applied, but current production quantities do not warrant an investment of this magnitude. The scallop configuration can be produced with standard carbide end mills on N.C. or tracer equipment. This approach was investigated by evaluating the two elements of contour milling (plunge and linear cuts). Costs, including tools and labor, were compared with HSS broaching.

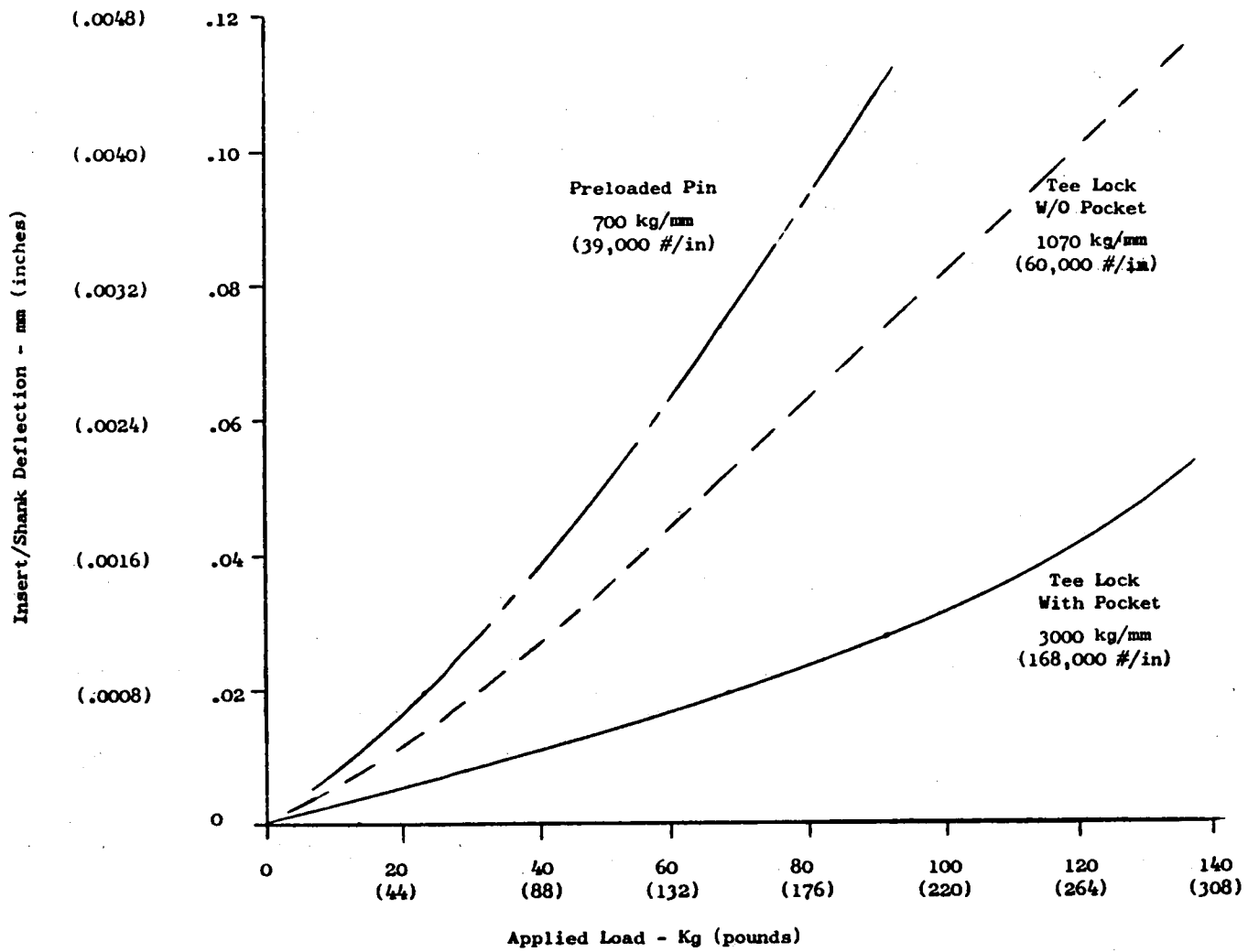


Figure 3-82. Stiffness Comparison of Tee Lock and Preloaded Pin Design.

Carbide end milling can greatly reduce the cost of producing scallops in René 95 when compared with HSS broaching. Chip making costs (tools and labor), ignoring set-up, inspection and other "down" time are listed below:

<u>Process</u>	<u>Shaft Mat'l</u>	<u>Relative Cost/Part</u>
HSS Broaching	In 718	1.0
Carbide Milling	René 95	0.72
HSS Broaching	René 95	25.0

Recommended Milling conditions are as follows:

<u>Parameter</u>	<u>Plunge Cuts</u>	<u>Linear Cuts</u>
Feed mm pt (ipt)	0.05 (0.002)	0.05 (0.002)
Speed cm/min (ft/min)	101.6 (40)	76-89 (30-35)
Depth mm (in)	---	Up to 2.54 mm (0.1 in.)
Expected life (per sharpening)	12 slots	greater than 38 cm (15 in.)

The simple model used herein for linear milling proved a good fit to the data (index of variation of 99%). Plunging, on the other hand, exhibited a degree of scatter in the results not compatible with good statistical analysis. Replicate tests would be required for satisfactory resolution. It was possible, however, to estimate the minimum number of pluges over the range of the experiment at 10.

Two experiments (plunge and linear) were run, using the set-ups shown in Figure 3-83 in each case as-HIP René 95 stock, 3.8 mm (0.15 inch) thick was milled with carbide cutters. The test designs and results are given in Table 3-43 and other machining conditions in Table 3-44. In the case of plunging, only feed and speed (depth not applicable) were investigated and a 3² factorial design (two variables at three levels) resulted in a reasonable number of tests. The linear milling experiment, including depth, was limited to 2 levels (2³ factorial) for brevity.

Analysis of the plunge life data (Table 3-43) resulted in an unsatisfactory fit (Index of variation of only 39%) to the data. One of the strongest factors was a highly remote second order interaction. Two suspect tests were repeated and the average life analyzed. This increased the fit to 51%, but yielded no statistically significant results. The average life was about 14 slots over the range evaluated. Replicate tests would be required to improve the fit to a point where the effects of feed and speed become clear.

Analysis of the linear milling data was more fruitful. A 99% fit, involving all three main effects, was obtained. Typical tool life data are plotted in Figure 3-84 for two feeds and depths of cut.

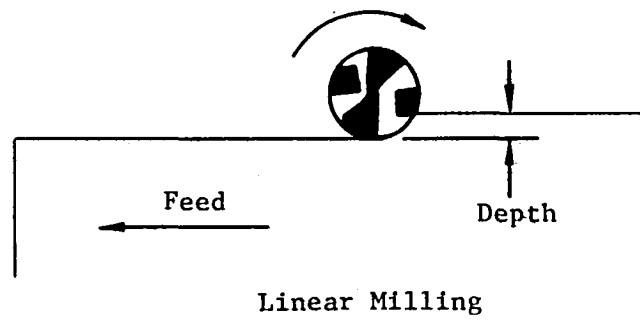
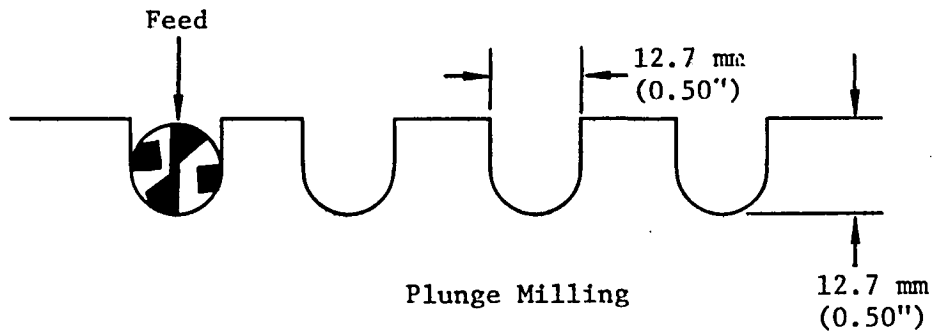
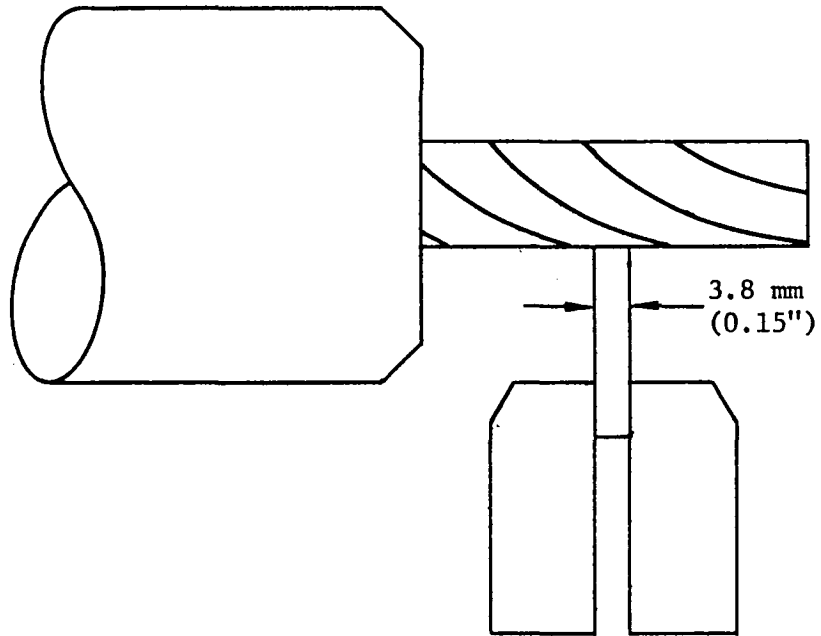


Figure 3-83. Milling Setups.

Table 3-43. Experimental Designs and Results.

I. Plunge Cuts

Test No.	Speed		Feed		Tool Life* No plunges
	m/min	(ft/min)	mm/t	in./t	
1	6.7	(22)	0.025	(0.001)	13.8
2	9.75	(32)	0.025	(0.001)	17.8, 13.0
3	12.2	(40)	0.025	(0.001)	11.0
4	6.7	(22)	0.038	(0.0015)	17.2
5	9.75	(32)	0.038	(0.0015)	16.0
6	12.2	(40)	0.038	(0.0015)	13.0
7	6.7	(22)	0.050	(0.002)	18.8
8	9.75	(32)	0.050	(0.002)	11.0, 11.0
9	12.0	(40)	0.050	(0.002)	14.0

II. Linear Cuts

Test No.	Speed		Feed		Depth		Tool Life	
	m/min	(ft/min)	mm/t	in./t	mm	(inches)	cm of cut	(in. of cut)
1	6.7	(22)	0.025	(0.001)	0.76	(0.030)	114	(44.8)
2	12.2	(40)	0.025	(0.001)	0.76	(0.030)	56	(22.1)
3	6.7	(22)	0.050	(0.002)	0.76	(0.030)	155	(61.2)
4	12.2	(40)	0.050	(0.002)	0.76	(0.030)	114	(44.9)
5	6.7	(22)	0.025	(0.001)	2.54	(0.100)	48	(18.8)
6	12.2	(40)	0.025	(0.001)	2.54	(0.100)	29	(11.4)
7	6.7	(22)	0.050	(0.002)	2.54	(0.100)	52	(20.5)
8	12.2	(40)	0.050	(0.002)	2.54	(0.100)	30	(11.9)

*Based on 0.254 mm (0.010") uniform wear

Table 3-44. Borazon Turning Design and Results.

2 x 2 x 3 Factorial Experiment

Test No.	m/s	Speed, (ft/min)	Feed		Depth,		Tool Life* (min)	DCL,		Failure Mode
			mm/r	(in./r)	mm	(in.)		mm	(in.)	
1	1.52	(300)	0.10	(0.004)	0.25	(0.010)	24.6	1.27	(0.050)	Wear
2	2.54	(500)	0.10	(0.004)	0.25	(0.010)	8.4	1.85	(0.073)	Wear
3	1.52	(300)	0.15	(0.006)	0.25	(0.010)	7.9	1.83	(0.072)	Wear
4	2.54	(500)	0.15	(0.006)	0.25	(0.010)	12.9	1.22	(0.048)	Wear
5	1.52	(300)	0.10	(0.004)	0.64	(0.025)	4.4	1.57	(0.062)	Nose Fracture
6	2.54	(500)	0.10	(0.004)	0.64	(0.025)	12.2	1.57	(0.060)	Wear
7	1.52	(300)	0.15	(0.006)	0.64	(0.025)	14.5	2.34	(0.092)	Wear
8	2.54	(500)	0.15	(0.006)	0.64	(0.025)	6.4	1.80	(0.070)	Wear
9	1.52	(300)	0.10	(0.004)	1.02	(0.040)	2.7	1.78	(0.070)	Nose Fracture
10	2.54	(500)	0.10	(0.004)	1.02	(0.040)	5.2	1.35	(0.053)	Wear
11	1.52	(300)	0.15	(0.006)	1.02	(0.040)	4.9	1.50	(0.059)	Edge Fracture
12	2.54	(500)	0.15	(0.006)	1.02	(0.040)	1.6	2.54	(0.100)	Nose Fracture

*Based on 0.030" uniform flank wear.

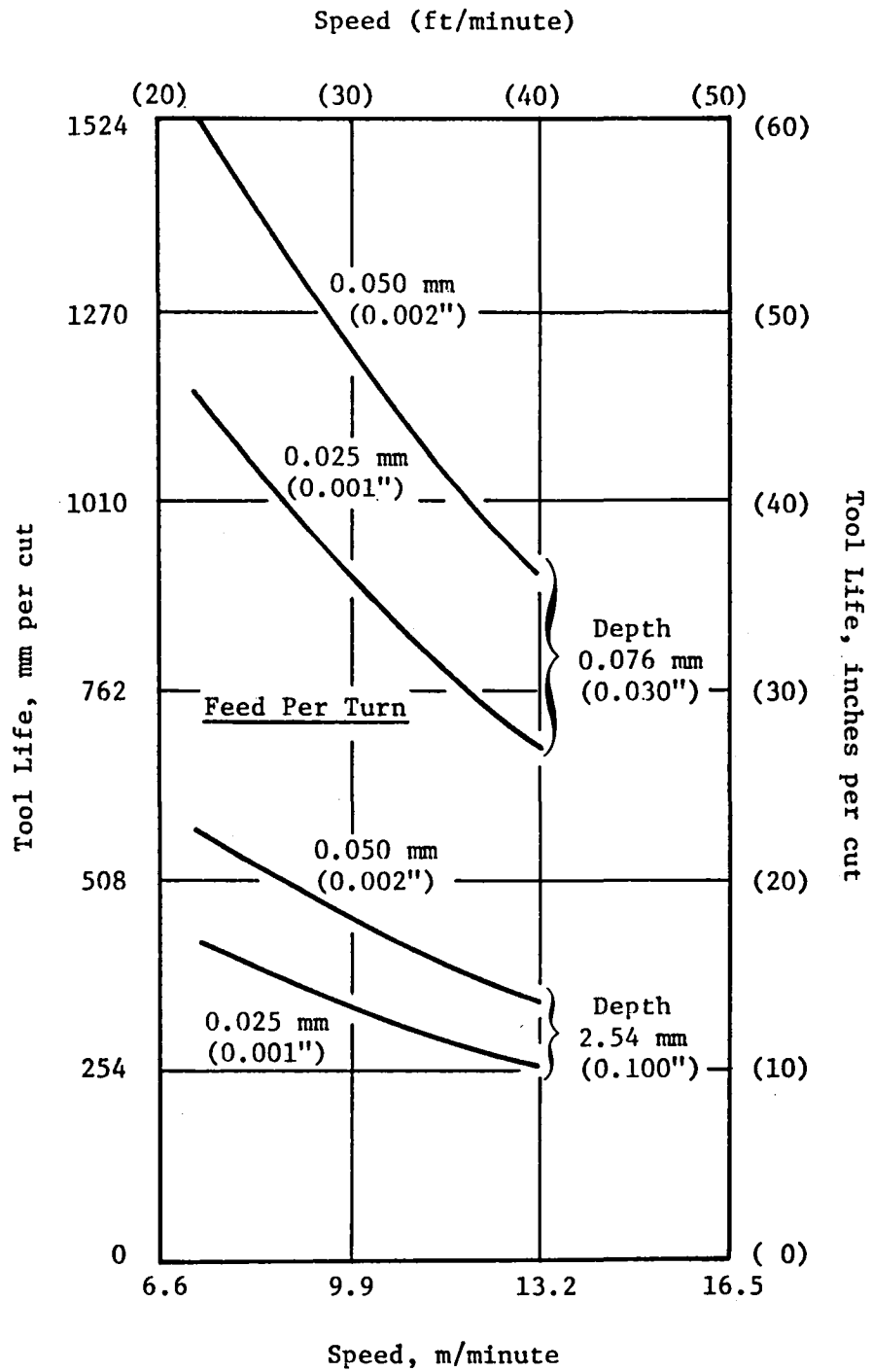


Figure 3-84. Tool Life-Linear Milling.

Tool life is not the only criterion for selecting machining parameters, but cost must also be considered.

The milling cost per pound of metal removed is 50 to 100 times as high as typical turning costs (for peripheral cuts in this size range). It will, of course, vary with the type of milling operation, cutter size, rigidity of set-up, etc.

Deep-Hole Drilling

The CF6 Aft Shaft contains a number of deep holes in the 1.5 mm (1/16 inch) and 6.35 mm (1/4 inch) diameter ranges. While these could be drilled in lower alloy content materials with conventional high-speed drills, standard practice in René 95 would be to EDM them and remove the recast layer with a carbide reamer. The purpose of this work was to evaluate the effectiveness of carbide drilling as an alternative process.

In drilling with both the 1.5 mm (1/16 inch) and 6.35 mm (1/4 inch) carbide drills, it was shown that holes of 3 diameters depth, such as those in the CF6-50 Aft Shaft, can be drilled with carbide tools at reasonable cost (tool and labor cost) whereas "EDM + ream" would cost more than twice as much.

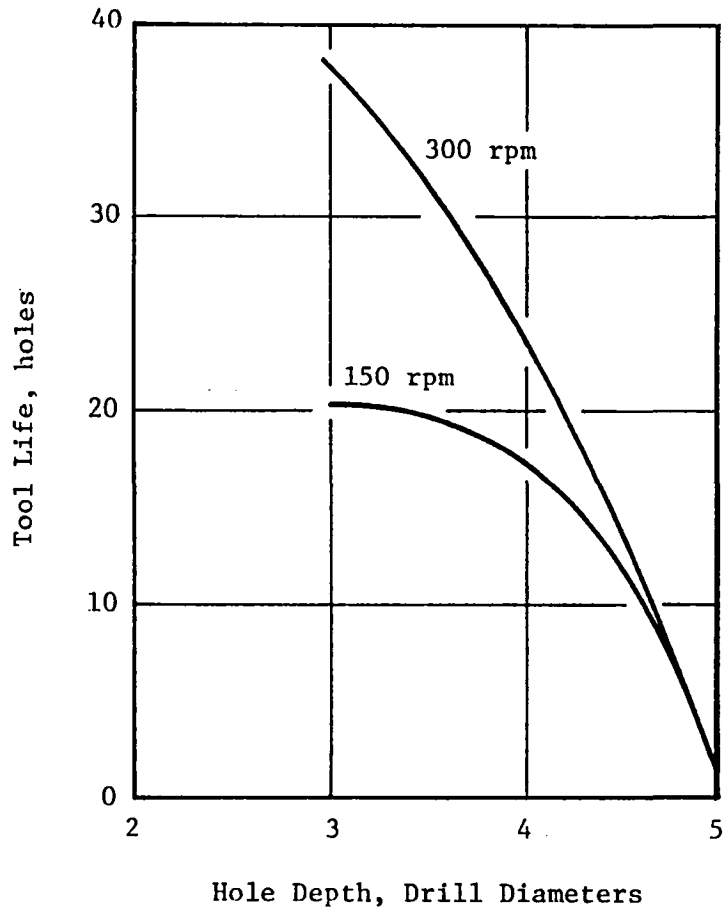
It was found that Master Spiral drills were superior to Twist drills and that 37 holes per sharpening could be expected at 300 rpm and 0.0635 mm (0.0025 inch) pr feed. Considering tool cost and labor, the relative cost perhole was found to be a minimum at 300 rpm and 0.102 mm (0.004 inch) pr. Maximum tool life therefore does not necessarily equate with minimum cost.

Vertical deviation during hole drilling (from a theoretical cylinder) is taken to include runout, taper, and local undercuts. The Master Spiral drill at recommended conditions produces about 0.1 mm (0.004 inch) vertical deviation and would probably dictate an additional reaming operation in most cases.

The effect of increased hole depth on drill life is shown in Figures 3-85 and 3-86. Life drops off appreciably at 4 diameters. In the 6.35 mm (1/4 inch) diameter holes, a depth of 5 diameters results in one hole; not an economic situation. In the latter test, the coolant was changed to a cutting oil, however no improvement was noted.

Turning of HIP and Forged René 95 Disks

Although HIP and Forge René 95 is usually turned with carbide, no systematic machining studies had been made to determine minimum cost conditions or possible advantages of Borazon tool materials.



*based on 0.25 mm (0.010") uniform wear and at 0.0635 mm per rev. (0.0025" per rev.) feed.

Figure 3-85. Effect of Hole Depth on Drill Life*, 6.35 mm (1/4") Diameter Carbide Drills.

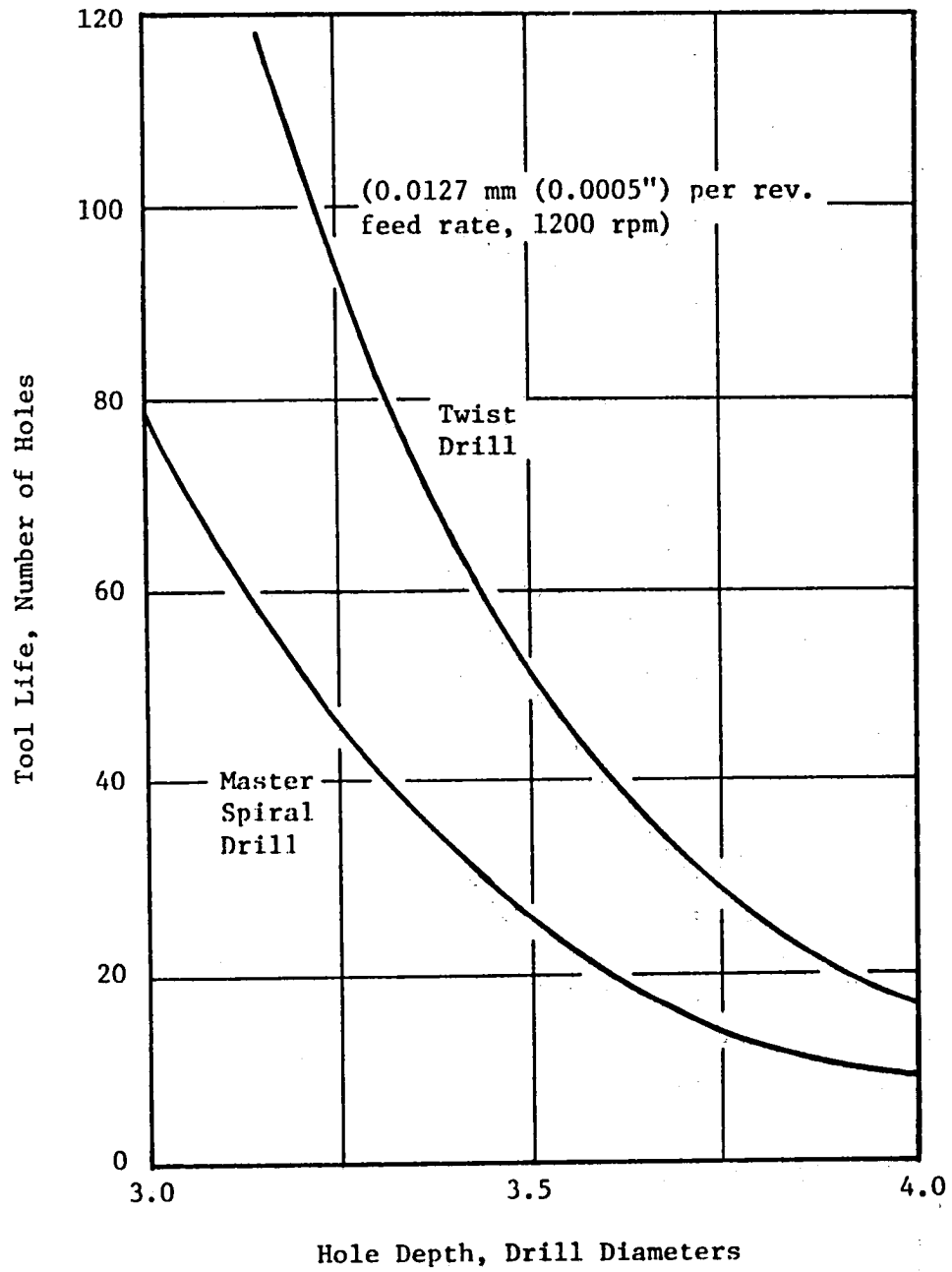


Figure 3-86. Effect of Hole Dept on Drill Life, 1.6 mm (1/16") Diameter Carbide Drills.

Preliminary turning with Borazon tools had demonstrated feasibility although cost effectiveness was in doubt. It was thought that changes in operating conditions or tool geometry might yield favorable results. Although turning tests with carbide were not extensive, the building-block technique used in design of the experiment yields a linear model sufficient for comparisons.

Borazon tools, in their present form, are not cost effective for turning this form of René 95, except for light cuts less than 0.5 mm (0.020 inch) in depth. Tests at 0.5 mm (0.025 inch) and 1 mm (0.040 inch) depth resulted in fracture in several cases; a condition not consistent with good machining practice. Changes in tool geometry were not fruitful.

Life experience with carbide tools in this limited experiment (8 tests) was significantly better than previously found when machining as-HIP René 95 (with carbide). This is not unexpected since the mechanical properties of this material were lower than those of the as-HIP René 95 tested. It may also be due to the limited carbide tests run to date. It does point up that material processing has a significant effect on machinability, and that all HIP forms cannot be considered to be the same. Based on relative machining costs the following turning conditions are recommended:

Type Cut	Tool Material	Depth mm (inches)	Feed mm (ipr)	Speed* (ft/min) m/mm
Finish	Borazon	0.13-0.51 (0.005-0.020)	0.10 (0.004)	(400) 121.9
Semi Finish	Carbide	0.51-1.02 (0.020-.040)	0.15-0.25 (0.006-0.010)	(70-90) 21.1-27.4
Rough	Carbide	1.02-3.12 (0.040-0.125)	0.20-0.36 (0.008-0.014)	(70-90) 21.3-27.4

*Even though a high speed may be cost effective, one must check the tool life (area) to assure completion of the cut without a tool change.

Two HIP and Forge René 95 Stage 5/9 disks were used for testing. They were HIP'd by Crucible and hot-die forged at Ladish. These forgings had typical René 95 properties. The properties also were about the same as for as-HIP René 95 material. The test setup was on a 4.06 m (16 inch) Lodge and Shipley variable speed lathe. Because the disk diameter was too large to clear the carriage, a heavy-duty tool post extension was built. Other constant conditions were as follows:

	Borazon	Carbide
Insert	TNG 3-1/2 32	TNG 432 (883)
Holder	CTBNR-85-4 (Mod)	MTANR-85
SCEA (degrees)	15	0
Coolant	Trimsol W/B @ 3:1	Trimsol W/B @ 3:1

The factorial experiment (2 x 2 x 3) shown in Table 3-44 was run in random order, using Borazon tools. Statistical analysis of the results was only able to pinpoint one significant variable (depth) due to scatter in the data and the relatively small size of the experiment. This often happens when the fracture mode is evident. The resulting tool life equation is:

$$\ln(L) = 2.702 - 1.078A - 0.631B - 1.097C - 0.334 B \times C$$

where: L is tool life, minutes
A is (speed - 70)/20
B is (feed - 0.010)/0.004
C is (depth - 0.060)/0.040

The feed/depth interaction is evident in that high feed yields greater life at light depth. This is, presumably due to the nose radius effect; thinning the chip. Note that tool life is given in terms of area turned, which is more useful than "minutes" when conditions vary widely.

4.0 HIP + FORGE PROCESSING

4.1 HOT DIE FORGING PREFORM SHAPE AND FORGING PARAMETERS

4.1.1 Die Cavity Design

The Stage 5 through 9 compressor disk forging is a shape designed to produce the five disks used to fabricate the inertia welded CFM56/F101 engine compressor spool. The similarity of the final shape of these disks dictates that a common forging shape for these parts is an efficient production process. The extremities of the composite part design were defined by superimposing the inertia weld part process shapes for all five stages and the forging shape then was designed about that composite drawing.

The general configuration of this near-net shape forging is shown in Figure 4-1. The smallest forging shape, considering the forging tolerances, is superimposed over the nominal dimensions for the composite (Stages 5-9 inclusive) inertia weld process shape. The sketch shows that the minimum forged part dimensions permit the forging to intersect the inertia weld part at one location on the rim. This situation was considered acceptable for ultrasonic inspection, since there was still sufficient material envelope beyond the final engineering part dimensions to allow ultrasonic inspection and inertia welding. As indicated in Figure 4-1 a bore test ring, labelled "T" was provided for mechanical test qualification of each forging. The average die cavity dimensions resulted in a calculated weight of about 30.8 kg (68 pounds) for this forging, although the actual forging weight is estimated at 32.6-33.6 kg (72-74 pounds) after consideration of flash and die closure tolerances.

The die design established by the General Electric and Ladish Companies in this task was approved by NASA and then used in subsequent tasks to manufacture the full-scale forging dies.

During the course of the MATE program, a redesign of the CFM56/F101 engine occurred. The effect of that redesign required a modification of the forging die which resulted in the dimensions shown in Figure 4-1. The forging dimensional modifications involved increasing the bore thickness by 2.54 mm (0.100 inch), decreasing the bore diameter by 1.3 cm (0.500 inch) and increasing the rim height by about 0.76 mm (0.03 inch). The change in forging weight of approximately four pounds was accommodated by modifying the die while using the selected preform design. There was sufficient excess weight in the preform design to permit a 3% increase in the die cavity weight after the design change.

4.1.2 Preform Shape Design

Design of the preform shape was established by the selected forging vendor, the Ladish Company, after dimensional agreements were reached on the forging process drawing. The concepts of preform design are proprietary to

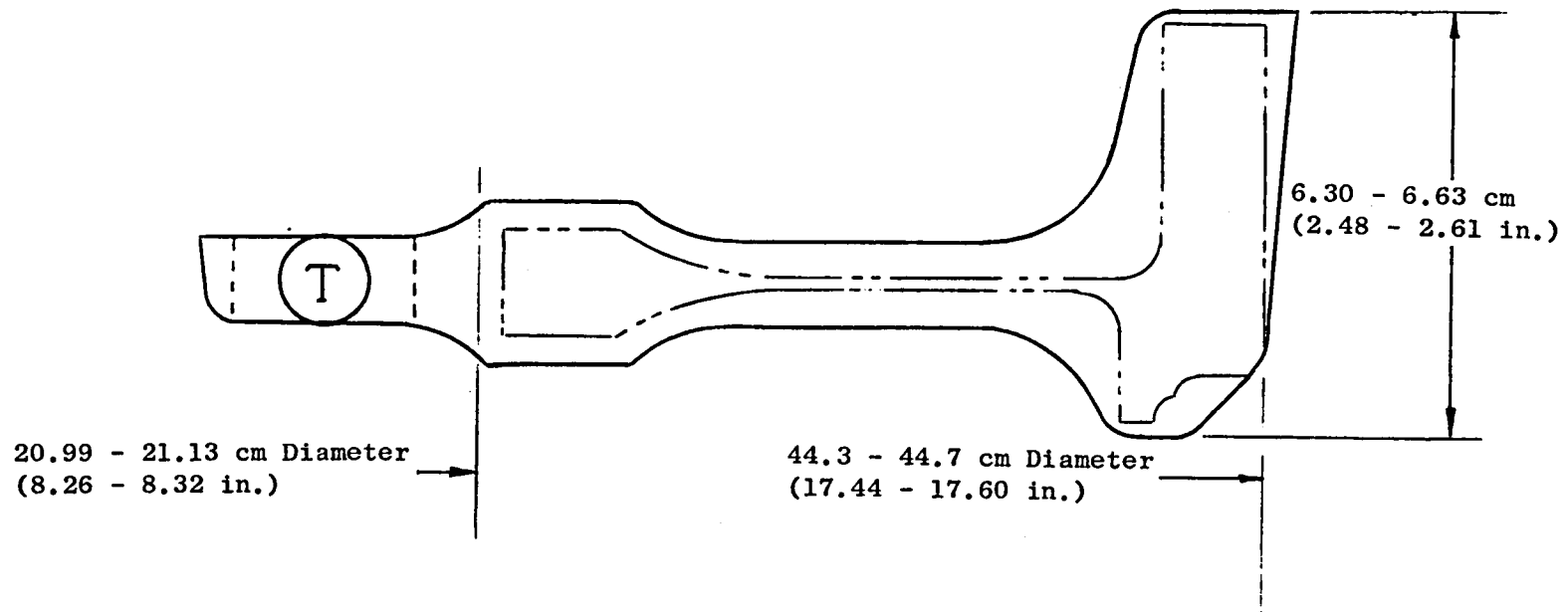


Figure 4-1. CFM56/F101 Stages 5-9 Compressor Rotor Disk Forging Configuration.

the Ladish Company since that design was based on experience prior to this program, but the basic configuration proposed was a hollow-center flat disk shape with a locating ring. Three preforms were designed using this basic configuration to provide reductions of 40%, 50%, and 60% in the forging parameter study. The results of the subscale study performed with these designs was planned to establish the configuration for the full-scale preforms.

4.1.3 CFM56/F101 Disk Hot Die Forging Parameter Development

A subscale forge parameter development study was conducted to establish the preferred forge reduction, forge temperature, and preforge heat-treatment cooling rate. Subscale preforms were machined from a compact produced by CarTech to the designs established for 40, 50, and 60% forge reductions. After selection of the preferred forge reduction, preforms were manufactured from this same material to evaluate the effect of variations in the preforge heat treatment cooling rate and the effect of variations in the forge temperature.

CarTech supplied the material for the subscale forge parameter development study. Thirteen centimeter (5 inch) diameter logs were prepared using the master powder blend B-093. That blend was the typical -60 mesh powder product produced by CarTech as characterized in Table 4-1. The cylindrical shapes (logs) were HIP compacted at Kawecki Berylco Industries (KBI) to CarTech's specifications.

The test facility used for the subscale forge parameter study was the minicompression tester built and used by the Ladish Company. It is a subscale facility quite similar in operation to the larger production isothermal forging press, except that loading in the subscale press is a manual rather than an automated remote handling process. Subscale molybdenum-base alloy dies were manufactured to 1/4 scale for the forging design shown in Figure 4-1 for these tests.

Forging Reduction Study

Preforms were machined from the CarTech logs to shapes which would yield 40, 50, or 60% forge reduction when forged in the Ladish 1/4-scale dies. These preforms were grain-growth preforge heat treated at 1190° C (2175° F) for four hours, and subsequently cooled at 93° C (200° F) hour to ~1056° C (1900° F) and then air cooled. A total of six preforms were forged, two for each percentage reduction. None of the six pieces exhibited significant forge cracking, although die fill was incomplete for the 60% forge reduction preforms. Metallographic evaluation of the subscale forgings showed that the 60% forge reduction provided the best combination of uniform metal flow and necklace microstructure throughout the part. Concern over the incomplete die fill of the 60% forge reduction prompted Ladish to conduct an additional subscale experiment with minor preform shape modifications designed to improve die-fill. That preform shape modification did improve die fill, while

Table 4-1. CarTech B-093 Characterization.

(Subscale Forge Parameter Development)

Chemical Analysis Results

	<u>Weight %</u>	<u>SPEC.</u>		<u>PPM</u>	<u>SPEC.</u>
Al	3.46	3.3-3.7	Si	400	2000 max
Ti	2.43	2.3-2.7	Mn	200	1500 max
Cb	3.61	3.3-3.7	S	50	150 max
Cr	13.29	12-14	P	<50	150 max
Co	8.08	7-9	Ta	<100	2000 max
Mo	3.56	3.3-3.7	Cu	200	-
W	3.39	3.3-3.7	Pb	<2	-
C	0.061	.04-.09	Bi	<0.5	-
Zr	0.052	.03-.07	O ₂	63	100 max
B	0.012	.006-.015	N ₂	10	50 max
Fe	0.23	0.5 max			

Particle Size Distribution

<u>Mesh Fraction</u>	<u>Weight %</u>
- 60,+ 80	6.8
- 80,+100	6.6
-100,+140	15.1
-140,+200	17.4
-200,+325	24.6
-325	29.5

Densities

Tap Density	5320 kg/m ³
Apparent Density	4290 kg/m ³

still maintaining the basic 60% forge reduction. Ladish was confident that complete die-fill could be achieved in the full-scale facility with the 60% reduction preform shape design because of a greater full-scale press capacity and improved metal flow with a thicker cross section. However, minor preform shape modifications were incorporated in the full-scale development to increase the die-fill probability.

Metallographic evaluation of the forged subscale preforms was used as the principal criterion for selection of the optimum preform shape, although this selection was further substantiated by mechanical property tests, as shown in Table 4-2. The goal for the subscale development was to achieve the necklace microstructure throughout the forging. The necklace microstructure is a duplex microstructure consisting of a necklace of fine recrystallized grains, ASTM No. 8 on Liner, surrounding larger elongated unrecrystallized grains ranging between ASTM Nos. 2 and 7. The total area of recrystallized fine grains in this necklace microstructure should range between about 10 and 60% of the observed surface plane. Typical microstructures for the 40, 50, and 60% forge reduction subscale parts are shown in Figure 4-2. All three forge reductions resulted in a necklace microstructure in the bore and web zone of these forgings, but only the 60% forge reduction provided sufficient metal flow to give the desired necklace microstructure in the rim zone as shown in Figure 4.2. The 60% reduction resulted in a uniform necklace microstructure throughout the forging and the superior combination of mechanical properties as shown in Table 4-2. It should be noted that all three forge reduction conditions resulted in acceptable room temperature tensile properties; however, a superior combination of stress rupture life and ductility was demonstrated in tests made on the 60% forge reduction part.

Forge Temperature Study

Forge parameter studies were conducted on subscale preforms machined from the CarTech log to the original 60% forge reduction shape. The first parameter, forge temperature, was evaluated by forging two preforms, one at 1093° C (2000° F) and one at 1121° C (2050° F) standard forge practice. These preforms were preforge heat treated to the same schedule as the subscale shape development preforms. Previously, the subscale preform forged at 1107° C (2025° F) in the shape development study had not exhibited any significant cracking, whereas now, both preforms in the forge temperature parameter study did show evidence of cracking, with more severe cracking on the 1093° C (2000° F) forged part than on the one forged at 1121° C (2050° F). Since cracking had not been anticipated to be a problem on either of these parts, a detailed analysis for the cause of the cracking was conducted. In the course of this investigation, it was noted that the back-up blocks for the sub-scale dies in the hot compression test machine were deformed, probably as the result of the earlier tests. While this misalignment, caused by the yielding of the back-up blocks, cannot be proven as the sole cause for cracking, it did raise doubts about the validity of the forge temperature experiment.

Table 4-2. Subscale Forge Development Mechanical Property Tests.

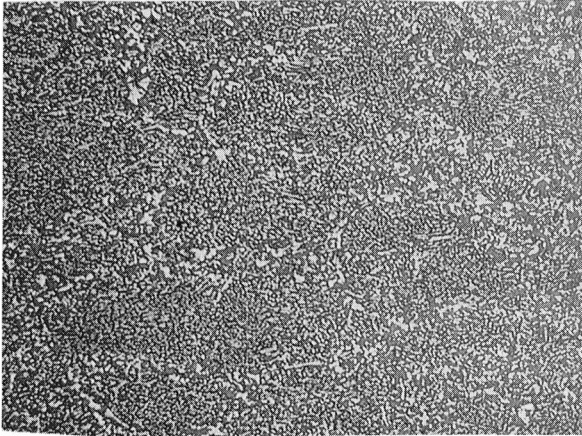
Forging Reduction	40%		50%		60%		Specification Minimums	
	MPa	(KSI)	MPa	(KSI)	MPa	(KSI)	MPa	(KSI)
Room Temperature Tensile*								
0.2% Yield Strength	1284	(186)	1116	(188)	1116	(188)	1227	(178)
Ultimate Tensile Strength	1682	(244)	1620	(235**)	1696	(246)	1565	(227)
Elong. (%)		(16)		(11**)		(16)		(10)
Red. Area (%)		(18)		(12**)		(20)		(12)
649° C/1034 MPa (1200° F/150 ksi) Stress Rupture***								
Life (Hrs)		6		47		53		25
Elong. (%)		7.9		4.4		5.0		2

*Specimens given Standard Heat Treat: (1093° C (2000° F) 1 Hr/Oil Quench + 760° C (1400° F) 16 Hrs/Air Cool

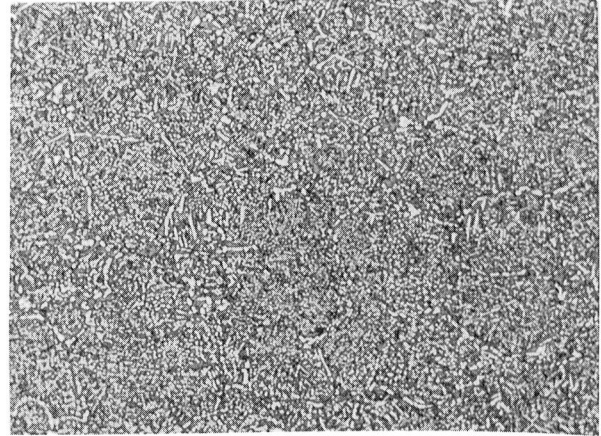
**Scribe Line Failure

***Specimens Aged At 760° C (1400° F) 16 Hrs/Air Cool After Forging, As Screening Test

A. 40% FORGE REDUCTION



BORE-WEB MT 16003

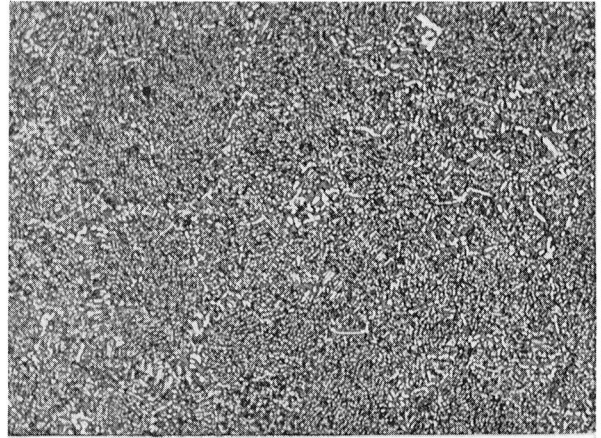


RIM MT 16002

B. 50% FORGE REDUCTION

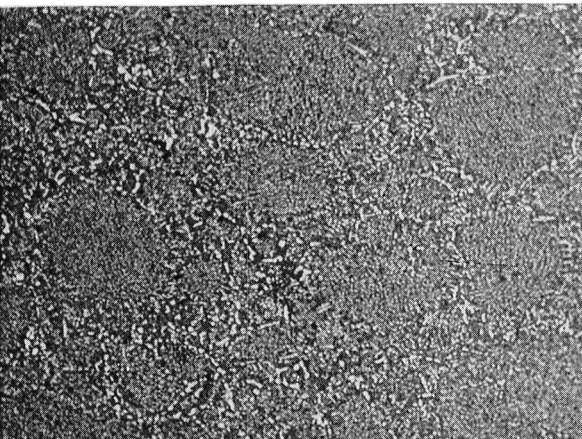


BORE-WEB MT 16005

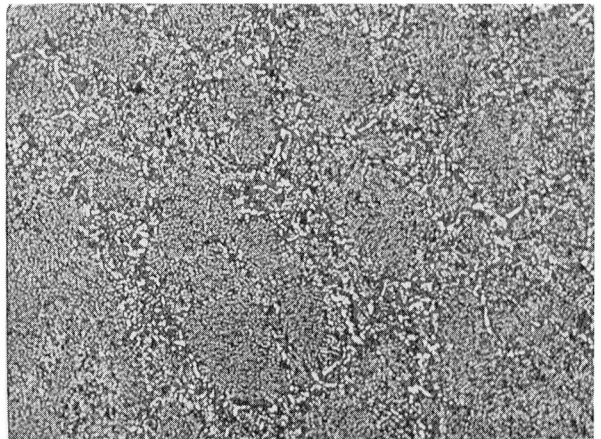


RIM MT 16004

C. 60% FORGE REDUCTION



BORE-WEB MT 16007



RIM MT 16006

Figure 4-2. Typical Subscale F101 Stage(s) 5-9 Compressor Disk(s) Forging Microstructures At 250X (Phosphoric Electrolytic Etch)

Preforge Heat-Treatment Cooling-Rate Study

Preparatory to the preforge heat treat cooling rate experiment, two preforms, one cooled at 56° C (100° F)/hour and one cooled at 278° C (500° F)/hour were manufactured. It was known, from cast plus wrought René 95 technology*, that increasing the cooling rate from the preforge heat treatment is conducive for producing the necklace microstructure. Similarly, it has been shown that very rapid cooling rates degrade forgeability. The goal was therefore to provide sufficient data to select a preferred preforge heat treatment cooling rate for the initial full-scale development forge trials.

The selection of the preforge heat treatment cooling rate based on the results of this study, like that of the forging temperature study, was complicated by cracking observed during forging. The initial preforms used to establish the 60% preform reduction shape received the 111° C/hr (200° F)/hr cooling rate from the preforge heat treatment and were forged at 1107° C (2025° F) without significant cracking. The subscale forgeability trials using 56° C (100° F)/hr and 260° C (500° F)/hr preforge heat treatment cooling rates with the 1107° C (2025° F) forge temperature did result in some cracking. The 38° C (100° F)/hr cooling rate preform exhibited a single crack, whereas the 278° C (500° F)/hr cooling rate preform exhibited multiple cracks. A necklace microstructure was achieved with the 278° C (500° F)/hr cooling rate preform, whereas the microstructure of the 56° C (100° F)/hr cooling rate preform was nearly a 100% fine grain condition with no apparent necklace structure. The conclusion drawn from these results was that the 278° C (500° F)/hr cooling rate significantly reduces forgeability, whereas the 56° C (100° F)/hr cooling rate is not sufficiently rapid to achieve the necklace microstructure. The 111° C (200° F)/hr cooling rate, on the other hand, produced both the necklace microstructure and provided acceptable forgeability. The anomaly indicated by the preform with the slower 56° C (100° F)/hr cooling rate which cracked while the 111° C (200° F)/hr cooling rate preform forged adequately, was thought to be due to variation within the as-received subscale log.

4.1.4 Full-Scale Forging Parameter Selection

Subscale forge parameter development and a single part full-scale demonstration (Task III) resulted in the selection of the following forging conditions.

- Forge Reduction - 60% reduction from the preform shape
- Forge Temperature - 1107° C (2025° F)
- Preforge Heat Treatment Cooling Rate - 111° C (200° F/hr)

*CE Shamblen, RE Allen, and FE Walker, "Effect of Processing and Microstructure on René 95", Met. Trans., Vol. 6A, November, 1975, pp 2073-82.

These parameters were shown to produce subscale parts without significant cracking and which had a uniform necklace microstructure throughout the part with acceptable mechanical properties. Lesser forge reductions did not produce sufficient flow at the rim to yield the desired microstructure. Cracking at the 1093° C (2000° F) forge temperature was definitely more severe, although some minor cracking was even observed at the 1121° C (2050° F) forge temperature in the subscale forge temperature parameter study. The cracking of these parts in the forge temperature study was initially attributed to a die misalignment problem, and it is entirely possible that this was a factor in the observed cracking. However, subsequent evaluations suggested that forgeability variations within the individual preforms may also have been a significant factor in the observed cracking. A preforge heat treatment cooling rate of 278° C (500° F)/hr definitely degraded forgeability, whereas a cooling rate as slow as 56° C (100° F)/hr did not result in the desired microstructure. Cracking of the subscale preforms in the preforge heat treatment parameter study also was believed to be attributable to variations (such as striations, prior particle boundary delineation or machining tolerances) in the individual preforms.

An evaluation of the cracking observed during processing of the forge parameter development preforms, the forgeable surface development preforms and the first full-scale demonstration part (Task III) was conducted. Most probable causes for the cracking were identified and corrective actions were implemented. This evaluation will be described in detail in Task III, Section 4.3. The corrective actions did not, however, alter the Task I conclusions, which demonstrated that the proposed forge parameters will yield the desired shape, necklace microstructure, and acceptable mechanical properties.

4.2 TASK II PROCESS DEVELOPMENT

4.2.1 Development Approach and Materials Characterization

A study was conducted to establish the processes necessary to produce near-net-shape forging preforms for the CFM56/F101 René 95 compressor disk forgings. The design of this preform was established in Task I of this program. Subscale (1/4 size) and full-scale shape development trials were conducted in this task to produce near-net-shape forging preforms. The subscale preform shape was developed to permit investigation of several surface preparation techniques to achieve a forgeable surface on near-net-shape preforms. The forgeable surface preparation technique developed on the subscale preforms was then to be demonstrated on preforms produced from the full-scale shape development trials.

Two powder (preform) suppliers were involved in the near-net-shape forgeable-surface preform study. These vendors were the Udimet Division of Special Metals (Udimet) and the Carpenter Technology Corporation (CarTech). General Electric and the Ladish Companies were involved in evaluation of the forgeable surface development studies, and forging of the subscale preforms were conducted at the Ladish Company on their minicompression test unit.

Udimet used four master powder blends (MPB) in the near-net-shape forgeable-surface preform development study. The subscale preform shape development parts and the initial subscale forgeable-surface development preforms were produced using MPB No. 76028. The first full scale shape development trial was also conducted using that master powder blend. A second subscale forgeable-surface development series of preforms was produced from MPB No. 76072. MPB No. 77024 was used for the second full-scale preform shape development trial and MPB No. 77042 was used for the final full-scale iterations. Characterization of two master powder blends (76028 and 76072) used in the subscale study is given in Table 4-3, whereas the other materials are described in later sections of this report.

CarTech used four MPB's in the preforms supplied for this program. The majority of the subscale shape development and the subscale forgeable-surface development was conducted using MPB NO. 93, but a limited number of these preforms were produced from MPB No. 107. In addition to the subscale preforms, CarTech initially supplied six oversized full-scale preforms to be machined to the design established in Task I for a preliminary full-scale evaluation. The oversized full-scale preforms also were produced from MPBs No. 93 and No. 107. MPB No. 139 was used to conduct the full-scale near-net-shape preform shape iterations and to produce the near-net-shape forging preforms for the Task III evaluation. MPB No. 146 was used to produce a three-piece preform multiple log to partially replace the initial six individual preforms after a forgeability problem was encountered. Characterization data for the two CarTech master powder blends (B93 and B107) used in the subscale study are given in Table 4-3, whereas characterization of the other full-scale part blends are presented in later sections. The first three blends were standard CarTech

Table 4-3. Subscale Forgeable Surface Development Master Powder Blends Characterization

Chemistry - Nominal Weight Percent

	<u>Udimet 76028</u>	<u>Udimet 76072</u>	<u>CarTech B93</u>	<u>CarTech B107</u>
Al	3.54	3.60	3.46	3.42
Ti	2.58	2.44	2.43	2.46
Cb	3.53	3.51	3.61	3.52
Cr	13.02	13.02	13.29	13.22
Co	8.08	8.13	8.08	8.06
Mo	3.42	3.40	3.56	3.50
W	3.46	3.47	3.39	3.51
C	0.062	0.051	0.061	0.072
Zr	0.037	0.042	0.052	0.051
B	0.013	0.012	0.012	0.012
Fe	0.21	0.12	0.23	0.23

Chemistry - Nominal ppm

Si	<100	<100	400	200
Mn	200	180	200	100
S	40	40	50	20
P	40	30	<50	<50
Ta	200	240	<100	<100
Cu	-	-	200	200
Pb	-	-	<2	<2
Bi	-	-	<0.5	<0.5
O2	84	80	63	81
N2	24	38	10	20
H2	1	6	---	4

Mesh Size Distribution - Weight Percent

+60	0	0	0	0
- 60, + 80	9.1	5.5	6.8	8.8
- 80, +100	8.3	5.7	6.6	9.0
-100 +140	19.8	14.3	15.1	15.6
-140, +200	18.1	16.9	17.4	18.0
-200, +325	19.1	21.6	24.6	22.0
-325	25.6	36.0	29.5	26.4

powder products, although the fourth blend (No. 146) modified the standard practice to permit cyclone fines to be used in that material.

Subsequent to identifying excessive cracking in the CarTech oversized preforms, three preform multiple logs produced from three Udimet master powder blends were machined and forged. Those blends, MPBs No. 77004, 77029, and 77032, were the standard Udimet powder product as is described later in this report.

4.2.2 Subscale Shape Development

The design of the full-scale near-net-shape forging preform was established in Task I. That design was basically a hollow-center right-cylinder shape with a locating ring which required a 60% forge reduction to fill the die cavity for the CFM56/F101 compressor disk forgings. Tolerances on the specified dimensions for the full-scale part were initially selected as typical forging tolerances, but the more realistic requirements were specified to be the minimum and maximum forging weights and the required height for the 60% forge reduction. Reducing the preform shape down to one-quarter scale was no problem, but specifying the dimensional tolerances for the one-quarter scale design was a problem in view of the available as-HIP shape making capabilities. Requirements for the tolerances were in the range of ± 0.50 mm (± 0.020 inch) on some dimensions for a direct scale-down of the full-scale preform. Since these tolerances were unrealistic, the decision was reached to specify only two major dimensional requirements on the subscale preforms. Those requirements were the rim dimension and the flatness of one face. The intent of the subscale test was to evaluate forgeability of the preform surface with various surface preparation techniques. That test was feasible with the rim diameter and one forging face available for evaluation by surface preparation of that rim and face. The other face could be machined to dimension for test if the preform were oversized. In the situations where this approach was used, the surface prepared face was consistently located to see the maximum forging deformation.

Since surface preparation techniques were to be used to achieve the forgeable-surface condition, the preform vendors had to modify the preform design supplied by Ladish to provide material for removal of the container-preform interaction zone. The intent of this study was that each vendor would modify the design to add the excess coverage required for the particular container material diffusion zone.

Both Udimet and CarTech conducted three shape iterations in developing the subscale preform shape. Both vendors also used the metal can approach with designs which included an OD and an ID seam weld. Achievement of the rim dimension requirement was adequate, but both vendors experienced problems in maintaining flatness of the faces of these preforms. Variations included an excessive height at the rim, a bulge at the mid radius, and occasionally a surface depression from what appeared to be an underfill condition. Flatness of the faces continued to be a problem in the subscale forgeable surface development program.

Forgeable Surface Process Development

Interaction zones between the container material and the powder during HIP compaction was recognized as a potential forgeability problem prior to initiating these studies. Limited investigations, prior to the MATE program, had shown diffusion zones after HIP to be as deep as ~0.50 mm (~20 mils) in the powder preform. The most common surface interaction metallographic observation was heavy prior particle boundary delineation by MC carbide precipitates. Such a condition is known to promote surface cracking and degrade forgeability of René 95 preforms. Therefore, the forgeable surface development study was planned to establish a process, excluding an expensive total surface machining step, to remove the container-preform interaction zone from near-net-shape preforms prior to forging.

Information on potentially viable surface preparation processes was supplied to the vendors by General Electric, and each vendor (Udimet and CarTech) proposed surface preparation processes to remove the container-preform interaction zone. At the time when the initial surface preparation processes were proposed, General Electric also was involved in evaluation of various finishing techniques. The initial surface preparation techniques proposed were heavily slanted towards mass-finish metal removal methods. However, after completion of the study on mass finish techniques and presenting the results to Udimet and CarTech, both vendors made changes in their proposed methods for metal removal. These changes were developed for two reasons. The first was that a simultaneous in-house development study at General Electric identified a solution for chemical milling which was capable of 0.013 - 0.025 mm (0.5-1.0 mil)/ minute metal removal on René 95 without pitting or intergranular attack. The second reason was recognition that the practical limit of the abrasive mass-finishing process for metal removal was only a depth of about 0.13 mm (5 mils.) Several mass finish surface preparation techniques were evaluated, but further development was discontinued on this program since removal was considered the minimum 0.13 mm (5 mil) metal clean-up necessary for forgeable surface development. The initially proposed and the revised surface preparation techniques for the first series of forgeable-surface development preforms are shown in Table 4-4.

Container material selection was initially thought to be an important consideration towards development of the near-net-shape forgeable-surface preform process because of the container to preform interdiffusion zone. Table 4-4 identifies the container materials proposed for subscale development, and a preliminary evaluation was conducted on the early preforms for comparison to SAE 1008 mild steel. A summary of those evaluations is presented in Table 4-5 which considers material cost, fabricability, and interaction zone depth in comparison to SAE 1008 mild steel.

SAE 1008 mild steel established the base line for cost and fabricability, but the metallographically apparent diffusion zone extended up to ~0.51 mm (~20 mils). The heavy prior particle boundary delineation by MC carbides only extended to about a 0.076 mm (3 mils) depth, but the gamma prime depletion zone extended to ~0.5 mm (~20 mils). Microprobe analysis traces on

Table 4-4. First Series Net-Shape Subscale Forging Preform Surface Preparation Conditions.

Preform Vendor/ Preform No.	Can Material	Can Removal	Surface Preparation	
			Initial Plan	Final Plan
Udimet/U1	SAE 1008 Steel	Machine	Machined - Baseline	Machined - Baseline
Udimet/U2	SAE 1008 Steel	Pickle	None	None
Udimet/U3	SAE 1008 Steel	Pickle	Mass Finish (Harperize)	Chemically-Mill ~ 0.127mm (5 Mils)
Udimet/U4	SAE 1008 Steel	Pickle	Deplate (Can and Surface)	Chemically-Mill ~ 0.51mm (20 Mils)
Udimet/U5	304 Stainless Steel	Pickle	None	None
Udimet/U6	304 Stainless Steel	Pickle	Mass Finish (Harperize)	Chemically-Mill ~ 0.127mm (5 Mils)
Udimet/U7	Armco Iron	Pickle	None	None
Udimet/U8	Armco Iron	Pickle	Mass Finish (Harperize)	Chemically-Mill ~ 0.127mm (5 Mils)
CarTech/C1	SAE 1008 Steel	Machine	Machined - Baseline	Machined - Baseline
CarTech/C2	SAE 1008 Steel	Pickle	None	None
CarTech/C3	SAE 1008 Steel	Pickle	Mass Finish (Harperize)	Chemically-Mill ~ 0.127mm (5 Mils)
CarTech/C4	SAE 1008 Steel	Pickle	Mass Finish (Harperize)	Chemically-Mill ~ 0.51mm (20 Mils)
CarTech/C5	Low Interstitial - FE Base	Pickle	None	None
CarTech/C6	Low Interstitial - FE Base	Pickle	Mass Finish (Harperize)	Chemically-Mill ~ 0.127mm (5 Mils)
CarTech/C7	NiPlate - SAE 1008 Steel	Pickle	None	None
CarTech/C8	Chromate Coating - SAE 1008	Pickle	None	None

Table 4-5. Container Material Characterization.

<u>Container Material</u>	<u>Approximate Cost Relative To SAE 1008 Steel</u>	<u>Fabri-cability</u>	<u>Metallographically Evident Diffusion Zone</u>
SAE 1008	1	OK	0.076mm ~ (3 Mils) Grain Boundary MC 0.51mm ~ (20 Mils) - γ' Depletion
Ferritic Stainless	2-3X	OK	0.025-0.051mm (1-2 Mils)
304 Stainless	5X	Difficult	0.051-0.076mm (2-3 Mils)
Ni 200	25X	Difficult	0.051mm (2 Mils)

specimens from the initial subscale shape trial parts indicated about 0.080 mm (3.5 mils) of iron diffusion from the mild-steel/René 95 interface, but the carbon trace could not be shown with the available microprobe analyzer. Later Ladish microprobe evaluations for a 304 stainless steel container indicated Fe diffusion into the preform to a depth of 1.5 mm (0.060 inches) and depletion of the elements Ti to 0.4 mm (0.016 inches) Al to 0.2 mm (0.008 inches) and Mo to 0.1 mm (0.004 inches.) The gamma prime element depletion observed by Ladish's microprobe results were not apparent in the earlier metallographic evaluations. Ferritic stainless steel, or low interstitial iron, exhibited acceptable fabricability, but the cost was 2-3 times that of SAE 1008 steel. The metallographically observed total interaction zone for ferritic stainless was only about 0.025-0.05 mm (1-2 mils,) which might offer an advantage over mild steel. Fabrication of the 304 stainless steel containers is feasible but more difficult than SAE 1008 steel. Further, 304 stainless costs about 5 times as much as SAE 1008 steel. Unalloyed nickel costs were 25 times that of SAE 1008 and in addition it was relatively difficult to fabricate. However, both 304 stainless and unalloyed nickel containers metallographically exhibited total diffusion zones of about 0.05 mm (2 mils) to show a potential advantage over SAE 1008 steel. The only conclusive advantage of the lower interstitial element iron and the 304 stainless steel is the reduction in the thickness of the heavy prior particle boundary MC carbide delineation zone, since Ladish's microprobe results suggest the gamma prime element depletion for 304 stainless steel is about the same as that observed for SAE 1008 mild steel. The inward diffusion of iron to 1.5 mm (0.060 inch) eventually set the metal removal requirement at that depth to assure elimination of contamination.

Each of the proposed container materials was evaluated while ignoring cost and fabricability considerations to determine the effect on forgeability, although it was recognized that all of these factors would be used in the final analyses to select a preform production process.

First Series Forgeable Surface Preform Evaluations

Udimet and CarTech produced the subscale containers shown in Table 4-6, filled these containers with René 95 powder, and HIP compacted them to preforms at 1121° C (2050° F) for two hours (minimum) at 103 MPa (15 kpsi.) The subscale preform shape was a flattened donut shape with a locating protrusion on one side at the inside diameter for the purpose of positioning in the die blocks prior to the forging upset. The weight of the subscale part was just over one pound. Udimet used their internal research and development autoclave to compact these preforms, whereas CarTech HIP compacted their preforms at KBI. The surface preparation for these preforms and the forgeability test results on the mini-compression tester at Ladish are summarized in Tables 4-6 and 4-7, and discussion of these results are given in the following paragraphs.

Two problems were encountered in the forgeability testing in respect to the mini-compression test facility. These initial forgeable surface preforms were forged prior to the Task I temperature parameter study and it is conceivable that the deformation of the back-up blocks for the subscale dies occurred during this experiment. Deformation of the back-up blocks led to a

Table 4-6. Net-Shape Subscale Forgeable Surface Hot Compression Test Metallographic Observations.

Preform Vendor No.	Can Material	Surface Preparation (1)	Forgeability		Metallographic Observations		
			Rating (2)	Comments	Reaction Zone		Comments
					mm	(mils)	
Udimet/U1	1008 Steel	Machined	4	Severe Axial Rim Cracking	0.076-0.132	3.0-5.2	Reaction Zone Shows PPB
Udimet/U2	1008 Steel	None	4	Severe Axial Rim Cracking	0.076-0.127	3.0-5.0	Reaction Zone Shows PPB
Udimet/U3	1008 Steel	Chemically Mill ~0.127mm (5 Mils)	1	Fill Tube Area Cracking	0.051-0.058	2.0-2.3	Reaction Zone Shows PPB
Udimet/U4	1008 Steel	Chemically Mill ~0.051mm (20 Mils)	4	Severe Axial Rim Cracking	0.033-0.061	1.3-2.4	Reaction Zone Shows PPB
Udimet/U5	304 SS	None	2	Fill Tube Area Cracking	0.076-0.132	3.0-5.2	Reaction Zone Shows PPB
Udimet/U6	304 SS	Chemically Mill ~0.127mm (5 Mils)	4	Severe Axial Rim Cracking	0.106-0.051	4.2-2.0	Reaction Zone Shows PPB
Udimet/U7	Armco Fe	None	4	Severe Axial Rim Cracking	0.081-0.178	3.2-7.0	Reaction Zone Shows PPB
Udimet/U8	Armco Fe	Chemically Mill ~0.127mm (5 Mils)	3	Severe Axial Rim Cracking	0.051-0.071	2.0-2.8	Reaction Zone Shows PPB
CarTech/C1	1008 Steel	Machined	0	Acceptable	0.013	0.5	Reaction Zone Shows PPB
CarTech/C2A	1008 Steel	None	1	Very Light Cracking	0.025	1.0	Reaction Zone Shows PPB
CarTech/C2B	1008 Steel	None	3	Light to Moderate Rim Cracking	0.041	1.6	Reaction Zone Shows PPB
CarTech/C2C	1008 Steel	None	4	Heavy Rim Cracking	0.041	1.6	Reaction Zone Shows PPB
CarTech/C3	1008 Steel	Chemically Mill ~0.127mm (5 Mils)	2	Light Rim Cracking-Notch Cracking	0.056	2.2	Reaction Zone Shows PPB
CarTech/C4	1008 Steel	Chemically Mill ~0.051mm (20 Mils)	3	Light to Moderate Rim Cracking	0.061	2.4	Reaction Zone Shows PPB
CarTech/C5	LI Fe Base	None	4	One Severe Rim Crack	0.013	0.5	Reaction Zone Shows PPB
CarTech/C6	LI Fe Base	Chemically Mill ~0.127mm (5 Mils)	2	Light Rim Cracking-Notch Effect	0.031	1.2	Reaction Zone Shows PPB
CarTech/C7	Ni-Plate 1008	None	4	Excessive Cracking	---	---	Either Container Leaked or Coating Caused Contamination
CarTech/C8	Chromate 1008	None	4	Very Severe Cracking	---	---	Either Container Leaked or Coating Caused Contamination
CarTech/C9	BN Coat 1008	None	3	Light to Moderate Rim Cracking	---	---	Reaction Zone Shows PPB

Notes:

(1) Can Removal by HNO₃ Pickle for 1008 Steel Containers

(2) Numerical Rating of Cracking Severity = 0 (Acceptable) to 4 (Excessive Cracking)

Table 4-7. Initial Net-Shape Forgeable Surface Hot Compression Test Evaluation Summary.

Preform Vendor No.	Can Material	Surface Preparation (1)	Forgeability Rating (2)	TIP		Filling Method	Minimum Input Wt.	Reaction Zone, mm (Mils)	Test Validity (3)
				Metallographic	$\Delta\%$				
Udimet/U1	1008	Machine	4	Excessive	5.02	Rim Fill	Below	0.089-0.132 (3.5-5.2)	Invalid
CarTech/C1	1008	Machine	0	Minor	0.10	Face Fill	OK	0.013 (0.5)	Valid
Udimet/U2	1008	None	4	Moderate	0.67	Rim Fill	OK	0.076-0.10 (3.0-4.0)	Questionable
CarTech/C2A	1008	None	1	Minor	0.01	Face Fill	OK	0.025 (1.0)	Valid
CarTech/C2B	1008	None	3	Minor	0.00	Face Fill	OK	0.041 (1.6)	Valid
CarTech/C2C	1008	None	4	Excessive	1.10	Face Fill	OK	0.041 (1.6)	Invalid
Udimet/U3	1008	Chemically Mill 0.127mm (5 Mils)	2	Moderate	0.42	Rim Fill	OK	0.051 (2.0)	Questionable
CarTech/C3	1008	Chemically Mill 0.127mm (5 Mils)	4	Minor	0.10	Face Fill	OK	0.056 (2.2)	Valid
Udimet/U4	1008	Chemically Mill 0.051mm (20 Mils)	4	Moderate	0.59	Rim Fill	Below	0.061 (2.4)	Questionable
CarTech/C4	1008	Chemically Mill 0.051mm (20 Mils)	3	Minor	0.00	Face Fill	OK	0.061 (2.4)	Valid
Udimet/U7	Armco FE	None	4	Moderate	0.65	Rim Fill	OK	0.081 (3.2)	Questionable
CarTech/C5	LI FE	None	4	Minor	0.06	Face Fill	OK	0.013 (0.5)	Valid
Udimet/U8	Armco FE	Chemically Mill 0.127mm (5 Mils)	3	Moderate	0.58	Rim Fill	OK	0.071 (2.8)	Questionable
CarTech/C6	LI FE	Chemically Mill 0.127mm (5 Mils)	2	Minor	0.01	Face Fill	OK	0.031 (1.2)	Valid
Udimet/U5	304 SS	None	2	Minor/Mod.	0.55	Rim Fill	OK	0.076-0.132 (3.0-5.2)	Questionable
Udimet/U6	304 SS	Chemically Mill 0.127mm (5 Mils)	4	Moderate	0.50	Rim Fill	Below	0.051 (2.0)	Questionable
CarTech/C7	1008, Ni Plate	None	4	Excessive	6.27	Face Fill	OK	---	Invalid
CarTech/C8	1008, Chromate	None	4	Excessive	3.66	Face Fill	OK	---	Invalid
CarTech/C9	1008, BN Coating	None	3	Minor	0.13	Face Fill	OK	0.013 (0.5)	Valid

Notes:
(1) Surface Preparation - Can Removed by Nitric Acid Pickle for all but Machined Preforms
(2) Forgeability Rating: 0 = Acceptable to 4 = Catastrophic Cracking
(3) This rating considers TIP values, can filling method, input weight, reaction zone and die misalignment

die misalignment situation which might contribute to initiation of cracks and could definitely enhance propagation of small surface cracks. The second concern was that the subscale die, as machined, had a small indentation which would leave a shallow ~0.13 mm (~0.005 inch) "bump" on the web-rim radius of each forged part. While this "bump" served to identify the rotational location of the preform in the die, it also tended to produce a notch effect in the forging. Preliminary trials by Ladish showed that machined good forgeability powder preforms forge well in spite of this notch, whereas marginal quality machined powder preforms (either from powder quality or from rapid cooling after preforge heat treatment) were more susceptible to cracking in this notch area. As such, the notch became (unintentionally) an additional quality check. The "bump" on the forging provided the clue toward suggesting that the back-up block deformation might be affecting the results, since most of the cracking observed consistently occurred at one side of the die.

Udimet First Series Forgeable Surface Preforms

Udimet supplied the eight subscale preforms shown in Table 4-4 for the initial forgeable surface development study. The containers for these preforms were vacuum filled via spouts near the rim, crimped and welded, and then 1121° C (2050° F) HIP compacted in Udimet's R&D autoclave at Ann Arbor, Michigan. The compacted preforms were found to be on the low side of the weight tolerance range. The low input weight and the rim fill spouts were both considered to be factors which could degrade forgeability. A low input weight preform requires greater metal flow in its thinner section to achieve equivalent die-fill in comparison to a heavier preform. In the case of rim fill spouts, the container-to-fill-spout weld often extends into the preform surface resulting in a notch at the rim of the preform. A notch in the preform could definitely reduce forgeability. In addition, rim filling was later found to present an unfavorable powder stratification pattern which could degrade forgeability.

The concern about rim filling develops from the observed phenomenon which has been given the name of striations. Striations result from powder stratification during container filling or from post filling handling.

Powder stratification is believed to be an unavoidable consequence of handling powder particles of varying sizes. As schematically shown in Figure 4-3, flowing powders are naturally classified as a result of the difference in particle volumes. Although the probability of striation formation was recognized early in the powder development studies, the belief existed that the post HIP preforge heat treatment at 2175° F to coarsen the grain size from ASTM 9-11 to ASTM 4-6 would recrystallize all powder particles and develop a uniform coarse grain size across prior powder particle boundaries. However, it was found that recrystallization does not always occur across particle boundaries in the fine particle stratification areas leaving discernable striations of fine and coarse powders (or fine and coarse grain sizes).

Recognizing that striations develop in the filling of the preform containers and that they remain evident through the HIP cycle and preforge heat

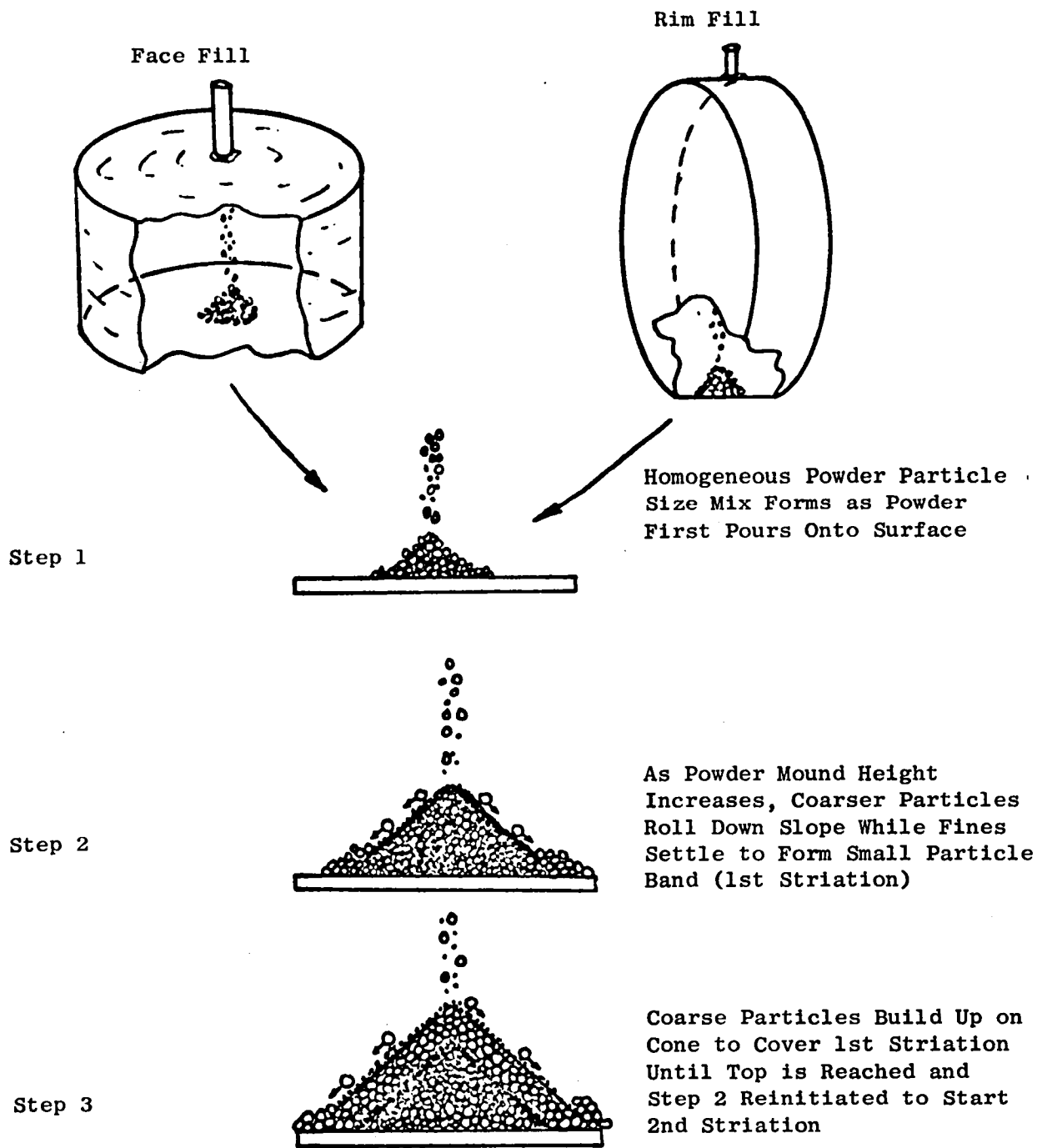


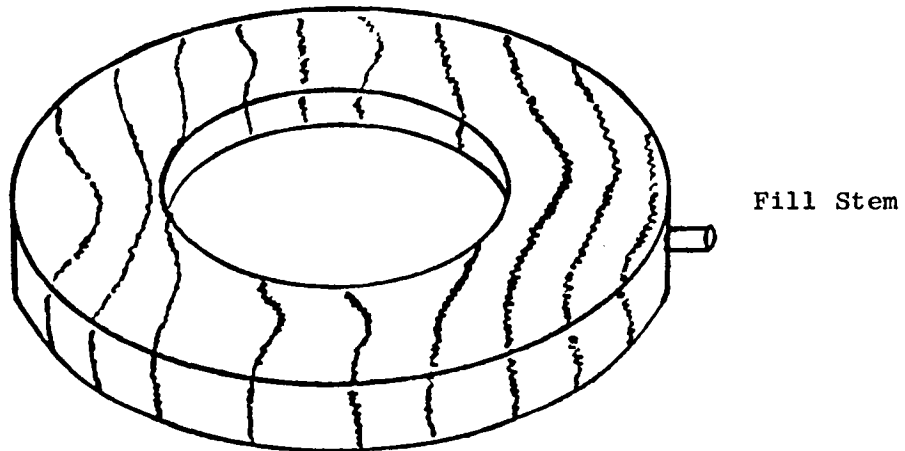
Figure 4-3. Schematic Diagram of Striation Development.

treatment, the question then arises as to what affect striations could exert on forgeability. Typical striation patterns developed for rim, 45° angle and face filling of single preforms are schematically characterized in Figure 4-4. Assuming, at this point, that striations could be planes of weakness during forging to initiate or propagate cracks, then the least desirable orientation would result from rim filling since the striations would be perpendicular to the major tensile stress during the forging process.

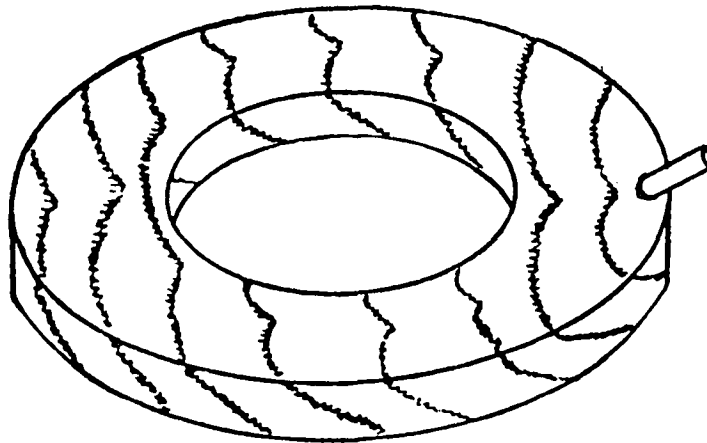
All of Udimet's preforms exhibited some cracking during forging in the minicompression test facility as summarized in Table 4-7. Typical examples of the cracking observed are shown in Figures 4-5, 4-6, and 4-7 to characterize the forgeability ratings reported in Table 4-7. Posttest analyses in an effort to explain the poor forgeability results are summarized in Table 4-7. When all the factors which could or did affect forgeability in the initial Udimet subscale forgeable surface development series were reviewed, it was very difficult to define exactly the conditions which caused cracking for each of the separate preforms. A summary of each of the results is described in the following paragraphs. The conclusion was reached from these data that selected experiments should be repeated in a second series of subscale forgeable-surface development preforms.

Udimet machined the U1 preform, but the low input weight limited the extent of machining and it was initially suspected that the container/preform carbon diffusion zone was not fully eliminated as shown by the 0.076-0.13 mm (3 to 5.2 mils) surface reaction zone on the forging (Table 4-6). Consequently, the remaining carbon diffusion zone, in the form of MC carbide prior particle boundaries, was believed to be one cause for cracking of that preform. Previous subscale forge trials on Udimet preforms outside of this contract had demonstrated acceptable forgeability. It was subsequently found as shown in Table 4-7 that U1 had an excessive TIP value (5.02%) indicating that preform leaked during HIP compaction. Therefore, the U1 result was considered invalid.

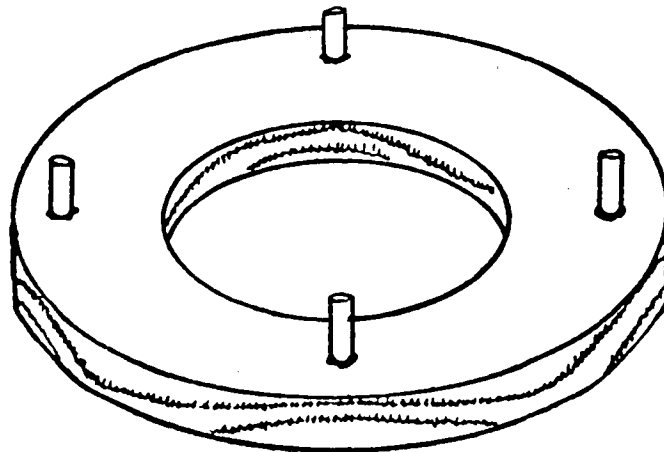
The U2, U3, and U4 SAE 1008 mild steel container preforms exhibited moderate TIP values (from 0.42% to 0.67%) and were therefore questionable in terms of can leaking. Metallographic observations of the surface reaction zones for the forged preforms U2, U3, and U4 are shown in Figure 4-8 which suggest that chemically milling was effective at eliminating the MC carbide reaction zone formed by carbon diffusion from the SAE 1008 steel container into the René 95 preform during the HIP compaction. Apparently a 0.025-0.076 mm (1 to 3 mil) gamma prime depletion zone results from the preforge heat treatment or heating the preform for forging in the minicompression test facility as observed on the U3 and U4 preforms, but the U2 preform with no chemically milling step also exhibited severe prior particle boundary delineation by a precipitate to a depth of about 3 mils. The validity of the U2, U3, and U4 tests is questionable because of the moderately high TIP values. In addition, U4 with the greatest metal removal by chemically milling had a minimum input weight.



(a) 90° (Rim) Fill: Striations Perpendicular to Maximum Forging Tensile Stress



(b) 45° Fill: Striations at 45° Angle to Maximum Forging Tensile Stress



(c) Horizontal Fill: Striations Nearly Parallel to Maximum Forging Tensile Stress

Figure 4-1. Striations Pattern Formation as a Function Container Filling Procedure.

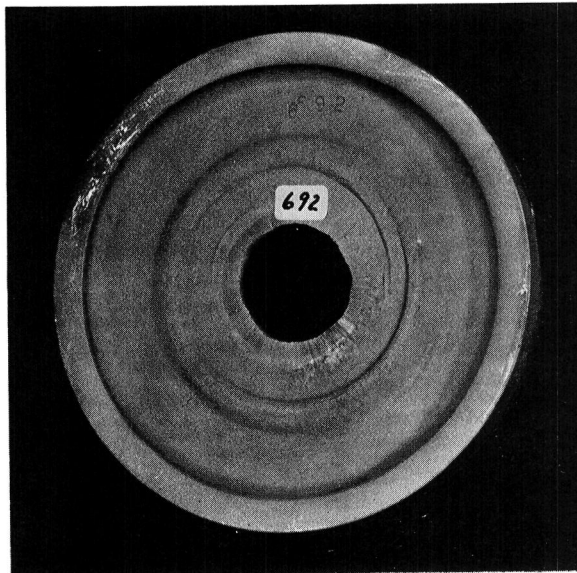
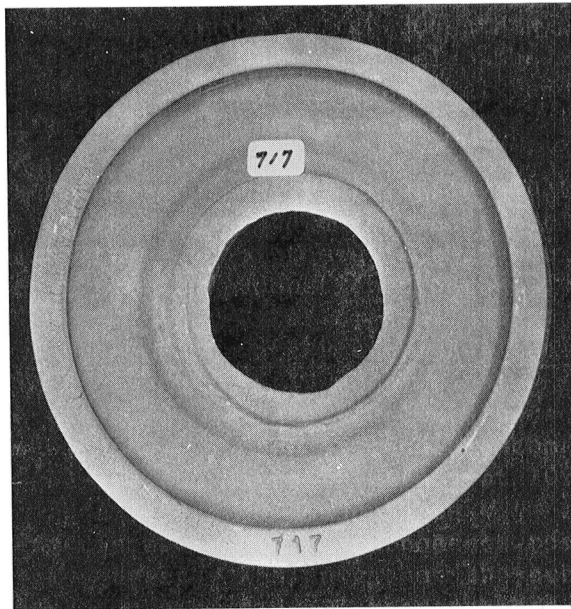
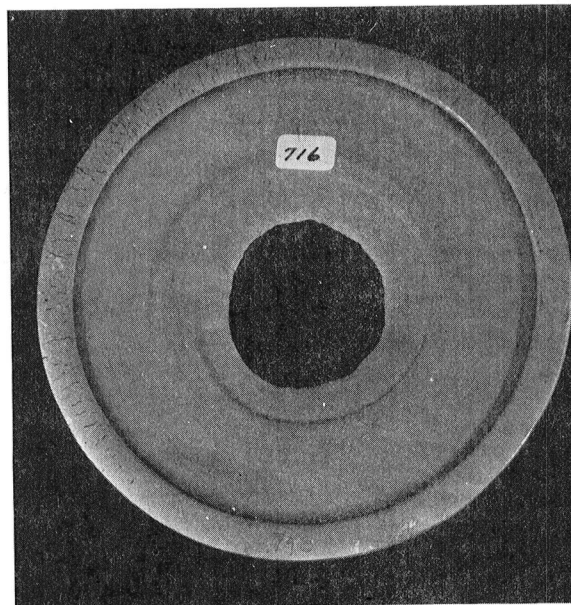


Figure 4-5. Acceptable Forgeability for Subscale
CFM56/F101 Stage 5-9 Compressor Disk
Forging



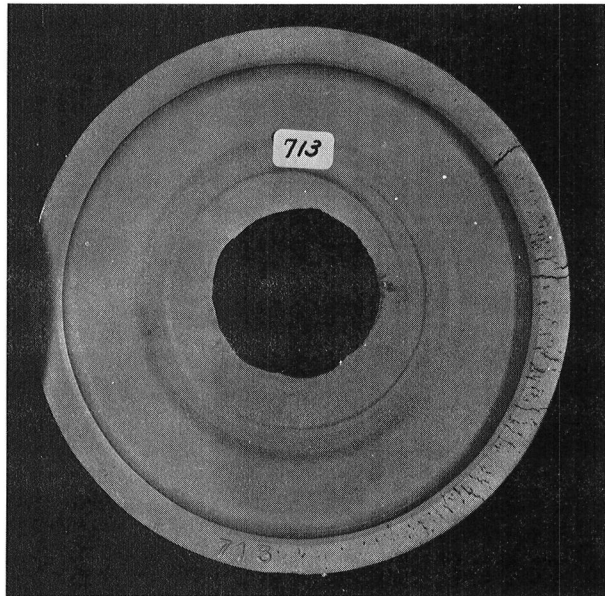
A



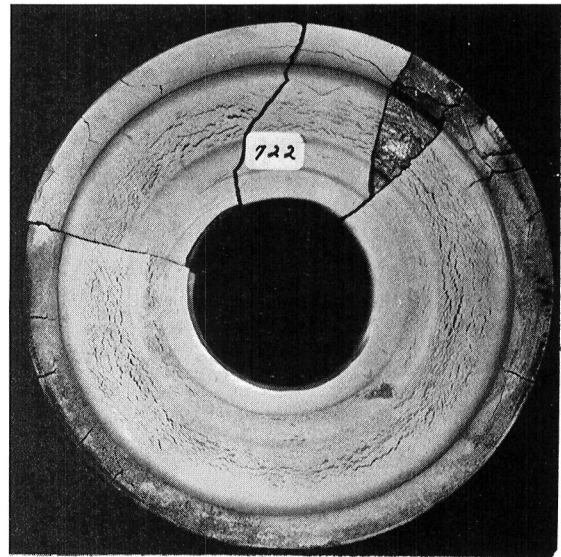
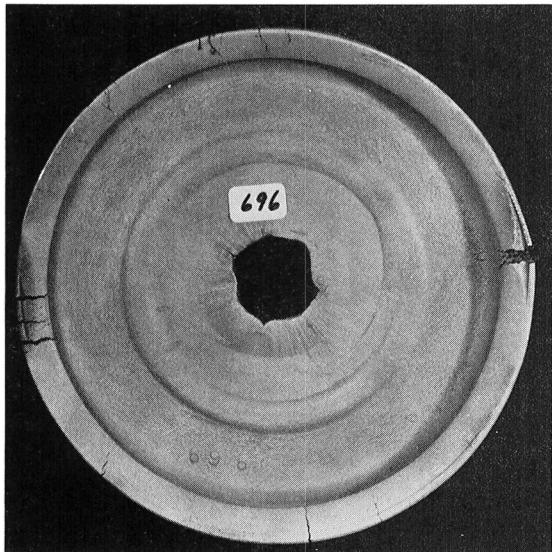
B

Figure 4-6. Subscale F101 Stage(s) 5-9 Compressor Disk(s) Forging with:

- (A) Condition 1: Very Light Cracking
- (B) Condition 2: Light Cracking



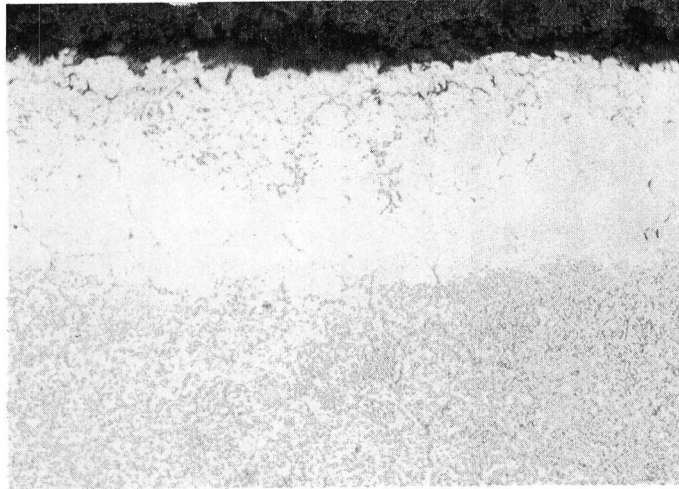
A



B

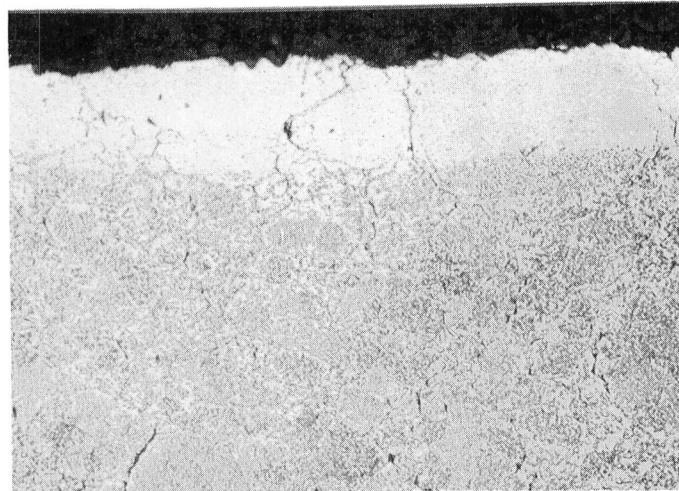
Figure 4-7. Subscale CFM56/F101 5-9 Compressor Disk Forging with:

- (A) Condition 3: Light to Moderate Cracking
- (B) Condition 4: Catastrophic Cracking



As Pickled
U2

Mount
18011



Chemically Milled
0.127 mm (0.005")
U3

Mount
18012



Chemically Milled
0.51 mm (0.020")
U4

Mount
18013

Figure 4-8. Udimet 1008 Can Material - 1st Subscale Run Forged Preforms Surface Reactions (Walker's Etch, 250X)

The 304 stainless steel as-canned preforms, U5 and U6, were delivered to General Electric. The same chemical milling solution was used to remove the can and to remove the additional 0.13 mm (5 mils) from the surface of U6. With this process, the rate of attack of 304 SS and René 95 are about the same, and, consequently, significant local removal of René 95 occurred while removing the can material. Chemical milling, at least with the solution used, was not found to be a practical approach for removal of 304 stainless steel cans on net-shape preforms. These preforms also exhibited moderate TIP values (0.50-0.55%) and were therefore possibly leakers. Observations of the forging surface reaction zones shown in Figure 4-9 again suggested the beneficial effect of chemical milling of the surface. Preform U6 was below the minimum desired weight which may have contributed to its cracking. The forgeability results for U5 and U6 were clouded because of the moderate TIP values and the underweight condition on U6.

The Armco Iron container preforms, U7 and U8, were pickled in nitric acid to remove the containers similar to the SAE 1008 mild steel container preforms. Chemical milling again appeared effective at reducing the surface reaction zone of the forging preform as observed after forging as shown in Figure 4-9. However, these preforms also exhibited severe cracking and these preforms had moderate TIP values.

In summary, all of the Udimet results were in doubt because of moderate to excessive TIP suggesting minor container leaks during HIP compaction. A repeat experiment was planned with corrective actions to eliminate these problems. The corrective actions planned by Udimet for the second series of sub-scale forgeable-surface development preforms were as follows:

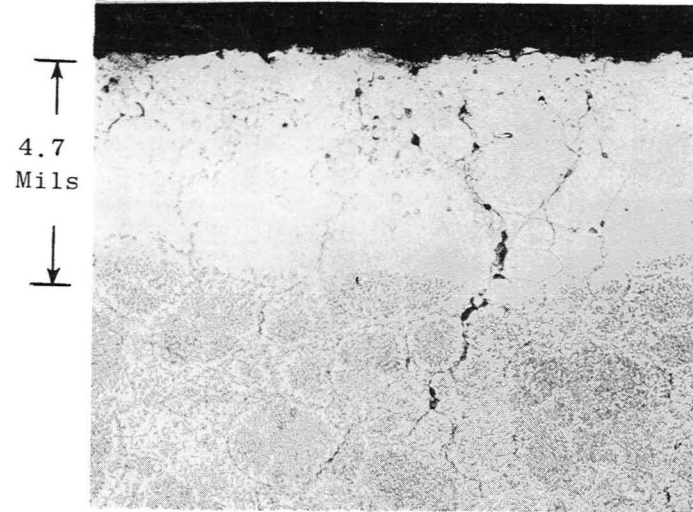
- Review process to minimize reactive contaminants in preforms.
- Modify container shape to make a thicker preform to avoid a minimum input weight problem.
- Modify process to achieve as nearly as possible a face filling condition.
- Conduct HIP compaction at 1204° C (2200° F.)
- Conduct TIP test for porosity on the fill-stem test material from each preform, as a check for leaks.

In addition, Ladish was to correct the back-up stack problem to achieve improved die alignment. Most of these corrective actions were obvious from the sub-scale study results, although some of the actions incorporated information from other sources. Minimization of reactive contaminants was planned to reduce the tendencies for prior particle boundary formation. However, the prior particle boundary delineation observed was believed to be attributable to container leaks. The preform weight and the fill spout location were discussed, but additional information on powder stratification effects and preferred location of the fill spout also entered into this recommendation. The 1204° C (2200° F) HIP compaction was based on previous evidence of superior forgeability for that process over the 1121° C (2050° F) process. The reason for the TIP test is obvious from the previous results with excessive TIP values.



18014

As
Pickled



45 250X 18010



18015

Chemically
Milled
0.127 mm
(0.005")



46 250X 18009

Armoco Fe Can Material

304 SS Can Material

Figure 4-9. Udimet 1st Subscale Run (250X)

CarTech First Series Forgeable Surface Preform Results

The CarTech subscale preforms (Tables 4-6 and 4-7) were prepared with fill spouts at the bore of the preform and most of these preforms exceeded the weight tolerance range. The excess weight was removed by machining the back side of the preform while leaving the maximum flow surface intact for the forgeability test. The only recognized qualification on the forgeability results for the CarTech preforms at the conclusion of this series was the previously described die-stack problem on the back-up blocks. However, later in this program (after conducting the second series specimens), a concern was identified in the adequacy of the HIP parameters with CarTech's process. That problem may likewise have been a factor in cracking of these subscale preforms.

The machined C1 preform forged satisfactorily, although, this was one of the earliest preforms forged and it may have been forged before the back-up blocks yielded. However, it was not possible to precisely define when the blocks yielded. The SAE 1008 steel canned preform results were quite similar to those of the Udimet preforms although the forgeability was slightly improved. The slightly improved forgeability may have been a result of the greater input weight of the CarTech preforms in comparison to those from Udimet. Three samples (C2A, B, and C) were forged after pickling to remove the can. Cracking, ranging from very light to heavy rim cracking, was observed. This cracking was not unexpected since the MC prior particle boundary layer was not fully removed. The C3 preform, after chemically milling 0.12 mm (5 mils) from the surface, forged satisfactorily except for light cracking in the area of the die notch. The C4 preform, after chemically milling 0.051 mm (20 mils) from the surface, exhibited light to moderate rim cracking and again the reason for this cracking was not understood unless there was a die-block misalignment effect. The inconsistency of these results warranted repeating at least the C3 and C4 forge tests after Ladish corrected the die stack problem, and CarTech agreed to supply the needed preforms for a repeat of the experiment.

The low interstitial Fe-base can material preforms, C5 and C6, were pickled to remove the can and the C6 preform was sent to General Electric for chemically milling 0.13 mm (5 mils) from the surface. The C5 preform, with merely the can material removed, exhibited one severe rim crack, presumably resulting from carbon diffusion forming an MC prior particle surface layer. The C6 pre-preform [with 0.13 mm (5 mils) removed from the surface by chemical milling] forged satisfactorily except for rim cracking from the die notch. Again, the degree of cracking may have been increased because of the die-stack problem.

The C7, C8, and C9 preforms with nickel plate, chromate coating, and boron nitride coating barrier layers, respectively, between the SAE 1008 can and the powder René 95 all cracked significantly during forging. Therefore, none of these three processes were repeated. Metallographic evaluation revealed the CarTech subscale preforms with coatings between the can and the René 95 powder, (C7 and C8) appeared to have had either container leaks during the HIP compaction or to have been contaminated by reaction with the coating. Excessive porosity or contamination seen throughout these preforms accounts for the severe cracking which was observed. These particular conditions were not planned for the repeat forgeable surface study, but because of this experience CarTech planned fill-stem TIP tests to evaluate for can leaks on all the repeat forgeable surface preforms.

When all the factors which could or did affect forgeability in the initial CarTech subscale forgeable surface development run were reviewed, it was very difficult to define the precise conditions which caused cracking for each of the separate preforms. Therefore, a repeat experiment, with appropriate corrective actions was warranted specifically, the corrective actions implemented by CarTech for the repeat experiment included:

- a. A review process to minimize reactive contaminants in preforms.
- b. Continued face filling of preforms to locate striations in the plane of the part.
- c. A plan to conduct TIP tests for porosity on the center test material from each preform, as a check for leaks.

Conclusions from the First Series Subscale Forgeable Surface Preform Tests

The results of the evaluation to determine the cause of cracking of the forgings made in the initial subscale forgeable surface development series identified the following possible reasons as shown below:

1. Excessive TIP (Thermally Induced Porosity)
2. Unfavorable striation orientation in the Udimet preforms
3. Low input weight and poor dimensional uniformity (predominately flatness)
4. Forging surface reaction zones on preforms that weren't chemically milled
5. Reactive contaminants or other causes for general prior particle boundary delineation
6. Die misalignment caused by yielding of the back-up blocks and the machining error region on the die cavity web-rim radius
7. Non-metallic inclusions

The test ring TIP evaluation is used to qualitatively identify preforms or forgings with an excessive gas content from either insufficient outgassing of the powder or container leakage during HIP compaction. The maximum TIP allowance is 0.3%, (that is, the density of the test sample shall not decrease by more than 0.3% after 1204° C (2200° F) 4 hour thermal exposure). The TIP measurements reported ranged from essentially zero to as high as 6.27%. Eleven of the 19 forging tests were above the desired 0.3% TIP limit.

Striations resulting from the powder fill technique were also a major concern for the Udimet preforms, which were rim filled. CarTech used a face fill technique with a solid center for these subscale preforms and this appeared to preferentially locate the striations in the plane of the preform for minimum effect on forgeability.

Input weight and dimensional uniformity were concerns on the preforms from both vendors. Three of the Udimet preforms were definitely below the minimum input weight, whereas the CarTech preforms were typically overweight to the extent that machining was required on one side to reduce the weight. Surface undulations were apparent on the preforms from both vendors. Thickness variations in the range of 1 mm (0.040 inch) were observed; this constituted on the order of 20 to 30% of the total preform thickness.

The forging surface reaction zone was evaluated as shown in Figures 4-6 and 4-7 as a possible cause since at one time it was considered that surface oxidation during the preforge heat treatment cycle could affect the subsequent forgeability. The reaction zone was found to be similar to the reaction zone observed on forgeable machined preforms. Therefore, it was concluded not to be a major factor in the forgeability results. Similarly, concern existed for the effect of reactive contaminants, die misalignment and nonmetallic inclusions on forgeability, but direct evidence of these as contributing factors was not found. Concern was expressed by CarTech on whether a satisfactory cleaning process was used to remove the surface oxide from the inside of the 1008 mild steel cans for the subscale preforms, although it is now believed that an adequate cleaning procedure has been developed.

Based on the excessive cracking observed in this initial subscale forgeable surface development program, a repeat subscale study was conducted to identify a surface preparation method precluding conventional machining for near net shape forging preforms.

Second Series Subscale Forgeable Surface Preforms

The corrective actions suggested from the results of the first forgeable-surface preform forging study were incorporated to produce a second series of preforms. The preforms prepared, the surface processing used, and the forgeability test results are shown in Table 4-8.

CarTech provided six preforms as shown in Table 4-8. Four of the preforms were produced using the standard SAE 1008 mild-steel containers, although CarTech reduced the thickness which resulted in an underweight condition. One preform was supplied using the low-interstitial iron (LI-Fe) container material and one preform using the SAE 1008 mild steel container with a boron-nitride (BN) barrier coating. These latter two preforms exhibited acceptable input weights. These six preforms were face filled using near-bore fill spouts and then HIP compacted at Kawecki Berylco Industries using the 1121° C (2050° F) 2 hours minimum 103 MPa (15 ksi) compaction parameters. Three of the SAE 1008 mild steel container preforms were surface prepared by chemically milling 0.5, 1.0 and 1.5 mm (20, 40, and 60 mils) from the surface, and one was forge evaluated with no surface preparation beyond pickling in HNO₃ to remove the container. The LI-Fe container was removed by pickling in HNO₃ and then chemically milling to remove 0.5 mm (20 mils) from the preform surface. TIP tests on these preforms gave acceptable levels, although the LI-Fe container preform indicated one value of 0.33% which was above the specification 0.30% maximum.

Forging of the CarTech preforms in this second series showed that cracking remained a significant problem. Although several of the preforms exhib-

Table 4-8. Second Series Subscale Preform Results.

	Vendor	Preform Number	Can Material	Surface Preparation(1) Plan	Initial Thickness		Final Approx. Thickness		Min. Input Wt.	Forge-ability Rating(4)	TIP (5) %
					mm	in	mm	in			
1	CarTech	C697	1008 MS	No Prep.	8.1	0.318	8.1	0.318	Below	2-3	0.29
2	CarTech	C742	1008 MS	Chemically Mill 0.5mm (20 Mils)	9.1	0.360	8.1	0.320	Below	1-2	0.29
3	CarTech	C771	1008 MS	Chemically Mill 1.0mm (40 Mils)	9.7	0.380	7.8	0.310	Below	3	0.28
4	CarTech	C762	1008 MS	Chemically Mill 1.5mm (60 Mils)	13.0	0.510	10.0	0.392	Below	4	0.23
5	CarTech	C801	LI FE	Chemically Mill 0.25mm (20 Mils)	11.8	0.465	10.1	0.427	OK	2-3	0.33
6	CarTech	C754	1008 MS/BN Coat	No Prep.	12.8	0.505	12.8	0.505	OK	1-2	0.19
7	Udimet	22-1 (2)	1008 MS	No Prep.	11.1	0.438	11.1	0.438	Below	2-3	OK
8	Udimet	22-2 (2)	1008 MS	No Prep.	11.1	0.438	11.1	0.438	OK	2-3	OK
9	Udimet	22-3 (2)	1008 MS	Chemically Mill 0.05mm (20 Mils)	11.1	0.439	10.6	0.394	OK	2-3	OK
10	Udimet	22-5 (2)	1008 MS	Chemically Mill 1.0mm (40 Mils)	11.2	0.442	8.9	0.352	Below	2-3	OK
11	Udimet	22-6	1008 MS	Chemically Mill 1.5mm (60 Mils)	11.2	0.440	8.0	0.313	Below	3	OK
12	Udimet	X-4 (3)	1008 MS	Chemically Mill 0.05mm (20 Mils)	10.5	0.415	9.5	0.375	Below	2-3	OK
13	Udimet	22-8 (2)	Armco Fe	No Prep.	11.1	0.438	11.1	0.438	OK	0	OK
14	Udimet	22-7 (2)	Armco Fe	Chemically Mill 0.05mm (20 Mils)	11.2	0.441	10.8	0.394	Below	1-2	OK
15	Udimet	Ni-10	Nickel	No Prep.	10.8	0.425	10.8	0.425	OK	2-3	OK
16	Udimet	UPD 2	1008 MS-OK	Chemically Mill 0.05mm (20 Mils)	10.8	0.425	9.7	0.380	Below	2-3	0.07
17	Udimet	UPD 3	1008 MS-Minor Voids	Chemically Mill 0.05mm (20 Mils)	10.8	0.422	9.5	0.373	Below	3-4	8.53
18	Udimet	UPD 1	1008 MS-Major Voids	Chemically Mill 0.05mm (20 Mils)	10.7	0.423	9.6	0.379	Below	4	2.37

Notes:
(1) Surface Preparation After Can Removal*Steel Cans Pickled in HNO₃
(2) 1204° P C (2200° F) HIP Rather Than 1121° C (2050° F) HIP
(3) 1121° C (2050° F) HIP + Re-HIP° at 1204° C (2200° F)
(4) 0 = Acceptable
4 = Severe Cracking
(5) TIP - Thermally Induced Porosity

ited an underweight condition which was known to degrade forgeability, even the LI-Fe preform which had an acceptable input weight exhibited cracking.

Udimet supplied nine subscale preforms for forgeable surface evaluation and three additional subscale preforms for evaluation of the effect of porosity (high TIP) on forgeability. Nine of the preforms were produced using SAE 1008 mild steel containers and all of these containers were rim filled since the Udimet process could not accommodate face filling. Two containers were processed from Armco iron and one from unalloyed nickel, and these also were rim filled. Five of the preforms in the SAE 1008 mild steel and the two Armco Fe container preforms were HIP compacted at 1204° C (2200° F), and one of the SAE 1008 mild steel container preforms was re-HIP compacted at 1204° C (2200° F) after a 1121° C (2050° F) HIP compaction. The three SAE 1008 mild steel container preforms for the porosity study remained from the first series with 1121° C (2050° F) HIP compaction. The containers, except for the unalloyed nickel, were stripped by pickling in a HNO₃ bath and then chemically milling was used to prepare the surfaces of these preforms as shown in Table 4-8.

The forgeability results on the second series of Udimet subscale preforms indicated some improvement over the first series tests in the degree of cracking, but cracking still remained a significant problem. Corrective actions had been implemented with respect to the TIP problem, and the 1204° C (2200° F) HIP temperature was used to improve forgeability. The tests on the three preforms for evaluation of the effect of TIP on forgeability did show increasing severity of the cracking when related to the metallographic observations characterized as "OK," "minor voids" and "major voids". However, even the preform with acceptable TIP exhibited significant cracking. TIP on the Udimet preforms was monitored by observation of the cut-off fill stem microstructure for porosity after a 1204° C (2200° F) exposure. Preform input weight remained a concern, since five of the nine surface preparation preforms were below the minimum desired weight. The best forgeability observed was on the Armco Fe container preforms. The preform with the container stripped by pickling forged acceptably, and after chemical milling of 0.5 mm (20 mils) from the surface, the second preform gave a 1-2 forgeability rating. Striations remained as a concern on these problems since Udimet continued their rim filling process, but distinct evidence of striations was not found.

Conclusions From the Second Series Forgeable Surface Preform Development Tests

Since cracking continued to be a significant problem in the second series of forgeable-surface development tests, it became increasingly evident that the shape reproducibility of the subscale preforms is apparently inadequate for a precise, reduced scale forgeability evaluation. The severe cracking problems observed for these subscale preforms are believed to have resulted from inadequate shape reproducibility which was accentuated by low input weights. All the preforms in this subscale study were HIP'ped to the same size and then chemically milled to remove the container-preform interdiffusion zone. The preforms became increasingly thinner and more underweight as metal removal was increased to assure elimination of the diffusion zone. Re-

duced weight is known to increase the severity of the forgeability test, and therefore the preforms with greater metal removal exhibited poorer forgeability. The surface undulations of the near-net-shape subscale preforms is also believed to be a factor in that ± 1.0 mm (40 mil) surface undulations from can rippling caused a 20-30% variation in the preform thickness. A surface depression undulation could be considered a mild notch in the forging preform. Surface undulations on the full-scale part would only account for about 5% thickness variations, and may have no effect on forgeability of thicker preforms. Assuming scale-down of the tests to be the real forgeability problem, then chemical milling might work as a surface preparation process on full-scale parts while subscale parts would crack simply because of inability to HIP an adequately flat subscale preform shape. A subscale test was therefore conducted to demonstrate that chemical milling was in fact an acceptable metal removal method and that it produced no detrimental effects on forgeability. Four subscale preforms were made from a Udimet 1204° C (2200° F) HIP log preform which was known to have acceptable forgeability. Two preforms were machined with a 1.5 mm (0.060 inch) envelope over the Ladish preform design. One blank was machined to the precise design size and another was machined undersize. The blanks machined with the 1.5 mm (0.060 inch) envelope were subsequently chemically milled to remove the excess, leaving a standard size preform. These four preforms all forged satisfactorily in the minicompressor test facility at Ladish.

Since satisfactory forgeability of the chemically milled subscale preforms was demonstrated, and the major forgeability problem is believed to exist with dimensional variations which may affect only the subscale forging, chemical milling was planned for full-scale near-net shape preform for forgeability demonstration. The degree of milling to be used on the full-scale preform was selected to be 1.5 mm (60 mils) metal removal to assure elimination of the total interaction zone with the container.

Conclusions From the Subscale Forgeability Surface Development

The conclusions drawn from the subscale forgeable surface development study were:

1. Chemical milling is an acceptable metal removal process to eliminate the container-powder interaction zone for near-net shape forging preforms.
2. 1204° C (2200° F) HIP René 95 preforms exhibit superior forgeability in comparison to the 1121° C (2050° F) HIP material.
3. Dimensional acceptability limits for full-scale preforms must be defined and met.
4. Test ring TIP evaluations of near-net-shape preforms is required prior to forging.
5. Container filling practices can result in powder particle size variations in the form of a striation pattern. The effect of these striations on mechanical properties should be evaluated.

6. Metallographically defined interdiffusion zones and forgeability results suggest that the low interstitial container materials (Armco Fe at Udimet and Li-Fe at CarTech) should be selected for full-scale development.
7. While the identification of the specific cause for cracking of each of the subscale forging preforms was not established, several factors were identified which were considered detrimental to forgeability. These included:
 - a. Dimensional Tolerances - major dimensions, surface undulations and notches from fill spout welds.
 - b. Input Weight - minimum weight must be exceeded
 - c. Die Alignment - back-up block problem caused misalignment
 - d. TIP - high porosity is detrimental
 - e. Striations - can at least contribute to crack propagation
 - f. Surface Reaction Zone - heavy prior particle boundary MC carbides act to initiate cracks during forging

4.2.3 Full-Scale Forging Preform Process Development

Chemical milling of the near-net-shape HIP compacts was the development process selected for the CFM56/F101 compressor disk forging preform production. The selection was made based on the results of the subscale forgeable surface development work and the judgment that it was the most viable approach for uniform metal removal to assure elimination of the container-to-preform interdiffusion zone. The following sections describe the scale-up of this process to produce full-scale forging preforms.

Shape Development

Ladish provided the full-scale preform design to Udimet and to CarTech to initiate the full-scale shape development trials. The decision was made to conduct shape iterations to the nominal preform design dimensions with an added 1.5 mm (0.060 inch) envelope to be removed by chemical milling. While less than an 0.75 mm (0.030 inch) envelope was required based on the observed interaction zones, the 1.5 mm (0.060 inch) envelope was selected to assure total removal including the Fe penetration observed on Ladish's microprobe results. The development plan included three shape iterations to produce the Ladish preform design with the 1.5 mm (0.060 inch) envelope. Both Udimet and CarTech used KBI as the HIP compaction source.

Initial Full-Scale Shape Trials

Udimet and CarTech used SAE 1008 mild steel containers to conduct the initial shape trials. CarTech's initial shape trial was conducted early in the MATE program using a single near-rim fill-spout preform loading procedure and a 1121° C (2050° F) HIP compaction cycle at KBI. Udimet's first shape

iteration, conducted later in the program, incorporated face filling through four near-rim face fill stems and 1204° C (2200° F) HIP compaction. Both vendors conducted these shape trials prior to the subscale recommendation to use Armco Fe or LI-Fe for the container material.

Udimet's first shape iteration was below the desired weight and dimensions. The preform weight after container removal was about 34.5 kg (76 lbs). After chemical milling to remove between 1.3 to 1.5 mm (0.050 to 0.060 inch) to eliminate the interdiffusion zone, however, this preform would weigh only about 31.7 kg (70 lbs). Dimensions were taken at 45° intervals for the rim diameter, bore diameter, locator diameter, rim thickness, midradius thickness and bore thickness. After chemical milling, this Udimet preform average rim diameter would have been ~1.27 mm (0.050 inch) oversized (acceptable), but the bore diameter would have been ~2.54 mm (0.100 inch) oversized (unacceptable). Similarly, after chemical milling, the average rim thickness would have been ~2.3 mm (0.090 inch) undersized and the average bore thickness ~0.75 mm (0.030 inch) undersized. The worst nonuniform underfill condition existed at a fill spout location. An approximately 0.5 mm (0.020 inch) depression, (both sides depressed) was evident at that underfill location and, based on subscale results, a high probability of cracking in that region would be anticipated during forging. Minor underfill was apparent at an adjacent fill stem, but the other two fill stems did not indicate this discrepancy.

CarTech's first shape iteration was similarly dimensionally discrepant, but the process was further judged unacceptable because of the unfavorable orientation of the powder fill stratification bands resulting from rim filling.

Both vendors modified their container design drawings to correct the dimensional deviations found in the initial trials to proceed into the second shape iterations.

Second Full-Scale Shape Trials

The second full-scale shape trials were conducted after completion of the subscale forgeable surface development studies and, thus, both vendors incorporated some of the resulting recommendations. Both Udimet and CarTech used the 1204° C (2200° F), 2 hours minimum 103 MPa (15 ksi) HIP compaction process. While CarTech modified their fill-spout orientation to more nearly achieve face-filling in this second iteration, Udimet assumed that 1204° C (2200° F) HIP compaction benefits were sufficient to overcome stratification problems and reverted to vacuum rim-filling from a single spout to alleviate the underfill problems encountered on the first shape trial. Both preform suppliers continued to use the SAE 1008 mild steel container material for the second shape trials because of sheet stock delivery problems for the Armco Fe and LI-Fe materials.

Preform measurements indicated that neither Udimet nor CarTech met the dimensional requirements of Ladish's preform drawing in the second shape iteration. The following dimensional deviations beyond Ladish's standard tolerances would result after the 1.5 mm (0.060 inch) chemical milling surface removal:

Check Measurement	Udimet	CarTech
Bore Dia. (in.)	0.5 mm (+0.02)(small)	Acceptable
Rim Dia. (in.)	0.75 mm (+0.030)(large)	-0.38 mm (-0.15)(small)
Thickness (in.)	Acceptable	+0.94 mm (+0.37)(large)

CarTech used two vacuum filling procedures to prepare preforms for this second shape trial. Two preforms were loaded from single rim fill spouts with the preform plane at about a 45° angle from the horizontal position, and the two remaining preforms were loaded from single face located fill spouts with the preform plane in the horizontal position. One of the 45° angle loaded preforms leaked during the 1204° C (2200° F) HIP cycle at KBI. The 1008 mild steel containers used for these preforms were removed by pickling for accurate dimensional analysis and striation observation. Striations were observed on the surface of the HIP compacted preform which was 45° angle rim loaded, although no striations were evident in either of the face-filled preforms.

Udimet elected to return to single fill stem, vacuum rim filling with the preform plane essentially vertical for this second shape iteration. Subsequently, forgeability of the 1204° C (2200° F) re-HIP CarTech preforms was found inadequate to eliminate the effect of striation cracking (Task III, this report). Therefore, Udimet returned to the face filling procedure for the third iteration.

Both Udimet and CarTech again modified their container designs to attempt to produce the Ladish preform shape with the 1.5 mm (0.060 inch) coverage in a third shape iteration. Both vendor's were reasonably confident that they could produce the shape in the third iteration, and therefore elected to produce a sufficient quantity of parts to provide the forging preforms for Task III production in this third trial.

Third Full-Scale Shape Trials

Both Udimet and CarTech employed face filling for the third shape trials, although Udimet provided a third preform using their rim fill process. Udimet used a low interstitial enameling iron to produce the containers for this third iteration, but CarTech continued to use SAE 1008 mild steel because of delivery problems on the LI-Fe material. The Udimet and CarTech preforms were HIP compacted in a single run at KBI using the 1204° C (2200° F), 2 hours (minimum) 103 MPa (15 ksi) cycle. It was subsequently found that these preforms probably did not reach the 1204° C (2200° F) temperature during HIP compaction as described later in this report.

Preliminary dimensions were obtained prior to can removal on these third shape iteration preforms to indicate the degree to which the Ladish preform shape had been achieved. Calculations were made with those dimensions by correcting for container removal and chemically milling to remove 1.5 mm (0.060 inch) from the surface which gave the following deviations beyond the Ladish drawing tolerances of 1.5 to -0.75 mm (+0.060 to -0.030 inch.)

Location/Measurement	Udimet	CarTech
Rim Diameter	Acceptable	Small by 0.7 mm (0.03")
Bore Diameter	Acceptable	Small by 0.35 mm (0.015")
Rim Thickness	Acceptable	Acceptable
Mid Radius Thickness	Acceptable	0.6, 0.28 mm (+0.022", 0.011") per side
Bore Thickness	1.5 mm (+0.06)	-0.75 mm (-0.03")
Weight	34 - 35.kg (75-77 lbs)	36 - 37 kg (80-82 lbs)

The Udimet preform dimensions and weight were considered acceptable, although the locator ring dimension would require machining of the locator prior to forging. Agreement was reached between Ladish and General Electric that the CarTech preform dimensional deviations would be accepted for forging, since the excess weight should produce adequate forgeability to the compressor disk shape.

Udimet produced three preforms in this third shape iteration. Two preforms were face filled in air with multiple fill stems and one was vacuum filled from a single rim fill stem. The air-filled preforms were evacuated at room temperature prior to sealing whereas the vacuum fill containers were sealed after filling. Udimet removed the containers by pickling in nitric acid prior to shipping these preforms to General Electric for chemical milling.

CarTech produced two multiple fill stem vacuum face-filled preforms. The fill spouts were sealed immediately after filling. After HIP compaction, CarTech stripped the SAE 1008 mild steel can by pickling in aqua-regia prior to shipping their preforms to General Electric for chemical milling.

These five preforms, three from Udimet and two from CarTech, were chemically milled at General Electric as described in the following section and were scheduled for forging in Task III. Problems subsequently identified for these parts precluded forging them to the F101 Stage 5-9 compressor disk shape.

Forgeable Surface Development - Full-Scale Parts

Forgeable surface development for the full-scale parts involved scaling up the chemical milling process. A facility was in place at General Electric to conduct the full-scale chemical milling operation on the forging preforms. Trial runs were conducted on one of the early shape iteration parts to demonstrate the process. Preliminary studies, as well as the results on the full-scale trial part, demonstrated the capability of the chemical milling process to remove between 0.013 mm (0.0005 inch) and 0.025 mm (0.001 inch) per minute from the surface without pitting or intergranular attack.

4.2.4 Alternate Approach to Near-Net-Shape Preforms

At the beginning of the program, the preform design anticipated by General Electric for the near-net-shape compressor disk forging design was a complex shape. A cross-section view of one side of the proposed ring preform might

have appeared as a "dog-bone" shape. However, that was not the preform shape recommended by Ladish in Task I based on prior forging experience. The generic shape recommended was a ring-type preform, but the cross-sectional view of one side of that ring was nearly rectangular with the only one protrusion required as a forge-die locating surface. This nearly rectangular cross-section ring preform design was in contrast to the more complex preform shape originally anticipated and increased the options for an economically viable processes to produce preforms beyond that of the near-net-shape single preforms. One process used to produce these compressor disk forging preforms is the preform-multiple log approach described in the following section.

Preform Multiple Log Approach

The nearly rectangular cross section of the ring-type preforms for the compressor disk forging is well suited to the approach of producing a long, hollow-center, cylindrical "log" from which several forging preforms can be sectioned. Multiple preform logs were produced by Udimet during the latter development tasks of the program forging studies, and this approach was found to be economically competitive with the near-net-shape preform process.

Economical use of material with this process requires close control of the OD and ID dimensions of the "log", but sufficient stock is required to machine away the container reaction zone and to accommodate the particular vendor's dimensional reproducibility of HIP shapes. Type 304 stainless steel containers have been used to minimize the container reaction zone. The top and bottom surfaces of the forging preforms require minimal preparation by machining after sectioning from the log, although some machining is required to produce the forging die locator. About 12.7 mm (0.5 inch) of excess material is provided at the top and the bottom of the preform multiple logs for quality control testing prior to forging.

Weight, Quality Control, and Cost Considerations

The preform-multiple log approach requires about 42.5 kg (94 lbs) of input René 95 powder per part compared to about 40.8 kg (90 lbs) of powder for the near-net-shape preform. These input weights both yield the 35.4 kg (78 lbs) required as input to the forging die cavity. Therefore, an additional 1.8 kg (4 lbs) of René 95 are required for the preform multiple log approach. However, that weight includes the end slices for quality control on the preform multiple log prior to forging. The quality control testing on single near-net-shape parts must either be conducted on the fill stem material or on the test ring material after forging. All of the typical quality control tests including density, TIP, microstructure, and oxygen analyses are difficult to obtain using only the fill spout sample.

Cost analysis by the Ladish Company indicated that the preform multiple log approach was significantly more cost effective than machining oversized single preforms. For the CFM56/F101 compressor disk forging preform it appeared about the same in cost as the near-net-shape preform process. However, on forgings with more complex preform shapes the near-net-shape preform process could prove more cost effective.

4.3 TASK III - MANUFACTURING

4.3.1 Forging Die Production

Ladish procured the molybdenum-base alloy die block materials from Sylvania Corporation and forged it in preparation to produce the full-scale CFM56/F101 compressor disk dies. The forged blocks were then machined to a configuration that would yield a part meeting the dimensional requirements of the compressor disk forging process drawing.

During the course of the MATE program, an engine redesign occurred for the CFM56/F101 compressor disks which required modification of the forging die cavity. Those dimensional changes were incorporated after forging the initial two development forge runs.

4.3.2 Oversized Preform Production

The program plan initially provided six oversized individual preforms to be machined for a forging demonstration prior to forging the full scale net-size preforms manufactured and processed by the forgeable surface development technique. The approximately 140 lb. oversized preforms were right cylinder ring shapes with a 17.5-inch outside diameter, a 8.0-inch inside diameter and a 2.5-inch thickness. Forgeability problems were encountered on these oversized preforms as described in the subsequent sections of this report, and replacement materials were produced and evaluated.

CarTech Forging Preforms

CarTech initially supplied six oversized single forging preforms for the full-scale demonstration of the compressor disk hot die forging system. The preforms were oversized which permitted machining to the selected preform shape after completion of the Task I preform shape study. Two preforms (C790 and C791) were produced using CarTech's master powder blend B-093, and four preforms (C792, C794, C795, and C796) were produced using master powder blend B-107.

Powder was loaded into SAE 1008 mild steel containers by vacuum filling with the container at a $\sim 45^\circ$ angle from horizontal. Since considerable machining was planned for these preforms, there was no concern about the interaction zone between the SAE 1008 mild steel containers. These preforms were HIP compacted at KBI using the then specified 1121°C (2050°F), 2 hours minimum 103 MPa (15 ksi) compaction cycle. After HIP compaction, one of the six preforms was given a preforge grain-coarsening heat treatment 1190°C (2175°F) / 4 hours with the Task I selected cooling rate of 111°C (200°F) per hour and then forge evaluated.

4 hours with the Task I selected cooling rate of 111°C (200°F) per hour and then forge evaluated.

Forgeability problems were encountered with the first of these six preforms and the remaining five preforms were given a re-HIP cycle at 1204° C (2200° F).

Details on the analysis of the cause of cracking of these parts which further characterizes these preforms is described in Section 4.3.5.

CarTech's Three-Piece Preform Multiple Log

Since forgeability problems were encountered with the six initial oversized individual forging preforms, CarTech elected to partially replace those parts with a three-piece preform multiple log later in the program. That container was manufactured using 304 stainless steel to produce three oversized preforms. A single face-fill stem was used to vacuum load powder into the container and the HIP compaction cycle was planned to be 1204° C (2200° F), 2 hours (minimum) at 103 MPa (15 ksi). This log was HIP compacted in the same autoclave as the third shape iteration near-net-shape preforms at KBI. René 95 powder used for this preform multiple log came from CarTech's master powder blend number B146. Processing of that powder was standard except that CarTech incorporated all of the fines to produce that blend. Characterization of blend B146 is shown in Table 4-9. The effects of adding the fines to B146 in comparison to the blends shown earlier was to increase the percentage of fines (-325 mesh powder) from the 26-30% range to 45%. A slightly higher oxygen level was also found for B146 master powder blend in comparison with B093 and B107.

Quality control tests at Ladish prior to forging on the top and bottom log slices (excess material) revealed an oxygen concentration problem on the three piece preform multiple log provided by CarTech. Oxygen concentrations exceeding the 150 ppm maximum specification limit were found at the rim-top of that log and sufficient data were generated to establish that an oxygen gradient existed. Those data are shown in Table 4-10. Metallographic evidence of excessive prior particle boundary precipitates, believed to be small oxide (Al_2O_3) particles, found at the rim of these preforms was consistent with the presence of oxygen gradients. The existence of these oxygen gradients raised concern regarding the forgeability of these preforms and an attempt was made to estimate the oxygen levels that would exist at the rim for each of the three preforms based on the gradient data.

The CarTech log diameter was such that 15.2 mm (0.6 inches) would be machined from the rim prior to forging. Based on the data in Table 4-10, the rim oxygen level for the top mult would be about 300 ppm. Similarly, the center mult was estimated to have a rim oxygen level of 150-200 ppm and the bottom mult was estimated to be in the 90-120 ppm range. The decision was made to forge these three preforms to observe the effect of oxygen level on the forgeability, although it was obvious that the part produced from at least the top mult would not meet the oxygen specification requirements.

The CarTech three-piece preform multiple log preforms were given the 1190° C (2175° F) preforge heat treatment and cooled at 110° C (200° F) per hour to produce the gamma prime distribution established in Task I to produce

Table 4-9. CarTech B146 Characterization.

(Three-Piece Preform Multiple Log)

Nominal Chemistry

	Wt %			ppm	
	<u>B146</u>	<u>SPEC</u>		<u>B146</u>	<u>SPEC</u>
Al	3.53		Si	100	
Ti	2.66		Mn	<100	
Cb	3.69		S	20	
Cr	13.10		P	<50	
Co	8.04		Ta	<100	
Mo	3.66		Cu	100	
W	3.82		Pb	<2	
C	0.040		Bi	<0.5	
Zr	0.050		O ₂	115	
B	0.010		N ₂	20	
Fe	0.20		H ₂	1	

Particle Size Distribution

<u>Mesh Fraction</u>	<u>Wt %</u>
- 60,+ 80	4.7
- 80,+100	4.1
-100,+140	10.4
-140,+200	14.3
-200,+325	21.0
-325	45.5
	<hr/>
Total:	100.0

Table 4-10. Oxygen Data - CarTech Three-Piece
Preform Multiple Log.

Material: Blend #B146
Reported Blend O₂ = 115 ppm (CarTech)

Depth - From Container Wall - (inches)	Oxygen Concentration (ppm)			
	Top Slice		Bottom Slice	
	12.7 mm (1/2 inch) from Top	12.7 mm (1/2 inch) from Bottom	12.7 mm (1/2 inch) from Top	12.7 mm (1/2 inch) from Bottom
	0°	180°	0°	180°
0	448	608	101	115
1/4	381	430	98	100
1/2	295	300	91	94
3/4	244	230	88	87

the necklace microstructure after forging: The forging of these three preforms and the postforging cracking analyses are described in Sections 4.3.4 and 4.3.5.

Udimet Preform Multiple Log

Concurrent with the CarTech production of the three-piece preform multiple log, Udimet produced a nine-piece preform multiple log for production of disk forgings. That log was a solid right-cylinder which was vacuum face-filled, although subsequent hollow center right-cylinder preform logs were produced. Standard Udimet René 95 powder was used for these logs which came from the master powder blends numbered 77004, 77029, and 77032. Characterization of the three blends is shown in Table 4-11.

These face-filled preform multiple logs were HIP compacted at KBI using Udimet's process for a 1204° C (2200° F), 2 hours minimum, 103 MPa (15 ksi) cycle. Cooling rates from the 1204° C (2200° F) HIP compaction cycle were estimated to be between 167° C to 278° C (300° F to 500° F) per hour, and microstructural observations of the gamma prime size and distribution on the preforms confirmed that the cooling rate was at least $> 111^{\circ} \text{C}$ (200° F)/hour. Therefore, the decision was made to bypass the preforge heat-treatment, since the 1204° C (2200° F) HIP compaction cycle ~56° C (~100° F) above the gamma prime solvus temperature provided the grain growth typically achieved by that heat treatment, and the autoclave cooling rate approximated that planned to give an acceptable gamma prime distribution.

Quality control tests on the Udimet preform-multiple log top and bottom slices did not indicate an oxygen gradient problem. Oxygen levels at the top-rim location were found to be as high as 200 ppm, but the planned machining to provide the preform dimensions brought the oxygen level well below the maximum specification limit of 150 ppm. Forging of these preforms is described in Section 4.3.4.

4.3.3 Net Size Preform Production

Processing of the near-net size forging preforms through HIP compaction and preliminary dimensional analyses was as described earlier. Those five preforms, two from CarTech and three from Udimet, were chemical milled at General Electric to produce the net size forging preforms. CarTech's preforms were made using MPB B-139, and Udimet's preforms were made using MPB 77042. These two master powder blends are characterized in Table 4-12 to be typical René 95 powder from these vendors.

The preforms were received at General Electric after pickling at Udimet or CarTech to remove the containers. The fill spouts were still evident on these parts and a flash-like protrusion existed on the rim and the bore at the container seams. The decision was made to remove the fill stems but to leave the flash-like protrusions in place through the chemical milling operation. The flash-like protrusion could be used for oxygen analyses after chemical milling and then the excess ground off prior to forging. Oxygen analyses were initiated on the fill spouts while the chemical milling process was conducted.

Table 4-11. Characterization of the Udimet Master Powder Blends.

(Preform Multiple Logs)

<u>Chemistry</u>	<u>Nominal Weight Percent</u>			<u>Specification</u>
	<u>77004</u>	<u>77029</u>	<u>77032</u>	
Al	3.58	3.47	3.53	3.3 - 3.7
Ti	2.48	2.51	2.56	2.3 - 2.7
Cb	3.50	3.65	3.52	3.3 - 3.7
Cr	13.30	12.64	12.83	12 - 14
Co	7.99	8.01	8.22	7 - 9
Mo	3.43	3.47	3.39	3.3 - 3.7
W	3.46	3.40	3.50	3.3 - 3.7
C	0.052	0.058	0.061	0.04 - 0.09
Zr	0.034	0.05	0.04	0.03 - 0.07
B	0.011	0.009	0.009	0.006 - 0.015
Fe	0.020	0.26	0.24	0.5 Max.

	<u>Nominal PPM</u>		
Si	<100	<100	<100
Mn	200	200	100
S	40	60	40
P	40	40	40
Ta	200	300	300
Cu	20	70	70
Pb	0.2	0.3	0.3
Bi	<0.1	<0.1	<0.1
O ₂	76	71	76
N ₂	35	26	26
H ₂	7	4	2

<u>Mesh Size Distribution</u>	<u>Weight Percent</u>		
+ 60	0.1	0	0
- 60,+ 80	5.5	4.1	4.6
- 80,+100	4.6	4.3	3.8
-100,+140	11.4	12.5	10.9
-140,+200	15.1	15.9	15.0
-200,+325	21.3	21.6	23.9
-325	42.0	41.6	41.8

Table 4-12. René Master Powder Blends Characterization.

(Near-Net-Shape Preforms)

<u>Chemistry</u>	<u>Nominal Weight Percent</u>	
	<u>CarTech B-139</u>	<u>Udimet #77042</u>
Al	3.49	3.48
Ti	2.54	2.54
Cb	3.59	3.54
Cr	13.02	12.81
Co	8.05	8.15
Mo	3.56	3.42
W	3.42	3.55
C	0.049	0.06
Zr	0.046	0.04
B	0.011	0.009
Fe	0.31	0.23

	<u>Nominal (PPM)</u>	
Si	300	<100
Mn	<100	200
S	40	40
P	60	40
Ta	<100	300
Cu	100	-
Pb	<2	-
Bi	<0.5	-
O ₂	80	88
N ₂	25	36
H ₂	2	4

<u>Mesh Size Distribution</u>	<u>Weight Percent</u>	
+ 60	0	0
- 60,+ 80	3.7	4.6
- 80,+100	5.1	4.6
-100,+140	13.1	10.6
-140,+200	18.7	13.8
-200,+325	29.0	22.8
-325	30.4	43.6

The two CarTech preforms were chemical milled to remove 1.5 mm (0.060 inch) from the surface without problems, but some difficulties were encountered in chemically milling the Udimet preforms. After 30 minutes in the chemical milling bath, each of the three Udimet preforms were found to exhibit nonuniform metal removal. At that point, those preforms were Harperized (mass finish technique) and grit blasted in an attempt to level the surface and to remove any barrier layer retarding the chemical milling action. Further chemical milling did result in more uniform attack, although the approximately 0.5 mm (0.020 inch) steps from the initial operation remained. No conclusive explanation for the differences in chemically milling of the CarTech and Udimet preforms was obtained. The known differences in the vendor processes was that CarTech used a SAE 1008 mild steel can, whereas Udimet used enamelling iron containers, and Udimet pickled in nitric acid while CarTech pickled in aqua-regia. Possibly the aqua regia pickle might have been more effective at removal of the interdiffusion zone which may have affected the rate of attack. Discussions with Ladish at that time led to the decision that they would hand-grind these Udimet preforms as required to level the surface prior to forging.

The oxygen results obtained on the fill spouts of the CarTech and Udimet near-net-shape preforms shown in Table 4-13 did lead to a concern on the oxygen levels in these parts. Two actions were taken as a result of finding fill stem oxygen levels in the range of 181 to 647 ppm. The first action was to take samples from the rim of each of the near-net-shape parts for oxygen analyses, and the second action was to cut-up the CarTech Task II full-scale second shape iteration part for an evaluation of the oxygen gradient. The results of these tests are also shown in Table 4-13 and confirmed that these near-net-shape preforms all exhibited an oxygen gradient. Metallographic evidence of near continuous prior particle boundary precipitates were found for these CarTech and Udimet preforms.

While recognizing the five near-net-shape preforms exhibited an oxygen gradient problem, the rim and bore flash-like parting lines were ground off and these parts shipped to Ladish for final dimensional analysis. Ladish's analyses indicated a problem with the locating rings on both vendor's preforms. The locating rings would have to be machined on the CarTech preforms because of an out-of-round condition, and a ring would have to be attached to the Udimet preforms since the location of the positioning ring was too far inward to correct by machining. In addition, Ladish confirmed that the chemical milling steps left on the Udimet preforms would have to be blended by grinding or by making a shallow machining surface cut prior to forging. A concern therefore existed that the Udimet preforms would be under the minimum acceptable forge weight after this additional surface removal.

Continued processing of the net shape preforms was placed in hold because of the oxygen gradient problem and the dimensional problems described. The decision was made to observe the forgeability for the CarTech three piece preform multiple log parts prior to continuation of processing. The poor forgeability of the CarTech preform multiple log parts described in Sections 4.3.4 and 4.3.5 subsequently led to the decision to stop work on these net-size preforms.

Table 4-13. Near-Net-Shape Preform Oxygen Analyses.

<u>Preform</u>	<u>Oxygen Concentration (ppm)</u>		
	<u>Fill Spout Sample</u>	<u>Rim Sample</u>	<u>Bore Sample</u>
CT992 (Vac-Face Fill)	181	269	138
CT993 (Vac-Face Fill)	205	229	-
UPD102-3 (Vac-Rim Rill)	446	272	109
UPD1-2-1 (Air-Face Fill)	455	323	-
UPD1-2-2 (Air-Face Fill)	647	421	-
CarTech - Second Shape Iteration	-	234 ± 39	112 + 16

<u>Depth from Rim mm (in.)</u>	<u>Oxygen Level (ppm)</u>
2.54 (0.10)	234 ± 39 (10 tests)
6.35 (0.25)	252, 244
10.92 (0.43)	151
17.02 (0.67)	117
40.60 (1.6)	113 ± 21 (4 tests)
Bore	112 ± 16 (6 tests)

4.3.4 Forging of Preforms

One of the six oversized 1121° C (2050° F HIP) full-scale preforms was preforge heat treated with a 111° C (200° F)/hr cooling rate, machined to the 60% forge reduction preform shape and forged at 1107° C (2025° F). Complete die fill was achieved, but cracking occurred which precluded use of that part. A preform design problem was found which resulted in excess flashing towards the inside diameter as shown in Figure 4-10. The presence of excess flash on future parts was corrected by a minor increase of the preform inside diameter. While the success in die fill confirmed application of the subscale preform design, the degree of cracking encountered (although not readily evident in Figure 4-8) presented a significant problem in this program.

Attempts to remove what was initially thought to be shallow cracking [depth ≤ 2 mm (≤ 0.1 inch)] in this initial part revealed that deeper cracking [depth ≥ 2 mm (≥ 0.1 inch)] and typically ≥ 0.6 mm to 1.5 mm (≥ 0.25 to 0.5 inch) had occurred in some locations. These deeper cracks were subsequently found to be associated with powder-fill stratification in bands as described in Section 4.3.5 which follows.

Nothing could be done at that time to modify the powder-fill striation band locations, but a re-HIP process at a higher temperature was proposed as a possible procedure to grow grains across the fine-grain (fine powder particle size) stratification bands. The remaining five preforms were given a re-HIP cycle at 1204° C (2200° F) using KBI autoclave. These preforms then were given the standard preforge heat treatment and cooled at $\sim 3^{\circ}\text{C}$ (200° F)/hr. Three of the five 1204° C (2200° F) re-HIP preforms were forged, and the results indicated that the cracking problem remained. Two of these parts forged at the standard 5 mm (0.2 in.)/min strain rate exhibited moderate to severe cracking, whereas the third part forged at a slower 2.54 mm (0.1 in.)/min strain rate exhibited mild to moderate cracking. Analyses were initiated on these forgings to define the cause of cracking as described in Section 4.3.5.

Three-Piece Preform Multiple Log

CarTech partially replaced the six individual preforms with a three-piece preform multiple log. That log was prepared by face filling and was HIP compacted at 1204° C (2200° F) as described earlier. Both of these changes were directed at alleviating the powder striation problem encountered in the prior six preforms. However, other problems were encountered with these log preforms. An oxygen gradient problem was identified as described earlier, and after forging, problems related to the HIP compaction temperature were found as discussed in Section 4.3.5.

Preforms were machined from the CarTech three-piece preform multiple log, given the preforge heat treatment with the 111° C (200° F)/hr cooling rate and then forged at Ladish. All three preforms exhibited some degree of cracking and none of these three forgings would yield an engine part. As shown

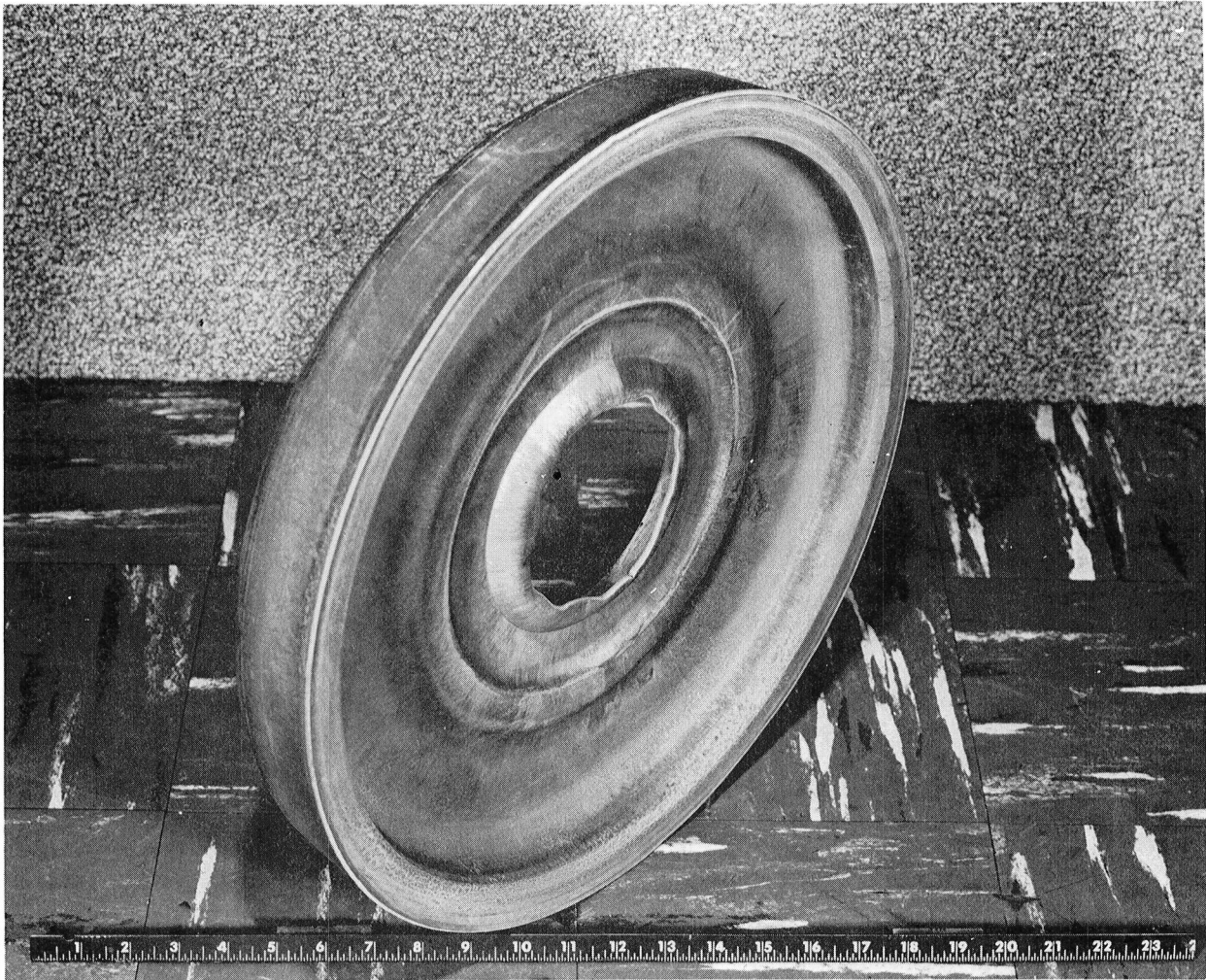


Figure 4-10. MATE CFM56/F101 Compressor Disk Forging

in Figure 4-11 the cracking in these forgings was not as catastrophic as in some of the subscale parts but was similar to the light to moderate cracking seen at that time. One forging exhibited shallow rim cracking ~5 mm (~0.2 inches deep), one had rim cracks with propagation over the rim face, and the third part contained a crack which penetrated the rim to a depth of about 38.1 mm (1.5 inches). Ladish found a preform identity problem for these three parts, but their records suggest that the forging exhibiting the least cracking is the bottom mult (the one containing the lowest oxygen content). Judgement prior to forging based on the oxygen gradient data was that the bottom and center mults would forge satisfactorily, whereas the top mult was expected to exhibit some cracking. Because of the unexpected degree of cracking, a study was initiated on these three parts to determine if the oxygen gradient and/or other factors resulted in the poor forgeability. Results of these analyses described in Section 4.3.5.

Udimet's Preform Multiple Logs

Udimet initially supplied a nine-piece solid-center preform multiple log for production hardware outside of the MATE program. As previously described, that log was vacuum face-filled and then was compacted at 1204° C (2200° F) HIP temperature at KBI. Since the cooling rate from the autoclave approximated that planned for the preforge heat treatment, no subsequent preforge heat treatment was used. Nine parts were machined to the preform shape and forged at Ladish. All nine parts forged successfully with no significant cracking. Two typical forgings are shown in Figure 4-12. That forging run confirmed the feasibility and production capability of the preform multiple log approach to produce preforms and near-net-shape isothermally forged compressor disks. The improved forgeability was believed to be largely due to process modifications developed during the MATE program including: (1) face filling of the log preforms to alleviate the powder particle size striation problem and (2) the use of the 1204° C (2200° F) HIP temperature.

Udimet subsequently supplied several hollow-center preform multiple logs for improved material utilization. Excellent forgeability results have continued with these face-filled preform multiple logs HIP compacted at 1204° C (2200° F). A total of approximately 64 forgings have been produced by this process to date. Mechanical properties obtained on these parts are presented in Section 4.3.6 of this report.

Net Size Forging Preforms

A review of the information available, including the analyses of the cracking problems in the CarTech and Udimet forgings was conducted prior to deciding the disposition of the five MATE net-size forging preforms. The final decision reached was not to forge these parts. The three major factors in that decision, as discussed in more detail in Section 4.3.5, were:



Figure 4-11. Compressor Disk Forgings Produced from the Cartech Three-Piece Preform Multiple Log

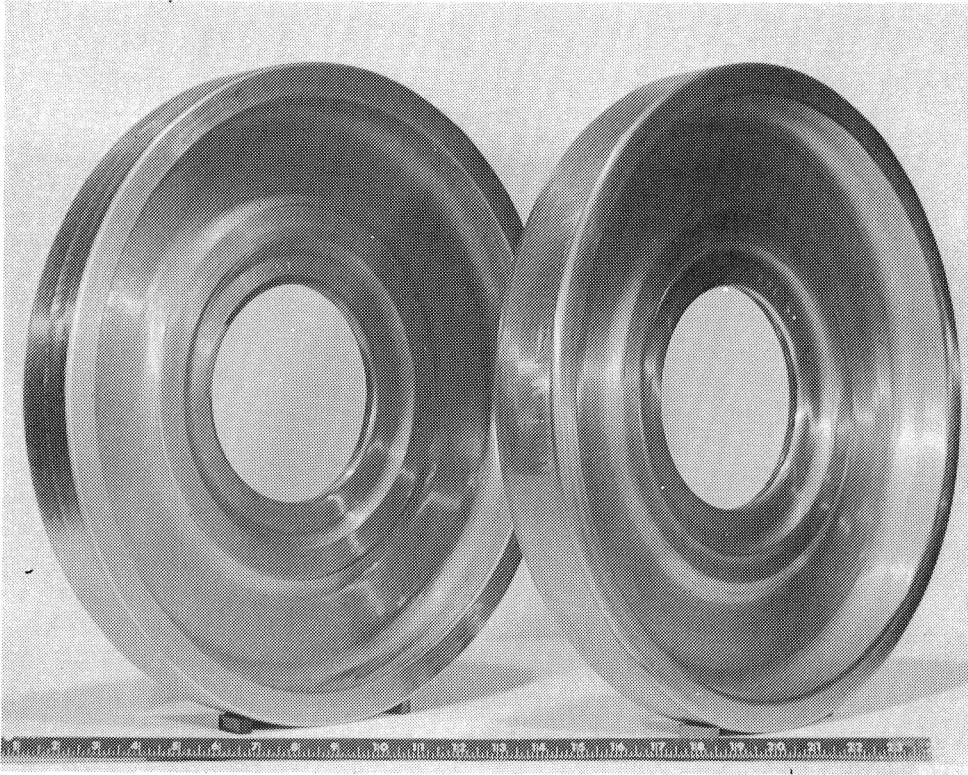


Figure 4-12. Stage 5-9 Compressor Disks Produced from
1204° C (2200° F) HIP Udimet Preforms

1. The HIP compaction cycle was not as desired since the micro-structure indicated the temperature achieved was below the gamma prime solvus $\sim 1149^{\circ}\text{C}$ ($\sim 2100^{\circ}\text{F}$) rather than as planned at 1204°C (2200°F). These preforms were in the same compaction run as CarTech's three piece log.
2. The preforms all exhibited excessive oxygen levels at the rim. Therefore, even if adequate forgeability was found, the parts would not meet specifications for engine test.
3. All of the preforms exhibited dimensional problems with respect to the locating ring surface.

4.3.5 Analyses Of Forge Cracking Problems

The analyses of the factors involved in cracking of the PM René 95 forgings were conducted contemporaneously as parts were forged for this project. The results are presented in the chronological order in which they occurred during the course of the project.

CarTech's Initial Six Oversized Forging Preforms

Macro and micro examinations were conducted on two of the cracked forgings produced from the CarTech oversized preforms. Forgings made from the original 1121°C (2050°F) HIP preform and one of the 1121°C (2050°F) HIP plus 1204°C (2200°F) re-HIP preforms were evaluated for powder striations and prior particle boundary precipitates. Macroetching in aqua-regia had revealed striations on the preforms as shown in Figure 4-13, although the pattern was not as distinct as has been previously observed on other parts.* Macroetching of the two forgings in a Super "0" etch ($80\%\text{HCl} + 20\%\text{H}_2\text{O}_2$) also revealed striations and that cracking had initiated and propagated² along these striations as shown in Figures 4-14 and 4-15. Figure 4-14 shows the original 1121°C (2050°F) HIP preform after forging and the severe grind-outs in an attempt to remove the striation cracks. The striation pattern in this part is apparent in the center of the picture as radial lines from the bore to the rim, and a faint pattern showing some of the bands approaching tangency to the bore was evident in the part. Figure 4-15 shows the rim intersection of the striation bands for the 1121°C (2050°F) HIP plus 1204°C (2200°F) re-HIP preform forging and the associated crack pattern.

Microstructural examination of both forgings also showed extensive prior particle boundary delineation with excessive gamma prime precipitation in the prior particle boundaries as shown in Figures 4-16 and 4-17. Scanning

*A.J. DeRidder, et. al., "Deformation Processing of Superalloy Hot Isostatic Press Preforms," presented at the 106th AIME Annular Meeting, Atlanta, Ga., March 6-10, 1977; (Figure 10).

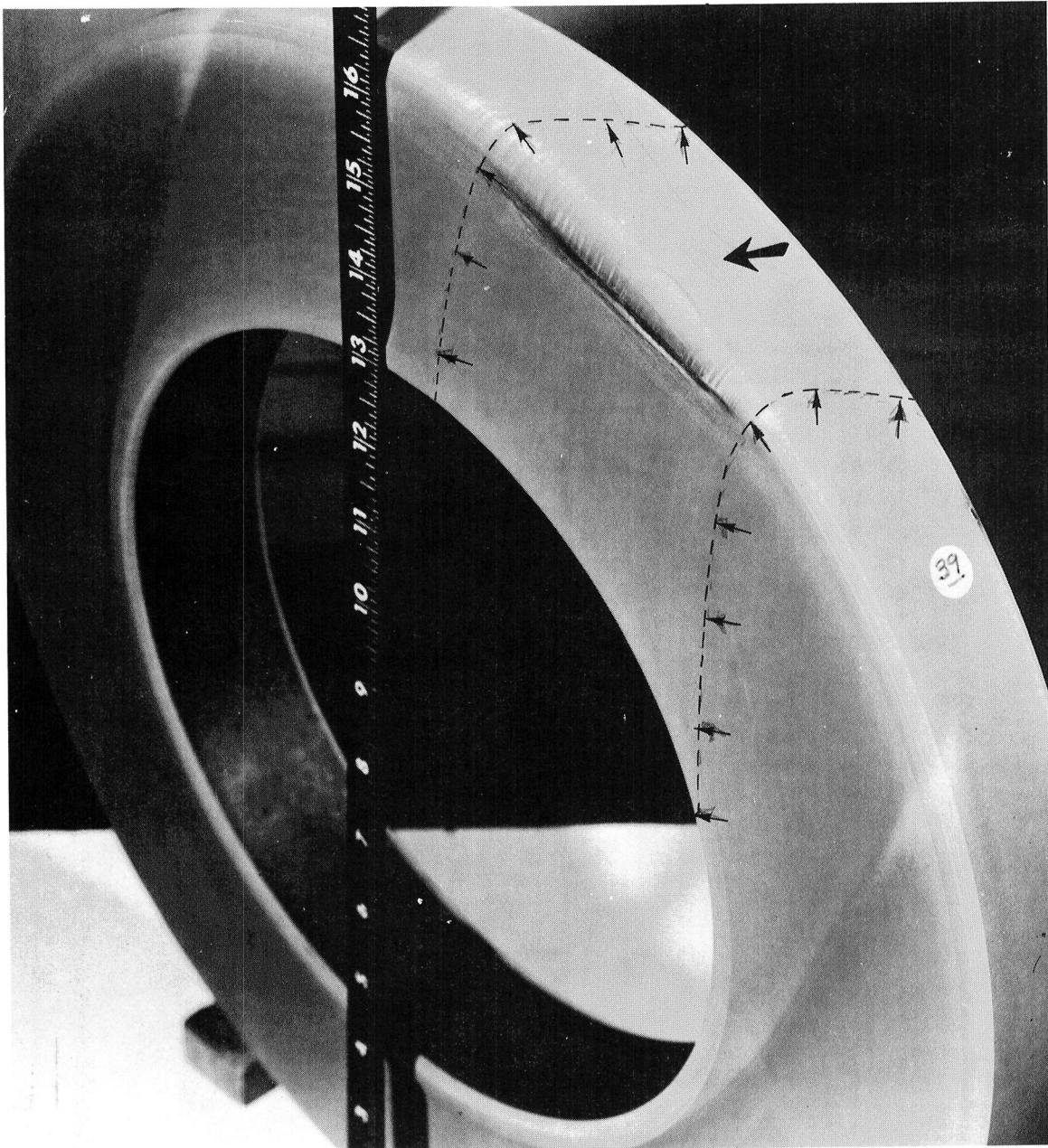


Figure 4-13. Stage 5-9 Compressor Disk Forging Preform Showing Powder Fill Striations

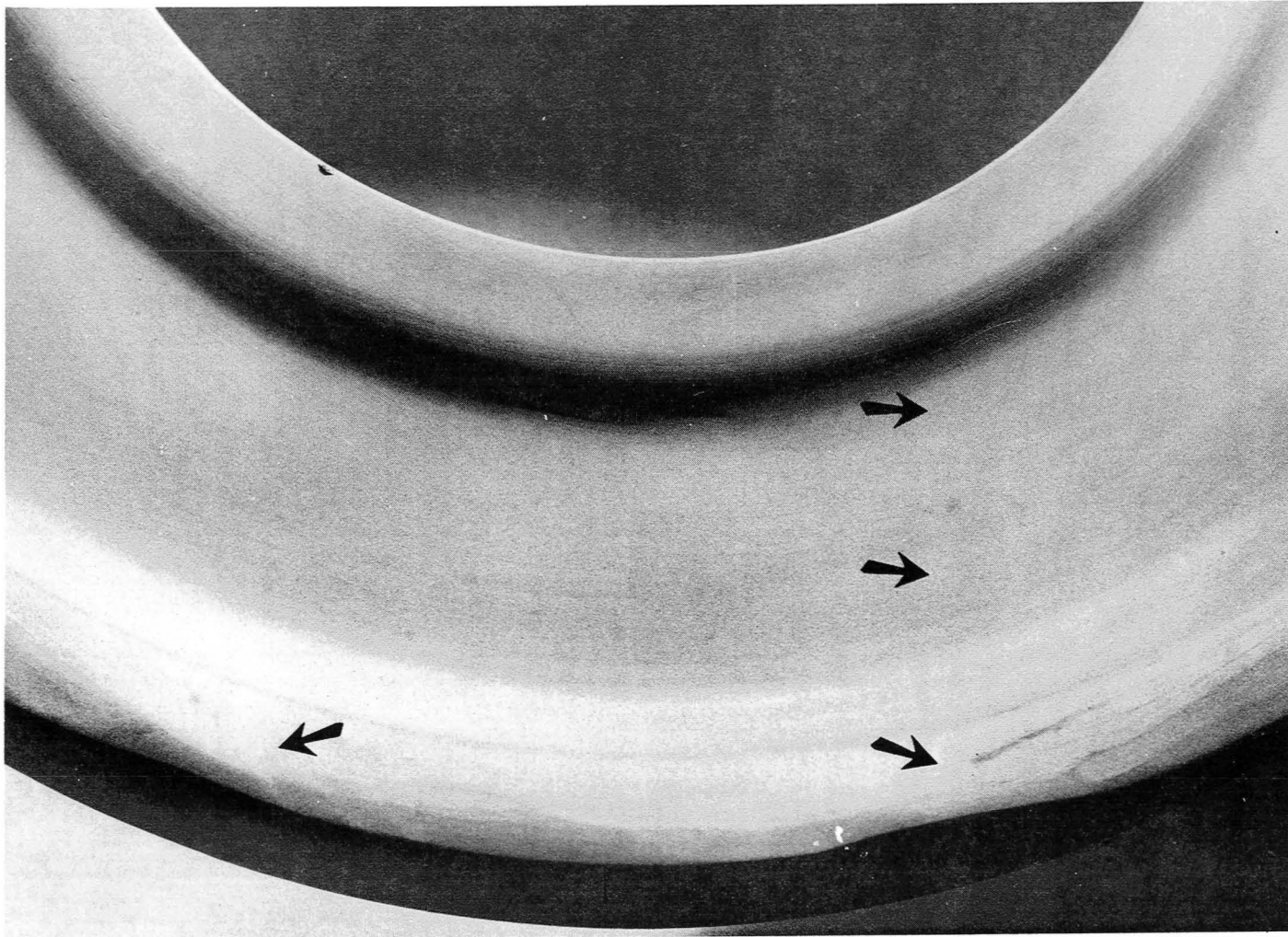
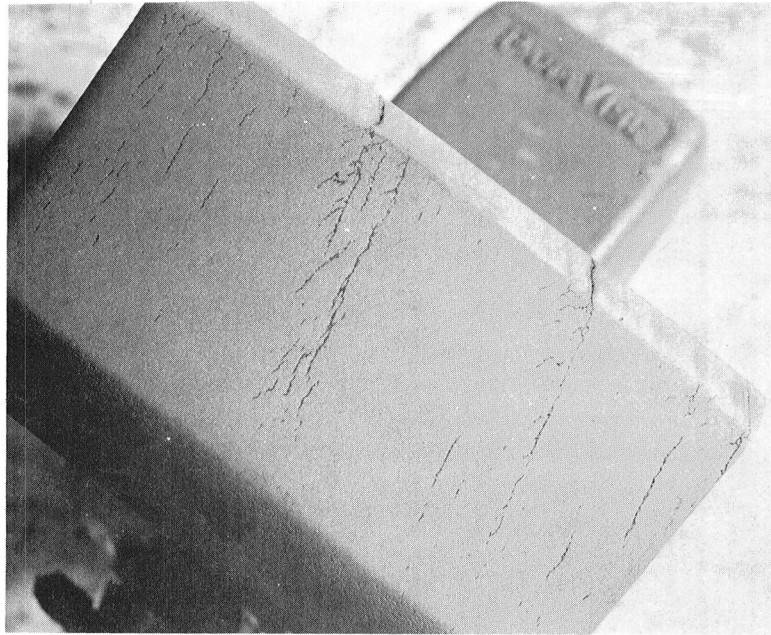
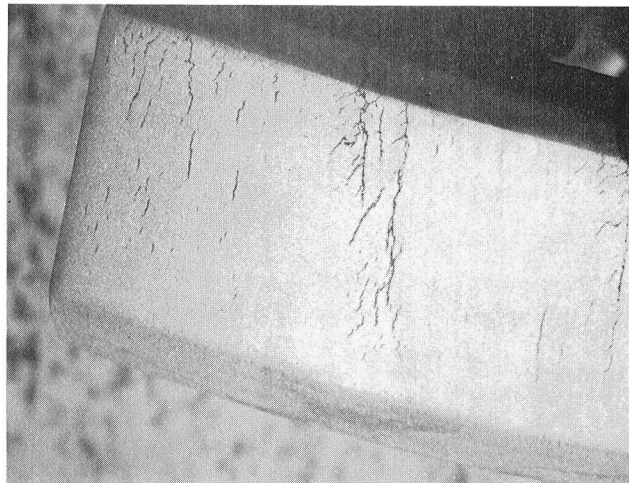


Figure 4-14. Section of Stage 5-9 Compressor Disk Forging Showing Striations and Attempt to Grind Out Striation Cracks at the Rim (Bottom)



~1X

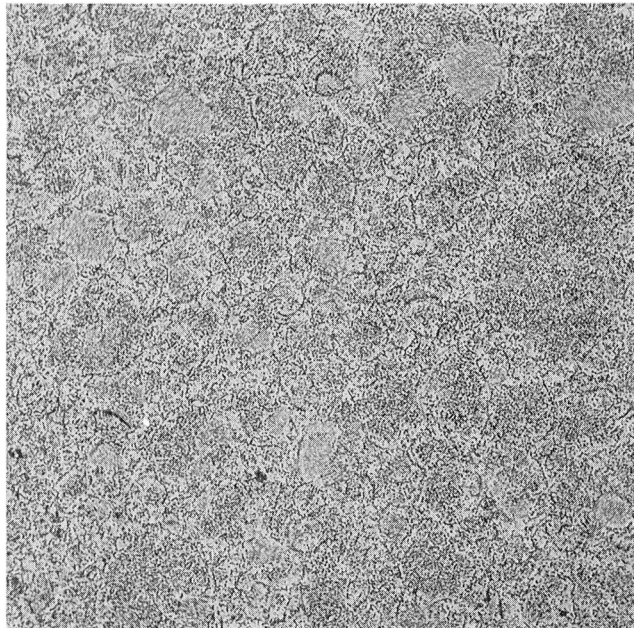
STRIATIONS APPARENT ONLY ON TOP TAPERED SURFACE



~1X

STRIATIONS APPARENT ON RIM SURFACE

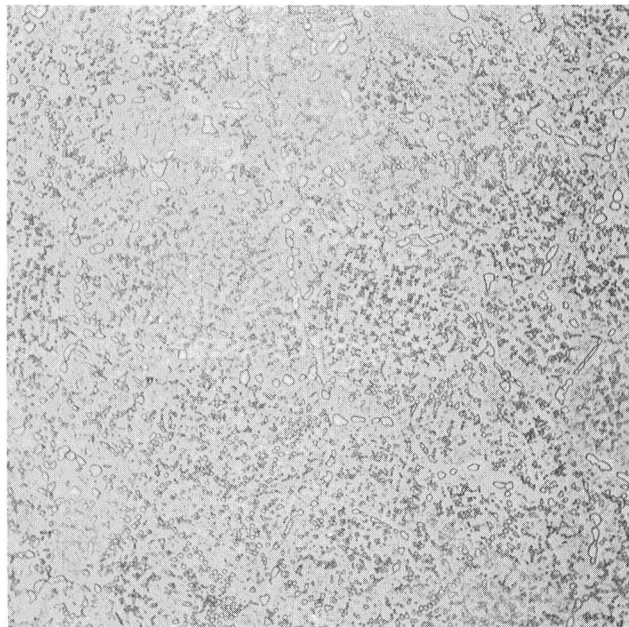
Figure 4-15. Section of the 1121° C (2050° F) HIP Plus 1204° C (2200° F) Re-HIP Preform Compressor Disk Forging Showing Striations and Associated Cracking



7-13376

100X

WALKER'S ETCHANT

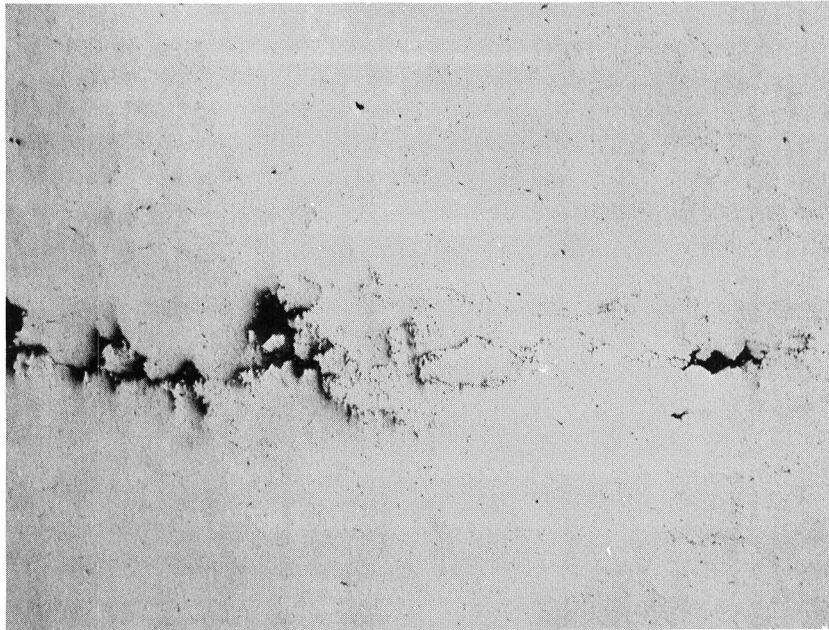


7-13376

500X

WALKER'S ETCHANT

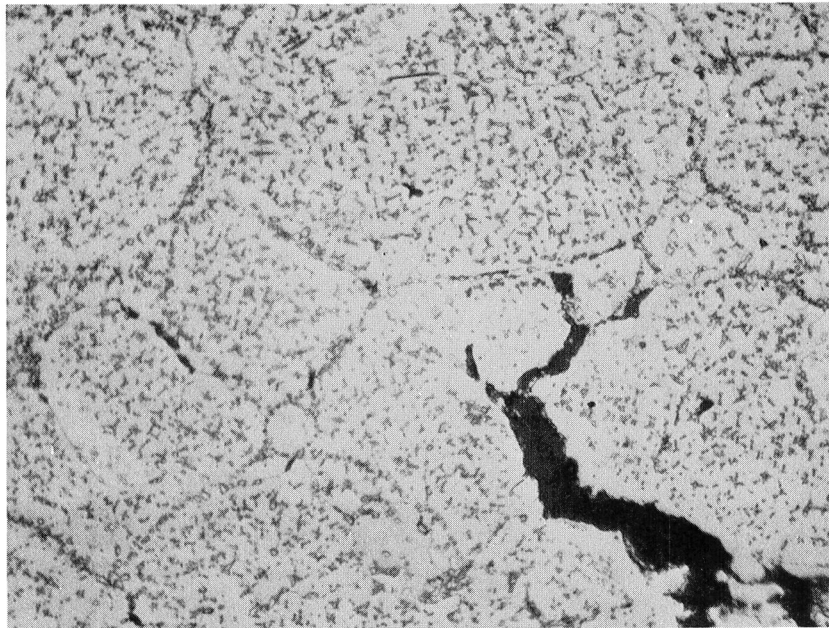
Figure 4-16. Compressor Disk Forging Microstructure After 1121° C (2050° F) HIP + 1190° C (2175° F) Preforge Heat Treatment + 1107° C (2025° F) Forge and Final Heat Treatment. Note Outlining of PPB



7-12674

AS POLISHED

100X



17-12677

SUPER "O" ETCHANT

500X

Figure 4-17. CFM56/F101 Compressor Disk Forging Microstructure After 1121° C (2050° F) HIP + 1204° C (2200° F) Re-HIP + 1190° C (2175° F) Preforge Heat Treatment + 1107° C (2025° F) Forge. Note Outlining of PPB

electron microscope EDAX analysis of these precipitates indicated only the expected gamma prime and carbide (Cb, Ti-C) phases present in the prior particle boundaries. No distinct microscopic evidence of the striations could be detected on these parts, although prior studies showed that striations result from powder particle size segregation. Fine powder particle bands typically appear as a striation in a matrix of a uniform powder particle size mixture. The observed striations were therefore assumed to be areas with an increased percentage of fine powder particles in comparison to the random mix matrix, but are difficult to identify microstructurally.

Concern existed on the extent of the prior particle boundary delineation with gamma prime and Cb, Ti-C carbides and the observed forge cracking at the prior particle boundaries as shown in Figure 4-17. Corrective action was taken on future CarTech preforms to minimize development of this excessive prior particle boundary precipitation by lowering the carbon level. Review of the chemistries of the CarTech, Udimet, and Crucible powders revealed that CarTech was consistently melting to the high end of carbon in the specification range (0.04 to 0.09 wt %), whereas the other vendors were typically at carbon levels in the 0.04 to 0.05 wt % range. However, the carbon level for this specific master powder blend (B093 and B107) was only in the 0.06 to 0.07 weight percent range. Since CarTech's powder preforms exhibited a greater tendency to show the prior particle boundary delineation in comparison to the preforms of the other two vendors, the decision was made to reduce CarTech's carbon level to the 0.04 to 0.05 wt % range for the powder in future preforms.

In summary, the cracking of the CarTech oversized preforms resulted from a combination of striation and prior particle boundary delineation problems. Corrective actions were defined for both problems as follows:

Striations: Face filling of the preforms was to be used to locate the powder particle separation bands nearly in the plane of the preform. When located in the plane of the preform, the striation bands are known to have minimal effect on forgeability.

Prior particle boundary precipitation: The carbon level was reduced from the 0.07-0.08 wt % range to the 0.04-0.05 wt % range to reduce the tendency towards prior particle boundary precipitate formation.

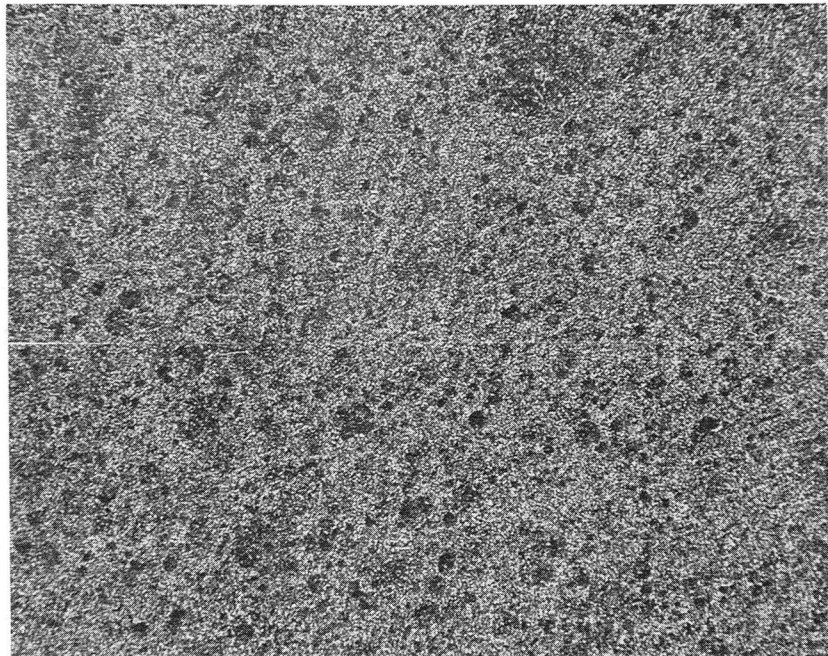
CarTech's Three Piece Preform Multiple Log

CarTech made changes in their production processes in an effort to eliminate the proposed causes of cracking observed in the initial oversized preforms. They produced a three-piece hollow right-cylinder preform multiple log to partially replace the six oversized preforms. The René 95 carbon level was reduced from ~0.06-0.07 weight percent to 0.04 weight percent (specification range 0.04 to 0.09 weight percent) to minimize PPB MC (Cb, Ti-C) carbides. Face filling of the containers was used to locate any striations in

the plane of the preforms, and a 1204° C (2200° F) HIP compaction cycle was planned based on the improved forgeability observed earlier for material processed at a higher HIP temperature. An oxygen gradient with top-rim oxygen levels to ~600 ppm was found in this preform log, but the decision was made to forge all three preforms, since the bottom mult exhibited an acceptable oxygen level (<150 ppm). All three of these preforms cracked during forging and the extensive study of the cracked forgings which was conducted to determine the cause of cracking is reported here. This study was conducted jointly by CarTech, Ladish, and General Electric to show that:

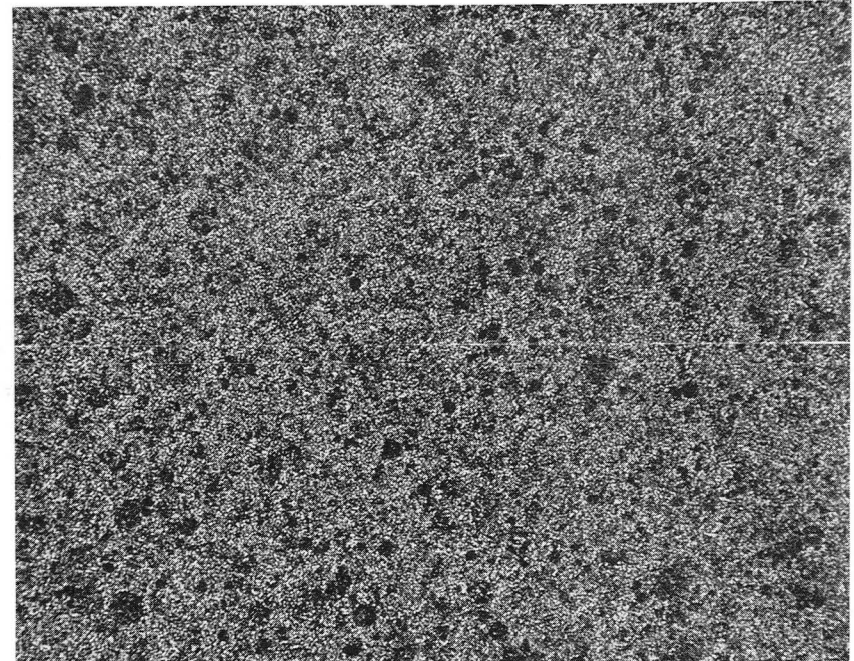
- As discussed in Section 4.3.2, CarTech added all of the -325 mesh fines to the powder in these preforms which had the effect of raising the overall oxygen level, but no conclusive link between the presence of fines and cracking was established.
- Metallographic examination indicated that the 1204° C (2200° F) HIP compaction temperature was not achieved, and thus the expected higher HIP temperature forgeability advantage was not obtained. This conclusion was based on the microstructure of the HIP compacted log which indicated that the actual HIP temperature was below the 1145° C (2090° F) gamma prime solvus. The microstructure of the CarTech MATE preforms in the HIP condition are shown in Figure 4-18 for comparison with the typical larger grain size Udimet 1204° C (2200° F) HIP preform multiple log microstructure in Figure 4-19. The HIP temperature control for the CarTech preforms was maintained only on the furnace control thermocouples, i.e.: there were no work load thermocouples. CarTech developed information at another HIP source comparing furnace to work-load thermocouples which suggested that the MATE preforms may have seen less than one-half hour at temperature. The microstructures of the intended 1204° C (2200° F) HIP compaction when compared to those of typical 1204° C (2200° F) HIP preforms suggests that the planned HIP temperature was not actually achieved. The implication of the previously stated conclusion that the 1204° C (2200° F) HIP temperature was not achieved, is that the known forgeability advantage after a 1204° C (2200° F) HIP compaction cycle also was not achieved.
- Cracking on these face filled preforms was not associated with striations. No evidence of powder filling striations was found.
- Oxygen level did not appear to be a major factor causing cracking since the acceptable-oxygen level preform also cracked. Oxygen levels greater than 200 ppm were not found in any of the three forgings.

Cracking was concluded to be a result of low 1093° C (2000° F) ductility (approximately 5% vs. desired >10% elongation) resulting from PPB delineation combined with the extensive metal flow required during forging the compressor part. The desired ductility value was an observation developed by



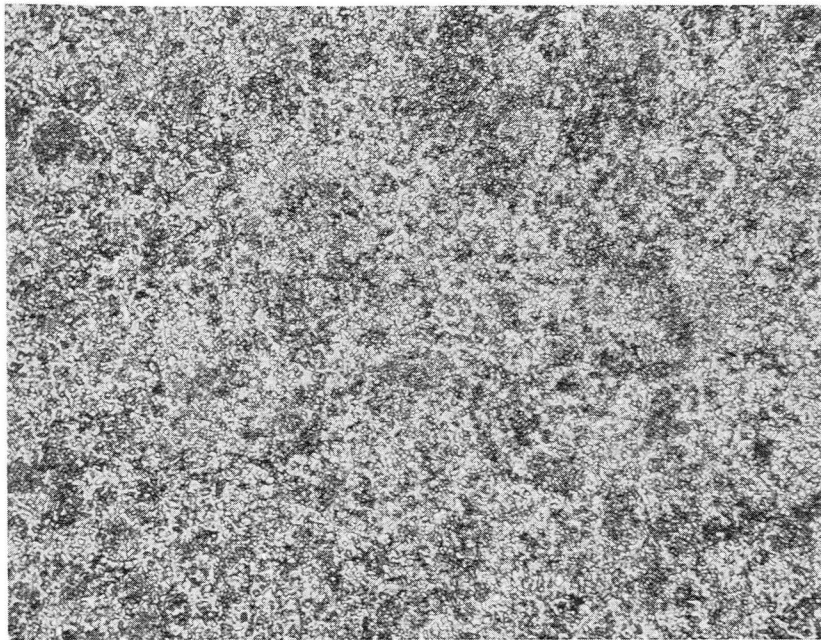
15075

100X



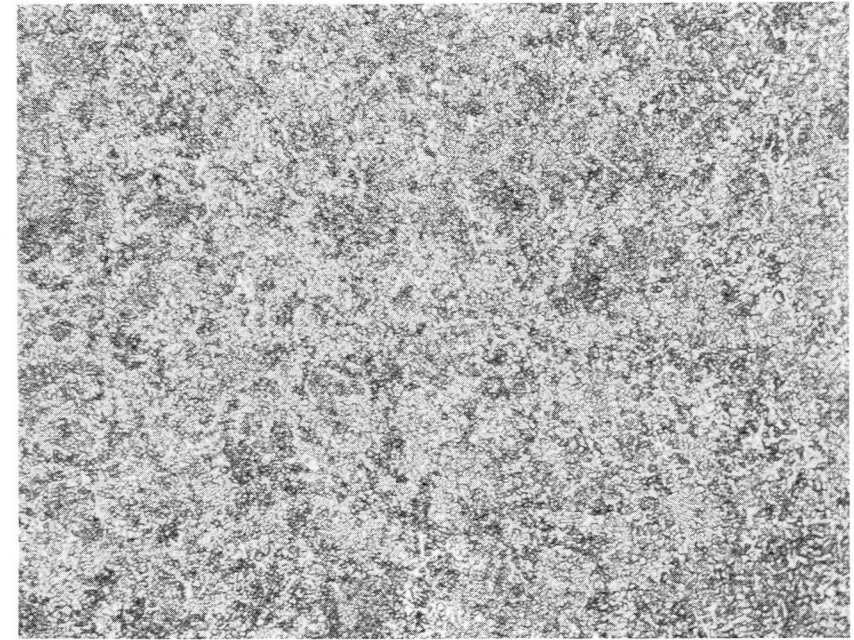
15077

100X



15078

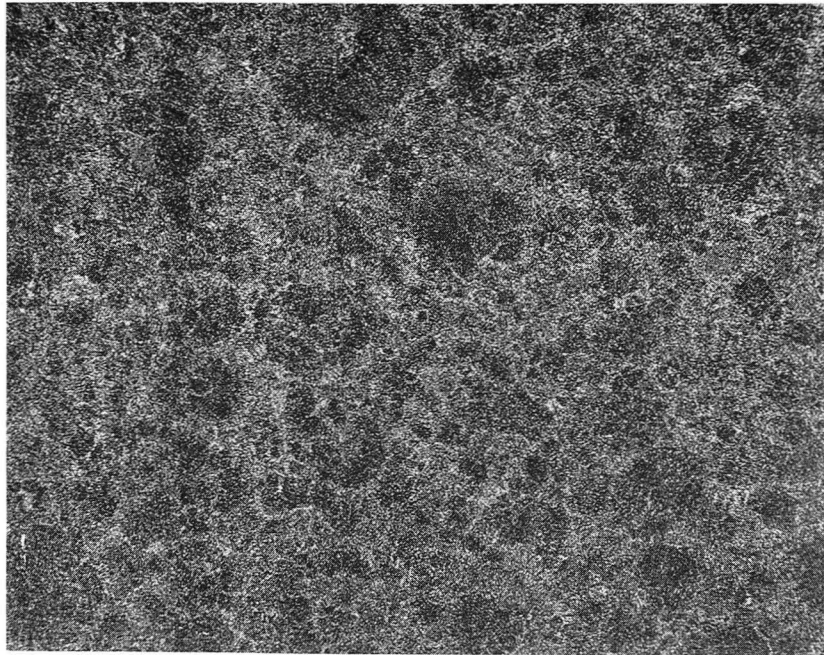
500X



15079

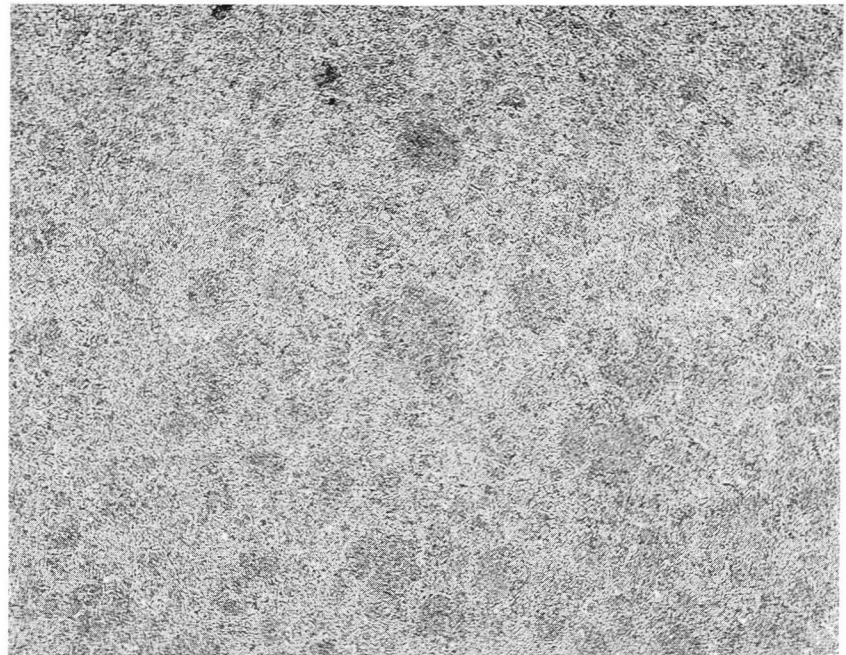
500X

Figure 4-18. Microstructures of the CarTech Preforms in the HIP Condition (Walker's Etchant).



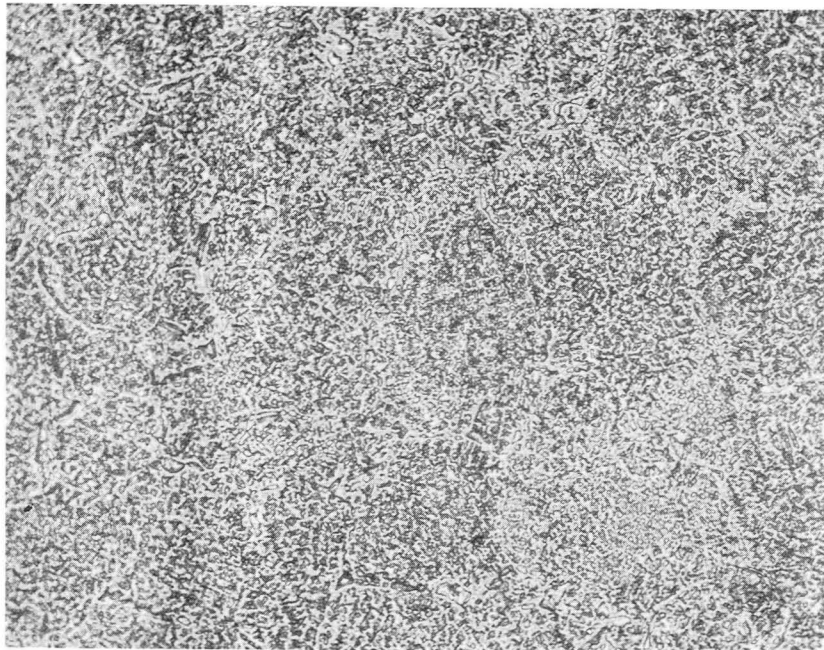
8-15897

100X

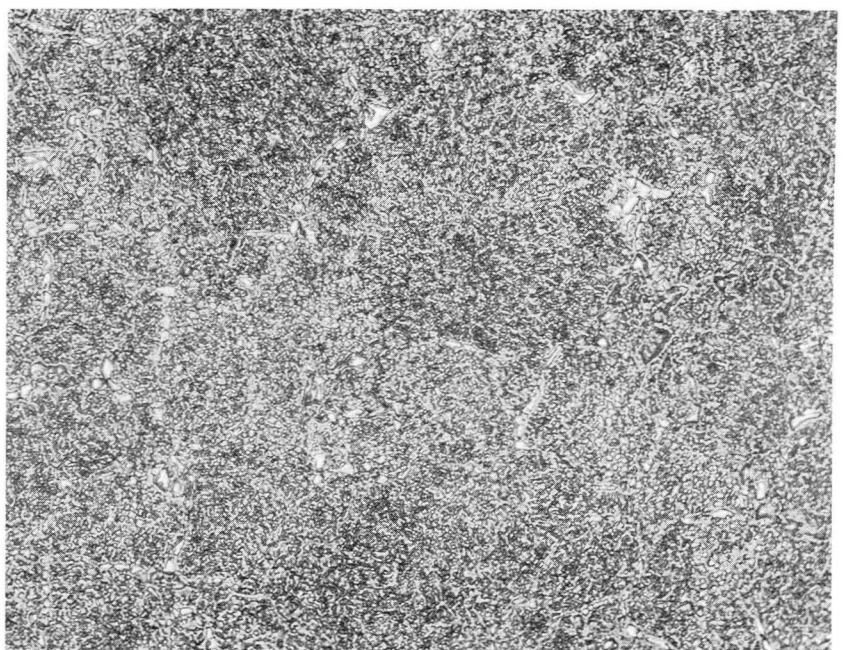


8-15898

100X



8-15898



8-15897

500X

Figure 4-19. Microstructure of the Udimet Preforms in the 1204° C (2200° F) HIP Condition (Walker's Etchant)

Ladish based on a limited number of 2000° F tensile tests on René 95 material from preforms which exhibited acceptable forgeability. Scanning electron micrographs of the fracture surfaces and metallographic evidence suggested prior particle boundary separation as the major cause of reduced ductility. PPB delineation was apparent in all three parts, including that part with an acceptable oxygen level. Typical microstructural evidence of the PPB delineation in these parts is shown in Figure 4-20 and the association with PPB separation cracking is shown in Figures 4-21 and 4-22.

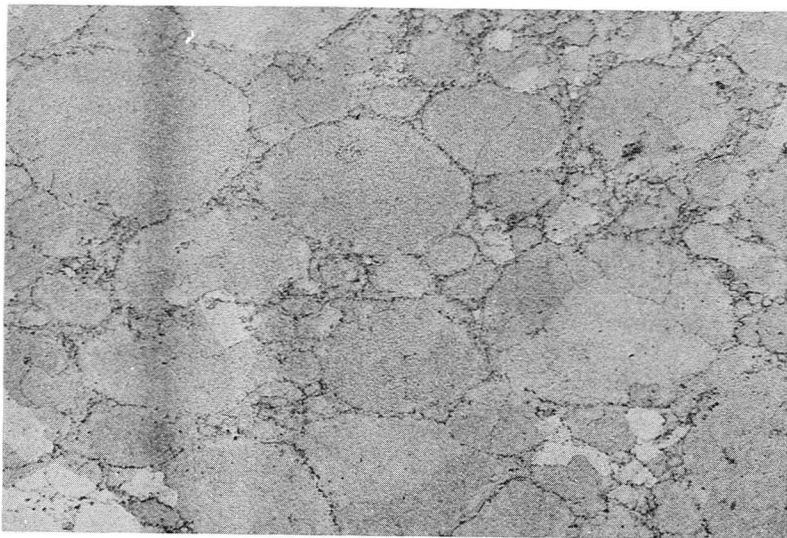
The PPB delineation source was concluded to be associated with powder handling practice and the specific HIP cycle attained on these parts. HIP compaction of CarTech powder without deleterious PPB delineation has been demonstrated on similar parts outside of the MATE program.

Corrective Action Investigations at CarTech

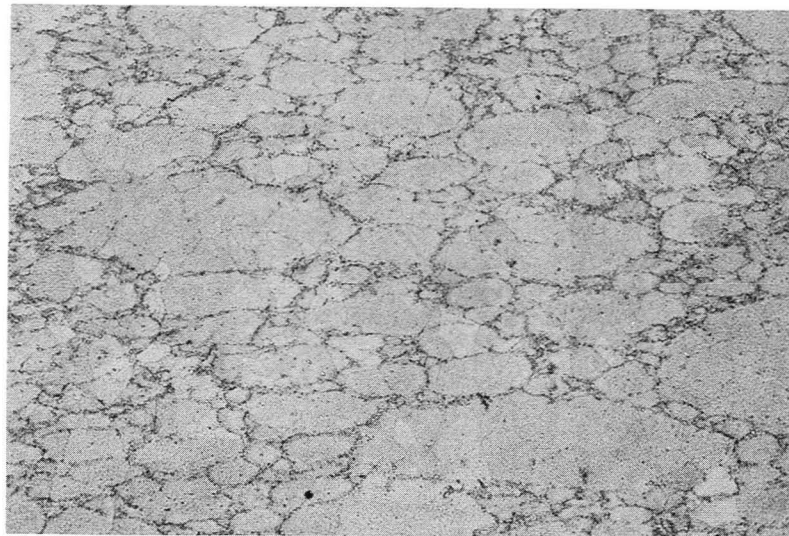
Low ductility in high temperature testing resulting from prior particle boundary delineation was recognized as the major preform production problem by CarTech, and they initiated corrective action investigations using the 1093° C (2000° F) tensile test ductility as the evaluation criterion. Preliminary results from that continuing investigation are shown in Table 4-14.

Tensile data on the C998 three-piece preform multiple log were conducted to establish baseline data. The 1093° C (2000° F) tensile elongation of that preform material was 20.3% in the HIP compacted condition. However, since the HIP compaction temperature planned to be 1204° C (2200° F) was actually less than 1150° C (2100° F), this result is for the fine grained material and the high ductility result is as anticipated. That material would have yielded a 100% fine grain microstructure if forged without the 1190° C (2175° F) preforge heat treatment, and it may have forged without significant cracking. The addition of the preforge heat treatment 1190° C (2175° F), 4 hours, plus cooling at a rate of 111° C (200° F) per hour to 1038° C (1900° F) and then air cooling increased the strength by about 68.9 MPa (10 ksi) and reduced the ductility to 5% elongation. As described earlier, the preforms cracked during forging in this condition. CarTech used a section of the C998 log material for re-HIP at 1204° C (2200° F) which produced a slight improvement in ductility (6.7% versus 5%) in comparison to the 1121° C (2050° F) HIP plus preforge heat treatment material.

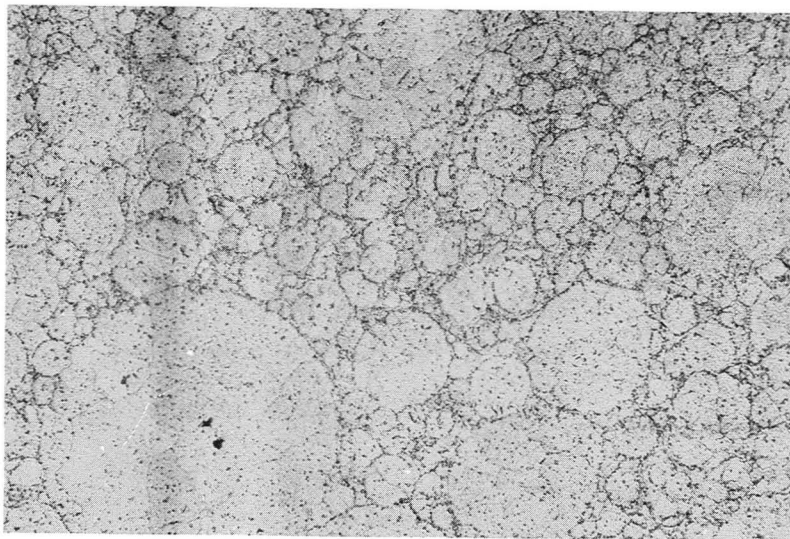
CarTech continued their evaluation using the 1033 compact produced from René 95 powder from lot A1382. That material, characterized in Table 4-15, differed from the earlier powder in at least two respects: it was processed to a low-oxygen level modified practice and in addition it was produced as minus 140 mesh. The 1121° C (2050° F) HIP compaction process was conducted with work load thermocouples being monitored to assure proper temperature control. The HIP temperature was selected for comparison with earlier CarTech results. The low oxygen 1033 compact material produced about the same strength level as the C998 log in the HIP compacted condition, but the ductility values (~33% elongation) were significantly higher. After



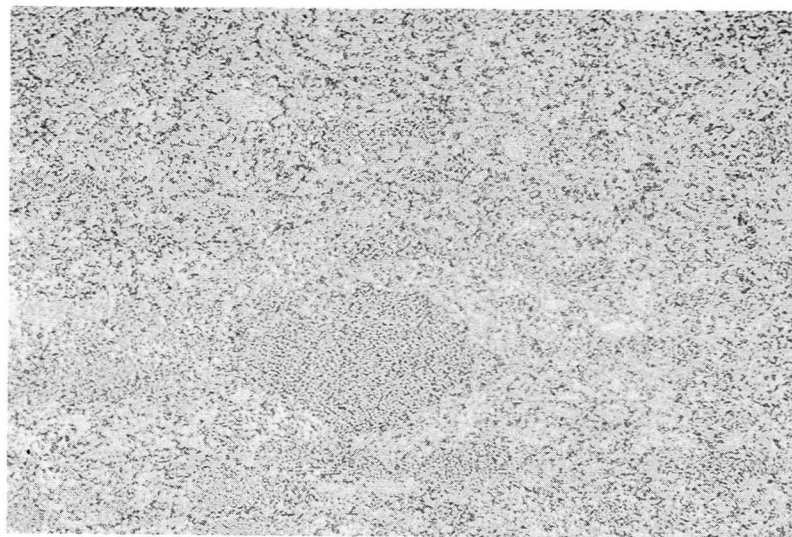
RIM - TOP S/N 9983



RIM - MID HEIGHT S/N 9983

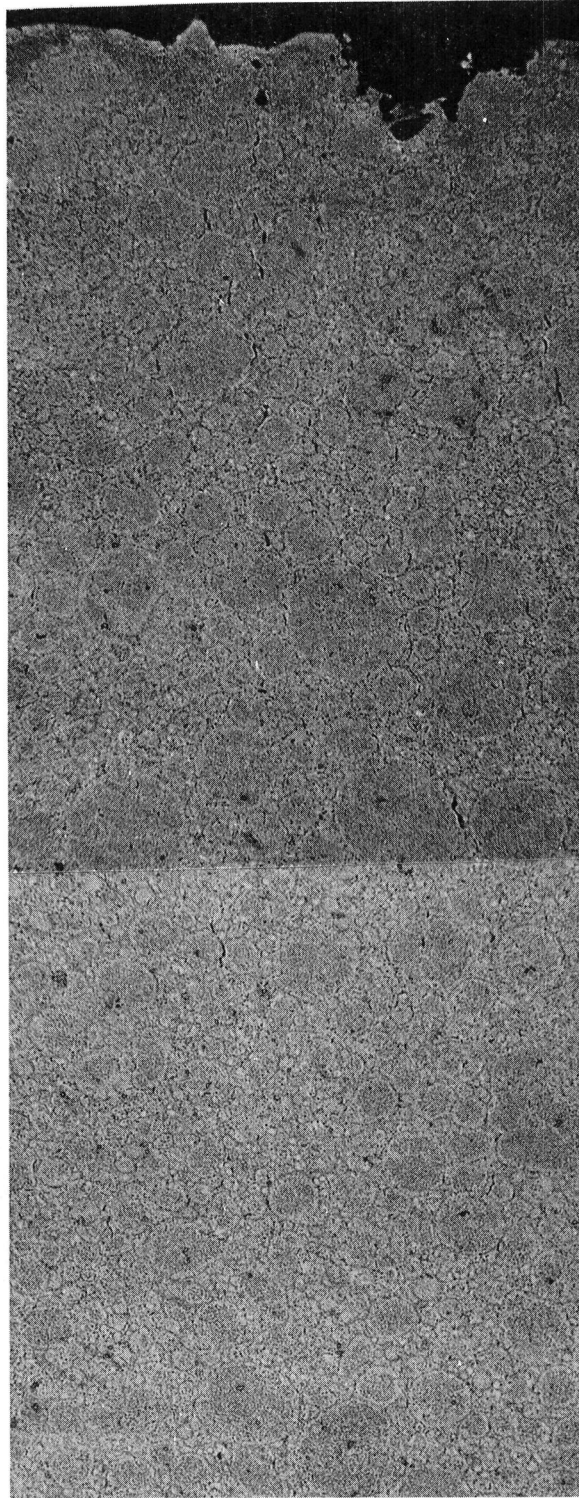


RIM - BOTTOM S/N 9981



BORE S/N 9982

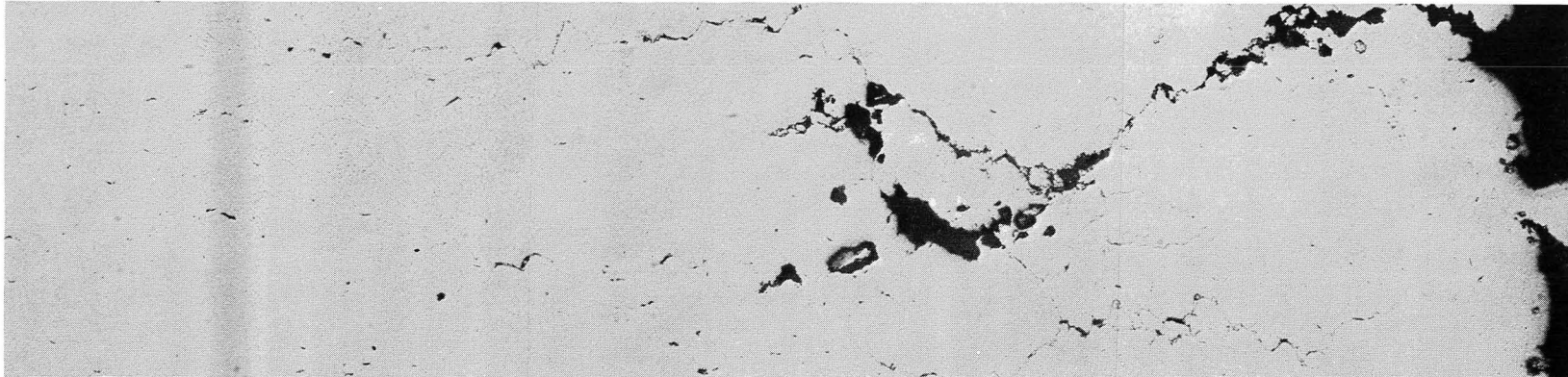
Figure 4-20. Typical Forged Microstructures of Compressor Disk Forgings Produced from CarTech Three-Piece Preform Multiple Log (Walker's Etch, 200X) - Note Prior Particle Delineation.



8-7527

100X

Figure 4-21. Illustration of Prior Particle Boundary Separation During Forging of CarTech Preforms (Forging S/N 9982, Walker's Etch).



(7527)

180x

Figure 4-22. Illustration of Prior Particle Boundary Separation Leading to Cracking During Forging of CarTech Preforms (Un-Etched Forging S/N 9982).

Table 4-14. 1093° C (2000° F) Tensile Data on CarTech Preforms.

Conditions: Gage Section: 4-78 mm (0.188 inch) diameter x 25.4 mm (1.0 inch) length
Strain Rate: 17 mm/mn/min (0.67 in./in./min)

Material	Condition	1093°C (2000°F) Tensile Properties		
		UTS MPa (KSI)	El (%)	RA (%)
MATE Log (C998)	Hip Compacted* - No Preforge HT	115.8 (16.8)	20.3	16.4
MATE Log (C998)	HIP Compacted Plus Preforge HT	115.8 (25.5)	5.0	6.5
MATE Log (C998)	Re-HIP at 1204°C (2200°F) at CarTech	186.8 (27.1)	6.7	8.6
Desired Ductility for Adequate Forgeability		-	10	10
1033 Compact	Low Oxygen Processes, 1121°C (2050°F) HIP Compacted - No Preforge Heat Treatment	113.1 (16.4)	32.9	33.3
1033 Compact	Low Oxygen Processed 1121°C (2050°F) HIP Compacted Plus Preforge Heat Treatment	184.8 (26.8)	8.4	8.8

*Planned 1204°C (2200°F) HIP compaction conditions not achieved.

Table 4-15. CarTech Al382 Material Characterization

	<u>Weight Percent</u>	<u>Specification</u>
<u>Chemistry</u>		
Al	3.52	3.30-3.70
Ti	2.54	2.30-2.70
Cb	3.68	3.30-3.70
Cr	12.94	12.00-14.00
Co	8.00	7.00-9.00
Mo	3.64	3.30-3.70
W	3.42	3.30-3.70
C	0.044	0.04-.09
Zr	0.07	0.03-.07
B	0.011	0.006-.015
Fe	0.35	0.50 Max
<u>Residual Elements</u>		
Si	300	2000 Max
Mn	<100	1500 Max
S	20	150 Max
P	<50	150 Max
Ta	<0.01	2000 Max
Cu	200	-
Pb	<2	5 Max
Bi	<0.5	0.5 Max
O ₂	29	150 Max
N ₂	20	50 Max
H ₂	2	10 Max
<u>Mesh Size Distribution</u>		
+60	0	
-60,+80	0	
-84,+100	0	
-100,+140	3.0	
-140,+200	17.8	
-200,+325	26.9	
-325	52.3	

preforge heat treatment of the 1121° C (2050° F) HIP 1033 compact, its ductility of 8.4% was closer to the 10% desired level than the C998 log. Metallographic observations at CarTech on the 1033 compact did not show the prior particle delineation problems encountered in the MATE C998 log.

Udimet's Preform Multiple Logs

Udimet's preform-multiple logs exhibited excellent forgeability. The mold face filling technique combined with the 1204° C (2200° F) HIP compaction process resulted in consistently excellent forgeability. Typical microstructures for these Ladish/Udimet preform CFM56/F101 compressor disk forgings are shown in Figure 4-23 to illustrate the absence of the prior particle delineation condition. A total of about 64 Udimet preforms have been forged to date with excellent results.

Decision Not to Forge the Net Size Forging Preforms

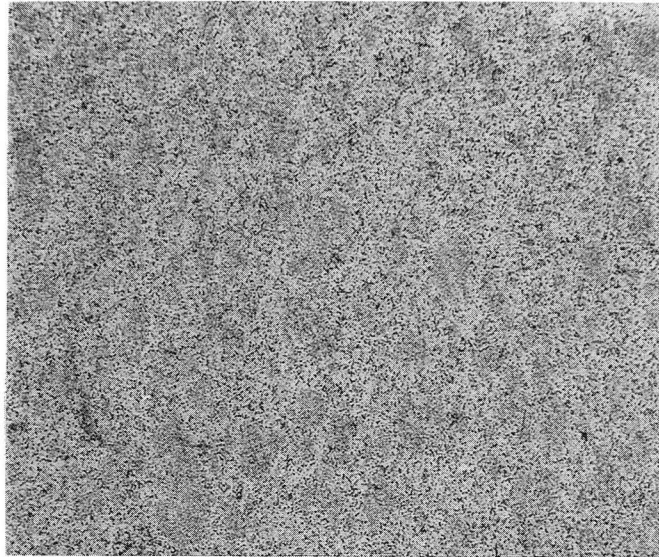
Further processing of the near-net-size forging preforms produced by CarTech and Udimet was not conducted. These preforms were all compacted in the same HIP run as the CarTech three piece preform multiple log. Excessive rim oxygen levels were found in these preforms, and the analysis of the cracked three-piece log preforms indicates that the actual HIP compaction temperature during this run was less than 1149° C (2100° F) rather than the planned 1204° C (2200° F). These factors suggest a high probability of cracking if these net size parts were to be forged.

4.3.6 Mechanical Property Evaluation

The mechanical property test plan for the CFM56/F101 compressor disks is shown in Table 4-16. Four forgings produced from Udimet preforms were included in this evaluation as follows:

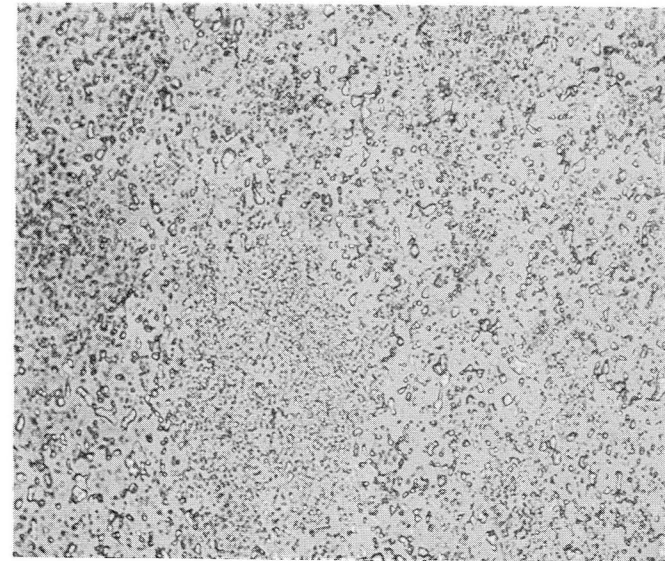
<u>Forging Designation</u>		<u>Preform Source and Master Powder Blend No.</u>
<u>Ladish</u>	<u>GE</u>	
DDA4	-	Udimet/77004
FWA67	MZS27657	Udimet/77029
FAH86	MZS27676	Udimet/77032
-	MZS27673	Udimet/77032

These blends were characterized to be standard Udimet -60 mesh powder as shown earlier. The preforms were HIP compacted at KBI using the 1204° C (2200° F), 2 hrs minimum, 103 MPa (15 ksi) cycle. Work load thermocouples were not used for compaction of these preforms, but Udimet's specification of the temperature-time cycle was adequate in achieving the desired preforge structure as typically shown in Figure 4-19.



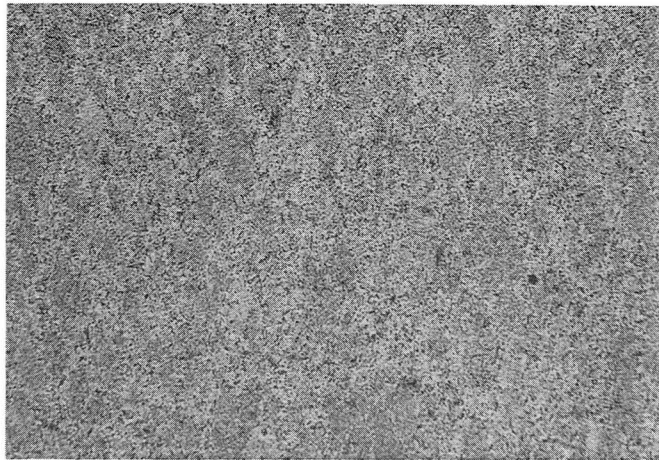
100X

H2200



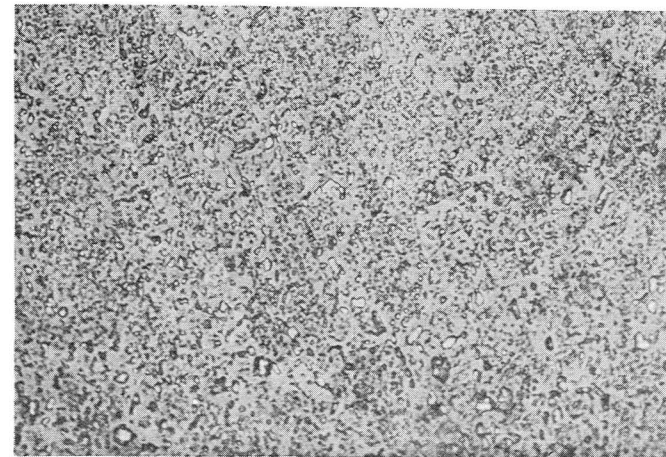
500X

H2200



100X

H2199



500X

H2199

Figure 4-23. Typical Forged Microstructures of the CFM56/F101 Forging (FAH 86) Produced from Udimet Preforms (Walker's Etch). Note Absence of Prior Particle Boundary Delineation

Table 4-16. Summary of Mechanical Property Tests on Hot Die Forged René 95 in Task III.

	<u>Ladish Product Acceptance Testing</u>	<u>Additional Testing (MZS 27673)</u>
<u>Tensile</u>		
• Room Temperature	36	0
• 204° C (400° F)	0	6
• 427° C (800° F)	0	6
• 538° C (1000° F)	0	6
• 649° C (1200° F)	36	0
<u>Stress Rupture</u>		
• 649° C/1034 MN/m ² (1200° F/150 ksi)	30	0
• 538-704° C (1000-1300° F) at stresses to produce failures in 100-1000 hrs.	0	9
<u>Creep</u>		
• 593° C/1034 MN/m ² (1100° F/150 ksi)	12	0
• 538-704° C (1000-1300° F) at stresses for 0.2% creep in 100-1000 hrs.	0	9
<u>Sustained Peak Low Cycle Fatigue, K_t=2, A=0.95</u>		
• 649° C/950 MN/m ² (1200° F/145 ksi)	6	0
• 649° C (1200° F) at stresses for 500-10,000 cycle life range	0	6
<u>Low Cycle Fatigue/Strain Control/A1=1</u>		
• Room Temperature	0	0
• 398° C (750° F)	3*	5**
• 427° C (800° F)	0	0
• 538° C (1000° F)	3*	5**
• 649° C (1200° F)	0	5**
<u>Residual Cyclic Life (K_R)/A=0.95</u>		
• 538° C (1000° F) - Crack 0.51 MMx1.52MM (.020"x.060") at 689 MN/m ² (100 ksi)	6	0
• Same, but varied stresses for 1000-10,000 cycle life range	0	4
<u>Dynamic Modulus of Elasticity</u>		
• Room Temperature - 816° C (1500° F)	0	2
<u>Density</u>	<u>8</u>	<u>12</u>
Total Tests	140	+ 75 = 215

*6.35 mm (0.25 inch) diameter test bars
 **10.16 mm (0.04 inch) diameter test bars

The serial numbered DDA4, and FAH86 forgings were all evaluated to the cut-up plan shown in Figure 4-24, and the MZS 27673 forging was cut-up as shown in Figure 4-25 for evaluation.

Test Results

The mechanical properties for the four PM René 95 compressor disk forgings evaluated were acceptable.

Tensile Data

Tensile data at room temperature and 1204° C (1200° F) on specimens from the source substantiation forgings and tensile data at 204° C, 427° C and 538° C (400° F, 800° F and 1000° F) on specimens from the MZS27673 forging are shown in Table 4-17 and in Figures 4-26 and 4-27. These data represent completion of the planned tensile tests. Of the 92 tests conducted only one below requirement value was found. That specimen, DDA-4-102, exhibited an 8% elongation value compared to the 10% requirement. Two retests on specimens taken adjacent to the 102 location for the DDA4 forging produced acceptable ductility values.

Stress Rupture

Stress rupture data at 649° C (1200° F) and 1034 MPa (150 ksi) on specimens from the three source substantiation forgings are given in Table 4-18. All of the test results met the requirements. Stress rupture testing in the 1000° F to 1300° F temperature range on specimens from the MZS27673 forging are shown in Table 4-19 and graphically in Figure 4-28.

Creep Data

Creep data at 593° C (1100° F) and 1034 MPa (150 ksi) on specimens from the three source substantiation forgings are reported in Table 4-20. The average creep deformation in 100 hours for these tests was about 0.1% which meets the program requirement of $\leq 0.2\%$. Creep tests in the 538° C (1000° F) to 704° C (1300° F) temperature range on specimens from the MZS27673 forging are shown in Table 4-21. Curves are shown in Figure 4-29 for the stress rupture life, the 0.2% plastic deformation time and the 0.1% plastic deformation conditions. Some data scatter was observed in the creep deformation results, but the lowest data point for 0.2% creep 649° C (1200° F), 565 MPa (82 ksi) was within a 0.7 parameter value of the average curve. A scatter band of about \pm one parameter value is typical of high temperature nickel-base alloys.

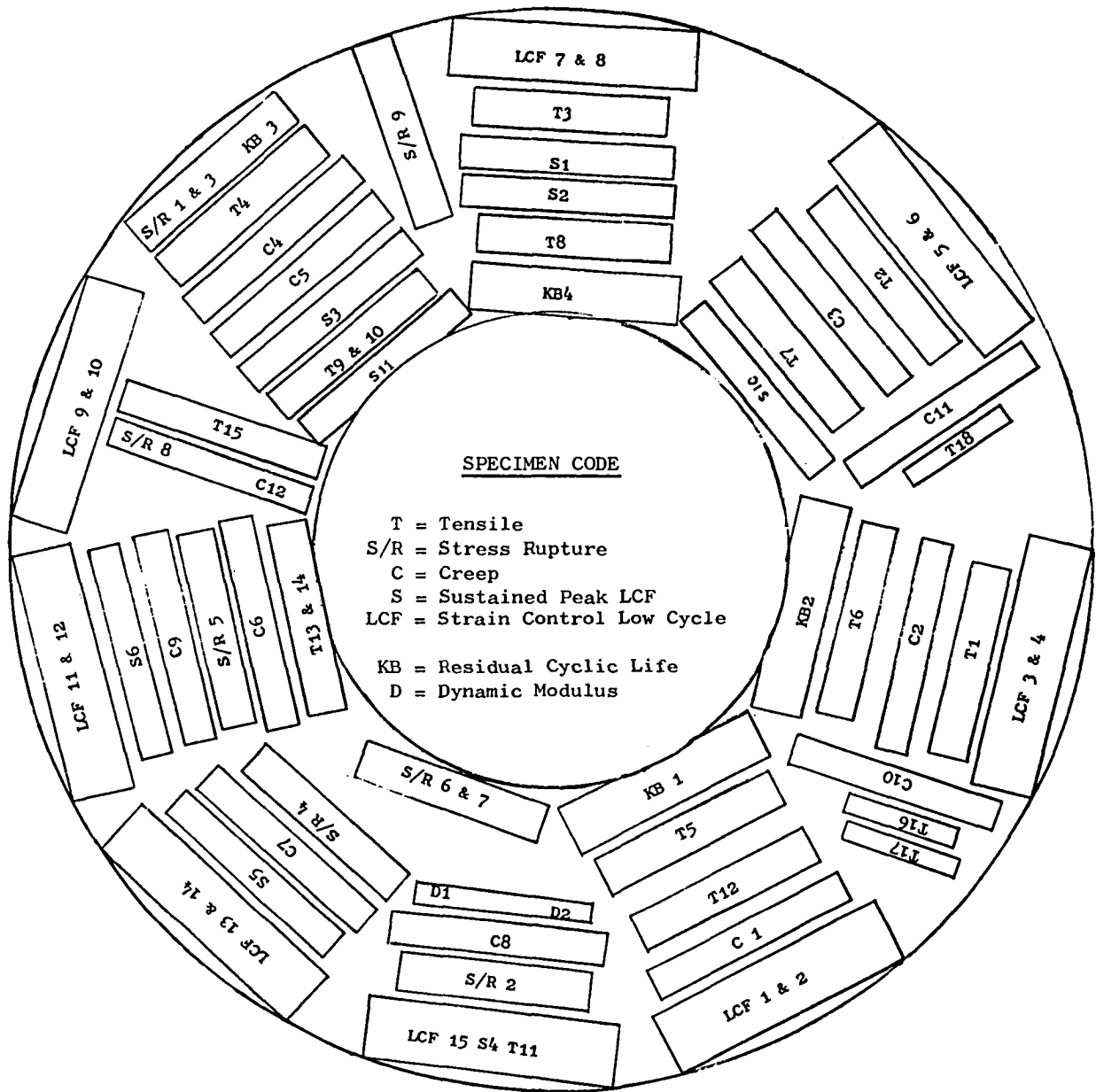


Figure 4-25. PM Rene' 95 HIP Plus Forge Compressor Stage 5-9 Disk (S/N MZS 27673) Forging Schematic Cutup Plan.

Table 4-17. Hot Die Forged PM René 95 Tensile Data.

Forging Serial No.	Test Temp.	Location	Orientation	Specimen	0.2% YS		UTS		El (%)	RA (%)
					MPa	(ksi)	MPa	(ksi)		
DDA 4	RT	Bore/Web	0-Tang	011TR	1311	(190.1)	1678	(243.4)	11	14
DDA 4	RT	Bore/Web	180-Tang	021TR	1312	(190.3)	1718	(249.2)	14	14
DDA 4	RT	Bore/Web	0-Tang	031	1318	(191.2)	1692	(245.4)	13	16
DDA 4	RT	Bore/Web	180-Tang	041	1301	(188.7)	1678	(243.4)	12	15
FWA67*	RT	Bore/Web	0-Tang	011TR	1296	(188.0)	1719	(249.3)	12	14
FWA67*	RT	Bore/Web	180-Tang	021TR	1313	(190.5)	1739	(252.2)	13	16
FWA67*	RT	Bore/Web	0-Tang	031	1309	(189.8)	1728	(250.7)	14	17
FWA67*	RT	Bore/Web	180-Tang	041	1291	(187.2)	1727	(250.5)	17	17
FAH86**	RT	Bore/Web	0-Tang	011TR	1333	(193.4)	1744	(252.9)	17	17
FAH86**	RT	Bore/Web	180-Tang	021TR	1329	(192.8)	1751	(253.9)	18	20
FAH86**	RT	Bore/Web	0-Tang	031	1293	(187.6)	1704	(247.2)	17	17
FAH86**	RT	Bore/Web	180-Tang	041	1306	(189.4)	1689	(244.9)	13	13
Average					1309	(189.9)	1714	(248.6)	14.1	15.7
DDA 4	RT	Bore/Web	0-Radial	072	1284	(186.3)	1633	(236.8)	10	13
DDA 4	RT	Bore/Web	180-Radial	082	1291	(187.3)	1713	(248.4)	16	18
FWA67	RT	Bore/Web	0-Radial	072	1300	(188.5)	1745	(253.1)	17	16
FWA67	RT	Bore/Web	180-Radial	082	1315	(190.7)	1748	(253.5)	19	20
FAH86	RT	Bore/Web	0-Radial	072	1288	(186.8)	1717	(249.0)	18	19
FAH86	RT	Bore/Web	180-Radial	082	1309	(189.8)	1740	(252.3)	19	21
Average					2394	(188.2)	1716	(248.9)	16.1	17.6
Room Temperature Bore/Web Average					1304	(189.1)	1715	(248.7)	15.1	16.6
Room Temperature Requirement Bore/Web					1207	(175.0)	1544	(224.0)	10	12

*FWA 67 = MZS 27657

**FAH 86 = MZS 27676

Table 4-17. Hot Die Forged PM René 95 Tensile Data (Continued)

Forging Serial No.	Test Temp.	Location	Orientation	Specimen	0.2% YS		UTS		E1 (%)	RA (%)
					MPa	(ksi)	MPa	(ksi)		
DDA 4	RT	Rim	0-Tang	051	1276	(185.1)	1611	(233.6)	10	13
DDA 4	RT	Rim	180-Tang	061	1243	(180.3)	1666	(241.6)	14	18
FWA 67	RT	Rim	0-Tang	051	1247	(180.9)	1694	(245.8)	18	19
FWA 67	RT	Rim	180-Tang	061	1222	(177.3)	1594	(231.2)	11	14
FAH 86	RT	Rim	0-Tang	051	1263	(183.2)	1696	(246.0)	17	17
FAH 86	RT	Rim	180-Tang	061	1249	(181.1)	1664	(241.3)	16	16
Average					1250	(181.3)	1654	(239.9)	14.0	16.0
DDA 4	RT	Rim	0-Radial	092	1293	(187.5)	1680	(243.7)	12	15
DDA 4	RT	Rim	180-Radial	102	1287	(186.7)	1564	(226.8)	8	12
DDA 4	RT	Rim	180-Radial	102A-RT	1271	(184.3)	1696	(246.0)	18	17
DDA 4	RT	Rim	180-Radial	102B-RT	1283	(186.1)	1703	(247.0)	18	18
FWA 67	RT	Rim	0-Radial	092	1300	(188.5)	1745	(253.1)	17	16
FWA 67	RT	Rim	180-Radial	102	1278	(185.3)	1713	(248.4)	20	21
FAH 86	RT	Rim	0-Radial	092	1267	(183.8)	1691	(245.3)	18	18
FAH 86	RT	Rim	180-Radial	102	1284	(186.2)	1678	(243.3)	14	16
Average					1283	(186.1)	1684	(244.2)	15.1	16.4
DDA 4	RT	Rim	0-Axial	113	1269	(184.1)	1627	(236.0)	11	15
DDA 4	RT	Rim	180-Axial	123	1258	(182.5)	1689	(245.0)	15	17
FWA 67	RT	Rim	0-Axial	113	1265	(183.4)	1689	(244.9)	16	17
FWA 67	RT	Rim	180-Axial	123	1259	(182.6)	1695	(245.8)	17	18
FAH 86	RT	Rim	0-Axial	113	1265	(183.5)	1731	(251.1)	14	17
FAH 86	RT	Rim	180-Axial	123	1284	(186.2)	1744	(253.0)	14	20
Average					1267	(183.7)	1696	(246.0)	14.4	17.3
Room Temperature All Rim Average					1266	(183.7)	1678	(243.4)	14.5	16.6
Room Temperature Requirement - Rim Tang-Radial					1179	(171.0)	1524	(221.0)	10	12
-Axial					1172	(170.0)	1310	(190.0)	2	5

Table 4-17. Hot Die Forged PM René 95 Tensile Data. (Continued)

Forging Serial No.	Test Temp.		Location	Orientation	Specimen	0.2% YS		UTS		El (%)	RA (%)
	(°C)	(°F)				MPa	(ksi)	MPa	(ksi)		
MZS27673	204	(400)	Web	Tang	T1	1202	(174.3)	1660	(240.8)	16.9	15.0
MZS27673	204	(400)	Web	Tang	T2	1223	(177.4)	1606	(233.0)	12.0	10.1
MZS27673	204	(400)	Web	Tang	T3	1217	(176.5)	1660	(240.8)	15.4	18.2
MZS27673	204	(400)	Bore	Tang	T10	1212	(175.8)	1619	(234.8)	13.5	15.7
MZS27673	204	(400)	Web	Radial	T16	1220	(176.9)	1646	(238.7)	13.6	12.1
MZS27673	204	(400)	Rim	Tang	T11	1213	(175.9)	1659	(240.6)	16.2	19.0
					Average	1214	(176.1)	1642	(238.2)	14.5	14.7
MZS27673	427	(800)		ng	T4	1194	(173.2)	1617	(234.6)	17.2	15.8
MZS27673	427	(800)	Web	Tang	T5	1162	(168.6)	1584	(229.7)	17.0	16.4
MZS27673	427	(800)	Web	Tang	T6	1198	(173.8)	1619	(234.8)	19.2	16.4
MZS27673	427	(800)	Bore	Tang	T13	1207	(175.0)	1625	(235.7)	16.5	19.0
MZS27673	427	(800)	Web	Radial	T15	1217	(176.9)	1619	(234.8)	16.4	18.6
MZS27673	427	(800)	Web/Rim	Radial	T17	1155	(167.5)	1589	(230.4)	16.6	17.2
					Average	1189	(172.5)	1608	(233.3)	17.1	17.2
MZS27673	538	(1000)	Web	Tang	T7	1162,	(168.5)	1605	(232.8)	16.3	17.5
MZS27673	538	(1000)	Web	Tang	T8	1158	(167.9)	1595	(231.3)	16.3	19.4
MZS27673	538	(1000)	Web	Tang	T12	1180	(171.2)	1626	(235.8)	17.2	18.2
MZS27673	538	(1000)	Bore	Tang	T9	1176	(170.6)	1612	(233.8)	16.7	16.8
MZS27673	538	(1000)	Bore	Tang	T14	1171	(169.9)	1615	(234.3)	16.5	19.7
MZS27673	538	(1000)	Web	Radial	T18	1179	(171.0)	1602	(232.3)	15.0	18.5
					Average	1171	(169.9)	1609	(233.4)	16.3	18.3

Table 4-17. Hot Die Forged PM René 95 Tensile Data (Continued).

Forging Serial No.	Test Temp.		Location	Orientation	Specimen	0.2% YS		UTS		E1 (%)	RA (%)
	(°C)	(°F)				MPa	(ksi)	MPa	(ksi)		
DDA 4	649	(1200)	Bore/Web	0-Tang	131TR	1217	(176.5)	1560	(226.3)	14	19
DDA 4	649	(1200)	Bore/Web	180-Tang	141TR	1209	(175.4)	1558	(226.9)	15	18
DDA 4	649	(1200)	Bore/Web	0-Tang	151	1189	(172.4)	1527	(221.5)	16	19
DDA 4	649	(1200)	Bore/Web	180-Tang	161	1174	(170.3)	1521	(220.6)	16	21
FWA 67	649	(1200)	Bore/Web	0-Tang	131TR	1218	(176.6)	1500	(217.6)	14	16
FWA 67	649	(1200)	Bore/Web	180-Tang	141TR	1205	(174.7)	1502	(217.8)	13	14
FWA 67	649	(1200)	Bore/Web	0-Tang	151	1189	(172.4)	1503	(218.0)	17	19
FWA 67	649	(1200)	Bore/Web	180-Tang	161	1185	(171.8)	1427	(207.0)	15	18
FAH 86	649	(1200)	Bore/Web	0-Tang	131TR	1224	(177.6)	1533	(222.4)	12	13
FAH 86	649	(1200)	Bore/Web	180-Tang	141TR	1223	(177.4)	1534	(222.5)	9	12
FAH 86	649	(1200)	Bore/Web	0-Tang	151	1169	(169.5)	1492	(216.4)	15	20
FAH 86	649	(1200)	Bore/Web	180-Tang	161	1183	(171.6)	1534	(222.5)	13	17
Average						1199	(173.9)	1516	(219.9)	13.9	16.9
DDA 4	649	(1200)	Bore/Web	0-Radial	192	1189	(172.4)	1543	(223.8)	14	17
DDA 4	649	(1200)	Bore/Web	180-Radial	202	1199	(173.9)	1545	(224.1)	16	20
FWA 67	649	(1200)	Bore/Web	0-Radial	192	1206	(174.9)	1507	(218.5)	13	16
FWA 67	649	(1200)	Bore/Web	180-Radial	202	1233	(178.8)	1521	(220.6)	13	15
FAH 86	649	(1200)	Bore/Web	0-Radial	192	1191	(172.7)	1524	(221.1)	14	15
FAH 86	649	(1200)	Bore/Web	180-Radial	202	1209	(175.3)	1524	(221.1)	11	13
Average						1205	(174.7)	1527	(221.5)	13.4	15.9
649° C (1200° F) All Bore/Web Average						1202	(174.3)	1522	(220.7)	13.6	16.4
649° C (1200° F) Requirement Bore/Web Tang & Radial						1117	(162.0)	1427	(207.0)	8	10

Table 4-17. Hot Die Forged PM René 95 Tensile Data (Concluded).

Forging Serial No.	Test Temp.		Location	Orientation	Specimen	0.2% YS		UTS		El (%)	RA (%)
	(°C)	(°F)				MPa	(ksi)	MPa	(ksi)		
DDA 4	649	(1200)	Rim	0-Tang	171	1189	(172.4)	1558	(225.9)	14	16
DDA 4	649	(1200)	Rim	180-Tang	181	1180	(171.2)	1555	(225.6)	12	13
FWA 67	649	(1200)	Rim	0-Tang	171	1136	(164.8)	1511	(219.2)	19	24
FWA 67	649	(1200)	Rim	180-Tang	181	1159	(172.5)	1507	(218.6)	19	20
FAH 86	649	(1200)	Rim	0-Tang	171	1151	(166.9)	1511	(219.1)	12	12
FAH 86	649	(1200)	Rim	180-Tang	181	1218	(176.6)	1511	(219.1)	14	16
Average						1177	(170.7)	1526	(221.3)	14.7	16.4
DDA 4	649	(1200)	Rim	0-Radial	212	1193	(173.0)	1565	(227.0)	14	16
DDA 4	649	(1200)	Rim	180-Radial	222	1185	(171.9)	1509	(218.8)	15	19
FWA 67	649	(1200)	Rim	0-Radial	212	1215	(176.5)	1510	(219.0)	15	16
FWA 67	649	(1200)	Rim	180-Radial	222	1193	(173.0)	1488	(215.8)	17	23
FAH 86	649	(1200)	Rim	0-Radial	212	1186	(172.0)	1518	(220.2)	13	19
FAH 86	649	(1200)	Rim	180-Radial	222	1191	(172.7)	1511	(219.2)	10	14
Average						1194	(173.2)	1517	(220.0)	13.8	17.6
DDA 4	649	(1200)	Rim	0-Axial	233	1198	(173.7)	1530	(221.9)	15	16
DDA 4	649	(1200)	Rim	180-Axial	243	1172	(170.0)	1544	(223.9)	16	20
FWA 67	649	(1200)	Rim	0-Axial	233	1166	(169.1)	1548	(224.5)	18	23
FWA 67	649	(1200)	Rim	180-Axial	243	1194	(173.2)	1559	(226.1)	16	21
FAH 86	649	(1200)	Rim	0-Axial	233	1196	(173.5)	1504	(218.2)	11	11
FAH 86	649	(1200)	Rim	180-Axial	243	1176	(170.5)	1505	(218.3)	12	13
Average						1184	(171.7)	1532	(222.2)	14.5	16.8
649° C (1200° F) All Rim Average						1185	(171.9)	1525	(221.2)	14.3	16.9
649° C (1200° F) Requirement Rim - Tang & Radial						1089	(158.0)	1407	(204.0)	8	10
Rim - Axial						1069	(155.0)	1241	(180.0)	2	5

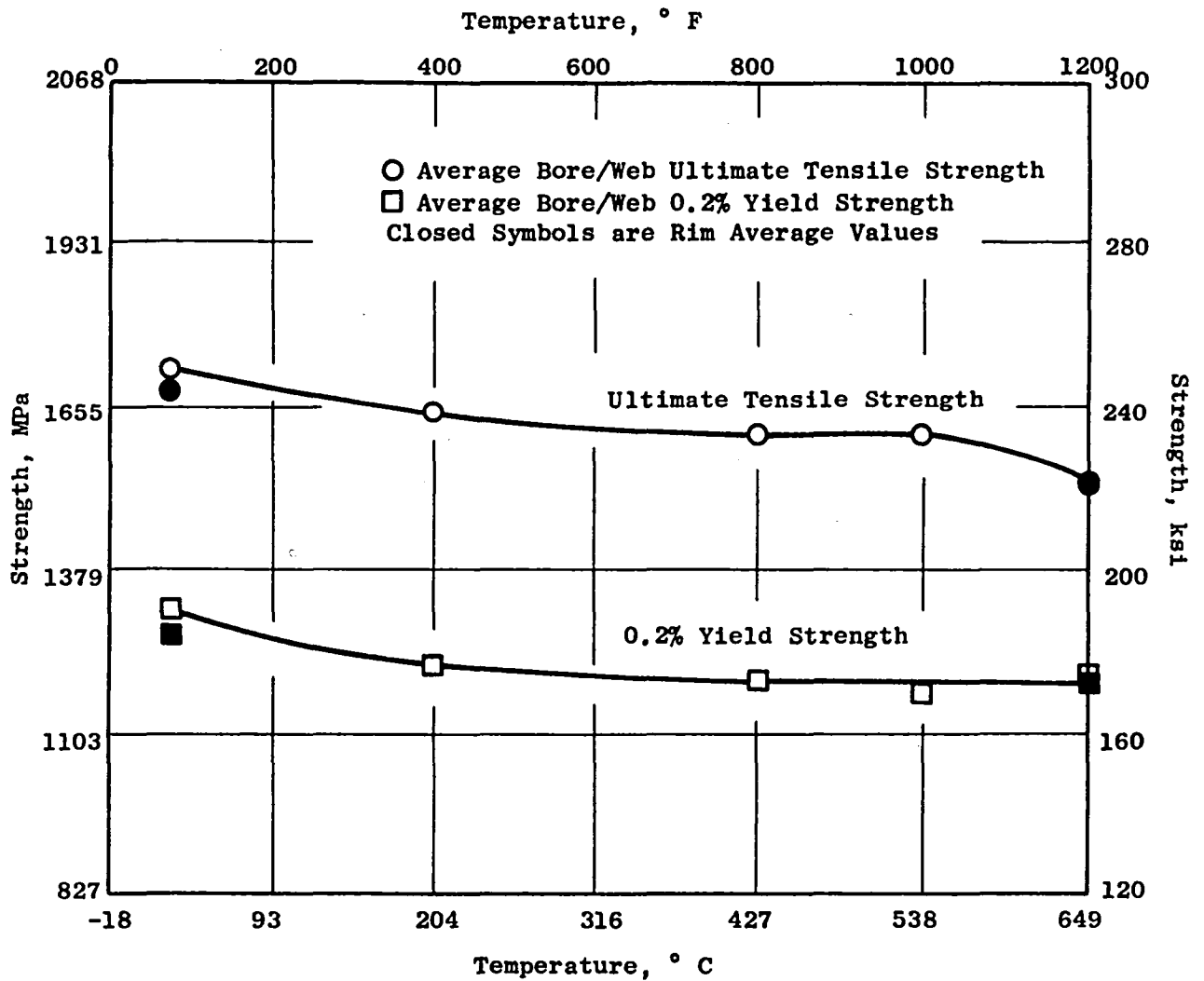


Figure 4-26. PM Rene' 95 HIP Plus Forge Average Tensile Data Strength Values.

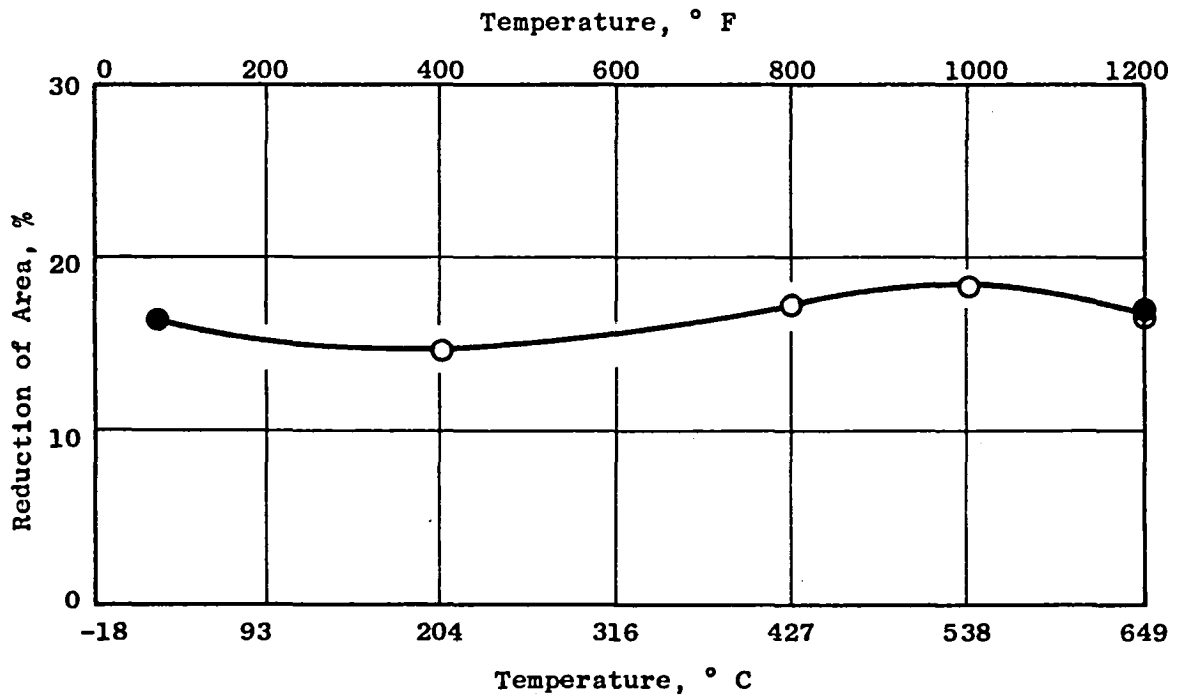
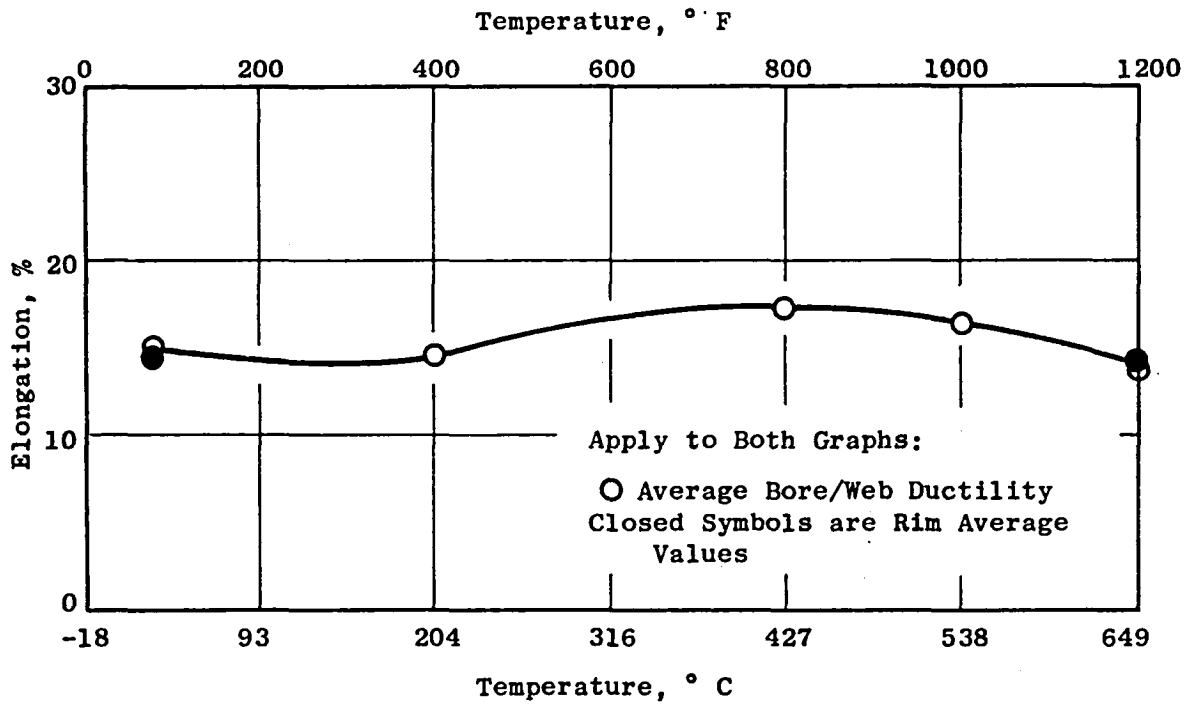


Figure 4-27. PM Rene' 95 HIP Plus Forge Average Tensile Ductility Values.

Table 4-18. Hot Die Forged PM René 95 Stress Rupture Data at 649° C/1034 MPa (1200° F/150 ksi).

<u>Forging</u>	<u>Location</u>	<u>Orientation</u>	<u>Specimen</u>	<u>Life (Hrs)</u>	<u>El (%)</u>
DDA 4	Bore/Web	0-Tang	251TR	132.0	4
DDA 4	Bore/Web	180-Tang	261TR	123.5	3
DDA 4	Bore/Web	0-Tang	271	85.8	5
DDA 4	Bore/Web	180-Tang	281	92.1	6
FWA 67	Bore/Web	0-Tang	251TR	137.6	4
FWA 67	Bore/Web	180-Tang	261TR	101.5	4
FWA 67	Bore/Web	0-Tang	271	130.0	9
FWA 67	Bore/Web	180-Tang	281	95.5	8
FAH 86	Bore/Web	0-Tang	251TR	72.0	4
FAH 86	Bore/Web	180-Tang	261TR	76.6	3
FAH 86	Bore/Web	0-Tang	271	77.4	5
FAH 86	Bore/Web	180-Tang	281	71.9	4
DDA 4	Bore/Web	0-Radial	312	79.0	4
DDA 4	Bore/Web	180-Radial	322	105.9	6
FWA 67	Bore/Web	0-Radial	312	137.6	7
FWA 67	Bore/Web	180-Radial	322	126.1	6
FHA 86	Bore/Web	0-Radial	312	78.4	6
FHA 86	Bore/Web	180-Radial	322	78.6	6
			Average	97.3	5.0
DDA 4	Rim	0-Tang	291	131.3	6
DDA 4	Rim	180-Tang	301	111.6	5
FWA 67	Rim	0-Tang	291	68.4	2
FWA 67	Rim	180-Tang	301	113.4	11
FHA 86	Rim	0-Tang	291	117.9	7
FHA 86	Rim	180-Tang	301	137.8	7
DDA 4	Rim	0-Radial	332	100.5	4
DDA 4	Rim	180-Radial	342	94.0	6
FWA 67	Rim	0-Radial	332	110.3	6
FWA 67	Rim	180-Radial	342	150.9	8
FAH 86	Rim	0-Radial	332	128.8	6
FAH 86	Rim	180-Radial	342	140.6	7
			Average	114.8	5.8
	Requirement			>25	>2.0

Table 4-19. Hot Die Forged PM René 95 Stress Rupture Data.

Specimen	Location/Orientation	Test Conditions				Test Results		LM Parameter C = 25	Notes
		Temp. °C	Temp. (°F)	Stress, MPa	Stress, (ksi)	Life (Hrs)	El (%)		
SR1	Bore-Tangential	538	(1000)	1519	(220)	FOL	13.2	<33.6	Removed
SR5	Web-Tangential	538	(1000)	1413	(205)	94.9	11.2	39.4	
SR8	Web-Radial	538	(1000)	1338	(194)	336.9	5.6	40.2	
SR3	Bore-Tangential	593	(1100)	1276	(185)	48.8	2.7	41.6	
SR2	Web-Tangential	593	(1100)	1117	(162)	2349.5	1.1	>44.3	
**	30 Tests AVE. -2 σ	649	(1200)	1034	(150)	104.0	5.3	44.9	
	AVE. -2 σ	649	(1200)	1034	(150)	64.1	2.6	44.5	
C8*	Web-Tangential	649	(1200)	882	(128)	968.7	4.4	46.4	
SR6	Bore-Tangential	704	(1300)	793	(115)	72.9	5.5	47.3	
SR9	Web-Radial	704	(1300)	690	(100)	237.3	7.6	48.2	
SR7	Bore-Tangential	704	(1300)	552	(80)	625.8	5.0	48.9	

*NOTE: Specimen SR4 loaded at 593° C/910.1 MPa (11000° F/132 ksi) rather than 649° C/910.1 MPa (1200° F/132 ksi) and was discontinued since estimated time to rupture was 36,000 hrs. Specimen SR4 was replaced by C8 (spare) which was run at 649° C/882.5 MPa (1200° F/128 ksi).

** Data from Table 4-18 (page 255)

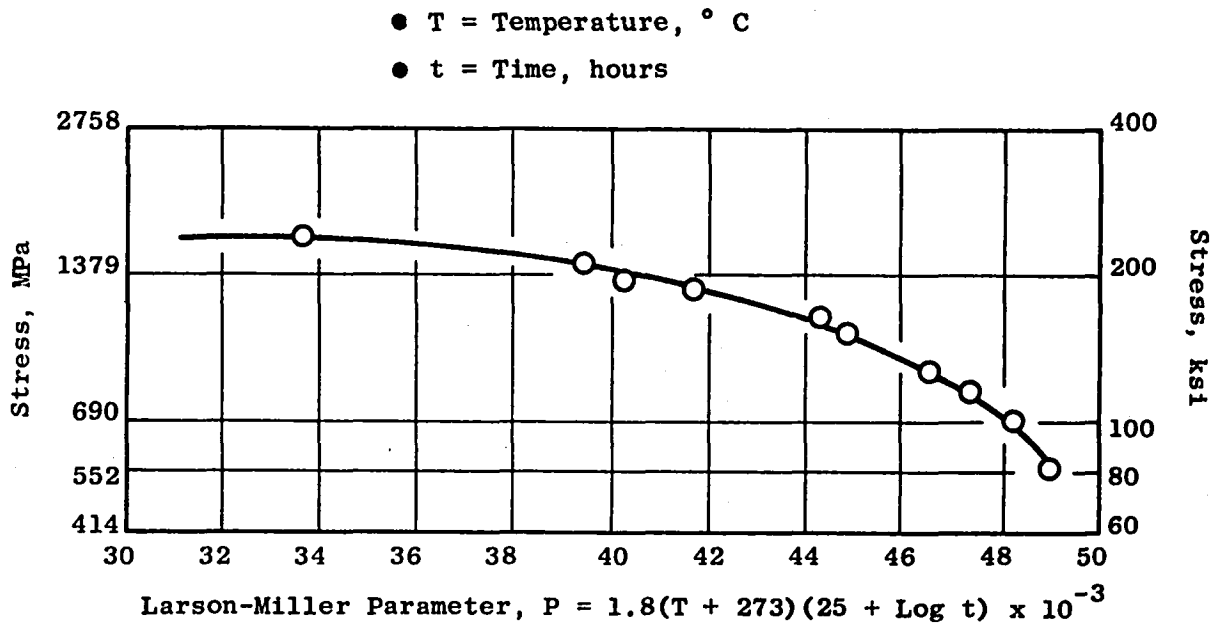


Figure 4-28. PM Rene' 95 HIP Plus Forge Stress Rupture Data.

Table 4-20. Hot Die Forged PM René 95 Creep Data At
593° C/1034 MPa (1100° F/150 ksi)

<u>Forging</u>	<u>Location</u>	<u>Orientation</u>	<u>Specimen</u>	<u>Duration (Hrs)</u>	<u>% Plastic Elongation</u>
DDA 4	Bore/Web	0-Tang	351	100	0.099
DDA 4	Bore/Web	180-Tang	361	100	0.13
FWA 67	Bore/Web	0-Tang	351	100	0.11
FWA 67	Bore/Web	180-Tang	361	100	0.13
FAH 86	Bore/Web	0-Tang	351	100	0.10
FAH 86	Bore/Web	180-Tang	361	100	0.07
Average					0.105 ± 0.023 (1σ)
DDA 4	Rim	0-Tang	371	100	0.13
DDA 4	Rim	180-Tang	381	100	0.07
FWA 67	Rim	0-Tang	371	100	0.06
FWA 67	Rim	180-Tang	381	100	0.06
FAH 86	Rim	0-Tang	371	100	0.13
FAH 86	Rim	180-Tang	381	100	0.13
Average					0.097 ± 0.037 (1σ)

Table 4-21. Hot Die Forged PM René 95 Creep Data.

Specimen	Location/Orientation	Test Conditions		Plastic Extension On Loading (%)	Time and LMP (C=25) For Plastic Deformation of:								Minimum Creep Rate (In./In./Hr)	Removal Conditions			
		Temp. (°C)	Temp. (°F)		Stress (MPa)	Stress (ksi)	0.05%		0.10%		0.20%			0.50%		Time (Hrs)	Elong. (%)
C1	Web-Tangential	538	(1000)	1241.0	(180)	0.35	POL*	-	POL	-	POL	<36.5	230	40.0	1.61x10 ⁻⁶	649	0.94
C10	Web-Radial	538	(1000)	1137.6	(165)	0.07	POL	-	20	38.4	E8830	42.3	-	-	1.10x10 ⁻⁷	920	0.11
Ladish	12 Tests	593	(1100)	1034.2	(150)	0.00	-	-	100	42.2	-	-	-	-	6.67x10 ⁻⁶	~100	0.10
C7	Web-Tangential	593	(1100)	965.3	(140)	0.00	750	43.5	E1750**	44.1	E4000+	44.6+	-	-	4.6 x10 ⁻⁷	979	Undetectable
C2	Web-Tangential	649	(1200)	792.9	(115)	0.00	225	45.4	555	46.0	E1215	46.6	-	-	1.80x10 ⁻⁶	865	0.15
C11	Web-Radial	649	(1200)	792.9	(115)	0.00	5	42.7	60	44.4	233	45.4	E745	46.3	5.71x10 ⁻⁶	339	0.27
C9	Web-Tangential	649	(1200)	620.5	(90)	0.00	8	43.0	60	44.4	360	45.8	E1970	46.9	1.89x10 ⁻⁶	528	0.23
C5	Web-Tangential	649	(1200)	565.4	(82)	0.00	20	43.7	75	44.6	E700	46.2	E1950	47.3	1.33x10 ⁻⁶	626	0.19
C3	Web-Tangential	704	(1300)	455.0	(66)	0.00	15	46.1	50	47.0	132	47.8	448	48.8	8.33x10 ⁻⁶	496	0.54
C12	Web-Radial	704	(1300)	344.7	(50)	0.00	30	46.6	190	48.0	E510	48.8	E1445	49.6	3.17x10 ⁻⁶	361	0.15
C6	Web-Tangential	704	(1300)	275.8	(40)	0.00	330	48.5	760	49.1	1575	49.6	-	-	1.23x10 ⁻⁶	1680	0.21

*POL = occurred during plastic extension on loading.
 **E = extrapolated time based on linearly graphed minimum creep rate.

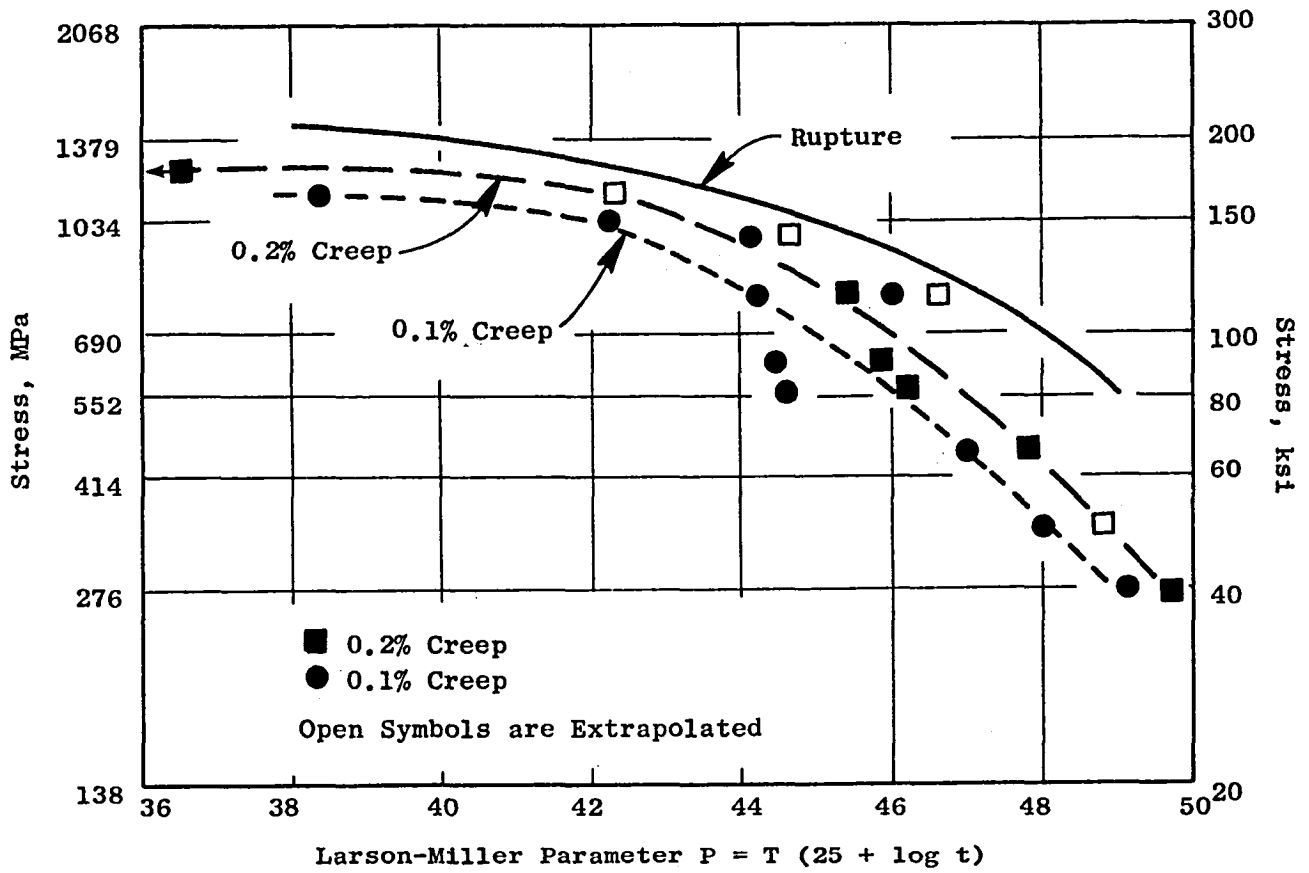


Figure 4-29. PM Rene '95 HIP Plus Forge Creep Data.

Cyclic Rupture Data

Notched ($K_t=2$) cyclic rupture data at 649° C (1200° F) $R=0$ ($A=1$) and 999.7 MPa (145 ksi) maximum stress are shown in Table 4-22. All of these tests met the 300 cycle minimum requirements, although the specimens for the DDA4 forging failed in the threaded section because of a machining error. That machining problem was corrected on the specimens from the other two forgings which produced an average notched section failure life of 1707 cycles. Cyclic rupture tests on specimens from the MZS27673 forging gave the results shown in Table 4-23. All of the cyclic rupture data are summarized in Figure 4-30. Data scatter to the high life region prevented establishing the average 10,000 cycle life maximum stress, but extrapolation of the data suggests that it is between 935 MPa and 965 MPa (135 and 140 ksi).

Strain Control Low Cycle Fatigue

Strain control low-cycle fatigue testing is reported in Tables 4-24 and 4-25. Table 4-24 gives the results on 6.35 mm (0.25 inch) diameter gage section bars from the three source substantiation forgings. Table 4-25 gives the results on 10.2 mm (0.4 inch) diameter gage section bars from the forging S/N MZS27673. Button head failures in the inertia welded Inco 718 ends were encountered on five of the 15 specimens tested. An attempt was made to complete these tests by machining threads in the Inco 718 shank sections of these bars for retest. The retests were all conducted at 538° C (1000° F) by mistake, whereas only two of the five should have been run at 538° C (1000° F). Specimen LCF 4 which was initially run at 399° C (750° F) gave an additional 1994 cycles at 538° C (1000° F), so its total life is probably greater than 41,105 cycles. Specimens LCF 10 and LCF 6, which were initially run at 538° C (1000° F) gave additional lives of 6065 and 7075, respectively, but LCF 10 failed in the Inco 718 threads. Therefore, the total life for LCF 10 is greater than 44,003 cycles, and the total life for LCF 6 is 77,522 cycles. Specimens LCF 12 and LCF 11, which were initially run at 649° C (1200° F) gave lives of 6062 cycles and 5200 cycles, respectively, when tested at 538° C (1000° F). However, both samples failed in the Inco 718 threads. Since these retests were conducted at a lower temperature, and since both specimens failed in the threads, these retests were not counted in the effective test cycles and the results are considered run-outs at the initial test condition. The strain-control low-cycle fatigue data are plotted as pseudo-stress versus cycles to failure curves in Figure 4-31.

Residual Cyclic Life Data

Residual cyclic life data at 538° C (1000° F) are shown in Table 4-26. Consistent achievement of the >5000 cycle life goal was demonstrated at 690 MPa (100 ksi) maximum stress with the initial 0.51 mm deep x 1.52 mm wide (0.020 inch x 0.060 inch) surface crack. The initial crack size was achieved by high-cycle fatigue loading the bar after producing a 0.13 mm deep x 0.52 mm wide (0.005 inch x 0.020 inch) EDM surface notch. Four residual cyclic life tests were also conducted on the MZS27673 forging at 538° C (1000° F) using stresses to produce failure lives in the range of 1000 to 10,000 cycles. The

Table 4-22. Hot Die Forged PM René 95 Cyclic Rupture Data.

Conditions: Temperature = 649° C (1200 F)
 Stress Ratio = R=0 (A=1.0)
 Max. Stress = 999.7 MPa (145 ksi)
 Load Cycle = 10-90-10 (Seconds)
 90 Seconds Loaded, 10 Seconds Intervals

<u>Forging</u>	<u>Location</u>	<u>Orientation</u>	<u>Specimen</u>	<u>Life (Cycles)</u>
DDA 4	Rim	0-Radial	342	>312*
DDA 4	Rim	180-Radial	402	>776*
FWA 67	Rim	0-Radial	342	1613
FWA 67	Rim	180-Radial	402	1665
FAH 86	Rim	0-Radial	342	1533
FAH 86	Rim	180-Radial	402	2062
			Average**	1707
			Requirement	>300

*Bars failing in threads because of machining error.

**DDA 4 tests not included.

Table 4-23. Hot Die Forged PM René 95 Cyclic Rupture Data

Conditions: Temperature = 649° C (1200° F)
 Stress Ratio = R=0 (A=1.0)
 Load Cycle = 10-90-10 (Seconds)
 90 Seconds Loaded, 10 Seconds Intervals
 Specimen K_t = 2.0
 Forging = MZS27673
 Max. Stress = Varied

<u>Location</u>	<u>Orientation</u>	<u>Specimen</u>	<u>Max. Stress</u>		<u>Life</u>
			MPa	(ksi)	(Cycles)
Rim	Tang	7354	1137.6	(165)	218
Web	Tang	7356	1068.7	(155)	451
Web/Rim	Tang	7353	1068.7	(155)	3060
Web	Tang	7351	999.7	(145)	1370
Web	Tang	7352	999.7	(145)	>30,107
Web	Tang	7355	965.3	(140)	4157

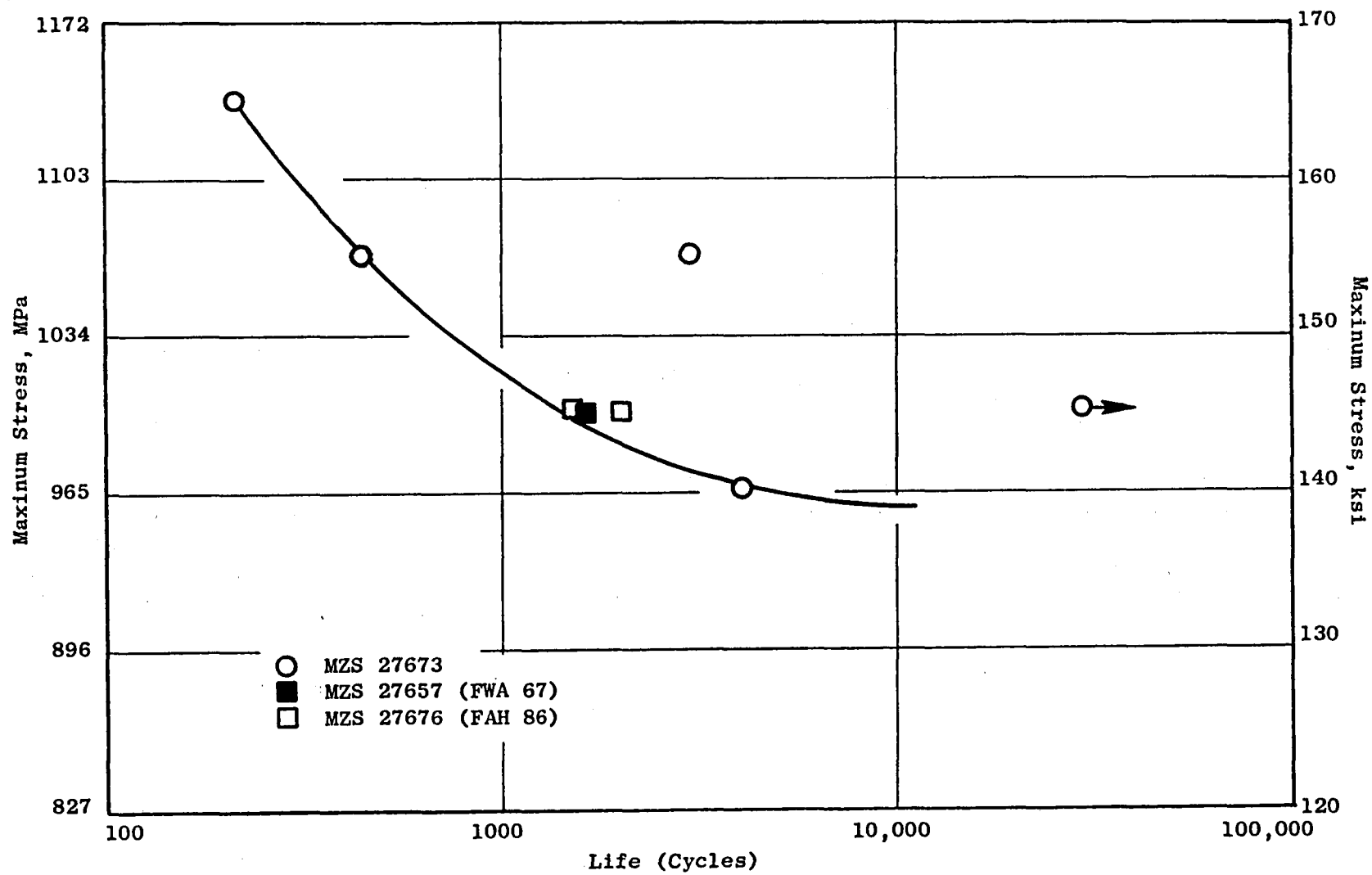


Figure 4-30. PM René 95 HIP Plus Forge Cycle Rupture Data at 649° C (1200° F),
 $A=1$, $K_t=2$, 10-90-10 Seconds.

Table 4-24. Hot Die Forged PM René 95 Strain Control Low Cycle Fatigue Data 6.35 mm (0.25 inch) Diameter, R = 0, (A = 1).

Forging	Specimen No.	Test Temp.		Strain Range (%)	E, TPa (106 psi)	Alternating Pseudo Stress,		Life (Cycles)	
		(°C)	(°F)			MPa	(ksi)	Ni	NF
DDA 4 (MZS--)	431 TR	399	750	0.972	.193 (28.0)	938	136.1	11,139	11,614
DDA 4 (MZS--)	441 Web	538	1000	0.788	.193 (28.0)	760	110.2	39,987	44,476
FAH 86 (MZS27676)	431	399	750	0.889	.200 (29.0)	889	128.9	-	10,739
FAH 86 (MZS27676)	441	538	1000	0.785	.192 (27.9)	774	112.2	-	15,535
FWA 67 (MZS27657)	431	399	750	0.926	.201 (29.2)	932	135.2	-	8,882
FWA 67	441	538	1000	0.786	.201 (29.2)	775	112.4	-	10,959

Table 4-25. Hot Die Forged PM René 95 Strain Control Low Cycle Fatigue Data - 10.16 mm (0.4 inch) Diameter, ($R = 0$, $A_e = 1$).

Forging = MZS27673

Specimen Number	Test Temp.		Strain Range (%)	E , TPa (10^6 psi)	Alternating Pseudo Stress		Life (Cycles)		Failure Initiation Location
	(°C)	(°F)			MPa	(ksi)	N_i	N_f	
LCF 1	399	(750)	1.127	.199 (28.9)	1123	(162.9)	3,600	3,649	Surface
LCF 5	399	(750)	0.901	.206 (29.9)	919	(133.3)	11,020	11,460	Surface
LCF 2	399	(750)	0.782	.198 (28.8)	776	(112.6)	18,700	19,073	Surface
LCF 4	399	(750)	0.708	.199 (28.9)	705	(102.3)	-	>39,111	Button Head Failure, Mach. Thds. & Cont.
	538	(1000*)	0.710	.185 (26.8)	631	(91.6)	-	(+1,994)	
LCF 3	399	(750)	0.621	.195 (28.3)	606	(87.9)	25,920	56,063	Internal
LCF 7	538	(1000)	0.901	.194 (28.2)	876	(127.1)	3,880	4,736	Surface
LCF 8	538	(1000)	0.784	.190 (27.6)	747	(108.3)	13,150	13,233	Surface
LCF 13	538	(1000)	0.722	.191 (27.7)	689	(100.0)	34,850	37,173	Internal
LCF 10	538	(1000)	0.659	.189 (27.4)	622	(90.2)	-	>37,938	Button Head Failure, Mach. Thds. & Cont.
	538	(1000)	0.660	.185 (26.9)	700	(87.0)	-	(+6,065)	Thread Failure
LCF 6	538	(1000)	0.598	.199 (28.9)	596	(86.5)	-	>70,447	Button Head Failure, Mach. Thds. & Cont.
	538	(1000)	0.600	.181 (26.3)	545	(79.0)	(+6,966)	(+7,075)	
LCF 9	649	(1200)	1.060	.181 (26.3)	964	(139.9)	1,879	2,053	Surface
LCF 14	649	(1200)	0.972	.188 (27.2)	911	(132.2)	7,000	7,185	Surface
LCF 15	649	(1200)	0.784	.177 (25.7)	694	(100.7)	22,950	23,165	Internal
LCF 12	649	(1200)	0.612	.177 (25.7)	576	(83.6)	-	>57,452	Button Head Failure, Mach. Thds. & Cont.
	538	(1000*)	0.620	.193 (28.0)	598	(86.8)	-	(+6,062)	Thread Failure
LCF 11	649	(1200)	0.611	.178 (25.8)	544	(78.9)	-	>89,026	Button Head Failure, Mach. Thds. & Cont.
	538	(1000*)	0.620	.184 (26.7)	571	(82.8)	-	(+5,200)	Thread Failure

*Retests improperly run at 538° C (1000° F).

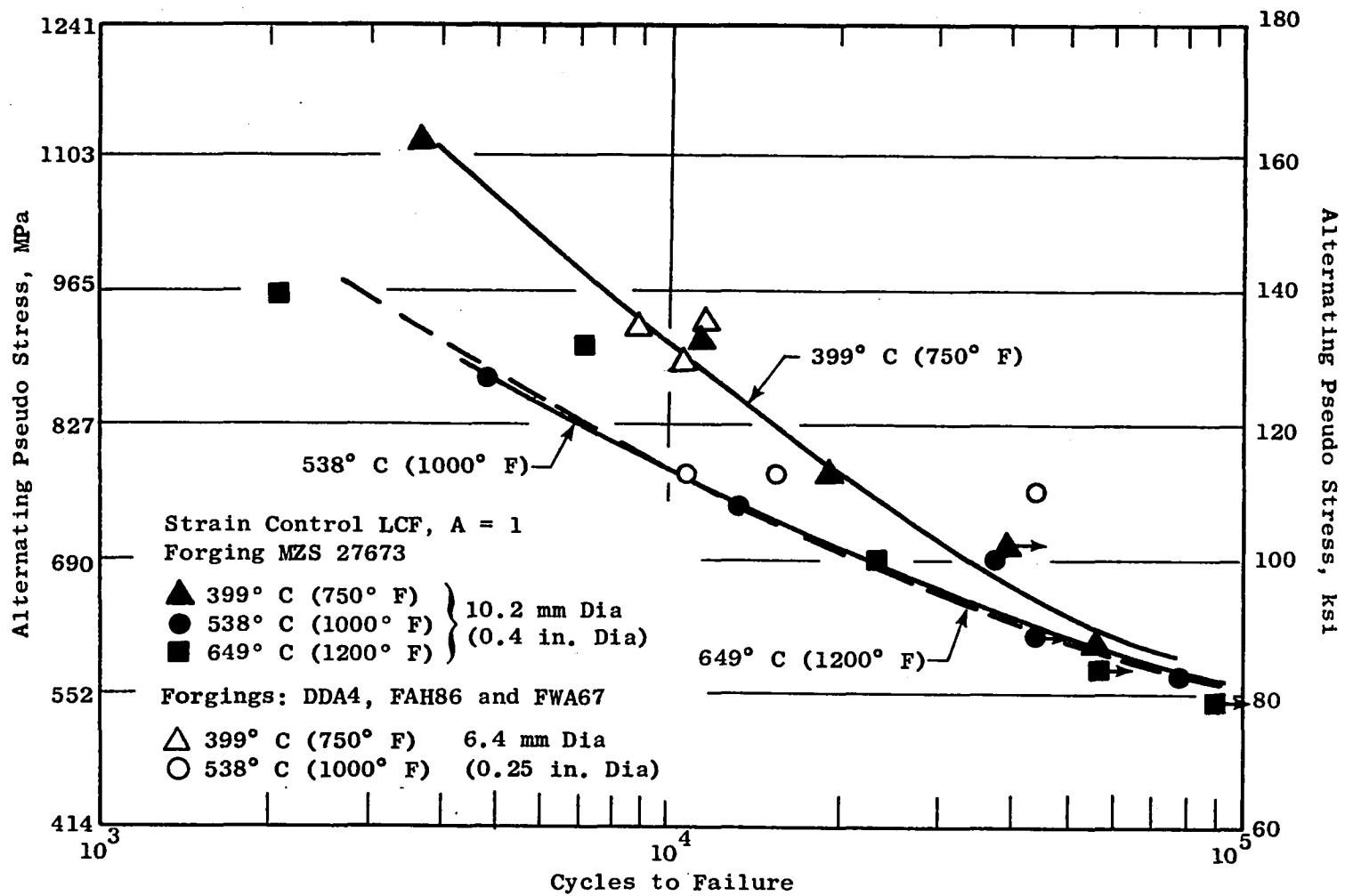


Figure 4-31. Hot Die Forged PM René 95 Strain Control Low Cycle Fatigue at $A_e = 1.0$.

Table 4-26. Hot Die Forged PM René Residual Cyclic Life Data.

Conditions: Temperature = 538° C (1000° F)
 Specimen = Rectangular Cross Section Gage of 15.24 mm (0.6 Inch)
 Width by 6.35 mm (0.25 Inch) Thickness
 Pre-Test Crack = 1.52 mm (0.06 Inch) Surface Width by ~.51 mm (0.02 Inch)
 Depth produced through EDM Slot plus High Cycle Fatigue.
 Crack pendicular to Stress at Center of 15.24 mm (0.6 Inch)
 Gage Width.
 Max. Stress = 689.5 MPa (100 ksi)
 Test = Low Cycle Fatigue at 20 CPM

Forging	Location	Orientation	Specimen	Actual Crack Size, mm (In.)		Life (Cycles)
				Width	Depth	
DDA 4	Bore	0-Tang	411	1.53 (0.0602)	.67 (0.0263)	7144
DDA 4	Bore	180-Tang	421	1.52 (0.0598)	.60 (0.0236)	7428
FWA 67	Bore	0-Tang	411	1.54 (0.0607)	.61 (0.0240)	7469
FWA 67	Bore	180-Tang	421	1.59 (0.0626)	.56 (0.0222)	9829
FAH 86	Bore	0-Tang	411	1.59 (0.0625)	.58 (0.0230)	7837
FAH 86	Bore	180-Tang	421	1.45 (0.0570)	.57 (0.0224)	9207
			Average	1.54 (0.0605)	.60 (0.0236)	8094
			Average - 3σ			5481
			Proposed Requirement	1.52 (0.06)	.51 (0.02)	>5000

results of the four tests on the MZS27673 forging including crack growth rate data are reported in Table 4-27. A graphical presentation of the data for all four forgings is shown in Figure 4-32. The crack growth rate (da/dn) versus stress intensity factor curve for the MZS27673 forging specimens is shown in Figure 4-33.

Dynamic Modulus of Elasticity Data

Two dynamic modulus of elasticity tests were conducted on specimens from the MZS27673 forging. The test results are shown in Table 4-28. The results were consistent and within the scatter band of previous data for cast plus wrought René 95 forging.

Density Data

Density tests were conducted on all the forgings for the HIP + Forge study as reported in Table 4-29. The initial density tests were conducted on end slices of the preform multiple logs for the evaluated forgings. In addition, the same samples were TIP tested with the results shown also in Table 4-29. Density values and TIP tests were conducted on each forging. All of the TIP results were within the specification allowance of <0.3%.

Table 4-27. Hot Die Forged PM René 95 Crack Growth Rate Data from the Residual Cyclic Life (KB) Specimen.

Specimen	Stress MPa (ksi)	Cycles	a, mm (In.)	2c, mm (In.)	K, MPa(M) ^{1/2} (ksi√In.)	Δa/ΔN, m/Cycle (In./Cycles)	Notes
KB2	551 (80)	0	.389 (.0153)	1.013 (.0399)	14.83 (13.5)	2.03 x 10 ⁻⁸ (8.00 x 10 ⁻⁷)	
KB2	551 (80)	54	.554 (.0218)	1.445 (.0569)	17.80 (16.2)	2.29 x 10 ⁻⁸ (9.00 x 10 ⁻⁶)	
KB2	551 (80)	806	.584 (.0230)	1.524 (.0600)	18.24 (16.6)	2.54 x 10 ⁻⁸ (1.00 x 10 ⁻⁶)	
KB2	551 (80)	1524	.584 (.0230)	1.524 (.0600)	18.24 (16.6)	2.64 x 10 ⁻⁸ (1.04 x 10 ⁻⁶)	
KB2	551 (80)	2690	.643 (.0253)	1.679 (.0661)	19.12 (17.4)	3.66 x 10 ⁻⁸ (1.44 x 10 ⁻⁶)	
KB2	551 (80)	4134	.681 (.0268)	1.778 (.0700)	19.78 (18.0)	5.64 x 10 ⁻⁸ (2.22 x 10 ⁻⁶)	
KB2	551 (80)	5553	.739 (.0291)	1.930 (.0760)	20.55 (18.7)	7.04 x 10 ⁻⁸ (2.77 x 10 ⁻⁶)	
KB2	551 (80)	6107	.828 (.0326)	2.162 (.0851)	21.76 (19.8)		(3.33 x 10 ⁻⁶)
KB2	551 (80)	6589	.846 (.0333)	2.207 (.0869)	21.98 (20.0)	8.46 x 10 ⁻⁸ (3.84 x 10 ⁻⁶)	
KB2	551 (80)	7536	.963 (.0379)	2.515 (.0990)	23.52 (21.4)	9.75 x 10 ⁻⁸ (4.54 x 10 ⁻⁶)	
KB2	551 (80)	10007	1.344 (.0529)	3.508 (.1381)	28.02 (25.5)	1.87 x 10 ⁻⁷ (7.35 x 10 ⁻⁶)	
KB2	551 (80)	(11500)	1.778 (.07)	4.041 (.1591)	30.33 (27.6)	3.73 x 10 ⁻⁷ (1.47 x 10 ⁻⁵)	Interpolated Value of a
KB2	551 (80)	(12500)	2.286 (.09)	4.864 (.1915)	33.63 (30.6)	6.35 x 10 ⁻⁷ (2.50 x 10 ⁻⁵)	Interpolated Value of a
KB2	551 (80)	(13500)	3.048 (.12)	6.096 (.2400)	38.36 (34.9)	1.02 x 10 ⁻⁶ (4.00 x 10 ⁻⁵)	Interpolated Value of a
KB2	551 (80)	14653	5.080 (.2000)	11.176 (.4400)	63.41 (57.7)	5.08 x 10 ⁻⁶ (2.00 x 10 ⁻⁴)	Failure at 14653 Cycles
KB1	620 (90)	0	.615 (.0242)	1.473 (.0580)	20.33 (18.5)	7.47 x 10 ⁻⁸ (2.94 x 10 ⁻⁸)	
KB1	620 (90)	313	.698 (.0275)	1.674 (.0659)	21.76 (19.8)	8.18 x 10 ⁻⁸ (3.22 x 10 ⁻⁶)	
KB1	620 (90)	1645	.815 (.0321)	1.956 (.0770)	23.52 (21.4)	1.06 x 10 ⁻⁷ (4.16 x 10 ⁻⁶)	
KB1	620 (90)	2245	.879 (.0346)	2.108 (.0830)	24.40 (22.2)	1.27 x 10 ⁻⁷ (5.00 x 10 ⁻⁶)	
KB1	620 (90)	2783	.952 (.0375)	2.283 (.0890)	25.39 (23.1)	1.41 x 10 ⁻⁷ (5.55 x 10 ⁻⁶)	
KB1	620 (90)	3391	1.039 (.0409)	2.492 (.0981)	26.60 (24.2)	1.64 x 10 ⁻⁷ (6.45 x 10 ⁻⁶)	
KB1	620 (90)	4139	1.196 (.0471)	2.868 (.1129)	28.57 (26.0)	2.31 x 10 ⁻⁷ (9.09 x 10 ⁻⁶)	
KB1	620 (90)	4508	1.313 (.0517)	3.150 (.1240)	30.00 (27.3)	3.18 x 10 ⁻⁷ (1.25 x 10 ⁻⁵)	
KB1	620 (90)	5342	1.755 (.0691)	3.734 (.1470)	32.86 (29.9)	4.22 x 10 ⁻⁷ (1.66 x 10 ⁻⁵)	
KB1	620 (90)	5894	1.890 (.0744)	3.937 (.1550)	33.74 (30.7)	7.06 x 10 ⁻⁷ (2.78 x 10 ⁻⁵)	
KB1	620 (90)	6302	2.377 (.0936)	4.572 (.1800)	36.60 (33.3)	1.02 x 10 ⁻⁶ (4.00 x 10 ⁻⁵)	
KB1	620 (90)	6766	2.977 (.1172)	5.461 (.2150)	40.44 (36.8)	1.27 x 10 ⁻⁶ (5.00 x 10 ⁻⁵)	
KB1	620 (90)	7185	3.729 (.1468)	6.403 (.2521)	44.62 (40.6)	2.36 x 10 ⁻⁶ (9.10 x 10 ⁻⁵)	
KB1	620 (90)	7598	5.055 (.1990)	9.398 (.3700)	60.99 (55.5)	5.08 x 10 ⁻⁶ (2.00 x 10 ⁻⁴)	Failure at 7598 cycles
KB4	758.4 (110)	0	.610 (.0240)	1.499 (.0590)	25.50 (23.2)	1.33 x 10 ⁻⁷ (5.25 x 10 ⁻⁶)	
KB4	758.4 (110)	340	.696 (.0274)	1.676 (.0660)	26.92 (24.5)	1.59 x 10 ⁻⁷ (6.25 x 10 ⁻⁶)	
KB4	758.4 (110)	784	.772 (.0304)	1.829 (.0720)	28.13 (25.6)	1.81 x 10 ⁻⁷ (7.14 x 10 ⁻⁶)	
KB4	758.4 (110)	1360	.843 (.0332)	1.961 (.0772)	29.23 (26.6)	2.12 x 10 ⁻⁷ (8.33 x 10 ⁻⁶)	
KB4	758.4 (110)	(2500)	1.143 (.045)	2.515 (.099)	33.08 (30.1)	5.08 x 10 ⁻⁷ (2.00 x 10 ⁻⁵)	Interpolated value of a
KB4	758.4 (110)	(3250)	1.422 (.056)	3.048 (.120)	36.60 (33.3)	6.35 x 10 ⁻⁷ (2.50 x 10 ⁻⁵)	Interpolated value of a
KB4	758.4 (110)	4997	4.521 (.1780)	8.839 (.3480)	70.88 (64.5)	~1.27 x 10 ⁻⁵ (~5.00 x 10 ⁻⁴)	Failure at 4997 cycles
KB3	965.3 (140)	0	.483 (.0190)	1.422 (.0560)	30.0 (27.3)	1.41 x 10 ⁻⁷ (5.55 x 10 ⁻⁶)	
KB3	965.3 (140)	150	.559 (.0220)	1.626 (.0640)	34.5 (31.4)	1.69 x 10 ⁻⁷ (6.67 x 10 ⁻⁶)	
KB3	965.3 (140)	700	.635 (.0250)	1.829 (.0720)	36.7 (33.4)	2.12 x 10 ⁻⁷ (3.33 x 10 ⁻⁶)	
KB3	965.3 (140)	1200	.665 (.0262)	1.930 (.0760)	38.0 (34.3)	2.82 x 10 ⁻⁷ (1.11 x 10 ⁻⁵)	
KB3	965.3 (140)	1700	.914 (.0360)	2.388 (.0940)	42.3 (38.5)	5.97 x 10 ⁻⁷ (2.35 x 10 ⁻⁵)	
KB3	965.3 (140)	2150	1.346 (.0530)	2.921 (.1150)	47.1 (42.9)	1.02 x 10 ⁻⁶ (4.00 x 10 ⁻⁵)	
KB3	965.3 (140)	2575	1.803 (.0710)	3.658 (.1440)	52.9 (48.1)	1.41 x 10 ⁻⁶ (5.56 x 10 ⁻⁵)	
KB3	965.3 (140)	2825	2.172 (.0855)	4.674 (.1840)	60.7 (55.2)	2.82 x 10 ⁻⁶ (1.11 x 10 ⁻⁴)	
KB3	965.3 (140)	(2900)	2.540 (.1000)	5.385 (.212)	65.8 (59.9)	4.22 x 10 ⁻⁶ (1.66 x 10 ⁻⁴)	Interpolated value of a
KB3	965.3 (140)	2910	3.175 (.1250)	6.147 (.2420)	71.2 (64.8)	1.69 x 10 ⁻⁵ (~6.67 x 10 ⁻⁴)	

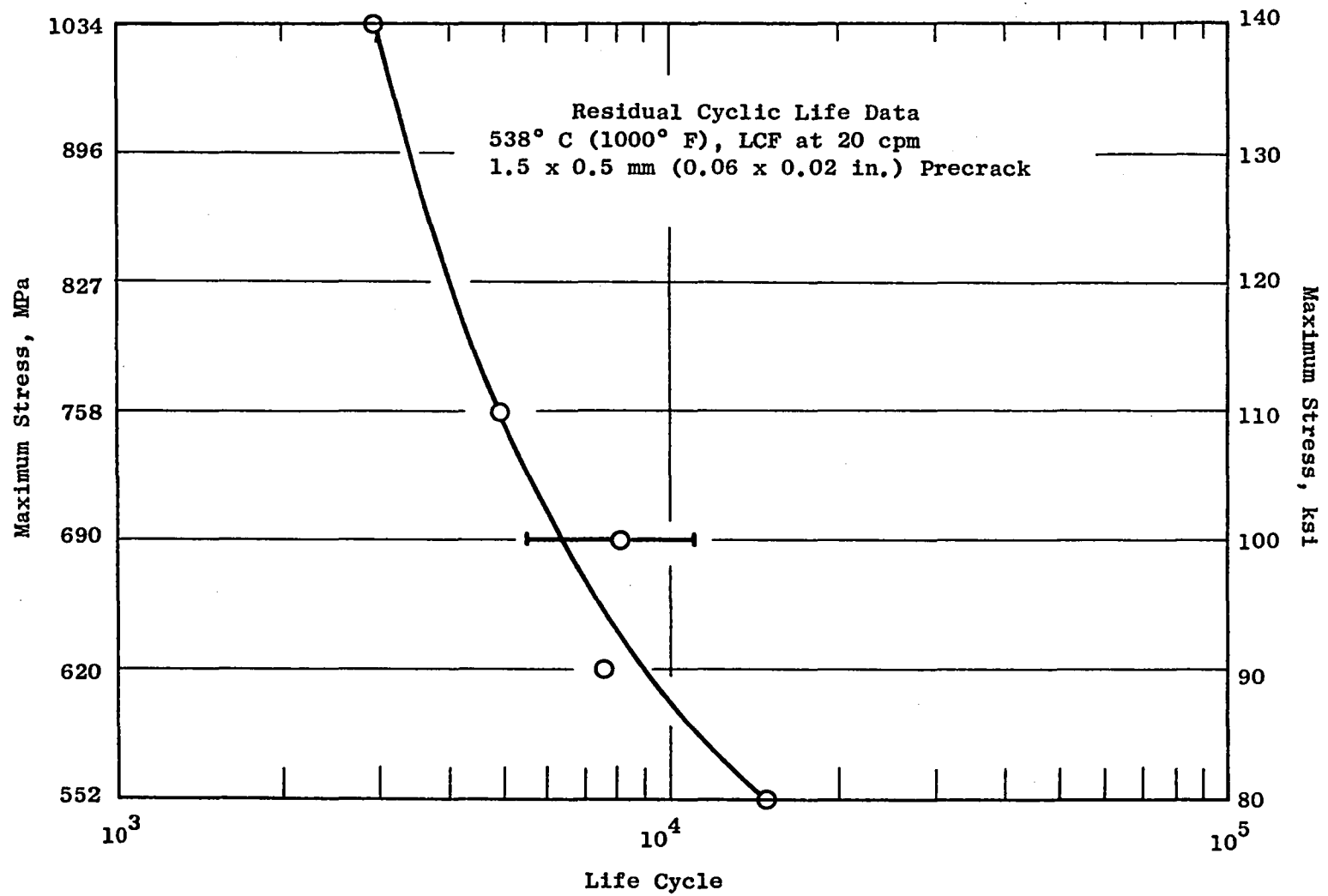


Figure 4-32. Maximum Stress Verses Cycles to Failure for the Residual Cyclic Life Specimens.

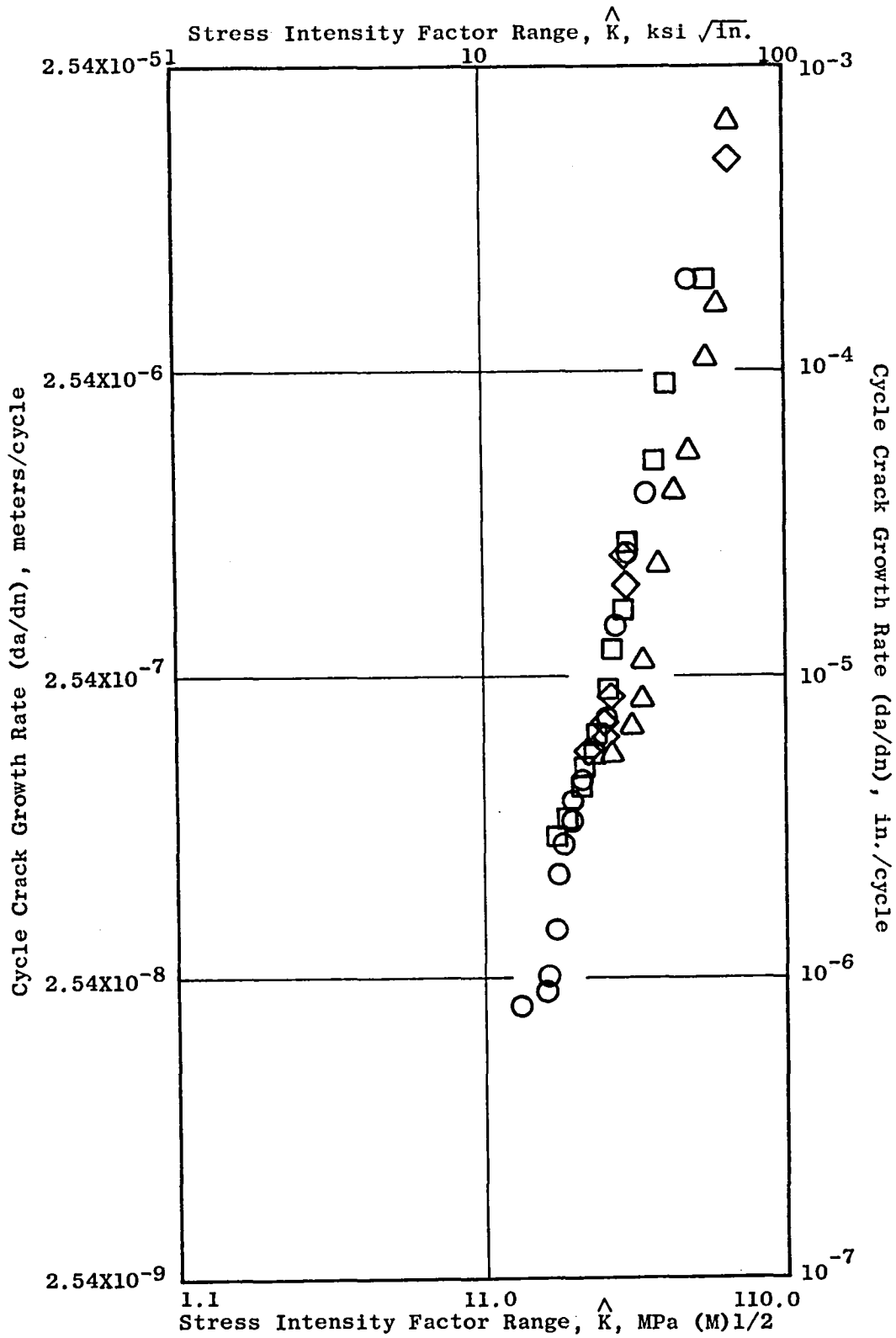


Figure 4-33. Crack Propagation Rate of HIP + Forged René 95, 538° C (1000° F), A = 0.95, 20 Hz.

Table 4-28. Hot Die Forged PM René 95
Dynamic Modulus Data.

Forging = MZS27673

Temperature		Dynamic Modulus, TPa ($\text{psi} \times 10^{-6}$)			
$^{\circ}\text{C}$	($^{\circ}\text{F}$)	73D1		73D2	
24.0	(1500)	.220	(31.98)	.220	(31.99)
151.6	(305)	.214	(30.98)	.214	(31.03)
310.0	(590)	.205	(29.72)	-	-
316.0	(600)	-	-	.206	(29.81)
482.0	(900)	.196	(28.47)	.196	(28.49)
649.0	(1200)	.185	(26.88)	.186	(26.98)
760.0	(1400)	.177	(25.70)	.178	(25.82)
815.0	(1500)	.172	(25.02)	.173	(25.10)

Table 4-29. Hot Die Forged PM René 95 Density Data.

Specimen		Density Values kg/m ³ (lbs/in. ³)				% Density Change (TIP)
		As Processed		After Tip Test*		
<u>Preform Multiple Log Tests</u>						
A7-685 (DDA 4)	Top	8274.5	(0.29872)	8259.3	(0.29817)	-0.184
A7-685 (DDA 4)	Bottom	8275.3	(0.29875)	8257.3	(0.29810)	-0.218
A7-2817 (S/N27657)	Top 0°	8280.3	(0.29893)	8267.6	(0.29845)	-0.161
A7-2817 (S/N27657)	Top 180°	8279.2	(0.29889)	8267.6	(0.29847)	-0.141
A7-2817 (S/N27657)	Bottom 0°	8280.0	(0.29892)	8268.7	(0.29851)	-0.137
A7-2817 (S/N27657)	Bottom 180°	8279.5	(0.29890)	8269.0	(0.29852)	-0.127
A7-3187 (S/N27673) (S/N27676)	Top 0°	8289.7	(0.29927)	8280.3	(0.29893)	-0.114
A7-3187 (S/N27673) (S/N27676)	Top 180°	8291.4	(0.29933)	8277.8	(0.29884)	-0.164
A7-3187 (S/N27673) (S/N27676)	Bottom 0°	8278.9	(0.29888)	8265.6	(0.29840)	-0.161
A7-3187 (S/N27673) (S/N27676)	Bottom 180°	8277.8	(0.29884)	8262.6	(0.29829)	-0.184
<u>Source Substantiation Forging Tests</u>						
DDA 4	571	8271.2	(0.29860)	8257.3	(0.29810)	-0.167
DDA 4	581	8273.1	(0.29867)	8260.4	(0.29821)	-0.154
S/N27657	571	8275.9	(0.29877)	8266.2	(0.29842)	-0.117
S/N27657	581	8275.3	(0.29875)	8265.6	(0.29840)	-0.117
S/N27676	572	8292.0	(0.29935)	8280.9	(0.29895)	-0.134
S/N27676	582	8292.2	(0.29936)	8277.3	(0.29882)	-0.180
<u>S/N27673 Additional Tests</u>						
Bore	0°	8251.5	(0.29789)	8241.8	(0.29754)	-0.117
Bore	180°	8252.9	(0.29794)	8246.8	(0.29772)	-0.074
Rim	0°	8258.2	(0.29813)	8234.6	(0.29728)	-0.285
Rim	180°	8259.3	(0.29817)	8239.6	(0.29746)	-0.238
Specification Allowable						-0.300

*1204° C (2200° F)/4 hour air exposure.

5.0 TASK IV - ENGINE DEMONSTRATION TEST

Two as-HIP HPT aft shafts were finish machined and were installed in a CF6-50 engine for land-based testing. The details of this test are classified as Category 2 FEDD data and will be reported in Volume II of this contract report.

HIP and forge stage 5-9 compressor disks were finish machined, inertia welded into a compressor rotor, and installed in a CFM56 engine for land-based engine testing. The details of this test are classified as Category 2 FEDD data and will be reported in Volume II of this contract report.

6.0 TASK V - POSTTEST ANALYSIS

The results of the posttest analysis of the as-HIP and HIP + Forge components are classified as Category 2 FEDD data. This analysis is to be reported in Volume II of this contract report.

7.0 ANALYSIS OF PROJECT RESULTS AND RECOMMENDATIONS

Analysis of Project Results

The results of the as-HIP processing for the CF6-50 HPT aft shaft are considered very successful. All target mechanical properties were achieved and commercially viable manufacturing processes were established. These processes should be applicable to as-HIP processing of other René 95 alloy engine components.

In comparison to a cast and wrought Inconel 718 alloy shaft, a 50% reduction in input weight was achieved for the as-HIP René 95 shape. In comparison to the same part in René 95 alloy, a 40% cost reduction could be obtained in comparison to cast and wrought material. However, no cost advantage was obtained in comparison to Inconel 718 in terms of 1979 dollars as shown in Figure 7-1. René 95 has undergone a greater inflationary increase in cost than Inconel 718 over the time period since 1974. One of the factors involved here has been the price spiral of cobalt. Since Inconel 718 does not contain cobalt, this has not affected its cost. The increased production volume of Inconel 718 has probably also served to hold down its relative cost. However, as-HIP processing using the techniques established here will have a high payoff when used to replace cast and wrought René 95.

For the HIP + Forge processing of René 95, an input weight reduction of 54% and a cost reduction of 35% (in 1979 dollars) was achieved for the Stage 5 through 9 CFM56/F101 disks. All target specification mechanical properties were achieved for these parts also. Although processing problems were encountered during the course of this project, the processes finally established have been successfully used in producing Stage 5 through 9 compressor disk forgings for the CFM56/F101 engine. HIP + Forged René 95 disks are now bill-of-material for these components on the CFM56/F101 engine.

Final Process Procedures

Appendices E and F present the acceptance criteria, process procedures, and lower limit mechanical properties for the as-HIP and HIP + Forged René 95 components respectively. These criteria and properties are those based on the processing procedures used and mechanical properties obtained during the Task III - Manufacturing phase of this program. For the HIP + Forge part, the properties obtained were essentially the same as those which would be expected for the same part produced by cast + wrought processes. For the as-HIP part, the mechanical property goals for this program were to meet or exceed Inconel 718 properties and the resultant lower limit properties were somewhat lower than for a similar part produced in René 95 by cast + wrought processes. However, as the Task II process development studies indicated, properties more nearly equivalent to cast + wrought or HIP + Forged René 95 could be obtained for as-HIP components by means of variations in HIP temperature and solution heat treat conditions (temperature and/or cooling rate).

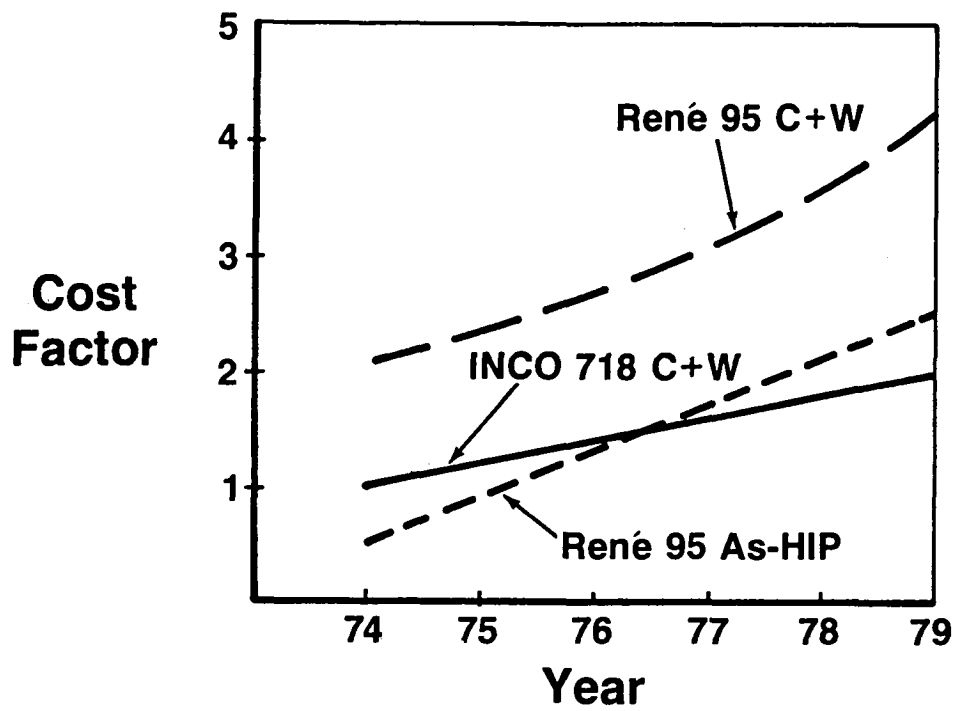


Figure 7-1. Cost Comparisons for As-HIP Rene'95.

Recommendations

Based on the results of this program, and the results of concurrent General Electric experience on René 95, as-HIP, and HIP + Forge components, René 95 components produced by the powder metallurgy processes established during the course of this MATE Project are recommended for producing René 95 components for use in commercial engines. René 95 produced by these techniques is now standard bill of material in the CFM56 and in several other engines now in the development stage.

8.0 CONCLUSIONS

HIP + Hot Die Forge Processes

1. Both the as-HIP and HIP + Hot Die forging processes established during this project have been shown capable of producing René 95 rotating engine hardware with acceptable mechanical properties at significantly reduced cost as compared to cast and wrought René 95. These processes were shown to be capable of implementation directly into the manufacture of commercial engine components.
2. The HIP + Hot Die forging process employed to make the René 95 CFM56/F101 Stage 5-9 compressor disk shape demonstrated the capability for a 54% weight reduction and a 35% cost reduction as compared to parts produced from conventionally cast and wrought René 95.
3. Individual near-net-shape HIP forging preforms were found to be cost effective on a selective basis; however, in the case of the stage 5-9 compressor disks produced in this project, a slice cut from a hollow HIP log was found to be more economical than an individually shaped preform. However, preform shapes can be successfully forged to finished shapes and might reflect a cost advantage for more complex final part configurations.
4. Chemical milling was shown to be a satisfactory surface preparation technique for subsequent hot die forging of HIP preform shapes.
5. Striations in René 95 HIP forging preforms resulting from variations in powder mesh size were found to degrade forgeability in the hot die forging process.
6. An increase in HIP temperature of René 95 forging preforms to 1200° C (2200° F), combined with the proper cooling rate from the HIP temperature, was found to result in improved forgeability.

As-HIP Processes

1. The ceramic mold process used to produce the as-HIP CF6-50 HPT aft shaft demonstrated a 2.5 mm (100 mil) near-net-shape envelope capability which translates to a 50% weight reduction and 40% cost reduction as compared to conventionally cast and wrought René 95 processes.
2. A tolerance of +28° C (+50° F) for HIP and solution heat treat temperatures is satisfactory for as-HIP René 95 powder processing. This is within the range of commercial powder consolidation process capability.
3. Oxide inclusions in as-HIP René 95 powder compacts greater than 0.15 mm (6 mils) in diameter were found to have an adverse effect on mechanical properties. Degradation increased with oxide inclusion size.

4. René 95 particle size distribution variation of -60, -60 + 150, and -150 mesh were found to have no significant effect on the mechanical properties measured during the course of this project.
5. HIP and heat treated surfaces can be satisfactorily prepared for ultrasonic inspection by Harperizing, without conventional machining.
6. Mechanical properties of as-HIP René 95 powder were not affected by an evenly distributed contamination with 0.1% of Astroloy powder (volume %).
7. An evenly distributed 0.1% by volume of M2 tool steel powder particles did reduce rupture life, ductility and fatigue life of as-HIP René 95.
8. Argon entrapment above the 0.3% thermal-induced-porosity level was found to reduce all properties of as-HIP René 95 powder. Degradation increased with the amount of argon and resultant increased porosity level.

9.0 GLOSSARY

Throughout the course of the contract, specialized terminology was used in contract reports as well as abbreviations which are not standard grammatical English. A list of these is presented in this Glossary.

Subcontractors

CarTech	=	The Carpenter Technology Corporation, Reading, Pennsylvania.
Crucible	=	Crucible, Inc., Materials Research Center (Division of Colt Industries) Pittsburgh, Pennsylvania.
Ladish	=	The Ladish Company, Cudahy, Wisconsin.
Udimet	=	Udimet Powder Division of Special Metals Company, Ann Arbor, Michigan.

Technical Terms

René 95	=	A nickel-base superalloy with the nominal composition (in weight percent) 0.08 C, 14.0 Cr, 8.0 Co, 3.5 Al, 2.5 Ti, 3.5 Mo, 3.5 W, 3.5 Nb, 0.010 B, 0.05 Zr.
HIP	=	Hot Isostatic Pressed.
Preform	=	A forging preform made by hot isostatic pressing René 95 powder.
H+F or HIP + Forge	=	A process in which René 95 powder is hot isostatically pressed into a preform which is subsequently hot die forged.
As-HIP	=	A process in which a shape is made by hot isostatic processing, heat treating, and machining the shape into a finished part.
NNS	=	Near Net Shape.
ECM	=	Electromechanical Machining.
AH	=	As-HIP.
SQ	=	Salt Quench.
P/M	=	Powder Metallurgy
HPT	=	High Pressure Turbine section of an aircraft gas turbine engine.
AC	=	Air cool from a heat treating temperature.

APPENDIX A

VENDOR CERTIFICATE OF TEST FOR CF6-50 HPT AFT SHAFT SM-586

Appendix A consists of vendor certificates of test for product acceptance data for the as-HIP René 95 CF6-50 HPT aft shaft serial number SM-586. The residual cyclic life, cyclic rupture, and creep tests were performed on shafts SM-582 and SM-590 and the data are presented elsewhere in this report.

CERTIFICATE OF TEST



P.O. BOX M • OAKDALE, PA. 15071

JOB ORDER NO.	196
ENTRY DATE	

CUSTOMER General Electric Company		PURCHASE ORDER NO. 200-4DK-10J22440		DATE 5/28/76	NEW <input type="checkbox"/>	X <input checked="" type="checkbox"/>
CUST. PART NO.		CUST. DWG. NO. 4013196-451		SPECIFICATION NO. C50TF64		END USE
POWDER HEAT NO.		MASTER BLEND NO. MB048		COMPACT NO. SM-586		SERIAL NO. COL00003
515-932 515-984		515-934 515-986		515-942 515-988		515-944 515-990
515-952 515-992		515-956 515-994		515-960 515-996		515-966 515-998
515-968 516-000		515-980 516-002				
						WANTED
						HIP CYCLE NO. CCMO 144

ITEM NO.	PIECES	WEIGHT	PRODUCT DESCRIPTION
03	1		CF6 High Pressure Turbine Rotor Rear Shaft

CHEMICAL ANALYSIS

* = LESS THAN

C	Mn	Si	Cr	Ni	Co	Fe	Mo	W	V	Cb	Ti	Al
.050	.01*	.08	12.86	Ba1	8.28	.05	3.53	3.42	-	3.50	2.49	3.61

B	Zr	S	P	Cu	O	N	H					
.009	.04	.005	.003*	-	65ppm	30ppm	2.4ppm					

HEAT TREATMENT: δ SOLVUS TEMP. 2135 °F
 SOLUTION TEMP. 2050 °F 1 HRS.
 QUENCH DELAY 20 Sec.
 QUENCH TEMP. 1500 °F QUENCH AGITATION Manual
 AGE TEMP. 1600 °F 1 HRS. + 1200 °F 16 HRS.

HEAT TREATMENT:
 AUST. _____ °F _____ MIN.
 TEMPER. _____ °F _____ HRS. + _____ HRS. + _____ HRS.
 HARDNESS Rc _____ MIN.

HARDNESS: Rc MIN. Rc MAX.

ANNEALED HARDNESS BHN

COMMENTS:
 Sun Steel performed the heat treatment.

COMMENTS:

SWORN TO AND SUBSCRIBED BEFORE ME

THE TEST RESULTS SHOWN IN THIS REPORT ARE CORRECT TO THE BEST OF OUR KNOWLEDGE AND BELIEF

THIS _____ DAY OF _____ 19____

COLT INDUSTRIES CRUCIBLE Inc

CERTIFIED

BY: _____

NOTARY PUBLIC

REPRESENTATIVE

CERTIFICATE OF TEST
MECHANICAL TESTING

JOB ORDER NO.

GE P.O.#200-4DK-10J22440
Dwg. No. 4013196-451
S/N COL00003
SM-586



P.O. BOX M • OAKDALE, PA. 15071

SAMPLE CODE	TEMP. °F	STRESS PSI	TYPE SAMPLE	LIFE Hrs.	ELONG. %	RA %	RUPTURE LIFE	CYCLES
6-15 (TR _A)	1200	100,000*	S/R		3.1	3.5	376.7	
6-25 (TR _B)	1200	100,000**	S/R		4.7	6.5	338.7	
31	1200	140,000	S/R		4.7	8.5	215.2	
32	1200	140,000	S/R		4.7	3.5	228.1	
41	700	40,000	Notched LCF (Metcut Report 433-25817-1)					24,046
42	700	"	(alternating) (K _t =3.5)					13,306
43R***	1000	"	"			"		6,021
44	1000	"	"			"		4,194
45	1000	"	"			"		9,999
46	1000	"	"			"		15,271

*Increased to 140,000 psi after 166.7 hours.
**Increased to 140,000 ksi after 167.1 hours.
***Specimen 43 was repeated due to equipment failure.

SAMPLE CODE	TEMP. °F	ULTIMATE PSI	YIELD .2% PSI	ELONG. %	RA %	INCLUSION (METALLIC)
6-11 (TR _A)	74	232,500	172,200	15.6	18.5	None observed
6-23 (TR _B)	74	230,500	171,300	15.0	17.4	INCLUSION (NON METALLIC)
6-12 (TR _A)	1200	214,100	154,400	12.5	19.0	None observed
6-24 (TR _B)	1200	201,600	159,500	8.0	14.2	INCIPIENT MELTING
11	74	233,500	171,900	15.6	18.5	None observed
12	74	233,700	173,700	15.6	17.1	None observed
13	74	237,300	176,700	17.2	18.9	MASTER BLEND TRACE ELEMENT ANAL.
14	74	232,000	175,700	14.0	16.4	SEE ATTACHED
15	74	234,500	174,900	16.0	18.4	MACRO ETCH INSPECTION
21	1200	213,600	155,300	9.4	13.6	Conducted by GE
22	1200	215,900	163,300	12.5	15.4	SONIC INSPECTION
23	1200	214,400	151,900	14.0	17.8	Conducted by GE
24	1200	211,600	160,500	15.0	18.6	PENETRANT INSPECTION
						Conducted by GE

MASTER BLEND SEIVE ANALYSIS		DENSITY DETERMINATION					
MESH SIZE	%	SAMPLE CODE	DENSITY LBS./IN. ³	TIP % CHANGE	STANDARD	% CHANGE HIP vs STD.	WHOLE PART
+ 60	0.5	MB048					
- 60 + 100	29.2	6-14 (TR _A at 90°)	.2979	.15	2981 lb/in. ³		
- 100 + 325	55.0	6-17 (TR _A at 270°)	.2980	.23			
		6-22 (TR _B at 0°)	.2979	.25			
- 325	15.3	6-27 (TR _B at 180°)	.2980	.25			

SWORN TO AND SUBSCRIBED BEFORE ME

THE TEST RESULTS SHOWN IN THIS REPORT ARE CORRECT TO THE BEST OF OUR KNOWLEDGE AND BELIEF.

THIS _____ DAY OF _____ 19 _____

COLT INDUSTRIES CRUCIBLE Inc

NOTARY PUBLIC

CERTIFIED BY: *M. L. Shoenberger*
REPRESENTATIVE
287

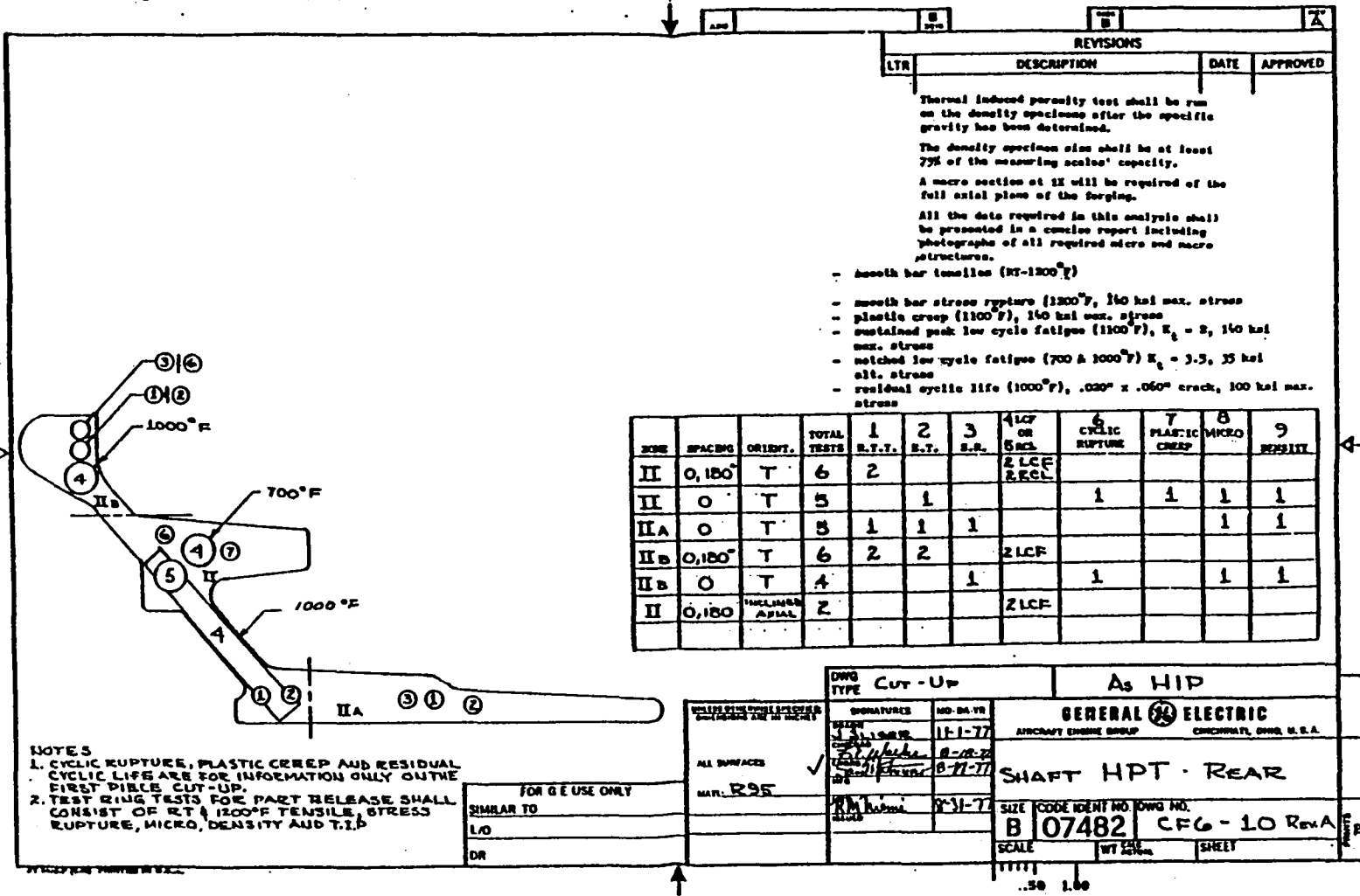


Figure 1. General Electric Cut-up Drawing for the Near-Net CF6 HPTR Aft Shaft.

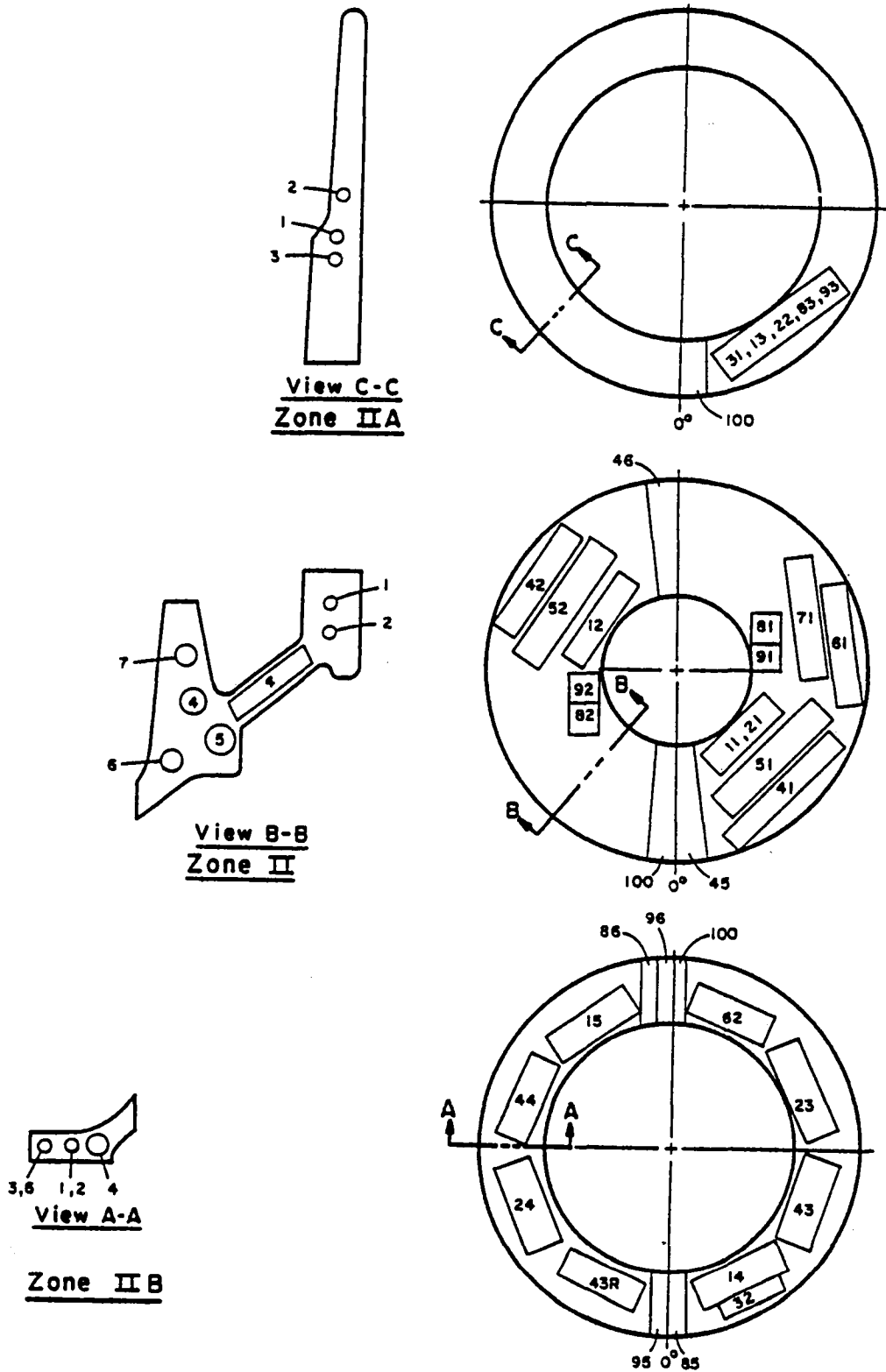


Figure 2. Cut-up Plan and Specimen Identification.

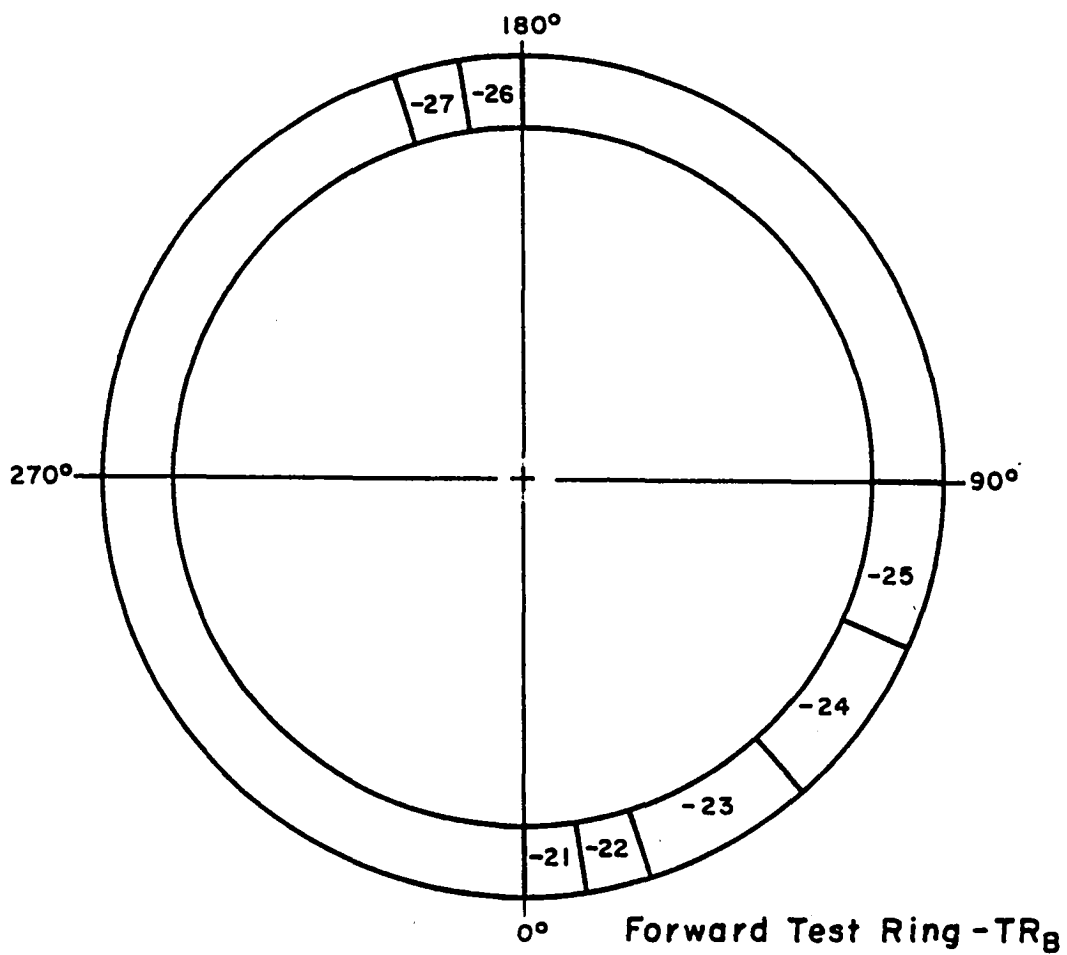
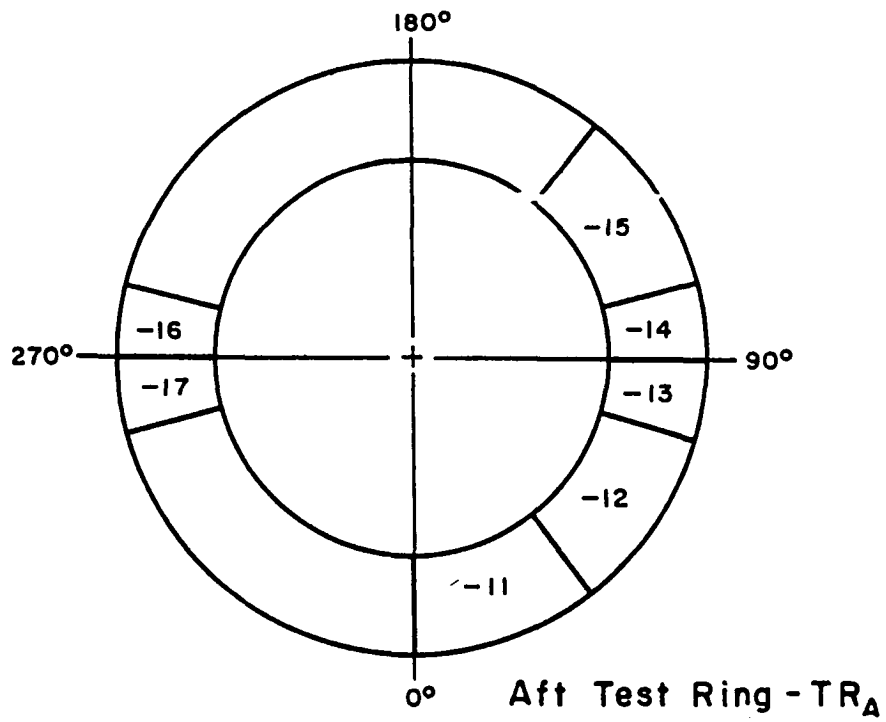


Table I. Density and TIP Data for the VSE cut-up SM-586

Sample Code	Location	As Heat Treated Density (lb/in. ³)	% TIP
91	Zone II - 90°	.2981	.24
92	Zone II - 270°	.2981	.22
93	Zone IIA - 0°	.2981	.22
95	Zone IIB - 0°	.2982	.26
96	Zone IIB - 180°	.2982	.25

Table IV. Trace Element Analyses of MB048

Analyses Performed at Accu-Labs Research, Inc.Chemistry Code No. ALR 107-4015-1Sample Identification No. CMRC 76-1789Master Blend or Heat No. MB048Date: November 22, 1976

Concentration for (ppm weight):

Uranium	<u> </u>	Cerium	<u> </u>	Copper	<u>7.3</u>
Thorium	<u>0.55</u>	Lanthanum	<u> </u>	Nickel	<u>Maj</u>
Bismuth	<u><0.10</u>	Barium	<u>0.55</u>	Cobalt	<u>Maj</u>
Lead	<u>0.17</u>	Cesium	<u> </u>	Iron	<u>790</u>
Thallium	<u><0.10</u>	Iodine	<u> </u>	Manganese	<u>10</u>
Mercury	<u>NR</u>	Tellurium	<u> </u>	Chromium	<u>Maj</u>
Gold	<u> </u>	Antimony	<u>0.97</u>	Vanadium	<u>5.7</u>
Platinum	<u> </u>	Tin	<u>1.4</u>	Titanium	<u>Maj</u>
Iridium	<u> </u>	Indium	<u> </u>	Scandium	<u> </u>
Osmium	<u> </u>	Cadmium	<u><1.0</u>	Calcium	<u>0.13</u>
Rhenium	<u> </u>	Silver	<u><0.15</u>	Potassium	<u>0.04</u>
Tungsten	<u>Maj</u>	Palladium	<u> </u>	Chlorine	<u>NR</u>
Tantalum	<u>12</u>	Rhodium	<u> </u>	Sulphur	<u>13</u>
Hafnium	<u>0.51</u>	Ruthenium	<u> </u>	Phosphorus	<u>NR</u>
Luycium	<u> </u>	Molybdenum	<u>Maj</u>	Silicon	<u>≈ 600</u>
Ytterbium	<u> </u>	Niobium	<u>Maj</u>	Aluminum	<u>Maj</u>
Thullium	<u> </u>	Zirconium	<u>610</u>	Magnesium	<u><0.41</u>
Erbium	<u> </u>	Yttrium	<u> </u>	Sodium	<u><0.10</u>
Holmium	<u> </u>	Strontium	<u> </u>	Fluorine	<u>NR</u>
Dysprosium	<u> </u>	Rubidium	<u> </u>	Oxygen	<u>NR</u>
Terbium	<u> </u>	Bromine	<u> </u>	Nitrogen	<u>NR</u>
Gadolinium	<u> </u>	Selenium	<u>0.21</u>	Carbon	<u>NR</u>
Europium	<u> </u>	Arsenic	<u>8.6</u>	Boron	<u>230</u>
Samarium	<u> </u>	Germanium	<u> </u>	Beryllium	<u> </u>
Neodymium	<u> </u>	Gallium	<u>11</u>	Lithium	<u> </u>
Praseodymium	<u> </u>	Zinc	<u>1.1</u>		

Notes: All elements not reported < 0.1 ppm weight.

292

NR - not reported.

APPENDIX B

VENDOR CERTIFICATE OF TEST FOR CF6-50 HPT AFT SHAFTS SM-582, SM-587,
SM-589, SM-590, AND SM-531

Appendix B presents certificate of test data for as-HIP CF6-50 HPT aft shaft serial numbers SM-582, SM-587, SM-589, SM-590, and SM-531 as reported by the vendor.

CERTIFICATE OF TEST



P.O. BOX M • OAKDALE, PA. 15071

JOB ORDER NO.	196
ENTRY DATE	

CUSTOMER General Electric Company		PURCHASE ORDER NO. 200-4DK-10J22440		DATE 5/28/76	NEW <input checked="" type="checkbox"/>	REPEAT <input type="checkbox"/>
CUST. PART NO.		CUST. DWG. NO. 4013196-451	SPECIFICATION NO. C50TF64		END USE	
POWDER HEAT NO.		MASTER BLEND NO. MB048	COMPACT NO.	SERIAL NO.	WANTED	
515-932	515-984		SM-582	COL00002		
515-934	515-986					
515-942	515-988		SM-587	COL00004		
515-944	515-990					
515-952	515-992		SM-589	COL00005		
515-956	515-994					
515-960	515-996		SM-590	COL00006		
515-966	515-998					
515-968	516-000				HIP CYCLE NO. 144	
515-980	516-002					

ITEM NO.	PIECES	WEIGHT	PRODUCT DESCRIPTION
03	4		CF6 High Pressure Turbine Rotor Rear Shaft

CHEMICAL ANALYSIS

* = LESS THAN

C	Mn	Si	Cr	Ni	Co	Fe	Mo	W	V	Cb	Ti	Al
.050	.01*	.08	12.86	Ba1	8.28	.05	3.53	3.42	-	3.50	2.49	3.61

B	Zr	S	P	Cu	O	N	H				
.009	.04	.005	.003*	-	65ppm	30ppm	2.4ppm				

HEAT TREATMENT: γ SOLVUS TEMP. 2135 °F
 SOLUTION TEMP. 2050 °F 1 HRS.
 QUENCH DELAY 20 Sec.
 QUENCH TEMP. 1500 °F QUENCH AGITATION Manual
 AGE TEMP. 1600 °F 1 HRS. + 1200 °F 16 HRS.

HEAT TREATMENT:
 AUST. _____ °F _____ MIN.
 TEMPER. _____ °F _____ HRS. + _____ HRS. + _____ HRS.
 HARDNESS Rc _____ MIN.

HARDNESS: Rc MIN. Rc MAX.

ANNEALED HARDNESS BHN

COMMENTS:
 Sun Steel performed the heat treatment.

COMMENTS:

SWORN TO AND SUBSCRIBED BEFORE ME

THE TEST RESULTS SHOWN IN THIS REPORT ARE CORRECT TO THE BEST OF OUR KNOWLEDGE AND BELIEF.

THIS _____ DAY OF _____ 19 _____

COLT INDUSTRIES CRUCIBLE Inc

CERTIFIED

BY: _____

REPRESENTATIVE

CERTIFICATE OF TEST
MECHANICAL TESTING

JOB ORDER NO.
196

GE P.O.#200-4DK-10J22440
Dwg. No. 4013196-451
S/N COL00002, 4, 5, 6
SM-582, 587, 589, 590



P.O. BOX M • OAKDALE, PA. 15071

SAMPLE CODE	TEMP. °F	STRESS PSI	TYPE SAMPLE	LIFE Hrs.	ELONG. %	RA %	RUPTURE LIFE	CYCLES
		Test Ring Cut-up Plan - see Figure 1 Stress Rupture Properties - see Table I						

SAMPLE CODE	TEMP. °F	ULTIMATE PSI	YIELD .2% PSI	ELONG. %	RA %	INCLUSION (METALLIC)	
		Tensile Properties - see Table II Dimensional Analyses - see Figure 2 and Table IV					None observed
						INCLUSION (NON METALLIC) None observed	
						INCIPIENT MELTING None observed	
						MASTER BLEND TRACE ELEMENT ANAL. SEE ATTACHED Table V	
						MACRO ETCH INSPECTION Conducted by GE	
						SONIC INSPECTION Conducted by GE	
						PENETRANT INSPECTION Conducted by GE	

MASTER BLEND SEIVE ANALYSIS		DENSITY DETERMINATION					
MESH SIZE	%	SAMPLE CODE	DENSITY LBS./IN. ³	TIP % CHANGE	STANDARD	% CHANGE HIP vs STD.	WHOLE PART
+ 60	0.5	MB048	Density - see Table III		.2981 lb/in. ³		
- 60 + 100	29.2						
- 100 + 325	55.0						
- 325	15.3						

SWORN TO AND SUBSCRIBED BEFORE ME
THIS _____ DAY OF _____ 19 _____

NOTARY PUBLIC

THE TEST RESULTS SHOWN IN THIS REPORT ARE CORRECT TO THE BEST OF OUR KNOWLEDGE AND BELIEF.
COLT INDUSTRIES CRUCIBLE Inc
CERTIFIED BY: *M. L. Shoenberger*
REPRESENTATIVE 295

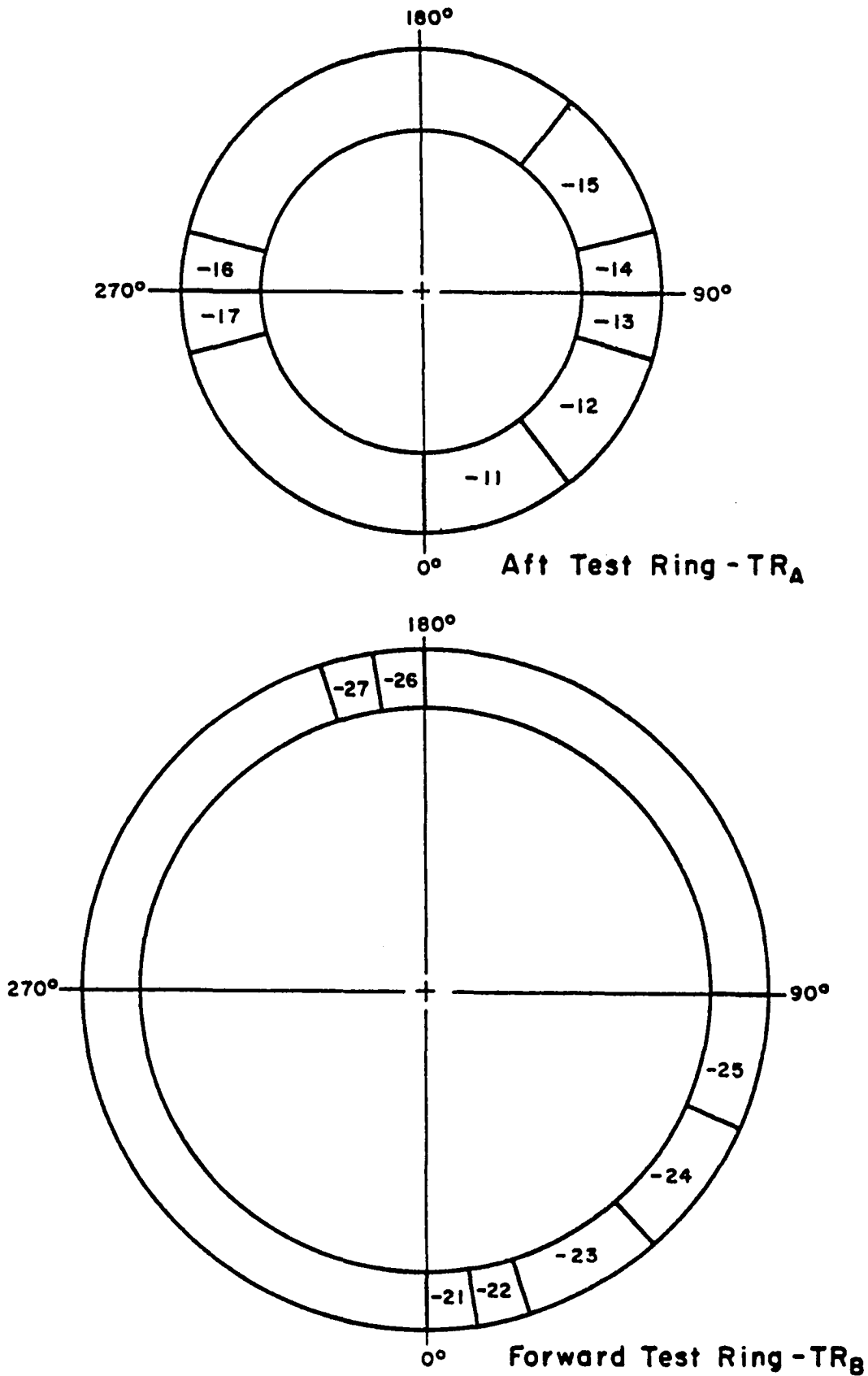


Figure 1. Test ring sectioning plan for CF6 aft shafts.

Table I. Stress Rupture Property Data

Part Identification	Serial Number	Sample Code ¹	Test Ring	Test Temp. (F)	Initial Stress (ksi)	Stress Increased After (hr) ²	Life (hr)	Elongation (%)	Reduction of Area (%)
SM-582	COL00002	2-15	TR _A	1200	100	173.4	345.0	4.7	7.5
SM-582	COL00002	2-25	TR _B	1200	100	162.4	276.0	4.7	7.0
SM-587	COL00004	7-15	TR _A	1200	100	166.9	341.2	3.1	7.5
SM-587	COL00004	7-25	TR _B	1200	100	163.4	321.4	5.5	5.5
SM-589	COL00005	9-15	TR _A	1200	100	169.2	392.0	6.3	6.5
SM-589	COL00005	9-25	TR _B	1200	100	165.2	353.2	7.8	8.5
SM-590	COL00006	0-15	TR _A	1200	100	162.1	322.0	3.1	3.5
SM-590	COL00006	0-25	TR _B	1200	100	166.2	310.8	4.7	5.0
Drawing Requirement #4013196-451				1200	100		25	6 ³	

¹Refer to Figure 1.

²Stress was increased to 140 ksi per Drawing #4013196-451.

³Only if failure occurs in less than 150 hours.

Table II. Tensile Property Data

Part Identification	Serial Number	Sample Code ¹	Test Ring	Test Temp. (F)	Ultimate Tensile Strength (ksi)	0.2% Yield Strength (ksi)	Elongation (%)	Reduction of Area (%)
SM-582	COL00002	2-11	TRA	74	232.5	168.9	18.7	21.0
SM-582	COL00002	2-23	TRB	74	228.9	169.6	15.0	18.1
SM-582	COL00002	2-12	TRA	1200	212.0	162.0	10.9	18.5
SM-582	COL00002	2-24	TRB	1200	209.2	158.0	14.0	18.2
SM-587	COL00004	7-11	TRA	74	230.0	172.5	14.0	17.5
SM-587	COL00004	7-23	TRB	74	228.9	171.0	15.6	17.9
SM-587	COL00004	7-12	TRA	1200	192.0	162.0	6.2	14.0
SM-587	COL00004	7-12A	TRA	1200	215.4	167.2	13.0	16.9
SM-587	COL00004	7-12B	TRA	1200	208.7	165.0	9.4	14.0
SM-587	COL00004	7-24	TRB	1200	209.0	156.7	12.0	17.9
SM-589	COL00005	9-11	TRA	74	231.7	168.9	17.2	19.5
SM-589	COL00005	9-23	TRB	74	231.3	168.4	18.7	19.9
SM-589	COL00005	9-12	TRA	1200	199.7	156.0	7.8	13.0
SM-589	COL00005	9-12A	TRA	1200	210.9	158.2	10.9	15.4
SM-589	COL00005	9-12B	TRA	1200	211.2	162.6	13.0	15.0
SM-589	COL00005	9-24	TRB	1200	210.0	156.6	14.0	19.5
SM-590	COL00006	0-11	TRA	74	228.4	171.0	14.1	17.9
SM-590	COL00006	0-23	TRB	74	205.8	171.7	8.0	12.0
SM-590	COL00006	0-23A	TRB	74	228.0	173.7	12.0	16.0
SM-590	COL00006	0-23B	TRB	74	225.5	174.0	11.0	14.8
SM-590	COL00006	0-12	TRA	1200	210.5	154.5	9.4	13.0
SM-590	COL00006	0-24	TRB	1200	208.2	161.8	10.0	14.6
Drawing Requirement #4013196-451				74	185.0	150.0	10	12
				1200	145.0	125.0	8	10

¹Refer to Figure 1.

Table III. Density and TIP Data

Part Identification	Serial Number	Sample Code ¹	Location ²	Test Ring	As Heat Treated Density ³ (lb/in. ³)	% TIP
SM-582	COL00002	2-14	90°	TRA	.2978	.23
SM-582	COL00002	2-17	270°	TRA	.2979	.21
SM-582	COL00002	2-22	0°	TRB	.2979	.22
SM-582	COL00002	2-27	180°	TRB	.2979	.23
SM-587	COL00004	7-14	90°	TRA	.2980	.19
SM-587	COL00004	7-17	270°	TRA	.2979	.17
SM-587	COL00004	7-22	0°	TRB	.2980	.23
SM-587	COL00004	7-27	180°	TRB	.2978	.24
SM-589	COL00005	9-14	90°	TRA	.2979	.22
SM-589	COL00005	9-17	270°	TRA	.2979	.26
SM-589	COL00005	9-22	0°	TRB	.2979	.25
SM-589	COL00005	9-27	180°	TRB	.2980	.25
SM-590	COL00006	0-14	90°	TRA	.2980	.23
SM-590	COL00006	0-17	270°	TRA	.2979	.17
SM-590	COL00006	0-22	0°	TRB	.2979	.22
SM-590	COL00006	0-27	180°	TRB	.2979	.18
Specification Requirement C50TF64					.2978 ⁴	.30

¹Refer to Figure 1.

²0° coincides with 0° from dimensional analyses.

³Standard density for MB048 = .2981 lb/in.³.

⁴99.9% of standard density - .2981 lb/in.³.

Table V. Trace Element Analyses

Analyses Performed at Accu-Labs Research, Inc.

Chemistry Code No. ALR 107-4015-1

Sample Identification No. CMRC 76-1789

Master Blend or Heat No. MB048

Date: November 22, 1976

Concentration for (ppm weight):

Uranium	<u> </u>	Cerium	<u> </u>	Copper	<u>7.3</u>
Thorium	<u>0.55</u>	Lanthanum	<u> </u>	Nickel	<u>Maj</u>
Bismuth	<u><0.10</u>	Barium	<u>0.55</u>	Cobalt	<u>Maj</u>
Lead	<u>0.17</u>	Cesium	<u> </u>	Iron	<u>790</u>
Thallium	<u><0.10</u>	Iodine	<u> </u>	Manganese	<u>10</u>
Mercury	<u>NR</u>	Tellurium	<u> </u>	Chromium	<u>Maj</u>
Gold	<u> </u>	Antimony	<u>0.97</u>	Vanadium	<u>5.7</u>
Platinum	<u> </u>	Tin	<u>1.4</u>	Titanium	<u>Maj</u>
Iridium	<u> </u>	Indium	<u> </u>	Scandium	<u> </u>
Osmium	<u> </u>	Cadmium	<u><1.0</u>	Calcium	<u>0.13</u>
Rhenium	<u> </u>	Silver	<u><0.15</u>	Potassium	<u>0.04</u>
Tungsten	<u>Maj</u>	Palladium	<u> </u>	Chlorine	<u>NR</u>
Tantalum	<u>12</u>	Rhodium	<u> </u>	Sulphur	<u>13</u>
Hafnium	<u>0.51</u>	Ruthenium	<u> </u>	Phosphorus	<u>NR</u>
Lutecium	<u> </u>	Molybdenum	<u>Maj</u>	Silicon	<u>≈ 600</u>
Ytterbium	<u> </u>	Niobium	<u>Maj</u>	Aluminum	<u>Maj</u>
Thullium	<u> </u>	Zirconium	<u>610</u>	Magnesium	<u><0.41</u>
Erbium	<u> </u>	Yttrium	<u> </u>	Sodium	<u><0.10</u>
Holmium	<u> </u>	Strontium	<u> </u>	Fluorine	<u>NR</u>
Dysprosium	<u> </u>	Rubidium	<u> </u>	Oxygen	<u>NR</u>
Terbium	<u> </u>	Bromine	<u> </u>	Nitrogen	<u>NR</u>
Gadolinium	<u> </u>	Selenium	<u>0.21</u>	Carbon	<u>NR</u>
Europium	<u> </u>	Arsenic	<u>8.6</u>	Boron	<u>230</u>
Samarium	<u> </u>	Germanium	<u> </u>	Beryllium	<u> </u>
Neodymium	<u> </u>	Gallium	<u>11</u>	Lithium	<u> </u>
Praseodymium	<u> </u>	Zinc	<u>1.1</u>		

Notes: All elements not reported < 0.1 ppm weight.
NR - not reported.

CERTIFICATE OF TEST



P.O. BOX M • OAKDALE, PA. 15071

JOB ORDER NO.	196
ENTRY DATE	

CUSTOMER General Electric Company		PURCHASE ORDER NO. 200-4DK-10J22440		DATE 5/28/76	NEW <input checked="" type="checkbox"/>	REPEAT <input type="checkbox"/>
CUST. PART NO.		CUST. DWG. NO. 4013196-451		SPECIFICATION NO. C50TF64		END USE
POWDER HEAT NO. 515-896 515-958 515-962 515-964 515-978		MASTER BLEND NO. MB047		COMPACT NO. SM-531		SERIAL NO. COL00001
				WANTED		HIP CYCLE NO. 101

ITEM NO.	PIECES	WEIGHT	PRODUCT DESCRIPTION
02	1		CF6 High Pressure Turbine Rotor Rear Shaft

CHEMICAL ANALYSIS

* = LESS THAN

C	Mn	Si	Cr	Ni	Co	Fe	Mo	W	V	Cb	Ti	Al
.05	.01	.08	12.86	Bal	8.23	.06	3.53	3.42	-	3.47	2.49	3.54

B	Zr	S	P	Cu	O	N	H				
.008	.04	.006	.003	-	76ppm	21ppm	2.4ppm				

HEAT TREATMENT: γ SOLVUS TEMP. 2120 °F
 SOLUTION TEMP. 2050 °F 1 HRS.
 QUENCH DELAY 20 Sec.
 QUENCH TEMP. 1500 °F QUENCH AGITATION Manual
 AGE TEMP. 1600 °F 1 HRS. + 1200 °F 16 HRS.

HEAT TREATMENT:
 AUST. _____ °F _____ MIN.
 TEMPER. _____ °F _____ HRS. + _____ HRS. + _____ HR.
 HARDNESS Rc _____ MIN.

HARDNESS: Rc MIN. Rc MAX.

ANNEALED HARDNESS BHN

COMMENTS:
Sun Steel performed the heat treatment.

COMMENTS:

SWGRN TO AND SUBSCRIBED BEFORE ME
 THIS _____ DAY OF _____ 19 _____

THE TEST RESULTS SHOWN IN THIS REPORT ARE CORRECT TO THE BEST OF OUR KNOWLEDGE AND BELIEF.
 COLT INDUSTRIES CRUCIBLE Inc

CERTIFIED BY: _____ REPRESENTATIVE

CERTIFICATE OF TEST
MECHANICAL TESTING

JOB ORDER NO.

196

GE P.O.#200-4DK-10J22440
Dwg. No. 4013196-451
S/N COL00001
SM-531



P.O. BOX M • OAKDALE, PA. 15071

SAMPLE CODE	TEMP. °F	STRESS PSI	TYPE SAMPLE	LIFE Hrs.	ELONG. %	RA %	RUPTURE LIFE	CYCLES
TRA 1-15	1200	100,000*	S/R		4.7	8.5	300.0 hr	
TRB 1-25	1200	100,000**	S/R		3.1	6.0	233.6 hr	
		*Increased to 140,000	psi after 162.0 hr					
		**Increased to 140,000	psi after 162.7 hr					
Test Ring Cut-up Plan - See Figure 1 Dimensional Analyses - See Figure 2 and Table I								

SAMPLE CODE	TEMP. °F	ULTIMATE PSI	YIELD .2% PSI	ELONG. %	RA %	INCLUSION (METALLIC)
TRA 1-11	RT	231,300	168,700	17.2	18.9	None observed
TRB 1-23	RT	229,500	169,300	16.0	18.8	INCLUSION (NON METALLIC)
TRA 1-12	1200	211,500	159,000	15.6	17.5	None observed
TRB 1-24	1200	211,000	156,300	16.0	16.8	INCIPIENT MELTING
						None observed
						MASTER BLEND TRACE ELEMENT ANAL.
						SEE ATTACHED Table II
						MACRO ETCH INSPECTION
						Conducted by GE
						SONIC INSPECTION
						Conducted by GE
						PENETRANT INSPECTION
						Conducted by GE

MASTER BLEND SEIVE ANALYSIS		DENSITY DETERMINATION					
MESH SIZE	%	SAMPLE CODE	DENSITY LBS./IN. ³	TIP % CHANGE	STANDARD	% CHANGE HIP vs STD.	WHOLE PART
+ 60	0.1						
- 60 + 100	26.9	MB047			.2980 lb/in. ³		
- 100 + 325	54.2	SM-531 (TRA)	.2979 (90°)	.13			
- 325	18.8	SM-531 (TR _B)	.2980 (270°)	.19			
			.2980 (0°)	.17			
			.2980 (180°)	.15			

SWORN TO AND SUBSCRIBED BEFORE ME

THE TEST RESULTS SHOWN IN THIS REPORT ARE CORRECT TO THE BEST OF OUR KNOWLEDGE AND BELIEF.

THIS _____ DAY OF _____ 19 _____

COLT INDUSTRIES CRUCIBLE Inc

NOTARY PUBLIC

CERTIFIED

BY:

M. L. Shoenberg
REPRESENTATIVE 303

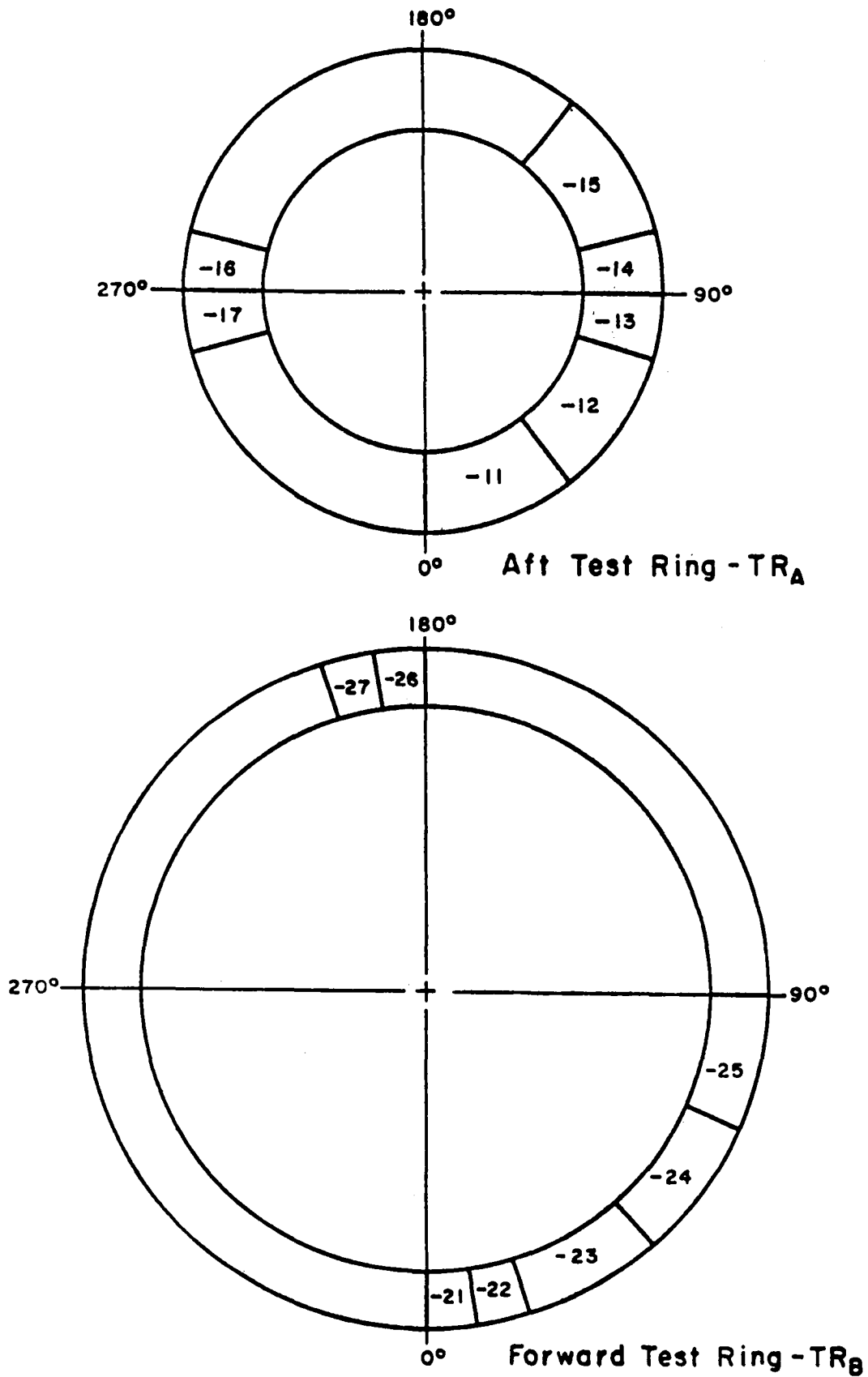


Figure 1. Test ring sectioning plan for CF6 aft shafts.

Table II. Trace Element Analyses

Analyses Performed at Accu-Labs Research, Inc.
 Chemistry Code No. 107-3688-1-1
 Sample Identification No. _____
 Master Blend or Heat No. MB047
 Date: 9/15/76

Concentration for (ppm weight):

Uranium		Cerium		Copper	30
Thorium	< 0.22	Lanthanum		Nickel	Major
Bismuth	< 0.10	Barium		Cobalt	Major
Lead	0.17	Cesium		Iron	790
Thallium	< 0.10	Iodine		Manganese	9.5
Mercury	NR	Tellurium	1.0	Chromium	Major
Gold		Antimony	3.0	Vanadium	11
Platinum		Tin	<1.0	Titanium	Major
Iridium		Indium		Scandium	
Osmium		Cadmium	<1.0	Calcium	0.07
Rhenium		Silver	<0.23	Potassium	0.04
Tungsten	Major	Palladium		Chlorine	NR
Tantalum	7.3	Rhodium		Sulphur	23
Hafnium	<0.57	Ruthenium		Phosphorus	NR
Lutecium		Molybdenum	Major	Silicon	560
Ytterbium		Niobium	Major	Aluminum	Major
Thullium		Zirconium	700	Magnesium	<0.41
Erbium		Yttrium		Sodium	<0.10
Holmium		Strontium		Fluorine	NR
Dysprosium		Rubidium		Oxygen	NR
Terbium		Bromine		Nitrogen	NR
Gadolinium		Selenium	0.51	Carbon	NR
Europium		Arsenic	14	Boron	71
Samarium		Germanium		Beryllium	
Neodymium		Gallium	11	Lithium	
Praseodymium		Zinc	2.4		

Notes: All elements not reported < 0.1 ppm weight.
 NR - not reported.

APPENDIX C

PROCESS PLAN FOR MANUFACTURING CF6-50 HPT AFT SHAFT

Appendix C presents the Crucible Inc. process plan for manufacturing the CF6-50 HPT aft shaft which resulted from this Project.

**PROCESS PLAN FOR PRODUCTION OF
GENERAL ELECTRIC CF6 HIGH PRESSURE
TURBINE AFT SHAFT**

GE Drawing No. 4013196-451

Process Code CMRC-002

**COLT INDUSTRIES
CRUCIBLE INC
MATERIALS RESEARCH CENTER
P. O. Box 88
Pittsburgh, Pennsylvania 15230**

August 15, 1977

PROCESS PLAN FOR PRODUCTION OF
GENERAL ELECTRIC CF6 HIGH PRESSURE
TURBINE AFT SHAFT

Drawing No.: 4013196-451
Part No.: 4013196-451 PO1
Process Code: CMRC-002

Process Description

I. Powder Manufacture

A. Applicable Specifications:

CMRC-002-1	GE C50TF64
CMRC-002-2	GE P29TF19
CMRC-002-3	GE P1TF47
CMRC-002-4	
CMRC-002-5	
CMRC-002-6	
CMRC-002-7	
CMRC-002-8	
CMRC-002-9	

B. Process:

Powder is produced by vacuum melting a charge of virgin, virgin + revert powder or revert powder and subsequent atomization with argon gas. The resulting powder is loaded into storage containers for subsequent processing. Each heat is screened to -60 mesh, passed through a magnetic particle separator, blended on itself, sampled, and returned to storage containers. Samples of each heat are qualified for use on the basis of composition, powder size, and cleanliness. Qualified heats are blended together to form a Master Blend. Master Blend samples are used to qualify the Master Blend on the basis of composition, trace element content, powder size, and cleanliness.

C. Process Controls:

1. Raw melting materials are procured from specific qualified commercial sources.
2. Refractories for containing and directing the liquid metal are specific materials purchased from specific qualified suppliers.
3. Melting and atomization are controlled with respect to addition sequence, vacuum level, temperature and gas pressure. Complete melting records are maintained.
4. Composition and trace elements are controlled by specific analytical techniques.
5. Powder heat quality is controlled with respect to composition, powder size, and cleanliness.
6. Powder Master Blend quality is controlled with respect to composition and cleanliness. Apparent density, sieve analysis, γ' solvus temperature, and HIP density are measured and recorded.
7. Controlled powder storage procedures.
8. Screening controlled with respect to equipment, cleaning, and procedure.
9. Blending controlled with respect to equipment, cleaning, procedure, blend size, blending time, and blending atmosphere.

II. Mold and Secondary Can Manufacture and Assembly

A. Applicable Specifications:

CMRC-002-10	GE C50TF64
CMRC-002-11	GE P7TF5
CMRC-002-12	

B. Process:

The process for preparing ceramic molds is essentially similar to the "lost wax" process utilized for casting molds. Wax patterns are prepared in accordance with the process drawing by machining or wax injection into a master die. The wax shape is coated with specific ceramic materials, dried and then heated to remove the wax and fire the ceramic shell. The shell is qualified for use by visual examination and powder purging to insure cleanliness and then capped until loading.

A secondary metal container is used to surround the ceramic mold.

C. Process Controls:

1. All raw materials are purchased from specific qualified sources.
2. Dimensional and weight measurements of wax pattern are made to insure compliance with the wax process drawing.
3. Visual examination of wax surface.
4. Wax storage within a controlled environment.
5. Mold slurries controlled with respect to viscosity, temperature and pH.
6. Mold drying controlled with respect to temperature and humidity.

7. Visual inspection of mold interior for surface defects, residual wax residue, and surface finish.
8. Powder purge of mold to insure cleanliness.

III. Powder Loading, Encapsulation, Outgassing, and Sealing

A. Applicable Specifications:

CMRC-002-13
GE C50TF64
GE P7TF5

B. Process:

Powder, prepared as in I above, is loaded in a clean room into the mold assembly as prepared in II above. The mold assembly is vibrated during loading. The process is continued until a predetermined weight of powder has been loaded into the mold cavity.

The powder filled assembly is then outgassed until a specific leak-out rate and vacuum level are obtained. The can is then sealed and the assembly is ready for HIP.

C. Process Controls:

1. Complete mold filling is controlled by an accurate determination of mold volume.

2. Adequate outgassing is controlled by measuring leak out rate and vacuum level.

IV. Consolidation and Container Removal

A. Applicable Specifications:

CMRC-002-14

CMRC-002-15

GE C50TF64

GE P7TF5

B. Process:

The sealed mold assembly, prepared as in III above, is loaded into the autoclave and hot-isostatically-pressed (HIP) at 2050 F under 15,000 psi pressure. Upon completion of the cycle, the charge is cooled in the autoclave and removed. The part is then removed from the mold assembly.

C. Process Controls:

1. HIP cycle is controlled with respect to heat-up rate, pressurization rate, and cycle time.
2. Temperature and pressure throughout the HIP cycle are continuously monitored and recorded.
3. Container removal is controlled on the basis of specific procedures to minimize part damage.

V. Post Consolidation Processing, Inspection and Evaluation

A. Applicable Specifications:

CMRC-002-4	GE C50TF64
CMRC-002-16	GE P3TF1
CMRC-002-17	GE P3TF2
CMRC-002-18	GE P7TF5

B. Process:

The consolidated part, processed as in IV above, is lightly grit blasted and spot ground, if necessary, to remove slight surface blemishes which may act as stress risers. The part is then dimensionally checked to insure compliance with process drawings. Integral fill tubes are removed and evaluated for density, TIP and microstructure.

Heat treatment is conducted without further surface preparation at a qualified heat treatment facility using the specified heat treatment cycle. Following heat treatment, test rings are removed and evaluated for density, TIP, microstructure and mechanical properties, per specification requirements. The part is then macroetched, dye penetrant inspected, and ultrasonically inspected per specification requirements.

C. Process Controls:

- 1. Heat treatment conducted at a qualified facility.**
- 2. Heat treatment cycle monitored and recorded.**
- 3. Shape verified by accurate measurement and target machining.**
- 4. HIP cycle verified by density measurement and microstructural evaluation of fill tube samples which are compared to approved standards.**
- 5. Part integrity and cleanliness are verified by dye penetrant and ultrasonic inspections to approved standards.**
- 6. Heat treatment cycle and part capability are verified by microstructural examination, density measurements, and mechanical property tests of test ring material.**

Issue Date 8/15/77

Revision No. _____

Revision Date _____

Process Specifications for Production
of
General Electric CF6 HPTR Rear Shaft
GE Drawing Number 4013196-451
Process Code CMRC-002

INDEX

Specification Number

CMRC-002-1	Raw Material Procurement
CMRC-002-2*	Melting and Atomizing Environment: Equipment, Crucibles and Refractories
CMRC-002-3*	Melting and Atomization
CMRC-002-4	Chemical Analysis Procedures for Superalloy Powder
CMRC-002-5	Powder Screening Procedure
CMRC-002-6	Powder Blending Procedure
CMRC-002-7	Powder Storage Procedure
CMRC-002-8	Powder Heat Quality Evaluation
CMRC-002-9	Master Blend Quality Evaluation
CMRC-002-10*	Wax Pattern Manufacture
CMRC-002-11*	Ceramic Mold Manufacture
CMRC-002-12*	Outer Metal Can Manufacture
CMRC-002-13*	Loading, Sealing and Outgassing Procedure
CMRC-002-14	HIP Procedure
CMRC-002-15	Container Removal and Inspection Procedure
CMRC-002-16	Heat Treatment Procedure
CMRC-002-17	Machining
CMRC-002-18	Mechanical Property and Non-Destructive Testing

*Restricted

APPENDIX D

PROCESS PLANS FOR MANUFACTURING CFM56 HIP + FORGE COMPRESSOR DISK
PREFORMS AND FORGINGS

Appendix D presents the vendor process plans for producing HIPPED forging preforms and the forging process plan for producing the CFM56 compressor disk forgings from these preforms.

SPECIAL METALS

An Allegheny Ludlum Industries Company

UDIMET POWDER DIVISION

2310 S. INDUSTRIAL HIGHWAY
ANN ARBOR, MICHIGAN 48104
TELEPHONE: 313 665-0669
TWX 810 223-6057

DEVELOPMENT CENTER

October 17, 1977

Cliff Shamblen
Mail Drop: E74
General Electric
Evendale Plant
Aircraft Engine Group
Cincinnati, Ohio 45215

Dear Cliff:

As of September 23, we have shipped to KBI three GE MATE preform containers to be hot isostatically pressed in Cartech's 2200°F/15 KSI/ 3 hr. cycle. The containers identified 0102-1 and 0102-2 were filled in air in a horizontal position through four fill tubes and container 0102-3 was rim filled by Udimet's standard vacuum can filling procedure.

CONTAINERS: The 14 gauge container material was purchased and certified as "enameling iron - decarburized .003 - maximum." A typical chemistry was given as .002% C, .18% Mn, .010% P, .020% S. The container shapes were produced by spin forming.

The containers were cleaned, welded and leak checked in accordance with the following paragraphs of Special Metals Rene 95 Standard Practice, SPII revision D: 3.1 - 3.6 describing the cleaning procedure, 4.1.1 - 4.1.2 container machining for fill tubes, 5.1.1 - 5.1.8 welding procedure and 6.1 - 6.5 leak checking. The only exception being the number and location of fill tubes on containers 1 and 2. These containers had four fill tubes equally spaced, 90° apart, and located mid-way across the flat container face.

The cleaning, welding, and leak checking procedure can be described as, prior to welding, the containers were degreased, any trace of oxidation removed and washed with acetone.

The components were fusion welded using TIG equipment. The fill tube was 0.049-in. wall, 3/4 in. OD seamless SAE 1015 steel and welded using a 308 stainless steel fill rod. During welding, the interior of the container



October 17, 1977

was purged with argon to prevent oxidation of the steel. The assembled containers were leak checked by pressurizing with 20 psig argon, submersing in a water-soap solution and checking for air bubbles.

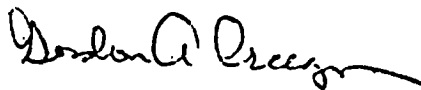
CONTAINER FILLING: Rene 95 powder, blend BN77042, was used to fill the containers. The chemistry and screen analysis are attached. Each container held between 84 and 85 pounds of -60 mesh powder. Containers 1 and 2 were filled in air while in a horizontal position. The powder in approximately two pound batches was loaded in alternating fill tubes. Vibration was required after the containers were 50% loaded. When loading was completed, three fill tubes were sealed with o-rings and KF blank-off fittings. The container was transferred to the evacuation station and pumped through the remaining fill tube.

The number three container was filled in accordance with Udimet's standard vacuum can filling procedure as outlined in Rene 95 Standard Practice, SPII revision D. The paragraphs describing this procedure are 8.1 - 8.4 and 8.5.2 - 8.13 powder filling, 9.1 - 9.1.10 transfer to evacuation station, 9.2.1 - 9.2.1.8 outgassing and 10.1 - 10.10 fill tube sealing. Basically, the container was vacuum filled with powder while maintaining a pressure of less than 15 microns of mercury on the system. The powder entered the containers by means of a vibrating feeding device which exposed individual particles to the vacuum. After filling, the container was valved off and transferred to the evacuation station for outgassing.

All three containers were outgassed under similar conditions. Sealing did not occur until the dynamic pressure was 4×10^{-5} torr or less and the leak rate was 5 microns per minute or less. The containers were sealed by crimping and fusion welding the fill tubes.

The containers are now at KBI for the 2200°F/15 KSI/3 hr. HIP cycle. When completed, the preforms will be returned to Ann Arbor for can removal by hot nitric acid and metallographic TIP testing. The preforms will then be shipped to GE Evendale for chem milling.

Sincerely,



Gordon A. Creeger
Research Metallurgist

GAC:vh

cc: W. B. Castledine

Attachment

CERTIFICATE OF TEST

SPECIAL METALS

An Allegheny Ludlum Industries Company

UDIMET POWDER DIVISION

3001 SOUTH STATE STREET
SUITE 1017
ANN ARBOR, MICHIGAN 48104
PHONE (313) 665-0666

TO: General Electric

SHIPPED TO: General Electric

ATTENTION:

CUSTOMER ORDER NO. _____

UPD ORDER NO. 0102

METAL POWDER TYPE _____

LOT NO. Blend BN77042

QUANTITY SHIPPED _____

MESH SIZE -60

SHIPPED VIA _____

PREPAID COLLECT

DATE SHIPPED _____

PACKING SLIP NO. _____

CHEMICAL ANALYSIS:

Al 3.48 %	B .009 %	C .06 %
Co 8.15 %	Cr 12.81 %	Cu N.D. %
Fe .23 %	Ni Balance %	O ₂ .0088 %
P .004 %	S .004 %	Si <.01 %
Ti 2.54 %	W 3.55 %	Zr .004 %
Mn .02 %	Cb 3.54 %	N ₂ .0036 %
Mo 3.42 %	Ta .03 %	H ₂ .0004 %

TYPICAL SIEVE ANALYSIS:

MESH	%
+60	0
+80	4.6
+100	4.6
+120	2.7
+140	7.9
+170	6.0
+200	7.8
+230	6.1
+270	7.2
+325	9.5
+400	11.0
+500	15.6
-500	16.9

COMMENTS:

BY M. R. Davis
M. R. Davis - Q. A. Supervisor
320

CARTECH MATE PROCESSING OUTLINE FOR NEAR NET SHAPE
F101/CFM56 STAGE 5-9 COMPRESSOR DISC FORGING PREFORMS

1. POWDER MANUFACTURE

- a. Composition & processing conform to General Electric Specifications C50TF65 & PlTF47.
- b. Powder is produced by vacuum induction remelting CarTech VIM ingot mulds and revert powder and gas atomizing with high purity argon.
- c. Powder is processed to produce blends of -60 mesh forging grade powder.

2. CANISTER MANUFACTURE

- a. Canister material is mild steel.
- b. Canister design is based upon shrinkage data obtained from previous shape iterations.
- c. Spun-shape forms are produced from a print of the desired canister design. A sample of mild steel used for spun-shaped components is submitted to CarTech for analysis.
- d. The spun-shape forms are inspected for conformance to desired dimensions. The forms are then cleaned, heli-arc welded and inspected for internal cleanliness, as-fabricated dimensions and vacuum integrity.
- e. The fabricated canisters are subject to a proprietary operation to enhance their internal cleanliness.

3. CANISTER FILLING

- a. Acceptable canister assemblies are identified with a canister number, tared and are vacuum filled with the appropriate -60 mesh Rene' 95 powder. The canisters are face-filled using dual fill tubes, to control the orientation of striations.
- b. Prior to and during the filling operation the powder is exposed to a vacuum of less than 5 microns Hg.

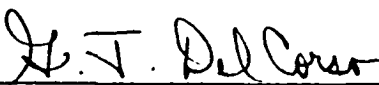
- c. After being filled with powder the canisters are sealed by crimping the evacuation tubes and burning through the crimped sections with an arc welder.
- d. The sealed canisters are inspected for dimensional acceptance and net fill weight.

4. CONSOLIDATION

- a. Acceptable canisters are sent to Kawecki Berylco Industries, Hazleton, Penna. for hot isostatic pressing.
- b. The hot isostatic pressing operation conforms to General Electric Specifications C50TF65 and P7TF5. The HIP temperature is 2200°F ± 25°F. The preforms are autoclave cooled subsequent to consolidation at 2200°F.

5. POST-CONSOLIDATION PROCESSING

- a. The as-compacted preforms are visually inspected for signs of leakage and are dimensioned to ascertain their size acceptability.
- b. The evacuation tube of the preforms are removed and are evaluated to determine their acceptability per General Electric specification C50TF65.
- c. Acceptably compacted preforms are pickled in modified Aqua-regia to remove all traces of the mild steel container. The preforms are then examined for striations and their net weights and preform dimensions of the preforms are noted. Acceptable preforms are shipped to General Electric for chem-milling.



Gregory J. Del Corso
Senior Project Metallurgist
Process Research

cjm

LADISH CO.

CLOSED IMPRESSION DIE FORGINGS TO 56,000 POUNDS
SEAMLESS ROLLED RINGS TO 28 FEET DIAMETER 350,000 POUNDS
FORGED AND SEAMLESS WELDING PIPE FITTINGS AND FLANGES
LARGE DIAMETER FLANGES - SAW BLADES
CORROSION RESISTANT PIPE FITTINGS, FLANGES AND VALVES
SANITARY FITTINGS, VALVES, PUMPS AND SPECIALTIES

CUDAHY, WISCONSIN, 53110

MILWAUKEE SUBURB - CABLE ADDRESS "LADISHCO"

*Controlled
Quality
Products*



TO MARK PROGRESS

September 20, 1977

General Electric Co.
Aircraft Engine Group
Bldg. 600
MAIL DROP A182
Cincinnati, OH 45215

C. Shambler

ATTENTION: ~~MR. ROGER BLUM~~

SUBJECT: Manufacturing Process Sheet Approval

Dear Roger:

Attached are five (5) copies of Ladish Co. revised Manufacturing Process Sheets for your part #4013084-314 P01 and P02. This process sheet applies only to the NASA MATE program, your purchase order #10J22426. Revised procedure incorporated a pre-treatment prior to forge.

Approval of process sheet 5042 Revision C by General Electric is requested.

Sincerely,

LADISH CO.

Bob Krueger

R. J. KRUEGER
ASSISTANT DIRECTOR
GOVERNMENT RELATIONS DIVISION

bp/att.

LADISH CO. METALLURGICAL DEPARTMENT

MFG. PROCESS

SHEET NO. 5042 Revision C

DATE 9/12/77

LADISH CONTROL NO. EX106	CUSTOMER General Electric	PART NO. 4013084-314 P01 & P02	DIE NO. EX106
	MATERIAL SPEC. C50TF65 Cl. B		STOCK SIZE Preform
MATERIAL René 95 P/M	*SIGNIFICANT OPERATIONS/ <u>C50TF65</u>	MATERIAL SOURCE(S) Special Metals	

Any specific forging operations may be repeated with Metallurgical Engineering approval to insure geometry control. Forge temperatures are individually selected to maintain optimum property response.

PROCESS SEQUENCE	METALLURGICAL DATA			
	HEATING EQUIPMENT	HEATING PROCEDURE	COOLING	GOVERNING SPEC.
1. Serialize				
2. Pretreat		2175°F./2 hrs.	Fc. cool	
3. Polish Preform as Necessary				
4. Sonic Test				(L) Info
5. Etch - Met. Release Required				8K23
6. Caustic Clean				
*7. Isothermal Forge		2100°F. Max.		
Caustic Clean				
9. Condition				
10. Etch				
11. Zyglo				(L) Info
*12. Solution Treat				C50TF65
13. Caustic Clean				
*14. Age				C50TF65
15. Brinell				C50TF65
16. Clean				
17. Part Test Ring				
*18. Product Test				C50TF65
19. Polish for Sonic - 90 RMS				
*20. Sonic Test per Print				P3TF1 Cl. A

† Secondary certification on file and equipped with L & N temperature controllers

PAGE 1 OF 2

324

LCO 2158 RI FC

AUTH. MET REP. 

R. Noel

AUTH. SALES REP. _____

APPENDIX E

MATERIAL ACCEPTANCE CRITERIA AND
LOWER LIMIT DATA CURVES FOR

as-HIP RENE 95

ACCEPTANCE CRITERIA FOR RENE 95 as-HIP PARTS

1. SCOPE:

1.1 Form: Hot isostatically pressed powder metallurgy product of an alloy known as Rene 95.

1.2 Application: For rotating turbine engine parts operating at temperatures up to about 650° C (1200° F).

2. APPLICABLE DOCUMENTS: The following documents form a part of this specification to the extent specified herein. Unless a certain issue is specified, the latest issue shall apply.

2.1 SAE Publications: Available from Society of Automotive Engineers, Inc., 400 Commonwealth Drive, Warrendale, PA 15096.

2.1.1 Aerospace Material Specifications:

AMS 2269 Chemical Check Analysis Limits, Wrought Nickel, and Nickel Base Alloys

AMS 2350 Standards and Test Methods

AMS 2630 Ultrasonic Inspection

2.2 ASTM Publications: Available from American Society for Testing and Materials, 1916 Race Street, Philadelphia, PA 19103.

ASTM E112 Estimating Average Grain Size of Metals

ASTM E354 Chemical Analysis of High-Temperature, Electrical, Magnetic, and Other Similar Iron, Nickel, and Cobalt-Base Alloys

2.3 Government Publications: Available from Commanding Officer, Naval Publications and Forms Center, 5801 Tabor Avenue, Philadelphia, PA 19120.

2.3.1 Federal Standards:

Federal Test Method Standard No. 151 - Metals; Test Methods.

3. TECHNICAL REQUIREMENTS:

3.1 Composition: Shall conform to the following percentages by weight, determined by wet chemical methods in accordance with ASTM E354, by spectrographic methods in accordance with Federal Test Method Standard No. 151, Method 112, or by other approved analytical methods.

3.1.1 Parts shall be produced from powder of a nickel-base alloy known as René 95 with the following chemical composition:

Chemical Composition, Percent

Carbon	0.04 - 0.09	Columbium.....	3.30 - 3.70
Manganese.....	0.15 Max	Zirconium.....	0.03 - 0.07
Silicon.....	0.20 Max	Titanium.....	2.30 - 2.70
Sulphur.....	0.015 Max	Aluminum.....	3.30 - 3.70
Phosphorus.....	0.015 Max	Boron.....	0.006 - 0.015
Chromium.....	12.00 - 14.00	Tungsten.....	3.30 - 3.70
Cobalt.....	7.00 - 9.00	Oxygen.....	0.15 Max
Molybdenum.....	3.30 - 3.70	Nitrogen.....	0.005 Max
Iron.....	0.50 Max	Hydrogen.....	0.001 Max
Tantalum.....	0.20 Max	Nickel.....	Remainder

3.1.2 Check Analysis: Composition variations shall meet the requirements of AMS 2269.

3.2 Powder:

René 95 powder shall be produced using the induction melt + argon atomize process and shall be screened to minus 60 mesh. Powder chemical composition shall meet the requirements of 3.1.1 and other powder characteristics shall be as agreed upon between purchaser and vendor.

3.3 Containerization:

The René 95 powder shall be canned prior to hot isostatic pressing using a procedure as agreed upon between purchaser and vendor.

3.4 Hot Isostatic Pressing (HIP):

The canned René 95 powder shall be HIPped at a temperature of 1121° C for a minimum of 2 hours at a pressure of 103.4 MPa (15,000 psi). The product shall be cooled in the autoclave. Other HIP process parameters shall be as agreed upon between purchaser and vendor.

3.5 Ultrasonic Inspection: The HIPped part shall undergo ultrasonic inspection in accordance with ASTM 2630 using a standard agreed upon by purchaser and vendor.

3.6 Dimensional Inspection: The part shall undergo dimensional inspection with the data conforming to the requirements agreed upon by purchaser and vendor.

4.0 CONDITION: The product shall be supplied in the heat treated condition as described in the following sections:

4.1 Heat Treatment:

All heat treat temperatures refer to metal temperature $\pm 14^{\circ}$ C ($\pm 25^{\circ}$ F). All times refer to time at temperature for the heaviest section. Parts shall be supplied in the solution treated and aged condition as specified below: Heat to 1121° C (2050° F) and hold for 1 hour, salt quench to 816° C (1500° F), and air cool to below 538° C (1000° F). Double age 1 hour at 816° C (1600° F) plus 16 hours at 649° C (1200° F) and air cool.

4.2 Mechanical Properties:

4.2.1 Tensile: Parts, heat treated per 4.1, shall meet the minimum tensile requirements shown in Table 4.2, as measured on test rings cut from the product in the tangential or radial directions, or as otherwise agreed upon between purchaser and vendor. Tensile properties for section sizes above 46.0 mm (1.8 inch) in thickness as heat treated shall be as agreed upon between purchaser and vendor.

4.2.2 Stress Rupture: Test specimens shall be tested at 648.9° C (1200° F) using the stress specified below, and shall have a 25-hour minimum life. Tests shall be continued to rupture, and elongation after rupture, measured at room temperature, shall be not less than 2% in 4D.

Stress, MPa (ksi)

965 (140)

4.3 Grain Size:

Parts shall have a uniform average grain size of ASTM No. 8 or finer.

4.4 Density:

After solution heat treatment and aging, the as-HIP part density measured by weighing a representative sample from the part shall meet or exceed 99.9% of 8249 kg/m^3 (0.298 lbs/in.^3). The density of a representative sample shall not decrease more than 0.3% after being exposed for 4 hours at 1204° C $\pm 8^{\circ}$ (2200° F $\pm 15^{\circ}$) in air, and air cooled.

4.5 Incipient Melting:

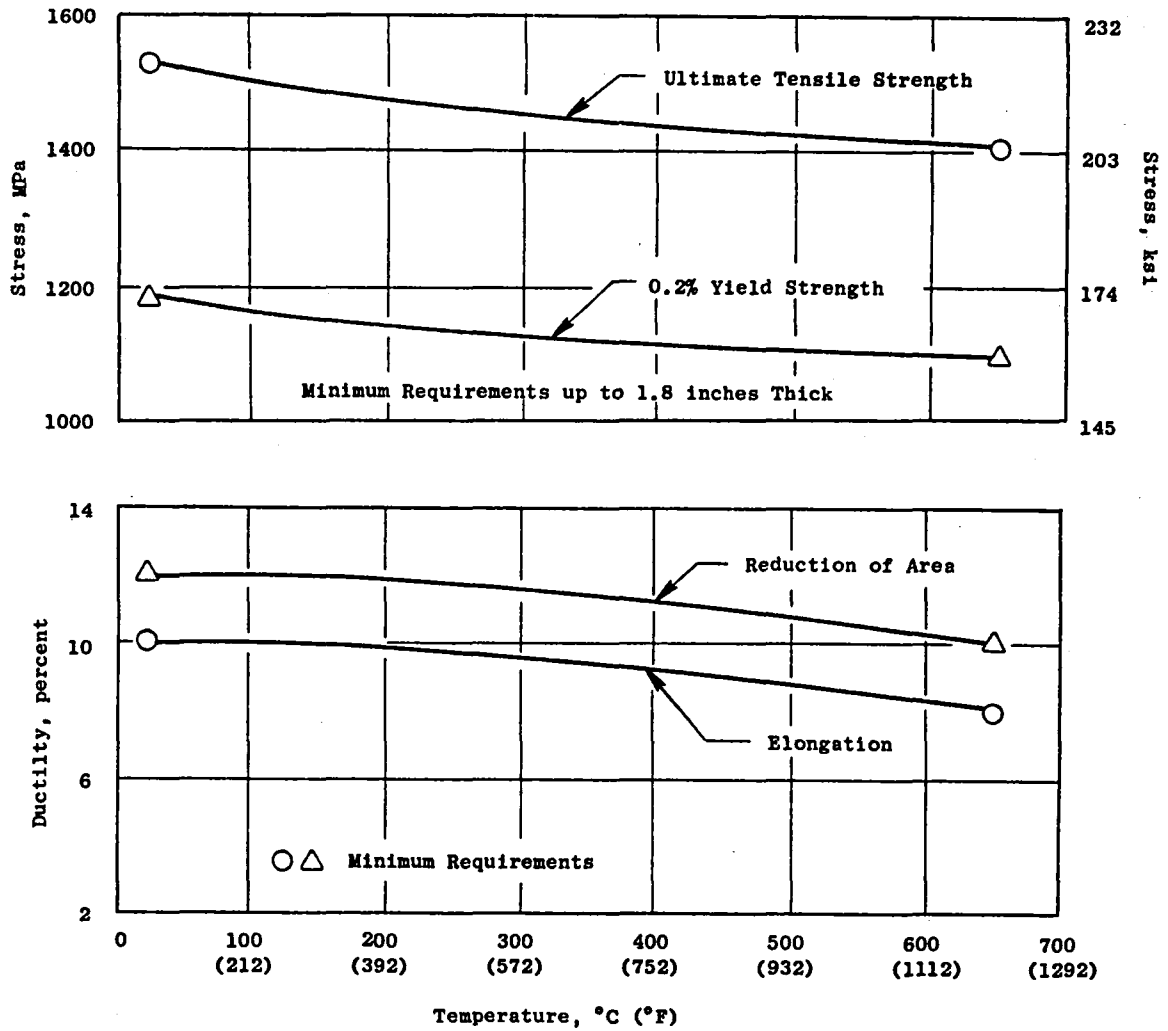
Parts shall exhibit no evidence of incipient melting.

4.6 Rejections:

Material not conforming to these acceptance criteria will be subject to rejection unless other agreements have been made between purchaser and vendor.

Table 4.2. Minimum Tensile Properties.

<u>Heat Treated Section Thickness</u>	<u>Room Temperature - MPa (ksi)</u>			
	<u>Ultimate Strength</u>	<u>0.2% Yield Strength</u>	<u>Elongation, Percent</u>	<u>Red. Area, Percent</u>
Up to 46.0 mm (1.8 inch)	1496 (217)	1145 (166)	10	12
	<u>1200° F - MPa (ksi)</u>			
Up to 46.0 mm (1.8 inch)	1365 (198)	1041 (151)	8	10



Material Acceptance Criteria Showing Lower Limits for As-HIP René 95.

APPENDIX F

MATERIAL ACCEPTANCE CRITERIA
AND LOWER LIMIT DATA CURVES FOR
HIP + FORGED RENE 95

ACCEPTANCE CRITERIA FOR RENE 95 HIP + FORGE PARTS

1. SCOPE:

1.1 Form: Hot isostatically pressed and forged powder metallurgy product of an alloy known as René 95.

1.2 Application: For rotating turbine engine parts operating at temperatures up to about 650° C (1200° F).

2. APPLICABLE DOCUMENTS: The following documents form a part of this specification to the extent specified herein. Unless a certain issue is specified, the latest issue shall apply.

2.1 SAE Publications: Available from Society of Automotive Engineers, Inc., 400 Commonwealth Drive, Warrendale, PA 15096.

2.1.1 Aerospace Material Specifications:

AMS 2269 Chemical Check Analysis Limits, Wrought Nickel, and Nickel Base Alloys

AMS 2350 Standards and Test Methods

AMS 2630 Ultrasonic Inspection

2.2 ASTM Publications: Available from American Society for Testing and Materials, 1916 Race Street, Philadelphia, PA 19103.

ASTM E112 Estimating Average Grain Size of Metals

ASTM E354 Chemical Analysis of High-Temperature, Electrical, Magnetic, and Other Similar Iron, Nickel, and Cobalt-Base Alloys.

2.3 Government Publications: Available from Commanding Officer, Naval Publications and Forms Center, 5801 Tabor Avenue, Philadelphia, PA 19120.

2.3.1 Federal Standards:

Federal Test Method Standard No. 151 - Metals; Test Methods.

3. TECHNICAL REQUIREMENTS:

3.1 Composition: Shall conform to the following percentages by weight, determined by wet chemical methods in accordance with ASTM E354, by spectrographic methods in accordance with Federal Test Method Standard No. 151, Method 112, or by other approved analytical methods.

3.1.1 Parts shall be produced from powder of a nickel-base alloy known as René 95 with the following chemical composition:

Chemical Composition, Percent

Carbon	0.04 - 0.09	Columbium.....	3.30 - 3.70
Manganese.....	0.15 Max	Zirconium.....	0.03 - 0.07
Silicon.....	0.20 Max	Titanium.....	2.30 - 2.70
Sulphur.....	0.015 Max	Aluminum.....	3.30 - 3.70
Phosphorus.....	0.015 Max	Boron.....	0.006 - 0.015
Chromium.....	12.00 - 14.00	Tungsten.....	3.30 - 3.70
Cobalt.....	7.00 - 9.00	Oxygen.....	0.015 Max
Molybdenum.....	3.30 - 3.70	Nitrogen.....	0.005 Max
Iron.....	0.50 Max	Hydrogen.....	0.001 Max
Tantalum.....	0.20 Max	Nickel.....	Remainder

3.1.2 Check Analysis: Composition variations shall meet the requirements of AMS 2269.

3.2 Powder:

René 95 powder shall be produced using the induction melt + argon atomize process and shall be screened to minus 60 mesh. Powder chemical composition shall meet the requirements of 3.1.1 and other powder characteristics shall be as agreed upon between purchaser and vendor.

3.3 Containerization:

The René 95 powder shall be canned prior to hot isostatic pressing using a procedure as agreed upon between purchaser and vendor.

3.4 Hot Isostatic Pressing (HIP):

The canned René 95 powder shall be HIPped at 1204° C (2200° F) for a minimum of 2 hours at a pressure of 103.4 MPa (15,000 psi). The product shall be cooled at a rate of 167° ± 55° C per hour (300° ± 100° F) to 871° C (1600° F) and rapidly cooled thereafter.

3.5 Microstructure:

The microstructure of each HIP lot shall be evaluated and the ASTM grain size of the product shall be in the range of ASTM 3 to 6 per ASTM-E112.

3.6 Forging:

The HIP billet sections or forging preforms shall be isothermally forged at a temperature of 1093° to 1121° C (2000° to 2050° F). HIP billet sections or forging preforms shall be designed to achieve a 50% to 60% reduction during forging.

- 3.7 Thermally Induced Porosity: A sample of the product shall be heated to a temperature of $1204^{\circ}\text{C} \pm 8^{\circ}$ ($2200^{\circ}\text{F} \pm 15^{\circ}$), held at the selected temperature for 4 hours, and air cooled. Microstructure after thermal exposure shall conform to the requirements agreed upon by purchaser and vendor. The density of the sample shall be measured before and after exposure and shall show no more than 0.3% density decrease after such exposure.
- 3.8 Ultrasonic Inspection: The HIP + Forged part shall undergo ultrasonic inspection in accordance with ASTM 2630 using a standard agreed upon by purchaser and vendor.
- 3.9 Dimensional Inspection: The part shall undergo dimensional inspection with the data conforming to the requirements agreed upon by purchaser and vendor.
- 4.0 CONDITION: The product shall be supplied in the heat treated condition as described in the following sections:
- 4.1 Heat Treatment:
- All heat treat temperatures refer to metal temperature $\pm 14^{\circ}\text{C}$ ($\pm 25^{\circ}\text{F}$). All times refer to time at temperature for the heaviest section.
- 4.1.2 Parts shall be supplied in the solution heat treated and aged condition as specified below:
- Heat to 1093°C (2000°F) and hold for 1 to 2 hours. Oil or salt quench from 1093°C (2000°F) with maximum bath temperature of 538°C (1000°F). Age at 760°C (1400°F) for 16 hours and air cool.
- 4.2 Mechanical Properties:
- 4.2.1 Tensile: Parts, heat treated per 4.1, shall meet the applicable minimum tensile requirements shown in Table 4.2, as measured on test rings cut from the product in the tangential or radial directions, or as otherwise agreed upon between purchaser and vendor. Tensile properties for section sizes above 46.0 mm (1.8 inch) in thickness as heat treated shall be as agreed upon between purchaser and vendor.
- 4.2.2 Stress Rupture: Test specimens shall be tested at 649°C (1200°F) using the stress specified below, and shall have a 25-hour minimum life. Tests shall be continued to rupture, and elongation after rupture, measured at room temperature, shall be not less than 2% in 4D.

Stress, MPa (ksi)
1030 (150)

4.3 Grain Size:

Parts shall have a duplex microstructure consisting of necklaces of fine recrystallized grains, ASTM No. 8 or finer, surrounding larger elongated unrecrystallized grains ranging between 10% and 60%. A schematic diagram of a typical structure is shown in Figure 1.

4.4 Incipient Melting:

Parts shall exhibit no evidence of incipient melting.

4.5 Rejections:

Material not conforming to these acceptance criteria will be subject to rejection unless other agreements have been made between the purchaser and vendor.

Table 4.2. Minimum Tensile Properties.

<u>Heat Treated Section Thickness</u>	<u>Room Temperature - MPa (ksi)</u>			
	<u>Ultimate Strength</u>	<u>0.2% Yield Strength</u>	<u>Elongation, Percent</u>	<u>Red. Area, Percent</u>
Up to 35.6 mm (1.4 inch)	1544 (224)	1207 (175)	10	12
>35.6 to 46.0 mm (1.4 to 1.8 inch)	1524 (221)	1179 (171)	10	12
	<u>1200° F - MPa (ksi)</u>			
Up to 35.6 mm (1.4 inch)	1427 (207)	1117 (162)	8	10
>35.6 to 46.0 mm (>1.4 to 1.8 inch)	1407 (204)	1089 (158)	8	10

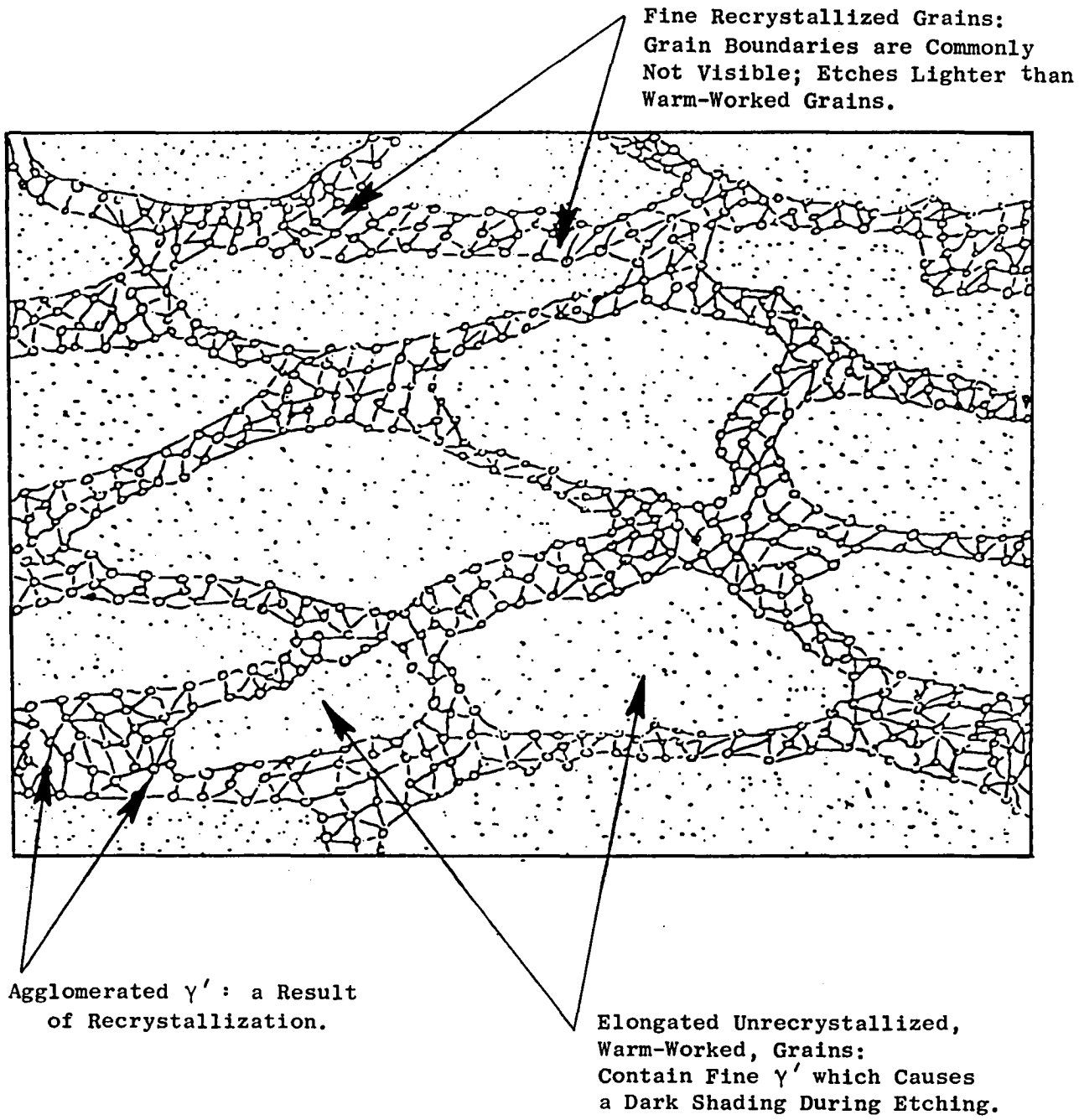
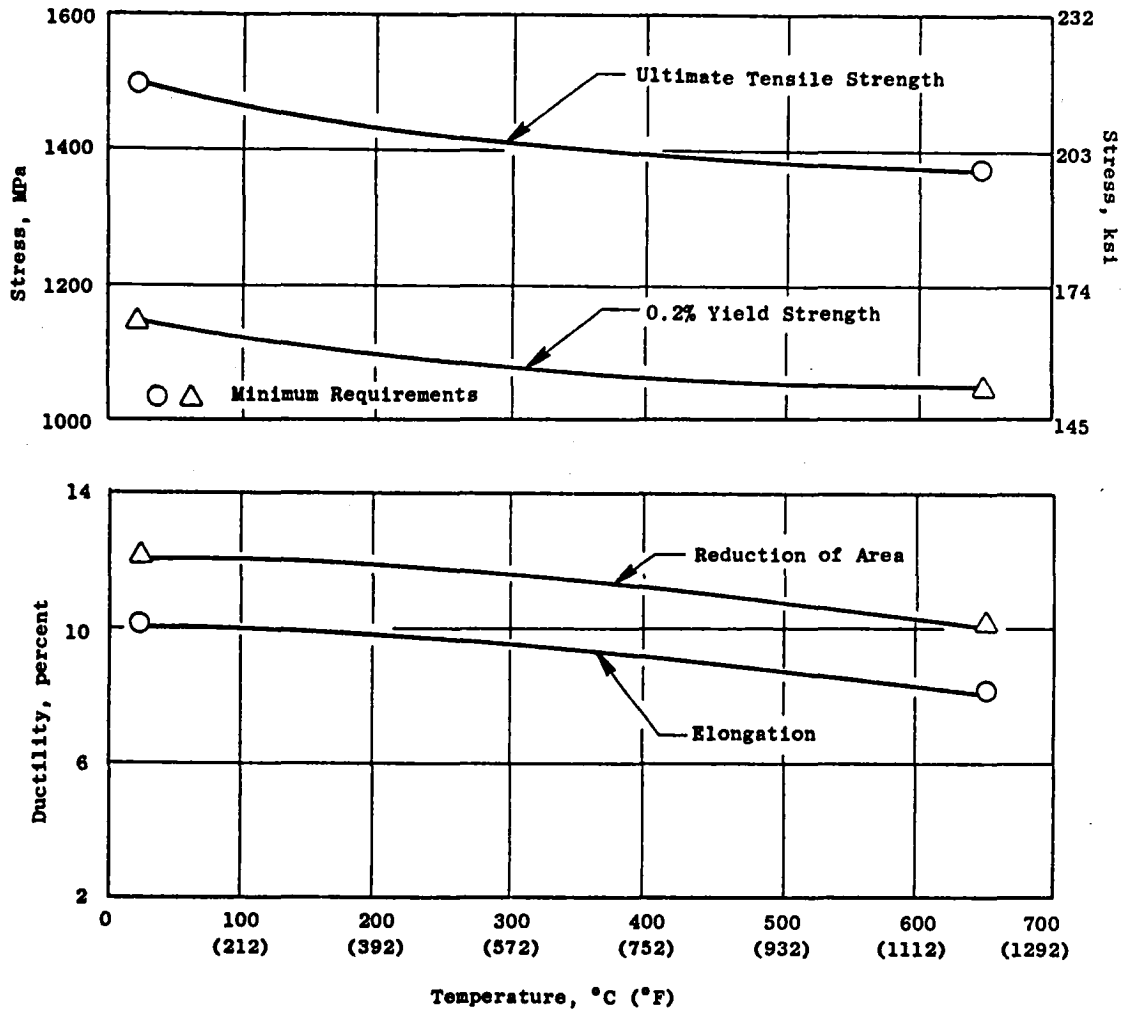


Figure 1. Idealized Sketch of a Power Metallurgy René 95 Microstructure at Approximately 500X.



Material Acceptance Criteria Showing Lower Limits for HIP + Forged René 95.

